frontiers

RESEARCH TOPICS

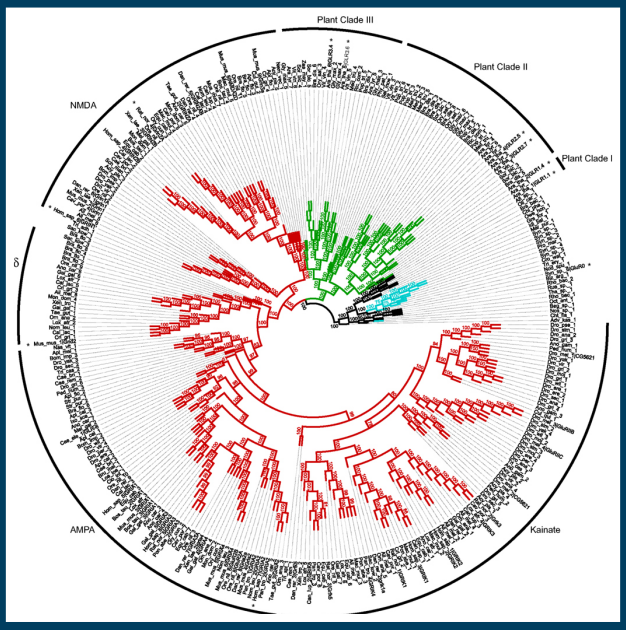

EVOLUTION OF MEMBRANE SIGNALING AND TRAFFICKING IN PLANTS

Topic Editors
Markus Geisler, Angus S. Murphy, and Heven Sze

frontiers in PLANT SCIENCE

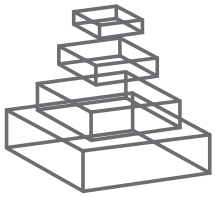

frontiers

ISSN 1664-8714
ISBN 978-2-88919-131-4
DOI 10.3389/978-2-88919-131-4

ABOUT FRONTIERS

Frontiers is more than just an open-access publisher of scholarly articles: it is a pioneering approach to the world of academia, radically improving the way scholarly research is managed. The grand vision of Frontiers is a world where all people have an equal opportunity to seek, share and generate knowledge. Frontiers provides immediate and permanent online open access to all its publications, but this alone is not enough to realize our grand goals.

FRONTIERS JOURNAL SERIES

The Frontiers Journal Series is a multi-tier and interdisciplinary set of open-access, online journals, promising a paradigm shift from the current review, selection and dissemination processes in academic publishing.
All Frontiers journals are driven by researchers for researchers; therefore, they constitute a service to the scholarly community. At the same time, the Frontiers Journal Series operates on a revolutionary invention, the tiered publishing system, initially addressing specific communities of scholars, and gradually climbing up to broader public understanding, thus serving the interests of the lay society, too.

DEDICATION TO QUALITY

Each Frontiers article is a landmark of the highest quality, thanks to genuinely collaborative interactions between authors and review editors, who include some of the world's best academicians. Research must be certified by peers before entering a stream of knowledge that may eventually reach the public - and shape society; therefore, Frontiers only applies the most rigorous and unbiased reviews.
Frontiers revolutionizes research publishing by freely delivering the most outstanding research, evaluated with no bias from both the academic and social point of view.
By applying the most advanced information technologies, Frontiers is catapulting scholarly publishing into a new generation.

WHAT ARE FRONTIERS RESEARCH TOPICS?

Frontiers Research Topics are very popular trademarks of the Frontiers Journals Series: they are collections of at least ten articles, all centered on a particular subject. With their unique mix of varied contributions from Original Research to Review Articles, Frontiers Research Topics unify the most influential researchers, the latest key findings and historical advances in a hot research area!
Find out more on how to host your own Frontiers Research Topic or contribute to one as an author by contacting the Frontiers Editorial Office: researchtopics@frontiersin.org

EVOLUTION OF MEMBRANE SIGNALING AND TRAFFICKING IN PLANTS

Topic Editors:
Markus Geisler, University of Fribourg, Switzerland
Angus S. Murphy, University of Maryland, USA
Heven Sze, University of Maryland, USA

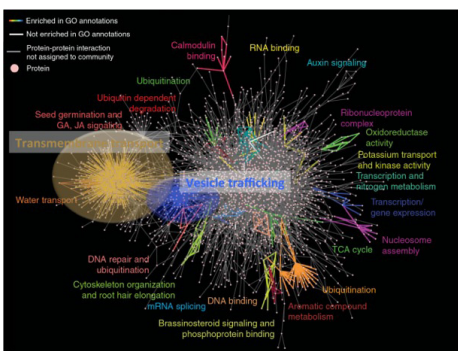

Membrane proteins are essential determinants of many biological processes in plants. They function in metabolic processes, signal transduction, transport of small molecules and polymers across endo- and plasma membranes, and intercompartmental trafficking of proteins, lipids, and cell wall components. During these integrative processes, dynamic interactions of membrane proteins with other membrane or soluble components are thought to provide a high degree of flexibility that usually characterizes higher plants. This concept is supported by the recent release of a first, partial Arabidopsis interactome by the Arabidopsis Interactome Mapping Consortium (http://www.sciencemag.org/content/333/6042/601.full.htm). The Arabidopsis interactome reveals a strong enrichment of a few network communities, including those for transmembrane transport and vesicle trafficking. Strikingly, the large transmembrane transport community shares a high amount of proteins with the vesicle trafficking community suggesting a strong physical and functional overlap and interaction.

Table of Contents

frontiers in
PLANT SCIENCE

EDITORIAL
published: 05 March 2013
doi: 10.3389/fpls.2013.00040

Evolution of membrane signaling and trafficking in plants

Markus Geisler*

Plant Biology – geislerLab, Department of Biology, University of Fribourg, Fribourg, Switzerland
**Correspondence: markus.geisler@unifr.ch*

Edited by:
Wendy A. Peer, University of Maryland, USA

Reviewed by:
Wendy A. Peer, University of Maryland, USA

Membrane proteins are essential determinants of many biological processes in plants. They function in metabolic processes, signal transduction, transport of small molecules and polymers across endo- and plasma membranes, and inter-compartmental trafficking of proteins, lipids, and cell wall components. During these highly integrative processes, dynamic interactions of membrane proteins with other membrane or soluble components are thought to provide a high degree of flexibility that usually characterizes higher plants. This concept is supported by the recent release of a first, partial Arabidopsis interactome by the Arabidopsis Interactome Mapping Consortium [http://interactome.dfci.harvard.edu/A_thaliana; (Arabidopsis Interactome Mapping Consortium, 2011)]. The Arabidopsis interactome reveals a strong enrichment of a few network communities, with the transmembrane transport community being the largest. Strikingly, the high degree of shared proteins among the transmembrane transport and trafficking communities suggests both physical interaction and functional overlap (see **Figure 1**).

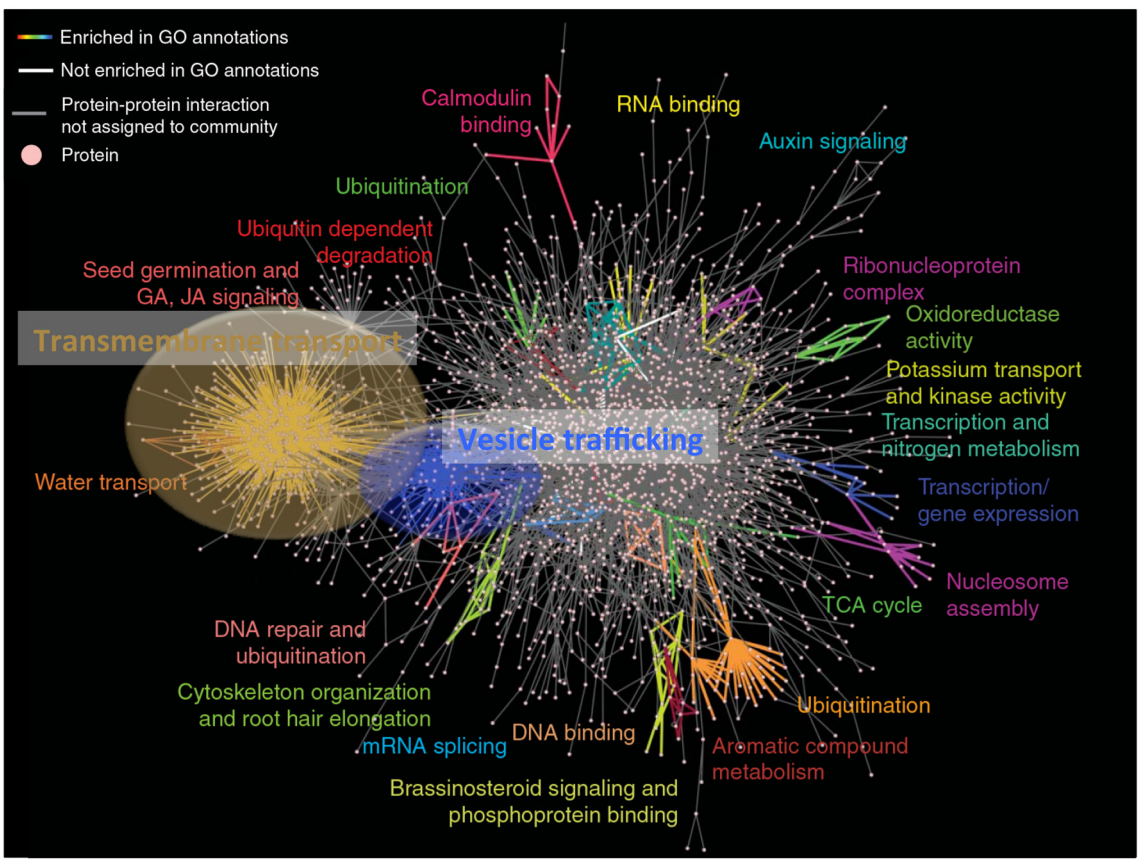

FIGURE 1 | The large transmembrane transport community (brown) shares a high amount of proteins with the vesicle trafficking community (blue) suggesting a strong physical and functional overlap and interaction. AI-1_{MAIN} communities enriched in gene ontology annotations are colored. Modified from Arabidopsis Interactome Mapping Consortium (2011).

With no surprise, this current research topic co-hosted by *Frontiers in Plant Transport and Traffic* and *Frontiers in Plant Physiology* reflects well this outcome of the *Arabidopsis* Interactome Mapping Consortium. It embraces outstanding current research efforts with a series of reviews and original papers that highlight conserved and plant-specific mechanisms of post-Golgi trafficking, exocytosis and endocytosis and the role of the actin cytoskeleton from an evolutionary perspective. This research topic is comprised of reviews on PILS and AUX/LAX transmembrane auxin carriers and reviews, original articles, and hypothesis and theory articles on plant channels, including potassium channels, slow and quick anion channels, and glutamate receptors. This research topic concludes with an integrated view on how membranes shape plant nodulation and Arbuscular mycorrhizae.

As such, this research topic is a timely update presenting advances in research in the evolution of membrane signaling and trafficking in plants, encompassed of outstanding contributions that address fundamental questions in these essential processes in plants.

ACKNOWLEDGMENTS

Work in the author's lab is supported by the Novartis Foundation, the *Pol de Recherche* of the University of Fribourg and the Swiss National Funds.

REFERENCES

Arabidopsis Interactome Mapping Consortium. (2011). Evidence for network evolution in an Arabidopsis interactome map. *Science* 333, 601–607.

Received: 28 January 2013; accepted: 13 February 2013; published online: 05 March 2013.
Citation: Geisler M (2013) Evolution of membrane signaling and trafficking in plants. Front. Plant Sci. ***4****:40. doi: 10.3389/fpls.2013.00040*
This article was submitted to Frontiers in Plant Traffic and Transport, a specialty of Frontiers in Plant Science.

frontiers in
PLANT SCIENCE

REVIEW ARTICLE
published: 28 August 2012
doi: 10.3389/fpls.2012.00197

Conserved and plant-unique mechanisms regulating plant post-Golgi traffic

Masaru Fujimoto*[1] *and Takashi Ueda*[1,2]

[1] *Department of Biological Sciences, Graduate School of Science, The University of Tokyo, Tokyo, Japan*
[2] *Japan Science and Technology Agency, Precursory Research for Embryonic Science and Technology, Kawaguchi, Japan*

Edited by:
Angus S. Murphy, University of Maryland, USA

Reviewed by:
Stephanie Robert, SLU/Umeå Plant Science Center, Sweden
Frantisek Baluska, University of Bonn, Germany

***Correspondence:**
Takashi Ueda, Department of Biological Sciences, Graduate School of Science, The University of Tokyo, 7-3-1 Hongo, Bunkyo-ku, Tokyo 113-0033, Japan.
e-mail: tueda@biol.s.u-tokyo.ac.jp

Membrane traffic plays crucial roles in diverse aspects of cellular and organelle functions in eukaryotic cells. Molecular machineries regulating each step of membrane traffic including the formation, tethering, and fusion of membrane carriers are largely conserved among various organisms, which suggests that the framework of membrane traffic is commonly shared among eukaryotic lineages. However, in addition to the common components, each organism has also acquired lineage-specific regulatory molecules that may be associated with the lineage-specific diversification of membrane trafficking events. In plants, comparative genomic analyses also indicate that some key machineries of membrane traffic are significantly and specifically diversified. In this review, we summarize recent progress regarding plant-unique regulatory mechanisms for membrane traffic, with a special focus on vesicle formation and fusion components in the post-Golgi trafficking pathway.

Keywords: coat protein complex, dynamin-related protein, membrane trafficking, Rab GTPase, tether, SNARE

INTRODUCTION

Eukaryotic cells are distinguished by the presence of internal membrane-bound organelles, including mitochondria, plastids, peroxisomes, and other single membrane-bound organelles. Two different underlying mechanisms have been proposed for the emergence of these organelles. Mitochondria and plastids, which have a double-membrane envelope in principle, arose respectively through the symbiotic incorporation of α-proteobacteria and cyanobacteria by the ancestral eukaryotic cell (Barbrook et al., 2006; Embley and Martin, 2006). In contrast, organelles bound by a single membrane layer [e.g., the endoplasmic reticulum (ER), Golgi apparatus, *trans*-Golgi network (TGN), plasma membrane (PM), and a series of endosomal compartments], are thought to have evolved autogenously from preexisting single membrane components in ancient proto-eukaryotic cells (Cavalier-Smith, 1987, 2002). These single membrane-bound organelles are connected with each other through a trafficking system mediated by vesicular and/or tubular membranous transport carriers, known as membrane trafficking. Membrane trafficking consists of several sequential processes: the formation of cargo-bearing vesicles or tubules from donor membranes, targeted delivery of transport carriers, and tethering of carriers to target membranes, followed by membrane fusion (**Figure 1**). These processes involve specific sets of regulatory machinery. For example, coat protein complexes (CPCs) and dynamin-related GTPases (DRPs) participate in the formation of vesicular or tubular carriers; CPCs facilitate cargo selection and membrane deformation, and DRPs take part in the tubulation and/or scission of donor membranes (**Figure 1**; Bonifacino and Glick, 2004; Praefcke and McMahon, 2004). Rab GTPase, a member of the Ras superfamily, tethers, and soluble *N*-ethylmaleimide-sensitive factor attachment protein receptors (SNAREs) are responsible for the targeting and subsequent tethering and fusion of carriers to target membranes (**Figure 1**; Chen and Scheller, 2001; Seabra and Wasmeier, 2004; Yu and Hughson, 2010). Each subfamily of these machinery components performs a function similar to that of other paralogs, but at a specific subcellular location or as part of a distinct transport pathway (Bonifacino and Glick, 2004).

Modern phylogenetic studies suggest that eukaryotes are comprised of five major supergroups: Amoebozoa; Opisthokonta; Archaeplastida; Excavata; and *St*ramenopiles, *Al*veolates and *R*hizaria together with *C*ryptophyte, *C*entrohelid, *T*elonemid, and *H*aptophyte (SAR + CCTH; Burki et al., 2009). Owing to the recent accumulation of genomic resources among these five supergroups, molecular evolutionary analyses have been yielding information about the emergence and establishment of membrane trafficking components. Comparative genomic and phylogenetic analyses of CPCs (Schledzewski et al., 1999), DRPs (Elde et al., 2005; Miyagishima et al., 2008), Rab GTPases (Brighouse et al., 2010; Elias et al., 2012), tethers (Koumandou et al., 2007), and SNAREs (Dacks and Doolittle, 2002; Yoshizawa et al., 2006) sampled from a broad range of eukaryotic lineages have revealed that similar sets of paralogous subgroups of these machinery components are often shared among these supergroups. This conservation suggests that the basic framework of membrane traffic was already established before the last common eukaryotic ancestor, which is commonly shared among extant descendant eukaryotic lineages (Dacks et al., 2009). However, these analyses also demonstrated that each eukaryotic lineage occasionally acquired lineage-specific new subgroups and/or expanded specific subfamilies, probably by lineage-specific gene multiplication and the accumulation of mutations. Such genes are predicted to be associated with the lineage-specific differentiation of organelle functions and membrane trafficking pathways.

The lineage-specific expansion and diversification of machinery components for membrane trafficking are also evident in plant

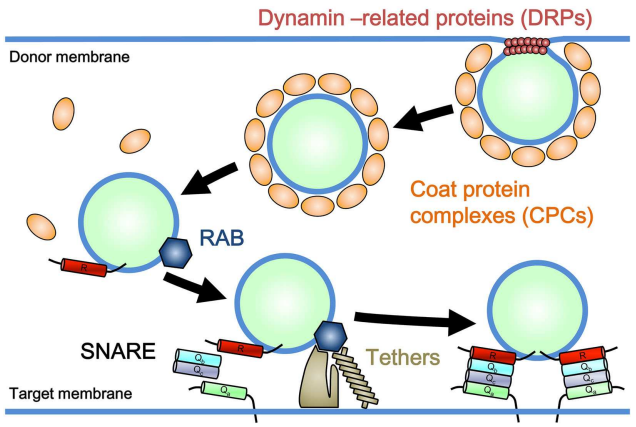

FIGURE 1 | Model for a general mechanism of membrane trafficking. Coat protein complexes (CPCs) and dynamin-related GTPases (DRPs) participate in the formation of vesicular or tubular carriers. CPCs facilitate cargo selection and membrane deformation, and DRPs take part in the tubulation and/or scission of donor membranes. Rab GTPase promotes the tethering of membrane carriers to the target membrane through effector molecules (Tethers), which is followed by SNARE-mediated membrane fusion.

lineages, especially in land plants (Embryophytes). For example, some specific Rab GTPase, component of tethering factors, and SNARE subfamilies are remarkably expanded and functionally diversified (Vernoud et al., 2003; Sanderfoot, 2007; Woollard and Moore, 2008; Saito and Ueda, 2009; Chong et al., 2010). Moreover, plant-unique molecular machineries, which are structurally distinct from closely related homologs conserved in a wide range of eukaryotic organisms, take part in fundamental membrane trafficking processes in plant cells (Ebine et al., 2008, 2011; Fujimoto et al., 2010; Van Damme et al., 2011). This review summarizes recent advances in the study of plant post-Golgi trafficking pathways, focusing on unique aspects of the plant system.

COAT PROTEIN COMPLEXES

A single round of trafficking between two organelles begin with the formation of transport vesicles from the donor organelle (**Figure 1**). In this process, cytosolic CPCs perform pivotal roles in membrane deformation and cargo recruitment. Three classes of CPCs are widely utilized in a range of eukaryotic organisms (Schledzewski et al., 1999; Singh and Gupta, 2004; Elde et al., 2005; Dacks and Field, 2007): coat protein complex II (COPII) mediates ER-to-Golgi trafficking, coat protein complex I (COPI) mediates intra-Golgi and Golgi-to-ER trafficking (Lee et al., 2004), and clathrin-based complexes are involved in multiple steps in post-Golgi trafficking (McMahon and Mills, 2004). These three CPCs are likely to have a common ancestral origin, which may be also the origin of the nuclear pore complex (Devos et al., 2004).

Clathrin-based complexes mainly comprise clathrin coats and adaptor molecules such as cargo- or lipid-binding proteins. The clathrin coat is made up of a three-legged structure called the triskelion, each leg of which consists of a heavy chain (CHC) and a light chain (CLC) (Brodsky et al., 2001). Triskelia assemble into a lattice surrounding the membrane bud on the TGN, PM, endosomes, and lysosomes/vacuoles, and concentrate adaptors bound with cargo, leading to the loading of proteins and lipids into forming vesicles (Crowther and Pearse, 1981; Hanover et al., 1984). Although the overall architecture is well conserved among clathrin coats in eukaryotic lineages, including plants (Coleman et al., 1987), the triskelion structure of the plant clathrin coat exhibits several distinct characteristics. The plant triskelion has a higher molecular mass and longer arms than the mammalian triskelion (Mersey et al., 1985; Depta and Robinson, 1986; Coleman et al., 1987; Depta et al., 1987), suggesting that unique properties were added to plant clathrin coats during evolution.

Adaptor protein (AP) complexes AP-1 through AP-5 are central organizers that mediate cargo recognition at forming vesicles in post-Golgi trafficking pathways (Pearse and Robinson, 1984; Dell'Angelica et al., 1997, 1999; Hirst et al., 1999, 2011; Robinson and Bonifacino, 2001). Each AP complex consists of four subunits called adaptins, which are large α/γ/δ/ε/ζ and β subunits, a medium μ subunit, and a small σ subunit (Boehm and Bonifacino, 2002; Hirst et al., 2011). During vesicle formation, AP complexes link the clathrin lattice and select membrane cargos and lipids. AP complexes also bind other accessory proteins, which in turn regulate the assembly and disassembly of the coat (Bonifacino and Traub, 2003). All of these AP complexes are observed among all eukaryotic lineages with sporadic secondary loss in some clades, indicating an ancient origin for all five complexes (Hirst et al., 2011). Currently, each AP complex is assigned to a distinctive location and function: bi-directional trafficking between endosomes and the TGN for AP-1 (Boehm and Bonifacino, 2002; Robinson et al., 2010), endocytosis from the PM for AP-2 (Bar et al., 2009; Jackson et al., 2010), traffic from early endosomes/TGN to late endosomes and lysosomes/vacuoles for AP-3 (Dell'Angelica, 2009; Niihama et al., 2009; Feraru et al., 2010), TGN-to-endosome trafficking for AP-4 (Burgos et al., 2010), and trafficking around the late endosomes for AP-5 (Hirst et al., 2011). Among these AP complexes, AP-1 and AP-2 have been demonstrated to interact with clathrin, while other complexes are thought to be able to act without associating with clathrin. The ancient origin of the AP complexes suggests that their functions are also conserved in plants, which should be verified in future studies.

In addition to the conserved AP complexes, land plants have a unique adaptor-like protein, TPLATE, which contains a domain similar to β-adaptin and interacts with clathrin (Van Damme et al., 2006, 2011). TPLATE is specifically targeted to the expanding cell plate and the particular region of the PM around the site of fusion between the expanding cell plate and the mother cell, to which clathrin is also localized (Van Damme et al., 2011). Thus, TPLATE is expected to act in clathrin-mediated endocytosis during cell plate formation. Restriction of the lateral diffusion of KNOLLE, a SNARE protein, at the PM of mother cells during cytokinesis and its removal from the PM are accomplished by clathrin-mediated endocytosis (Segui-Simarro et al., 2004; Boutte et al., 2010). KNOLLE is a possible cargo of TPLATE-mediated endocytosis.

DYNAMIN-RELATED PROTEINS

Dynamin-related proteins (DRPs) are large GTPases that regulate membrane fission, fusion, and tubulation during diverse cellular

activities such as endocytosis, cytokinesis, vacuolar sorting, fission and fusion of mitochondria, biogenesis of peroxisomes, and the maintenance of ER morphology (Praefcke and McMahon, 2004; Hu et al., 2009). In many cases, distinct DRP proteins are assigned to fulfill different cellular functions. However, in *Trypanosoma brucei*, a protist belonging to the Excavata supergroup, a single DRP mediates both mitochondrial division and post-Golgi trafficking, including endocytosis (Chanez et al., 2006). By contrast, in the SAR + CCTH supergroup, the DRP protein that acts in endomembrane trafficking has not been found thus far, while DRPs acting in mitochondrial and/or plastid divisions have been identified in this supergroup (Miyagishima et al., 2008; van Dooren et al., 2009). These lines of evidence might suggest that an ancient function of DRPs was the regulation of membrane remodeling associated with mitochondrial endosymbiosis, although it is also plausible that DRPs for membrane trafficking were secondarily lost during evolution of the SAR + CCTH lineage. It has also been reported that some bacterial species possess DRP-like proteins that are able to deform lipid bilayers, implying a possible prokaryotic origin of this protein family (Low and Lowe, 2006; Burmann et al., 2011).

Among DRP family members, dynamin is the best-characterized member that acts in clathrin-mediated trafficking in animal cells (Sever, 2002). During clathrin-coated vesicle (CCV) formation, dynamin assembles into helical or ring-shaped structures at the neck of clathrin-coated buds (Takei et al., 1995), and constricts, severing the bud neck membrane in a GTP hydrolysis-dependent manner (Sweitzer and Hinshaw, 1998; Macia et al., 2006). Animal dynamin contains five distinct domains: the *N*-terminal GTPase domain; a middle domain that mediates intermolecular interaction during self-assembly; a GTPase-effector domain (GED), which stimulates the GTPase activity required to enact structural change in a dynamin polymer; a pleckstrin homology (PH) domain, which mediates binding to the membrane phosphoinositide; and a proline-rich domain (PRD), which is required for the recruitment of dynamin to clathrin-coated pits (Heymann and Hinshaw, 2009). The former three domains are conserved among almost all DRP proteins. DRPs with a domain configuration similar to that of dynamin, which also harbor the two additional domains, have been observed only in metazoa and land plants (Chanez et al., 2006; Miyagishima et al., 2008; Heymann and Hinshaw, 2009).

Most land plants' genomes contain six types of DRPs: DRP1-DRP4, DRP5A, and DRP5B (Hong et al., 2003; Miyagishima et al., 2008). Of these subfamilies, two structurally different DRPs, DRP1, and DRP2, are involved in clathrin-dependent trafficking events including endocytosis and cell plate formation (**Figure 2**; Hong et al., 2003; Kang et al., 2003; Collings et al., 2008; Fujimoto et al., 2008, 2010; Konopka et al., 2008; Taylor, 2011). DRP2 shares overall domain organization with animal dynamin, while DRP1 lacks the PH domain and PRD; a DRP with a similar structure is only found in green plants (Hong et al., 2003). In spite of the similarity in the overall domain structure between plant DRP2 and animal dynamin, the GTPase domain of animal dynamin exhibits greater similarity to the GTPase domains of DRP1 members than to that of DRP2 (e.g., 66% identity to *A. thaliana* DRP1A, and 27% identity to *A. thaliana* DRP2B). These lines of evidence raise the possibility that complementary functions of plant DRP2 and DRP1 are required to fulfill the function in clathrin-mediated trafficking events, which animal dynamin executes by itself. In a consistent manner, these two subfamilies of DRPs interact with each other and assemble together with clathrin at discrete foci at the PM (Fujimoto et al., 2010). Cooperative action of two structurally distinct DRPs in the same membrane scission event has not been reported in other organisms; thus, plants appear to have developed a unique mechanism for endocytic vesicle formation.

Rab GTPases

Rab GTPases, which comprise the largest family in the Ras superfamily, act as molecular switches to regulate the targeting and tethering of transport carriers to target membranes by cycling between GTP-bound active and GDP-bound inactive states (**Figure 1**; Saito and Ueda, 2009). The activation of Rab GTPases occurs with the exchange of bound GDP for GTP, which is catalyzed by guanine nucleotide exchange factor (GEF). GTP-bound Rab GTPases interact with specific effector molecules that evoke downstream reactions including the tethering of transport carriers to target membranes by tethers (Grosshans et al., 2006). Tethering between two membranes is mediated by a group of multi-subunit complexes (e.g., HOPS, TRAPP, and Exocyst) and/or long fibrous proteins (e.g., EEA1 and p115/Uso1p), most of which act as effectors of Rab GTPases (Cai et al., 2007; Markgraf et al., 2007). Because Rab GTPases exhibit a much greater degree of phylogenetic diversification than other tethering components, they are thought to be vital players in the diversification of the endomembrane system (Dacks and Field, 2007; Gurkan et al., 2007; Elias, 2010). Recent comprehensive genomic analysis has suggested that the last common eukaryotic ancestor harbored at least 23 groups of Rab GTPases (Elias et al., 2012) – substantially more than have been found in many extant eukaryotic organisms, including plants. Thus, the secondary loss of Rab GTPases (and the acquisition of new ones) occurred in a wide range of eukaryotes during evolution.

Plant Rab GTPases also appear to have followed a unique path of diversification and evolution. The genome of *A. thaliana* contains 57 Rab GTPases that are classified into eight groups (RABA–RABH). Each group exhibits a high degree of similarity to animal RAB1, RAB2, RAB5, RAB6, RAB7, RAB8, RAB11, or RAB18 (Rutherford and Moore, 2002; Vernoud et al., 2003). Most land plants possess these eight groups in theory, with a few additional members of unknown function in basal land plants (Rensing et al., 2008; Banks et al., 2011). Compared with other eukaryotic lineages, one distinct feature of the land plant Rab GTPase is extreme expansion of the RABA/RAB11 group (Rutherford and Moore, 2002). In *A. thaliana*, 26 of 57 Rab GTPases belong to this group, which are further divided into six subgroups, RABA1 through RABA6 (Rutherford and Moore, 2002). In contrast, three of 66 and two of 11 RAB GTPases in *Homo sapiens* and *Saccharomyces cerevisiae*, respectively, are members of the RAB11 group (Pereira-Leal and Seabra, 2001; Stenmark and Olkkonen, 2001).

Yeast and animal RAB11 members function at multiple steps of post-Golgi trafficking pathways (Benli et al., 1996; Ullrich et al., 1996; Jedd et al., 1997; Chen et al., 1998; Strickland and Burgess, 2004). In addition, in land plants, RABA members have been shown to localize around the TGN (Ueda et al., 1996; de Graaf et al., 2005; Chow et al., 2008; Szumlanski and Nielsen, 2009),

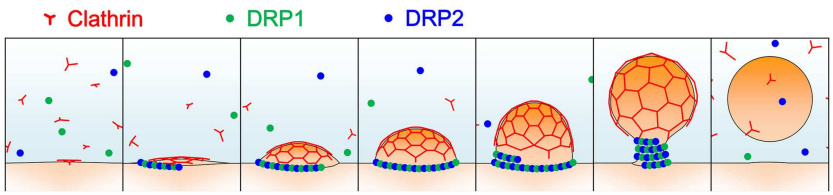

FIGURE 2 | A schematic illustration of clathrin-coated vesicle formation in land plants. Light blue represents the cytosol; orange, and red lines represent the donor membrane and the clathrin coat, respectively; and green and blue dots represent DRP1 and DRP2 proteins, respectively.

which also acts as the early endosome in plant cells (Dettmer et al., 2006; Viotti et al., 2010). The diversity of RABA/RAB11 members in land plants suggests that plant-unique functions are assigned to members of this group, some of which are demonstrated by recent studies. For example, RABA2 and A3 are involved in cell plate formation (Chow et al., 2008), and RABA1 and RABA4 are required for normal tip growth of pollen tubes and root hairs (Preuss et al., 2004; de Graaf et al., 2005; Szumlanski and Nielsen, 2009). It has also been proposed that the function of RABA is associated with the biogenesis and degradation of the cell wall during fruit development (Zainal et al., 1996; Lu et al., 2001; Abbal et al., 2008; Lycett, 2008).

The diversification of the RAB5 group is another distinctive feature of the plant Rab GTPase. RAB5 is a broadly conserved Rab GTPase, and regulates a wide range of early endocytic trafficking in animal cells (Somsel Rodman and Wandinger-Ness, 2000; Benmerah, 2004). Orthologs of animal *RAB5* are also conserved in all plant species whose genomes have been sequenced thus far, with the exception of a unicellular rhodophyte, *Cyanidioschyzon merolae* (Matsuzaki et al., 2004). Land plants also harbor another plant-unique type of RAB5 molecule, the ARA6/RABF1 group, which is structurally distinct from conventional RAB5 (Ebine and Ueda, 2009). The *A. thaliana* genome has three RAB5-related genes: two conventional type *RAB5*, *RHA1*/*RABF2a*, and *ARA7*/*RABF2b*; and one plant-unique *RAB5*, *ARA6*/*RABF1* (Ueda et al., 2001). All of the three RAB5s in *A. thaliana* have been detected on multivesicular endosomes (MVEs) using electron microscopy (Haas et al., 2007), and are activated by the same GEF, VPS9a (Goh et al., 2007). However, the subcellular localizations of two types of RAB5 did not overlap completely when their localization was compared in the same cell (Ueda et al., 2004), and the overexpression of constitutively active ARA6 and ARA7 conferred different effects on a partial loss-of-function mutant of *VPS9a*, *vps9a-2* (Goh et al., 2007).

Recently, we have successfully demonstrated the functional diversification between these conventional and plant-unique types of RAB5 in *A. thaliana*. Genetic, biochemical, and imaging analyses indicated that ARA6 acts in the trafficking pathway from MVEs to the PM, while conventional RAB5 is involved in the trafficking pathway between MVEs and vacuoles (Ebine et al., 2011). The *ara6* mutation resulted in hypersensitivity to salinity and osmotic stresses, and overexpression of constitutive active ARA6 conferred salinity stress tolerance to *A. thaliana* plants (Ebine et al., 2011, 2012). Possible involvement of *ARA6* homologs in the stress response has also been reported for other land plant species (Bolte et al., 2000; Zhang et al., 2009). Considering with that *ARA6* homologs are well conserved among land plants and rather sporadic in algal lineages, it may be adaptive for land plants to retain the trafficking pathway involving the ARA6-type RAB5 for survival in terrestrial conditions.

Another class of small GTPase, Rho-like GTPases of plants (ROP), has recently been demonstrated to have regulatory roles in plant membrane trafficking, which is required for the auxin-mediated establishment of cell polarity (Chen et al., 2012; Lin et al., 2012; Nagawa et al., 2012). Directional transport of auxin depends on a family of auxin efflux carriers known as PIN-FORMED (PIN) proteins, which undergo constitutive endocytic recycling (Dhonukshe et al., 2007, 2008; Kleine-Vehn et al., 2011). In the roots, auxin affects its own transport by inhibiting the clathrin-mediated endocytosis of PIN1 and PIN2, which is mediated by Auxin Binding Protein 1 (ABP1; Paciorek et al., 2005; Robert et al., 2010), as well as the downstream signaling molecules ROP6 and ROP-interactive CRIB motif containing protein 1 (RIC1; Chen et al., 2012; Lin et al., 2012). In addition, ROP and RIC have been shown to act in the morphogenesis of leaf epidermal cells. Auxin and ABP1 promote interdigitation of epidermal pavement cells by activating a signaling pathway involving ROP2 and RIC4 (Fu et al., 2005; Xu et al., 2010), which causes the accumulation of cortical actin microfilaments, thereby resulting in the local inhibition of clathrin-dependent endocytosis and asymmetric distribution of PIN1 (Nagawa et al., 2012). Rho GTPase-mediated inhibition of endocytosis is also centrally involved in the establishment of cell polarity in animal systems (Izumi et al., 2004; Harris and Tepass, 2008). Thus, the plant appears to have developed its multicellular body plan by recruiting the common mechanism of polarity regulation, as well as by adding plant-specific innovations such as ABP1 and RICs (Napier et al., 2002; Nagawa et al., 2010).

TETHERS

Some of proteins that mediate the tethering of transport vesicles to target membranes also appear to be diversified in a unique way in plants. A comparative genomic analysis suggested that each tethering complex has an ancient and independent origin; a set of non-homologous tethering complexes is conserved across all eukaryotic lineages, with frequent secondary losses (Koumandou et al., 2007). Acquisition of the non-homologous tethering complexes may be the other driving force for the diversification of membrane trafficking pathways, in addition to the paralogous expansion observed in the Rab and SNARE families.

While the obvious orthologs of long fibrous tethers have not been found, the components of tethering complexes are well conserved in plants (Koumandou et al., 2007). In *A. thaliana*,

components of the HOPS/CORVET complexes residing on vacuolar membranes and pre-vacuolar compartments are involved in vacuolar biogenesis and transport to vacuoles (Rojo et al., 2001, 2003; Niihama et al., 2009). The TRAPP complex, which is further divided into TRAPPI and TRAPPII, is required for cell plate formation (Thellmann et al., 2010). The importance of the exocyst complex in various secretion-related events, including tip growth of pollen tubes and root hairs, hypocotyl elongation, deposition of seed coat pectin, pollen acceptance at the stigma, and pathogen responses, has also been reported (Cole et al., 2005; Synek et al., 2006; Hala et al., 2008; Chong et al., 2010; Kulich et al., 2010; Pecenkova et al., 2011). The GARP complex is also involved in pollen tube growth (Lobstein et al., 2004; Guermonprez et al., 2008), as well as resistance to heat and osmotic stresses (Lee et al., 2006).

Among the tethering complexes in land plants, the exocyst complex appears to be assigned to uniquely diversified functions in exocytosis-related events. The exocyst consists of eight evolutionarily conserved subunits, SEC3, SEC5, SEC6, SEC8, SEC10, SEC15, EXO70, and EXO84, whose assembly mediates the tethering of secretory vesicles to the target PM during the last step of exocytosis (Munson and Novick, 2006). Among the exocyst subunits, the EXO70 family exhibits remarkable expansion in land plants. In contrast to a single copy of the *EXO70* gene in most of opisthokonta genomes, multiple *EXO70* genes have been observed in a variety of land plant genomes: 13 in *Physcomitrella patens*; 23 in *A. thaliana* and *Populus trichocarpa*; and 41 in *Oryza sativa* (Chong et al., 2010), which can be divided into three families comprising nine subfamilies (Elias et al., 2003; Synek et al., 2006; Chong et al., 2010).

Although the functions of the majority of EXO70 family proteins remain unknown, several *A. thaliana* EXO70 members are localized to endosomal compartments including the TGN/early endosome (Chong et al., 2010). Recently, a unique function of an *A. thaliana* EXO70 family member, Exo70E2, has been reported. EXO70E2 was localized to spherical double-membrane structures resembling autophagosomes and were named exocyst-positive organelles (EXPOs; Wang et al., 2010). Intriguingly, standard markers for conventional organelles (including the Golgi apparatus; TGN and early endosomes; MVE/late endosomes; and autophagosomes) did not occur on EXPOs (Wang et al., 2010), and brefeldin A and wortmannin did not affect EXPO distribution. EXPOs have been suggested to mediate a form of unconventional protein secretion unique to land plants: the transport of cytosolic proteins to the cell exterior (Wang et al., 2010). Additional studies of other EXO70 family members, as well as functional analyses of other exocyst components, would lead to understanding the unique and diverse exocytic mechanisms that plants have acquired during the course of evolution.

SNARE FAMILY PROTEINS

At the final step of a single round of trafficking, SNARE family proteins, which are evolutionarily conserved integral or peripheral membrane proteins, execute membrane fusion between transport carriers and target membranes (**Figure 1**; Jahn and Scheller, 2006; Wickner and Schekman, 2008; Saito and Ueda, 2009). The SNARE family consists of four subgroups, Qa-, Qb-, Qc-, and R-SNAREs, which are classified according to the presence of a conserved glutamine (Q) or arginine (R) residue in a particular helical domain called the SNARE domain. In general, Q- and R-SNAREs reside on distinct membrane compartments, and three Q-SNAREs (Qa, Qb, and Qc) and an R-SNARE assemble into a tight complex in specific combinations, leading to membrane fusion between two compartments. Most SNARE proteins, except for SNAP-25-like members, contain one SNARE domain in their polypeptides (Jahn and Scheller, 2006). Recent comprehensive genomic analyses have indicated that a significant increase in the number of SNARE family members occurred with the acquisition of developmental complexity – for example, from unicellular to multicellular organisms (there are 17 SNAREs in *C. merolae*, 24 in *S. cerevisiae*, 26 in *Chlamydomonas reinhardtii*, 38 in *H. sapiens*, and 63 in *A. thaliana*; Dacks and Doolittle, 2002; Yoshizawa et al., 2006; Sanderfoot, 2007; Dacks et al., 2008). This increase is in good agreement with the hypothesis that multiplication followed by the functional diversification of key components of membrane trafficking, including SNAREs, is a prerequisite for the diversification of membrane trafficking pathways (Dacks and Doolittle, 2002; Yoshizawa et al., 2006; Dacks and Field, 2007; Dacks et al., 2008), which in turn should be required to support increasingly complex body plans and life cycles.

One remarkable feature of the post-Golgi SNARE in land plants is the functional diversification of the PM-localized Qa-SNARE, the SYP1 group, which consists of nine members in *A. thaliana*. Phylogenetic relationships to animal and fungal orthologs suggest that SYP1 group members are involved in membrane fusion at the PM (Sanderfoot, 2007); some members of SYP1 group have been reported to perform specialized functions at the PM. For example, SYP111/KNOLLE is expressed in mitotic cells and plays an essential role in membrane fusion at forming cell plates during cytokinesis (Lukowitz et al., 1996; Lauber et al., 1997). SYP121/PEN1/SYR1, another SYP1 member, takes part in K^+ uptake through the control of K^+ channel gating (Honsbein et al., 2009; Grefen et al., 2010). This protein also participates in the non-host defense response against attack by fungal pathogens (Collins et al., 2003; Assaad et al., 2004). SYP132 appears to be centrally involved in bacterial infection and symbiosis: the silencing of a SYP132 ortholog in *Nicotiana benthamiana* resulted in impaired multiple responses against bacterial pathogens (Kalde et al., 2007), and an ortholog of SYP132 in *Medicago truncatula* localizes to the PM surrounding infection threads and the infection droplet membrane (Catalano et al., 2007).

In addition to the functional diversification of SYP1 group members, another distinct feature of post-Golgi SNAREs in land plants is the expansion of the VAMP7 R-SNARE group (Sanderfoot, 2007; Ebine and Ueda, 2009). R-SNAREs are divided into two groups, longins and brevins; longins contain an N-terminal longin domain, while brevins lack this domain (Filippini et al., 2001). Land plants harbor only longin-type R-SNARE members, which are further classified into three major groups: VAMP7, YKT6, and SEC22. While vertebrates have only one or a few VAMP7 proteins that participate in secretory and endocytic trafficking (Chaineau et al., 2009), the VAMP7 group of *A. thaliana* consists of 12 members, which are further divided into three subgroups: VAMP71, VAMP72, and VAMP727 (Uemura et al., 2004).

A phylogenic analysis has suggested that VAMP71 is a prototype from which VAMP72 and VAMP727 have been derived (Sanderfoot, 2007). VAMP71 members localize to the vacuolar membrane (Uemura et al., 2004) and are involved in salt and drought stress responses (Leshem et al., 2006, 2010). VAMP72 members localize to the TGN and function in the secretory pathway, including cell plate formation (Zhang et al., 2011). Although VAMP727 exhibits high sequence similarity to other VAMP72 members, it harbors a unique structural characteristic: VAMP727 has an insertion comprising acidic amino acid clusters in the longin domain (Ebine and Ueda, 2009; Vedovato et al., 2009). This type of VAMP7 member is well conserved in seed plants; however, it has not found in lycophytes or moss thus far, indicating relatively recent emergence of this subfamily.

VAMP727 localizes on the RAB5-positive MVE/pre-vacuolar compartment, and mediates membrane fusion between the pre-vacuolar compartment and vacuolar membranes by forming a complex with Qa-SYP22/VAM3, Qb-VTI11, and Qc-SYP51 (Ebine et al., 2008). This complex is essential for the efficient transport of storage proteins to protein storage vacuoles during the process of seed maturation. Moreover, VAMP727 also mediates membrane fusion at the PM by forming a complex with Qa-SYP121/PEN1 (Ebine et al., 2011), which is under the control of the plant-unique RAB5 ARA6. These lines of evidence may indicate that the plant explored novel trafficking pathways from the MVE to the vacuole and PM by acquiring these two plant-unique molecules, leading to the current complex and unique post-Golgi trafficking network in angiosperms.

PERSPECTIVES

Plants have elaborated a distinctive post-Golgi trafficking system through the acquisition of plant-specific machinery components of membrane trafficking, such as TPLATE, DRP1/2, ARA6, and VAMP727, as well as the functional expansion of evolutionarily conserved components, as observed for RAB11, EXO70, and SYP1 groups. However, many unsolved questions must be answered to elucidate the precise function and regulatory mechanism of the plant-unique trafficking system. For example, with what APs does TPLATE form a complex to mediate CCV formation? Does the TPLATE complex-mediated CCV formation involve DRP proteins? Why do land plants require two structurally distinct DRPs for CCV formation? Do they in fact polymerize into the same ring- or helix-shaped structure?

Regarding the molecular machinery involved in membrane tethering and fusion, key questions also remain to be elucidated. What effector molecules mediate ARA6 function to fulfill higher-ordered functions, such as salinity stress tolerance? Is the ARA6 function revealed in *A. thaliana* shared by all ARA6 group members throughout the plant lineages? Why and how did plants expand the RAB11 group, and how are different functions of RAB11 members exerted in spite of their high sequence similarity? What is the mechanism of molecular evolution of the VAMP727 group, and what is the molecular function of the acidic insertion? Additional studies using model systems like *A. thaliana* are obviously needed to answer these questions, and would also be required to challenge distinct lineages of plants, including basal lineages (e.g., ferns, mosses, liverworts, and algae), to yield information regarding aspects of diversity and evolution of membrane trafficking. Future experimental studies employing a wide variety of plant species, together with comprehensive genomics analysis *in silico*, will help us to understand how current plant membrane trafficking pathways have evolved.

REFERENCES

Abbal, P., Pradal, M., Muniz, L., Sauvage, F. X., Chatelet, P., Ueda, T., and Tesniere, C. (2008). Molecular characterization and expression analysis of the Rab GTPase family in Vitis vinifera reveal the specific expression of a VvRabA protein. *J. Exp. Bot.* 59, 2403–2416.

Assaad, F. F., Qiu, J. L., Youngs, H., Ehrhardt, D., Zimmerli, L., Kalde, M., Wanner, G., Peck, S. C., Edwards, H., Ramonell, K., Somerville, C. R., and Thordal-Christensen, H. (2004). The PEN1 syntaxin defines a novel cellular compartment upon fungal attack and is required for the timely assembly of papillae. *Mol. Biol. Cell* 15, 5118–5129.

Banks, J. A., Nishiyama, T., Hasebe, M., Bowman, J. L., Gribskov, M., dePamphilis, C., Albert, V. A., Aono, N., Aoyama, T., Ambrose, B. A., Ashton, N. W., Axtell, M. J., Barker, E., Barker, M. S., Bennetzen, J. L., Bonawitz, N. D., Chapple, C., Cheng, C., Correa, L. G. G., Dacre, M., DeBarry, J., Dreyer, I., Elias, M., Engstrom, E. M., Estelle, M., Feng, L., Finet, C., Floyd, S. K., Frommer, W. B., Fujita, T., Gramzow, L., Gutensohn, M., Harholt, J., Hattori, M., Heyl, A., Hirai, T., Hiwatashi, Y., Ishikawa, M., Iwata, M., Karol, K. G., Koehler, B., Kolukisaoglu, U., Kubo, M., Kurata, T., Lalonde, S., Li, K., Li, Y., Litt, A., Lyons, E., Manning, G., Maruyama, T., Michael, T. P., Mikami, K., Miyazaki, S., Morinaga, S., Murata, T., Mueller-Roeber, B., Nelson, D. R., Obara, M., Oguri, Y., Olmstead, R. G., Onodera, N., Petersen, B. L., Pils, B., Prigge, M., Rensing, S. A., Riano-Pachon, D. M., Roberts, A. W., Sato, Y., Scheller, H. V., Schulz, B., Schulz, C., Shakirov, E. V., Shibagaki, N., Shinohara, N., Shippen, D. E., Sorensen, I., Sotooka, R., Sugimoto, N., Sugita, M., Sumikawa, N., Tanurdzic, M., Theissen, G., Ulvskov, P., Wakazuki, S., Weng, J. K., Willats, W. W., Wipf, D., Wolf, P. G., Yang, L., Zimmer, A. D., Zhu, Q., Mitros, T., Hellsten, U., Loque, D., Otillar, R., Salamov, A., Schmutz, J., Shapiro, H., Lindquist, E., Lucas, S., Rokhsar, D., and Grigoriev, I. V. (2011). The Selaginella genome identifies genetic changes associated with the evolution of vascular plants. *Science* 332, 960–963.

Bar, M., Sharfman, M., Schuster, S., and Avni, A. (2009). The coiled-coil domain of EHD2 mediates inhibition of LeEix2 endocytosis and signaling. *PLoS ONE* 4, e7973. doi:10.1371/journal.pone.0007973

Barbrook, A. C., Howe, C. J., and Purton, S. (2006). Why are plastid genomes retained in non-photosynthetic organisms? *Trends Plant Sci.* 11, 101–108.

Benli, M., Doring, F., Robinson, D. G., Yang, X., and Gallwitz, D. (1996). Two GTPase isoforms, Ypt31p and Ypt32p, are essential for Golgi function in yeast. *EMBO J.* 15, 6460–6475.

Benmerah, A. (2004). Endocytosis: signaling from endocytic membranes to the nucleus. *Curr. Biol.* 14, R314–R316.

Boehm, M., and Bonifacino, J. S. (2002). Genetic analyses of adaptin function from yeast to mammals. *Gene* 286, 175–186.

Bolte, S., Schiene, K., and Dietz, K. J. (2000). Characterization of a small GTP-binding protein of the rab 5 family in Mesembryanthemum crystallinum with increased level of expression during early salt stress. *Plant Mol. Biol.* 42, 923–936.

Bonifacino, J. S., and Glick, B. S. (2004). The mechanisms of vesicle budding and fusion. *Cell* 116, 153–166.

Bonifacino, J. S., and Traub, L. M. (2003). Signals for sorting of transmembrane proteins to endosomes and lysosomes. *Annu. Rev. Biochem.* 72, 395–447.

Boutte, Y., Frescatada-Rosa, M., Men, S., Chow, C. M., Ebine, K., Gustavsson, A., Johansson, L., Ueda, T., Moore, I., Jurgens, G., and Grebe, M. (2010). Endocytosis restricts Arabidopsis KNOLLE syntaxin to the cell division plane during late cytokinesis. *EMBO J.* 29, 546–558.

Brighouse, A., Dacks, J. B., and Field, M. C. (2010). Rab protein evolution and the history of the eukaryotic endomembrane system. *Cell. Mol. Life Sci.* 67, 3449–3465.

Brodsky, F. M., Chen, C. Y., Knuehl, C., Towler, M. C., and Wakeham, D. E. (2001). Biological basket weaving: formation and function of clathrin-coated vesicles. *Annu. Rev. Cell Dev. Biol.* 17, 517–568.

Burgos, P. V., Mardones, G. A., Rojas, A. L., Dasilva, L. L., Prabhu, Y., Hurley, J. H., and Bonifacino, J. S. (2010). Sorting of the Alzheimer's disease amyloid precursor protein mediated by the AP-4 complex. *Dev. Cell* 18, 425–436.

Burki, F., Inagaki, Y., Brate, J., Archibald, J. M., Keeling, P. J., Cavalier-Smith, T., Sakaguchi, M., Hashimoto, T., Horak, A., Kumar, S., Klaveness, D., Jakobsen, K. S., Pawlowski, J., and Shalchian-Tabrizi, K. (2009). Large-scale phylogenomic analyses reveal that two enigmatic protist lineages, telonemia and centroheliozoa, are related to photosynthetic chromalveolates. *Genome Biol. Evol.* 1, 231–238.

Burmann, F., Ebert, N., Van Baarle, S., and Bramkamp, M. (2011). A bacterial dynamin-like protein mediating nucleotide-independent membrane fusion. *Mol. Microbiol.* 79, 1294–1304.

Cai, H., Reinisch, K., and Ferro-Novick, S. (2007). Coats, tethers, Rabs, and SNAREs work together to mediate the intracellular destination of a transport vesicle. *Dev. Cell* 12, 671–682.

Catalano, C. M., Czymmek, K. J., Gann, J. G., and Sherrier, D. J. (2007). Medicago truncatula syntaxin SYP132 defines the symbiosome membrane and infection droplet membrane in root nodules. *Planta* 225, 541–550.

Cavalier-Smith, T. (1987). The origin of eukaryotic and archaebacterial cells. *Ann. N. Y. Acad. Sci.* 503, 17–54.

Cavalier-Smith, T. (2002). The phagotrophic origin of eukaryotes and phylogenetic classification of Protozoa. *Int. J. Syst. Evol. Microbiol.* 52, 297–354.

Chaineau, M., Danglot, L., and Galli, T. (2009). Multiple roles of the vesicular-SNARE TI-VAMP in post-Golgi and endosomal trafficking. *FEBS Lett.* 583, 3817–3826.

Chanez, A. L., Hehl, A. B., Engstler, M., and Schneider, A. (2006). Ablation of the single dynamin of T. brucei blocks mitochondrial fission and endocytosis and leads to a precise cytokinesis arrest. *J. Cell. Sci.* 119, 2968–2974.

Chen, W., Feng, Y., Chen, D., and Wandinger-Ness, A. (1998). Rab11 is required for trans-golgi network-to-plasma membrane transport and a preferential target for GDP dissociation inhibitor. *Mol. Biol. Cell* 9, 3241–3257.

Chen, X., Naramoto, S., Robert, S., Tejos, R., Lofke, C., Lin, D., Yang, Z., and Friml, J. (2012). ABP1 and ROP6 GTPase signaling regulate clathrin-mediated endocytosis in Arabidopsis roots. *Curr. Biol.* 22, 1326–1332.

Chen, Y. A., and Scheller, R. H. (2001). SNARE-mediated membrane fusion. *Nat. Rev. Mol. Cell Biol.* 2, 98–106.

Chong, Y. T., Gidda, S. K., Sanford, C., Parkinson, J., Mullen, R. T., and Goring, D. R. (2010). Characterization of the Arabidopsis thaliana exocyst complex gene families by phylogenetic, expression profiling, and subcellular localization studies. *New Phytol.* 185, 401–419.

Chow, C. M., Neto, H., Foucart, C., and Moore, I. (2008). Rab-A2 and Rab-A3 GTPases define a trans-golgi endosomal membrane domain in Arabidopsis that contributes substantially to the cell plate. *Plant Cell* 20, 101–123.

Cole, R. A., Synek, L., Zarsky, V., and Fowler, J. E. (2005). SEC8, a subunit of the putative Arabidopsis exocyst complex, facilitates pollen germination and competitive pollen tube growth. *Plant Physiol.* 138, 2005–2018.

Coleman, J., Evans, D., Hawes, C., Horsley, D., and Cole, L. (1987). Structure and molecular-organization of higher-plant coated vesicles. *J. Cell. Sci.* 88, 35–45.

Collings, D. A., Gebbie, L. K., Howles, P. A., Hurley, U. A., Birch, R. J., Cork, A. H., Hocart, C. H., Arioli, T., and Williamson, R. E. (2008). Arabidopsis dynamin-like protein DRP1A: a null mutant with widespread defects in endocytosis, cellulose synthesis, cytokinesis, and cell expansion. *J. Exp. Bot.* 59, 361–376.

Collins, N. C., Thordal-Christensen, H., Lipka, V., Bau, S., Kombrink, E., Qiu, J. L., Huckelhoven, R., Stein, M., Freialdenhoven, A., Somerville, S. C., and Schulze-Lefert, P. (2003). SNARE-protein-mediated disease resistance at the plant cell wall. *Nature* 425, 973–977.

Crowther, R. A., and Pearse, B. M. (1981). Assembly and packing of clathrin into coats. *J. Cell Biol.* 91, 790–797.

Dacks, J. B., and Doolittle, W. F. (2002). Novel syntaxin gene sequences from Giardia, Trypanosoma and algae: implications for the ancient evolution of the eukaryotic endomembrane system. *J. Cell. Sci.* 115, 1635–1642.

Dacks, J. B., and Field, M. C. (2007). Evolution of the eukaryotic membrane-trafficking system: origin, tempo and mode. *J. Cell. Sci.* 120, 2977–2985.

Dacks, J. B., Peden, A. A., and Field, M. C. (2009). Evolution of specificity in the eukaryotic endomembrane system. *Int. J. Biochem. Cell Biol.* 41, 330–340.

Dacks, J. B., Poon, P. P., and Field, M. C. (2008). Phylogeny of endocytic components yields insight into the process of nonendosymbiotic organelle evolution. *Proc. Natl. Acad. Sci. U.S.A.* 105, 588–593.

de Graaf, B. H., Cheung, A. Y., Andreyeva, T., Levasseur, K., Kieliszewski, M., and Wu, H. M. (2005). Rab11 GTPase-regulated membrane trafficking is crucial for tip-focused pollen tube growth in tobacco. *Plant Cell* 17, 2564–2579.

Dell'Angelica, E. C. (2009). AP-3-dependent trafficking and disease: the first decade. *Curr. Opin. Cell Biol.* 21, 552–559.

Dell'Angelica, E. C., Mullins, C., and Bonifacino, J. S. (1999). AP-4, a novel protein complex related to clathrin adaptors. *J. Biol. Chem.* 274, 7278–7285.

Dell'Angelica, E. C., Ohno, H., Ooi, C. E., Rabinovich, E., Roche, K. W., and Bonifacino, J. S. (1997). AP-3: an adaptor-like protein complex with ubiquitous expression. *EMBO J.* 16, 917–928.

Depta, H., Freundt, H., Hartmann, D., and Robinson, D. G. (1987). Preparation of a homogeneous coated vesicle fraction from bean-leaves. *Protoplasma* 136, 154–160.

Depta, H., and Robinson, D. G. (1986). The isolation and enrichment of coated vesicles from suspension-cultured carrot cells. *Protoplasma* 130, 162–170.

Dettmer, J., Hong-Hermesdorf, A., Stierhof, Y. D., and Schumacher, K. (2006). Vacuolar H+-ATPase activity is required for endocytic and secretory trafficking in Arabidopsis. *Plant Cell* 18, 715–730.

Devos, D., Dokudovskaya, S., Alber, F., Williams, R., Chait, B. T., Sali, A., and Rout, M. P. (2004). Components of coated vesicles and nuclear pore complexes share a common molecular architecture. *PLoS Biol.* 2, e380. doi:10.1371/journal.bio.0020380

Dhonukshe, P., Aniento, F., Hwang, I., Robinson, D. G., Mravec, J., Stierhof, Y. D., and Friml, J. (2007). Clathrin-mediated constitutive endocytosis of PIN auxin efflux carriers in Arabidopsis. *Curr. Biol.* 17, 520–527.

Dhonukshe, P., Tanaka, H., Goh, T., Ebine, K., Mahonen, A. P., Prasad, K., Blilou, I., Geldner, N., Xu, J., Uemura, T., Chory, J., Ueda, T., Nakano, A., Scheres, B., and Friml, J. (2008). Generation of cell polarity in plants links endocytosis, auxin distribution and cell fate decisions. *Nature* 456, 962–966.

Ebine, K., Fujimoto, M., Okatani, Y., Nishiyama, T., Goh, T., Ito, E., Dainobu, T., Nishitani, A., Uemura, T., Sato, M. H., Thordal-Christensen, H., Tsutsumi, N., Nakano, A., and Ueda, T. (2011). A membrane trafficking pathway regulated by the plant-specific RAB GTPase ARA6. *Nat. Cell Biol.* 13, 853–859.

Ebine, K., Miyakawa, N., Fujimoto, M., Uemura, T., Nakano, A., and Ueda, T. (2012). Endosomal trafficking pathway regulated by ARA6, a RAB5 GTPase unique to plants. *Small GTPases* 3, 0–4.

Ebine, K., Okatani, Y., Uemura, T., Goh, T., Shoda, K., Niihama, M., Morita, M. T., Spitzer, C., Otegui, M. S., Nakano, A., and Ueda, T. (2008). A SNARE complex unique to seed plants is required for protein storage vacuole biogenesis and seed development of Arabidopsis thaliana. *Plant Cell* 20, 3006–3021.

Ebine, K., and Ueda, T. (2009). Unique mechanism of plant endocytic/vacuolar transport pathways. *J. Plant Res.* 122, 21–30.

Elde, N. C., Morgan, G., Winey, M., Sperling, L., and Turkewitz, A. P. (2005). Elucidation of clathrin-mediated endocytosis in tetrahymena reveals an evolutionarily convergent recruitment of dynamin. *PLoS Genet.* 1, e52. doi:10.1371/journal.pgen.0010052

Elias, M. (2010). Patterns and processes in the evolution of the eukaryotic endomembrane system. *Mol. Membr. Biol.* 27, 469–489.

Elias, M., Brighouse, A., Castello, C. G., Field, M. C., and Dacks, J. B. (2012). Sculpting the endomembrane system in deep time: high resolution phylogenetics of Rab GTPases. *J. Cell. Sci.* 125, 2500–2508.

Elias, M., Drdova, E., Ziak, D., Bavlnka, B., Hala, M., Cvrckova, F., Soukupova, H., and Zarsky, V. (2003). The exocyst complex in plants. *Cell Biol. Int.* 27, 199–201.

Embley, T. M., and Martin, W. (2006). Eukaryotic evolution, changes and challenges. *Nature* 440, 623–630.

Feraru, E., Paciorek, T., Feraru, M. I., Zwiewka, M., De Groodt, R., De Rycke, R., Kleine-Vehn, J., and Friml, J. (2010). The AP-3 beta adaptin mediates the biogenesis and

function of lytic vacuoles in Arabidopsis. *Plant Cell* 22, 2812–2824.
Filippini, F., Rossi, V., Galli, T., Budillon, A., D'Urso, M., and D'Esposito, M. (2001). Longins: a new evolutionary conserved VAMP family sharing a novel SNARE domain. *Trends Biochem. Sci.* 26, 407–409.
Fu, Y., Gu, Y., Zheng, Z., Wasteneys, G., and Yang, Z. (2005). Arabidopsis interdigitating cell growth requires two antagonistic pathways with opposing action on cell morphogenesis. *Cell* 120, 687–700.
Fujimoto, M., Arimura, S., Nakazono, M., and Tsutsumi, N. (2008). Arabidopsis dynamin-related protein DRP2B is co-localized with DRP1A on the leading edge of the forming cell plate. *Plant Cell Rep.* 27, 1581–1586.
Fujimoto, M., Arimura, S., Ueda, T., Takanashi, H., Hayashi, Y., Nakano, A., and Tsutsumi, N. (2010). Arabidopsis dynamin-related proteins DRP2B and DRP1A participate together in clathrin-coated vesicle formation during endocytosis. *Proc. Natl. Acad. Sci. U.S.A.* 107, 6094–6099.
Goh, T., Uchida, W., Arakawa, S., Ito, E., Dainobu, T., Ebine, K., Takeuchi, M., Sato, K., Ueda, T., and Nakano, A. (2007). VPS9a, the common activator for two distinct types of Rab5 GTPases, is essential for the development of Arabidopsis thaliana. *Plant Cell* 19, 3504–3515.
Grefen, C., Chen, Z., Honsbein, A., Donald, N., Hills, A., and Blatt, M. R. (2010). A novel motif essential for SNARE interaction with the K(+) channel KC1 and channel gating in Arabidopsis. *Plant Cell* 22, 3076–3092.
Grosshans, B. L., Ortiz, D., and Novick, P. (2006). Rabs and their effectors: achieving specificity in membrane traffic. *Proc. Natl. Acad. Sci. U.S.A.* 103, 11821–11827.
Guermonprez, H., Smertenko, A., Crosnier, M. T., Durandet, M., Vrielynck, N., Guerche, P., Hussey, P. J., Satiat-Jeunemaitre, B., and Bonhomme, S. (2008). The POK/AtVPS52 protein localizes to several distinct post-Golgi compartments in sporophytic and gametophytic cells. *J. Exp. Bot.* 59, 3087–3098.
Gurkan, C., Koulov, A. V., and Balch, W. E. (2007). An evolutionary perspective on eukaryotic membrane trafficking. *Adv. Exp. Med. Biol.* 607, 73–83.
Haas, T. J., Sliwinski, M. K., Martinez, D. E., Preuss, M., Ebine, K., Ueda, T., Nielsen, E., Odorizzi, G., and Otegui, M. S. (2007). The Arabidopsis AAA ATPase SKD1 is involved in multivesicular endosome function and interacts with its positive regulator LYST-INTERACTING PROTEIN5. *Plant Cell* 19, 1295–1312.
Hala, M., Cole, R., Synek, L., Drdova, E., Pecenkova, T., Nordheim, A., Lamkemeyer, T., Madlung, J., Hochholdinger, F., Fowler, J. E., and Zarsky, V. (2008). An exocyst complex functions in plant cell growth in Arabidopsis and tobacco. *Plant Cell* 20, 1330–1345.
Hanover, J. A., Willingham, M. C., and Pastan, I. (1984). Kinetics of transit of transferrin and epidermal growth factor through clathrin-coated membranes. *Cell* 39, 283–293.
Harris, K. P., and Tepass, U. (2008). Cdc42 and Par proteins stabilize dynamic adherens junctions in the Drosophila neuroectoderm through regulation of apical endocytosis. *J. Cell Biol.* 183, 1129–1143.
Heymann, J. A. W., and Hinshaw, J. E. (2009). Dynamins at a glance. *J. Cell. Sci.* 122, 3427–3431.
Hirst, J., Barlow, L. D., Francisco, G. C., Sahlender, D. A., Seaman, M. N., Dacks, J. B., and Robinson, M. S. (2011). The fifth adaptor protein complex. *PLoS Biol.* 9, e1001170. doi:10.1371/journal.pbio.1001170
Hirst, J., Bright, N. A., Rous, B., and Robinson, M. S. (1999). Characterization of a fourth adaptor-related protein complex. *Mol. Biol. Cell* 10, 2787–2802.
Hong, Z., Bednarek, S. Y., Blumwald, E., Hwang, I., Jurgens, G., Menzel, D., Osteryoung, K. W., Raikhel, N. V., Shinozaki, K., Tsutsumi, N., and Verma, D. P. (2003). A unified nomenclature for Arabidopsis dynamin-related large GTPases based on homology and possible functions. *Plant Mol. Biol.* 53, 261–265.
Honsbein, A., Sokolovski, S., Grefen, C., Campanoni, P., Pratelli, R., Paneque, M., Chen, Z., Johansson, I., and Blatt, M. R. (2009). A tripartite SNARE-K+ channel complex mediates in channel-dependent K+ nutrition in Arabidopsis. *Plant Cell* 21, 2859–2877.
Hu, J., Shibata, Y., Zhu, P. P., Voss, C., Rismanchi, N., Prinz, W. A., Rapoport, T. A., and Blackstone, C. (2009). A class of dynamin-like GTPases involved in the generation of the tubular ER network. *Cell* 138, 549–561.
Izumi, G., Sakisaka, T., Baba, T., Tanaka, S., Morimoto, K., and Takai, Y. (2004). Endocytosis of E-cadherin regulated by Rac and Cdc42 small G proteins through IQGAP1 and actin filaments. *J. Cell Biol.* 166, 237–248.
Jackson, L. P., Kelly, B. T., Mccoy, A. J., Gaffry, T., James, L. C., Collins, B. M., Honing, S., Evans, P. R., and Owen, D. J. (2010). A large-scale conformational change couples membrane recruitment to cargo binding in the AP2 clathrin adaptor complex. *Cell* 141, 1220–1229.
Jahn, R., and Scheller, R. H. (2006). SNAREs – engines for membrane fusion. *Nat. Rev. Mol. Cell Biol.* 7, 631–643.
Jedd, G., Mulholland, J., and Segev, N. (1997). Two new Ypt GTPases are required for exit from the yeast trans-Golgi compartment. *J. Cell Biol.* 137, 563–580.
Kalde, M., Nuhse, T. S., Findlay, K., and Peck, S. C. (2007). The syntaxin SYP132 contributes to plant resistance against bacteria and secretion of pathogenesis-related protein 1. *Proc. Natl. Acad. Sci. U.S.A.* 104, 11850–11855.
Kang, B. H., Busse, J. S., and Bednarek, S. Y. (2003). Members of the Arabidopsis dynamin-like gene family, ADL1, are essential for plant cytokinesis and polarized cell growth. *Plant Cell* 15, 899–913.
Kleine-Vehn, J., Wabnik, K., Martiniere, A., Langowski, L., Willig, K., Naramoto, S., Leitner, J., Tanaka, H., Jakobs, S., Robert, S., Luschnig, C., Govaerts, W., Hell, S. W., Runions, J., and Friml, J. (2011). Recycling, clustering, and endocytosis jointly maintain PIN auxin carrier polarity at the plasma membrane. *Mol. Syst. Biol.* 7, 540.
Konopka, C. A., Backues, S. K., and Bednarek, S. Y. (2008). Dynamics of Arabidopsis dynamin-related protein 1C and a clathrin light chain at the plasma membrane. *Plant Cell* 20, 1363–1380.
Koumandou, V. L., Dacks, J. B., Coulson, R. M., and Field, M. C. (2007). Control systems for membrane fusion in the ancestral eukaryote; evolution of tethering complexes and SM proteins. *BMC Evol. Biol.* 7, 29. doi:10.1186/1471-2148-7-29
Kulich, I., Cole, R., Drdova, E., Cvrckova, F., Soukup, A., Fowler, J., and Zarsky, V. (2010). Arabidopsis exocyst subunits SEC8 and EXO70A1 and exocyst interactor ROH1 are involved in the localized deposition of seed coat pectin. *New Phytol.* 188, 615–625.
Lauber, M. H., Waizenegger, I., Steinmann, T., Schwarz, H., Mayer, U., Hwang, I., Lukowitz, W., and Jurgens, G. (1997). The Arabidopsis KNOLLE protein is a cytokinesis-specific syntaxin. *J. Cell Biol.* 139, 1485–1493.
Lee, C. F., Pu, H. Y., Wang, L. C., Sayler, R. J., Yeh, C. H., and Wu, S. J. (2006). Mutation in a homolog of yeast Vps53p accounts for the heat and osmotic hypersensitive phenotypes in Arabidopsis hit1-1 mutant. *Planta* 224, 330–338.
Lee, M. C., Miller, E. A., Goldberg, J., Orci, L., and Schekman, R. (2004). Bi-directional protein transport between the ER and Golgi. *Annu. Rev. Cell Dev. Biol.* 20, 87–123.
Leshem, Y., Golani, Y., Kaye, Y., and Levine, A. (2010). Reduced expression of the v-SNAREs AtVAMP71/AtVAMP7C gene family in Arabidopsis reduces drought tolerance by suppression of abscisic acid-dependent stomatal closure. *J. Exp. Bot.* 61, 2615–2622.
Leshem, Y., Melamed-Book, N., Cagnac, O., Ronen, G., Nishri, Y., Solomon, M., Cohen, G., and Levine, A. (2006). Suppression of Arabidopsis vesicle-SNARE expression inhibited fusion of H2O2-containing vesicles with tonoplast and increased salt tolerance. *Proc. Natl. Acad. Sci. U.S.A.* 103, 18008–18013.
Lin, D., Nagawa, S., Chen, J., Cao, L., Chen, X., Xu, T., Li, H., Dhonukshe, P., Yamamuro, C., Friml, J., Scheres, B., Fu, Y., and Yang, Z. (2012). A ROP GTPase-dependent auxin signaling pathway regulates the subcellular distribution of PIN2 in Arabidopsis roots. *Curr. Biol.* 22, 1319–1325.
Lobstein, E., Guyon, A., Ferault, M., Twell, D., Pelletier, G., and Bonhomme, S. (2004). The putative Arabidopsis homolog of yeast vps52p is required for pollen tube elongation, localizes to Golgi, and might be involved in vesicle trafficking. *Plant Physiol.* 135, 1480–1490.
Low, H. H., and Lowe, J. (2006). A bacterial dynamin-like protein. *Nature* 444, 766–769.
Lu, C., Zainal, Z., Tucker, G. A., and Lycett, G. W. (2001). Developmental abnormalities and reduced fruit softening in tomato plants expressing an antisense Rab11 GTPase gene. *Plant Cell* 13, 1819–1833.
Lukowitz, W., Mayer, U., and Jurgens, G. (1996). Cytokinesis in the Arabidopsis embryo involves the syntaxin-related KNOLLE gene product. *Cell* 84, 61–71.
Lycett, G. (2008). The role of Rab GTPases in cell wall metabolism. *J. Exp. Bot.* 59, 4061–4074.
Macia, E., Ehrlich, M., Massol, R., Boucrot, E., Brunner, C., and Kirchhausen, T. (2006). Dynasore,

a cell-permeable inhibitor of dynamin. *Dev. Cell* 10, 839–850.

Markgraf, D. F., Peplowska, K., and Ungermann, C. (2007). Rab cascades and tethering factors in the endomembrane system. *FEBS Lett.* 581, 2125–2130.

Matsuzaki, M., Misumi, O., Shin, I. T., Maruyama, S., Takahara, M., Miyagishima, S. Y., Mori, T., Nishida, K., Yagisawa, F., Yoshida, Y., Nishimura, Y., Nakao, S., Kobayashi, T., Momoyama, Y., Higashiyama, T., Minoda, A., Sano, M., Nomoto, H., Oishi, K., Hayashi, H., Ohta, F., Nishizaka, S., Haga, S., Miura, S., Morishita, T., Kabeya, Y., Terasawa, K., Suzuki, Y., Ishii, Y., Asakawa, S., Takano, H., Ohta, N., Kuroiwa, H., Tanaka, K., Shimizu, N., Sugano, S., Sato, N., Nozaki, H., Ogasawara, N., Kohara, Y., and Kuroiwa, T. (2004). Genome sequence of the ultrasmall unicellular red alga Cyanidioschyzon merolae 10D. *Nature* 428, 653–657.

McMahon, H. T., and Mills, I. G. (2004). COP and clathrin-coated vesicle budding: different pathways, common approaches. *Curr. Opin. Cell Biol.* 16, 379–391.

Mersey, B. G., Griffing, L. R., Rennie, P. J., and Fowke, L. C. (1985). The isolation of coated vesicles from protoplasts of soybean. *Planta* 163, 317–327.

Miyagishima, S. Y., Kuwayama, H., Urushihara, H., and Nakanishi, H. (2008). Evolutionary linkage between eukaryotic cytokinesis and chloroplast division by dynamin proteins. *Proc. Natl. Acad. Sci. U.S.A.* 105, 15202–15207.

Munson, M., and Novick, P. (2006). The exocyst defrocked, a framework of rods revealed. *Nat. Struct. Mol. Biol.* 13, 577–581.

Nagawa, S., Xu, T., Lin, D., Dhonukshe, P., Zhang, X., Friml, J., Scheres, B., Fu, Y., and Yang, Z. (2012). ROP GTPase-dependent actin microfilaments promote PIN1 polarization by localized inhibition of clathrin-dependent endocytosis. *PLoS Biol.* 10, e1001299. doi:10.1371/journal.pbio.1001299

Nagawa, S., Xu, T., and Yang, Z. (2010). RHO GTPase in plants: conservation and invention of regulators and effectors. *Small GTPases* 1, 78–88.

Napier, R. M., David, K. M., and Perrot-Rechenmann, C. (2002). A short history of auxin-binding proteins. *Plant Mol. Biol.* 49, 339–348.

Niihama, M., Takemoto, N., Hashiguchi, Y., Tasaka, M., and Morita, M. T. (2009). ZIP genes encode proteins involved in membrane trafficking of the TGN-PVC/vacuoles. *Plant Cell Physiol.* 50, 2057–2068.

Paciorek, T., Zazimalova, E., Ruthardt, N., Petrasek, J., Stierhof, Y. D., Kleine-Vehn, J., Morris, D. A., Emans, N., Jurgens, G., Geldner, N., and Friml, J. (2005). Auxin inhibits endocytosis and promotes its own efflux from cells. *Nature* 435, 1251–1256.

Pearse, B. M., and Robinson, M. S. (1984). Purification and properties of 100-kd proteins from coated vesicles and their reconstitution with clathrin. *EMBO J.* 3, 1951–1957.

Pecenkova, T., Hala, M., Kulich, I., Kocourkova, D., Drdova, E., Fendrych, M., Toupalova, H., and Zarsky, V. (2011). The role for the exocyst complex subunits Exo70B2 and Exo70H1 in the plant-pathogen interaction. *J. Exp. Bot.* 62, 2107–2116.

Pereira-Leal, J. B., and Seabra, M. C. (2001). Evolution of the Rab family of small GTP-binding proteins. *J. Mol. Biol.* 313, 889–901.

Praefcke, G. J., and McMahon, H. T. (2004). The dynamin superfamily: universal membrane tubulation and fission molecules? *Nat. Rev. Mol. Cell Biol.* 5, 133–147.

Preuss, M. L., Serna, J., Falbel, T. G., Bednarek, S. Y., and Nielsen, E. (2004). The Arabidopsis Rab GTPase RabA4b localizes to the tips of growing root hair cells. *Plant Cell* 16, 1589–1603.

Rensing, S. A., Lang, D., Zimmer, A. D., Terry, A., Salamov, A., Shapiro, H., Nishiyama, T., Perroud, P. F., Lindquist, E. A., Kamisugi, Y., Tanahashi, T., Sakakibara, K., Fujita, T., Oishi, K., Shin, I. T., Kuroki, Y., Toyoda, A., Suzuki, Y., Hashimoto, S., Yamaguchi, K., Sugano, S., Kohara, Y., Fujiyama, A., Anterola, A., Aoki, S., Ashton, N., Barbazuk, W. B., Barker, E., Bennetzen, J. L., Blankenship, R., Cho, S. H., Dutcher, S. K., Estelle, M., Fawcett, J. A., Gundlach, H., Hanada, K., Heyl, A., Hicks, K. A., Hughes, J., Lohr, M., Mayer, K., Melkozernov, A., Murata, T., Nelson, D. R., Pils, B., Prigge, M., Reiss, B., Renner, T., Rombauts, S., Rushton, P. J., Sanderfoot, A., Schween, G., Shiu, S. H., Stueber, K., Theodoulou, F. L., Tu, H., Van De Peer, Y., Verrier, P. J., Waters, E., Wood, A., Yang, L., Cove, D., Cuming, A. C., Hasebe, M., Lucas, S., Mishler, B. D., Reski, R., Grigoriev, I. V., Quatrano, R. S., and Boore, J. L. (2008). The Physcomitrella genome reveals evolutionary insights into the conquest of land by plants. *Science* 319, 64–69.

Robert, S., Kleine-Vehn, J., Barbez, E., Sauer, M., Paciorek, T., Baster, P., Vanneste, S., Zhang, J., Simon, S., Covanova, M., Hayashi, K., Dhonukshe, P., Yang, Z., Bednarek, S. Y., Jones, A. M., Luschnig, C., Aniento, F., Zazimalova, E., and Friml, J. (2010). ABP1 mediates auxin inhibition of clathrin-dependent endocytosis in Arabidopsis. *Cell* 143, 111–121.

Robinson, M. S., and Bonifacino, J. S. (2001). Adaptor-related proteins. *Curr. Opin. Cell Biol.* 13, 444–453.

Robinson, M. S., Sahlender, D. A., and Foster, S. D. (2010). Rapid inactivation of proteins by rapamycin-induced rerouting to mitochondria. *Dev. Cell* 18, 324–331.

Rojo, E., Gillmor, C. S., Kovaleva, V., Somerville, C. R., and Raikhel, N. V. (2001). VACUOLELESS1 is an essential gene required for vacuole formation and morphogenesis in Arabidopsis. *Dev. Cell* 1, 303–310.

Rojo, E., Zouhar, J., Kovaleva, V., Hong, S., and Raikhel, N. V. (2003). The AtC-VPS protein complex is localized to the tonoplast and the prevacuolar compartment in arabidopsis. *Mol. Biol. Cell* 14, 361–369.

Rutherford, S., and Moore, I. (2002). The Arabidopsis Rab GTPase family: another enigma variation. *Curr. Opin. Plant Biol.* 5, 518–528.

Saito, C., and Ueda, T. (2009). Chapter 4: functions of RAB and SNARE proteins in plant life. *Int. Rev. Cell Mol. Biol.* 274, 183–233.

Sanderfoot, A. (2007). Increases in the number of SNARE genes parallels the rise of multicellularity among the green plants. *Plant Physiol.* 144, 6–17.

Schledzewski, K., Brinkmann, H., and Mendel, R. R. (1999). Phylogenetic analysis of components of the eukaryotic vesicle transport system reveals a common origin of adaptor protein complexes 1, 2, and 3 and the F subcomplex of the coatomer COPI. *J. Mol. Evol.* 48, 770–778.

Seabra, M. C., and Wasmeier, C. (2004). Controlling the location and activation of Rab GTPases. *Curr. Opin. Cell Biol.* 16, 451–457.

Segui-Simarro, J. M., Austin, J. R. II, White, E. A., and Staehelin, L. A. (2004). Electron tomographic analysis of somatic cell plate formation in meristematic cells of Arabidopsis preserved by high-pressure freezing. *Plant Cell* 16, 836–856.

Sever, S. (2002). Dynamin and endocytosis. *Curr. Opin. Cell Biol.* 14, 463–467.

Singh, B., and Gupta, R. S. (2004). Genomic organization and linkage via a bidirectional promoter of the AP-3 (adaptor protein-3) mu3A and AK (adenosine kinase) genes: deletion mutants of AK in Chinese hamster cells extend into the AP-3 mu3A gene. *Biochem. J.* 378, 519–528.

Somsel Rodman, J., and Wandinger-Ness, A. (2000). Rab GTPases coordinate endocytosis. *J. Cell. Sci.* 113(Pt 2), 183–192.

Stenmark, H., and Olkkonen, V. M. (2001). The Rab GTPase family. *Genome Biol.* 2, REVIEWS3007.

Strickland, L. I., and Burgess, D. R. (2004). Pathways for membrane trafficking during cytokinesis. *Trends Cell Biol.* 14, 115–118.

Sweitzer, S. M., and Hinshaw, J. E. (1998). Dynamin undergoes a GTP-dependent conformational change causing vesiculation. *Cell* 93, 1021–1029.

Synek, L., Schlager, N., Elias, M., Quentin, M., Hauser, M. T., and Zarsky, V. (2006). AtEXO70A1, a member of a family of putative exocyst subunits specifically expanded in land plants, is important for polar growth and plant development. *Plant J.* 48, 54–72.

Szumlanski, A. L., and Nielsen, E. (2009). The Rab GTPase RabA4d regulates pollen tube tip growth in Arabidopsis thaliana. *Plant Cell* 21, 526–544.

Takei, K., Mcpherson, P. S., Schmid, S. L., and De Camilli, P. (1995). Tubular membrane invaginations coated by dynamin rings are induced by GTP-gamma S in nerve terminals. *Nature* 374, 186–190.

Taylor, N. G. (2011). A role for Arabidopsis dynamin related proteins DRP2A/B in endocytosis; DRP2 function is essential for plant growth. *Plant Mol. Biol.* 76, 117–129.

Thellmann, M., Rybak, K., Thiele, K., Wanner, G., and Assaad, F. F. (2010). Tethering factors required for cytokinesis in Arabidopsis. *Plant Physiol.* 154, 720–732.

Ueda, T., Matsuda, N., Anai, T., Tsukaya, H., Uchimiya, H., and Nakano, A. (1996). An Arabidopsis gene isolated by a novel method for detecting genetic interaction in yeast encodes the GDP dissociation inhibitor of Ara4 GTPase. *Plant Cell* 8, 2079–2091.

Ueda, T., Uemura, T., Sato, M. H., and Nakano, A. (2004). Functional differentiation of endosomes in Arabidopsis cells. *Plant J.* 40, 783–789.

Ueda, T., Yamaguchi, M., Uchimiya, H., and Nakano, A. (2001). Ara6, a plant-unique novel type Rab GTPase, functions in the endocytic

pathway of Arabidopsis thaliana. *EMBO J.* 20, 4730–4741.

Uemura, T., Ueda, T., Ohniwa, R. L., Nakano, A., Takeyasu, K., and Sato, M. H. (2004). Systematic analysis of SNARE molecules in Arabidopsis: dissection of the post-Golgi network in plant cells. *Cell Struct. Funct.* 29, 49–65.

Ullrich, O., Reinsch, S., Urbe, S., Zerial, M., and Parton, R. G. (1996). Rab11 regulates recycling through the pericentriolar recycling endosome. *J. Cell Biol.* 135, 913–924.

Van Damme, D., Coutuer, S., De Rycke, R., Bouget, F. Y., Inze, D., and Geelen, D. (2006). Somatic cytokinesis and pollen maturation in Arabidopsis depend on TPLATE, which has domains similar to coat proteins. *Plant Cell* 18, 3502–3518.

Van Damme, D., Gadeyne, A., Vanstraelen, M., Inze, D., Van Montagu, M. C., De Jaeger, G., Russinova, E., and Geelen, D. (2011). Adaptin-like protein TPLATE and clathrin recruitment during plant somatic cytokinesis occurs via two distinct pathways. *Proc. Natl. Acad. Sci. U.S.A.* 108, 615–620.

van Dooren, G. G., Reiff, S. B., Tomova, C., Meissner, M., Humbel, B. M., and Striepen, B. (2009). A novel dynamin-related protein has been recruited for apicoplast fission in Toxoplasma gondii. *Curr. Biol.* 19, 267–276.

Vedovato, M., Rossi, V., Dacks, J. B., and Filippini, F. (2009). Comparative analysis of plant genomes allows the definition of the "Phytolongins": a novel non-SNARE longin domain protein family. *BMC Genomics* 10, 510. doi:10.1186/1471-2164-10-510

Vernoud, V., Horton, A. C., Yang, Z., and Nielsen, E. (2003). Analysis of the small GTPase gene superfamily of Arabidopsis. *Plant Physiol.* 131, 1191–1208.

Viotti, C., Bubeck, J., Stierhof, Y. D., Krebs, M., Langhans, M., Van Den Berg, W., Van Dongen, W., Richter, S., Geldner, N., Takano, J., Jurgens, G., De Vries, S. C., Robinson, D. G., and Schumacher, K. (2010). Endocytic and secretory traffic in Arabidopsis merge in the trans-Golgi network/early endosome, an independent and highly dynamic organelle. *Plant Cell* 22, 1344–1357.

Wang, J., Ding, Y., Hillmer, S., Miao, Y., Lo, S. W., Wang, X., Robinson, D. G., and Jiang, L. (2010). EXPO, an exocyst-positive organelle distinct from multivesicular endosomes and autophagosomes, mediates cytosol to cell wall exocytosis in Arabidopsis and tobacco cells. *Plant Cell* 22, 4009–4030.

Wickner, W., and Schekman, R. (2008). Membrane fusion. *Nat. Struct. Mol. Biol.* 15, 658–664.

Woollard, A. A., and Moore, I. (2008). The functions of Rab GTPases in plant membrane traffic. *Curr. Opin. Plant Biol.* 11, 610–619.

Xu, T., Wen, M., Nagawa, S., Fu, Y., Chen, J. G., Wu, M. J., Perrot-Rechenmann, C., Friml, J., Jones, A. M., and Yang, Z. (2010). Cell surface- and rho GTPase-based auxin signaling controls cellular interdigitation in Arabidopsis. *Cell* 143, 99–110.

Yoshizawa, A. C., Kawashima, S., Okuda, S., Fujita, M., Itoh, M., Moriya, Y., Hattori, M., and Kanehisa, M. (2006). Extracting sequence motifs and the phylogenetic features of SNARE-dependent membrane traffic. *Traffic* 7, 1104–1118.

Yu, I. M., and Hughson, F. M. (2010). Tethering factors as organizers of intracellular vesicular traffic. *Annu. Rev. Cell Dev. Biol.* 26, 137–156.

Zainal, Z., Tucker, G. A., and Lycett, G. W. (1996). A rab11-like gene is developmentally regulated in ripening mango (Mangifera indica L.) fruit. *Biochim. Biophys. Acta* 1314, 187–190.

Zhang, L., Tian, L. H., Zhao, J. F., Song, Y., Zhang, C. J., and Guo, Y. (2009). Identification of an apoplastic protein involved in the initial phase of salt stress response in rice root by two-dimensional electrophoresis. *Plant Physiol.* 149, 916–928.

Zhang, L., Zhang, H., Liu, P., Hao, H., Jin, J. B., and Lin, J. (2011). Arabidopsis R-SNARE proteins VAMP721 and VAMP722 are required for cell plate formation. *PLoS ONE* 6, e26129. doi:10.1371/journal.pone.0026129

Conflict of Interest Statement: The authors declare that the research was conducted in the absence of any commercial or financial relationships that could be construed as a potential conflict of interest.

Received: 28 May 2012; accepted: 08 August 2012; published online: 28 August 2012.

*Citation: Fujimoto M and Ueda T (2012) Conserved and plant-unique mechanisms regulating plant post-Golgi traffic. Front. Plant Sci. **3**:197. doi: 10.3389/fpls.2012.00197*

This article was submitted to Frontiers in Plant Traffic and Transport, a specialty of Frontiers in Plant Science.

frontiers in
PLANT SCIENCE

REVIEW ARTICLE
published: 02 October 2012
doi: 10.3389/fpls.2012.00219

Endocytic signaling in leaves and roots: same rules different players

Christian Craddock* and Zhenbiao Yang*

Center for Plant Cell Biology, Department of Botany and Plant Sciences, University of California, Riverside, CA, USA

Edited by:
Angus S. Murphy, University of Maryland, USA

Reviewed by:
Liwen Jiang, The Chinese University of Hong Kong, Hong Kong
Yi Ma, University of Connecticut, USA

****Correspondence:***
Christian Craddock and Zhenbiao Yang, Center for Plant Cell Biology, Department of Botany and Plant Sciences, University of California, Riverside, CA, USA.
e-mail: christian.craddock@ucr.edu; zhenbiao.yang@ucr.edu

To take up proteins and other components required by the cell, cells internalize a portion of the plasma membrane (PM), which invaginates to form a closed vesicle within the cytoplasm in a process known as endocytosis. The major plant endocytic mechanism is mediated by clathrin, a protein that is necessary to generate a coated vesicle on the inner side of the PM. These vesicles bud away from the membrane generating a vesicle whose contents originated from outside of the cell and they can selectively concentrate or exclude compounds. The process is therefore of key importance to plant growth, development, signaling, polarity, and nutrient delivery. Rho family small GTPases are conserved molecular switches that function in many signaling events. Plants possess only a single Rho-like GTPase (ROP) family. ROPs are known to be involved in the control of cell polarity by regulating endocytosis. To contend with the high levels of regulation required for such processes, plants have evolved specific regulators, including the Rop-interactive CRIB motif-containing protein (RIC) effectors. Recent findings have demonstrated that ROP dynamics and the cytoskeleton (including actin microfilaments and microtubules) are interwoven. In this review, we summarize the current understanding of endocytosis in plants, with particular regard to the signaling pathways.

Keywords: auxin, ABP1, ROP RIC actin, endocytosis clathrin, microtubules

INTRODUCTION

The generation of planar cell polarity (PCP) is a process involving the distribution of cellular structures or molecules asymmetrically. PCP establishment requires a mechanism for the formation of both intra-cell polarity and inter-cell polarity.

Rho-like GTPases (ROPs) from plants are the sole signaling small GTPases in plants and it is therefore expected that they have a role in numerous signaling events. ROPs are already known to participate in signaling pathways that regulate cytoskeletal organization and vesicular trafficking, and as a consequence have an impact on cell polarization, polar growth, and cell morphogenesis. Microtubules (MTs) and actin microfilaments (F-actin) are the two major cytoskeletal elements that play a key role in many cellular processes, including cell polarity and endocytosis.

In plants, the phytohormone auxin has a cardinal role in the coordination of many physiological functions, including growth and the development of cells and organs (Benkova et al., 2003; Friml et al., 2003; Blilou et al., 2005; Vieten et al., 2005; Weijers et al., 2005; Scarpella et al., 2006; Wisniewska et al., 2006; Grieneisen et al., 2007; Gao et al., 2008; Yang, 2008). To function, auxin must be dynamic both spatially and temporally (Santner and Estelle, 2009; Vanneste and Friml, 2009). In multicellular plants, this process is in part mediated by the polar distribution of the auxin efflux carriers PIN-FORMED (PIN) proteins, which are required for polar auxin transport and the formation of auxin gradients.

Asymmetric endocytosis and the recycling of PINs localized at the plasma membrane (PM) contribute to the polar localization of PINs (Geldner et al., 2003; Dhonukshe et al., 2008). More recently, auxin has been implicated as a self-organizing signal that causes the polarization of PIN proteins. The auxin signal that appears to regulate downstream ROPs involved in PCP is mediated through auxin binding protein 1 (ABP1). ABP1 has been proposed to regulate clathrin-mediated endocytosis in roots, and the ROP-dependent pavement cell (PC) interdigitation in leaves (Robert et al., 2010; Xu et al., 2010, 2011).

The signaling mechanisms involved in the formation of cell polarity, including ROPs, their close relationship with the cytoskeleton and endocytic trafficking are the focus of this review. The above-mentioned mechanisms are all conserved in plants and animals, and consequently advances in knowledge in the plant system may synergize advances in understanding similar mechanisms and processes in mammalian systems.

SIGNALING AND ENDOCYTOSIS IN PAVEMENT CELLS

The formation of the jigsaw puzzle like shape of *Arabidopsis* leaf PCs epitomizes a long-standing question in cell and developmental biology. How does a field of cells precisely coordinate uniform cell polarity? Importantly, the interdigitation of PCs provides an excellent system for the investigation because interdigitation is a non-essential process. It is therefore possible to study the signaling mechanism with the use of overexpressing or knockout plant lines.

In leaf PCs, the auxin cell surface receptor ABP1 mediates auxin signaling to coordinately activate two mutually exclusive ROP signaling pathways. They are activated in complementary lobe and indent regions on adjacent sides of the cell (**Figure 1**). A lobe in a cell corresponds to an indent in the adjacent cell. ROP2 and ROP4 promote lobe formation and are functionally redundant; ROP2 is

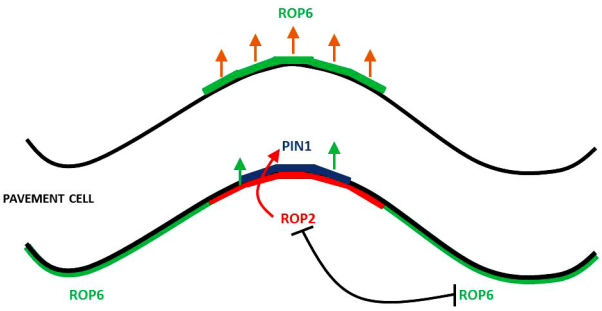

FIGURE 1 | Rho-like GTPase activation regions and PIN1 localization in leaf PCs. ROP2 promotes the localization of PIN1 to the lobe tip which initiates a positive feedback loop in this region. The mutual exclusivity of ROP2 and ROP6 help restrict PIN1 to the lobe region.

the dominant ROP in lobe promotion and it is common to refer to ROP2 and ROP4 simply as ROP2. ROP6 is responsible for the promotion of indentations (Fu et al., 2002, 2005). Both ROP2 and ROP6 localize to and are activated at the PM (Xu et al., 2010, 2011). The localization of the auxin efflux carrier PIN1 to the lobe tips requires localized ROP2, indicating the existence of a localized auxin–ROP2–PIN1–auxin positive feedback loop that could be responsible for the generation and maintenance of localized auxin levels (Xu et al., 2010). However, it remains to be established how auxin-activated ROP2 regulates PIN1 polarization. ROP2 regulates the formation of multipolarity through its activation of RIC4 (Fu et al., 2005), a member of the ROP interacting CRIB motif-containing (RIC) family of ROP effector proteins (Wu et al., 2001). RIC4 induces the formation of cortical F-actin in the tips of PCs (Fu et al., 2005).

In the indenting zone, ROP6 activates RIC1, leading to the formation of well-ordered MT arrays, which promote indentation and inhibit ROP2 activation (Fu et al., 2005, 2009).

ROP2 inactivates RIC1, which causes the suppression of well-ordered cortical MTs, thus preventing outgrowth as MTs are excluded from outgrowing lobe tips (Fu et al., 2002, 2005). With the local activation of ROP2–PIN1 in the lobe region, ROP6 is suppressed at this site, given that the ROP2 and ROP6 pathways are mutually exclusive (Fu et al., 2009). Within an indent region, ROP6 activates RIC1, which leads to the creation of highly ordered MT arrays, which promote further indentation and inhibit ROP2 activity (Fu et al., 2005, 2009). It is hypothesized that the mutual inhibition between the ROP2 and ROP6 pathways transforms the initial uniform pool of auxin into localized extracellular auxin pools that enable the sustainment of ROP2 and ROP6 activity on opposing sides of the extracellular pool of auxin. It is thought that this interdigitated patterning of ROP2 and ROP6 activation could give rise to the lobe and indentation patterning that is observed between neighboring cells. It was recently shown that the rapid activation of the antagonizing ROP2 and ROP6 pathways require ABP1-dependent auxin perception (Xu et al., 2010). This work demonstrated that exogenous auxin promotes interdigitation in PCs, whereas a reduction in endogenous auxin suppresses interdigitation (Xu et al., 2010). Auxin inhibits PIN internalization (Paciorek et al., 2005; Dhonukshe et al., 2008), and consistent with this, the localization of PIN1 to the lobe tips (Fu et al., 2005) was found to be dependent on ROP2, which is activated in the same PM region where PIN1 is located (Xu et al., 2010). The evidence is suggestive that PIN1-directed auxin efflux is involved in the positive feedback regulation of ROP2 (Fu et al., 2002, 2005). This model is consistent with that of roots and guard cells, where constitutive activation of ROPs inhibited the internalization of the endocytosis marker FM-64 (Bloch et al., 2005; Sorek et al., 2010; Hwang et al., 2011). ROP2 was found to inhibit PIN1 endocytosis in the lobe regions of PCs. A series of elegant studies using the Dendra2 photo-convertible fluorescent protein revealed that in wild type, PIN1 endocytosis was found to occur in the indentation regions but not in the lobe regions. In contrast, expression of dominant negative ROP2 induced PIN1 endocytosis in the lobe region. Following the transient expression of PIN1–GFP in *rop2* mutant PCs, revealed that ROP2 is required for the inhibitory effect of auxin on PIN1 endocytosis. A final experiment using *ric4* mutant knock down and PIN1–GFP demonstrated that RIC4 has a role in promoting the accumulation of cortical F-actin in the lobe region and in turn inhibiting PIN1 endocytosis through RIC4-dependent F-actin. Recent data, summarized in **Figure 2**, show that the ROP2/RIC4 pathway inhibits clathrin-dependent PIN1 endocytosis thereby leading to PIN1 polarization. The direction of auxin movement is dependent on PIN auxin transporters, which constantly undertake endocytic recycling (Dhonukshe et al., 2007, 2008; Kleine-Vehn et al., 2011), with the polar location of PIN at the PM determining the direction of auxin flow between cells (Petrasek et al., 2006).

Although the nature and morphology of the recycling endosome remains elusive, plant early endosomes (EEs) and late endosomes (LEs) have been shown to correspond to the *trans*-Golgi network (TGN) and multivesicular bodies (MVBs), respectively. Endosomes are cellular organelles that appear to be involved in both the endocytic and biosynthetic pathways in plants (De Matteis and Luini, 2008; Foresti and Denecke, 2008). In the endocytic pathway, EEs receive internalized material from the PM and either recycle it back to the cell surface or target it for degradation, thereby acting as an important protein sorting station in the endocytic pathway, which is fundamental to ensure establishment and maintenance of cell polarity and homeostasis (Geldner, 2004; Geldner et al., 2004; Lam et al., 2007b; Otegui and Spitzer, 2008). In addition, EEs play a role in the biosynthetic pathway as they can receive newly synthesized material from the TGN and either sort it to the endosome/lysosome or recycle it back to the PM via the recycling endosome (De Matteis and Luini, 2008).

Studies using the endocytic tracer FM4-64, indicate that the VHA1-labeled TGN is an EE given that it displays detectable steady state levels of FM4-64 prior to the labeling of the PVC (Dettmer et al., 2006; Lam et al., 2007a). These studies in conjunction with morphological observations that both the TGN and the EE can present clathrin budding profiles (Payne and Schekman, 1985; Hillmer et al., 1988; Pearse and Robinson, 1990) further support the TGN and EEs being the same compartment (Geldner, 2004; Lam et al., 2007a).

Proteins within the EEs that are destined for degradation are sorted into another subdomain, which will form MVB/LEs (Murk et al., 2002). MVBs/LEs mediate the delivery of vacuolar-destined

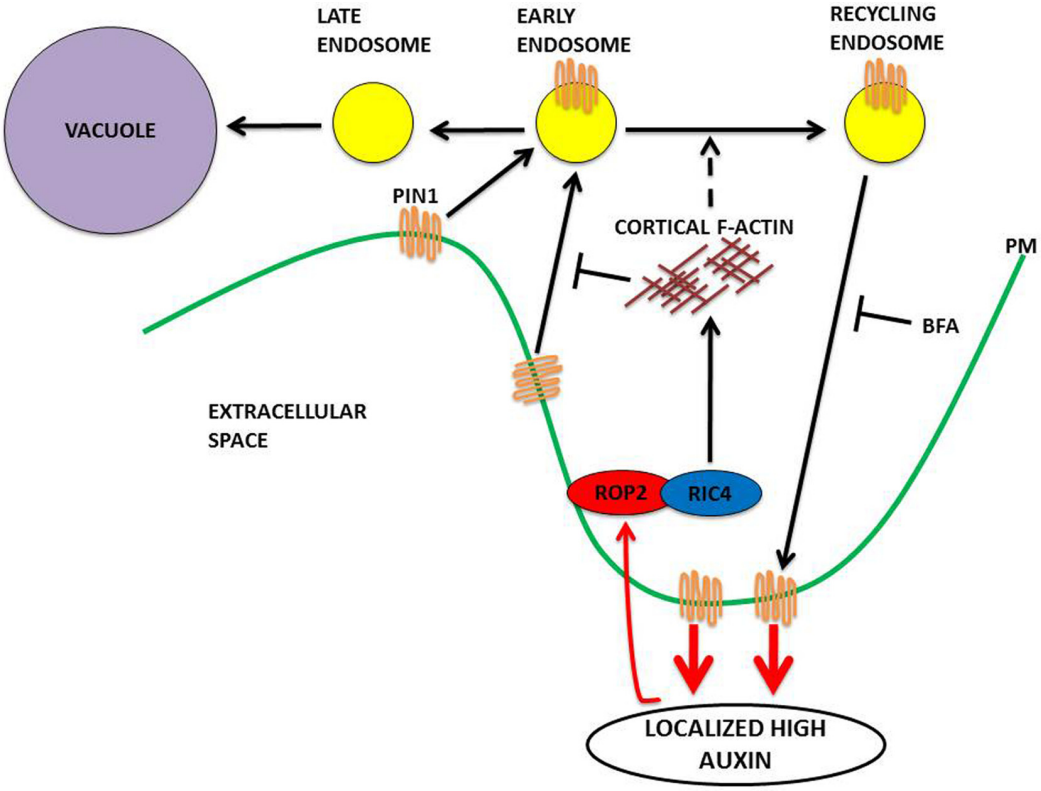

FIGURE 2 | A model in PCs for PIN1 polarization to the lobe regions of PCs via a ROP signaling mechanism. ROP2 is activated by extracellular auxin in the lobe region. The activated ROP2–RIC4 pathway leads to the inhibition of PIN1 internalization through RIC4-dependent cortical F-actin, leading to PIN1 polarization at the lobe. The PIN1-based export of auxin leads to further ROP2 activation for completion of this feed-forward cycle. Recent data (Nagawa et al., 2012) indicates that the activated ROP2–RIC4 pathway has a role in the promotion of endosomal trafficking from early endosomes to recycling endosomes (Brefeldin A inhibits ADP ribosylation factor GEF and prevents endosomal recycling, the accumulation of internalized PIN1 in aggregates known as BFA bodies in plant cells). Endocytosed material can then be recycled back to the PM. Material maintained in early endosomes as they mature becomes internalized in late endosomes. The multivesicular structure of the late endosomes allows membrane fusion with the vacuole. Proteins within the late endosomes are delivered to the vacuole for degradation.

proteins to the vacuole through fusion with the tonoplast. It was shown that LE/MVBs contain visibly distinct morphological regions together with membrane domains enriched in two GTPases, Rab7, and Rab9, that regulate late endocytic traffic and LE/MVB to EE/TGN recycling, respectively (Gruenberg, 2001; Barbero et al., 2002), inferring that LEs/MVBs derive from TGN/EEs. Earlier evidence indeed demonstrated that the formation of LEs/MVBs from EEs/TGN is induced by the ubiquitination of receptors, as illustrated by the epidermal growth factor (EGF; Hicke and Riezman, 1996). More recent evidence also points toward LEs/MVBs being derived through the maturation of EEs/TGN (Scheuring et al., 2011). Importantly, their experiments suggest that the inhibition of clathrin-mediated transport does not halt the transport of soluble cargo bearing vacuolar sorting determinants to the vacuole. Therefore the widely held concept of the anterograde trafficking of proteins occurring via the recognition of sorting signals and trafficking through vesicles moving between stable compartments is not supported by this evidence. Instead the evidence supports the idea that anterograde trafficking occurs in the absence of CCVs and the recycling of receptors (Scheuring et al., 2011).

REGULATION OF ENDOCYTOSIS IN ROOTS

In roots, the mechanisms underlying apical and basal polarization appear similar to the coordination of polarity in leaves. In roots, recent findings have shown that a signal module composed of auxin, ABP1, ROP6/RIC1, clathrin, PIN1/PIN2 act as an integral component of the feedback regulation of auxin transport during root development.

Recent evidence indicates that ROP6 affects endocytosis and is involved in PIN internalization (Chen et al., 2012). Subsequent experiments revealed that the uptake of FM4-64 increased in the roots of *rop6* or *ric1* mutant plant lines, whereas uptake was reduced in the presence of constitutive *rop6* expression (Chen et al., 2012). In addition, visualization of clathrin heavy chain with the aforementioned plant lines revealed that ROP6 signaling negatively regulates clathrin-mediated endocytosis (Chen et al., 2012). *rop6* and *ric1* mutants displayed lower levels of sensitivity to auxin indicating the ROP6/RIC1 pathway is involved in and acts downstream of both auxin regulation and ABP1 signaling in the regulation of clathrin-mediated endocytosis in roots (Chen et al., 2012). The role of the ROP6/RIC1 pathway in endocytosis roots is similar to the regulation of PC interdigitation in leaves

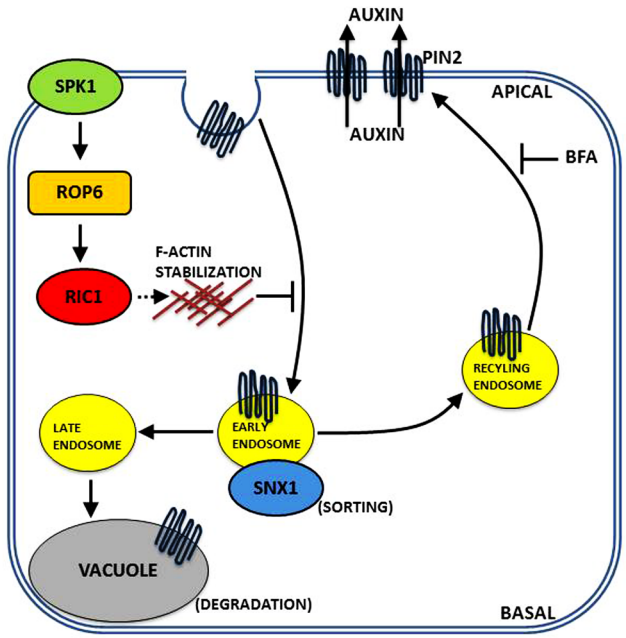

FIGURE 3 | A model in roots for PIN2 polar distribution via a ROP signaling mechanism. Data indicate that the auxin-mediated inhibition of polar PIN2 internalization is regulated by the SPK1–ROP6–RIC1 pathway. Auxin is proposed to activate the SPK1–ROP6–RIC1 pathway and inhibit PIN2 internalization. The localized inhibition of PIN2 internalization via ROP6 signaling causes PIN2 to be retained in the PM, which generates a positive feedback mechanism for maintaining polar PIN2 distribution to the PM.

(Xu et al., 2010; Nagawa et al., 2012). Both pathways possess the auxin feedback module composed of auxin–ABP1–ROP–clathrin-mediated endocytosis-PIN1/PIN2 localization, although there are key differences in how the individual steps are performed. In PCs, auxin acts via ABP1 to activate the ROP2 pathway and inhibits clathrin-dependent endocytosis leading to PIN1 polarization at the lobe (Xu et al., 2010; Nagawa et al., 2012). In roots, ABP1 seems to act as a positive regulator of clathrin-mediated endocytosis, whereas auxin acts as the inhibitor (Chen et al., 2012). The relatively mild phenotype displayed in the analyzed ROP6 genotypes indicates functional redundancy with other ROPs such as ROP9 and ROP11 (Bloch et al., 2005). Very recent findings have begun to link auxin signaling to PIN-mediated pattern formation and morphogenesis in roots. A genetic screen found that the absence of SPIKE1 leads to increased lateral root density and retarded gravitropic responses matching the phenotype observed in *pin2* knockouts (Lin et al., 2012). Mutant *spk1* plants induced PIN2 internalization that could not be suppressed by auxin, equivalent to *rop6* and *ric1* mutants. Moreover, SPIKE1 was required for auxin induction of ROP6 activation.

The current model for the polar distribution of PIN2 via the ROP-based signaling pathway is presented in **Figure 3**.

CONCLUSION

Recent findings suggest that PIN internalization by ROP-based auxin signaling is a mechanism responsible for the regulation of polar auxin trafficking in plants. The ROP2/RIC4 pathway being responsible for the induction of F-actin in PCs which leads to the inhibition of PIN1 internalization necessary for PIN1 polarization to the lobe tips (Nagawa et al., 2012). The ROP6/RIC1 pathway functions in roots to inhibit PIN2 internalization through the stabilization of F-actin. A key distinction is that ABP1 activates the ROP pathway in PCs (Xu et al., 2010; Nagawa et al., 2012), whereas in roots ABP1 is responsible for inactivation of the ROP pathway (Chen et al., 2012). Future studies will hopefully elucidate whether this finding is due to differences in auxin concentration required to activate the ROP pathways in different tissues.

Whilst recent advances strongly suggest that the ROP-based auxin signaling that regulates PIN internalization is a widespread mechanism for the modulation of auxin transport in plants, key questions remain. Including for example the involvement of the ABP1 pathway in cytoskeletal dynamics and cell polarity. A resourceful use of biochemistry, forward and reverse genetics, and imaging are necessary to identify the remaining components to obtain a fuller understanding of the signaling events regulating endocytosis in plants.

ACKNOWLEDGMENTS

The authors thank Irene Lavagi for editing this manuscript and providing thoughtful comments. We thank past and present members of the Yang laboratory for stimulating discussions and the generation of data that made this review possible. The work is supported by funding from the National Institute of General Medical Sciences (R01GM081451 and R01GM100130) and the Department of Energy (DE-FG02-04ER15555) to Zhenbiao Yang.

REFERENCES

Barbero, P., Bittova, L., and Pfeffer, S. R. (2002). Visualization of Rab9-mediated vesicle transport from endosomes to the trans-Golgi in living cells. *J. Cell Biol.* 156, 511–518.

Benkova, E., Michniewicz, M., Sauer, M., Teichmann, T., Seifertová, D., Jürgens, G., and Friml, J. (2003). Local, efflux-dependent auxin gradients as a common module for plant organ formation. *Cell* 115, 591–602.

Blilou, I., Xu, J., Wildwater, M., Willemsen, V., Paponov, I., Friml, J., Heidstra, R., Aida, M., Palme, K., and Scheres, B. (2005). The PIN auxin efflux facilitator network controls growth and patterning in *Arabidopsis* roots. *Nature* 433, 39–44.

Bloch, D., Lavy, M., Efrat, Y., Efroni, I., Bracha-Drori, K., Abu-Abied, M., Sadot, E., and Yalovsky, S. (2005). Ectopic expression of an activated RAC in *Arabidopsis* disrupts membrane cycling. *Mol. Biol. Cell* 16, 1913–1927.

Chen, X., Naramoto, S., Robert, S., Tejos, R., Löfke, C., Lin, D., Yang, Z., and Friml, J. (2012). ABP1 and ROP6 GTPase signaling regulate clathrin-mediated endocytosis in *Arabidopsis* roots. *Curr. Biol.* 22, 1326–1332.

De Matteis, M. A., and Luini, A. (2008). Exiting the Golgi complex. *Nat. Rev. Mol. Cell Biol.* 9, 273–284.

Dettmer, J., Hong-Hermesdorf, A., Stierhof, Y.-D., and Schumacher. K. (2006). Vacuolar H+-ATPase activity is required for endocytic and secretory trafficking in *Arabidopsis*. *Plant Cell* 18, 715–730.

Dhonukshe, P., Aniento, F., Hwang, I., Robinson, D. G., Mravec, J., Stierhof, Y. D., and Friml, J. (2007). Clathrin-mediated constitutive endocytosis of PIN auxin efflux carriers in *Arabidopsis*. *Curr. Biol.* 17, 520–527.

Dhonukshe, P., Tanaka, H., Goh, T., Ebine, K., Mähönen, A. P., Prasad, K., Blilou, I., Geldner, N., Xu, J., Uemura, T., Chory, J., Ueda, T., Nakano, A., Scheres, B., and Friml, J. (2008). Generation of cell polarity in plants links endocytosis, auxin distribution and cell fate decisions. *Nature* 456, 962–966.

Foresti, O., and Denecke, J. (2008). Intermediate organelles of the plant secretory pathway: identity and function. *Traffic* 9, 1599–1612.

Friml, J., Vieten, A., Sauer, M., Weijers, D., Schwarz, H., Hamann, T., Offringa, R., and Jürgens, G. (2003). Efflux-dependent auxin gradients establish the apical-basal axis of *Arabidopsis*. *Nature* 426, 147–153.

Fu, Y., Gu, Y., Zheng, Z., Wasteneys, G., and Yang, Z. (2005). *Arabidopsis* interdigitating cell growth requires two antagonistic pathways with opposing action on cell morphogenesis. *Cell* 120, 687–700.

Fu, Y., Li, H., and Yang, Z. (2002). The ROP2 GTPase controls the formation of cortical fine F-actin and the early phase of directional cell expansion during *Arabidopsis* organogenesis. *Plant Cell* 14, 777–794.

Fu, Y., Xu, T., Zhu, L., Wen, M., and Yang, Z. (2009). A ROP GTPase signaling pathway controls cortical microtubule ordering and cell expansion in *Arabidopsis*. *Curr. Biol.* 19, 1827–1832.

Gao, X., Nagawa, S., Wang, G., and Yang, Z. (2008). Cell polarity signaling: focus on polar auxin transport. *Mol. Plant* 1, 899–909.

Geldner, N. (2004). The plant endosomal system – its structure and role in signal transduction and plant development. *Planta* 219, 547–560.

Geldner, N., Anders, N., Wolters, H., Keicher, J., Kornberger, W., Muller, P., Delbarre, A., Ueda, T., Nakano, A., and Jürgens, G. (2003). The *Arabidopsis* GNOM ARF-GEF mediates endosomal recycling, auxin transport, and auxin-dependent plant growth. *Cell* 112, 219–230.

Geldner, N., Richter, S., Vieten, A., Marquardt, S., Torres-Ruiz, R. A., Mayer, U., and Jürgens, G. (2004). Partial loss-of-function alleles reveal a role for GNOM in auxin transport-related, post-embryonic development of *Arabidopsis*. *Development* 131, 389–400.

Grieneisen, V. A., Xu, J., Marée, A. F., Hogeweg, P., and Scheres, B. (2007). Auxin transport is sufficient to generate a maximum and gradient guiding root growth. *Nature* 449, 1008–1013.

Gruenberg, J. (2001). The endocytic pathway: a mosaic of domains. *Nat. Rev. Mol. Cell Biol.* 2, 721–730.

Hicke, L., and Riezman, H. (1996). Ubiquitination of a yeast plasma membrane receptor signals its ligand-stimulated endocytosis. *Cell* 84, 277–287.

Hillmer, S., Freundt, H., and Robinson, D. G. (1988). The partially coated reticulum and its relationship to the Golgi apparatus in higher plant cells. *Eur. J. Cell Biol.* 47, 206–212.

Hwang, J. U., Jeon, B. W., Hong, D., and Lee, Y. (2011). Active ROP2 GTPase inhibits ABA- and CO2-induced stomatal closure. *Plant Cell Environ.* 34, 2172–2182.

Kleine-Vehn, J., Wabnik, K., Martinière, A., Langowski, L., Willig, K., Naramoto, S., Leitner, J., Tanaka, H., Jakobs, S., Robert, S., Luschnig, C., Govaerts, W., Hell, S. W., Runions, J., and Friml, J. (2011). Recycling, clustering, and endocytosis jointly maintain PIN auxin carrier polarity at the plasma membrane. *Mol. Syst. Biol.* 7, 540.

Lam, S. K., Siu, C. L., Hillmer, S., Jang, S., An, G., Robinson, D. G., and Jiang, L. (2007a). Rice SCAMP1 defines clathrin-coated, *trans*-Golgi-located tubular-vesicular structures as an early endosome in tobacco BY-2 cells. *Plant Cell* 19, 296–319.

Lam, S. K., Tse, Y. C., Robinson, D. G., and Jiang, L. (2007b). Tracking down the elusive early endosome. *Trends Plant Sci.* 12, 497–505.

Lin, D., Nagawa, S., Chen, J., Cao, L., Chen, X., Xu, T., Li, H., Dhonukshe, P., Yamamuro, C., Friml, J., Scheres, B., Fu, Y., and Yang, Z. (2012). A ROP GTPase-dependent auxin signaling pathway regulates the subcellular distribution of PIN2 in *Arabidopsis* roots. *Curr. Biol.* 22, 1319–1325.

Murk, J. L., Stoorvogel, W., Kleijmeer, M. J., and Geuze, H. J. (2002). The plasticity of multivesicular bodies and the regulation of antigen presentation. *Semin. Cell Dev. Biol.* 13, 303–311.

Nagawa, S., Xu, T., Lin, D., Dhonukshe, P., Zhang, X., Friml, J., Scheres, B., Fu, Y., and Yang, Z. (2012). ROP GTPase-dependent actin microfilaments promote PIN1 polarization by localized inhibition of clathrin-dependent endocytosis. *PLoS Biol.* 10, e1001299. doi: 10.1371/journal.pbio.1001299

Otegui, M. S., and Spitzer, C. (2008). Endosomal functions in plants. *Traffic* 9, 1589–1598.

Paciorek, T., Zazimalova, E., Ruthardt, N., Petrásek, J., Stierhof, Y. D, Kleine-Vehn, J., Morris, D. A., Emans, N., Jürgens, G., Geldner, N., and Friml, J. (2005). Auxin inhibits endocytosis and promotes its own efflux from cells. *Nature* 435, 1251–1256.

Payne, G. S., and Schekman, R. (1985). A test of clathrin function in protein secretion and cell growth. *Science* 230, 1009–1014.

Pearse, B. M., and Robinson, M. S. (1990). Clathrin, adaptors, and sorting. *Annu. Rev. Cell Biol.* 6, 151–171.

Petrasek, J., Mravec, J., Bouchard, R., Blakeslee, J. J., Abas, M., Seifertová, D., Wisniewska, J., Tadele, Z., Kubes, M., Covanová, M., Dhonukshe, P., Skupa, P., Benková, E., Perry, L., Krecek, P., Lee, O. R., Fink, G. R., Geisler, M., Murphy, A. S., Luschnig, C., Zazímalová, E., and Friml, J. (2006). PIN proteins perform a rate-limiting function in cellular auxin efflux. *Science* 312, 914–918.

Robert, S., Kleine-Vehn, J., Barbez, E., Sauer, M., Paciorek, T., Baster, P., Vanneste, S., Zhang, J., Simon, S., Čovanová, M., Hayashi, K., Dhonukshe, P., Yang, Z., Bednarek, S. Y., Jones, A. M., Luschnig, C., Aniento, F., Zažímalová, E., and Friml, J. (2010). ABP1 mediates auxin inhibition of clathrin-dependent endocytosis in *Arabidopsis*. *Cell* 143, 111–121.

Santner, A., and Estelle, M. (2009). Recent advances and emerging trends in plant hormone signalling. *Nature* 459, 1071–1078.

Scarpella, E., Marcos, D., Friml, J., and Berleth, T. (2006). Control of leaf vascular patterning by polar auxin transport. *Genes Dev.* 20, 1015–1027.

Scheuring, D., Viotti, C., Krüger, F., Künzl, F., Sturm, S., Bubeck, J., Hillmer, S., Frigerio, L., Robinson, D. G., Pimpl, P., and Schumacher, K. (2011). Multivesicular bodies mature from the *trans*-Golgi network/early endosome in *Arabidopsis*. *Plant Cell* 23, 3463–3481.

Sorek, N., Segev, O., Gutman, O., Bar, E., Richter, S., Poraty, L., Hirsch, J. A., Henis, Y. I., Lewinsohn, E., Jürgens, G., and Yalovsky, S. (2010). An *S*-acylation switch of conserved G domain cysteines is required for polarity signaling by ROP GTPases. *Curr. Biol.* 20, 914–920.

Vanneste, S., and Friml, J. (2009). Auxin: a trigger for change in plant development. *Cell* 136, 1005–1016.

Vieten, A., Vanneste, S., Wisniewska, J., Benková, E., Benjamins, R., Beeckman, T., Luschnig, C., and Friml, J. (2005). Functional redundancy of PIN proteins is accompanied by auxin-dependent cross-regulation of PIN expression. *Development* 132, 4521–4531.

Weijers, D., Sauer, M., Meurette, O., Friml, J., Ljung, K., Sandberg, G., Hooykaas, P., and Offringa, R. (2005). Maintenance of embryonic auxin distribution for apical-basal patterning by PIN-FORMED-dependent auxin transport in *Arabidopsis*. *Plant Cell* 17, 2517–2526.

Wisniewska, J., Xu, J., Seifertová, D., Brewer, P. B., Ruzicka, K., Blilou, I., Rouquié, D., Benková, E., Scheres, B., and Friml, J. (2006). Polar PIN localization directs auxin flow in plants. *Science* 312, 883.

Wu, G., Gu, Y., Li, S., and Yang, Z. (2001). A genome-wide analysis of *Arabidopsis* Rop-interactive CRIB motif-containing proteins that act as Rop GTPase targets. *Plant Cell* 13, 2841–2856.

Xu, T., Nagawa, S., and Yang, Z. (2011). Uniform auxin triggers the Rho GTPase-dependent formation of interdigitation patterns in pavement cells. *Small GTPases* 2, 227–232.

Xu, T., Wen, M., Nagawa, S., Fu, Y., Chen, J. G., Wu, M. J., Perrot-Rechenmann, C., Friml, J., Jones, A. M., and Yang, Z. (2010). Cell surface- and rho GTPase-based auxin signaling controls cellular interdigitation in *Arabidopsis*. *Cell* 143, 99–110.

Yang, Z. (2008). Cell polarity signaling in *Arabidopsis*. *Annu. Rev. Cell. Dev. Biol.* 24, 551–575.

Conflict of Interest Statement: The authors declare that the research was conducted in the absence of any commercial or financial relationships that could be construed as a potential conflict of interest.

Received: 30 June 2012; accepted: 05 September 2012; published online: 02 October 2012.

Citation: Craddock C and Yang Z (2012) Endocytic signaling in leaves and roots: same rules different players. Front. Plant Sci. ***3****:219. doi: 10.3389/fpls.2012.00219*

This article was submitted to Frontiers in Plant Traffic and Transport, a specialty of Frontiers in Plant Science.

frontiers in
PLANT SCIENCE

ORIGINAL RESEARCH ARTICLE
published: 18 July 2012
doi: 10.3389/fpls.2012.00159

Evolution of the land plant exocyst complexes

Fatima Cvrčková[1]*, Michal Grunt[1], Radek Bezvoda[1], Michal Hála[1,2], Ivan Kulich[1], Anamika Rawat[1] and Viktor Žárský[1,2]

[1] *Department of Experimental Plant Biology, Faculty of Sciences, Charles University, Prague, Czech Republic*
[2] *Institute of Experimental Botany, Academy of Sciences of the Czech Republic, Prague, Czech Republic*

Edited by:
Markus Geisler, University of Fribourg, Switzerland

Reviewed by:
Jürgen Kleine-Vehn, University of Natural Resources and Life Sciences Vienna, Austria
Frantisek Baluska, University of Bonn, Germany

****Correspondence:***
Fatima Cvrčková, Department of Experimental Plant Biology, Faculty of Sciences, Charles University, Viničná 5, CZ 128 44 Praha 2, Czech Republic. e-mail: fatima.cvrckova@natur.cuni.cz

Exocyst is an evolutionarily conserved vesicle tethering complex functioning especially in the last stage of exocytosis. Homologs of its eight canonical subunits – Sec3, Sec5, Sec6, Sec8, Sec10, Sec15, Exo70, and Exo84 – were found also in higher plants and confirmed to form complexes *in vivo*, and to participate in cell growth including polarized expansion of pollen tubes and root hairs. Here we present results of a phylogenetic study of land plant exocyst subunits encoded by a selection of completely sequenced genomes representing a variety of plant, mostly angiosperm, lineages. According to their evolution histories, plant exocyst subunits can be divided into several groups. The core subunits Sec6, Sec8, and Sec10, together with Sec3 and Sec5, underwent few, if any fixed duplications in the tracheophytes (though they did amplify in the moss *Physcomitrella patens*), while others form larger families, with the number of paralogs ranging typically from two to eight per genome (Sec15, Exo84) to several dozens per genome (Exo70). Most of the diversity, which can be in some cases traced down to the origins of land plants, can be attributed to the peripheral subunits Exo84 and, in particular, Exo70. As predicted previously, early land plants (including possibly also the Rhyniophytes) encoded three ancestral Exo70 paralogs which further diversified in the course of land plant evolution. Our results imply that plants do not have a single "Exocyst complex" – instead, they appear to possess a diversity of exocyst variants unparalleled among other organisms studied so far. This feature might perhaps be directly related to the demands of building and maintenance of the complicated and spatially diverse structures of the endomembranes and cell surfaces in multicellular land plants.

Keywords: exocyst, phylogeny, land plants, co-evolution, gene duplication

INTRODUCTION

Exocyst, or the Sec6/8 complex, is an evolutionarily conserved heterooligomeric protein complex, generally believed to function especially in the last stage of exocytosis – i.e., vesicle tethering, preceding fusion of trans-Golgi network-derived vesicles with the plasmalemma, although additional, also mostly vesicle trafficking-related, exocyst roles have been described (reviewed, e.g., in He and Guo, 2009; Zhang et al., 2010; Heider and Munson, 2012). The eight canonical exocyst subunits, Sec3, Sec5, Sec6, Sec8, Sec10, Sec15, Exo70, and Exo84, were originally identified in yeast (TerBush et al., 1996; Guo et al., 1999). Subsequently, their homologs were found also in metazoans (Guo et al., 1997; Kee et al., 1997) and higher plants (Eliáš et al., 2003). Angiosperm exocyst subunits form complexes *in vivo* (Hála et al., 2008), and participate in exocytosis- or vesicle trafficking-dependent processes, such as cell growth including both tip growth and diffuse surface expansion (Cole et al., 2005; Wen et al., 2005; Synek et al., 2006; Hála et al., 2008), cell division (Fendrych et al., 2010), delivery of materials to the periplasm and cell wall (Wang et al., 2010), biogenesis of specialized cell wall structures such as the myxosperm seed coat (Kulich et al., 2010), pathogen response (Pečenková et al., 2011), and mycorrhiza (Genre et al., 2012). The Exo70 subunit has been also previously implicated in the pollen-stigma interaction in *Brassica* and *Arabidopsis* (Samuel et al., 2009), though its specific role remains controversial (Kitashiba et al., 2011) and the observed phenotypes may be rather due to a generalized secretion defect affecting stigma function (Synek et al., 2006).

Exocyst belongs, together with related COG, GARP, and DSL1 complexes, to the large, evolutionarily ancient family of eukaryotic quatrefoil vesicle tethering complexes (Whyte and Munro, 2002; Koumandou et al., 2007). Structural studies (recently reviewed by Hertzog and Chavrier, 2011) and theoretical sequence-based modeling revealed common structural elements involving rod-like helical bundles in all eight subunits, and a model of exocyst architecture based on aggregation of these bundles has been proposed (Munson and Novick, 2006; Croteau et al., 2009). Electron microscopy observations consistent with this model have been made also in the case of the putative plant exocyst (Seguí-Simmaro et al., 2004). Bundled Sec6, Sec8, Sec10 subunits probably form a core of the complex. At least in the yeast model, Sec6 also participates in its anchoring to the target membrane, and the remaining, more peripherally located subunits mediate interactions with membrane vesicles destined for delivery (as in the case of Sec15, interacting with the vesicle-borne Sec4 GTPase), with the target membrane and associated small GTPases of the Rho family (Sec3 and Exo70), and possibly with other structural or

regulatory proteins (Songer and Munson, 2009). The Exo70 subunit, which can bind to phosphoinositides, is crucial for targeting the complex to the destination membrane also in metazoans (He et al., 2007). Exo84 is also required for proper localization of the exocyst in yeast (Zhang et al., 2005). Surprisingly, the function of these subunits is not restricted to participation in exocytosis, as Exo70 and Exo84 subunits also participate in pre-mRNA splicing (Awashi et al., 2001; Dellago et al., 2011).

While exocyst subunits are encoded by a single gene in yeast or at most a few paralogs in metazoans, a puzzling number of plant isoforms has been identified in particular for the Exo70 subunit, which is encoded by 23 distinct loci in *Arabidopsis thaliana* (Eliáš et al., 2003; Synek et al., 2006). Some other subunits are also encoded by duplicated or triplicated (as in case of *A. thaliana* Exo84) loci. However, the only published phylogenetic studies of the plant exocyst so far are devoted solely to the Exo70 subunit (Eliáš et al., 2003; Synek et al., 2006) or restricted to a very limited species selection (Chong et al., 2010). With growing number of sequenced genomes, and increasing quality of genomic sequence annotations, a broader coverage of plant lineages can now be achieved. Here we present the results of a phylogenetic analysis of the canonical exocyst subunits encoded by 10 land plant genomes representing dicot and monocot angiosperms, a lycophyte (*Selaginella moellendorffii*) and a moss (*Physcomitrella patens*), and propose an evolutionary scenario consistent with our results.

MATERIALS AND METHODS

IDENTIFICATION OF EXOCYST SUBUNIT SEQUENCES

The collection of exocyst subunit sequences has been assembled by exhaustive mining of multiple data sources. For each subunit, a "seed" collection was generated as a non-redundant union of sequences originating from *A. thaliana*, *Arabidopsis lyrata*, *Populus trichocarpa*, *Vitis vinifera*, *Oryza sativa* var. *japonica*, *O. sativa* var. *indica* (omitted in case of Exo70 to keep the project at a manageable scale), *Sorghum bicolor*, *Brachypodium distachyon* and *P. patens*, and identified on the basis of their annotation among (i) components of the exocyst complex as recorded in the COG section of the STRING protein interaction database[1] (Sklarczyk et al., 2011) and (ii) reference sequences from GenBank (Benson et al., 2012). BLAST (McGinnis and Madden, 2004) searches of species-specific portions of the non-redundant section of GenBank and several species-specific resources (see below) have been employed to identify additional sequences from the above listed species, as well as from *S. moellendorffii* and selected members of the genus *Solanum* (see Results).

The additional databases mined included Uniprot (The Uniprot Consortium, 2012), Phytozome[2] (Goodstein et al., 2012), and JGI[3] for multiple species, Solgenomics[4] (Bombarely et al., 2011) and PGSC[5] (Potato Genome Sequencing Consortium, 2011) for *Solanaceae*, The Arabidopsis Information Resource[6] (Lamesch et al., 2012) for *Arabidopsis,* and COSMOSS[7] (Lang et al., 2005) for *Physcomitrella*. Final round of searches was performed between February and May 2012.

Redundancies within the collection were removed on the basis of pairwise BLAST alignments. In case of multiple protein predictions originating from the same locus, protein sequences closest to the most frequent splicing variety were chosen. In some cases, predicted protein sequences were revised based on re-evaluation of the available gene models, taking into account multiple methods of splicing prediction, ESTs, and homologous sequences as described previously (Grunt et al., 2008). The complete collection of sequences including the revised ones is available in the Supplement.

Additional BLAST searches of non-redundant GenBank sequences where performed to identify homologs of outlier sequences as described in Results.

PROTEIN SEQUENCE ALIGNMENTS

For initial estimation of sequence similarity and detection of possible problems with gene structure prediction (i.e., missing or extraneous exons), the interactive MACAW tool (Schuler et al., 1991; Lawrence et al., 1993), or the automated tools ClustalX (Thompson et al., 1997) and KALIGN (Lassmann and Sonnhammer, 2006) have been employed to generate preliminary versions of multiple protein sequence alignments. Final alignments for all subunits except Exo70 have been constructed manually with the aid of BioEdit (Hall, 1999), taking into account the preliminary alignments.

In case of the more numerous and more diverse Exo70 sequences, a similar manual approach has been employed first with a complete collection of *A. thaliana*, *A. lyrata,* and *P. trichocarpa* sequences, resulting in a "skeleton" alignment into which additional sequences in batches of up to 10 have been merged using the "realign selected sequences" feature of ClustalX; the alignments were manually adjusted after each batch using BioEdit with similarity shading for guidance, where considered appropriate.

Because of the admittedly subjective method of alignment construction, we are including the final alignments that have been used for phylogeny reconstruction in the Supplement. We have also performed parallel phylogeny estimations (as described below) with a manually constructed alignment and a KALIGN-constructed one for the Exo84 subunit, producing trees of essentially identical topology (i.e., sharing all significant branches, though differing somewhat in branch length and bootstrap support).

To identify conserved motifs in the divergent Exo70 N-termini, N-terminal sequence portions upstream of the conserved part used in phylogenetic analysis (see below) have been aligned *de novo* using ClustalX. Conserved sequence motifs have been identified visually after removal of obviously non-aligned sequences, manually adjusted in BioEdit and colored using the Dayhoff matrix (as implemented in BioEdit) for presentation.

PHYLOGENETIC ANALYSES

For phylogram construction, alignments except Exo70 were stripped of all columns containing gaps. For Exo70, which is more

[1] http://string-db.org/
[2] http://www.phytozome.net/
[3] http://genome.jgi.doe.gov/
[4] http://solgenomics.net/
[5] http://potatogenomics.plantbiology.msu.edu/
[6] http://www.arabidopsis.org
[7] http://www.cosmoss.org/

divergent than the remaining subunits (especially in its N-terminal part) and where several sequences were C- or N-truncated, only the unreliably aligned N-terminal portion and regions containing gaps in multiple sequences were removed prior to phylogenetic tree calculation.

Trees were computed by the maximum likelihood (ML) method using PHYML v3.0 aLRT (Guindon and Gascuel, 2003; Anisimova and Gascuel, 2006) at Phylogeny.fr (Dereeper et al., 2008) with default settings, using the aLRT test to estimate internal branch reliability. Independently, phylograms were constructed also by the neighbor-joining (NJ) method using ClustalX with 1000 bootstrap samples. Trees were visualized with the aid of the MEGA5 software (Tamura et al., 2011) and manually colored using CorelDraw for presentation.

K_a/K_s ESTIMATIONS

Nucleotide sequences corresponding to selected Exo70 subunits (see Results) have been retrieved from GenBank, and portions corresponding to reliably aligned protein parts have been realigned manually using BioEdit in the "toggle nucleotide to protein" mode to re-create the protein alignment used to calculate the phylogenetic trees. Resulting nucleotide sequence alignments have been analyzed using Selecton (Stern et al., 2007) to obtain codon-specific values of non-synonymous to synonymous mutation rates, providing information on residue-specific selection in the history of the examined sequences.

RESULTS

AN INVENTORY OF EXOCYST SUBUNITS IN 10 PLANT SPECIES

We performed exhaustive searches of sequenced genomes of eight angiosperm and two non-seed plant species with the aim to identify all genes encoding putative exocyst subunits. Among the angiosperms, we included the eudicots *A. thaliana*, *A. lyrata*, poplar (*P. trichocarpa*), and grapevine (*V. vinifera*) as representatives of the rosids. To gain insight also into the asterid lineage, we attempted to find the exocyst subunits in the publicly available tomato (*Solanum lycopersicon*) genome and cDNA sequences, which, however, did not yet cover the complete genome at the time of analysis. In particular, we found no sequences corresponding to Sec5 and Sec8. We therefore located the missing subunits in data from two potato species (*S. phureja* and *S. tuberosum*, respectively); we shall refer to these asterids collectively as *Solanum* sp. From the monocot class, four grass species (rice – *O. sativa*, represented by both *japonica* and *indica* varieties, sorghum – *S. bicolor*, and the model grass *B. distachyon*) have been included. Finally, we also analyzed genome data from one "lower" vascular plant – the lycophyte *S. moellendorffii*, and from the model moss *P. patens*. In total, we have collected 392 distinct protein sequences corresponding to presumed exocyst subunits (**Table 1**).

In agreement with the expected essential character of the exocyst in plants and with previous reports, all genomes encoded at least one copy of each subunit, and most of the subunits were encoded by one or a few loci, except Exo70, which always formed an extensive family of paralogs. Among the remaining subunits, we could upon closer inspection distinguish genuine single-copy or low copy subunits that were never present in more than two versions in the vascular plants (this was the case for Sec3, Sec5, Sec6, Sec8, and Sec10), and intermediate size gene families with more than two and less than eight paralogs in at least one of the species (Sec15 and Exo84). We shall further discuss these three groups separately.

LOW COPY SUBUNITS: SEC3, SEC5, SEC6, SEC8, AND SEC10

The first group of subunits includes Sec3 (in *A. thaliana* encoded by two genes in tandem – AtSEC3A/At1g47550/Arath1_Sec3 and AtSEC3B/At1g47560/Arath2_Sec3), Sec5 (again two *A. thaliana* genes – AtSEC5A/At1g76850/Arath1_Sec5 and AtSEC5B/At1g21170/Arath2_Sec5), Sec6, Sec8, and Sec10 (all encoded by single genes in *A. thaliana* – AtSEC6/At1g71820/Arath_Sec6, AtSEC8/At3g10380/Arath_Sec8 and AtSEC10/At5g12370/Arath_Sec10 – but see comments on possible Sec10 duplication below). Though these subunits are single-copy in some species, each of them is duplicated in at least one angiosperm genome, and all but Sec6 are triplicated in *P. patens*, showing that there is no strict functional requirement on keeping only a single protein version in cells. In fact, multiple splicing variants have been proposed

Table 1 | Numbers of exocyst subunit paralogs encoded by the studied plant genomes.

	Sec3	Sec5	Sec6	Sec8	Sec10	Sec15	Exo70	Exo84
A. thaliana	2	2	1	1	1	2	23	3
A. lyrata	2	2	1	1	1	2	23	3
P. trichocarpa	2	2	2	2	2	5	29	8
Solanum sp.	2[2]	1[3]	1[2]	1[4]	1[2]	2[2]	22[2]	4[2]
V. vinifera	1	1	2	1	1	2	15	3
O. sativa[1]	2(2)	1(1)	1(1)	1(1)	1(1)	4(4)	47	3(3)
S. bicolor	2	1	1	1	1	3	31	3
B. distachyon	2	1	1	1	1	3	27	3
S. moellendorffi	2	1	2	2	2	1	8	2
P. patens	3	3	1	3	3	2	13	7

The complete list of the 392 analyzed genes or proteins including database accession numbers, as well as protein sequences and sequence alignments used in phylogeny calculations, is provided as Supplementary Material.

[1]japonica variety, with numbers for indica in brackets; [2]S. lycopersicon; [3]S. phureja; [4]S. tuberosum.

for most *Arabidopsis* subunits in the recent genome annotation (Lamesch et al., 2012).

Tandem duplications affecting angiosperm exocyst genes are apparently not restricted to *Arabidopsis* Sec3. The *A. thaliana* genomic assembly might be problematic in the area around Sec10, since inspection of available GenBank sequences suggests a possible tandem duplication of the Sec10 locus differing by a couple of silent mutations and variant non-coding ends. The duplicated gene appears to be transcribed (see GenBank cDNAs AF479280.1 and AK318699.1 which are in good mutual agreement but differ from the reference genome sequence, though they encode an identical protein). Also in tomato, we found a single possibly functional Sec10 locus and three closely related pseudogenes with multiple stop codons, two of them in tandem (the pseudogenes are not included in the phylogeny; see Supplementary Material for accession numbers).

As a rule, protein sequences of the low copy subunits consist of a single well-defined domain, are well conserved along the whole length (exceptions will be discussed below) and their phylogenetic trees (**Figure 1**) exhibit striking overall mutual similarity. Within the angiosperms, all gene duplications except monocot Sec3 appear to be relatively recent, resulting in within-species paralogs that share at least 80% of identical amino acids in the most distant pair of the *A. thaliana* Sec5 paralogs. Duplicated paralogs cannot be matched among genomes more distant than the two rice varieties, or the two *Arabidopsis* species. The only exception from this pattern of apparently late gene duplications is the Sec3 subunit that has obviously split into two paralogous lineages early in the evolution of monocots or at least grasses.

Rice and *Arabidopsis* versions of any of the low copy subunits share between 59% (Arath1_Sec5 vs. OrysaJ_Sec5) and 81% (Arath_Sec6 vs. OrysaJ_Sec6) of identical amino acids. The Sec6, Sec10, and Sec8 subunits, believed to form the central core of the complex (Munson and Novick, 2006; Croteau et al., 2009), are the best conserved ones. Notably, one of the ancient Sec3 branches (the clade "monocot 1" in **Figure 1**) has considerably diverged from the cluster of dicot sequences and the remaining monocot clade, suggesting a possible release of selection pressure followed by neo- or subfunctionalization. Compared to the degree of conservation found in the angiosperms, the *Physcomitrella* paralogs exhibit major within-genome differences, with the most distant paralogs Phypa1_Sec10 and Phypa3_Sec10 sharing only 51% of identical amino acids.

Two sequences deviate from the standard overall conserved domain structure of the relevant low copy subunits and can be perhaps viewed as "structural outliers" of their corresponding gene families. In the case of the *A. lyrata* Sec3 paralog Araly2_Sec3, the N-terminal part of the conserved domain is replaced by a domain related to a family of RING box/E3 ligases, encoded by a single-exon and flanked at least from one side by a sequence related to Copia-like retroelements, suggesting a very recent retrotransposition-mediated gene fusion. However, this domain combination appears to be unique in the whole of GenBank, and there are no ESTs documenting that this gene is expressed *in planta*; therefore, its functionality and biological significance remains problematic.

The second structural outlier is the *P. patens* Sec10 paralog Phypa2_Sec10, noticed in our previous study (Grunt et al., 2008) because of its unique combination of a N-terminally located Sec10 domain with the formin-specific FH2 domain at the C-end of the protein (see sequence Phypa5 in Grunt et al., 2008). An alternative splicing prediction separates these two domains into two distinct proteins (a short version corresponding to standard Sec10 is included in our phylogeny). The combination of Sec10 and FH2 domains is again unique in GenBank. However, there is a partial cDNA of the formin end (GenBank BY987890.1) indicating gene expression in the moss, albeit it is unclear which splice variants are biologically relevant.

INTERMEDIATE SIZE FAMILIES: SEC15 AND EXO84

The second group of subunits consists of two gene families, Sec15 (with two *A. thaliana* paralogs – AtSEC15A/At3g56640/Arath1_Sec15 and AtSEC15B/At4g02350/Arath2_Sec15) and Exo84 (with three paralogs in *A. thaliana* – AtEXO84a/At5g49830/Arath2_Exo84, AtEXO84b, At1g10385/Arath3_Exo84, and AtEXO84c/At1g10180/Arath1_Exo84). In other studied genomes, Sec15 is encoded by two to five subunits (except *S. moellendorffii*, where only a single protein was found) and Exo84 by three to eight (again except *S. moellendorffii* with only two genes). In both cases the highest number was found in *P. trichocarpa*, and the final poplar subunit count may be even higher, since there is cDNA evidence of additional transcripts encoding proteins identical to the Sec15 paralogs included in our analysis but differing in their non-translated ends, reminiscent of the situation in *A. thaliana* Sec10 (see Supplementary Material).

Phylogenetic trees of both families indicate that at least a part of the observed diversity is ancient, and can be traced back at least to the origins of angiosperms (**Figure 2**). Both gene families can be split into two branches in seed plants, with multiple additional within-branch amplifications. In Sec15, most of these later amplification events (generating two clusters of poplar genes in both branches and a pair of rice genes in the B branch) appear to be fairly recent, reminiscent of those detected for low copy subunits. However, a duplication of the A subunit apparently occurred early in the monocot lineage (no later than at the emergence of grasses), resulting in two monocot- or grass-specific subfamilies, A1 and A2.

In Exo84, the situation is somewhat more complex. Clearly defined A and B branches (named according to the corresponding *A. thaliana* subunits) were found only in the dicots, while related monocot sequences form a rather compact cluster, probably closer to the A branch than to B. The dicot A and B branches and the monocot cluster will be further referred to as the A/B clade (**Figure 2**). Monocot A/B sequences also bear traces of early gene duplication preceding the radiation of grasses, but clearly distinct from the event that produced the A and B branches and followed by little actual sequence divergence (the rice A/B sequences OrysaJ1_Exo84 and OrysaJ2_Exo84 share 78% of identical amino acids). Besides of the A/B clade, a second ancient branch (the C clade) is shared by all examined angiosperms and contains, as a rule, products of single-copy genes with exception of an apparently recent cluster of three poplar sequences. Two mutually related dicot outliers (the CX sequences) are apparently related to the C clade, and proteins similar to them have been predicted also in

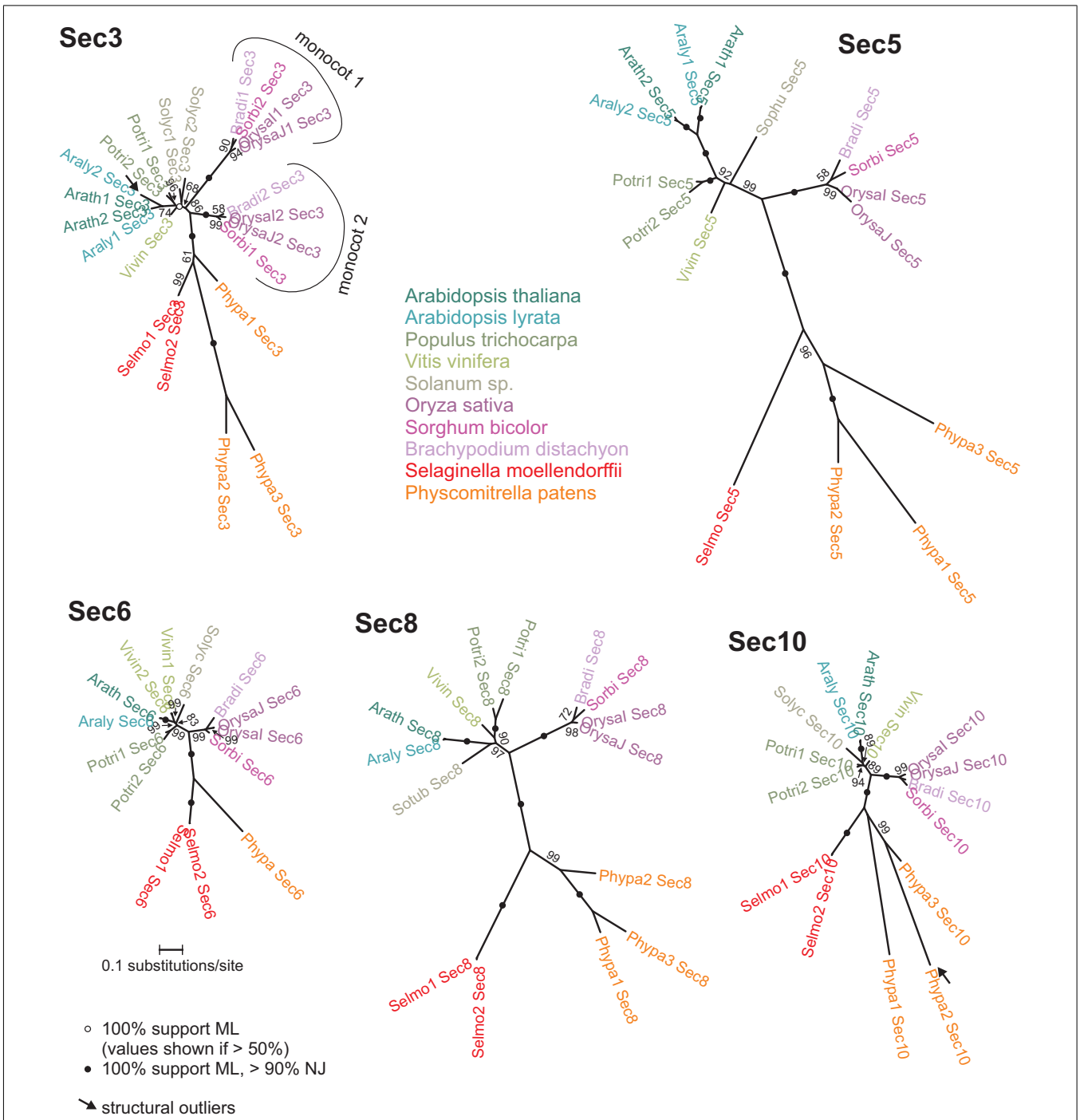

FIGURE 1 | Unrooted maximum likelihood (ML) phylograms of the low copy Exocyst subunits. All SH-like support values above 50% from the aLRT test are shown. Consistent trees were obtained also using the neighbor-joining (NJ) method with 1000 bootstrap samples; nodes with high support by both ML and NJ algorithms are marked by black dots. Arrows denote "structural outliers," i.e., sequences deviating from the standard domain organization of typical representatives of the protein family. All trees are at the same scale.

Ricinus communis (GenBank XM_002526525.1) and *Glycine max* (GenBank XM_003541318.1). A genomic DNA sequence fragment from *V. vinifera* (GenBank AM443616.2) contains patches of a possible ORF similar to the CX sequences in an area annotated as non-coding. While the grapevine genome annotation may require updating, it is also possible that these patches are vestiges of a lost gene that may have had a wider distribution.

In contrast to the angiosperms, the lycophyte and moss Sec15 sequences exhibit only minimum diversification, while Exo84 underwent duplication in *S. moellendorffii* and extensive

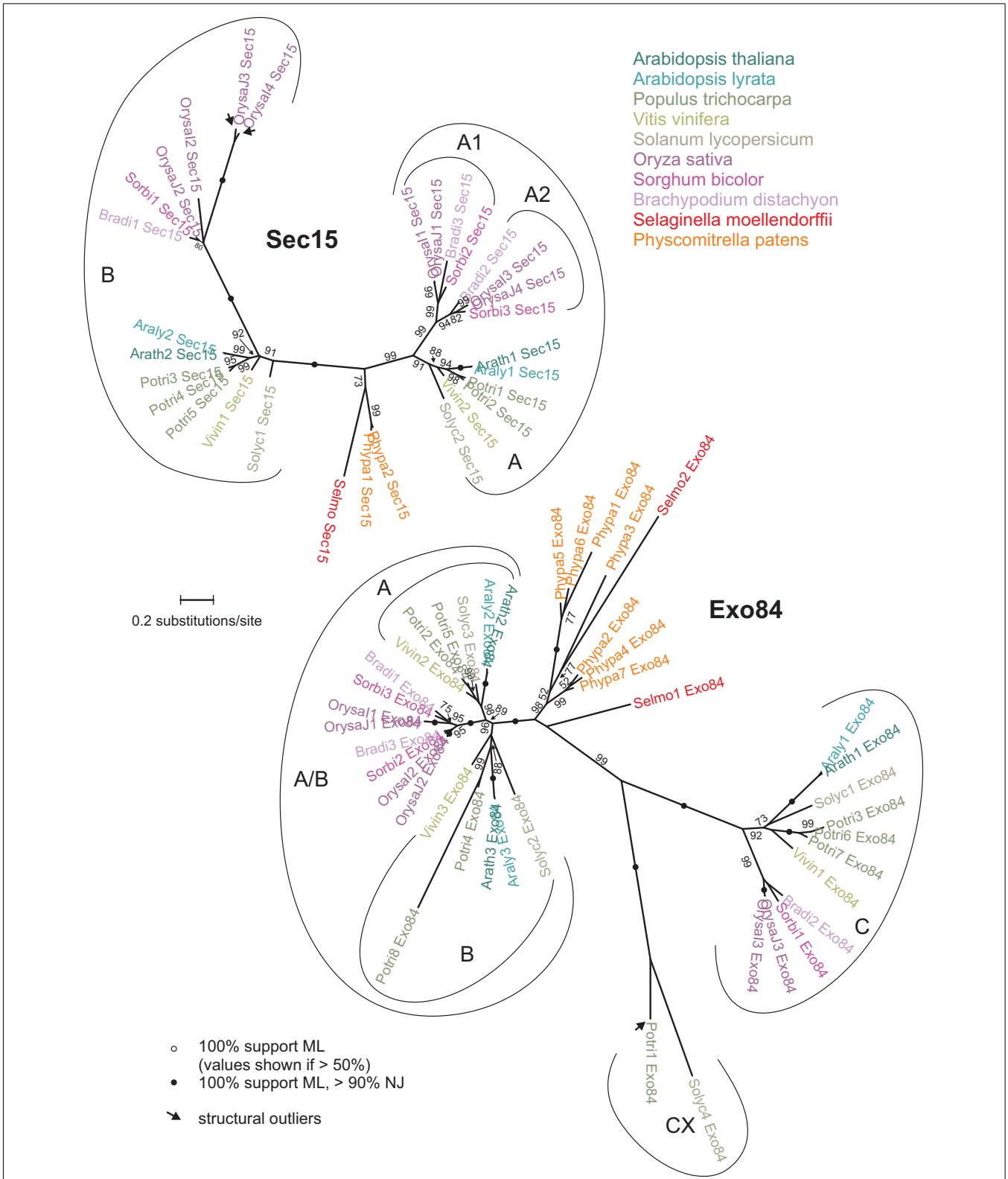

FIGURE 2 | Unrooted maximum likelihood (ML) phylograms of Sec15 and Exo84. All SH-like support values above 50% are shown. Consistent trees were obtained also using the neighbor-joining (NJ) method; nodes with high support by both ML and NJ algorithms are marked by black dots. Arrows denote "structural outliers" (see **Figure 1**). Both trees are at the same scale.

amplification, producing seven rather diversified paralogs, in *P. patens*. While the branching order is not reliable in the non-angiosperm sequences, the resulting tree does not exclude the possibility that the two major Exo84 clades might have appeared already at the base of the vascular plants.

Compared to the low copy subunits, Sec15 and Exo84 sequences exhibit greater diversity, with *Arabidopsis* AtSec15A and AtSec15B sharing 48%, AtExo84A and AtExo84B 59%, and AtExo84B and AtExo84C only 34% of identical amino acids. Nevertheless, the angiosperm branches of the phylogram appear to be rather compact, and the only conspicuously diversified poplar Exo84B paralog, Potri8_Exo84, may not be expressed, as we could not find any corresponding ESTs.

All sequences from each family can be aligned reliably along the whole length, with only three exceptions. The predicted rice Sec15 paralogs OrysaJ3_Sec15 and OrysaI4_Sec15 are missing a C-terminal part of the characteristic Sec15 domain and have instead an unrelated sequence. No homologs with such a gene organization have been found in GenBank, and there are no ESTs matching these genes. Together with the long distance from the rest of B clade Sec15 sequences, indicating relaxed selection, this suggest that these *O. sativa* Sec15 outliers may actually correspond to a pseudogene that has arisen not long before the separation of the *japonica* and *indica* varieties and that is now in the process of decay. The third structural outlier, Potri1_Exo84, one of the outlier CX sequences with a long C-terminal extension, also lacks cDNA or EST support, and it is thus not clear if it is expressed at all.

THE ENORMOUS DIVERSITY OF EXO70 PARALOGS

The large Exo70 family consists of 23 paralogs in *A. thaliana*, representing eight previously identified clades (Synek et al., 2006): AtExo70A1/At5g03540/ArathA1_Exo70, AtExo70A2/At5g52340/ArathA2_Exo70, and AtExo70A3/At5g52350/ArathA3_Exo70 in clade A, AtExo70B1/At5g58430/ArathB1_Exo70 and AtExo70B2/At1g07000/ArathB2_Exo70 in clade B, AtExo70C1/At5g13150/ArathC1_Exo70 and AtExo70C2/At5g13990/ArathC2_Exo70 in clade C, AtExo70D1/At1g72470/ArathD1_Exo70, AtExo70D2/At1g54090/ArathD2_Exo70, and AtExo70D3/At3g14090/ArathD3_Exo70 in clade D, AtExo70E1/At3g29400/ArathE1_Exo70 and AtExo70E2/At5g61010/ArathE2_Exo70 in clade E, AtExo70F1/At5g50380/ArathF1_Exo70 in clade F, AtExo70G1/At4g31540/ArathG1_Exo70 and AtExo70G2/At1g51640/ArathG2_Exo70 in clade G, and eight paralogs – AtExo70H1/At3g55150/ArathH1_Exo70, AtExo70H2/At2g39380/ArathH2_Exo70, AtExo70H3/At3g09530/ArathH3_Exo70, AtExo70H4/At3g09520/ArathH4_Exo70, AtExo70H5/At2g28640/ArathH5_Exo70, AtExo70H6/At1g07725/ArathH6_Exo70, AtExo70H7/At5g59730/ArathH7_Exo70, and AtExo70H8/At2g28650/ArathH8_Exo70 – in clade H. In other studied plants, the number ranges from eight in *Selaginella* to 47 in rice (**Table 2**; see Supplementary Material for a full list of genes), albeit the final count might still change in the genomes whose annotation is still under development (especially *Solanum* sp.).

Unlike the other seven subunits, Exo70 paralogs are rather diverse and their N-terminal part of up to 300 amino acids could not be aligned reliably throughout all the 238 studied sequences. We have used only the well-aligned portion to construct a phylogram (**Figure 3**) that essentially corroborates the previous reports but brings some additional new insights. Our analysis confirms the existence of three major Exo70 lineages Exo70.1, Exo70.2, and Exo70.3 that contain both angiosperm and "lower plant" sequences, as well as the nine clades (A–I) with members of both monocot and dicot origin (Synek et al., 2006). The clade I, restricted only to some angiosperms (it is, e.g., missing in both *Arabidopsis* species), clusters within a branch that includes the compact angiosperm G clade and a group of moss sequences, but none from *Selaginella*, suggesting loss in the lycophyte lineage. We will refer to this wider branch, corresponding to the previously proposed Exo70.3 lineage, as the G/I clade.

Remarkable is the major expansion of a monocot- or grass-specific branch of the F family, the FX clade. Apparently, a single family of Exo70 subunits underwent major expansion in both monocots and dicots. Reverse transcription might have contributed to gene amplification in case of the abundant dicot H clade with a large proportion of single-exon genes (Synek et al., 2006; Chong et al., 2010), but not in case of the monocot FX with a large proportion of multi-exon genes (Chong et al., 2010). Somewhat surprisingly, a very distant paralog OrysaFX8_Exo84, which clusters within the F branch but outside the genuine FX clade,

Table 2 | Numbers of Exo70 paralogs encoded by the studied genomes (in total and in the individual clades).

	All	A	B	C	D	E	F (FX)	G/I	H	BNG[1]
A. thaliana	23	3	2	2	3	2	1(0)	2	8	–
A. lyrata	23	3	2	2	3	2	1(0)	2	8	–
P. trichocarpa	29	4	2	3	2	6	2(0)	5	5	–
S. lycopersicon	22	3	1	3	2	2	1(0)	4	6	–
V. vinifera	15	2	1	1	1	2	1(0)	4	3	–
O. sativa	47	4	3	3	2	1	26 (19)	3	5	–
S. bicolor	31	3	3	2	2	1	16 (12)	3	1	–
B. distachyon	27	5	2	2	2	1	11(6)	3	1	–
S. moellendorffi	8	4	–	–	–	–	–	–	–	4
P. patens	13	3	–	–	–	–	–	4	–	6

[1] *Basal non-angiosperm group.*

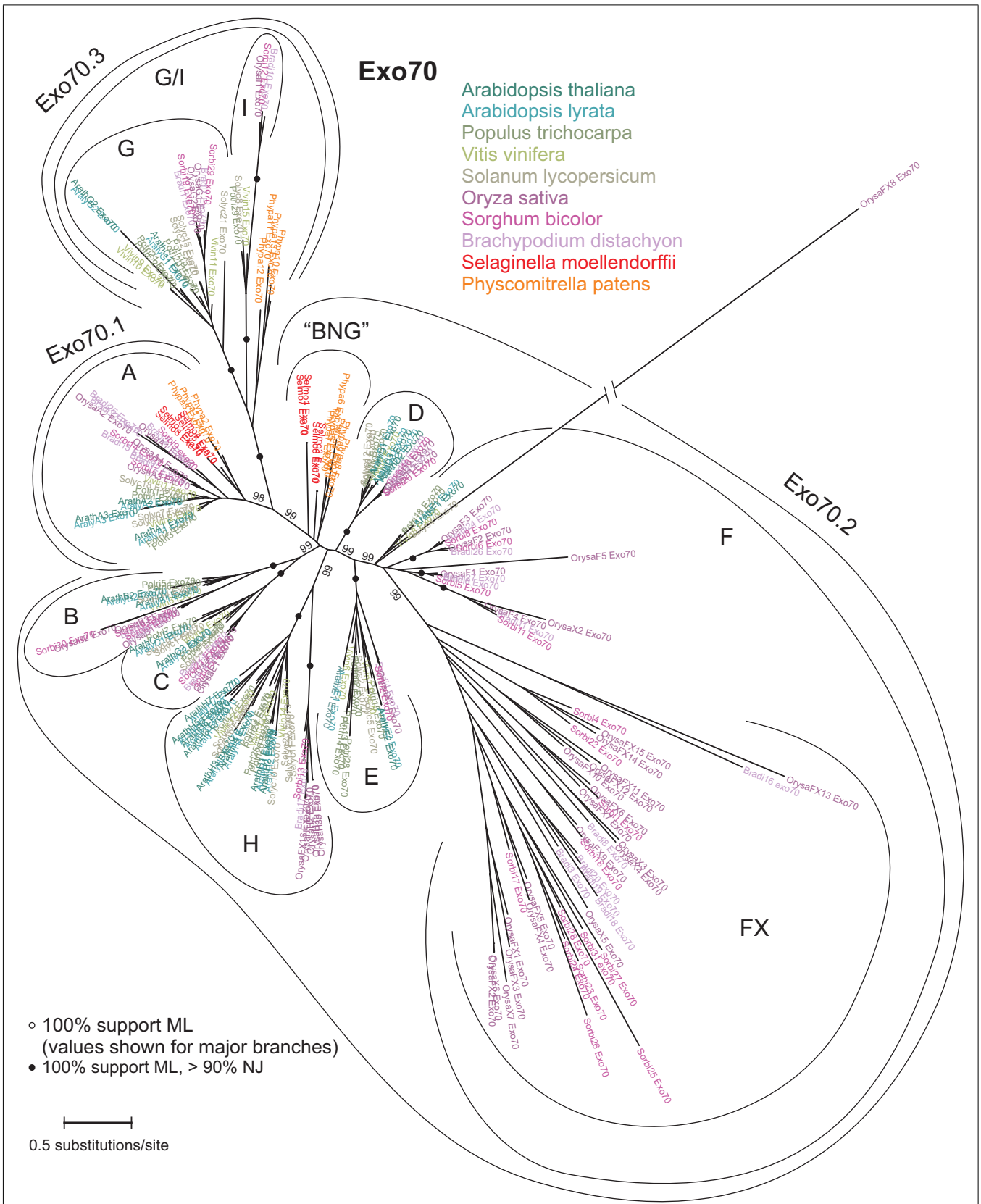

FIGURE 3 | Unrooted maximum likelihood (ML) phylogram of Exo70. SH-like support values above 50% are shown only for major branches for the sake of legibility. A tree obtained using the neighbor-joining (NJ) method was consistent with the ML one except of placing the FX branch outside the F clade; nodes with high support by both ML and NJ algorithms are marked by black dots. "BNG" denotes the basal non-angiosperm group of Exo70 paralogs.

is supported by a full-length cDNA (GenBank AK109785.1) and there are even two closely related ESTs from *Lolium perenne* (GenBank GR511301.1) and *L. temulentum* (GenBank DT673816.1), indicating that this outlier is functional and possibly specific for some grasses.

Duplicated genes tend to be rapidly eliminated by natural selection if they bring no advantage in terms of fitness. Question thus arises why there are so many Exo70 varieties maintained across large evolutionary distances. One possibility would be sub- or neofunctionalization of the conserved Exo70 domain itself. We have thus examined representative *A. thaliana* Exo70 sequences for traces of positive (diversifying) selection by estimation of the residue-specific ratio of non-synonymous to synonymous mutation rates (K_a/K_s). For this analysis, we chose two sequence collection – eight representatives of the main clades (AtExo70A1, AtExo70B1, AtExo70C1, AtExo70D1, AtExo70E1, AtExo70F1, AtExo70G1, and AtExo70H1) to identify markers of selection generating or enhancing between-clade differences, and eight representatives of the H clade (AtExo70H1, AtExo70H2, AtExo70H3, AtExo70H4, AtExo70H5, AtExo70H6, AtExo70H7, and AtExo70H8) to find traces of selection favoring within-clade differences. However, in both cases there was only evidence of purifying selection throughout the length of the sequence, but no positive selection, and we thus conclude that differences within the conserved part of the Exo70 subunits are not likely to play a decisive part in determining the function of the individual paralogs.

Functional diversification, however, may be due to the variable N-terminal sequences. We thus examined these regions in more detail and uncovered two sequence motifs conserved in many, but not all, Exo70 paralogs (**Figure 4**). Distribution of these motifs (see Supplementary Material) suggests that they are ancestral, and that they have been lost or eroded in some of the sequences. Motif 2 is present in most, if not all members of all stable Exo70 clades with exception of FX, and also in the members of the "basal non-angiosperm group," i.e., in the sequences of lower plant origin with unclear mutual relationships that belong to the Exo70.2 supergroup. The more N-terminally located motif 1 was found in most members of the basal non-angiosperm group and of the A, E, and G/I clades. It is present also in members of the F branch except FX, and also except the distant F outlier OrysaFX8_Exo70. This suggests that Motif 1 is also ancestral but was lost in some angiosperm clades within the Exo70.2 supergroup. The presence of the conserved motifs indicates that the variable Exo70 N-termini have largely evolved through a process of mutations and selection rather than domain-shuffling, although this does not have to be the rule in all cases (especially the origin of the diverse and mutually largely unrelated N-termini of the FX proteins remains unclear).

DISCUSSION

The present study provides the first attempt to reconstruct evolution of the land plant, especially angiosperm, exocyst complex in the broader context of higher plant evolution. Our previous works (Eliáš et al., 2003; Synek et al., 2006) have focused only on the most abundant subunit, Exo70, and the only previous phylogenetic study addressing all the eight canonical exocyst subunits in plants (Chong et al., 2010) was based on only four species – *Arabidopsis*, rice and poplar as the representatives of angiosperms, and the moss *P. patens*, allowing only a limited possibility of generalization. We have included a broader and more representative collection of genomes, including a moss (*P. patens*), a lycophyte, i.e., a non-seed vascular plant (*S. moellendorffii*), and eight angiosperms (unfortunately, there is, to date, no sufficiently well-covered gymnosperm genome for an exhaustive search). The angiosperms are represented by five dicotyledonous and three grass species covering a

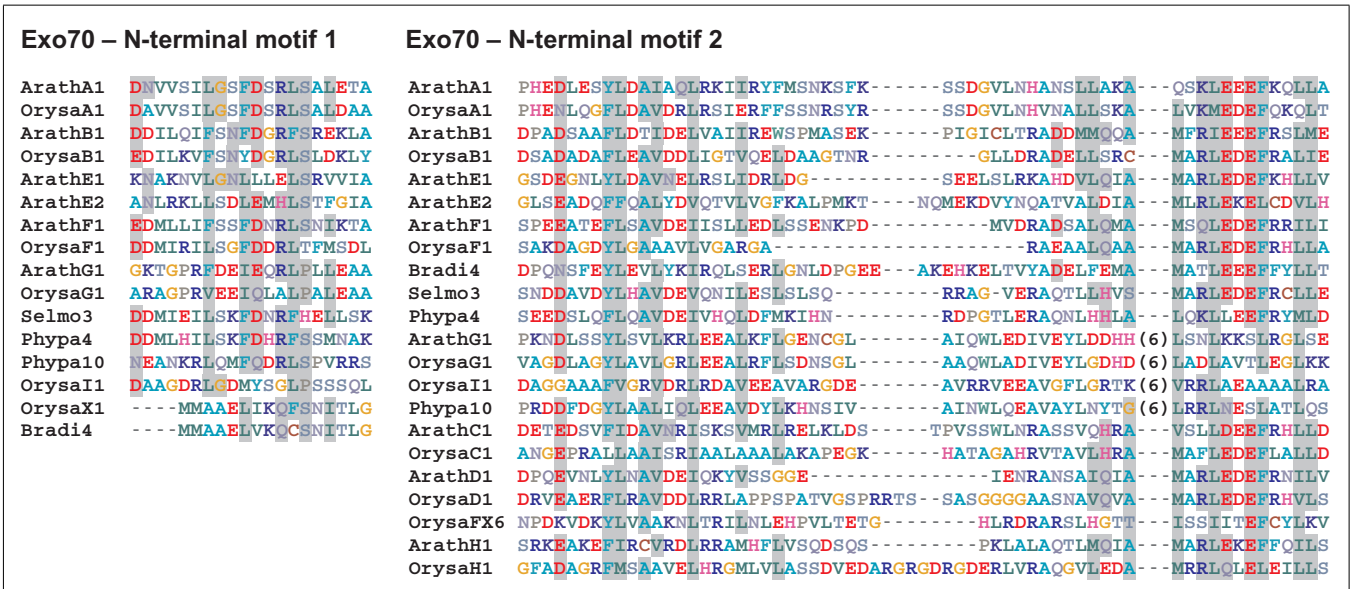

FIGURE 4 | Alignment of representative examples of the N-terminal conserved motifs found within the variable N-terminal part of Exo70 sequences. Motif 1 is located no more than 70 amino acids from the N terminus and always upstream of motif 2; motif 2 begins less than 250 amino acids from the N terminus. Residues conserved among 75% or more of the sequences containing the motif are shown on a gray background (residue conservation was determined using the Dayhoff matrix). Numbers in brackets indicate the length of variable insertions removed for clarity.

rather broad range of diversity (see the simplified scheme of plant evolution in **Figure 5**). Among dicots, the closest are the two *Arabidopsis* species (*A. thaliana* and *A. lyrata*) that have separated approximately five millions of years ago (Koch et al., 2000). Poplar (*P. trichocarpa*) is included as somewhat more distant representative of the rosid clade, grapevine (*V. vinifera*) as a basal rosid, and several members of the genus *Solanum* (where, unfortunately, no genome is annotated well enough to provide data for all subunits) are representing the asterids. The coverage of the monocot clade is narrower, as all the available genomes belong to grasses. Thus, although we propose some possible monocot-specific features of the exocyst family in this paper on the basis of data from three grass species (*O. sativa*, *S. bicolor*, and *B. distachyon*), we do not know at present if such features are present also in non-grass monocots.

In total, we have analyzed nearly 400 exocyst subunit sequences. Our list, however, may not be complete especially in case of the *Solanum* sp. sequences, where genomic annotation is still under development, and some loci may have been missed. It is not surprising that our inventory yielded novel genes especially in the Exo70 family in addition to those reported previously for *P. trichocarpa* and *O. sativa* (Chong et al., 2010). On the other hand, in the absence of gene expression data and experimental observations, distinction between functional genes and pseudogenes may be somewhat blurry, especially in case of the extensive Exo70 family, containing numerous single-exon members that apparently underwent reverse transcription at some point in the course of their evolution (Synek et al., 2006). Thus, the determined numbers of subunits might still somewhat change in the future, even in well-characterized models (see the possible undocumented duplication of the *Arabidopsis* Sec10 locus). Also allelic diversity in heterozygous diploids may have resulted in identification of extraneous loci in particular in the case of *S. moellendorffii*, where most genes appear to have two closely related paralogs, albeit this species is believed to be one of the few plants without a recent history of whole-genome duplications (Jiao et al., 2011).

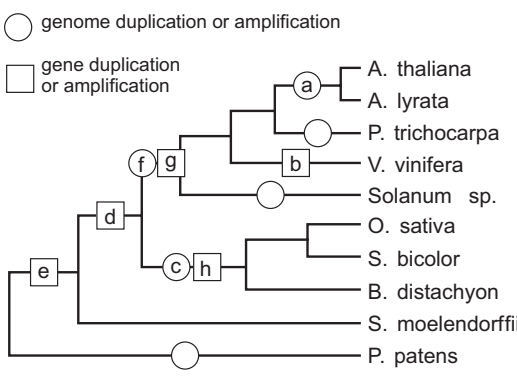

FIGURE 5 | A possible scenario of exocyst evolution in the context of land plant evolution and the history of genome duplications. Selected genome duplication and gene amplification events that may have founded specific subfamilies of exocyst subunits are denoted by letters. (a) Duplication of *Arabidopsis* sp. Sec5; (b) Duplication of grapevine Sec6; (c) Origin of two Sec3 clades (monocot1 and monocot2), and of the Sec15 clades A1 and A2; (d) Origin of Sec15 clades A and B; (e) Origin of Exo84 clades A/B and C/CX; (f) Separation of the Exo84 clades A and B, as well as C and CX, the later subsequently lost in some descendants; (g) Amplification of dicot Exo70 clade H; (h) Amplification of the monocot Exo70 clade FX.

We have found that a subgroup of exocyst subunits, corresponding to the previously proposed core of the complex (Munson and Novick, 2006; Croteau et al., 2009), underwent little or no amplification in the vascular plants, though even these subunits have amplified to a some extent in non-seed plants. These low copy subunits, in particular Sec6, Sec8, and Sec10, but to a somewhat lesser extent also Sec5 and Sec3, exhibit evolutionary trees that are not only topologically similar but also obviously correlated in terms of branch length, which is consistent with co-evolution driven by the requirement of maintaining mutual compatibility of closely interacting complex subunits (Juan et al., 2008; Lovell and Robertson, 2010). The remaining subunits Sec15, Exo84, and in particular Exo70, exhibit greater diversity consistent with their function on the periphery of the complex, providing an interface to a variety of interactors that may be specific to particular lineages or even to particular paralogs.

Whole-genome duplications have played an important part in the evolution of land plants (Van de Peer et al., 2009; Jiao et al., 2011). They also provided an obvious source of "raw materials" for evolution of divergent paralog families of the exocyst subunits. We were able to pinpoint several of the proposed ancient genome duplication or polyploidization events in a widely accepted scenario of land plant evolution (Soltis et al., 2008; Van de Peer et al., 2009; Jiao et al., 2011; Woodhouse et al., 2011) as possible sources of distinct exocyst subunit clades especially in the Sec15 and Exo84 families (**Figure 5**). However, it has to be stressed that not every gene duplication coincident with a genome duplication must be a result of that duplication. For instance, the tandem duplication of *A. thaliana* Sec3 appears to be a local event, while equally distant *A. thaliana* Sec5 paralogs are obviously a product of a whole-genome duplication (see data from Woodhouse et al., 2011).

The greatest part of the putative exocyst diversity is due to the extremely amplified Exo70 subunit that apparently existed in at least three paralogs already in the common ancestor of land plants including Rhyniophytes, and diversified into seven clades prior to the separation of the monocot and dicot lineages (Synek et al., 2006). Reverse transcription may have contributed to early amplification of some clades, which contain mostly single-exon genes, among them also the dicot clade H that has expanded into an extensive family of paralogs. No such expansion, however, took place in the monocots, which have only a few H-type Exo70s. Instead, a branch of the multi-exon F family has amplified and diversified substantially, producing the monocot-specific FX clade.

While there is considerable sequence divergence among the Exo70 paralogs, we found no evidence of positive selection operating across their conserved part. An obvious source of functional diversity, however, would be the variable sequences at both ends of the Exo70 subunits. A possible participation of C-terminal motifs in differential binding to membrane phosphoinositides has been already proposed (Žárský et al., 2009). Here we have uncovered two obviously ancestral N-terminal motifs that document that the N-terminal segments, though highly diversified, have evolved from a common ancestor at least in most of the sequences, without contribution of major domain-shuffling events. Nevertheless,

they have possibly built up enough diversity to mediate interactions with a variety of cellular components, ensuring thus the apparently required functional diversification.

Assuming that the alternative paralogs of exocyst subunits are co-expressed, and that they can freely combine into complexes (which is by no means guaranteed), literally hundreds of distinct exocysts may exist within plant cells. Were the subunit combinations unrestricted (i.e., each Sec15 paralog working with each Exo84 and each Exo70), *Arabidopsis* would be capable of producing 552 distinct exocyst variants, and rice stunning 1128 variants. Alternative splicing may provide an additional source of exocyst diversity. Even in metazoans, an array of Exo70 splicing variants was uncovered, dependent on cell type and age of the tissue (Dellago et al., 2011). It is therefore possible that also in animals hidden multiplicity of exocysts may exist depending on the splice-isoforms of Exo70 (and possibly also other subunits). On the other hand, the actual numbers of plant exocyst varieties are undoubtedly much lower than the numbers of possible subunit combinations, since not all paralogs are co-expressed, and some may be expressed only under special circumstances or not at all. Nevertheless, we cannot avoid asking what is the biological relevance (or selective advantage) of such a profusion of exocyst varieties.

One possible reason may be the need to maintain and manage a variety of qualitatively distinct membranes – not only of intracellular compartments, but also within the cell cortex whose lateral mobility is restricted by the cell wall. Distinct exocyst variants in the same cell, defined especially by different "landmarking" Exo70 subunits, may participate in delimiting specific plasmalemma domains ("activated cortical domains") engaging in distinctly regulated membrane turnover. Together with the underlying cytoplasm (in particular the connected recycling endosomes defined by distinct Rab11 paralogs), the activated cortical domains form larger functional units (recycling domains) that may play a central part in the control of different cortical or endomembrane domains of the many-sided plant cells (see detailed discussion in Žárský et al., 2009; Žárský and Potocký, 2010). Another possibility is functional separation of the diverse complexes in time and/or in tissue or organ space through controlled gene expression of subunit variants optimized for a particular set of circumstances (e.g., specific cell differentiation stages, tissues, or environmental conditions). Participation of Exo84B in the establishment of mycorrhiza (Genre et al., 2012) and, in particular, of distinct Exo70 variants in pathogen response (Pečenková et al., 2011) shows that this indeed appears to be the case. Remarkably, one of the *Arabidopsis* Exo70 paralogs involved in pathogen response is member of the H clade, expanded specifically in the dicots, and it is thus tempting to speculate about a possible analogous role of the even more diversified monocot FX clade.

In summary, both our data and recent experimental observations show that plants do not have "an exocyst complex," but an enormous variety of diverse exocyst complexes, and that this feature is at least as old as the land plants. Unraveling its functional significance will continue to provide interesting challenges for the plant cell biology of the near future.

ACKNOWLEDGMENTS

This work has been supported by the European Community 7th Framework Programme (FP7/2007–2013) Grant No. 238640 PLANTORIGINS, the Grant Agency of the Czech Republic (P305/11/1629), the Ministry of Education of the Czech Republic (MSM 0021620858), and the Charles University in Prague (SVV 265203/2012).

SUPPLEMENTARY MATERIAL

The Supplementary Material for this article can be found online at http://www.frontiersin.org/Plant_Traffic_and_Transport/abstract/31437

Cvrckova_S1.xls | List of the 392 exocyst subunit sequences analyzed, including database accession numbers, phylogenetic classification and domain composition (Microsoft Excel file).

Cvrckova_S2.zip | Protein sequences and alignments used for phylogenetic analyses (compressed Zip file containing protein sequences in text format – ∗.txt and alignment sequences in FASTA format – ∗.fst).

REFERENCES

Anisimova, M., and Gascuel, O. (2006). Approximate likelihood ratio test for branchs: a fast, accurate and powerful alternative. *Syst. Biol.* 55, 539–552.

Awashi, S., Palmer, R., Castro, M., Mobarak, C. D., and Ruby, S. W. (2001). New roles for the Snp1 and Exo84 proteins in yeast pre-mRNA splicing. *J. Biol. Chem.* 276, 31004–31015.

Benson, D. A., Karsch-Mizrachi, I., Clark, K., Lipman, D. J., Ostell, J., and Sayers, E. W. (2012). GenBank. *Nucleic Acids Res.* 40, D48–D53.

Bombarely, A., Menda, N., Buels, R. M., Strickler, S., Fischer-York, T., Pujar, A., Leto, J., Gosselin, J., and Mueller, L. A. (2011). The sol genomics network (solgenomics.net): growing tomatoes using perl. *Nucleic Acids Res.* 39, D1149–D1155.

Chong, Y. T., Gidda, S. K., Sanford, C., Parkinson, J., Mullen, R. T., and Goring, D. R. (2010). Characterization of the *Arabidopsis thaliana* exocyst complex gene families by phylogenetic, expression profiling, and subcellular localization studies. *New Phytol.* 185, 401–419.

Cole, R. A., Synek, L., Žárský, V., and Fowler, J. E. (2005). SEC8, a subunit of the putative *Arabidopsis* exocyst complex, facilitates pollen germination and competitive pollen tube growth. *Plant Physiol.* 138, 2005–2018.

Croteau, N. J., Furgason, M. L. M., Devos, D., and Munson, M. (2009). Conservation of helical bundle structure between the exocyst subunits. *PLoS ONE* 4, e4443. doi:10.1371/journal.pone.0004443

Dellago, H., Löscher, M., Ajuh, P., Ryder, U., Kaisermayer, C., Grillari-Voglauer, R., Fortschegger, K., Gross, S., Gstraunthaler, A., Borth, N., Eisenhaber, F., Lamond, A. I., and Grillari, J. (2011). Exo70, a subunit of the exocyst complex, interacts with SNEV(hPrp19/hPso4) and is involved in pre-mRNA splicing. *Biochem. J.* 438, 81–91.

Dereeper, A., Guignon, V., Blanc, G., Audic, S., Buffet, S., Chevenet, F., Dufayard, J. F., Guindon, S., Lefort, V., Lescot, M., Claverie, J. M., and Gascuel, O. (2008). Phylogeny.fr: robust phylogenetic analysis for the non-specialist. *Nucleic Acids Res.* 36, W465–W469.

Eliáš, M., Drdová, E., Žiak, D., Bavlnka, B., Hála, M., Cvrčková, F., Soukupová, H., and Žárský, V. (2003). The exocyst complex in plants. *Cell Biol. Int.* 27, 199–201.

Fendrych, M., Synek, L., Pečenková, T., Toupalová, H., Cole, N., Drdová, E., Nebesářová, J., Šedinová, M., Hála, M., Fowler, J. E., and Žárský, V. (2010). The *Arabidopsis* exocyst complex is involved in cytokinesis and cell plate maturation. *Plant Cell* 22, 3053–3065.

Genre, A., Ivanov, S., Fendrych, M., Faccio, A., Žárský, V., Bisseling, T., and Bonfante, P. (2012). Multiple exocytotic markers accumulate at the sites of perifungal membrane biogenesis in arbuscular mycorrhizas. *Plant Cell Physiol.* 53, 244–255.

Goodstein, D. M., Shu, S., Howson, R., Neupane, R., Hayes, R. D., Fazo, J., Mitros, T., Dirks, W., Hellsten,

U., Putnam, N., and Rokshar, D. S. (2012). Phytozome: a comparative platform for green plant genomics. *Nucleic Acids Res.* 40, D1178–D1186.

Grunt, M., Žárský, V., and Cvrčková, F. (2008). Roots of angiosperm formins: the evolutionary history of plant FH2 domain-containing proteins. *BMC Evol. Biol.* 8, 115. doi:10.1186/1471-2148-8-115

Guindon, S., and Gascuel, O. (2003). A simple, fast an accurate algorithm to estimate large phylogenies by maximum likelihood. *Syst. Biol.* 52, 696–704.

Guo, W., Grant, A., and Novick, P. (1999). Exo84p is an exocyst protein essential for secretion. *J. Biol. Chem.* 274, 23558–23564.

Guo, W., Roth, D., Gatti, E., and Novick, P. (1997). Identification and characterization of homologues of the exocyst component Sec10p. *FEBS Lett.* 404, 135–139.

Hála, M., Cole, R. A., Synek, L., Drdová, E., Pečenková, T., Nordheim, A., Lamkemeyer, T., Madlung, J., Hochholdinger, F., Fowler, J. E., and Žárský, V. (2008). An exocyst complex functions in plant cell growth in *Arabidopsis* and tobacco. *Plant Cell* 20, 1330–1345.

Hall, T. A. (1999). BioEdit: a user-friendly biological sequence alignment editor and analysis program for Windows 95/98/NT. *Nucl. Acids Symp. Ser.* 41, 95–98.

He, B., and Guo, W. (2009). The exocyst complex in polarized exocytosis. *Curr. Opin. Cell Biol.* 21, 537–542.

He, B., Xi, F., Zhang, X., Zhang, J., and Guo, W. (2007). Exo70 interacts with phospholipids and mediates the targeting of the exocyst to the plasma membrane. *EMBO J.* 26, 4053–4065.

Heider, M. R., and Munson, M. (2012). Exorcising the exocyst complex. *Traffic* 13, 898–907.

Hertzog, M., and Chavrier, P. (2011). Cell polarity during motile processes: keeping on track with the exocyst complex. *Biochem. J.* 433, 403–409.

Jiao, Y., Wickett, N. J., Ayyampalayam, S., Chanderbali, A. S., Landherr, L., Ralph, P. E., Tomsho, L. P., Hu, Y., Liang, H., Soltis, P. S., Soltis, D. E., Clifton, S. W., Schlarbaum, S. E., Schuster, S. C., Ma, H., Leebens-Mack, J., and de Pamphilis, C. W. (2011). Ancestral polyploidy in seed plants and angiosperms. *Nature* 473, 97–100.

Juan, D., Pazos, F., and Valencia, A. (2008). Co-evolution and co-adaptation in protein networks. *FEBS Lett.* 582, 1225–1230.

Kee, Y., Yoo, J. S., Hazuka, C. D., Peterson, K. E., Hsu, S. C., and Scheller, R. H. (1997). Subunit structure of the mammalian exocyst complex. *Proc. Natl. Acad. Sci. U.S.A.* 94, 14438–14443.

Kitashiba, H., Liu, P., Nishio, T., Nasrallah, J. B., and Nasrallah, M. E. (2011). Functional test of *Brassica* self-incompatibility modifiers in *Arabidopsis thaliana*. *Proc. Natl. Acad. Sci. U.S.A.* 108, 18173–18178.

Koch, M. A., Haubold, B., and Mitchell-Olds, T. (2000). Comparative evolutionary analysis of chalcone synthase and alcohol dehydrogenase loci in *Arabidopsis, Arabis*, and related genera (Brassicaceae). *Mol. Biol. Evol.* 17, 1483–1498.

Koumandou, V. L., Dacks, J. B., Coulson, R. M., and Field, M. C. (2007). Control systems for membrane fusion in the ancestral eukaryote; evolution of tethering complexes and SM proteins. *BMC Evol. Biol.* 7, 29. doi:10.1186/1471-2148-7-29

Kulich, I., Cole, R. A., Drdová, E., Cvrčková, F., Soukup, A., Fowler, J. E., and Žárský, V. (2010). Arabidopsis exocyst subunits SEC8 and EXO70A1 and exocyst interactor ROH1 are involved in the localized deposition of seed coat pectin. *New Phytol.* 188, 615–625.

Lamesch, P., Berardini, T. Z., Li, D., Swarbreck, D., Wilks, C., Sasidharan, R., Muller, R., Dreher, K., Alexander, D. L., Garcia-Hernandez, M., Karthikeyan, A. S., Lee, C. H., Nelson, W. D., Ploetz, L., Singh, S., Wensel, A., and Huala, E. (2012). The *Arabidopsis* information resource (TAIR): improved gene annotation and new tools. *Nucleic Acids Res.* 40, D1202–D1210.

Lang, D., Eisinger, J., Reski, R., and Rensing, S. (2005). Representation and high-quality annotation of the *Physcomitrella patens* transcriptome demonstrates a high proportion of proteins involved in metabolism among mosses. *Plant Biol.* 7, 238–250.

Lassmann, T., and Sonnhammer, E. L. (2006). Kalign, Kalignvu and Mumsa: web servers for multiple sequence alignment. *Nucleic Acids Res.* 34, W596–W599.

Lawrence, C. E., Altschul, S. F., Boguski, M. S., Liu, J. S., Neuwald, A. F., and Wootton, J. C. (1993). Detecting subtle sequence signals: a Gibbs sampling strategy for multiple alignment. *Science* 262, 208–214.

Lovell, S. C., and Robertson, D. L. (2010). An integrated view of molecular co-evolution in protein-protein interactions. *Mol. Biol. Evol.* 27, 2567–2575.

McGinnis, S., and Madden, T. L. (2004). BLAST: at the core of a powerful and diverse set of sequence analysis tools. *Nucleic Acids Res.* 32, W20–W25.

Munson, M., and Novick, P. (2006). The exocyst defrocked, a framework of rods revealed. *Nat. Struct. Mol. Biol.* 13, 577–581.

Pečenková, T., Hála, M., Kulich, I., Kocourková, D., Drdová, E., Fendrych, M., Toupalová, H., and Žárský, V. (2011). The role for the exocyst complex subunits Exo70B2 and Exo70H1 in the plant-pathogen interaction. *J. Exp. Bot.* 62, 2107–2116.

Potato Genome Sequencing Consortium. (2011). Genome sequence and analysis of the tuber crop potato. *Nature* 475, 189–195.

Samuel, M. A., Chong, Y. T., Haasen, K. E., Aldea-Brydges, M. G., Stone, S. L., and Goring, D. R. (2009). Cellular pathways regulating responses to compatible and self-incompatible pollen in *Brassica* and *Arabidopsis* stigmas intersect at Exo70A1, a putative component of the exocyst complex. *Plant Cell* 21, 2655–2671.

Schuler, G. D., Altschul, S. F., and Lipman, D. J. (1991). A workbench for multiple alignment construction analysis. *Proteins* 9, 180–190.

Seguí-Simmaro, J. M., Austin, J. R., White, E. A., and Staehelin, L. A. (2004). Electron tomographic analysis of somatic cell plate formation in meristematic cells of *Arabidopsis* preserved by high-pressure freezing. *Plant Cell* 16, 836–856.

Sklarczyk, D., Franceschini, A., Kuhn, M., Simonovic, M., Roth, A., Minguez, P., Doerks, T., Stark, M., Muller, J., Bork, P., Jensen, L. J., and von Mering, C. (2011). The STRING database in 2011: functional interaction networks of proteins, globally integrated and scored. *Nucleic Acids Res.* 39, D561–D568.

Soltis, D. E., Bell, C. D., Kim, S., and Soltis, P. S. (2008). Origin and early evolution of angiosperms. *Ann. N. Y. Acad. Sci.* 1133, 3–25.

Songer, J. A., and Munson, M. (2009). Sec6p anchors the assembled exocyst aomplex at sites of secretion. *Mol. Biol. Cell* 20, 973–982.

Stern, A., Doron-Faigenboim, A., Erez, E., Martz, E., Bacharach, E., and Pupko, T. (2007). Selecton 2007: advanced models for detecting positive and purifying selection using a Bayesian inference approach. *Nucleic Acids Res.* 35, W506–W511.

Synek, L., Schlager, N., Eliáš, M., Quentin, M., Hauser, M. T., and Žárský, V. (2006). AtEXO70A1, a member of a family of putative exocyst subunits specifically expanded in land plants, is important for polar growth and plant development. *Plant J.* 48, 54–72.

Tamura, K., Peterson, D., Peterson, N., Stecher, G., Nei, M., and Kumar, S. (2011). MEGA5: molecular evolutionary genetics analysis using maximum likelihood, evolutionary distance, and maximum parsimony methods. *Mol. Biol. Evol.* 28, 2731–2739.

TerBush, D. R., Maurice, T., Roth, D., and Novick, P. (1996). The exocyst is a multiprotein complex required for exocytosis in *Saccharomyces cerevisiae*. *EMBO J.* 15, 6483–6494.

The Uniprot Consortium. (2012). Reorganizing the protein space at the Universal Protein Resource (UniProt). *Nucleic Acids Res.* 40, D71–D75.

Thompson, J. D., Gibson, T. J., Plewniak, F., Jeanmougin, F., and Higgins, D. G. (1997). The ClustalX windows interface: flexible strategies for multiple sequence alignment aided by quality analysis tools. *Nucleic Acids Res.* 24, 4876–4882.

Van de Peer, Y., Maere, S., and Meyer, A. (2009). The evolutionary significance of ancient genome duplications. *Nat. Rev. Genet.* 10, 725–732.

Wang, J., Ding, Y., Wang, J., Hillmer, S., Miao, Y., Lo, S. W., Wang, X., Robinson, D. G., and Jiang, L. (2010). EXPO, an exocyst-positive organelle distinct from multivesicular endosomes and autophagosomes, mediates cytosol to cell wall exocytosis in *Arabidopsis* and tobacco cells. *Plant Cell* 22, 4009–4030.

Wen, T. J., Hochholdinger, F., Sauer, M., Bruce, W., and Schnable, P. S. (2005). The roothairless1 gene of maize encodes a homolog of sec3, which is involved in polar exocytosis. *Plant Physiol.* 138, 1637–1643.

Whyte, J. R., and Munro, S. (2002). Vesicle tethering complexes in membrane traffic. *J. Cell Sci.* 115, 2627–2657.

Woodhouse, M. R., Tang, H., and Freeling, M. (2011). Different gene families in *Arabidopsis thaliana* transposed in different epochs and at different frequencies throughout the rosids. *Plant Cell* 23, 4241–4253.

Žárský, V., Cvrčková, F., Potocký, M., and Hála, M. (2009). Exocytosis and cell polarity in plants – exocyst and recycling domains. *New Phytol.* 183, 255–272.

Žárský, V., and Potocký, M. (2010). Recycling domains in plant cell

morphogenesis: small GTPase effectors, plasma membrane signalling and the exocyst. *Biochem. Soc. Trans.* 38, 723–728.

Zhang, X., Zajac, A., Zhang, J., Wang, P., Li, M., Murray, J., TerBush, D. R., and Guo, W. (2005). The critical role of Exo84p in the organization and polarized localization of the exocyst complex. *J. Biol. Chem.* 280, 20356–20364.

Zhang, Y., Liu, C. M., Emons, A. M. C., and Ketelaar, T. (2010). The plant exocyst. *J. Integr. Plant Biol.* 52, 138–146.

Conflict of Interest Statement: The authors declare that the research was conducted in the absence of any commercial or financial relationships that could be construed as a potential conflict of interest.

Received: 13 June 2012; paper pending published: 25 June 2012; accepted: 29 June 2012; published online: 18 July 2012.
*Citation: Cvrčková F, Grunt M, Bezvoda R, Hála M, Kulich I, Rawat A and Žárský V (2012) Evolution of the land plant exocyst complexes. Front. Plant Sci. **3**:159. doi: 10.3389/fpls.2012.00159*
This article was submitted to Frontiers in Plant Traffic and Transport, a specialty of Frontiers in Plant Science.

frontiers in
PLANT SCIENCE

REVIEW ARTICLE
published: 24 August 2012
doi: 10.3389/fpls.2012.00188

Bundling actin filaments from membranes: some novel players

Clément Thomas*

Laboratory of Molecular and Cellular Oncology, Department of Oncology, Public Research Centre for Health (CRP-Santé), Luxembourg, Luxembourg

Edited by:
Markus Geisler, University of Fribourg, Switzerland

Reviewed by:
Benoit Lacroix, State University of New York at Stony Brook, USA
Frantisek Baluska, University of Bonn, Germany

****Correspondence:***
Clément Thomas, Laboratory of Molecular and Cellular Oncology, Department of Oncology, Public Research Centre for Health (CRP-Santé), 84 Val Fleuri, L-1526 Luxembourg, Luxembourg.
e-mail: clement.thomas@crp-sante.lu

Progress in live-cell imaging of the cytoskeleton has significantly extended our knowledge about the organization and dynamics of actin filaments near the plasma membrane of plant cells. Noticeably, two populations of filamentous structures can be distinguished. On the one hand, fine actin filaments which exhibit an extremely dynamic behavior basically characterized by fast polymerization and prolific severing events, a process referred to as actin stochastic dynamics. On the other hand, thick actin bundles which are composed of several filaments and which are comparatively more stable although they constantly remodel as well. There is evidence that the actin cytoskeleton plays critical roles in trafficking and signaling at both the cell cortex and organelle periphery but the exact contribution of actin bundles remains unclear. A common view is that actin bundles provide the long-distance tracks used by myosin motors to deliver their cargo to growing regions and accordingly play a particularly important role in cell polarization. However, several studies support that actin bundles are more than simple passive highways and display multiple and dynamic roles in the regulation of many processes, such as cell elongation, polar auxin transport, stomatal and chloroplast movement, and defense against pathogens. The list of identified plant actin-bundling proteins is ever expanding, supporting that plant cells shape structurally and functionally different actin bundles. Here I review the most recently characterized actin-bundling proteins, with a particular focus on those potentially relevant to membrane trafficking and/or signaling.

Keywords: actin bundling, fimbrins, formins, LIM proteins, SCAB1, THRUMIN1, V-ATPases, villins

INTRODUCTION

Actin is one of the most abundant, ubiquitous, and conserved proteins in eukaryotes. In the cell, globular actin subunits polymerize into actin filaments which themselves assemble into higher order structures, such as orthogonal networks and parallel bundles (**Figure 1**). This system, referred to as the actin cytoskeleton, exhibits an extraordinary high degree of plasticity allowing the formation, destruction, and recycling of diverse filamentous structures within a short time scale, and offers countless possibilities to cells. The primary level of the regulation of actin cytoskeleton organization and dynamics consists in various (>100) actin-binding proteins which control, in time and space, actin filament nucleation, elongation, stabilization, capping, severing, and crosslinking (Pollard et al., 2000; Winder and Ayscough, 2005). In animal and yeast cells, cortical actin filaments and the plasma membrane undergo a dynamic interplay (Pollard and Cooper, 2009). For instance, the coordinated polymerization of actin filaments against the membrane provides the force necessary to modify cell shape and promote cell locomotion and division. As a consequence, dysfunctions in the actin polymerization machinery or in its regulation frequently results in diseases, including cancers (Van Troys et al., 2008a). Although related mechanisms are not excluded in plant cells, they are obviously not prevalent. The rigid plant cell wall precludes any modification of the cell boundary by an actin polymerization-based process. However, actin filaments are in close proximity with the cell membrane in plant cells too.

Recent studies combining advanced imaging approaches, such as variable-angle epifluorescence microscopy (VAEM), spinning disc confocal microscopy, and reliable fluorescent actin markers have advanced our understanding of the organization and dynamics of the actin cytoskeleton near the cell cortex (Staiger et al., 2009; Khurana et al., 2010; Smertenko et al., 2010; Henty et al., 2011; Wang et al., 2011; Toth et al., 2012; **Figure 1**). Cortical filaments arrange into complex networks whose stochastic behavior is largely consistent with the predictions of a biomimetic system (Michelot et al., 2007; Staiger et al., 2009; Blanchoin et al., 2010). Single filaments randomly polymerize at extremely high growth rates (1.7 μm/s in hypocotyl epidermal cells from *Arabidopsis* seedlings) and exhibit prominent buckling and straightening behavior. Most filaments are short-lived (<30 s), which was demonstrated to be primarily due to prolific severing activity rather than to filament end depolymerization. Beside single filaments, thicker and longer bundles adopt less convoluted configurations and tend to align with the long axis of the cell (Staiger et al., 2009; Smertenko et al., 2010; Henty et al., 2011). In comparison with finer filaments, thick fibers experience slower but qualitatively similar dynamics. Indeed, they elongate, buckle,

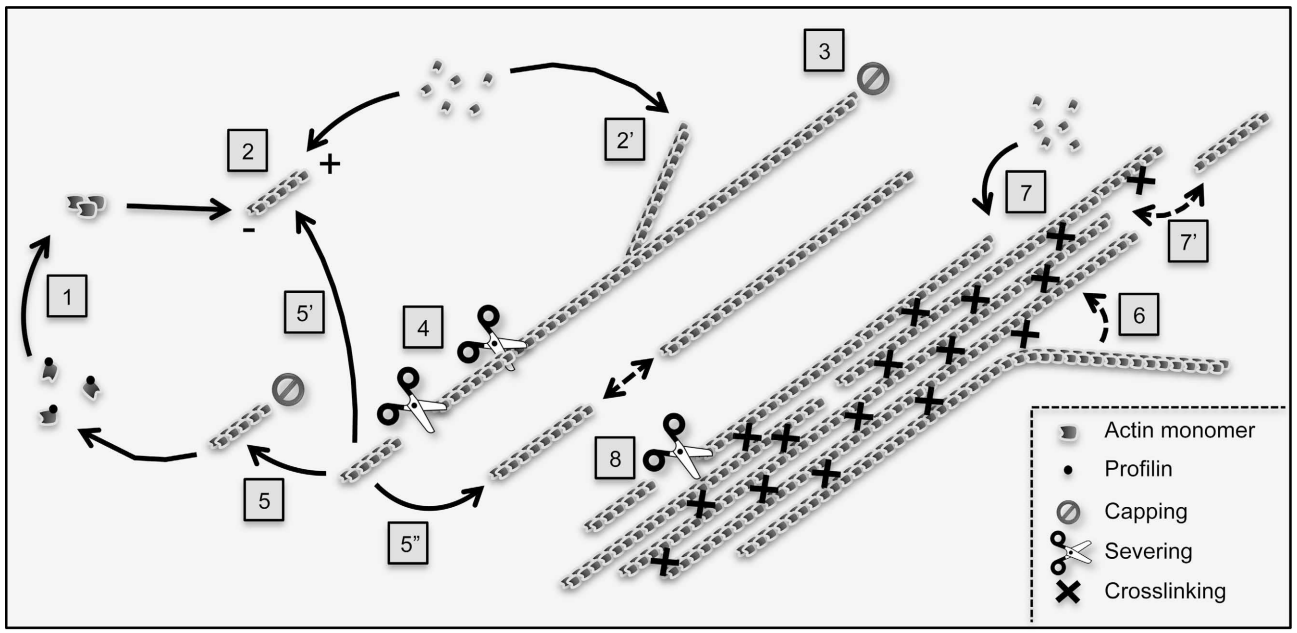

FIGURE 1 | Main reactions controlling actin filament dynamics and organization in plant cells. The G-actin monomer binding protein profilin inhibits spontaneous actin nucleation in the cytoplasm. Nucleation is promoted *de novo* (1) by nucleating proteins such as formins. In addition, non-processive formins, such as *Arabidopsis* AtFH1, can also induce nucleation from the side of pre-existing filaments, a process which likely contributes to the initiation of actin bundles (not illustrated; Michelot et al., 2006; Blanchoin et al., 2010). Following nucleation, actin filaments undergo fast polymerization (2) and (2′) before being capped (3). The aging section of actin filaments (which contains ADP-loaded actin subunits, not shown) is fragmented by severing proteins such as actin-depolymerizing factors (4). The resulting fragments can be capped at their barbed end and depolymerize from their pointed (–) end to replenish the pool of monomers (5). Alternatively, they can re-elongate through polymerization (5′) although this process rarely occurs immediately following severing, suggesting intense barbed end capping activity (Staiger et al., 2009). Finally, actin fragments can serve as building blocks to assemble novel filaments by an end-joining mechanism (5″). Actin filaments are crosslinked into bundles by bundling proteins (right part of the cartoon). Both *in vitro* and live cell TIRFM-based analyses support that actin bundles form by a "catch and zipper" mechanism (6) (Khurana et al., 2010). Actin bundles subsequently grow by elongation of filaments at their ends (7) as well as by end-association of pre-existing filaments (7′), a process which might be facilitated by bundling proteins. Like single filaments, actin bundles are severed although at a lower frequency (Khurana et al., 2010; Smertenko et al., 2010). Current data support that unipolar bundles (here-exemplified) predominate in plant cells. However, the existence of bundles containing actin filaments of mixed polarity is not excluded.

bundle, and are severed (Staiger et al., 2009; Blanchoin et al., 2010; Smertenko et al., 2010). Although actin filament severing emerges as the leading driver of actin cytoskeleton remodeling, an additional mechanism involving filament bundling, unbundling, and myosin-dependent sliding events was suggested to contribute to the permanent reorganization of the cortical actin network (Smertenko et al., 2010). Using VAEM and quantitative approaches, Henty et al. (2011) provided, for the first time, direct evidence of the contribution of an ABP, namely *Arabidopsis* actin depolymerizing factor 4 (AtADF4), to actin stochastic dynamics *in vitro*. In agreement with the biochemical actin severing activity of AtADF4, hypocotyl epidermal cells from *adf4* knockout mutants exhibited a 2.5–3-fold decrease in the rate of severing, as well as increased filament lengths and lifetimes. The loss of AtADF4 also led to excessive actin bundling and cell growth in the apical region of the hypocotyl, where active cell expansion takes place.

Actin bundles have been repeatedly reported to play a critical role in cell morphogenesis (Baluska et al., 2001; Smith and Oppenheimer, 2005; Thomas et al., 2009; Higaki et al., 2010a). The relationships between the extent of actin bundling and cell growth are however complex as illustrated by contradictory observations. For instance, the growing epidermal cells from petioles of *adf4* mutants also exhibit enhanced bundling but, contrarily to hypocotyl epidermal cells, are shorter than in wild-type plants (Henty et al., 2011). Some studies have established that in specific cells, such as rice coleoptiles, increased actin bundling negatively impacts cell elongation (Nick et al., 2009; Nick, 2010). As an underlying mechanism, it has been proposed that actin bundling prevents efficient delivery of auxin-efflux carriers to their site of action at the plasma membrane, a process which would require a more unbundled actin configuration (Nick, 2010). Actin bundles most likely impact cell growth by different ways. Indeed, actin bundling can alter turgor pressure, the main physical driver of cell expansion (Szymanski and Cosgrove, 2009), by modifying the thickness of the cell wall and the shape of the transvacuolar strands and vacuole (e.g., Staiger et al., 1994; Higaki et al., 2010a,b, 2011). Finally, there is much evidence that actin bundles serve as main tracks used by myosin motors to drive endomembrane compartments over long distances to sites of growth (Smith and Oppenheimer, 2005; Thomas et al., 2009; Higaki et al., 2010a). Interestingly, the organization and

dynamics of the actin cytoskeleton significantly differ in isotropically and anisotropically growing cells, and this was confirmed by recent quantitative analyses using VAEM (Smertenko et al., 2010). Therefore, the role of actin bundling in cell growth appears multiple and cell-type dependent.

In animal cells, the assembly of actin bundles is required for the formation and/or function of various specialized cellular structures, such as filopodia, lamellipodia, stress fibers, microvilli, and invadopodia (Stevenson et al., 2012). In most of these structures, actin bundles are in close connection with the cell membrane and, in some cases, with the extracellular environment referred to as the extracellular matrix. For instance, the α-actinin-induced actin bundles that constitute the ventral stress fibers of non-muscle cells are anchored to focal adhesions at each of their extremities. Focal adhesions transmit the force generated by myosin II-dependent stress fiber contraction to the extracellular matrix, allowing to pull the cell body during cell migration (Vicente-Manzanares et al., 2009; Ciobanasu et al., 2012). Key players of focal adhesions are the cell surface membrane receptors integrins around which assemble complex networks made of about 160 proteins that contribute to link the extracellular matrix to the actin cytoskeleton and to create a high-performance environmental sensing system (Geiger et al., 2009). Plants lack most focal adhesion components, including true integrin homologs. However, there is no doubt that plant cells perceive and transduce many external signals from their cell wall to their cytoskeleton (Baluska et al., 2003; Drobak et al., 2004; Humphrey et al., 2007; Fu, 2010; Higaki et al., 2011). Day et al. (2011) recently comprehensively reviewed the potential roles played by the actin cytoskeleton in the organization and activation of host responses to biotic stress. One of the earliest and well-documented responses of plant cells to fungal or oomycete pathogens is a reorganization of the actin cytoskeleton and endomembrane components which both focus at the site of infection (e.g., Kobayashi et al., 1994; Leckie et al., 1995; Xu et al., 1998; Opalski et al., 2005; Takemoto et al., 2006; Day et al., 2011). Such reorganization is thought to culminate in the formation of cell wall appositions rich in antimicrobial compounds (Hardham et al., 2007). During this process actin filaments become more bundled, suggesting an important role for actin-bundling proteins in the dynamic relocalization of organelles during interactions with pathogens. Interestingly, Hardham et al. (2008) could mimic pathogen-induced actin remodeling by applying a gentle and local pressure on the surface of *Arabidopsis* cotyledon epidermal cells, indicating that the actin cytoskeleton can readily reorganize (3–5 min after stimulation) in response to the physical force exerted by pathogens. Considering the continuous and fast remodeling of the cortical actin array observed in both growing and non-growing epidermal cells, an emerging and seducing idea is that cortical actin plays a sentinel role capable of initiating basal defense against pathogen-induced diseases or abiotic stress, such as mechanical stress, within short time scales (Staiger et al., 2009). How actin filaments and bundles communicate with the cell membrane and cell wall largely remains enigmatic.

Since our last review on actin bundling in plants (Thomas et al., 2009), more than fifteen additional plant actin-bundling proteins were isolated and characterized. Several of those belong to the previously known villin, formin, fimbrin, and LIM protein families, whereas others define novel families. Some of these proteins are likely direct linkers between actin bundles and the cell or organelle membranes. Here we review the last advances in plant actin-bundling proteins with a particular interest for those that further move ahead our comprehension about how actin bundles physically or functionally interact with membranes.

FORMINS

Over the last years, formins have emerged as a large and major family of plant actin nucleating factors with critical functions in cell growth and division (Blanchoin and Staiger, 2008). Beside their core nucleating activity, plant formins display additional actin regulatory activities including nucleation, capping, severing, and bundling (Staiger and Blanchoin, 2006). The *Arabidopsis* formin AtFH1 (Banno and Chua, 2000), was the first plant formin reported to promote the formation of actin bundles both in live cells and *in vitro* (Cheung and Wu, 2004; Michelot et al., 2005). Its overexpression in pollen tubes stimulates the formation of actin bundles from the cell membrane and locally induces membrane deformation, suggesting that a proper density and distribution of actin bundles is critical for membrane assembly and/or maintenance, and that formins play substantial roles in these processes (Cheung and Wu, 2004). Mechanistic studies, employing total internal reflection fluorescence microscopy (TIRFM), revealed that AtFH1 functions as a non-processive formin which moves from the barbed end to the side of an actin filament after the nucleation event, and that this property is involved in AtFH1 actin bundling activity (Michelot et al., 2006). Recently, several other plant formins were shown to promote the formation of actin bundles in an autonomous manner, including *Arabidopsis* AtFH4, AtFH8, and AtFH14 (Deeks et al., 2010; Li et al., 2010; Xue et al., 2011), and rice OsFH5 (Yang et al., 2011; Zhang et al., 2011a).

Interaction of class I plant formins with a membrane is predicted by the characteristic membrane-targeting domain present in their N-terminal region which consists in a signal peptide followed by a transmembrane domain (Deeks et al., 2002; Blanchoin and Staiger, 2008). Accordingly, most class I formins examined so far were shown to accumulate at the cell periphery or in membrane-rich structures such as the cell plate using immunocytochemistry and/or GFP-fusion strategies (Cheung and Wu, 2004; Favery et al., 2004; Van Damme et al., 2004; Deeks et al., 2005; Ingouff et al., 2005; Cheung et al., 2010). Interestingly, AtFH8-GPF localizes primarily to the nuclear envelope in interphase cells, suggesting functional differences among class I formins (Xue et al., 2011). In addition, biochemical analyses indicate that pollen-specific AtFH3 lacks the ability to generate actin bundles *in vitro* (Ye et al., 2009). Nevertheless, with or without intrinsic actin-bundling activities, class I formins were convincingly demonstrated to promote actin bundling *in vivo* (Cheung and Wu, 2004; Ye et al., 2009; Cheung et al., 2010). Indeed, both gain- and loss-of-function genetic studies pointed out a central role of AtFH3 in regulating the long and thick actin bundles running along the pollen tube shank and in controlling the direction and velocity of cytoplasmic streaming (Ye et al., 2009). Therefore, AtFH3 likely cooperates with pollen actin-bundling proteins to assemble the tracks required for long

distance actomyosin-dependent movement. Beside AtFH3, the pollen tube tip-enriched formin AtFH5 was found to play more specific functions in the formation of the subapical actin structure often referred to as the cortical actin fringe, and in membrane-targeted vesicular trafficking (Cheung et al., 2010).

It is noteworthy that class I formins exhibit divergent and potentially highly glycosylated extracellular domains, and accordingly represent excellent candidates for mediating extracellular stimuli to the actin cytoskeleton (Cvrckova, 2000; Blanchoin and Staiger, 2008), e.g., during the guidance of pollen tube growth in response to female tissue signals (Cheung and Wu, 2004). In this context, Martiniere et al. (2011) recently provided compelling evidence that the extracellular domain of AtFH1 is anchored to the cell wall and thereby reduces the lateral mobility of AtFH1. Domain analyses highlighted the central role in AtFH1 immobilization of a short, 15 amino acid-long, domain which includes a signature peptide of extensins, a class of cell wall-associated hydroxyproline-rich glycoproteins (Banno and Chua, 2000; Showalter et al., 2010). Although the biochemical nature of formin-cell wall interactions has not been resolved yet, it is tempting to propose that cell wall heterogeneity is responsible for targeting formins to specific plasma membrane subdomains. For instance, the accumulation of AtFH4 in cell-to-cell contact areas and of AtFH5 in the pollen-tube apical dome (Deeks and Hussey, 2005; Cheung et al., 2010) might reflect specificities in cell wall composition at these locations. Interestingly, the extracellular domain responsible for anchoring AtFH1 to the cell wall was required for AtFH1-mediated actin cytoskeleton remodeling in overexpression experiments (Martiniere et al., 2011). Although this remains speculative, anchoring of AtFH1 has been suggested to contribute to the formation and/or stabilization of AtFH1 functional dimers. Together these data support that AFH1, and most likely other class I formins, provide stable anchor points for the actin cytoskeleton at the cell membrane and can induce actin remodeling upon external signal perception. It is noteworthy that time lapse imaging analyses suggested that some of the AtFH5-nucleated and membrane-anchored actin filaments in the subapical region of pollen tubes are fragmented and released to the cytoplasm, providing precursors of some long actin bundles in the core cytoplasm (Cheung et al., 2010). Membrane-associated formins might therefore also indirectly contribute to the formation of more internal actin structures.

In addition to their function as interface between cell membrane and actin cytoskeleton, plant formins recently emerged as central links between actin filaments and microtubules. For instance, class I AtFH4, class II AtFH14, and the closely related rice OsFH5 bind to and bundle both actin filaments and microtubules and are accordingly expected to functionally coordinate the corresponding cytoskeletons (Deeks et al., 2010; Li et al., 2010; Yang et al., 2011; Zhang et al., 2011a). There is accumulating evidence that such coordination is crucial for many developmental processes such as intracellular transport, directional cell growth, and cell division (e.g., Fu et al., 2005; Collings, 2008; Wightman and Turner, 2008; Crowell et al., 2009; Petrasek and Schwarzerova, 2009). A recent quantitative study using VAEM revealed that microtubule depolymerization induces faster elongation and shortening of actin filaments, suggesting that actin dynamics at the cell cortex are modulated by microtubules (Smertenko et al., 2010). Although the underlying mechanism remains unknown, it seems reasonable to speculate that some formin family members are involved. Interestingly, endogenous OsFH5 localizes to specific regions at the chloroplast surface (Zhang et al., 2011a). Like other class II formins, OsFH5 possesses an N-terminal phosphate tensin (PTEN)-like domain instead of the typical transmembrane domain of most class I formins. Transient expression experiments indicate that the PTEN-like domain of FH5 is sufficient to target a fluorescent protein reporter to the chloroplast outer surface of tobacco cells, suggesting that it is responsible for the anchoring of OsFH5 to chloroplasts. Therefore OsFH5 emerges as a potential linker between actin filaments/bundles, microtubules, and chloroplasts, and might accordingly contribute to chloroplast motility, a process that has been proposed to rely on both cytoskeletons at least in some species (e.g., Chuong et al., 2006).

THRUMIN1

Chloroplasts change their subcellular location in response to light. They move toward weak light to optimize light capture for photosynthesis and away from intense light to minimize photodamage, the latter process being referred to as the avoidance response (Kasahara et al., 2002; Suetsugu and Wada, 2007). In plants, organelle movement primarily relies on class XI myosins which are predicted to transport their cargos along cytosplasmic actin bundles (Avisar et al., 2008; Peremyslov et al., 2008; Sparkes et al., 2008). Although myosin inhibitor studies support that chloroplast movement also depends on myosin activity to some extent (e.g., Paves and Truve, 2007), recent data indicate that chloroplasts primarily use another type of actin-based mechanism to rapidly change their direction in response to light. A population of so-called chloroplast actin filaments (cp-actin filaments) was shown to anchor chloroplasts to the plasma membrane suggesting that they are involved in light-induced chloroplast repositioning (Kadota et al., 2009; Suetsugu et al., 2010a,b). In this context, THRUMIN1 was recently identified as a novel actin-bundling protein with a potential critical role in linking phototropin photoreceptor activity at the plasma membrane and actin-dependent chloroplast movements (Whippo et al., 2011).

Compared to wild-type plants, *thrumin1* mutants exhibit slower and more randomized chloroplast movements in response to light stimuli. *In vitro* biochemical analyses indicate that THRUMIN1 binds to actin filaments in a direct manner and promotes the formation of actin bundles. Consistent with these data and the previously reported association of THRUMIN1 with the plasma membrane (Alexandersson et al., 2004), YFP-fused THRUMIN1 (THRUMIN1-YFP) extensively decorates the filamentous actin cytoskeleton along the plasma membrane, and in association with chloroplasts (Whippo et al., 2011). Upon stimulation of the chloroplast avoidance response by a localized blue-light irradiation, THRUMIN1-YFP further accumulates along actin filaments and apparently increases actin-bundling locally. The underlying mechanism was proven to be dependent on the phototropin blue-light photoreceptors PHOT1 and PHOT2. Indeed, no elevation of THRUMIN1-YFP fluorescence occurred in *phot1phot2* double mutants upon blue light stimulation. Together these data support that THRUMIN1

promotes the formation of actin bundles from the plasma membrane in response to light and in a phototropin-dependent manner. However, the exact role of such actin bundles in chloroplast movement remains to be established. In addition, how THRUMIN1 cooperates with CHUP1, a chloroplast outer envelope ABP involved in cp-actin filament formation (Oikawa et al., 2003, 2008; Schmidt Von Braun and Schleiff, 2008a,b; Kadota et al., 2009), to remodel the actin cytoskeleton and drive chloroplast movement upon light perception by PHOT1 and PHOT2 are central questions that should be addressed in future studies. As already stated in the previous section, class II formins represent additional potential linkers between chloroplasts and actin bundles (Zhang et al., 2011a).

VACUOLAR H^+-ATPases B SUBUNITS

Vacuolar H^+-ATPases (V-ATPases) are evolutionary-conserved multisubunit complexes that consist in a cytosolic ATP-hydrolyzing V_1 subcomplex and a membrane-associated proton-translocating V_0 subcomplex (Nishi and Forgac, 2002; Nelson, 2003; Ma et al., 2011). They mediate ATP-dependent transport of protons across plasma and intracellular membranes and thereby contribute to (1) the acidification of the lumen of various organelles such as vacuoles, secretory vesicles, endosomes, Golgi apparatus, and lysosomes and (2) the production of the energy required for various coupled transport processes. Accordingly, V-ATPases are involved in a wide range of critical processes including membrane trafficking and fusion, and cell expansion (Schumacher et al., 1999; Padmanaban et al., 2004; Dettmer et al., 2006; Brux et al., 2008). In mammals and yeast, both B and C subunits of the V_1 subcomplex were previously reported to directly bind to F-actin with high affinity (Lee et al., 1999; Holliday et al., 2000; Vitavska et al., 2003, 2005; Chen et al., 2004; Zuo et al., 2008).

Functional studies support that the actin binding activity of V-ATPase B and C subunits is not involved in the regulation of V-ATPase assembly or activity. However, under stress conditions, it provides a significant survival advantage in yeast, supporting that it is biologically relevant (Xu and Forgac, 2001; Zuo et al., 2008). In addition, several studies have highlighted that the targeting of V-ATPases to specific sites relies on their interaction with the actin cytoskeleton (Lee et al., 1999; Adams et al., 2006; Zuo et al., 2006). Carnell et al. (2011) recently suggested a novel and elegant model in which nucleation-promoting factor WASH-dependent actin polymerization on mature lysosomes from *Dictyostelium* would sort V-ATPases to recycling vesicles, leading to subsequent lysosome neutralization and exocytosis. In the absence of WASH, no polymerization would occur and V-ATPases would remain on the lysosome, which in turn would remain acidic and unable to exocytose. Such a model assumes that the actin-binding activity of V-ATPases functions as tags for actin-mediated sorting.

A similar mechanism in plant cells is plausible since homologs of V-ATPases (Zimniak et al., 1988; Krebs et al., 2010), ARP2/3 complex and associated nucleation-promoting factors have been identified (Deeks and Hussey, 2005; Szymanski, 2005). In addition, the three *Arabidopsis* V-ATPase B subunits (*At*AVB1, *At*VAB2, and *At*VAB3) were recently shown to display direct actin binding and bundling activities *in vitro* (Ma et al., 2012). Therefore, the multiple actin-binding sites responsible for the *in vitro* actin bundling activity of *At*AVB1-3 may confer these proteins an increased affinity for actin filaments/bundles and trigger their clustering and/or recycling upon actin polymerization. Such a scenario of an actin-mediated sorting mechanism in plants remains however highly hypothetical. As an alternative, plant V-ATPases might serve as more passive points for anchoring organelles to actin bundles. A last possibility is that *At*AVB1-3 function in a complex dissociated form in the cytoplasm, and therefore contribute to increase actin-bundling upon V-ATPase complex dissociation. Obviously, much work is required to examine each of these possibilities. Nevertheless, V-ATPases emerge as potential additional links between the actin cytoskeleton and membrane trafficking.

SCAB1

Stomatal movement is driven by modifications in turgor pressure of the guard cells. Stomata open when the guard cell volume increases, and they close when the guard cell volume decreases. It is well established that stomatal closure and opening involves reorganization of the actin cytoskeleton at the cell cortex and that such reorganization plays a key role in stomatal movement (e.g., Kim et al., 1995; Eun and Lee, 1997; Liu and Luan, 1998; Hwang and Lee, 2001; Lemichez et al., 2001; Macrobbie and Kurup, 2007; Choi et al., 2008; Gao et al., 2008). Recently, Higaki et al. (2010b) developed a novel quantitative image analysis method allowing a more detailed and reliable characterization of the changes in actin configurations during the diurnal cycles of *Arabidopsis* guard cells. Data confirmed previous observations that actin filaments adopt a well-organized and radial orientation in open stomata and a more longitudinal orientation in closed stomata. They also provide clear evidence that actin-bundling transiently increases during stomatal opening, and drastically reduces once this process is completed. Interestingly, the abnormally thick and long-lasting actin bundles induced by the expression of a mouse talin-derived actin reporter compromised stomatal opening. This is in good agreement with previous pharmacological and genetic studies indicating that changes in actin dynamics control stomatal movement (Kim et al., 1995; Liu and Luan, 1998; Dong et al., 2001; Lemichez et al., 2001; Macrobbie and Kurup, 2007).

Higaki et al. (2010a,b) suggest that unbundling of actin bundles (rather than their complete depolymerization; Liu and Luan, 1998) stimulates membrane trafficking and increases the number of activated potassium channels in the plasma membrane, which in turn promotes an increase of turgor pressure. In this context, a novel plant-specific actin-bundling protein, termed STOMATAL CLOSURE-RELATED ACTIN BINDING PROTEIN 1 (SCAB1), was isolated from a genetic screen aimed at identifying *Arabidopsis* mutants defective in stomatal movement (Zhao et al., 2011). *In vitro* biochemical data revealed that SCAB1 is a simple actin bundling protein unable to promote actin nucleation or capping. Depletion of SCAB1 reduces actin filament stability, delays the switch from a radial to a longitudinal actin filament configuration in guard cells during stomatal closure, and reduces stomatal closure sensitivity to abscisic acid, H_2O_2, and $CaCl_2$. In contrast, the overexpression of *SCAB1* increases actin filament stability and promotes excessive bundling. Both *SCAB1* knockout

and overexpressing lines exhibit a retardation of stomatal closure, suggesting that proper levels of SCAB1 and actin bundling are required for normal stomatal movements.

Structural and domain analyses indicate that SCAB1 functions as a single actin-binding domain protein that dimerizes through its central coiled coils to achieve the bivalent organization required for actin filament crosslinking (Zhang et al., 2012). Contrary to some other ABPs, SCAB1 activities are insensitive to pH and Ca^{2+} *in vitro* (Zhao et al., 2011). Nevertheless, the SCAB1 C-terminal pleckstrin homology domain was shown to weakly bind to inositol phosphates, suggesting a possible SCAB1 regulation by phosphoinositides at the cell membrane (Zhang et al., 2012). In addition to its potential impact on potassium channel density at the membrane of guard cells, actin bundling might also play a structural role in the control of the vacuolar shape and volume. Indeed, the radial actin filament configuration in open stomata allows the vacuole to occupy a maximal volume. In contrast, the long and heavy bundles spanning along the longitudinal axis of the guard cells of closed stomata might contribute to reduce the vacuole volume. Although the exact roles of actin bundles and the newly discovered actin bundling protein SCAB1 in stomatal movement remain to be established, there is accumulating evidence that they are central players.

VILLINS

Plant villins define a class of multifunctional ABPs which can combine several actin regulatory activities, including actin filament severing, barbed-end capping, and bundling activities. The *Arabidopsis* genome contains five villin genes (*AtVLN1-5*), each of which being highly expressed in a wide range of tissues (Klahre et al., 2000; Huang et al., 2005). Whereas atypical AtVLN1 was reported to function as a simple and calcium-insensitive bundling protein (Huang et al., 2005; Khurana et al., 2010), recent biochemical work supports that the rest of the family, including AtVLN2-5, retains the full set of typical villin activities and is calcium-responsive (Khurana et al., 2010; Zhang et al., 2010, 2011b; Bao et al., 2012; van der Honing et al., 2012). The analysis of AtVLN4 and AtVLN5 loss-of-function mutants (Zhang et al., 2010, 2011b) confirmed the predicted roles of villins in the formation and/or stabilization of the long actin bundles running along the shank of pollen tubes and root hairs (e.g., Yokota et al., 1998, 2003; Tominaga et al., 2000; Ketelaar et al., 2002). These studies also further validated the primary role of such actin bundles in the intracellular transport of organelles and vesicles in tip-growing cells (e.g., Miller et al., 1999; Sheahan et al., 2004; Lovy-Wheeler et al., 2005; Ye et al., 2009). Interestingly, the fact that beside their bundling activity, AtVLN4 and AtVLN5 possess calcium-dependent actin severing and capping activities suggests that they also actively contribute to assembling and disassembling the typical short actin bundle-based structures observed in the subapical region of pollen tubes and root hairs (Zhang et al., 2010, 2011b). As these structures remain at a constant distance from the growing cell tip, they inevitably undergo continuous cycles of disassembly/reassembly, a process which is thought to be primarily regulated by changes in the concentration of ions including $[Ca^{+}]$ and $[H^{+}]$, and reactive oxygen species (Holdaway-Clarke and Hepler, 2003; Knight, 2007; Cheung and Wu, 2008).

The analysis of *vln2vln3* double T-DNA insertion mutants supports that AtVLN2 and AtVLN3 together play a major role in the generation of thick actin bundles in tissues other than pollen and root hairs, and that such bundles are involved in the regulation of directional organ growth (van der Honing et al., 2012). Indeed, unlike single *vln2* and *vln3* mutants, double mutants exhibit much thinner actin bundles as compared to wild type plants, and develop twisted leaves, stems, siliques, and roots. Only full-length AtVLN3, but not a truncated version lacking the headpiece region which is required for actin bundling *in vitro*, could rescue both actin and developmental phenotypes of *vln2vln3* double mutants, supporting that villin-induced thick bundles are required for proper regulation of coordinated cell expansion. It is noteworthy that cell shape and size and plant growth rates are similar in control and double mutant plants, indicating that cell expansion itself is unaffected. Surprisingly, another recent study, which also focused on *vln2vln3* double T-DNA insertion mutants (Bao et al., 2012), reported a morphological phenotype differing from the one described by van der Honing et al. (2012). In this study, the inflorescence stem of *vln2vln3* seedlings developed a pendent phenotype which was correlated to defects in sclerenchyma development (Bao et al., 2012). Although petioles were modestly twisted, this malformation was obviously milder than the prominent twisted phenotype exhibited by various organs of van der Honing's double mutants. Both the pendent and faint twisted phenotypes of Bao's double mutants could be rescued by the expression of either VLN2 or VLN3. In addition, quantitative analyses indicate that xylem fiber cells of double mutant inflorescence stems contain abnormally fine actin bundles, supporting van der Honing's conclusions that VLN2 and VLN3 work as effective and functionally redundant actin-bundling proteins *in vitro*. The morphological differences between the Bao and van der Honing phenotypes remain intriguing and might reflect the presence of truncated forms of VLN3 (the same *vln2* mutant is used as a parental line in both studies) and/or the use of dissimilar plant growth conditions.

LIM PROTEINS

Plant LIM proteins or LIMs (the acronym LIM derived from the first letter of the three first identified LIM domain-containing proteins, namely LIN-11, ISl1, and MEC-3; Way and Chalfie, 1988; Freyd et al., 1990; Karlsson et al., 1990) define a ubiquitous family of actin-bundling proteins. Since our first report on tobacco NtWLIM1 describing the promotion of actin-bundle formation both *in vitro* and in live cells (Thomas et al., 2006, 2007), several additional LIMs, including the six *Arabidopsis* AtLIMs (Papuga et al., 2010; Ye and Xu, 2012), lilium LlLIM1 (Wang et al., 2008), and tobacco NtWLIM2 (Moes et al., 2012), were biochemically characterized and recognized as actin-bundling proteins. Contrary to formins and villins, no other actin-regulatory activity has been attributed to any plant LIM protein so far, supporting that they function as simple actin bundlers. In Papuga et al. (2010), we showed that the actin bundling activity of the three pollen-enriched *Arabidopsis* LIMs (AtPLIM2a–c) is regulated by pH and calcium (AtPLIM2c), whereas that of the three widely-expressed LIMs (AtWLIM1, AtWLIM2a, and AtWLIM2b) is not. These data are particularly relevant considering the central roles

previously proposed for pH and calcium gradients/oscillations in the regulation of ABPs activities and cytoskeletal organization during pollen tube elongation (Staiger et al., 2010). Using an *Arabidopsis* cell suspension-based system, we could demonstrate that the interaction of PLIMs with the actin cytoskeleton can be specifically and reversibly inhibited by a controlled increase of the intracellular pH (Papuga et al., 2010). Overexpression of LlLIM1 modifies the actin cytoskeleton architecture in growing pollen tubes of lily, disturbs endomembrane trafficking, including the Golgi apparatus and endo/exocytic vesicles, and impairs normal targeting of signaling molecules, including phosphatidylinositol-4,5-bisphosphate, phospholipase C, and diacyl glycerol (Wang et al., 2008). As an additional proof of the biological functions of LIMs in pollen, the partial co-suppression of the three AtPLIMs by an RNAi approach was recently shown to provoke important defects in pollen development and tube growth (Ye and Xu, 2012).

Beside their cytosplasmic functions, plant LIMs were repeatedly reported to enter the nucleus, although their roles in this compartment have been comparatively less studied (Mundel et al., 2000; Kawaoka and Ebinuma, 2001; Briere et al., 2003; Thomas et al., 2006; Papuga et al., 2010). One of the first hints of the nuclear roles of plant LIMs was the identification of tobacco NtWLIM1 as a *trans* factor binding to a PAL-box motif of the horseradish *C2 peroxidase* (*prxC2*) gene whose product is involved in phenylpropanoid biosynthesis (Kawaoka et al., 1992, 2000). Supporting the biological relevance of this finding, transgenic tobacco plants with an antisense *NtWLIM1* exhibited abnormally low levels of transcripts of several key phenylpropanoid pathway genes as well as a 27% reduction in lignin content (Kawaoka et al., 2000; Kaothien et al., 2002). We recently evaluated the nuclear functions of the tobacco NtWLIM2 and found that NtWLIM2 can specifically and directly bind to the conserved octamer *cis*-element of the histone *AtH4A748* promoter and activate the corresponding promoter in live cell reporter-based experiments (Moes et al., 2012). Similar activities were also shown for the *Arabidopsis* homolog of NtWLIM2, namely AtWLIM2a, whereas the more distant NtWLIM1 and AtWLIM1 proteins were unable to bind to and to activate the *AtH4A748* promoter, suggesting a specialization of LIM protein subfamilies in their nuclear targets.

Like all the other plant LIMs previously characterized, NtWLIM2 decorates the actin cytoskeleton in live cells, and binds to and bundles actin filaments *in vitro* (Moes et al., 2012). Interestingly, we observed that the NtWLIM2 nuclear fraction readily increases after cell treatment with the F-actin disrupting drug latrunculin B, suggesting that the compartmentalization of NtWLIM2 is modulated by the cytoskeletal status of the cell. It is noteworthy that the mammalian counterparts of plant LIMs, namely the cysteine-rich proteins (CRP1-3) were also reported to shuttle between the cytoplasm and the nucleus where they function as co-activators of genes involved in muscle differentiation (Arber et al., 1994; Arber and Caroni, 1996; Kong et al., 1997; Chang et al., 2003, 2007). In addition, some data support that CRP3 translocates to the nucleus in response to mechanical cues (Boateng et al., 2007, 2009) and that both CRP2 and CRP3 are involved in the stretch response and the regulation of the cell contractile force through their interaction with actin stress fibers (Knoll et al., 2002; Kim-Kaneyama et al., 2005). It is therefore tempting to propose that plant LIMs function as sensors able to perceive mechanical signals and to regulate in turn the mechanical properties of the cell by regulating gene expression (Kawaoka et al., 2000; Kaothien et al., 2002) and remodeling the actin cytoskeleton. In addition, recent expression analyses have highlighted that a subset of poplar LIMs is up-regulated in tension wood (Arnaud et al., 2012), further indicating a connection between plant LIMs and mechanical stress. Such a hypothesis is currently tested in our lab.

FIMBRINS

Fimbrins (also known as plastins in humans) define an evolutionary-conserved family of actin bundling proteins whose activities, biological functions, and roles in diseases have been extensively analyzed in animals/humans and yeast (e.g., Bretscher, 1981; Samstag and Klemke, 2007; Al Tanoury et al., 2010; Skau et al., 2011; Morley, 2012; Shinomiya, 2012). The *Arabidopsis* genome encodes five fimbrins (AtFIM1-5; Staiger and Hussey, 2004). Although the structural bases underlying the actin binding and crosslinking activities of AtFIM1 were characterized in detail, only few studies have directly addressed the biological functions of plant fimbrins (Kovar et al., 2000, 2001; Klein et al., 2004; Wang et al., 2004). Wu et al. (2010) recently provided evidence that pollen-enriched AtFIM5 is required for the proper organization of the actin cytoskeleton in pollen grains and growing pollen tubes. The loss of AtFIM5 disorganizes the typical longitudinal configuration of actin bundles in the shank of the pollen tube and causes some bundles to invade the extreme tip. Such aberrant cytoskeletal organization in turn alters the pattern and velocity of cytoplasmic streaming. Biochemical data revealed that AtFIM5 is a calcium-insensitive actin bundling factor. Although the mechanism by which the loss-of-function of an actin-bundling protein leads to an increase in actin bundles a the tip of pollen tubes remains obscure, together these data highlight an important role for FIM5 in maintaining the normal actin organization and/or dynamics in pollen tubes.

SB401

SB401 is a pollen-specific protein from *Solanum berthaultii* (Liu et al., 1997) which was previously reported to bind to and bundle both microtubules and actin filaments and proposed to function as a linker between microtubule and actin cytoskeletons (Huang et al., 2007). In agreement with its higher *in vitro* affinity for microtubules, SB401 was observed to preferentially interact with the microtubule cytoskeleton in immunolabeled pollen tubes. However, recent *in vitro* biochemical analyses support that phosphorylation of SB401 by casein kinase II specifically inhibits SB401 microtubule regulatory activities, suggesting that phosphorylation can switch the protein toward its actin regulatory function(s) (Liu et al., 2009). Future work should validate SB401 cytoskeleton regulatory activities in a live cell context and provide an insight into its biological function(s) in potato pollen tubes.

AtADF9

Members of the ADF/cofilin family are well-established ABPs able to bind both actin monomers and filaments and whose main

Table 1 | List of the actin bundling promoting proteins cited in this article.

Name	Remarkable features	Reported subcellular locations	Identified or suggested biological functions	Key references
FORMINS				
AtFH1	Non-processive formin; anchors in the cell wall	Cell membrane	Pollen tube growth, cell expansion	Cheung and Wu, 2004; Michelot et al., 2005, 2006; Martiniere et al., 2011
AtFH3	Lacks *in vitro* actin bundling activity	Nuclear envelope; cell plate	Pollen tube growth polarity	Ye et al., 2009
AtFH4	Bundles both AFs and MTs; AtFH4-GFP co-aligns the ER and MTs	Cell membrane at cell-to-cell contacts; ER membrane	Cell expansion	Deeks et al., 2005, 2010
AtFH5	*In vitro* actin bundling activity not reported so far	Growing cell plate; cell membrane in the pollen tube tip	Cell cytokinesis; pollen tube growth	Ingouff et al., 2005; Cheung et al., 2010
AtFH8	AtFH8(FH1FH2) induces stellar structures *in vitro*	Cell membrane at cell-to-cell contacts; nuclear envelope	Primary root growth; lateral root initiation; cell expansion and division	Deeks et al., 2005; Yi et al., 2005; Xue et al., 2011
AtFH14	Bundles both AFs and MTs; crosslinks AFs and MTs together	Preprophase band; phragmoplast	Cell division	Li et al., 2010
OsFH5	Bundles both AFs and MTs	Chloroplast surface	Cell expansion	Yang et al., 2011; Zhang et al., 2011a
AtTHRUMIN1	Light-dependent actin bundling activity	Cell membrane	Chloroplast movement	Whippo et al., 2011
AtAVB1-3	Part of the V-ATPase multimeric complex	Endomembrane system	–	Ma et al., 2012
AtSCAB1	Dimerizes; likely regulated by phosphoinositides	Cytoplasm	Stomatal movement	Zhao et al., 2011; Zhang et al., 2012
VILLINS				
LIP-135-ABP and LIP-115-ABP	Ca^{2+} sensitive; bundle AFs with uniform polarity	Cytoplasm	Direction of cytoplasmic streaming in pollen tubes and root hair cells	Yokota et al., 1998, 2000, 2003, 2005; Yokota and Shimmen, 1999; Tominaga et al., 2000
AtVLN1	Ca^{2+} insensitive; lacks severing and capping activities	–	–	Huang et al., 2005; Khurana et al., 2010
AtVLN2	Ca^{2+} sensitive; has severing and capping activities	Cytoplasm	Directional organ growth; Sclerenchyma development	Bao et al., 2012; van der Honing et al., 2012
AtVLN3	Ca^{2+} sensitive; has severing and capping activities; can sever AtVLN1-induced bundles *in vitro*	Cytoplasm	Directional organ growth; Sclerenchyma development	Khurana et al., 2010; Bao et al., 2012; van der Honing et al., 2012
AtVLN4	Ca^{2+} sensitive; has severing and capping activities	Cytoplasm	Root hair growth and cytoplasmic streaming	Zhang et al., 2011b
AtVLN5	Ca^{2+} sensitive; has severing and capping activities	Cytoplasm	Pollen tube growth	Zhang et al., 2010
LIM PROTEINS				
NtWLIM1	Interacts directly with DNA	Cytoplasm; nucleus	Gene expression (lignin biosynthesis)	Kawaoka et al., 2000; Kaothien et al., 2002; Thomas et al., 2006, 2007
NtWLIM2	Interacts directly with DNA; dimerizes	Cytoplasm; nucleus	Gene expression (Histones)	Moes et al., 2012

(Continued)

Table 1 | Continued

Name	Remarkable features	Reported subcellular locations	Identified or suggested biological functions	Key references
AtWLIM1, 2a and b	Ca^{2+} and pH insensitive	Cytoplasm; nucleus	–	Papuga et al., 2010
AtPLIM2a and b	Only pH sensitive	Cytoplasm; nucleus	Pollen tube growth	Papuga et al., 2010; Ye and Xu, 2012
AtPLIM2c	Ca^{2+} and pH sensitive	Cytoplasm; nucleus	Pollen tube growth	Papuga et al., 2010; Ye and Xu, 2012
LILIM1	Ca^{2+} and pH sensitive	Cytoplasm; nucleus	Pollen tube growth	Wang et al., 2008
FIMBRINS				
AtFIM1	Ca^{2+} insensitive	Cytoplasm	Cytoplasmic streaming	Kovar et al., 2000, 2001
AtFIM5	Ca^{2+} insensitive	Cytoplasm	Pollen tube germination and growth	Wu et al., 2010
OTHER ABP FAMILIES				
Sb401	Bundles both AFs and MTs; activity possibly switched toward actin bundling by phosphorylation; genus-specific protein	Cytoplasm; cell cortex	–	Huang et al., 2007; Liu et al., 2009
AtADF9	Expression induced by hormones; lacks conventional ADF AF severing activity	Cytoplasm; nucleus	Gene expression (repression of flowering); development	Burgos-Rivera et al., 2008; Tholl et al., 2011

In the column "Reported subcellular locations," the term "cytoplasm" means no association with any specific organelle. Note that, in some cases, the "Identified or suggested biological functions" is not directly related to the actin bundling activity of the protein, e.g., nuclear functions. AFs, actin filaments; ER, endoplasmic reticulum; MT, microtubules.

function is to increase actin dynamics (Staiger and Blanchoin, 2006; Ono, 2007; Van Troys et al., 2008b; Bernstein and Bamburg, 2010). Whereas vertebrates typically possess three ADFs/cofilins, plant ADF families are particularly large. Indeed, *Arabidopsis* expresses 11 functional ADFs (AtADF1-11) which can be divided into 5 subclasses according to their tissular expression and phylogeny (Ruzicka et al., 2007). Recently, time-lapse TIRFM analyses provided direct evidence that subclass I AtADF1 and AtADF4 sever actin filaments *in vitro* (Khurana et al., 2010; Henty et al., 2011), an activity displayed by most animal, protozoa, and yeast ADFs/cofilins (e.g., Andrianantoandro and Pollard, 2006; Chan et al., 2009). In agreement with these data and the role predicted for actin severing in the stochastic dynamics of plant actin filaments (Michelot et al., 2007; Blanchoin et al., 2010; Staiger et al., 2010), Henty et al. (2011) established that *Arabidopsis adf4* knockout mutants exhibit a 2.5-fold reduced severing frequency as well as other characteristics of reduced actin dynamics in the cortical region of hypocotyl epidermal cells.

We recently compared the biochemical activities of *Arabidopsis* ADFs from different subclasses (unpublished data). We found that, contrary to other ADFs, subclass III AtADF9 is unable to enhance actin depolymerization *in vitro* (Tholl et al., 2011). Instead, AtADF9 stabilizes and crosslinks actin filaments into large bundles. By transiently expressing GFP-tagged and untagged AtADF9 recombinant proteins in tobacco BY2 cells, we confirmed the actin-bundling activity of AtADF9 in a live cell context. Indeed, contrary to AtADF1 which induced many breaks in the actin cytoskeleton, AtADF9 reduced the density and increased the thickness of actin fibers. Interestingly, similar data were obtained with AtADF5 (unpublished data), the other member of *Arabidopsis* ADF subclass III. Future work should identify the structural features responsible for the unconventional activities of subclass III ADFs, and compare the developmental and actin cytoskeleton phenotypes of *adf5* and *adf9* mutants to those recently reported for the knockout mutant of the conventional ADF AtADF4 (Henty et al., 2011).

Table 1 lists the actin bundling proteins cited in the present article and emphasizes some of their important features.

CONCLUSIONS

The growing number and diversity of actin-bundling proteins identified in plants indicate that, like animals, plants elaborate various types of actin-bundles with specific structural features and distinct functions (**Table 1**). This implies that the functions of actin bundles extend beyond the traditional definition of stable tracks for long distance intracellular transport. The characterization of novel types of actin-bundling proteins points out potential functions for actin bundles in stomatal movement, ion channel trafficking and/or activities, and chloroplast movement. In addition, actin bundles most likely play an important role in the regulation of hormone carriers cycling between plasma membrane and intracellular compartments (Nick, 2010). The specific actin bundling proteins involved in this process as well as their mode of regulation however remain to be identified.

Precise actin filament dynamics and organization near the plant cell cortex have been resolved only recently, and the

elucidation of the roles of actin filaments and bundles at this location will keep researchers busy during the years to come. Future work should establish why epidermal plant cells keep their cortical actin network so dynamic and whether the other cell types do the same. A number of actin-bundling proteins reviewed in this article support the existence of a physical linkage between actin bundles and membranes. Among those, formins emerge as key multifunctional ABPs able to initiate polymerization and bundling of filaments from diverse types of subcellular locations including the cell membrane. Noticeably, the recent work by Martiniere et al. (2011) provides compelling evidence that the *Arabidopsis* formin AtAFH1 is anchored by its predicted extracellular domain within the cell wall and bridges the latter to the actin cytoskeleton. A next important step consists in identifying the external signals that target the extracellular domain of class I formins and in characterizing how such signals modulate the intracellular activities of formins. In addition, one can expect that, following the pioneering work on AtADF4 by Henty et al. (2011), the exact contribution of formins to actin nucleation and bundling near the cell cortex, and more generally to the actin stochastic dynamics, will be soon characterized. During the reviewing process of the present article, a publication by Deeks et al. (2012) reporting the identification of a novel and plant-specific superfamily of ABPs termed Networked (NET) was released. Localization analyses strongly suggest that the *Arabidopsis* NET proteins function as linkers between the actin cytoskeleton and diverse types of membranes, including specific subdomains of the plasma membrane, the tonoplast and the nuclear membrane. There is no doubt that such an exciting discovery will boost the field and contribute to a better understanding of how AFs and actin bundles are coupled to membranes in plant cells.

ACKNOWLEDGMENTS

Work in the author's lab is supported by the Ministry of Culture, Higher Education, and Research and the National Research Fund from Luxembourg (project: HUMCRP, C10/BM/784171).

REFERENCES

Adams, D. S., Robinson, K. R., Fukumoto, T., Yuan, S., Albertson, R. C., Yelick, P., Kuo, L., McSweeney, M., and Levin, M. (2006). Early, H+-V-ATPase-dependent proton flux is necessary for consistent left-right patterning of non-mammalian vertebrates. *Development* 133, 1657–1671.

Alexandersson, E., Saalbach, G., Larsson, C., and Kjellbom, P. (2004). Arabidopsis plasma membrane proteomics identifies components of transport, signal transduction and membrane trafficking. *Plant Cell Physiol.* 45, 1543–1556.

Al Tanoury, Z., Schaffner-Reckinger, E., Halavatyi, A., Hoffmann, C., Moes, M., Hadzic, E., Catillon, M., Yatskou, M., and Friederich, E. (2010). Quantitative kinetic study of the actin-bundling protein L-plastin and of its impact on actin turn-over. *PLoS ONE* 5:e9210. doi: 10.1371/journal.pone.0009210

Andrianantoandro, E., and Pollard, T. D. (2006). Mechanism of actin filament turnover by severing and nucleation at different concentrations of ADF/cofilin. *Mol. Cell* 24, 13–23.

Arber, S., and Caroni, P. (1996). Specificity of single LIM motifs in targeting and LIM/LIM interactions *in situ*. *Genes Dev.* 10, 289–300.

Arber, S., Halder, G., and Caroni, P. (1994). Muscle LIM protein, a novel essential regulator of myogenesis, promotes myogenic differentiation. *Cell* 79, 221–231.

Arnaud, D., Dejardin, A., Leple, J. C., Lesage-Descauses, M. C., Boizot, N., Villar, M., Benedetti, H., and Pilate, G. (2012). Expression analysis of LIM gene family in poplar, toward an updated phylogenetic classification. *BMC Res. Notes* 5, 102.

Avisar, D., Prokhnevsky, A. I., Makarova, K. S., Koonin, E. V., and Dolja, V. V. (2008). Myosin XI-K is required for rapid trafficking of Golgi stacks, peroxisomes, and mitochondria in leaf cells of *Nicotiana benthamiana*. *Plant Physiol.* 146, 1098–1108.

Baluska, F., Jasik, J., Edelmann, H. G., Salajova, T., and Volkmann, D. (2001). Latrunculin B-induced plant dwarfism: plant cell elongation is F-actin-dependent. *Dev. Biol.* 231, 113–124.

Baluska, F., Samaj, J., Wojtaszek, P., Volkmann, D., and Menzel, D. (2003). Cytoskeleton-plasma membrane-cell wall continuum in plants. Emerging links revisited. *Plant Physiol.* 133, 482–491.

Banno, H., and Chua, N. H. (2000). Characterization of the arabidopsis formin-like protein AFH1 and its interacting protein. *Plant Cell Physiol.* 41, 617–626.

Bao, C., Wang, J., Zhang, R., Zhang, B., Zhang, H., Zhou, Y., and Huang, S. (2012). Arabidopsis VILLIN2 and VILLIN3 act redundantly in sclerenchyma development via bundling of actin filaments. *Plant J.* doi: 10.1111/j.1365-313X.2012.05044.x. [Epub ahead of print].

Bernstein, B. W., and Bamburg, J. R. (2010). ADF/cofilin: a functional node in cell biology. *Trends Cell Biol.* 20, 187–195.

Blanchoin, L., Boujemaa-Paterski, R., Henty, J. L., Khurana, P., and Staiger, C. J. (2010). Actin dynamics in plant cells: a team effort from multiple proteins orchestrates this very fast-paced game. *Curr. Opin. Plant Biol.* 13, 714–723.

Blanchoin, L., and Staiger, C. J. (2008). Plant formins: diverse isoforms and unique molecular mechanism. *Biochim. Biophys. Acta*. 1803, 201–206.

Boateng, S. Y., Belin, R. J., Geenen, D. L., Margulies, K. B., Martin, J. L., Hoshijima, M., De Tombe, P. P., and Russell, B. (2007). Cardiac dysfunction and heart failure are associated with abnormalities in the subcellular distribution and amounts of oligomeric muscle LIM protein. *Am. J. Physiol. Heart Circ. Physiol.* 292, H259–H269.

Boateng, S. Y., Senyo, S. E., Qi, L., Goldspink, P. H., and Russell, B. (2009). Myocyte remodeling in response to hypertrophic stimuli requires nucleocytoplasmic shuttling of muscle LIM protein. *J. Mol. Cell. Cardiol.* 47, 426–435.

Bretscher, A. (1981). Fimbrin is a cytoskeletal protein that crosslinks F-actin *in vitro*. *Proc. Natl. Acad. Sci. U.S.A.* 78, 6849–6853.

Briere, C., Bordel, A. C., Barthou, H., Jauneau, A., Steinmetz, A., Alibert, G., and Petitprez, M. (2003). Is the LIM-domain protein HaWLIM1 associated with cortical microtubules in sunflower protoplasts? *Plant Cell Physiol.* 44, 1055–1063.

Brux, A., Liu, T. Y., Krebs, M., Stierhof, Y. D., Lohmann, J. U., Miersch, O., Wasternack, C., and Schumacher, K. (2008). Reduced V-ATPase activity in the trans-Golgi network causes oxylipin-dependent hypocotyl growth Inhibition in Arabidopsis. *Plant Cell* 20, 1088–1100.

Burgos-Rivera, B., Ruzicka, D. R., Deal, R. B., McKinney, E. C., King-Reid, L., and Meagher, R. B. (2008). ACTIN DEPOLYMERIZING FACTOR9 controls development and gene expression in Arabidopsis. *Plant Mol. Biol.* 68, 619–632.

Carnell, M., Zech, T., Calaminus, S. D., Ura, S., Hagedorn, M., Johnston, S. A., May, R. C., Soldati, T., Machesky, L. M., and Insall, R. H. (2011). Actin polymerization driven by WASH causes V-ATPase retrieval and vesicle neutralization before exocytosis. *J. Cell Biol.* 193, 831–839.

Chan, C., Beltzner, C. C., and Pollard, T. D. (2009). Cofilin dissociates Arp2/3 complex and branches from actin filaments. *Curr. Biol.* 19, 537–545.

Chang, D. F., Belaguli, N. S., Chang, J., and Schwartz, R. J. (2007). LIM-only protein, CRP2, switched on smooth muscle gene activity in adult cardiac myocytes. *Proc. Natl. Acad. Sci. U.S.A.* 104, 157–162.

Chang, D. F., Belaguli, N. S., Iyer, D., Roberts, W. B., Wu, S. P., Dong, X. R., Marx, J. G., Moore, M. S., Beckerle, M. C., Majesky, M. W., and Schwartz, R. J. (2003). Cysteine-rich LIM-only proteins CRP1 and CRP2 are potent smooth muscle differentiation cofactors. *Dev. Cell* 4, 107–118.

Chen, S. H., Bubb, M. R., Yarmola, E. G., Zuo, J., Jiang, J., Lee, B. S., Lu, M., Gluck, S. L., Hurst, I. R., and Holliday, L. S. (2004). Vacuolar H+-ATPase binding to microfilaments: regulation in response to phosphatidylinositol 3-kinase activity and detailed characterization of the actin-binding site in subunit B. *J. Biol. Chem.* 279, 7988–7998.

Cheung, A. Y., Niroomand, S., Zou, Y., and Wu, H. M. (2010). A transmembrane formin nucleates subapical actin assembly and controls tip-focused growth in pollen tubes. *Proc. Natl. Acad. Sci. U.S.A.* 107, 16390–16395.

Cheung, A. Y., and Wu, H. M. (2004). Overexpression of an Arabidopsis formin stimulates supernumerary actin cable formation from pollen tube cell membrane. *Plant Cell* 16, 257–269.

Cheung, A. Y., and Wu, H. M. (2008). Structural and signaling networks for the polar cell growth machinery in pollen tubes. *Annu. Rev. Plant Biol.* 59, 547–572.

Choi, Y., Lee, Y., Jeon, B. W., and Staiger, C. J. (2008). Phosphatidylinositol 3- and 4-phosphate modulate actin filament reorganization in guard cells of day flower. *Plant Cell Environ.* 31, 366–377.

Chuong, S. D., Franceschi, V. R., and Edwards, G. E. (2006). The cytoskeleton maintains organelle partitioning required for single-cell C4 photosynthesis in Chenopodiaceae species. *Plant Cell* 18, 2207–2223.

Ciobanasu, C., Faivre, B., and Le Clainche, C. (2012). Actin dynamics associated with focal adhesions. *Int. J. Cell Biol.* 2012, 941292.

Collings, D. (2008). "Crossed-wires: interactions and cross-talk between the microtubule and microfilament networks in plants," in *Plant Microtubules, Plant Cell Monographs,* ed N. Peter (Berlin: Springer), 47–79.

Crowell, E. F., Bischoff, V., Desprez, T., Rolland, A., Stierhof, Y. D., Schumacher, K., Gonneau, M., Hofte, H., and Vernhettes, S. (2009). Pausing of Golgi bodies on microtubules regulates secretion of cellulose synthase complexes in Arabidopsis. *Plant Cell* 21, 1141–1154.

Cvrckova, F. (2000). Are plant formins integral membrane proteins? *Genome Biol.* 1, RESEARCH001.

Day, B., Henty, J. L., Porter, K. J., and Staiger, C. J. (2011). The pathogen-actin connection: a platform for defense signaling in plants. *Annu. Rev. Phytopathol.* 49, 483–506.

Deeks, M. J., Calcutt, J. R., Ingle, E. K., Hawkins, T. J., Chapman, S., Richardson, A. C., Mentlak, D. A., Dixon, M. R., Cartwright, F., Smertenko, A. P., Oparka, K., and Hussey, P. J. (2012). A Superfamily of Actin-Binding Proteins at the Actin-Membrane Nexus of Higher Plants. *Curr. Biol.* doi: 10.1016/j.cub.2012.06.041. [Epub ahead of print].

Deeks, M. J., Cvrckova, F., Machesky, L. M., Mikitova, V., Ketelaar, T., Zarsky, V., Davies, B., and Hussey, P. J. (2005). Arabidopsis group Ie formins localize to specific cell membrane domains, interact with actin-binding proteins and cause defects in cell expansion upon aberrant expression. *New Phytol.* 168, 529–540.

Deeks, M. J., Fendrych, M., Smertenko, A., Bell, K. S., Oparka, K., Cvrckova, F., Zarsky, V., and Hussey, P. J. (2010). The plant formin AtFH4 interacts with both actin and microtubules, and contains a newly identified microtubule-binding domain. *J. Cell Sci.* 123, 1209–1215.

Deeks, M. J., and Hussey, P. J. (2005). Arp2/3 and SCAR: plants move to the fore. *Nat. Rev. Mol. Cell Biol.* 6, 954–964.

Deeks, M. J., Hussey, P. J., and Davies, B. (2002). Formins: intermediates in signal-transduction cascades that affect cytoskeletal reorganization. *Trends Plant Sci.* 7, 492–498.

Dettmer, J., Hong-Hermesdorf, A., Stierhof, Y. D., and Schumacher, K. (2006). Vacuolar H+-ATPase activity is required for endocytic and secretory trafficking in Arabidopsis. *Plant Cell* 18, 715–730.

Dong, C. H., Xia, G. X., Hong, Y., Ramachandran, S., Kost, B., and Chua, N. H. (2001). ADF proteins are involved in the control of flowering and regulate F-actin organization, cell expansion, and organ growth in Arabidopsis. *Plant Cell* 13, 1333–1346.

Drobak, B. K., Franklin-Tong, V. E., and Staiger, C. J. (2004). The role of the actin cytoskeleton in plant cell signaling. *New Phytol.* 163, 13–30.

Eun, S. O., and Lee, Y. (1997). Actin filaments of guard cells are reorganized in response to light and abscisic acid. *Plant Physiol.* 115, 1491–1498.

Favery, B., Chelysheva, L. A., Lebris, M., Jammes, F., Marmagne, A., De Almeida-Engler, J., Lecomte, P., Vaury, C., Arkowitz, R. A., and Abad, P. (2004). Arabidopsis formin AtFH6 is a plasma membrane-associated protein upregulated in giant cells induced by parasitic nematodes. *Plant Cell* 16, 2529–2540.

Freyd, G., Kim, S. K., and Horvitz, H. R. (1990). Novel cysteine-rich motif and homeodomain in the product of the Caenorhabditis elegans cell lineage gene lin-11. *Nature* 344, 876–879.

Fu, Y. (2010). The actin cytoskeleton and signaling network during pollen tube tip growth. *J. Integr. Plant Biol.* 52, 131–137.

Fu, Y., Gu, Y., Zheng, Z., Wasteneys, G., and Yang, Z. (2005). Arabidopsis interdigitating cell growth requires two antagonistic pathways with opposing action on cell morphogenesis. *Cell* 120, 687–700.

Gao, X. Q., Chen, J., Wei, P. C., Ren, F., and Wang, X. C. (2008). Array and distribution of actin filaments in guard cells contribute to the determination of stomatal aperture. *Plant Cell Rep.* 27, 1655–1665.

Geiger, B., Spatz, J. P., and Bershadsky, A. D. (2009). Environmental sensing through focal adhesions. *Nat. Rev. Mol. Cell Biol.* 10, 21–33.

Hardham, A. R., Jones, D. A., and Takemoto, D. (2007). Cytoskeleton and cell wall function in penetration resistance. *Curr. Opin. Plant Biol.* 10, 342–348.

Hardham, A. R., Takemoto, D., and White, R. G. (2008). Rapid and dynamic subcellular reorganization following mechanical stimulation of Arabidopsis epidermal cells mimics responses to fungal and oomycete attack. *BMC Plant Biol.* 8, 63.

Henty, J. L., Bledsoe, S. W., Khurana, P., Meagher, R. B., Day, B., Blanchoin, L., and Staiger, C. J. (2011). Arabidopsis actin depolymerizing factor4 modulates the stochastic dynamic behavior of actin filaments in the cortical array of epidermal cells. *Plant Cell* 23, 3711–3726.

Higaki, T., Kojo, K. H., and Hasezawa, S. (2010a). Critical role of actin bundling in plant cell morphogenesis. *Plant Signal. Behav.* 5, 1–5.

Higaki, T., Kutsuna, N., Sano, T., Kondo, N., and Hasezawa, S. (2010b). Quantification and cluster analysis of actin cytoskeletal structures in plant cells: role of actin bundling in stomatal movement during diurnal cycles in Arabidopsis guard cells. *Plant J.* 61, 156–165.

Higaki, T., Kurusu, T., Hasezawa, S., and Kuchitsu, K. (2011). Dynamic intracellular reorganization of cytoskeletons and the vacuole in defense responses and hypersensitive cell death in plants. *J. Plant Res.* 124, 315–324.

Holdaway-Clarke, T. L., and Hepler, P. K. (2003). Control of pollen tube growth: role of ion gradients and fluxes. *New Phytol.* 159, 539–563.

Holliday, L. S., Lu, M., Lee, B. S., Nelson, R. D., Solivan, S., Zhang, L., and Gluck, S. L. (2000). The amino-terminal domain of the B subunit of vacuolar H+-ATPase contains a filamentous actin binding site. *J. Biol. Chem.* 275, 32331–32337.

Huang, S., Jin, L., Du, J., Li, H., Zhao, Q., Ou, G., Ao, G., and Yuan, M. (2007). SB401, a pollen-specific protein from *Solanum berthaultii*, binds to and bundles microtubules and F-actin. *Plant J.* 51, 406–418.

Huang, S., Robinson, R. C., Gao, L. Y., Matsumoto, T., Brunet, A., Blanchoin, L., and Staiger, C. J. (2005). Arabidopsis VILLIN1 generates actin filament cables that are resistant to depolymerization. *Plant Cell* 17, 486–501.

Humphrey, T. V., Bonetta, D. T., and Goring, D. R. (2007). Sentinels at the wall: cell wall receptors and sensors. *New Phytol.* 176, 7–21.

Hwang, J. U., and Lee, Y. (2001). Abscisic acid-induced actin reorganization in guard cells of dayflower is mediated by cytosolic calcium levels and by protein kinase and protein phosphatase activities. *Plant Physiol.* 125, 2120–2128.

Ingouff, M., Fitz Gerald, J. N., Guerin, C., Robert, H., Sorensen, M. B., Van Damme, D., Geelen, D., Blanchoin, L., and Berger, F. (2005). Plant formin AtFH5 is an evolutionarily conserved actin nucleator involved in cytokinesis. *Nat. Cell Biol.* 7, 374–380.

Kadota, A., Yamada, N., Suetsugu, N., Hirose, M., Saito, C., Shoda, K., Ichikawa, S., Kagawa, T., Nakano, A., and Wada, M. (2009). Short actin-based mechanism for light-directed chloroplast movement in Arabidopsis. *Proc. Natl. Acad. Sci. U.S.A.* 106, 13106–13111.

Kaothien, P., Kawaoka, A., Ebinuma, H., Yoshida, K., and Shinmyo, A. (2002). Ntlim1, a PAL-box binding factor, controls promoter activity of the horseradish wound-inducible peroxidase gene. *Plant Mol. Biol.* 49, 591–599.

Karlsson, O., Thor, S., Norberg, T., Ohlsson, H., and Edlund, T. (1990). Insulin gene enhancer binding protein Isl-1 is a member of a novel class of proteins containing both a homeo- and a Cys-His domain. *Nature* 344, 879–882.

Kasahara, M., Kagawa, T., Oikawa, K., Suetsugu, N., Miyao, M., and Wada, M. (2002). Chloroplast avoidance movement reduces photodamage in plants. *Nature* 420, 829–832.

Kawaoka, A., and Ebinuma, H. (2001). Transcriptional control of lignin biosynthesis by tobacco LIM protein. *Phytochemistry* 57, 1149–1157.

Kawaoka, A., Kaothien, P., Yoshida, K., Endo, S., Yamada, K., and Ebinuma, H. (2000). Functional

analysis of tobacco LIM protein Ntlim1 involved in lignin biosynthesis. *Plant J.* 22, 289–301.

Kawaoka, A., Sato, S., Nakahara, K., Matsushima, N., Okada, N., Sekine, M., Shinmyo, A., and Takano, M. (1992). Expression and promoter activity of genes for isozymes of horseradish peroxidase. *Plant Cell Physiol.* 33, 1143–1150.

Ketelaar, T., Faivre-Moskalenko, C., Esseling, J. J., De Ruijter, N. C., Grierson, C. S., Dogterom, M., and Emons, A. M. (2002). Positioning of nuclei in Arabidopsis root hairs: an actin-regulated process of tip growth. *Plant Cell* 14, 2941–2955.

Khurana, P., Henty, J. L., Huang, S., Staiger, A. M., Blanchoin, L., and Staiger, C. J. (2010). Arabidopsis VILLIN1 and VILLIN3 have overlapping and distinct activities in actin bundle formation and turnover. *Plant Cell* 22, 2727–2748.

Kim, M., Hepler, P. K., Eun, S. O., Ha, K. S., and Lee, Y. (1995). Actin filaments in mature guard cells are radially distributed and involved in stomatal movement. *Plant Physiol.* 109, 1077–1084.

Kim-Kaneyama, J. R., Suzuki, W., Ichikawa, K., Ohki, T., Kohno, Y., Sata, M., Nose, K., and Shibanuma, M. (2005). Uni-axial stretching regulates intracellular localization of Hic-5 expressed in smooth-muscle cells *in vitro*. *J. Cell Sci.* 118, 937–949.

Klahre, U., Friederich, E., Kost, B., Louvard, D., and Chua, N. H. (2000). Villin-like actin-binding proteins are expressed ubiquitously in Arabidopsis. *Plant Physiol.* 122, 35–48.

Klein, M. G., Shi, W., Ramagopal, U., Tseng, Y., Wirtz, D., Kovar, D. R., Staiger, C. J., and Almo, S. C. (2004). Structure of the actin crosslinking core of fimbrin. *Structure (Camb.)* 12, 999–1013.

Knight, M. R. (2007). New ideas on root hair growth appear from the flanks. *Proc. Natl. Acad. Sci. U.S.A.* 104, 20649–20650.

Knoll, R., Hoshijima, M., Hoffman, H. M., Person, V., Lorenzen-Schmidt, I., Bang, M. L., Hayashi, T., Shiga, N., Yasukawa, H., Schaper, W., McKenna, W., Yokoyama, M., Schork, N. J., Omens, J. H., McCulloch, A. D., Kimura, A., Gregorio, C. C., Poller, W., Schaper, J., Schultheiss, H. P., and Chien, K. R. (2002). The cardiac mechanical stretch sensor machinery involves a Z disc complex that is defective in a subset of human dilated cardiomyopathy. *Cell* 111, 943–955.

Kobayashi, I., Kobayashi, Y., and Hardham, A. R. (1994). Dynamic reorganization of microtubules and microfilaments in flax cells during the resistance response to flax rust infection. *Planta* 195, 237–247.

Kong, Y., Flick, M. J., Kudla, A. J., and Konieczny, S. F. (1997). Muscle LIM protein promotes myogenesis by enhancing the activity of MyoD. *Mol. Cell. Biol.* 17, 4750–4760.

Kovar, D. R., Gibbon, B. C., McCurdy, D. W., and Staiger, C. J. (2001). Fluorescently-labeled fimbrin decorates a dynamic actin filament network in live plant cells. *Planta* 213, 390–395.

Kovar, D. R., Staiger, C. J., Weaver, E. A., and McCurdy, D. W. (2000). AtFim1 is an actin filament crosslinking protein from *Arabidopsis thaliana*. *Plant J.* 24, 625–636.

Krebs, M., Beyhl, D., Gorlich, E., Al-Rasheid, K. A., Marten, I., Stierhof, Y. D., Hedrich, R., and Schumacher, K. (2010). Arabidopsis V-ATPase activity at the tonoplast is required for efficient nutrient storage but not for sodium accumulation. *Proc. Natl. Acad. Sci. U.S.A.* 107, 3251–3256.

Leckie, C. P., Callow, J. A., and Green, J. R. (1995). Reorganization of the endoplasmic reticulum in pea leaf epidermal cells infected by the powdery mildew fungus *Erysiphe pisi*. *New Phytol.* 131, 211–221.

Lee, B. S., Gluck, S. L., and Holliday, L. S. (1999). Interaction between vacuolar H(+)-ATPase and microfilaments during osteoclast activation. *J. Biol. Chem.* 274, 29164–29171.

Lemichez, E., Wu, Y., Sanchez, J. P., Mettouchi, A., Mathur, J., and Chua, N. H. (2001). Inactivation of AtRac1 by abscisic acid is essential for stomatal closure. *Genes Dev.* 15, 1808–1816.

Li, Y., Shen, Y., Cai, C., Zhong, C., Zhu, L., Yuan, M., and Ren, H. (2010). The type II Arabidopsis formin14 interacts with microtubules and microfilaments to regulate cell division. *Plant Cell* 22, 2710–2726.

Liu, B. Q., Jin, L., Zhu, L., Li, J., Huang, S., and Yuan, M. (2009). Phosphorylation of microtubule-associated protein SB401 from *Solanum berthaultii* regulates its effect on microtubules. *J. Integr. Plant Biol.* 51, 235–242.

Liu, J., Seul, U., and Thompson, R. (1997). Cloning and characterization of a pollen-specific cDNA encoding a glutamic-acid-rich protein (GARP) from potato *Solanum berthaultii*. *Plant. Mol. Biol.* 33, 291–300.

Liu, K., and Luan, S. (1998). Voltage-dependent K+ channels as targets of osmosensing in guard cells. *Plant Cell* 10, 1957–1970.

Lovy-Wheeler, A., Wilsen, K. L., Baskin, T. I., and Hepler, P. K. (2005). Enhanced fixation reveals the apical cortical fringe of actin filaments as a consistent feature of the pollen tube. *Planta* 221, 95–104.

Ma, B., Qian, D., Nan, Q., Tan, C., An, L., and Xiang, Y. (2012). Arabidopsis vacuolar H+-ATPase (V-ATPase) B subunits are involved in actin cytoskeleton remodeling via binding to, bundling, and stabilizing F-actin. *J. Biol. Chem.* 287, 19008–19017.

Ma, B., Xiang, Y., and An, L. (2011). Structural bases of physiological functions and roles of the vacuolar H(+)-ATPase. *Cell. Signal.* 23, 1244–1256.

Macrobbie, E. A., and Kurup, S. (2007). Signalling mechanisms in the regulation of vacuolar ion release in guard cells. *New Phytol.* 175, 630–640.

Martiniere, A., Gayral, P., Hawes, C., and Runions, J. (2011). Building bridges: formin1 of Arabidopsis forms a connection between the cell wall and the actin cytoskeleton. *Plant J.* 66, 354–365.

Michelot, A., Berro, J., Guerin, C., Boujemaa-Paterski, R., Staiger, C. J., Martiel, J. L., and Blanchoin, L. (2007). Actin-filament stochastic dynamics mediated by ADF/cofilin. *Curr. Biol.* 17, 825–833.

Michelot, A., Derivery, E., Paterski-Boujemaa, R., Guerin, C., Huang, S., Parcy, F., Staiger, C. J., and Blanchoin, L. (2006). A novel mechanism for the formation of actin-filament bundles by a nonprocessive formin. *Curr. Biol.* 16, 1924–1930.

Michelot, A., Guerin, C., Huang, S., Ingouff, M., Richard, S., Rodiuc, N., Staiger, C. J., and Blanchoin, L. (2005). The formin homology 1 domain modulates the actin nucleation and bundling activity of Arabidopsis FORMIN1. *Plant Cell* 17, 2296–2313.

Miller, D. D., De Ruijter, N. C., Bisseling, T., and Emons, A. M. (1999). The role of actin in root hair morphogenesis: studies with lipochito-oligosaccharide as a growth stimulator and cytochalasin as an actin perturbing drug. *Plant J.* 17, 141–154.

Moes, D., Gatti, S., Hoffmann, C., Dieterle, M., Moreau, F., Neumann, K., Schumacher, M., Diederich, M., Grill, E., Shen, W. H., Steinmetz, A., and Thomas, C. (2012). A LIM domain protein from tobacco involved in actinbundling and histone gene transcription. *Mol. Plant*. doi: 10.1093/mp/SSS075. [Epub ahead of print].

Morley, S. C. (2012). The actin-bundling protein L-plastin: a critical regulator of immune cell function. *Int. J. Cell Biol.* 2012, Article ID: 935173.

Mundel, C., Baltz, R., Eliasson, A., Bronner, R., Grass, N., Krauter, R., Evrard, J. L., and Steinmetz, A. (2000). A LIM-domain protein from sunflower is localized to the cytoplasm and/or nucleus in a wide variety of tissues and is associated with the phragmoplast in dividing cells. *Plant Mol. Biol.* 42, 291–302.

Nelson, N. (2003). A journey from mammals to yeast with vacuolar H+-ATPase (V-ATPase). *J. Bioenerg. Biomembr.* 35, 281–289.

Nick, P. (2010). Probing the actin-auxin oscillator. *Plant Signal. Behav.* 5, 94–98.

Nick, P., Han, M. J., and An, G. (2009). Auxin stimulates its own transport by shaping actin filaments. *Plant Physiol.* 151, 155–167.

Nishi, T., and Forgac, M. (2002). The vacuolar (H+)-ATPases–nature's most versatile proton pumps. *Nat. Rev. Mol. Cell Biol.* 3, 94–103.

Oikawa, K., Kasahara, M., Kiyosue, T., Kagawa, T., Suetsugu, N., Takahashi, F., Kanegae, T., Niwa, Y., Kadota, A., and Wada, M. (2003). Chloroplast unusual positioning1 is essential for proper chloroplast positioning. *Plant Cell* 15, 2805–2815.

Oikawa, K., Yamasato, A., Kong, S. G., Kasahara, M., Nakai, M., Takahashi, F., Ogura, Y., Kagawa, T., and Wada, M. (2008). Chloroplast outer envelope protein CHUP1 is essential for chloroplast anchorage to the plasma membrane and chloroplast movement. *Plant Physiol.* 148, 829–842.

Ono, S. (2007). Mechanism of depolymerization and severing of actin filaments and its significance in cytoskeletal dynamics. *Int. Rev. Cytol.* 258, 1–82.

Opalski, K. S., Schultheiss, H., Kogel, K. H., and Huckelhoven, R. (2005). The receptor-like MLO protein and the RAC/ROP family G-protein RACB modulate actin reorganization in barley attacked by the biotrophic powdery mildew fungus *Blumeria graminis* f.sp. hordei. *Plant J.* 41, 291–303.

Padmanaban, S., Lin, X., Perera, I., Kawamura, Y., and Sze, H. (2004). Differential expression of vacuolar H+-ATPase subunit c genes in tissues active in membrane trafficking and their roles in plant growth

as revealed by RNAi. *Plant Physiol.* 134, 1514–1526.

Papuga, J., Hoffmann, C., Dieterle, M., Moes, D., Moreau, F., Tholl, S., Steinmetz, A., and Thomas, C. (2010). Arabidopsis LIM proteins: a family of actin bundlers with distinct expression patterns and modes of regulation. *Plant Cell* 22, 3034–3052.

Paves, H., and Truve, E. (2007). Myosin inhibitors block accumulation movement of chloroplasts in *Arabidopsis thaliana* leaf cells. *Protoplasma* 230, 165–169.

Peremyslov, V. V., Prokhnevsky, A. I., Avisar, D., and Dolja, V. V. (2008). Two class XI myosins function in organelle trafficking and root hair development in Arabidopsis. *Plant Physiol.* 146, 1109–1116.

Petrasek, J., and Schwarzerova, K. (2009). Actin and microtubule cytoskeleton interactions. *Curr. Opin. Plant Biol.* 12, 728–734.

Pollard, T. D., Blanchoin, L., and Mullins, R. D. (2000). Molecular mechanisms controlling actin filament dynamics in nonmuscle cells. *Annu. Rev. Biophys. Biomol. Struct.* 29, 545–576.

Pollard, T. D., and Cooper, J. A. (2009). Actin, a central player in cell shape and movement. *Science* 326, 1208–1212.

Ruzicka, D. R., Kandasamy, M. K., McKinney, E. C., Burgos-Rivera, B., and Meagher, R. B. (2007). The ancient subclasses of Arabidopsis actin depolymerizing factor genes exhibit novel and differential expression. *Plant J.* 52, 460–472.

Samstag, Y., and Klemke, M. (2007). Ectopic expression of L-plastin in human tumor cells: diagnostic and therapeutic implications. *Adv. Enzyme Regul.* 47, 118–126.

Schmidt Von Braun, S., and Schleiff, E. (2008a). The chloroplast outer membrane protein CHUP1 interacts with actin and profilin. *Planta* 227, 1151–1159.

Schmidt Von Braun, S., and Schleiff, E. (2008b). Moving the green: CHUP1 and chloroplast movement-an obvious relationship? *Plant Signal. Behav.* 3, 488–489.

Schumacher, K., Vafeados, D., McCarthy, M., Sze, H., Wilkins, T., and Chory, J. (1999). The Arabidopsis det3 mutant reveals a central role for the vacuolar H(+)-ATPase in plant growth and development. *Genes Dev.* 13, 3259–3270.

Sheahan, M. B., Staiger, C. J., Rose, R. J., and McCurdy, D. W. (2004). A green fluorescent protein fusion to actin-binding domain 2 of Arabidopsis fimbrin highlights new features of a dynamic actin cytoskeleton in live plant cells. *Plant Physiol.* 136, 3968–3978.

Shinomiya, H. (2012). Plastin family of actin-bundling proteins: its functions in leukocytes, neurons, intestines, and cancer. *Int. J. Cell Biol.* 2012, 213492.

Showalter, A. M., Keppler, B., Lichtenberg, J., Gu, D., and Welch, L. R. (2010). A bioinformatics approach to the identification, classification, and analysis of hydroxyproline-rich glycoproteins. *Plant Physiol.* 153, 485–513.

Skau, C. T., Courson, D. S., Bestul, A. J., Winkelman, J. D., Rock, R. S., Sirotkin, V., and Kovar, D. R. (2011). Actin filament bundling by fimbrin is important for endocytosis, cytokinesis, and polarization in fission yeast. *J. Biol. Chem.* 286, 26964–26977.

Smertenko, A. P., Deeks, M. J., and Hussey, P. J. (2010). Strategies of actin reorganisation in plant cells. *J. Cell Sci.* 123, 3019–3028.

Smith, L. G., and Oppenheimer, D. G. (2005). Spatial control of cell expansion by the plant cytoskeleton. *Annu. Rev. Cell Dev. Biol.* 21, 271–295.

Sparkes, I. A., Teanby, N. A., and Hawes, C. (2008). Truncated myosin XI tail fusions inhibit peroxisome, golgi, and mitochondrial movement in tobacco leaf epidermal cells: a genetic tool for the next generation. *J. Exp. Bot.* 59, 2499–2512.

Staiger, C. J., and Blanchoin, L. (2006). Actin dynamics: old friends with new stories. *Curr. Opin. Plant Biol.* 9, 554–562.

Staiger, C. J., and Hussey, P. J. (2004). "Actin and actin-modulating proteins," in *The Plant Cytoskeleton in Cell Differentiation and Development,* ed P. J. Hussey (Oxford, UK: Blackwell Publishing), 32–80.

Staiger, C. J., Poulter, N. S., Henty, J. L., Franklin-Tong, V. E., and Blanchoin, L. (2010). Regulation of actin dynamics by actin-binding proteins in pollen. *J. Exp. Bot.* 61, 1969–1986.

Staiger, C. J., Sheahan, M. B., Khurana, P., Wang, X., McCurdy, D. W., and Blanchoin, L. (2009). Actin filament dynamics are dominated by rapid growth and severing activity in the Arabidopsis cortical array. *J. Cell Biol.* 184, 269–280.

Staiger, C. J., Yuan, M., Valenta, R., Shaw, P. J., Warn, R. M., and Lloyd, C. W. (1994). Microinjected profilin affects cytoplasmic streaming in plant cells by rapidly depolymerizing actin microfilaments. *Curr. Biol.* 4, 215–219.

Stevenson, R. P., Veltman, D., and Machesky, L. M. (2012). Actin-bundling proteins in cancer progression at a glance. *J. Cell Sci.* 125, 1073–1079.

Suetsugu, N., Yamada, N., Kagawa, T., Yonekura, H., Uyeda, T. Q., Kadota, A., and Wada, M. (2010a). Two kinesin-like proteins mediate actin-based chloroplast movement in *Arabidopsis thaliana*. *Proc. Natl. Acad. Sci. U.S.A.* 107, 8860–8865.

Suetsugu, N., Dolja, V. V., and Wada, M. (2010b). Why have chloroplasts developed a unique motility system? *Plant Signal. Behav.* 5, 1190–1196.

Suetsugu, N., and Wada, M. (2007). Chloroplast photorelocation movement mediated by phototropin family proteins in green plants. *Biol. Chem.* 388, 927–935.

Szymanski, D. B. (2005). Breaking the WAVE complex: the point of Arabidopsis trichomes. *Curr. Opin. Plant Biol.* 8, 103–112.

Szymanski, D. B., and Cosgrove, D. J. (2009). Dynamic coordination of cytoskeletal and cell wall systems during plant cell morphogenesis. *Curr. Biol.* 19, R800– R811.

Takemoto, D., Jones, D. A., and Hardham, A. R. (2006). Re-organization of the cytoskeleton and endoplasmic reticulum in the Arabidopsis pen1-1 mutant inoculated with the non-adapted powdery mildew pathogen, *Blumeria graminis* f. sp. hordei. *Mol. Plant Pathol.* 7, 553–563.

Tholl, S., Moreau, F., Hoffmann, C., Arumugam, K., Dieterle, M., Moes, D., Neumann, K., Steinmetz, A., and Thomas, C. (2011). Arabidopsis actin-depolymerizing factors (ADFs) 1 and 9 display antagonist activities. *FEBS Lett.* 585, 1821–1827.

Thomas, C., Hoffmann, C., Dieterle, M., Van Troys, M., Ampe, C., and Steinmetz, A. (2006). Tobacco WLIM1 is a novel F-actin binding protein involved in actin cytoskeleton remodeling. *Plant Cell* 18, 2194–2206.

Thomas, C., Moreau, F., Dieterle, M., Hoffmann, C., Gatti, S., Hofmann, C., Van Troys, M., Ampe, C., and Steinmetz, A. (2007). The LIM domains of WLIM1 define a new class of actin bundling modules. *J. Biol. Chem.* 282, 33599–33608.

Thomas, C., Tholl, S., Moes, D., Dieterle, M., Papuga, J., Moreau, F., and Steinmetz, A. (2009). Actin bundling in plants. *Cell. Motil. Cytoskeleton* 66, 940–957.

Tominaga, M., Yokota, E., Vidali, L., Sonobe, S., Hepler, P. K., and Shimmen, T. (2000). The role of plant villin in the organization of the actin cytoskeleton, cytoplasmic streaming and the architecture of the transvacuolar strand in root hair cells of Hydrocharis. *Planta* 210, 836–843.

Toth, R., Gerding-Reimers, C., Deeks, M. J., Menninger, S., Gallegos, R. M., Tonaco, I. A., Hubel, K., Hussey, P. J., Waldmann, H., and Coupland, G. (2012). Prieurianin/endosidin 1 is an actin-stabilizing small molecule identified from a chemical genetic screen for circadian clock effectors in *Arabidopsis thaliana*. *Plant J.* 71, 338–352.

Van Damme, D., Bouget, F. Y., Van Poucke, K., Inze, D., and Geelen, D. (2004). Molecular dissection of plant cytokinesis and phragmoplast structure: a survey of GFP-tagged proteins. *Plant J.* 40, 386–398.

van der Honing, H. S., Kieft, H., Emons, A. M., and Ketelaar, T. (2012). Arabidopsis VILLIN2 and VILLIN3 are required for the generation of thick actin filament bundles and for directional organ growth. *Plant Physiol.* 158, 1426–1438.

Van Troys, M., Vandekerckhove, J., and Ampe, C. (2008a). "Actin and actin-binding proteins in cancer progression and metastasis," in *Actin-Binding Proteins and Disease, Protein Reviews,* eds C. G. Dos Remedios and D. Chhabra (New York, NY: Springer), 229–277.

Van Troys, M., Huyck, L., Leyman, S., Dhaese, S., Vandekerkhove, J., and Ampe, C. (2008b). Ins and outs of ADF/cofilin activity and regulation. *Eur. J. Cell Biol.* 87, 649–667.

Vicente-Manzanares, M., Ma, X., Adelstein, R. S., and Horwitz, A. R. (2009). Non-muscle myosin II takes centre stage in cell adhesion and migration. *Nat. Rev. Mol. Cell Biol.* 10, 778–790.

Vitavska, O., Merzendorfer, H., and Wieczorek, H. (2005). The V-ATPase subunit C binds to polymeric F-actin as well as to monomeric G-actin and induces cross-linking of actin filaments. *J. Biol. Chem.* 280, 1070–1076.

Vitavska, O., Wieczorek, H., and Merzendorfer, H. (2003). A novel role for subunit C in mediating binding of the H+-V-ATPase to the actin cytoskeleton. *J. Biol. Chem.* 278, 18499–18505.

Wang, H. J., Wan, A. R., and Jauh, G. Y. (2008). An actin binding protein,

LlLIM1, mediates Ca and H regulation of actin dynamics in pollen tubes. *Plant Physiol.* 47, 1619–1636.

Wang, X. L., Gao, X. Q., and Wang, X. C. (2011). Stochastic dynamics of actin filaments in guard cells regulating chloroplast localization during stomatal movement. *Plant Cell Environ.* 34, 1248–1257.

Wang, Y. S., Motes, C. M., Mohamalawari, D. R., and Blancaflor, E. B. (2004). Green fluorescent protein fusions to Arabidopsis fimbrin 1 for spatio-temporal imaging of F-actin dynamics in roots. *Cell. Motil. Cytoskeleton* 59, 79–93.

Way, J. C., and Chalfie, M. (1988). mec-3, a homeobox-containing gene that specifies differentiation of the touch receptor neurons in *C. elegans Cell* 54, 5–16.

Whippo, C. W., Khurana, P., Davis, P. A., Deblasio, S. L., Desloover, D., Staiger, C. J., and Hangarter, R. P. (2011). THRUMIN1 is a light-regulated actin-bundling protein involved in chloroplast motility. *Curr. Biol.* 21, 59–64.

Wightman, R., and Turner, S. R. (2008). The roles of the cytoskeleton during cellulose deposition at the secondary cell wall. *Plant J.* 54, 794–805.

Winder, S. J., and Ayscough, K. R. (2005). Actin-binding proteins. *J. Cell Sci.* 118, 651–654.

Wu, Y., Yan, J., Zhang, R., Qu, X., Ren, S., Chen, N., and Huang, S. (2010). Arabidopsis FIMBRIN5, an actin bundling factor, is required for pollen germination and pollen tube growth. *Plant Cell* 22, 3745–3763.

Xu, J. R., Staiger, C. J., and Hamer, J. E. (1998). Inactivation of the mitogen-activated protein kinase Mps1 from the rice blast fungus prevents penetration of host cells but allows activation of plant defense responses. *Proc. Natl. Acad. Sci. U.S.A.* 95, 12713–12718.

Xu, T., and Forgac, M. (2001). Microtubules are involved in glucose-dependent dissociation of the yeast vacuolar [H+]-ATPase *in vitro*. *J. Biol. Chem.* 276, 24855–24861.

Xue, X. H., Guo, C. Q., Du, F., Lu, Q. L., Zhang, C. M., and Ren, H. Y. (2011). AtFH8 is involved in root development under effect of low-dose latrunculin B in dividing cells. *Mol. Plant* 4, 264–278.

Yang, W., Ren, S., Zhang, X., Gao, M., Ye, S., Qi, Y., Zheng, Y., Wang, J., Zeng, L., Li, Q., Huang, S., and He, Z. (2011). BENT UPPERMOST INTERNODE1 encodes the class II formin FH5 crucial for actin organization and rice development. *Plant Cell* 23, 661–680.

Ye, J., and Xu, M. (2012). Actin bundler PLIM2s are involved in the regulation of pollen development and tube growth in Arabidopsis. *J. Plant Physiol.* 169, 516–522.

Ye, J., Zheng, Y., Yan, A., Chen, N., Wang, Z., Huang, S., and Yang, Z. (2009). Arabidopsis Formin3 directs the formation of actin cables and polarized growth in pollen tubes. *Plant Cell* 21, 3868–3884.

Yi, K., Guo, C., Chen, D., Zhao, B., Yang, B., and Ren, H. (2005). Cloning and functional characterization of a formin-like protein (AtFH8) from Arabidopsis. *Plant Physiol.* 138, 1071–1082.

Yokota, E., Takahara, K., and Shimmen Ki, T. T. (1998). Actin-bundling protein isolated from pollen tubes of lily. Biochemical and immunocytochemical characterization. *Plant Physiol.* 116, 1421–1429.

Yokota, E., and Shimmen, T. (1999). The 135-kDa actin-bundling protein from lily pollen tubes arranges F-actin into bundles with uniform polarity. *Planta* 209, 264–266.

Yokota, E., Muto, S., and Shimmen, T. (2000). Calcium-calmodulin suppresses the filamentous actin-binding activity of a 135-kilodalton actin-bundling protein isolated from lily pollen tubes. *Plant Physiol.* 123, 645–654.

Yokota, E., Vidali, L., Tominaga, M., Tahara, H., Orii, H., Morizane, Y., Hepler, P. K., and Shimmen, T. (2003). Plant 115-kDa actin-filament bundling protein, P-115-ABP, is a homologue of plant villin and is widely distributed in cells. *Plant Cell Physiol.* 44, 1088–1099.

Yokota, E., Tominaga, M., Mabuchi, I., Tsuji, Y., Staiger, C. J., Oiwa, K., and Shimmen, T. (2005). Plant villin, Lily P-135-ABP, possesses G-actin binding activity and accelerates the polymerization and depolymerization of actin in a Ca2+-sensitive manner. *Plant Cell Physiol.* 46, 1690–1703.

Zhang, H., Qu, X., Bao, C., Khurana, P., Wang, Q., Xie, Y., Zheng, Y., Chen, N., Blanchoin, L., Staiger, C. J., and Huang, S. (2010). Arabidopsis VILLIN5, an actin filament bundling and severing protein, is necessary for normal pollen tube growth. *Plant Cell* 22, 2749–2767.

Zhang, W., Zhao, Y., Guo, Y., and Ye, K. (2012). Plant actin-binding protein SCAB1 is dimeric actin cross-linker with atypical pleckstrin homology domain. *J. Biol. Chem.* 287, 11981–11990.

Zhang, Z., Zhang, Y., Tan, H., Wang, Y., Li, G., Liang, W., Yuan, Z., Hu, J., Ren, H., and Zhang, D. (2011a). RICE MORPHOLOGY DETERMINANT encodes the type II formin FH5 and regulates rice morphogenesis. *Plant Cell* 23, 681–700.

Zhang, Y., Xiao, Y., Du, F., Cao, L., Dong, H., and Ren, H. (2011b). Arabidopsis VILLIN4 is involved in root hair growth through regulating actin organization in a Ca(2+) -dependent manner. *New Phytol.* 190, 667–682.

Zhao, Y., Zhao, S., Mao, T., Qu, X., Cao, W., Zhang, L., Zhang, W., He, L., Li, S., Ren, S., Zhao, J., Zhu, G., Huang, S., Ye, K., Yuan, M., and Guo, Y. (2011). The plant-specific actin binding protein SCAB1 stabilizes actin filaments and regulates stomatal movement in Arabidopsis. *Plant Cell* 23, 2314–2330.

Zimniak, L., Dittrich, P., Gogarten, J. P., Kibak, H., and Taiz, L. (1988). The cDNA sequence of the 69-kDa subunit of the carrot vacuolar H+-ATPase. Homology to the beta-chain of F0F1-ATPases. *J. Biol. Chem.* 263, 9102–9112.

Zuo, J., Jiang, J., Chen, S. H., Vergara, S., Gong, Y., Xue, J., Huang, H., Kaku, M., and Holliday, L. S. (2006). Actin binding activity of subunit B of vacuolar H+-ATPase is involved in its targeting to ruffled membranes of osteoclasts. *J. Bone Miner Res.* 21, 714–721.

Zuo, J., Vergara, S., Kohno, S., and Holliday, L. S. (2008). Biochemical and functional characterization of the actin-binding activity of the B subunit of yeast vacuolar H+-ATPase. *J. Exp. Biol.* 211, 1102–1108.

Conflict of Interest Statement: The author declares that the research was conducted in the absence of any commercial or financial relationships that could be construed as a potential conflict of interest.

Received: 03 July 2012; paper pending published: 19 July 2012; accepted: 01 August 2012; published online: 24 August 2012.

*Citation: Thomas C (2012) Bundling actin filaments from membranes: some novel players. Front. Plant Sci. **3**:188. doi: 10.3389/fpls.2012.00188*

This article was submitted to Frontiers in Plant Traffic and Transport, a specialty of Frontiers in Plant Science.

frontiers in
PLANT SCIENCE

REVIEW ARTICLE
published: 11 December 2012
doi: 10.3389/fpls.2012.00274

Multiple roles for membrane-associated protein trafficking and signaling in gravitropism

Allison K. Strohm[1,2], Katherine L. Baldwin[1,2] and Patrick H. Masson[1]*

[1] Laboratory of Genetics, University of Wisconsin-Madison, Madison, WI, USA
[2] Graduate Program in Cellular and Molecular Biology, University of Wisconsin-Madison, Madison, WI, USA

Edited by:
Markus Geisler, University of Fribourg, Switzerland

Reviewed by:
Stephanie Robert, Swedish University of Agricultural Sciences/Umeå Plant Science Centre, Sweden
Nadine Paris, Centre National de la Recherche Scientifique, France

***Correspondence:**
Patrick H. Masson, Laboratory of Genetics, University of Wisconsin-Madison, 425G Henry Mall, Madison, WI 53706, USA.
e-mail: phmasson@wisc.edu

Gravitropism is a process that allows plant organs to guide their growth relative to the gravity vector. It requires them to sense changes in their orientation and generate a biochemical signal that they transmit to the tissues that drive organ curvature. Trafficking between the plasma membrane and endosomal compartments is important for all of these phases of the gravitropic response. The sedimentation of starch-filled organelles called amyloplasts plays a key role in sensing reorientation, and vacuolar integrity is required for amyloplast sedimentation in shoots. Other proteins associated with the vesicle trafficking pathway contribute to early gravity signal transduction independently of amyloplast sedimentation in both roots and hypocotyls. Phosphatidylinositol signaling, which starts at the plasma membrane and later affects the localization of auxin efflux facilitators, is a likely second messenger in the signal transduction phase of gravitropism. Finally, membrane-localized auxin influx and efflux facilitators contribute to a differential auxin gradient across the gravistimulated organs, which directs root curvature.

Keywords: gravitropism, *Arabidopsis*, endomembrane, vacuole, trafficking, PIN, phosphatidylinositol, auxin transport

INTRODUCTION TO GRAVITROPISM

Gravitropism is a dynamic process that involves the perception of an organ's abnormal orientation within the gravity field, a transduction of the corresponding information into a biochemical signal, the transmission of this signal to a site of response, and organ curvature. Proper curvature therefore requires the coordination of multiple cellular activities including signal transduction, phytohormone transport, and cell expansion. Published work discussed in this review, mostly on *Arabidopsis*, indicates that protein trafficking through the endomembrane system plays a critical role in all of these processes.

Gravitropism begins with signal perception. In *Arabidopsis* roots, the specialized cells that sense gravity, or statocytes, are located in the root tips within the columella region of the cap (Blancaflor et al., 1998; Tsugeki and Fedoroff, 1999; Kiss, 2000); in shoots, the endodermis contains the statocytes (Fukaki et al., 1998). Both root columella and shoot endodermal cells contain dense, starch-filled amyloplasts that sediment to the lower sides of the statocytes upon gravistimulation (Caspar and Pickard, 1989; Kiss et al., 1989; Leitz et al., 2009). After amyloplast sedimentation, an auxin gradient is generated (part of the biochemical signal discussed above) and transmitted so that the auxin concentration on the lower side of the organ is higher than the concentration along its upper side (Ottenschlager et al., 2003). This typically promotes downward curvature of roots and upward curvature of shoots (Salisbury et al., 1988; Young et al., 1990).

The steps connecting amyloplast sedimentation and auxin redistribution in the signal transduction phase of gravitropism are still unclear, although several genes have been implicated in this phase. The molecular and functional analysis of some of these genes has suggested roles for endomembrane trafficking in this process. One possible model for signal perception involves the activation of stretch-activated mechanosensitive ion channels within membranes pressed upon by sedimenting amyloplasts (Leitz et al., 2009). Alternatively, in the ligand-receptor model, the activation of a transduction pathway occurs through productive interactions between sedimenting plastid-borne molecules and receptors associated with lower membranes (Braun, 2002). Lastly, in the hydrostatic pressure model, cellular machinery detects a pressure differential between the upper and lower sides of the statocytes caused by the weight of the entire protoplast on the cell wall (Staves, 1997). There is also substantial evidence for root gravity sensing outside of the columella cells that could involve an amyloplast-independent mechanism (Wolverton et al., 2002).

Researchers have proposed that several secondary messengers contribute to the signal transduction phase of gravitropism. For example, Ca^{2+} changes occur in response to gravistimulation, although studies have not found them in the columella cells (Plieth and Trewavas, 2002; Toyota et al., 2008). Cytosolic pH changes, however, do occur in the columella cells upon gravistimulation, and changing the pH alters the gravitropic response (Scott and Allen, 1999; Monshausen et al., 2011). Inositol 1,4,5-triphosphate ($InsP_3$) also appears to contribute to the formation of the auxin gradient possibly through a role in vesicle trafficking (Perera et al., 1999; Wang et al., 2009).

In contrast to the signal perception phase of gravitropism, how a plant generates, maintains, and transmits the auxin gradient, as well as how this gradient dictates differential cell expansion, are better understood. The auxin efflux facilitators PIN-FORMED 3 (PIN3) and PIN7 show a distinct relocalization to the lower side of the root cap columella cells in response to gravistimulation that initiates the differential flow of auxin toward the lower

flank of the root (Friml et al., 2002b; Kleine-Vehn et al., 2010). Other auxin transporters help to generate and propagate this gradient along the root, and protein trafficking is critical in this step. Auxin then may bind to one of two proposed auxin receptor classes, the AUXIN-BINDING PROTEIN 1 (ABP1) receptor or the TRANSPORT-INHIBITOR-RESISTANT 1 (TIR1)/AUXIN SIGNALING F-BOX (AFB) proteins. TIR1/AFB receptors bind auxin in a complex with an Aux/indole-3-acetic acid (IAA) regulatory protein, which is degraded upon auxin binding (Dharmasiri et al., 2005; Kepinski and Leyser, 2005). This de-represses auxin-response factors, which can then activate or suppress target genes to cause differential cell expansion on the upper and lower sides of roots and shoots. Although its mechanism of action is less clear, ABP1 is required for auxin responses at the plasma membrane and auxin-responsive gene expression changes, and it has been proposed to coordinate cell division and cell expansion (Shi and Yang, 2011). For more information on the overall gravitropic response, please see a recent review (Morita, 2010; Strohm et al., 2012).

ENDOMEMBRANE SYSTEM COMPONENTS ARE IMPORTANT FOR GRAVITY PERCEPTION AND EARLY GRAVITY SIGNAL TRANSDUCTION

Endomembrane system components are required for normal shoot and root gravitropism in *Arabidopsis*. Endocytotic pathways mediate the transport of proteins from the plasma membrane in order to control their recycling via the endosome or their degradation. Many proteins targeted to vacuoles are transported from the ER, to the Golgi, and then to the vacuole, although a Golgi-independent pathway also exists. Furthermore, some endocytosed plasma membrane proteins are also targeted to the vacuole. Prevacuolar compartments (PVCs), also called multivesicular bodies (MVBs), mediate Golgi or plasma membrane to vacuole transport. For more information, see a recent review on this process (Reyes et al., 2011). Genetic screens for shoot gravitropism mutants revealed a contribution of vesicular trafficking to vacuoles in gravitropism. Similarly, a screen designed to find compounds that reduced hypocotyl gravitropic responses identified several small molecules that link gravitropism and endomembrane trafficking. Although characterization of the proteins that interact with these molecules is still underway, two of the compounds reduce gravitropic responses and disrupt the endomembrane system despite having no apparent effect on auxin, suggesting an auxin-independent role for endomembrane trafficking in gravitropism (Surpin et al., 2005).

VACUOLAR INTEGRITY IS ESSENTIAL FOR AMYLOPLAST SEDIMENTATION IN SHOOTS

Four *shoot gravitropism* (*sgr*) mutants have been identified that share similar phenotypes and suggest a connection between vacuole integrity, amyloplast sedimentation, and shoot gravitropic responses. SGR3/VAM3 and SGR4/VTI11/ZIG are SNARES, which are named for SNAP (soluble NSF attachment protein) receptors and are small proteins that mediate vesicle fusion. They are divided into vesicle-SNAREs (v-SNAREs), which are located on vesicle membranes, and target-SNARES (t-SNAREs), which are located on target membranes. SGR3 is a t-SNARE (Sato et al., 1997), and SGR4 is a v-SNARE (Zheng et al., 1999). SGR8/GRV2/KAM2 is a DnaJ domain-containing peripheral membrane protein that localizes to late endosomes (Silady et al., 2004, 2008). Lastly, *SGR2* encodes a vacuole-localized protein homologous to the bovine testis phosphatidic acid-preferring phospholipase A1 (PA-PLA1; Kato et al., 2002).

sgr2, sgr3, sgr4, and sgr8 share reduced shoot gravitropic responses, abnormal amyloplast localization, and altered vacuole structures

sgr2, *sgr3*, *sgr4*, and *sgr8* mutants all exhibit strongly reduced shoot gravitropic responses but normal or slightly enhanced phototropic and root gravitropic responses; *sgr2* and *sgr4* mutants also display very slow hypocotyl gravitropism (Fukaki et al., 1996b; Yamauchi et al., 1997; Kato et al., 2002; Yano et al., 2003; Silady et al., 2004). All of these mutants show a generally intact tissue structure consisting of a single layer of epidermis, three to four layers of cortex, and one layer of endodermis, although the *sgr2*, *sgr4*, and *sgr8* mutants show some pleiotropic phenotypes including altered cell size and shape (Kato et al., 2002; Yano et al., 2003; Silady et al., 2004). This suggests that these genes are likely to function directly in gravitropism and do not simply have missing or disorganized statocytes.

In wild-type plants, amyloplasts in shoot endodermal cells are found sedimented on the lower sides of the cells (Morita et al., 2002). They are wrapped in thin, tunnel-like cytoplasmic layers surrounded by vacuolar membranes that are called transvacuolar strands, which pass through the vacuole and are connected to the peripheral cytoplasm. Amyloplasts can pass through these transvacuolar strands (Saito et al., 2005). However, in *sgr2*, *sgr3*, *sgr4*, and *sgr8* mutants, the endodermal amyloplasts are found throughout both the upper and lower sides of the cells where they localize outside of the vacuole (instead of within the transvacuolar strands), often pressed against the cell periphery (Morita et al., 2002; Yano et al., 2003; Silady et al., 2004). At least *sgr2* and *sgr4* amyloplasts can be stained with potassium iodide, suggesting that they do accumulate starch, although a few amyloplasts appeared to contain slightly less starch than wild-type (Morita et al., 2002). Together, these data suggest that altered amyloplast localization, rather than reduced starch accumulation, results in the abnormal gravitropic responses of these mutants.

sgr2, *sgr3*, *sgr4*, and *sgr8* also all show altered vacuolar phenotypes. *sgr2* and *sgr4* both have aberrant vacuolar components in the cytoplasm, although these compartments differ between mutants (Morita et al., 2002). *sgr3* vacuolar membranes form irregular curves and do not properly surround the amyloplasts (Yano et al., 2003). *sgr8* mutants have irregularly shaped vacuoles and aggregates of endosomes, which suggests that they might not properly fuse the tonoplast and vesicular membranes (Silady et al., 2008).

Golgi-to-vacuole targeting is critical for proper amyloplast localization in shoots

SGR2, *SGR3*, *SGR4*, and *SGR8* are all expressed in all tissues examined, and at least for *SGR2*, *SGR3*, and *SGR4*, expression in the endodermis is sufficient to rescue the gravitropic defects of the mutants (Zheng et al., 1999; Morita et al., 2002; Yano et al., 2003; Silady et al., 2004). This indicates that these proteins' contribution to gravitropism occurs within the statocytes. In root cells, SGR4 colocalizes with ELP, a vacuolar cargo receptor located on the

trans-Golgi network, as well as with PEP12, a t-SNARE located at the PVC (Zheng et al., 1999). Experiments have shown that SGR4 can substitute for yeast Vti1p in vesicle transport from the Golgi to the PVC (Zheng et al., 1999). SGR3 localizes to the vacuole or the PVC, and coimmunoprecipitation experiments suggest that it forms a complex with SGR4 (Yano et al., 2003). Similarly, SGR8 plays a role in trafficking from the PVC to the tonoplast (Silady et al., 2008). Together, these data suggest that trafficking from the Golgi to the vacuole plays an important role in shoot and hypocotyl gravitropism, possibly by providing a cellular environment that is favorable to amyloplast sedimentation upon gravistimulation.

The putative phospholipase SGR2 also localizes to vacuolar membranes (Morita et al., 2002). It is therefore possible that SGR3, SGR4, or SGR8 directly mediates the localization of SGR2 or that another cargo protein transported by SGR3, SGR4, or SGR8 is important for the localization or activity of SGR2. Alternatively, SGR2 may contribute to gravitropism independently of SGR3, SGR4, and SGR8. While the exact function of SGR2 is still unclear, it is possible that it mediates the degradation of phospholipids that dictate the composition of membranes in order to modify their properties. This could consequently result in altered amyloplast sedimentation and slow gravitropic curvature. Another possibility is that cleavage of phospholipids by SGR2 creates signaling molecules required for gravitropism (Kato et al., 2002; Morita et al., 2002).

Unlike amyloplasts in shoots, those in root columella cells are not enveloped in vacuolar membranes and move through the cytoplasm instead of within transvacuolar strands (Zheng and Staehelin, 2001; Leitz et al., 2009). There is also no large central vacuole in columella cells like there is in shoot endodermal cells. Consistent with these observations, none of the mutations identified thus far as affecting root gravitropism have been associated with defects in vacuolar biogenesis or function.

SOME ENDOMEMBRANE SYSTEM-ASSOCIATED PROTEINS MEDIATE EARLY GRAVITY SIGNAL TRANSDUCTION INDEPENDENTLY OF AMYLOPLAST SEDIMENTATION

ALTERED RESPONSE TO GRAVITY 1 (*ARG1*/*RHG*) and its paralog *ARG1-LIKE 2* (*ARL2*/*GPS4*) encode DnaJ-domain-containing peripheral membrane proteins that are necessary for full root and hypocotyl gravitropism (Fukaki et al., 1997; Sedbrook et al., 1999; Boonsirichai et al., 2003; Guan et al., 2003; Luesse et al., 2010). GFP-ARG1 fusions localize to components of the vesicle trafficking pathway including the ER, the Golgi, and vesicles near the plasma membrane, as well as the cell plate. Additionally, upon treatment with brefeldin A (BFA), which disrupts vesicle trafficking, cMyc-ARG1 accumulates in BFA-induced compartments as do many proteins known to be associated with vesicle trafficking (Boonsirichai et al., 2003). ARG1 and ARL2 are required for the relocalization of PIN3 to the new lower sides of the columella cells upon gravistimulation, and at least ARG1 is required for the gravity-induced cytoplasmic alkalinization of the columella cells. Both of these processes are important in generating an auxin gradient (Boonsirichai et al., 2003; Harrison and Masson, 2008). These genes are especially interesting because *arg1* and *arl2* mutants display normal phototropism, amyloplast starch accumulation, amyloplast sedimentation, responses to phytohormones, and responses to auxin transport inhibitors (Fukaki et al., 1997; Sedbrook et al., 1999; Guan et al., 2003; Stanga et al., 2009). Although the specific molecular function of ARG1 and ARL2 remains unclear, these data suggest that they play a role in the early gravity signal transduction steps that connect amyloplast sedimentation and auxin redistribution.

PHOSPHATIDYLINOSITOL SIGNALING MEDIATES VESICLE TRAFFICKING, AUXIN GRADIENT FORMATION, AND THE GRAVITROPIC RESPONSE

Phosphatidylinositol monophosphate 5-kinase (PIP5K) catalyzes the synthesis of phosphatidylinositol 4,5-bisphosphate (PIP_2), a plasma membrane-localized phospholipid. PIP_2 is then cleaved by phospholipase C (PLC) to produce the second messenger $InsP_3$, which diffuses throughout the cell, and diacylglycerol (DAG), which stays in the membrane. Inositol polyphosphate 5-phosphatases (InsP 5-ptases) dephosphorylate $InsP_3$ to stop its activity. In animals, $InsP_3$ can trigger Ca^{2+} release from the ER and the vacuole, and Ca^{2+} itself is another possible second messenger in gravity signal transduction in plants (Plieth and Trewavas, 2002; Monshausen et al., 2011). Additional research in both animals and plants has shown that PIP_2 can bind actin-interacting enzymes, endocytic and exocytic-related proteins, ion channels, and regulators of vesicle trafficking. Please see the following reviews for additional information (Wasteneys and Galway, 2003; Haucke, 2005).

$InsP_3$ MAY ACT AS A SECOND MESSENGER IN GRAVITROPISM SIGNALING

Multiple lines of evidence point to a role for phosphatidylinositol signaling in gravity signal transduction. $InsP_3$ levels increase threefold on both the upper and lower sides of gravistimulated oat pulvini after only 15 s. Over the next 30 min, $InsP_3$ fluxes continue, resulting in a threefold increase in the levels on the upper compared to the lower side. After about an hour, $InsP_3$ returns to its basal level (Perera et al., 2001). Several other observations also support a role for $InsP_3$ in gravitropism. Phosphatidylinositol 4-phosphate 5-kinase levels increase in the lower halves of gravistimulated pulvini, suggesting that PIP_2 biosynthesis increases in this region (Perera et al., 1999). Additionally, inhibiting PLC also blocks the long-term $InsP_3$ increase and reduces gravitropic bending (Perera et al., 2001). Some genes show $InsP_3$-dependent changes in expression in response to gravitropic and/or phototropic stimuli, suggesting that this second messenger may play a key role in coordinating these two responses (Salinas-Mondragon et al., 2010).

Arabidopsis inflorescence stems can perceive a change in orientation while at 4°C but cannot respond until after they are returned to room temperature (Fukaki et al., 1996a). $InsP_3$ changes are similar in plants gravistimulated at 4°C and at room temperature, and plants expressing a constitutively active InsP 5-ptase show decreased bending after gravistimulation at 4°C and a subsequent return to room temperature (Perera et al., 2001, 2006). These results support the hypothesis that phosphatidylinositol signaling functions early in gravity signal transduction.

PLANTS CARRYING MUTATIONS IN GENES ASSOCIATED WITH PHOSPHATIDYLINOSITOL SIGNALING SHOW ALTERED GRAVITROPIC AND AUXIN-RELATED PHENOTYPES

PIP5K and InsP 5-ptases are each encoded by 15 genes in *Arabidopsis*. *pip5k2* seedlings have decreased PIP_2 levels, and *5-ptase13* mutants are likely to have a decreased ability to dephosphorylate $InsP_3$ (Wang et al., 2009; Mei et al., 2012). Therefore, it is not surprising that these mutants share many opposite phenotypes. *pip5k2* seedlings respond slowly to gravity, while *5-ptase13* mutants show an enhanced response (Wang et al., 2009; Mei et al., 2012). In agreement with this finding, plants expressing a constitutively active InsP 5-ptase do not exhibit the characteristic $InsP_3$ increase in response to gravistimulation and show decreased gravitropic bending (Perera et al., 2006). *pip5k2* mutants are more sensitive to the polar auxin transport inhibitor 1-N-naphthylphthalamic acid (NPA) than are wild-type plants, which suggests impaired polar auxin transport in this mutant (Mei et al., 2012). In contrast, *5-ptase13* mutants show a reduced response to NPA, which indicates increased polar auxin transport (Wang et al., 2009). Plants carrying the constitutively active InsP 5-ptase also show decreased basipetal auxin transport (Perera et al., 2006). Indeed, a greater percentage of *5-ptase13* mutants and a smaller percentage of *pip5k2* mutants generate an asymmetric auxin gradient in roots in response to gravistimulation compared to wild-type seedlings, resulting in altered gravitropic phenotypes (Wang et al., 2009; Mei et al., 2012).

PHOSPHATIDYLINOSITOL SIGNALING AFFECTS VESICLE TRAFFICKING AND PIN PROTEIN TURNOVER

Phosphatidylinositol signaling is required for proper vesicle trafficking that leads to the establishment of an auxin gradient. PIN auxin efflux facilitators play important roles in controlling the direction and rate of auxin fluxes that allow for differential cell expansion upon gravistimulation (see The PIN Family of Auxin Efflux Facilitators). Normally PIN proteins cycle between the plasma membrane and endosomal compartments. This process is sensitive to BFA and requires clathrin-mediated endocytosis (Steinmann et al., 1999; Friml et al., 2002b; Geldner et al., 2003; Dhonukshe et al., 2007; Kleine-Vehn et al., 2010). Compared to wild-type, *5-ptase13* mutants have an increased ability to internalize the endocytosis marker FM4-64, are less sensitive to BFA, and show faster resumption of PIN1 and PIN2 polar localization at the plasma membrane after BFA removal (Wang et al., 2009). In contrast, *pip5k2* mutants show a decreased ability to internalize FM4-64, increased sensitivity to BFA, slower recovery after BFA removal, and decreased cycling of PIN2 and PIN3 (Mei et al., 2012). The phosphatidylinositol-3-kinase (PI3K) inhibitor wortmannin also results in altered PIN protein localization and gravitropic defects (Jaillais et al., 2006; Kleine-Vehn et al., 2008). Together, these data indicate a role for phosphatidylinositol signaling in vesicle trafficking that affects PIN protein turnover and the generation of the auxin gradient that is required for differential cell elongation in response to a gravity stimulus. It remains possible, however, that the *5-ptase13* and *pip5k2* mutants have altered membrane lipid composition, which is known to affect PIN cycling (Men et al., 2008).

AUXIN TRANSPORT ACROSS CELL MEMBRANES RESULTS IN AN AUXIN GRADIENT THAT DIRECTS DIFFERENTIAL CELL EXPANSION

The major natural auxin, IAA, is a weak acid that can diffuse through membranes only when protonated (Rubery and Sheldrake, 1974; Raven, 1975). The pH in the apoplast remains low, and so a proportion of IAA molecules are protonated, which allows them to diffuse across the membrane into the cytoplasm (Rubery and Sheldrake, 1974; Raven, 1975). Additional apoplastic IAA can be actively imported by the AUX1 and LIKE-AUX1 (LAX) permeases and at least one ATP-binding cassette (ABC) transporter/P-glycoprotein (PGP) (Marchant et al., 1999; Santelia et al., 2005; Yang et al., 2006; Yang and Murphy, 2009; Péret et al., 2012). Once in the cytoplasm, far fewer IAA molecules are protonated, being exposed to more neutral pH, and active auxin efflux mediated by PIN proteins and some ABC transporters is required (**Figure 1F**). The polar localization of these proteins at the plasma membrane can dictate directional auxin transport within cell files (Wisniewska et al., 2006). In vertically growing roots, this results in the flow of auxin down the vasculature to the columella cells where it is redirected along the outer layers of the root in what is termed the reverse fountain model of auxin transport (Swarup and Bennett, 2003). Upon gravistimulation, the PIN3 and PIN7 auxin efflux carriers switch from a non-polar localization to a preferential distribution at the lower side of the plasma membrane (Friml et al., 2002b; Kleine-Vehn et al., 2010). This causes auxin to accumulate in the lower sides of shoots and roots where it alters cell expansion rates to cause organ curvature (Salisbury et al., 1988; Young et al., 1990). Vesicle trafficking therefore plays a critical role in mediating this auxin gradient through its effects on the abundance, activity, and subcellular localization of auxin efflux and influx carriers. Membrane composition and differences in the sensitivity of certain cells to auxin over time also influence curvature kinetics (Willemsen et al., 2003; Benjamins and Scheres, 2008).

THE PIN FAMILY OF AUXIN EFFLUX FACILITATORS

There are eight PIN proteins in *Arabidopsis*, and at least five of them function directly or indirectly in gravitropism. This is achieved through their asymmetric localization at the plasma membrane, which can determine the direction of auxin flow (Wisniewska et al., 2006). These proteins often have overlapping functions; when one protein is non-functional, auxin-dependent ectopic expression of other PIN proteins can sometimes compensate for the loss (Blilou et al., 2005; Vieten et al., 2005).

PIN proteins are required for the generation and propagation of the gravity-induced auxin gradient

PIN1 localizes to the rootward sides of the cells that form the vasculature whereas PIN4 localizes to the rootward sides of the proximal meristem cells; the latter also shows non-polar localization in the columella cells (Friml et al., 2002a). These patterns suggest that PIN1 and PIN4 play indirect roles in gravitropism by contributing to auxin efflux through the vasculature to the columella cells (Gälweiler et al., 1998; Geldner et al., 2001; Friml et al., 2002a). This is important for auxin to be transported to the root tip so that it can later be distributed laterally across the cap and up to the elongation zones upon gravistimulation.

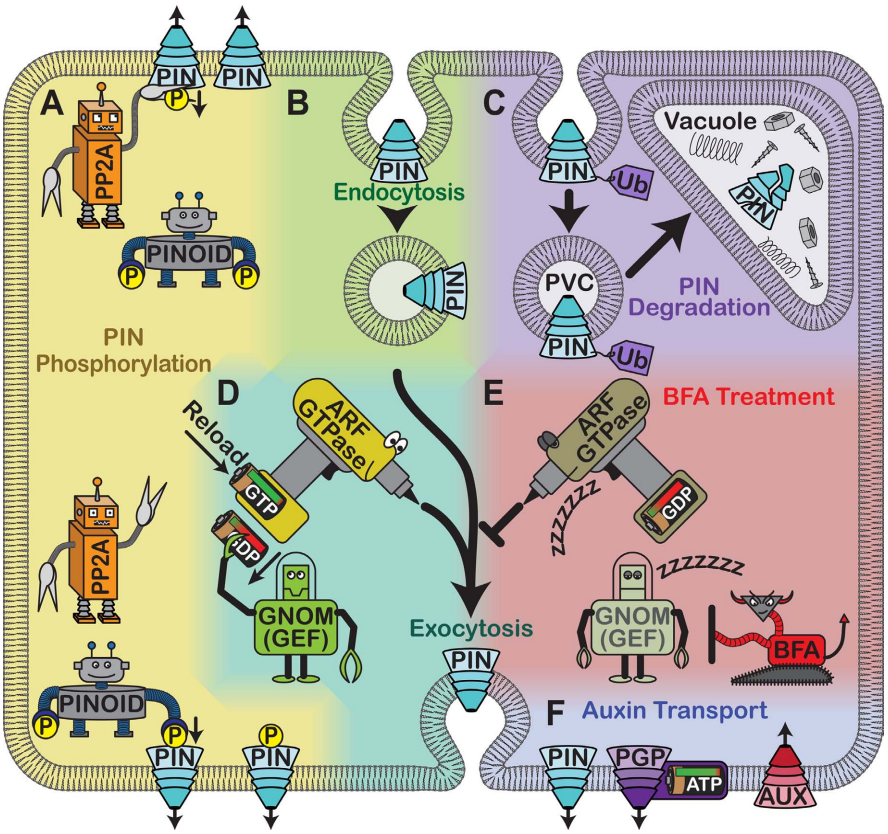

FIGURE 1 | Cellular control of auxin carriers. (A) Phosphorylation by PINOID kinase and dephosphorylation by PP2A regulate PIN protein localization. **(B)** PIN proteins are removed from the plasma membrane through clathrin-mediated endocytosis into endocytic compartments. **(C)** PIN proteins may also be ubiquitylated and targeted to the vacuole via PVCs for degradation. **(D)** Alternatively, following endocytosis PIN proteins may be exocytosed in a selective, polar manner that requires the activity of an unidentified ARF GTPase. The activity of the GTPase is controlled by a GEF called GNOM, which removes the used GDP and allows fresh GTP to reload. **(E)** Treating plants with BFA inhibits GNOM, which likely inactivates the ARF GTPase. As a result, PIN proteins accumulate in intracellular aggregates termed BFA bodies. **(F)** Auxin can be actively transported across the plasma membrane. PIN proteins are gradient-powered auxin efflux carriers. Members of the ABC transporter family are ATP-driven and act as either auxin influx or efflux facilitators. AUX1 and its relative LAX are auxin influx carriers that use an existing ion gradient to allow auxin into cells.

While mutations in *PIN4* cause root meristem disorganization that makes it difficult to analyze their gravitropic responses, *pin1* mutants have normal roots with no gravitropic defects, suggesting that other *PIN*s are able to compensate for the loss of this gene (Friml et al., 2002a).

In contrast, PIN3 and PIN7 may function immediately upon gravistimulation to generate the initial auxin gradient across the cap. PIN3 is normally expressed in the upper S1 and S2 layers of the columella cells, while PIN7 localizes to the S2 and S3 tiers. However, PIN7 expands its expression into the S1 layer in *pin3* mutants, suggesting its ability to compensate for the loss of PIN3 (Kleine-Vehn et al., 2010). In roots growing vertically, these proteins show a generally non-polar localization in the columella cells, but upon gravistimulation they are internalized and resorted into vesicles that direct them to the lower plasma membrane. This gravity-induced relocalization of the PIN3 and PIN7 proteins within the statocytes may be responsible for the development of a lateral auxin gradient across the cap, with accumulation on the new lower side of the root (Friml et al., 2002b; Kleine-Vehn et al., 2010). Consistent with this conclusion, the *pin3* and *pin7* mutants show gravitropism defects, and the *pin3 pin7* double mutant shows stronger defects than either single mutant (Friml et al., 2002b; Kleine-Vehn et al., 2010).

PIN2/EIR1/AGR1/WAV6 localizes to the shootward sides of lateral root cap and epidermal cells where it plays a critical role in transporting auxin from the cap to the elongation zone both in vertically growing roots and upon gravistimulation. It also localizes to the rootward sides of the cortical cells in the meristem, where it may play a negative regulatory role that allows for optimal auxin fluxes in this region (Müller et al., 1998; Blilou et al., 2005; Abas et al., 2006; Rahman et al., 2010). Here it may also contribute to an auxin reflux loop through the root epidermal and cortical cells in which the auxin maximum that forms on the lower side of the root is reinforced. *pin2* mutants do not establish an auxin gradient upon gravistimulation and therefore exhibit gravitropic defects (Luschnig et al., 1998; Müller et al., 1998; Abas et al., 2006).

PIN protein regulation affects gravitropic responses

PIN proteins can be regulated at the levels of transcription, protein stability, subcellular localization, and transport activity (Petrásek

and Friml, 2009). Because auxin efflux requires a membrane H^+ gradient and because PIN proteins do not have recognizable ATP-binding motifs, PIN proteins are thought to be gradient-driven secondary transporters (Krecek et al., 2009). However, they can act together with ATP-dependent ABC transporters when needed (Blakeslee et al., 2007).

Guanine nucleotide exchange factors regulate PIN protein localization. Intracellular trafficking is required for the polar localization of PIN proteins, which cycle between the plasma membrane and endosomal compartments (Steinmann et al., 1999; **Figure 1B**). GNOM is a GTP–GDP exchange factor (GEF) for ADP ribosylation factor (ARF) small G-proteins, which are important for cargo selection and vesicle budding (**Figure 1D**). BFA binds to ARF-GEF/ARF-GDP complexes and prevents ARF activation (Peyroche et al., 1999; Robineau et al., 2000). When this happens, PIN1 and PIN3 endocytosis continues, but these proteins are no longer secreted, causing them to accumulate in intracellular compartments (Geldner et al., 2001; Kleine-Vehn et al., 2010; **Figure 1E**). Therefore, BFA treatment blocks the relocalization of PIN3 to the lower membrane upon reorientation, alters auxin transport, and reduces gravitropism (Geldner et al., 2001; Kleine-Vehn et al., 2010; Rahman et al., 2010). Plants expressing a BFA-resistant version of GNOM, however, show proper PIN1 and PIN3 localization, robust auxin gradients after gravistimulation, and normal gravitropism even in the presence of BFA (Geldner et al., 2003; Kleine-Vehn et al., 2010). This confirms that GNOM regulates PIN1 and PIN3 localization and demonstrates that ARF-GEFs can modulate certain endosomal trafficking routes. BFA also partially affects PIN2 localization, suggesting that the gravitropic defects associated with BFA treatment might not be due entirely to its effects on PIN1 and PIN3 (Geldner et al., 2003).

SPIKE1 (SPK1) acts as a GEF for Rho-like GTPase from Plants 6 (ROP6; Basu et al., 2008). In *spk1* mutants, PIN2 levels at the plasma membrane are decreased. Consistent with this, *spk1* mutants show a less robust auxin gradient upon reorientation and a slow gravitropic response (Lin et al., 2012). Plants carrying mutations in *ROP6* or its effector *ROP-INTERACTIVE CRIB MOTIF 1* (*RIC1*) share some of these phenotypes, whereas ROP6 overexpression causes an increased gravitropic response (Chen et al., 2012; Lin et al., 2012). Normally auxin increases active ROP6 levels, but this does not happen in *spk1* mutants. Additionally, while exogenous application of the synthetic auxin 1-naphthalene acetic acid (1-NAA) normally prevents BFA-induced PIN2 accumulation in internal BFA compartments, *spk1*, *rop6*, and *ric1* mutants do not show this effect (Lin et al., 2012). These data suggest that SPK1, ROP6, and RIC1 inhibit PIN2 internalization through their effects on auxin signaling.

Protein degradation, protein phosphorylation, and small peptides also regulate PIN2 localization. PIN2 is also clearly regulated at the protein stability level. Upon gravistimulation, PIN2 is internalized and degraded preferentially on the upper side of the root, which is required for the generation of the auxin gradient. When BFA or the proteasome inhibitor MG132 is applied, this asymmetry is disrupted and PIN2 levels increase; this correlates with gravitropism defects (Abas et al., 2006). PIN2 endocytosis and targeting to the vacuole are normally triggered by ubiquitylation (**Figure 1C**). However, in *pin2* mutants in which six or more potential ubiquitylation sites are mutated, PIN2 is not internalized and targeted to the vacuole upon gravistimulation. Therefore, PIN2 levels stay constant at the plasma membrane in these mutants, and these seedlings do not form a robust auxin gradient upon reorientation (Leitner et al., 2012). Short-term auxin treatment also interferes with intracellular PIN2 accumulation, but long-term treatment causes PIN2 internalization and degradation (Abas et al., 2006). This may reflect a feedback mechanism in which PIN2 is degraded after the auxin level reaches a threshold, preventing additional auxin transport and excessive root curvature. Ubiquitylation could control the rate of PIN2 degradation in this process.

BFA inhibits the targeting of PIN2 to the vacuole, which suggests the involvement of an ARF-GEF. However, plants expressing the BFA-resistant GNOM showed BFA-sensitive PIN2 vacuolar targeting, indicating that the ARF-GEF of interest is not GNOM. Like GNOM, SORTING NEXIN 1 (SNX1) localizes to endosomal compartments and is BFA-sensitive; however only SNX1 is sensitive to the PI3K inhibitor wortmannin (Jaillais et al., 2006; Kleine-Vehn et al., 2008). *snx1* mutants resemble weak allele *gnom* mutants, and *snx1 gnom* double mutants show enhanced abnormal phenotypes compared to the single mutants (Jaillais et al., 2006). This suggests that these genes function in different pathways but contribute to some of the same developmental processes. Upon wortmannin-treatment, PIN2 and SNX1 colocalize in compartments, and PIN2 levels at the plasma membrane are reduced in *snx1* mutants (Jaillais et al., 2006; Kleine-Vehn et al., 2008). However, SNX1 does not appear to directly mediate the localization or recycling of PIN2 (Kleine-Vehn et al., 2008). Instead, wortmannin likely causes PIN protein mislocalization through its interference with sorting between the PVC and the Golgi (Matsuoka et al., 1995). Proper PIN2 localization depends on its targeting to the vacuole where it is degraded, and wortmannin blocks this (Jaillais et al., 2006; Kleine-Vehn et al., 2008). Accordingly, long-term wortmannin treatment results in phenotypes reminiscent of altered auxin transport, including defective root and hypocotyl gravitropism (Jaillais et al., 2006). SNX1 may therefore contribute to a feedback mechanism involved in PIN2 retrieval for recycling through its ability to mediate PIN2 translocation from the PVC to the vacuole.

PIN protein localization also depends on its phosphorylation state, which is mediated in part by the serine-threonine kinase PINOID (PID) and type 2A protein phosphatase (PP2A), which act antagonistically (Michniewicz et al., 2007 **Figure 1A**). PP2A subunits are encoded by multiple genes including *ROOTS CURL IN NPA 1* (*RCN1*). Plants that overexpress PID, *rcn1* mutants, and wild-type plants treated with the phosphatase inhibitor cantharidin all show increased shootward auxin transport, delayed auxin gradient formation upon gravistimulation, and randomized root growth; these phenotypes are rescued by blocking polar auxin transport (Christensen et al., 2000; Benjamins et al., 2001; Rashotte et al., 2001). The elevated auxin transport in these plants probably leads to auxin depletion in the root meristem, which prevents auxin gradient formation (Benjamins et al., 2001; Rashotte et al., 2001). This increased auxin transport is attributed to a rootward

to shootward shift in the localization of some PIN proteins (Friml et al., 2004). PINOID and RCN1 partially colocalize with PIN proteins and mediate the phosphorylation states of their central hydrophilic loops (Michniewicz et al., 2007). This means that they can affect PIN2-mediated auxin fluxes upon gravistimulation (Shin et al., 2005). More specifically, PP2A and a PINOID kinase family member are known to mediate the polar targeting of PIN2 in meristematic cortical cells, which is necessary for a full gravitropic response (Rahman et al., 2010). These experiments show that the phosphorylation status of PIN proteins affects their localizations and in turn their abilities to regulate gravitropism.

In addition to intracellular trafficking, protein degradation, and phosphorylation, a recent study suggests that small secretory peptides can also regulate PIN protein localization and affect gravitropism. *GOLVEN* (*GLV*) genes encode these peptides, and overexpression or knockdown of these genes generally results in reduced root and hypocotyl gravitropism. Treatment with some of these peptides, which act locally, also correlates with reduced auxin gradient formation upon reorientation and results in gravitropic defects. *pin2* mutants are resistant to GLV peptide treatment, and PIN2 levels increase in the membrane fractions of wild-type plants treated with GLV peptides (Whitford et al., 2012). Therefore, it is thought that the GLV peptides, along with auxin, mediate PIN2 trafficking in order to generate the auxin gradient necessary for root curvature.

PIN proteins may promote growth in the organ curvature phase of gravitropism

Auxin can inhibit the internalization of many PIN proteins and prevent their constitutive cycling. This results in increased levels of PIN proteins at the plasma membrane, and so auxin stimulates its own efflux from cells. After gravistimulation, the inhibition of endocytosis corresponds with the formation of the auxin gradient (Paciorek et al., 2005). Therefore, the increased level of plasma membrane-associated PIN2 on the lower flank of gravistimulated roots may further enhance the auxin gradient.

Auxin also triggers cell wall loosening that is necessary for cell elongation during root curvature. In *Arabidopsis*, PIN1 mediates local auxin accumulation, and its polar localization corresponds to the direction of mechanical stress in shoot apices (Heisler et al., 2010). Work done in tomatoes shows that as tissue becomes more strained during growth, PIN1 shows an increase in overall abundance and a preferential localization at the plasma membrane. This contributes to auxin accumulation, which then promotes growth in a feed-forward loop. One possible mechanism for this is that local cell wall strain increases plasma membrane tension, which promotes exocytosis and blocks endocytosis. This could increase the amount of membrane-localized PIN1 relative to cytoplasmically-localized PIN1, although more complex models are also possible (Nakayama et al., 2012). It is possible that a similar process takes place upon gravistimulation, although this has not yet been addressed experimentally. For example, tissue strain during curvature could increase plasma membrane-localized PIN2 levels on the lower side of the root. This would increase the auxin concentration in this region and further inhibit curvature in a feed-forward manner.

THE ABC TRANSPORTER FAMILY OF AUXIN EFFLUX AND INFLUX FACILITATORS

Members of the family of ATP-binding cassette (ABC) transporters couple ATP hydrolysis with the import and export of molecules such as xenobiotics, ions, sugars, lipids, peptides, and hormones including auxin across cell membranes. There are several lines of evidence that these proteins play critical roles in maintaining the auxin gradient that results in gravitropism.

ABC transporters regulate auxin fluxes

Multiple pieces of evidence support a role for several ABC-type transporters in auxin transport. First, the *Arabidopsis* PGP19/MDR1/ABCB19 protein and its closest relative ABCB1 directly act as auxin transporters when expressed in mammalian and yeast cells as well as in protoplast assays (Geisler et al., 2005; Yang and Murphy, 2009). Furthermore, *abcb19* single mutants and to a greater extent *abcb19 abcb1* double mutants show decreased rootward auxin transport (Noh et al., 2001; Lewis et al., 2007). Similarly, plants carrying mutations in *ABCB4/PGP4/MDR4*, another ABC-type transporter with sequence similarity to *ABCB1* and *ABCB19*, show decreased shootward auxin transport (Santelia et al., 2005; Terasaka et al., 2005; Lewis et al., 2007).

Interestingly, ABCB1 shows a distinct polar localization in different cell types at the upper edge of the distal elongation zone. In the endodermal cells its localization is always shootward, and in the cortical cells it is most often shootward (Geisler et al., 2005). A similar result was found for ABCB19 (Blakeslee et al., 2007). On the other hand, ABCB4 shows rootward localization in the epidermal cells at the upper edge of the distal elongation zone while displaying apolar localization in S3 columella and adjacent root cap cells (Terasaka et al., 2005). These distinct localization patterns may help generate differential levels of auxin accumulation in different cells.

A phenotypic analysis of these mutants is also compatible with a role for these proteins in auxin transport. Indeed, *abcb19* and *abcb19 abcb1* mutants show epinastic, or downward-folding, cotyledons and first true leaves as do wild-type plants when treated with exogenous auxin (Noh et al., 2001). This is likely due to the improper accumulation of auxin in the cotyledons. These mutants also show increased sensitivity to 1-NAA, decreased sensitivity to NPA, and decreased auxin-responsive DR5::GUS expression (Geisler et al., 2005; Lin and Wang, 2005).

Together, these studies strongly suggest that these transporters help maintain proper auxin flow patterns, and additional work has shown that interactions between ABC transporters and other proteins play important roles in this process. Genetic interactions have been observed between *ABCB*s and *PIN*s, and coimmunoprecipitation and yeast two-hybrid experiments have shown that both ABCB1 and ABCB19 interact with PIN1 (Blakeslee et al., 2007). Additionally, *abcb19* and especially *abcb19 abcb1* mutants show diffuse, punctate, and discontinuous PIN1 localization, which is likely to result in randomized directions of auxin efflux (Noh et al., 2003). Heterologous coexpression studies have also shown that the rate of auxin transport is increased when these proteins colocalize compared to when only one of them is present. In contrast, when PIN2 and either ABCB1, ABCB4, or ABCB19 are coexpressed in HeLa cells, IAA efflux decreases when compared

to when only one protein is expressed (Blakeslee et al., 2007). AGC kinases also mediate both PIN protein polarity and the auxin efflux activity of ABCB1 and ABCB19, suggesting that they regulate crosstalk between these auxin transporters (Christie et al., 2011; Henrichs et al., 2012). From these experiments, it appears that the ABC transporters and PIN proteins function separately but synergistically to provide both the specificity and the high rate of long-distance auxin transport.

Additionally, the immunophilin-like integral membrane protein required for brassinosteroid perception or signaling, TWISTED DWARF 1, interacts with both ABCB1 and ABCB19 (Geisler et al., 2003). *twd1* mutants exhibit epinastic cotyledons and a strong reduction in polar auxin transport like *abcb1 abcb19* double mutants, suggesting that ABCB1 and ABCB19 form a complex with TWD1 (Geisler et al., 2003). It is possible that TWD1 regulates the transport activity of ABCB1 and ABCB19 or that it mediates ABCB–PIN interactions.

ABC transporters are required for normal gravitropic responses

Several experiments show that ABC transporters function in the auxin transport phase of gravitropism. Interestingly, *abcb19* hypocotyls respond to gravistimulation twice as quickly as wild-type plants, and they also exhibit an enhanced phototropic response (Noh et al., 2003). Similarly, the *abcb4* mutant shows a faster root gravitropic response than wild-type plants (Lewis et al., 2007). Experiments using the auxin-responsive DR5::GUS construct showed that these mutants form a more robust asymmetric auxin gradient across the root tip than wild-type plants (Lin and Wang, 2005; Lewis et al., 2007). The altered auxin efflux may therefore result in a steeper, although transient, auxin gradient upon gravistimulation. One possible explanation for this comes from studies showing that *PIN2* mRNA levels decrease with distance from the root tip, while *ABCB4* mRNA levels increase (Birnbaum et al., 2003). If this correlates with their contributions to auxin transport, the reduced shootward auxin transport as a result of the loss of *ABCB19* or *ABCB4* may cause auxin buildup in the elongation zone where it leads to an enhanced curvature response (Lewis et al., 2007). Surprisingly, despite the large reduction in rootward auxin transport, root gravitropic responses of *abcb19* mutants are normal (Lewis et al., 2007). This could be due to compensation by other ABC transporters or PIN proteins.

A screen for compounds that reduce hypocotyl gravitropic responses identified a molecule called Gravacin that also causes decreased auxin sensitivity, decreased auxin transport, and endomembrane system defects (Surpin et al., 2005; Rojas-Pierce et al., 2007). Subsequent work showed that *abcb19* and *twd1*, but not *abcb1*, are resistant to Gravacin (Rojas-Pierce et al., 2007). Gravacin targets *ABCB19* and disrupts the ABCB19–PIN1 complexes, thereby interfering with their auxin transport activity (Rojas-Pierce et al., 2007). Using Gravacin to perturb ABCB19 but not PIN proteins may be useful in further characterizing the role of ABC transporters in auxin fluxes and gravitropism.

THE AUX AND LAX FAMILY OF AUXIN IMPORT CARRIER PROTEINS

In addition to auxin efflux, auxin flow into cells also contributes to the auxin gradient. While auxin influx can occur by diffusion, the auxin influx carriers AUX1 and LAX can also actively import IAA (Marchant et al., 1999; Yang et al., 2006; Yang and Murphy, 2009; Péret et al., 2012). Active auxin influx into particular cells might maintain proper auxin fluxes by counteracting auxin diffusion into other cells. *aux1*, but not *lax*, mutants are agravitropic, suggesting functional specialization within this gene family (Bennett et al., 1996; Péret et al., 2012). Because *aux1* mutants are defective in active auxin uptake, they are therefore resistant to exogenous IAA and the auxin 2,4-dichlorophenoxyacetic acid (2,4-D), but not 1-NAA, which can diffuse easily through membranes (Maher and Martindale, 1980; Bennett et al., 1996). Similarly, 1-NAA, but not 2,4-D, rescues the *aux1* agravitropic root phenotype (Marchant et al., 1999). It is likely that 1-NAA is taken up by the root and redirected by an auxin efflux facilitator such as PIN2, which is expressed in the cortical and epidermal root tip cells like *AUX1* (Müller et al., 1998; Marchant et al., 1999).

AUX1 functions in the signal transmission and curvature response phases, not the perception phase, of gravitropism. This is suggested by its expression in the regions of the root that respond to gravity (Marchant et al., 1999). Consistent with this result, AUX1 expression in only the lateral root cap and epidermal cells is sufficient to rescue the *aux1* agravitropic phenotype (Swarup et al., 2005). This suggests that AUX1 contributes to gravitropism by facilitating shootward auxin transport from the root cap to the elongation zone (Swarup et al., 2005).

AUX1 also affects pH changes upon gravistimulation, suggesting a relationship between pH and auxin in gravitropism. Shortly after reorientation, wild-type roots show a decrease in pH on the upper side of the extracellular root surface and an increase on the lower side; this gradient occurs in the root cap as well as throughout the elongation zone (Monshausen et al., 2011). It might contribute to cell wall loosening to allow for cell expansion or even to signal transmission itself. *aux1* mutants, however, do not show this pH change. In fact, even when growing vertically, *aux1* mutant extracellular root surfaces are uniformly acidic instead of showing dynamic pH fluctuations like wild-type roots. Both the pH gradient and the pH dynamics are rescued by introducing AUX1 into only the lateral root cap and epidermal cells (Monshausen et al., 2011). It is possible that the pH gradient contributes to feedback mechanisms that regulate the gravity response by affecting AUX1-mediated auxin uptake.

CONCLUSION

Upon gravistimulation, amyloplasts sediment to the lower sides of the statocytes. In endodermal cells, SGR proteins play a key role in this process by maintaining vacuolar membrane integrity. The amyloplasts then trigger a signal transduction cascade that may involve protons, calcium, and phosphatidylinositol signaling, which begins at the plasma membrane. Phosphatidylinositol signaling affects the cycling of auxin transporters, and changes in their localization at the plasma membrane cause auxin to accumulate in the lower side of the root and shoot. Here it affects cell elongation and causes the plant to realign itself with the gravity vector (**Figure 2**).

Therefore, through their roles in amyloplast sedimentation, phosphatidylinositol signaling, and auxin carrier localization,

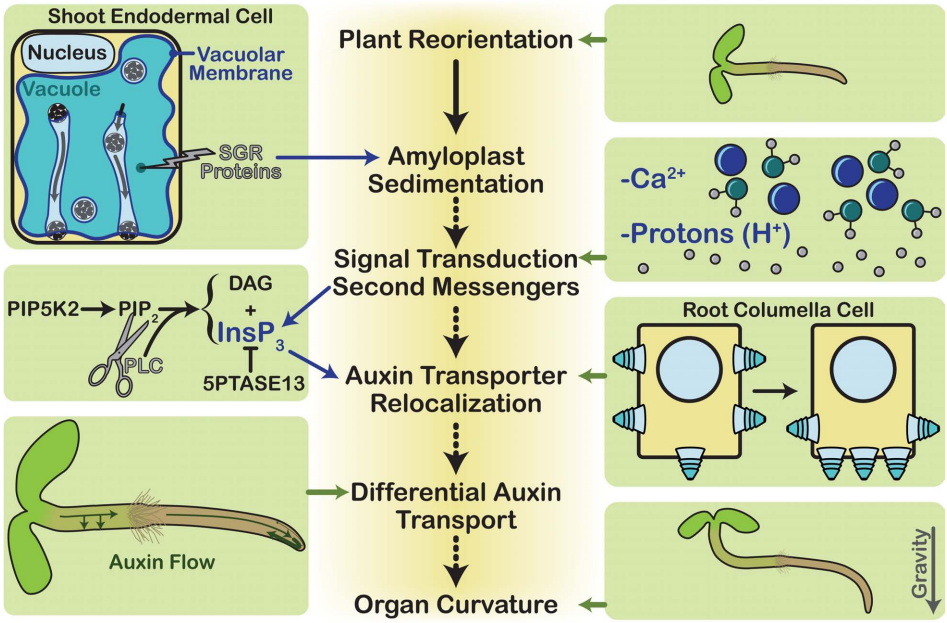

FIGURE 2 | Gravitropism overview. The steps of gravitropism are shown down the center core of the diagram. During plant reorientation, a plant is rotated relative to the gravity vector. This results in the sedimentation of dense amyloplasts within the statocytes. In roots the statocytes are the columella cells, whereas in stems they are the endodermal cells. Each endodermal cell contains a large vacuole, and the amyloplasts must traverse it by tunneling through transvacuolar strands in order to reach the new lower side of the cell. This requires proper vacuole structure, which the SGR proteins mediate. Amyloplast sedimentation is then thought to activate signal transduction through second messengers, possibly calcium ions or protons. Another second messenger is $InsP_3$, which is produced by cleavage of the phospholipid, PIP_2. In a process that is not completely understood, the second messengers activate the relocalization of auxin transporters, such as PIN3 and PIN7 in the columella cells. The new polarized distribution of these auxin efflux carriers changes the flow of auxin throughout the plant. This differential auxin transport affects cell elongation rates, thereby resulting in organ curvature as the plant grows.

membranes contribute in multiple ways to all phases of gravitropism. The evolution of these complex processes allows plants to adapt to changing environments and to integrate their responses to gravity with those to a wide variety of other stimuli including touch and moisture gradients. Future work in this area will continue to clarify how membrane-associated signaling and trafficking contribute to gravitropism and other areas of plant growth and development.

ACKNOWLEDGMENTS

This review was made possible due to grants to Patrick H. Masson from the National Science Foundation (#IOS-0821884 and #IOS-1121694) and the College of Agricultural and Life Sciences HATCH program. Allison K. Strohm is supported by a National Science Foundation Graduate Research Fellowship. We thank Sebastian Bednarek and Marisa Otegui for their helpful comments on the manuscript.

REFERENCES

Abas, L., Benjamins, R., Malenica, N., Paciorek, T., Wisniewska, J., Wirniewska, J., et al. (2006). Intracellular trafficking and proteolysis of the *Arabidopsis* auxin-efflux facilitator PIN2 are involved in root gravitropism. *Nat. Cell Biol.* 8, 249–256.

Basu, D., Le, J., Zakharova, T., Mallery, E. L., and Szymanski, D. B. (2008). A SPIKE1 signaling complex controls actin-dependent cell morphogenesis through the heteromeric WAVE and ARP2/3 complexes. *Proc. Natl. Acad. Sci. U.S.A.* 105, 4044–4049.

Benjamins, R., Quint, A., Weijers, D., Hooykaas, P., and Offringa, R. (2001). The PINOID protein kinase regulates organ development in *Arabidopsis* by enhancing polar auxin transport. *Development* 128, 4057–4067.

Benjamins, R., and Scheres, B. (2008). Auxin: the looping star in plant development. *Annu. Rev. Plant Biol.* 59, 443–465.

Bennett, M. J., Marchant, A., Green, H. G., May, S. T., Ward, S. P., Millner, P. A., et al. (1996). *Arabidopsis* AUX1 gene: a permease-like regulator of root gravitropism. *Science* 273, 948–950.

Birnbaum, K., Shasha, D. E., Wang, J. Y., Jung, J. W., Lambert, G. M., Galbraith, D. W., et al. (2003). A gene expression map of the *Arabidopsis* root. *Science* 302, 1956–1960.

Blakeslee, J. J., Bandyopadhyay, A., Lee, O. R., Mravec, J., Titapiwatanakun, B., Sauer, M., et al. (2007). Interactions among PIN-FORMED and P-glycoprotein auxin transporters in *Arabidopsis*. *Plant Cell* 19, 131–147.

Blancaflor, E. B., Fasano, J. M., and Gilroy, S. (1998). Mapping the functional roles of cap cells in the response of *Arabidopsis* primary roots to gravity. *Plant Physiol.* 116, 213–222.

Blilou, I., Xu, J., Wildwater, M., Willemsen, V., Paponov, I., Friml, J., et al. (2005). The PIN auxin efflux facilitator network controls growth and patterning in *Arabidopsis* roots. *Nature* 433, 39–44.

Boonsirichai, K., Sedbrook, J. C., Chen, R., Gilroy, S., and Masson, P. H. (2003). ALTERED RESPONSE TO GRAVITY is a peripheral membrane protein that modulates gravity-induced cytoplasmic alkalinization and lateral auxin transport in plant statocytes. *Plant Cell* 15, 2612–2625.

Braun, M. (2002). Gravity perception requires statoliths settled on specific plasma membrane areas in characean rhizoids and protonemata. *Protoplasma* 219, 150–159.

Caspar, T., and Pickard, B. G. (1989). Gravitropism in a starchless mutant of *Arabidopsis*: implications for the starch-statolith theory of gravity sensing. *Planta* 177, 185–197.

Chen, X., Naramoto, S., Robert, S., Tejos, R., Löfke, C., Lin, D., et al. (2012). ABP1 and ROP6 GTPase signaling regulate clathrin-mediated endocytosis in *Arabidopsis* roots. *Curr. Biol.* 22, 1326–1332.

Christensen, S. K., Dagenais, N., Chory, J., and Weigel, D. (2000). Regulation of auxin response by the protein kinase PINOID. *Cell* 100, 469–478.

Christie, J. M., Yang, H., Richter, G. L., Sullivan, S., Thomson, C. E., Lin, J., et al. (2011). phot1 inhibition of ABCB19 primes lateral auxin fluxes in the shoot apex required for phototropism. *PLoS Biol.* 9:e1001076. doi: 10.1371/journal.pbio.1001076

Dharmasiri, N., Dharmasiri, S., and Estelle, M. (2005). The F-box protein TIR1 is an auxin receptor. *Nature* 435, 441–445.

Dhonukshe, P., Aniento, F., Hwang, I., Robinson, D. G., Mravec, J., Stierhof, Y. D., et al. (2007). Clathrin-mediated constitutive endocytosis of PIN auxin efflux carriers in *Arabidopsis*. *Curr. Biol.* 17, 520–527.

Friml, J., Benková, E., Blilou, I., Wisniewska, J., Hamann, T., Ljung, K., et al. (2002a). AtPIN4 mediates sink-driven auxin gradients and root patterning in *Arabidopsis*. *Cell* 108, 661–673.

Friml, J., Wisniewska, J., Benková, E., Mendgen, K., and Palme, K. (2002b). Lateral relocation of auxin efflux regulator PIN3 mediates tropism in *Arabidopsis*. *Nature* 415, 806–809.

Friml, J., Yang, X., Michniewicz, M., Weijers, D., Quint, A., Tietz, O., et al. (2004). A PINOID-dependent binary switch in apical-basal PIN polar targeting directs auxin efflux. *Science* 306, 862–865.

Fukaki, H., Fujisawa, H., and Tasaka, M. (1996a). Gravitropic response of inflorescence stems in *Arabidopsis thaliana*. *Plant Physiol.* 110, 933–943.

Fukaki, H., Fujisawa, H., and Tasaka, M. (1996b). SGR1, SGR2, SGR3: novel genetic loci involved in shoot gravitropism in *Arabidopsis thaliana*. *Plant Physiol.* 110, 945–955.

Fukaki, H., Fujisawa, H., and Tasaka, M. (1997). The RHG gene is involved in root and hypocotyl gravitropism in *Arabidopsis thaliana*. *Plant Cell Physiol.* 38, 804–810.

Fukaki, H., Wysocka-Diller, J., Kato, T., Fujisawa, H., Benfey, P. N., and Tasaka, M. (1998). Genetic evidence that the endodermis is essential for shoot gravitropism in *Arabidopsis thaliana*. *Plant J.* 14, 425–430.

Gälweiler, L., Guan, C., Müller, A., Wisman, E., Mendgen, K., Yephremov, A., et al. (1998). Regulation of polar auxin transport by AtPIN1 in *Arabidopsis* vascular tissue. *Science* 282, 2226–2230.

Geisler, M., Blakeslee, J. J., Bouchard, R., Lee, O. R., Vincenzetti, V., Bandyopadhyay, A., et al. (2005). Cellular efflux of auxin catalyzed by the *Arabidopsis* MDR/PGP transporter AtPGP1. *Plant J.* 44, 179–194.

Geisler, M., Kolukisaoglu, H. U., Bouchard, R., Billion, K., Berger, J., Saal, B., et al. (2003). TWISTED DWARF1, a unique plasma membrane-anchored immunophilin-like protein, interacts with *Arabidopsis* multidrug resistance-like transporters AtPGP1 and AtPGP19. *Mol. Biol. Cell* 14, 4238–4249.

Geldner, N., Anders, N., Wolters, H., Keicher, J., Kornberger, W., Muller, P., et al. (2003). The *Arabidopsis* GNOM ARF-GEF mediates endosomal recycling, auxin transport, and auxin-dependent plant growth. *Cell* 112, 219–230.

Geldner, N., Friml, J., Stierhof, Y. D., Jürgens, G., and Palme, K. (2001). Auxin transport inhibitors block PIN1 cycling and vesicle trafficking. *Nature* 413, 425–428.

Guan, C., Rosen, E. S., Boonsirichai, K., Poff, K. L., and Masson, P. H. (2003). The ARG1-LIKE2 gene of *Arabidopsis* functions in a gravity signal transduction pathway that is genetically distinct from the PGM pathway. *Plant Physiol.* 133, 100–112.

Harrison, B. R., and Masson, P. H. (2008). ARL2, ARG1 and PIN3 define a gravity signal transduction pathway in root statocytes. *Plant J.* 53, 380–392.

Haucke, V. (2005). Phosphoinositide regulation of clathrin-mediated endocytosis. *Biochem. Soc. Trans.* 33, 1285–1289.

Heisler, M. G., Hamant, O., Krupinski, P., Uyttewaal, M., Ohno, C., Jönsson, H., et al. (2010). Alignment between PIN1 polarity and microtubule orientation in the shoot apical meristem reveals a tight coupling between morphogenesis and auxin transport. *PLoS Biol.* 8:e1000516. doi: 10.1371/journal.pbio.1000516

Henrichs, S., Wang, B., Fukao, Y., Zhu, J. Charrier, L., Bailly, A., et al. (2012). Regulation of ABCB1/PGP1-catalysed auxin transport by linker phosphorylation. *EMBO J.* 31, 2965–2980.

Jaillais, Y., Fobis-Loisy, I., Miège, C., Rollin, C., and Gaude, T. (2006). AtSNX1 defines an endosome for auxin-carrier trafficking in *Arabidopsis*. *Nature* 443, 106–109.

Kato, T., Morita, M. T., Fukaki, H., Yamauchi, Y., Uehara, M., Niihama, M., et al. (2002). SGR2, a phospholipase-like protein, and ZIG/SGR4, a SNARE, are involved in the shoot gravitropism of *Arabidopsis*. *Plant Cell* 14, 33–46.

Kepinski, S., and Leyser, O. (2005). The *Arabidopsis* F-box protein TIR1 is an auxin receptor. *Nature* 435, 446–451.

Kiss, J. Z., Hertel, R., and Sack, F. D. (1989). Amyloplasts are necessary for full gravitropic sensitivity in roots of *Arabidopsis thaliana*. *Planta* 177, 198–206.

Kiss, J. Z. (2000). Mechanisms of the early phases of plant gravitropism. *CRC Crit. Rev. Plant Sci.* 19, 551–573.

Kleine-Vehn, J., Ding, Z., Jones, A. R., Tasaka, M., Morita, M. T., and Friml, J. (2010). Gravity-induced PIN transcytosis for polarization of auxin fluxes in gravity-sensing root cells. *Proc. Natl. Acad. Sci. U.S.A.* 107, 22344–22349.

Kleine-Vehn, J., Leitner, J., Zwiewka, M., Sauer, M., Abas, L., Luschnig, C., et al. (2008). Differential degradation of PIN2 auxin efflux carrier by retromer-dependent vacuolar targeting. *Proc. Natl. Acad. Sci. U.S.A.* 105, 17812–17817.

Krecek, P., Skupa, P., Libus, J., Naramoto, S., Tejos, R., Friml, J., et al. (2009). The PIN-FORMED (PIN) protein family of auxin transporters. *Genome Biol.* 10, 249.

Leitner, J., Petrásek, J., Tomanov, K., Retzer, K., Pařezová, M., Korbei, B., et al. (2012). Lysine63-linked ubiquitylation of PIN2 auxin carrier protein governs hormonally controlled adaptation of *Arabidopsis* root growth. *Proc. Natl. Acad. Sci. U.S.A.* 109, 8322–8327.

Leitz, G., Kang, B.-H., Schoenwaelder, M. E. A., and Staehelin, L. A. (2009). Statolith sedimentation kinetics and force transduction to the cortical endoplasmic reticulum in gravity-sensing *Arabidopsis* columella cells. *Plant Cell* 21, 843–860.

Lewis, D. R., Miller, N. D., Splitt, B. L., Wu, G., and Spalding, E. P. (2007). Separating the roles of acropetal and basipetal auxin transport on gravitropism with mutations in two *Arabidopsis* multidrug resistance-like ABC transporter genes. *Plant Cell* 19, 1838–1850.

Lin, D., Nagawa, S., Chen, J., Cao, L., Chen, X., Xu, T., et al. (2012). A ROP GTPase-dependent auxin signaling pathway regulates the subcellular distribution of PIN2 in *Arabidopsis* roots. *Curr. Biol.* 22, 1319–1325.

Lin, R., and Wang, H. (2005). Two homologous ATP-binding cassette transporter proteins, AtMDR1 and AtPGP1, regulate *Arabidopsis* photomorphogenesis and root development by mediating polar auxin transport. *Plant Physiol.* 138, 949–964.

Luesse, D. R., Schenck, C. A., Berner, B. K., Justus, B., and Wyatt, S. E. (2010). GPS4 is allelic to ARL2: implications for gravitropic signal transduction. *Gravit. Space Biol.* 23, 95–96.

Luschnig, C., Gaxiola, R. A., Grisafi, P., and Fink, G. R. (1998). EIR1, a root-specific protein involved in auxin transport, is required for gravitropism in *Arabidopsis thaliana*. *Genes Dev.* 12, 2175–2187.

Maher, E. P., and Martindale, S. J. (1980). Mutants of *Arabidopsis thaliana* with altered responses to auxins and gravity. *Biochem. Genet.* 18, 1041–1053.

Marchant, A., Kargul, J., May, S. T., Muller, P., Delbarre, A., Perrot-Rechenmann, C., et al. (1999). AUX1 regulates root gravitropism in *Arabidopsis* by facilitating auxin uptake within root apical tissues. *EMBO J.* 18, 2066–2073.

Matsuoka, K., Bassham, D. C., Raikhel, N. V., and Nakamura, K. (1995). Different sensitivity to wortmannin of two vacuolar sorting signals indicates the presence of distinct sorting machineries in tobacco cells. *J. Cell Biol.* 130, 1307–1318.

Mei, Y., Jia, W.-J., Chu, Y.-J., and Xue, H.-W. (2012). *Arabidopsis* phosphatidylinositol monophosphate 5-kinase 2 is involved in root gravitropism through regulation of polar auxin transport by affecting the cycling of PIN proteins. *Cell Res.* 22, 581–597.

Men, S., Boutté, Y., Ikeda, Y., Li, X., Palme, K., Stierhof, Y.-D., et al. (2008). Sterol-dependent endocytosis mediates post-cytokinetic acquisition of PIN2 auxin efflux carrier polarity. *Nat. Cell Biol.* 10, 237–244.

Michniewicz, M., Zago, M. K., Abas, L., Weijers, D., Schweighofer, A., Meskiene, I., et al. (2007). Antagonistic regulation of PIN phosphorylation by PP2A and PINOID directs auxin flux. *Cell* 130, 1044–1056.

Monshausen, G. B., Miller, N. D., Murphy, A. S., and Gilroy, S. (2011). Dynamics of auxin-dependent Ca^{+} and pH signaling in root growth revealed by integrating high-resolution imaging with automated computer vision-based analysis. *Plant J.* 65, 309–318.

Morita, M. T. (2010). Directional gravity sensing in gravitropism. *Annu. Rev. Plant Biol.* 61, 705–720.

Morita, M. T., Kato, T., Nagafusa, K., Saito, C., Ueda, T., Nakano, A., et al. (2002). Involvement of the vacuoles of the endodermis in the early process of shoot gravitropism in *Arabidopsis*. *Plant Cell* 14, 47–56.

Müller, A., Guan, C., Gälweiler, L., Tänzler, P., Huijser, P., Marchant, A., et al. (1998). AtPIN2 defines a locus of *Arabidopsis* for root gravitropism control. *EMBO J.* 17, 6903–6911.

Nakayama, N., Smith, R. S., Mandel, T., Robinson, S., Kimura, S., Boudaoud, A., et al. (2012). Mechanical regulation of auxin-mediated growth. *Curr. Biol.* 22, 1468–1476.

Noh, B., Bandyopadhyay, A., Peer, W. A., Spalding, E. P., and Murphy, A. S. (2003). Enhanced gravi- and phototropism in plant mdr mutants mislocalizing the auxin efflux protein PIN1. *Nature* 423, 999–1002.

Noh, B., Murphy, A. S., and Spalding, E. P. (2001). Multidrug resistance-like genes of *Arabidopsis* required for auxin transport and auxin-mediated development. *Plant Cell* 13, 2441–2454.

Ottenschlager, I., Wolff, P., Wolverton, C., Bhalerao, P., Sandberg, G., Ishikawa, H., et al. (2003). Gravity-regulated differential auxin transport from columella to lateral root cap cells. *Proc. Natl. Acad. Sci. U.S.A.* 100, 2987–2991.

Paciorek, T., Zazimalova, E., Ruthardt, N., Petrasek, J., Stierhof, Y. D., Kleine-Vehn, J., et al. (2005). Auxin inhibits endocytosis and promotes its own efflux from cells. *Nature* 435, 1251–1256.

Perera, I. Y., Heilmann, I., and Boss, W. F. (1999). Transient and sustained increases in inositol 1,4,5-trisphosphate precede the differential growth response in gravistimulated maize pulvini. *Proc. Natl. Acad. Sci. U.S.A.* 96, 5838–5843.

Perera, I. Y., Heilmann, I., Chang, S. C., Boss, W. F., and Kaufman, P. B. (2001). A role for inositol 1,4,5-trisphosphate in gravitropic signaling and the retention of cold-perceived gravistimulation of oat shoot pulvini. *Plant Physiol.* 125, 1499–1507.

Perera, I. Y., Hung, C.-Y., Brady, S., Muday, G. K., and Boss, W. F. (2006). A universal role for inositol 1,4,5-trisphosphate-mediated signaling in plant gravitropism. *Plant Physiol.* 140, 746–760.

Petrásek, J., and Friml, J. (2009). Auxin transport routes in plant development. *Development* 136, 2675–2688.

Peyroche, A., Antonny, B., Robineau, S., Acker, J., Cherfils, J., and Jackson, C. L. (1999). Brefeldin A acts to stabilize an abortive ARF-GDP-Sec7 domain protein complex: involvement of specific residues of the Sec7 domain. *Mol. Cell* 3, 275–285.

Péret, B., Swarup, K., Ferguson, A., Seth, M., Yang, Y., Dhondt, S., et al. (2012). AUX/LAX genes encode a family of auxin influx transporters that perform distinct functions during *Arabidopsis* development. *Plant Cell* 24, 2874–2885.

Plieth, C., and Trewavas, A. J. (2002). Reorientation of seedlings in the earth's gravitational field induces cytosolic calcium transients. *Plant Physiol.* 129, 786–796.

Rahman, A., Takahashi, M., Shibasaki, K., Wu, S., Inaba, T., Tsurumi, S., et al. (2010). Gravitropism of *Arabidopsis thaliana* roots requires the polarization of PIN2 toward the root tip in meristematic cortical cells. *Plant Cell* 22, 1762–1776.

Rashotte, A. M., DeLong, A., and Muday, G. K. (2001). Genetic and chemical reductions in protein phosphatase activity alter auxin transport, gravity response, and lateral root growth. *Plant Cell* 13, 1683–1697.

Raven, J. A. (1975). Transport of indoleacetic acid in plant cells in relation to pH and electrical potential gradients, and its significance for polar IAA transport. *New Phytol.* 74, 163–172.

Reyes, F. C., Buono, R., and Otegui, M. S. (2011). Plant endosomal trafficking pathways. *Curr. Opin. Plant Biol.* 14, 666–673.

Robineau, S., Chabre, M., and Antonny, B. (2000). Binding site of brefeldin A at the interface between the small G protein ADP-ribosylation factor 1 (ARF1) and the nucleotide-exchange factor Sec7 domain. *Proc. Natl. Acad. Sci. U.S.A.* 97, 9913–9918.

Rojas-Pierce, M., Titapiwatanakun, B., Sohn, E. J., Fang, F., Larive, C. K., Blakeslee, J., et al. (2007). *Arabidopsis* P-glycoprotein19 participates in the inhibition of gravitropism by gravacin. *Chem. Biol.* 14, 1366–1376.

Rubery, P. H., and Sheldrake, A. R. (1974). Carrier-mediated auxin transport. *Planta* 118, 101–121.

Saito, C., Morita, M. T., Kato, T., and Tasaka, M. (2005). Amyloplasts and vacuolar membrane dynamics in the living graviperceptive cell of the *Arabidopsis* inflorescence stem. *Plant Cell* 17, 548–558.

Salinas-Mondragon, R. E., Kajla, J. D., Perera, I. Y., Brown, C. S., and Sederoff, H. W. (2010). Role of inositol 1,4,5-triphosphate signalling in gravitropic and phototropic gene expression. *Plant Cell Environ.* 33, 2041–2055.

Salisbury, F. B., Gillespie, L., and Rorabaugh, P. (1988). Gravitropism in higher plant shoots. V. Changing sensitivity to auxin. *Plant Physiol.* 88, 1186–1194.

Santelia, D., Vincenzetti, V., Azzarello, E., Bovet, L., Fukao, Y., Düchtig, P., et al. (2005). MDR-like ABC transporter AtPGP4 is involved in auxin-mediated lateral root and root hair development. *FEBS Lett.* 579, 5399–5406.

Sato, M. H., Nakamura, N., Ohsumi, Y., Kouchi, H., Kondo, M., Hara-Nishimura, I., et al. (1997). The AtVAM3 encodes a syntaxin-related molecule implicated in the vacuolar assembly in *Arabidopsis thaliana*. *J. Biol. Chem.* 272, 24530–24535.

Scott, A. C., and Allen, N. S. (1999). Changes in cytosolic pH within *Arabidopsis* root columella cells play a key role in the early signaling pathway for root gravitropism. *Plant Physiol.* 121, 1291–1298.

Sedbrook, J. C., Chen, R., and Masson, P. H. (1999). ARG1 (altered response to gravity) encodes a DnaJ-like protein that potentially interacts with the cytoskeleton. *Proc. Natl. Acad. Sci. U.S.A.* 96, 1140–1145.

Shi, J.-H., and Yang, Z.-B. (2011). Is ABP1 an auxin receptor yet? *Mol. Plant* 4, 635–640.

Shin, H., Shin, H.-S., Guo, Z., Blancaflor, E. B., Masson, P. H., and Chen, R. (2005). Complex regulation of *Arabidopsis* AGR1/PIN2-mediated root gravitropic response and basipetal auxin transport by cantharidin-sensitive protein phosphatases. *Plant J.* 42, 188–200.

Silady, R. A., Ehrhardt, D. W., Jackson, K., Faulkner, C., Oparka, K., and Somerville, C. R. (2008). The GRV2/RME-8 protein of *Arabidopsis* functions in the late endocytic pathway and is required for vacuolar membrane flow. *Plant J.* 53, 29–41.

Silady, R. A., Kato, T., Lukowitz, W., Sieber, P., Tasaka, M., and Somerville, C. R. (2004). The gravitropism defective 2 mutants of *Arabidopsis* are deficient in a protein implicated in endocytosis in *Caenorhabditis elegans*. *Plant Physiol.* 13.6, 3095–3103: discussion 3002.

Stanga, J. P., Boonsirichai, K., Sedbrook, J. C., Otegui, M. S., and Masson, P. H. (2009). A role for the TOC complex in *Arabidopsis* root gravitropism. *Plant Physiol.* 149, 1896–1905.

Staves, M. P. (1997). Cytoplasmic streaming and gravity sensing in Chara internodal cells. *Planta* 203, S79–84.

Steinmann, T., Geldner, N., Grebe, M., Mangold, S., Jackson, C. L., Paris, S., et al. (1999). Coordinated polar localization of auxin efflux carrier PIN1 by GNOM ARF GEF. *Science* 286, 316–318.

Strohm, A. K., Baldwin, K. L., and Masson, P. H. (2012). Molecular mechanisms of root gravity sensing and signal transduction. *Wiley Interdiscip. Rev. Dev. Biol.* 1, 276–285.

Surpin, M., Rojas-Pierce, M., Carter, C., Hicks, G. R., Vasquez, J., and Raikhel, N. V. (2005). The power of chemical genomics to study the link between endomembrane system components and the gravitropic response. *Proc. Natl. Acad. Sci. U.S.A.* 102, 4902–4907.

Swarup, R., and Bennett, M. (2003). Auxin transport: the fountain of life in plants? *Dev. Cell* 5, 824–826.

Swarup, R., Kramer, E. M., Perry, P., Knox, K., Leyser, H. M. O., Haseloff, J., et al. (2005). Root gravitropism requires lateral root cap and epidermal cells for transport and response to a mobile auxin signal. *Nat. Cell Biol.* 7, 1057–1065.

Terasaka, K., Blakeslee, J. J., Titapiwatanakun, B., Peer, W. A., Bandyopadhyay, A., Makam, S. N., et al. (2005). PGP4, an ATP binding cassette P-glycoprotein, catalyzes auxin transport in *Arabidopsis thaliana* roots. *Plant Cell* 17, 2922–2939.

Toyota, M., Furuichi, T., Tatsumi, H., and Sokabe, M. (2008). Critical consideration on the relationship between auxin transport and calcium transients in gravity perception of *Arabidopsis* seedlings. *Plant Signal. Behav.* 3, 521–524.

Tsugeki, R., and Fedoroff, N. V. (1999). Genetic ablation of root cap cells in *Arabidopsis*. *Proc. Natl. Acad. Sci. U.S.A.* 96, 12941–12946.

Vieten, A., Vanneste, S., Wisniewska, J., Benková, E., Benjamins, R., Beeckman, T., et al. (2005). Functional redundancy of PIN proteins is accompanied by auxin-dependent cross-regulation of PIN expression. *Development* 132, 4521–4531.

Wang, Y., Lin, W.-H., Chen, X., and Xue, H.-W. (2009). The role of *Arabidopsis* 5PTase13 in root gravitropism through modulation of vesicle trafficking. *Cell Res.* 19, 1191–1204.

Wasteneys, G. O., and Galway, M. E. (2003). Remodeling the cytoskeleton for growth and form: an overview with some new views. *Annu. Rev. Plant Biol.* 54, 691–722.

Whitford, R., Fernandez, A., Tejos, R., Pérez, A. C., Kleine-Vehn, J., Vanneste, S., et al. (2012). GOLVEN secretory peptides regulate auxin carrier turnover during plant gravitropic responses. *Dev. Cell* 22, 678–685.

Willemsen, V., Friml, F., Grebe, M., van den Toorn, A., Palme, K., and Scheres, B. (2003). Cell polarity and PIN protein positioning in *Arabidopsis* require STEROL

METHYLTRANSFERASE1 function. *Plant Cell* 15, 612–625.

Wisniewska, J., Xu, J., Seifertová, D., Brewer, P. B., Ruzicka, K., Blilou, I., et al. (2006). Polar PIN localization directs auxin flow in plants. *Science* 312, 883.

Wolverton, C., Ishikawa, H., and Evans, M. L. (2002). The kinetics of root gravitropism: dual motors and sensors. *J. Plant Growth Regul.* 21, 102–112.

Yamauchi, Y., Fukaki, H., Fujisawa, H., and Tasaka, M. (1997). Mutations in the SGR4, SGR5 and SGR6 loci of *Arabidopsis thaliana* alter the shoot gravitropism. *Plant Cell Physiol.* 38, 530–535.

Yang, H., and Murphy, A. S. (2009). Functional expression and characterization of *Arabidopsis* ABCB, AUX 1 and PIN auxin transporters in *Schizosaccharomyces pombe*. *Plant J.* 59, 179–191.

Yang, Y., Hammes, U. Z., Taylor, C. G., Schachtman, D. P., and Nielsen, E. (2006). High-affinity auxin transport by the AUX1 influx carrier protein. *Curr. Biol.* 16, 1123–1127.

Yano, D., Sato, M., Saito, C., Sato, M. H., Morita, M. T., and Tasaka, M. (2003). A SNARE complex containing SGR3/AtVAM3 and ZIG/VTI11 in gravity-sensing cells is important for *Arabidopsis* shoot gravitropism. *Proc. Natl. Acad. Sci. U.S.A.* 100, 8589–8594.

Young, L. M., Evans, M. L., and Hertel, R. (1990). Correlations between gravitropic curvature and auxin movement across gravistimulated roots of *Zea mays*. *Plant Physiol.* 92, 792–796.

Zheng, H. Q., and Staehelin, L. A. (2001). Nodal endoplasmic reticulum, a specialized form of endoplasmic reticulum found in gravity-sensing root tip columella cells. *Plant Physiol.* 125, 252–265.

Zheng, H., von Mollard, G. F., Kovaleva, V., Stevens, T. H., and Raikhel, N. V. (1999). The plant vesicle-associated SNARE AtVTI1a likely mediates vesicle transport from the trans-Golgi network to the prevacuolar compartment. *Mol. Biol. Cell* 10, 2251–2264.

Conflict of Interest Statement: The authors declare that the research was conducted in the absence of any commercial or financial relationships that could be construed as a potential conflict of interest.

Received: 07 September 2012; accepted: 21 November 2012; published online: 11 December 2012.

*Citation: Strohm AK, Baldwin KL and Masson PH (2012) Multiple roles for membrane-associated protein trafficking and signaling in gravitropism. Front. Plant Sci. **3**:274. doi: 10.3389/fpls.2012.00274*

This article was submitted to Frontiers in Plant Traffic and Transport, a specialty of Frontiers in Plant Science.

frontiers in
PLANT SCIENCE

REVIEW ARTICLE
published: 12 October 2012
doi: 10.3389/fpls.2012.00227

Evolution and structural diversification of PILS putative auxin carriers in plants

Elena Feraru[1], Stanislav Vosolsobě[2], Mugurel I. Feraru[1], Jan Petrášek[2,3] and Jürgen Kleine-Vehn[1]*

[1] Department of Applied Genetics and Cell Biology, University of Natural Resources and Life Sciences, Vienna, Austria
[2] Department of Faculty of Science, Experimental Plant Biology, Charles University, Prague, Czech Republic
[3] Institute of Experimental Botany of the Academy of Sciences of the Czech Republic, Prague, Czech Republic

Edited by:
Markus Geisler, University of Fribourg, Switzerland

Reviewed by:
Viktor Zarsky, Charles University, Czech Republic
Eric M. Kramer, Bard College at Simon's Rock, USA

****Correspondence:***
Jürgen Kleine-Vehn, Department of Applied Genetics and Cell Biology, University of Natural Resources and Life Sciences, Muthgasse 18, A-1190 Vienna, Austria.
e-mail: juergen.kleine-vehn@boku.ac.at

The phytohormone auxin contributes to virtually every aspect of the plant development. The spatiotemporal distribution of auxin depends on a complex interplay between auxin metabolism and intercellular auxin transport. Intracellular auxin compartmentalization provides another link between auxin transport processes and auxin metabolism. The PIN-LIKES (PILS) putative auxin carriers localize to the endoplasmic reticulum (ER) and contribute to cellular auxin homeostasis. PILS proteins regulate intracellular auxin accumulation, the rate of auxin conjugation and, subsequently, affect nuclear auxin signaling. Here, we investigate sequence diversification of the PILS family in *Arabidopsis thaliana* and provide insights into the evolution of these novel putative auxin carriers in plants. Our data suggest that PILS proteins are conserved throughout the plant lineage and expanded during higher plant evolution. PILS proteins diversified early during plant evolution into three clades. Besides the ancient Clade I encompassing non-land plant species, PILS proteins evolved into two clades. The diversification of Clade II and Clade III occurred already at the level of non-vascular plant evolution and, hence, both clades contain vascular and non-vascular plant species. Nevertheless, Clade III contains fewer non- and increased numbers of vascular plants, indicating higher importance of Clade III for vascular plant evolution. Notably, PILS proteins are distinct and appear evolutionarily older than the prominent PIN-FORMED auxin carriers. Moreover, we revealed particular PILS sequence divergence in *Arabidopsis* and assume that these alterations could contribute to distinct gene regulations and protein functions.

Keywords: PILS proteins, auxin, evolution, phylogeny, auxin metabolism, auxin homeostasis

INTRODUCTION

Plant development is particularly flexible due to its postembryonic growth behavior, allowing individual adjustment of the body plan according to the environment (Finet and Jaillais, 2012). The phytohormone auxin is crucial for these adaptive responses and, hence, has drawn enormous research attention (Teale et al., 2008). The importance of auxin for plant development seems to be also reflected in the complex regulation of auxin perception and its spatiotemporal distribution (Vanneste and Friml, 2009). Up to date three auxin receptor classes have been suggested to jointly regulate auxin-signaling output. Most auxin responses have been assigned to the F-box proteins TRANSPORT INHIBITOR RESPONSE1/AUXIN SIGNALING F-BOX (TIR1/AFB). Auxin binding to the co-receptors TIR1/AFB and the AUXIN/INDOLE-3-ACETIC ACID (Aux/IAA) will initiate the proteasome-dependent degradation of the transcriptional repressors Aux/IAAs. The subsequent release of AUXIN RESPONSE FACTOR (ARF) transcription factors eventually leads to the transcriptional reprogramming of the respective cell (Leyser, 2006; Chapman and Estelle, 2009). Another F-box protein S-PHASE KINASE-ASSOCIATED PROTEIN 2A (SKP2A) also binds to auxin and might contribute to auxin-dependent modulation of the cell cycle (Jurado et al., 2010). Rapid and non-genomic auxin effects appear to be mainly perceived by the AUXIN BINDING PROTEIN1 (ABP1; Jones and Venis, 1989; Robert et al., 2010; Xu et al., 2010). However, ABP1 action might also affect auxin-dependent gene transcription and cell cycle regulation (Braun et al., 2008; Tromas et al., 2009).

Beside the complex cell type-dependent regulation of auxin signaling, also auxin metabolism is multifaceted. Several redundant auxin biosynthesis pathways determine auxin levels in various tissues and the decay/inactivation of auxin is regulated via oxidation or mostly reversible conjugation (Woodward and Bartel, 2005; Ruiz Rosquete et al., 2012; Zhao, 2012). Auxin metabolism is highly dynamic and has pronounced importance for the spatiotemporal regulation of auxin.

Intercellular (polar) auxin transport also determines cellular auxin levels (Zazímalová et al., 2010). The most prominent auxin carriers are AUXIN-RESISTANT1/LIKE AUX1 (AUX/LAX) influx carriers, ATP BINDING CASSETTE (ABC) auxin transporters of a MULTIDRUG RESISTANCE (MDR) subfamily, and the PIN-FORMED (PIN) auxin carriers (Bennett et al., 1996; Chen et al., 1998; Gälweiler et al., 1998; Luschnig et al., 1998; Müller et al., 1998; Utsuno et al., 1998; Geisler et al., 2005). PIN proteins have a

particular developmental importance as their polar localization at a given cell side determines the direction of the intercellular auxin flow (Wisniewska et al., 2006). PIN proteins can be grouped into two subclasses according to the length of the central hydrophilic loop. Canonical PIN1-type auxin efflux carriers have a long loop, localize to the plasma membrane (PM) and perform a rate-limiting function in cellular auxin efflux (Petrásek et al., 2006). In contrast, PIN5 and PIN8 have a dramatically reduced central hydrophilic loop, localize to the endoplasmic reticulum (ER) and regulate intracellular auxin compartmentalization and homeostasis (Mravec et al., 2009; Bosco et al., 2012; Ding et al., 2012).

We have recently discovered a novel putative auxin carrier family of seven members in *Arabidopsis thaliana* (Barbez et al., 2012) and designated them as PIN-LIKES (PILS), because their predicted protein topology is highly similar to the topology of the PIN proteins. Similar to PIN proteins, PILS contain the so-called Interpro auxin carrier domain, an *in silico* defined domain to predict auxin transport function. Functional PILS5-GFP fusion proteins localize to the ER and stimulate intracellular auxin accumulation in plant and yeast cells (Barbez et al., 2012). PILS2 and PILS5 activity increases amide auxin conjugates, thereby reducing the free auxin levels, and negatively affecting nuclear auxin signaling (Barbez et al., 2012). Our current working model proposes that PILS2 and PILS5 proteins regulate auxin compartmentalization into the ER lumen, where auxin might be the substrate for compartmentalized auxin metabolism (**Figure 1**). It needs to be experimentally tested whether PILS proteins affect nuclear auxin signaling mainly by limiting the excess of auxin to diffuse into the nucleus or by the effect on presumably compartmentalized auxin conjugation. This mode of action is reminiscent to auxin carrier PIN5 that has been shown to regulate intracellular auxin homeostasis by modulating auxin compartmentalization and metabolism at the ER (Mravec et al., 2009). Further research will address whether the distinct protein families have redundant and interchangeable function at the ER.

PILS overexpression strongly distorts plant patterning and development, while *pils2* and *pils5* loss of function mutants show comparably weaker defects in plant growth regulation. Moderate PILS5 gain and *pils2pils5* loss of function phenotypes can be largely explained by low and high auxin content, respectively. For example, PILS5 overexpressors have reduced free auxin levels/signaling, shorter hypocotyls and fewer lateral roots, while *pils2pils5* double mutants display higher free auxin levels, enhanced hypocotyl growth and lateral rooting. In contrast, PILS5 gain and*pils2pils5* loss of function leads to reduced and enhanced root growth, which might be not related to the overall changes in auxin content, but could indicate a more specific PILS2 and PILS5 function in the cellular regulation of root growth (Barbez et al., 2012).

The identification of PILS proteins and their role in auxin homeostasis at the ER reveal the molecular complexity of intracellular auxin compartmentalization and its eminent importance for the plant development. Here we present *in silico* analysis to further reveal insight into the organization and regulation of this novel family of putative auxin transport facilitators.

MATERIAL AND METHODS

SEQUENCE INFORMATION

Sequences were downloaded from PLAZA[1], NCBI[2] by using tblastx program (Altschul et al., 1997; nr/nt database, PILS and PIN sequences from *A. thaliana* as queries) or Phytozome[3] servers. The information and the ID of the presented sequences can be found in the Supplementary Data.

ONLINE SERVERS

The online available servers used to perform *in silico* analyses of PILSes are found at: http://www.arabidopsis.org (chromosome localization; alternative splicing), http://bioinformatics.psb.ugent.be/plaza/ (intron/exon organization; sequence information), www.genevestigator.com (expression), http://bar.utoronto.ca/efp/cgi-bin/efpWeb.cgi (expression), http://www.enzim.hu/hmmtop/index.php (prediction of protein topology), http://biophysics.biol.uoa.gr/TMRPres2D (visual representation of transmembrane protein models), http://weblogo.berkeley.edu/logo.cgi (sequence logo), http://www.cbs.dtu.dk/services/NetPhos/ (prediction of phosphorylation sites), http://www.cbs.dtu.dk/services/NetPhosK (prediction of phosphorylation sites), http://www.ebi.ac.uk/Tools/msa/clustalw2/ (multiple amino acid sequences alignment), http://blast.ncbi.nlm.nih.gov/ (sequence information), http://www.phytozome.net/ (sequence information), http://www.r-project.org/ (analysis of collinearity).

ANALYSIS OF COLLINEARITY

We investigated possible collinearity among *A. thaliana PILS* genes by comparing 200 surrounding translated genes for each *PILS*. The comparison was performed for pairs of *PILS* genes by using blastp program (Altschul et al., 1997). The homology was

[1]http://bioinformatics.psb.ugent.be/plaza/
[2]http://www.ncbi.nlm.nih.gov/
[3]http://www.phytozome.net/

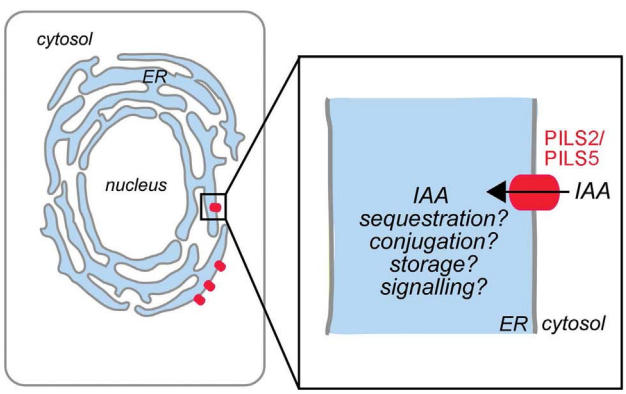

FIGURE 1 | Model of PILS protein function in *Arabidopsis thaliana*. PILS2 and PILS5 proteins localize to the ER and mediate intracellular auxin accumulation. We hypothesize that PILS proteins are putative auxin carriers that regulate the auxin transport from the cytosol into the lumen of the ER (black arrow). PILS activity affects auxin metabolism and might control the cytoplasmic availability of auxin (adapted from Barbez et al., 2012).

determined according to *E-value* from blast results. The analysis was performed in R environment[4].

PHYLOGENETIC ANALYSIS

A multiple alignment was built by using Muscle in MEGA5 software (Tamura et al., 2011). Only the conserved domains were used and all positions with less than 80% site coverage were eliminated. The evolutionary history was inferred by using the Maximum Likelihood method based on the Whelan and Goldman (2001) + Freq. model with discrete Gamma distribution (five categories, *G* parameter = 3.0640) for analysis of PILS amino acid sequences or on the Whelan and Goldman model with discrete Gamma distribution (five categories, *G* parameter = 2.9920) for analysis of PIN-PILS dataset. The trees are drawn to scale, with branch lengths measured in the number of substitutions per site. The PILS analysis involved 42 amino acid sequences and 322 positions in the final dataset. The PIN-PILS analysis involved 67 amino acid sequences and 354 positions. Evolutionary analyses were conducted in MEGA5 (Tamura et al., 2011). For the sequence alignments see Figures S2 and S3 in Supplementary Material.

RESULTS

PHYLOGENY OF PILS PROTEINS

Using available online tools, we previously showed that PILS proteins are highly conserved among plant species (Barbez et al., 2012). To further investigate the evolution of PILS protein diversification, we analyzed PILS protein sequences from all sequenced taxa of Viridiplantae. The PILS family is present in all the 26 available sequenced genomes and is represented by 202 genes (**Table 1**; Van Bel et al., 2012; confirmed by reciprocal blast, Altschul et al., 1997). PILS family obviously diversified in the different plant lineages (**Table 1**). Ancient species, such as algae (1–2), mosses (5), and spike mosses (8), have 1–8 *PILS* genes, while seed plants, such as *Oryza* (6), *Zea* (10), *Medicago* (13), or *Populus* (18), have 6 to 18 *PILS* genes (**Table 1**). The steadily increasing number in seed plants suggests that *PILS* genes have duplicated independently in several plant lineages and indicate a more diversified function of PILS proteins in higher plants.

To assess the evolutionary relationship among PILS proteins, we constructed phylogenetic trees with PILS sequences from selected model organisms such as available green algae, *Physcomitrella*, *Selaginella*, *Picea*, *Brachypodium*, *Oryza*, *Medicago*, *Arabidopsis*, and *Populus* sequences (**Figure 2**; Figure S1 in Supplementary Material; for sequence alignment see Figure S2 in Supplementary Material). The phylogenetic tree presented in **Figure 2** shows that PILSes from Viridiplantae can be grouped into three evolutionary clades: Clade I, Clade II, and Clade III.

The available green algae genomes from the lineage *Chlorophyta* have a relatively low number of only one or two *PILS* genes per species. All these PILS algae orthologs cluster together and define the Clade I that contains the so far oldest known *PILS* genes of the Viridiplantae (**Figure 2**). We could also identify putative *PILS* genes in the genomes of sequenced algae from lineage Streptophyta from which the land plants evolved. However, we did not include these sequences in the phylogenetic analysis because they were incomplete (only EST fragments are currently available).

The evolutionary Clade II and III already emerged early during non-vascular plant evolution and both contain PILS sequences from Embryophytes (land plants; **Figure 2**). The main lineages of land plants are mosses, liverworts, hornworts, lycophytes, ferns, gymnosperms, and angiosperms. Clade II includes the well-conserved PILS2- and PILS6-like subclades, including orthologs of PILS2 and PILS6 from *Physcomitrella*, *Selaginella*, *Brachypodium*, or *Oryza* (**Figure 2**).

Clade III encompasses the PILS1/PILS3/PILS4- and PILS5/PILS7-like subclades and displays particular expansion in higher seed plants (**Figure 2**; Figure S1 in Supplementary Material). Accordingly, this clade encompasses also most *Brachypodium* and *Oryza* orthologs (**Figure 2**; Figure S1 in Supplementary Material). Interestingly, one *Physcomitrella* and two *Selaginella* PILS sequences are present at the root of the Clade III (**Figure 2**). The relatively low number of moss and the relative over amount of higher plant sequences in Clade III may suggest particular importance of this clade in vascular plant evolution.

Table 1 | Size of *PILS* gene families in different plant species.

Lineage	Species	Number of genes*
Eukaryota		
Viridiplantae		
Chlorophyta	*Micromonas* sp.	1
	Micromonas pusilla	1
	Ostreococcus lucimarinus	1
	Ostreococcus tauri	1
	Chlamydomonas reinhardtii	2
	Volvox carteri	2
Bryophyta	*Physcomitrella patens*	5
Lycopodiophyta	*Selaginella moellendorffii*	8
Euphyllophyta		
Monocots	*Oryza sativa japonica*	6
	Oryza sativa indica	6
	Sorghum bicolor	7
	Brachypodium distachyon	8
	Zea mays	10
Dicots	*Carica papaya*	4
	Arabidopsis lyrata	6
	Arabidopsis thaliana	7
	Ricinus communis	7
	Fragaria vesca	8
	Manihot esculenta	9
	Lotus japonicus	12
	Medicago truncatula	13
	Vitis vinifera	13
	Malus domestica	14
	Theobroma cacao	16
	Glycine max	17
	Populus trichocarpa	18

**Gene information and sequences were retrieved from PLAZA platform (Van Bel et al., 2012) and candidates were evaluated by reciprocal blasts (Altschul et al., 1997).*

[4]http://www.r-project.org/

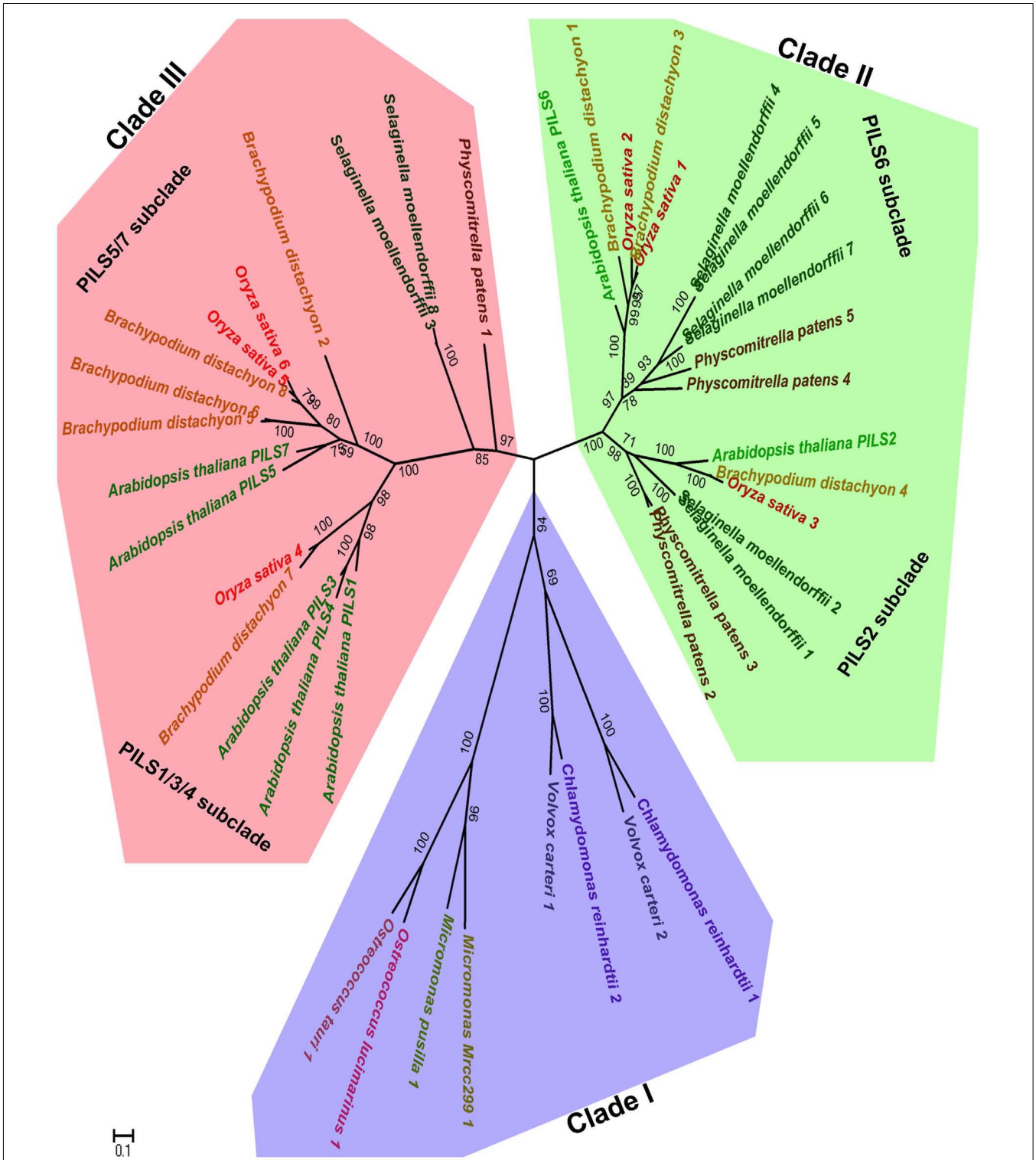

FIGURE 2 | Phylogeny of PILS proteins. The phylogenetic tree of PILS proteins can be divided into three clades: Clade I (blue), Clade II (green), and Clade III (red). The *Arabidopsis* PILSes are found in the Clade II and Clade III, while Clade I is represented only by PILS proteins from algae. The Maximum Likelihood molecular phylogenetic analysis was performed in MEGA5 (Tamura et al., 2011) by using 42 amino acid PILS sequences from algae, *Physcomitrella*, *Selaginella*, *Brachypodium*, *Oryza*, and *Arabidopsis* as explained in the Materials and Methods.

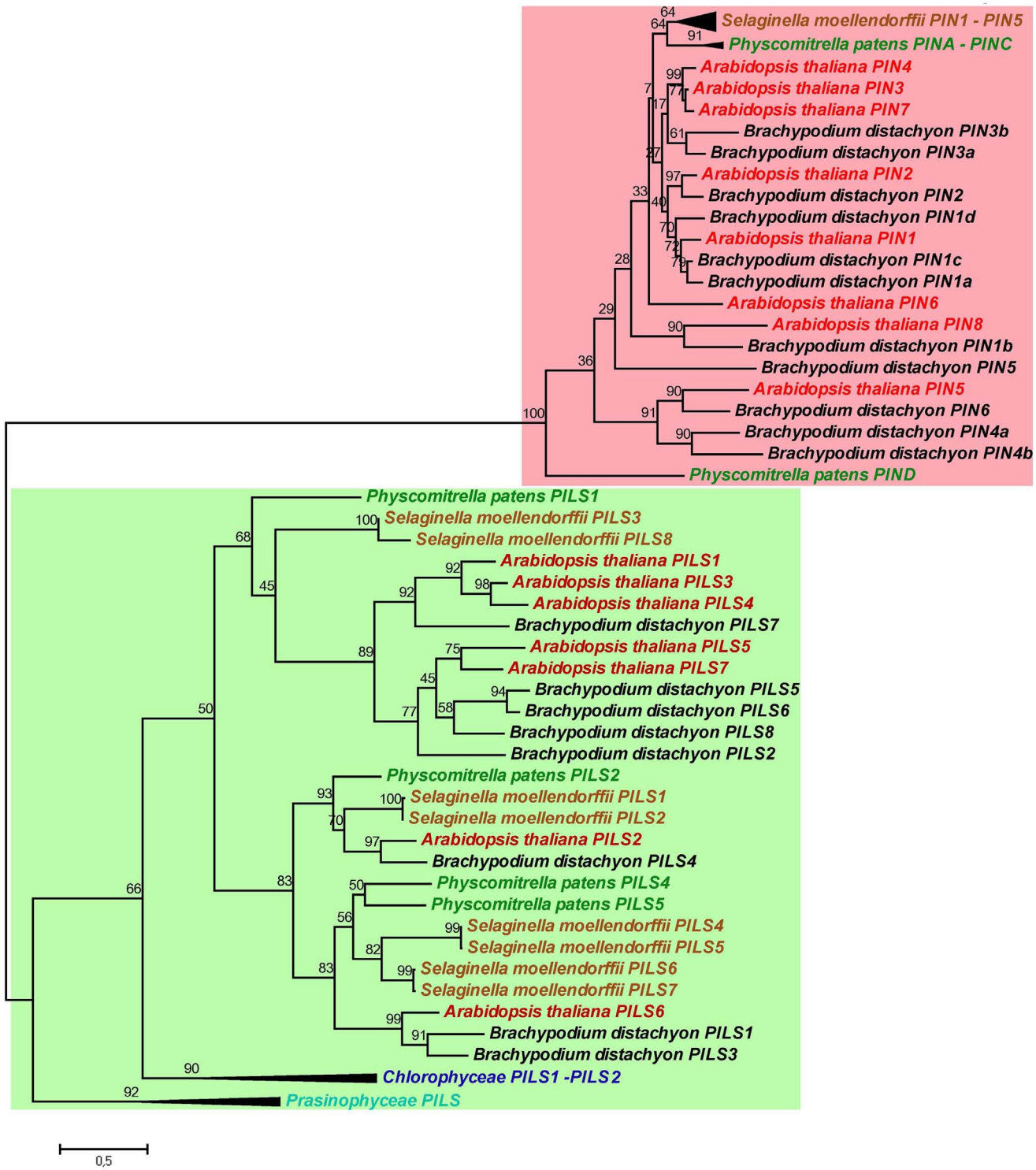

FIGURE 3 | Phylogeny of PILS and PIN proteins. PILS proteins are evolutionarily distinct of PIN proteins. Note the two separated subtrees. The Maximum Likelihood phylogenetic analysis was performed in MEGA5 (Tamura et al., 2011) by using PILS and PIN amino acid sequences from algae, *Physcomitrella*, *Selaginella*, *Brachypodium*, and *Arabidopsis*. For a better visualization the algae and sometimes the *Physcomitrella* and *Selaginella* branches were collapsed.

Our analysis reveals that PILS proteins are evolutionarily conserved throughout plant evolution and might uncover the versatile importance of compartmentalized auxin homeostasis throughout the plant kingdom.

PILS PROTEINS ARE EVOLUTIONARILY DISTINCT OF PIN PROTEINS

The canonical PIN proteins act in the cellular efflux of auxin at the plasma membrane, but the most ancient members of PIN proteins (PIN5-type) localize to the ER and regulate the subcellular compartmentalization of auxin and auxin metabolism (Mravec et al., 2009). Hence, both PILS and PIN5-like proteins localize to the ER and regulate auxin homeostasis, presumably by mediating auxin transport at the ER (Mravec et al., 2009; Barbez et al., 2012; Bosco et al., 2012; Ding et al., 2012).

Next, we investigated the evolutionary relationship between PILS and PIN proteins (**Figure 3**; for sequence alignment see Figure S3 in Supplementary Material). The phylogenetic analysis of PILS and PIN sequences from algae, moss, spikemoss, and several Angiosperms revealed that PILSes and PINs form two distinct phylogenetic clades (**Figure 3**). Although having a similar predicted protein structure and possibly similar function at the ER, PIN and PILS proteins are evolutionarily distinct in plants. In contrast to PILSes, we could not find any PIN sequence in the genomes of *Chlorophyta* algae, such as *Chlamydomonas*, *Micromonas*, *Ostreococcus*, *or Volvox*. Notably, a truncated PIN sequence has been found in the genome of *Spirogyra* (De Smet et al., 2011). These findings indicate that PILS proteins are more conserved during plant evolution and seem evolutionarily older than PIN proteins. Therefore, we assume that the PILS proteins are central to the evolution of intracellular auxin transport, which presumably has preceded the evolution of PIN-dependent intercellular and intracellular auxin transport.

PILS DIVERSIFICATION IN *ARABIDOPSIS THALIANA*

The seven *Arabidopsis PILS* genes are placed on chromosome 1, 2, and 5 (**Figure 4**). *PILS1* to *PILS4* are found on chromosome 1, *PILS5* on chromosome 2, while *PILS6* and *PILS7* are both placed at the ends of the chromosome 5 (**Figure 4**). *PILS3* and *PILS4* are neighboring genes at the bottom arm of the chromosome 1 (**Figure 4**), indicating that *PILS3* and *PILS4* may resulted from a gene duplication event. To investigate *PILS* paralogs in *A. thaliana* we performed comparative sequence analysis of genes that surround the seven *PILS* genes (**Figure 5**). Rows of 200 translated genes surrounding each of the seven *PILS* genes were analyzed in pairs by blastp program (Altschul et al., 1997) and homology between all genes in all unique pairs of gene rows were determined according to *E-value* from blast results. Pairs of gene rows with high diagonal homology were assigned as collinearity. In the *PILS1/PILS3/PILS4* group we found very high collinearity between *PILS3* and *PILS4* (**Figure 5A**). These genes appear to be products of very recent gene duplication. Between *PILS1* and the *PILS3/PILS4* pair we also found high collinearity (**Figures 5B,C**) and assume that these genes arose during full-genome duplication at Brassicaceae family level (20 million years ago; *Mya*). Only very weak or no collinearity was detectable between *PILS5* and *PILS7* (**Figure 5D**).

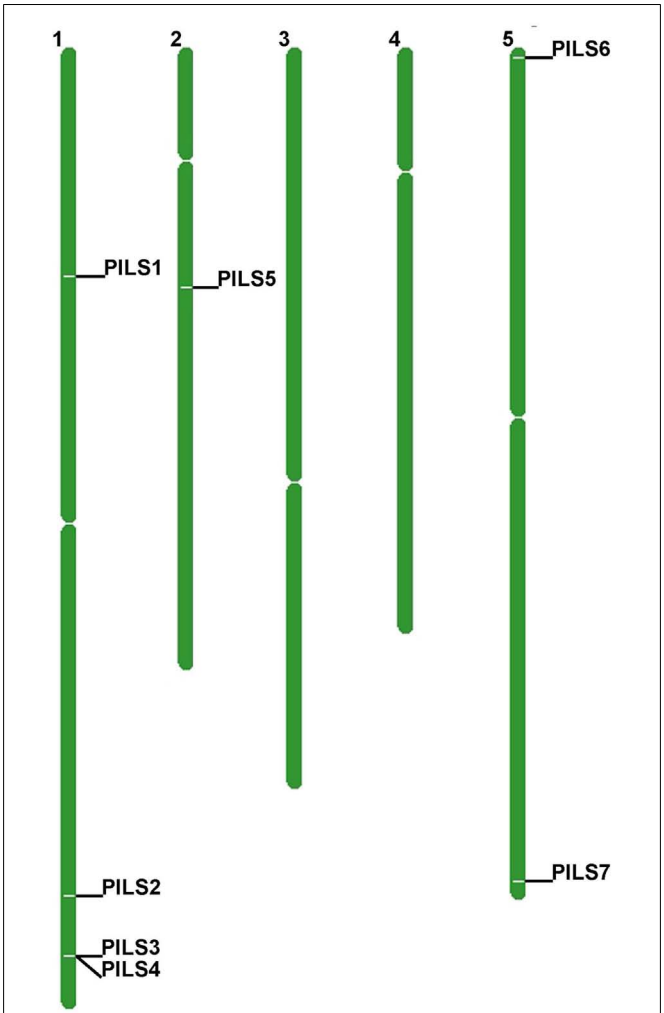

FIGURE 4 | Chromosomal distribution of *Arabidopsis thaliana PILS* genes. *A. thaliana PILS* genes are found on chromosome 1, 2, and 5.

To further elaborate on the recent duplication of *PILS3* and *PILS4*, we analyzed the microevolutionary relationship between PILS sequences of *A. thaliana* and *A. lyrata* (Figure S1 in Supplementary Material). *A. lyrata* is the closest known relative of *A. thaliana* and has a genome of eight chromosomes and six PILS proteins (Van Bel et al., 2012). In contrast, *A. thaliana* has five chromosomes and seven PILS proteins (Barbez et al., 2012; Van Bel et al., 2012). It has been shown that the reduction of genome size in *A. thaliana* is the result of chromosomes fusion that presumably occurred about 5 *Mya* (Yogeeswaran et al., 2005). The phylogenetic analysis revealed that all six *A. lyrata* PILSes have highly similar orthologs in *A. thaliana*, while *AtPILS4* is a lineage-specific gene (Figure S1 in Supplementary Material). This indicates that *AtPILS4* is a duplicated gene that has arisen after the separation of *A. thaliana* from *A. lyrata* 5 *Mya*.

Next we addressed the sequence diversifications among the *A. thaliana* PILS proteins and performed a ClustalW Multiple sequence alignment (Larkin et al., 2007; **Table 2**; for sequence

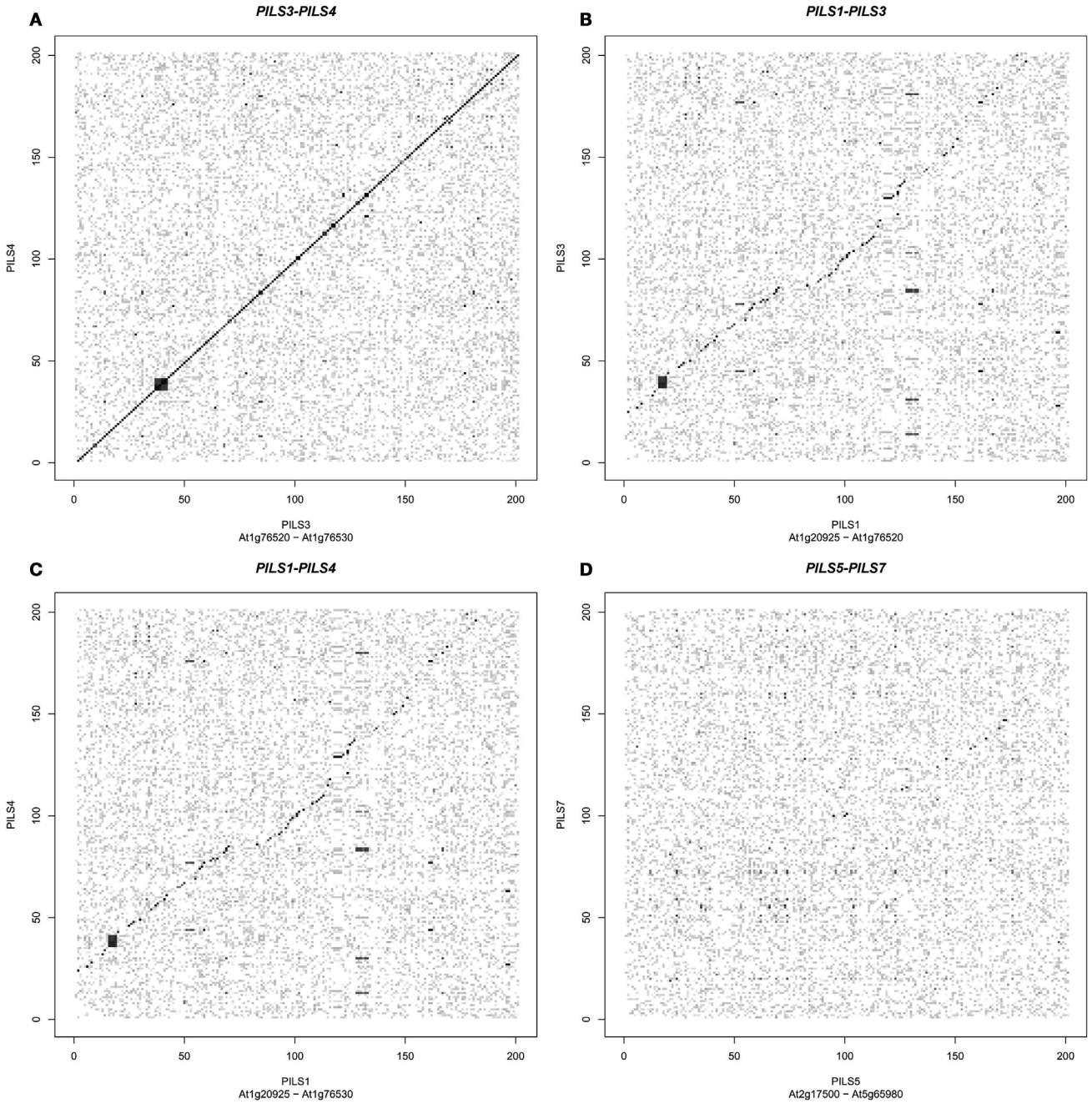

FIGURE 5 | Origin of *PILS* paralogs in *Arabidopsis thaliana*. (A–D) *PILS* genes show high collinearity between gene pairs *PILS3*/*PILS4* **(A)**, *PILS1*/*PILS3* **(B)**, and *PILS1*/*PILS4* **(C)**. No or only very weak collinearity could be detected between *PILS5* and *PILS7* **(D)**.

alignment see Figure S4 in Supplementary Material). PILS3/PILS4 showed the highest identity (82%), followed by PILS1/PILS3 (69%), PILS5/PILS7 (64%), and PILS1/PILS4 (61%; **Table 2**). Interestingly, PILS2 and PILS6 showed sequence identity of only 39% (**Table 2**). Taking together, the amino acid identity proposes that *A. thaliana* PILS proteins belong to three subgroups: (i) PILS1/PILS3/PILS4, (ii) PILS5/PILS7, and (iii) PILS2/PIL6.

PILS GENE REGULATION AND ORGANIZATION IN *ARABIDOPSIS THALIANA*

To get further insight into the regulation of PILS activity, we analyzed *in silico PILS* gene organization and expression. *A. thaliana PILS* gene transcripts organization is pretty well-conserved regarding the number and size of the exons (**Figure 6**). *PILS3* to *PILS6* genes contain nine exons with more or less conserved size and placements (**Figure 6**). In contrast, *PILS1*, *PILS2*, and *PILS7* have

Table 2 | Percentages* of *Arabidopsis thaliana* PILS amino acid sequence identity calculated by ClustalW multiple sequence alignment (Larkin et al., 2007).

							PILS7
						31	PILS6
					31	64	PILS5
				39	28	43	PILS4
			82	41	31	43	PILS3
		32	28	29	39	30	PILS2
	28	69	61	40	29	42	PILS1
PILS1	PILS2	PILS3	PILS4	PILS5	PILS6	PILS7	

**The identity percentages were calculated as the identities between two PILS sequences, divided by the length of the alignment.*

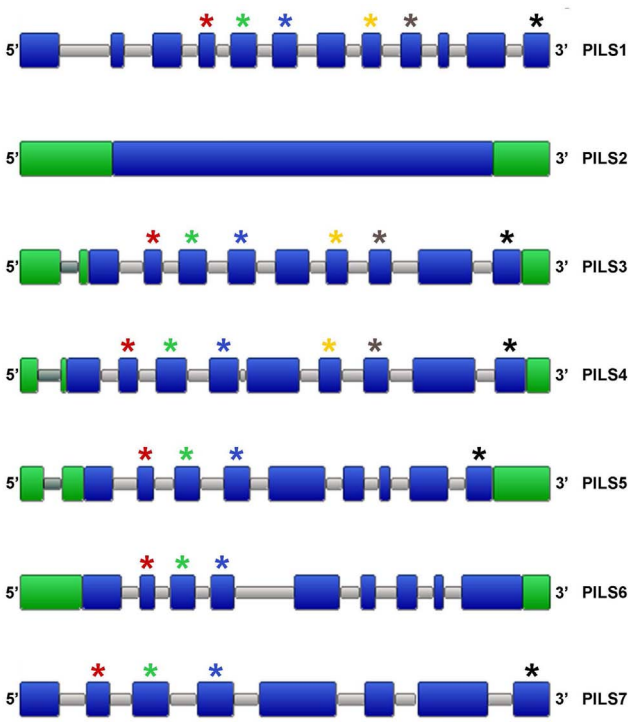

FIGURE 6 | Organization of *Arabidopsis thaliana PILS* genes. Schematic intron/exon representation of *A. thaliana PILS* genes (Van Bel et al., 2012). Exons and introns are depicted in blue and gray, respectively. 3′ UTR and 5′ UTR are in green. Stars are showing exons of similar sizes (nucleotides): red (80), green (125), blue (122), yellow (93), gray (101), and black (125).

a divergent exon/intron structure. *PILS1* has 12 exons, *PILS7* bares eight exons and *PILS2* is even intron less. The size of exon number 2 (80 nucleotides), 3 (125 nucleotides), and 4 (122 nucleotides) is largely kept in *AtPILS* genes and encode for a highly conserved region of the predicted transmembrane helices 2–4 (109 aa in total). Also a C-terminal transmembrane domain seems to be encoded by the last exon (125 nucleotides) in almost all *AtPILS* genes (**Figure 6**).

Next, we analyzed the intron/exon organization of *PILS* genes from algae, *Physcomitrella*, *Selaginella*, and several Angiosperms. Our results show that *PILS* intron/exon organization is largely conserved among *PILS* orthologous (**Figure 7**). The variations of 1–2 more or less exons may be the result of insertions, deletions, or both processes along the lineage evolution. The subfamily of *PILS2* genes is most particular, because they display single-exon genes in Angiosperms and *Selaginella* and 3-exons genes in *Physcomitrella* (**Figure 7**). Thus, *PILS* genes belong to two structural groups with 1–3 exons (*PILS2* orthologs and *PILS* genes from *Ostreococcus* and *Micromonas*) and 7–12 exons (all the other *PILSes*; **Figure 7**).

PILS gene activity can be detected in all tissues of *A. thaliana* as shown by RT-PCR (Barbez et al., 2012) or by micro array-based online tools such as Genevestigator[5]. *PILS* genes display either relatively low (*PILS1*, *PILS4*, *PILS7*), medium (*PILS6*) or high (*PILS2*, *PILS3*, and *PILS5*) expression levels (see text footnote 5). *PILS2*-to-*AtPILS6* are expressed in seedlings, leaves, and flowers (**Figure 8**; Barbez et al., 2012; see text footnote 5). *PILS4* displays the strongest expression in the rosette leaves (Barbez et al., 2012). *PILS6* transcripts are particularly abundant in the stem and together with *PILS5* in the cauline leaves and flowers, while *PILS2* is highest in siliques (Barbez et al., 2012). Interestingly, some *PILS* gene products were excluded from certain tissues. *PILS1* was found to be expressed only in flowers, *PILS2* and *PILS3* are not expressed in the stem, *PILS5* is absent in the rosette leaves, stem, and siliques, while *PILS6* and *PILS7* were present in all plant organs but not in siliques (Barbez et al., 2012). Except *PILS1*, all the other *PILSes* were expressed in seedlings, with *PILS5* and *PILS2* having the highest expression (Barbez et al., 2012). *PILS2*-to-*PILS6* showed expression in pollen with *PILS5* being the most abundant (see text footnote 5). Based on these evidences it seems that *PILS* genes show specific and partially overlapping expression patterns in all plant tissues.

Alternative splicing might furthermore contribute to the regulatory complexity and diversity for *PILS* gene activity. *PILS3* and *PILS5* appear to bear two and four alternative transcripts, respectively[6]. In both cases the alternative gene splicing seems to occur in the 5′ region and may modulate *PILS3* and *PILS5* function. However, the importance of *PILS* transcript splicing remains to be demonstrated.

The pronounced differences in the expression levels and tissue distributions might indicate that PILS-mediated regulation of plant growth and development may be largely determined by gene regulation.

PILS PROTEIN ORGANIZATION IN *ARABIDOPSIS THALIANA*

The temporal and spatial regulation of *PILS* genes will give rise to tissue specific distribution of distinct PILS proteins. Next we analyzed predicted PILS protein organization and searched for domains to speculate on PILS function. PILS proteins range in size from 390 (43 kDa; PILS3) to 472 (52 kDa; PILS1) amino acids. However, the predicted protein topology is highly similar for all PILS proteins. PILS proteins are presumably characterized by two hydrophobic transmembrane regions found at N- and C-termini (**Figure 9A**; Tusnády and Simon, 1998, 2001; Spyropoulos et al., 2004). The two transmembrane regions flank a short hydrophilic

[5]www.genevestigator.com
[6]http://www.arabidopsis.org

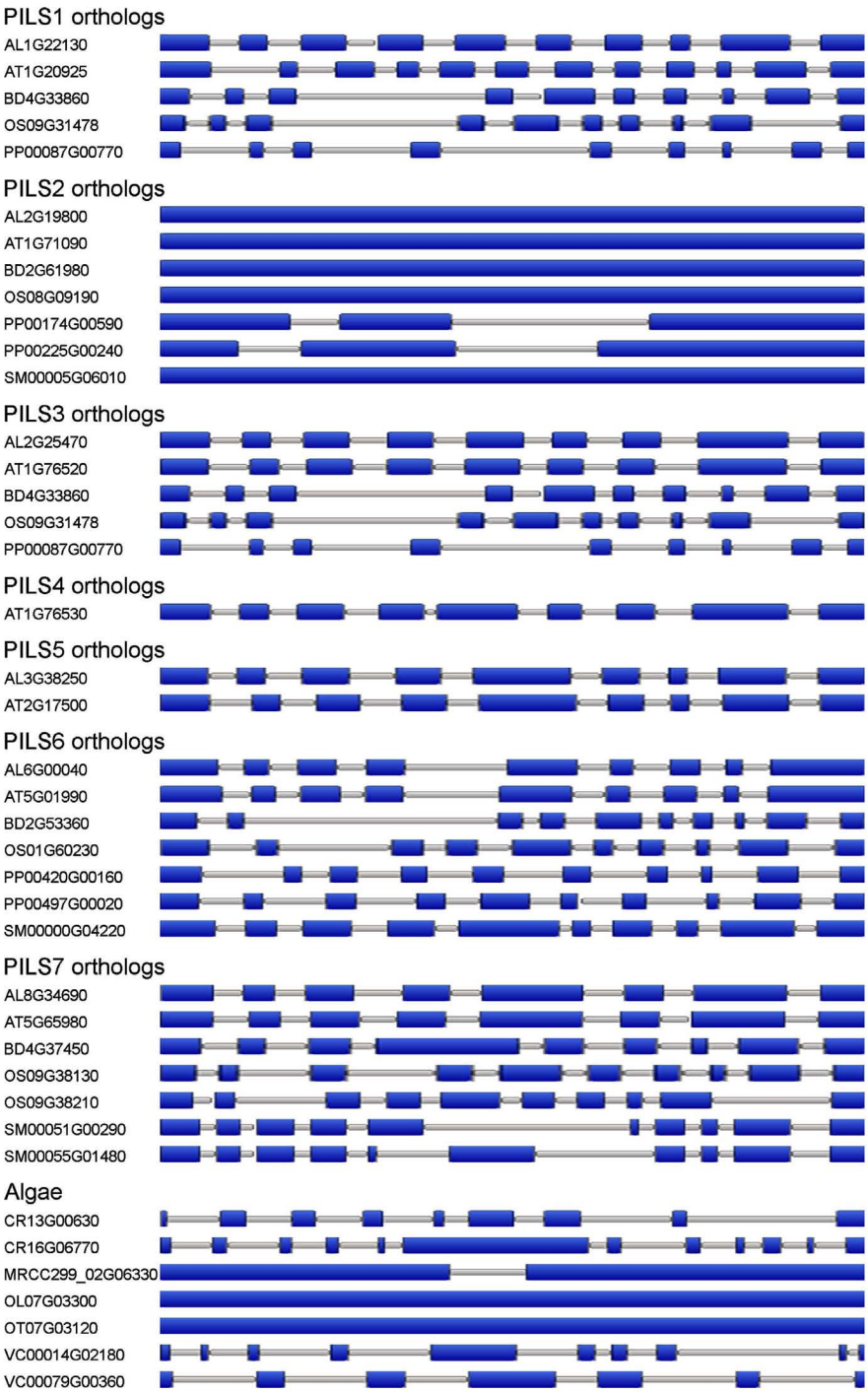

FIGURE 7 | Organization of *PILS* orthologs. Schematic intron/exon representation of *PILS* genes from *Arabidopsis lyrata* (AL), *Arabidopsis thaliana* (AT), *Brachypodium distachyon* (BD), *Chlamydomonas reinhardtii* (CR), *Micromonas* (MRCC299), *Oryza sativa* (OS), *Ostreococcus lucimarinus* (OL), *Ostreococcus tauri* (OT), *Physcomitrella patens* (PP), *Selaginella moellendorffii* (SM), and *Volvox carteri* (VC; Van Bel et al., 2012). Exons are depicted in blue boxes, introns in gray lines.

region (loop) with a presumable cytosolic orientation (**Figure 9A**). Each hydrophobic region appears to be organized in five transmembrane helices that are very similar and highly conserved among the PILS proteins (**Figure 9**). In contrast, the loop is less conserved and is the most divergent part of the PILS sequences. We assume that the transmembrane domains have central roles in

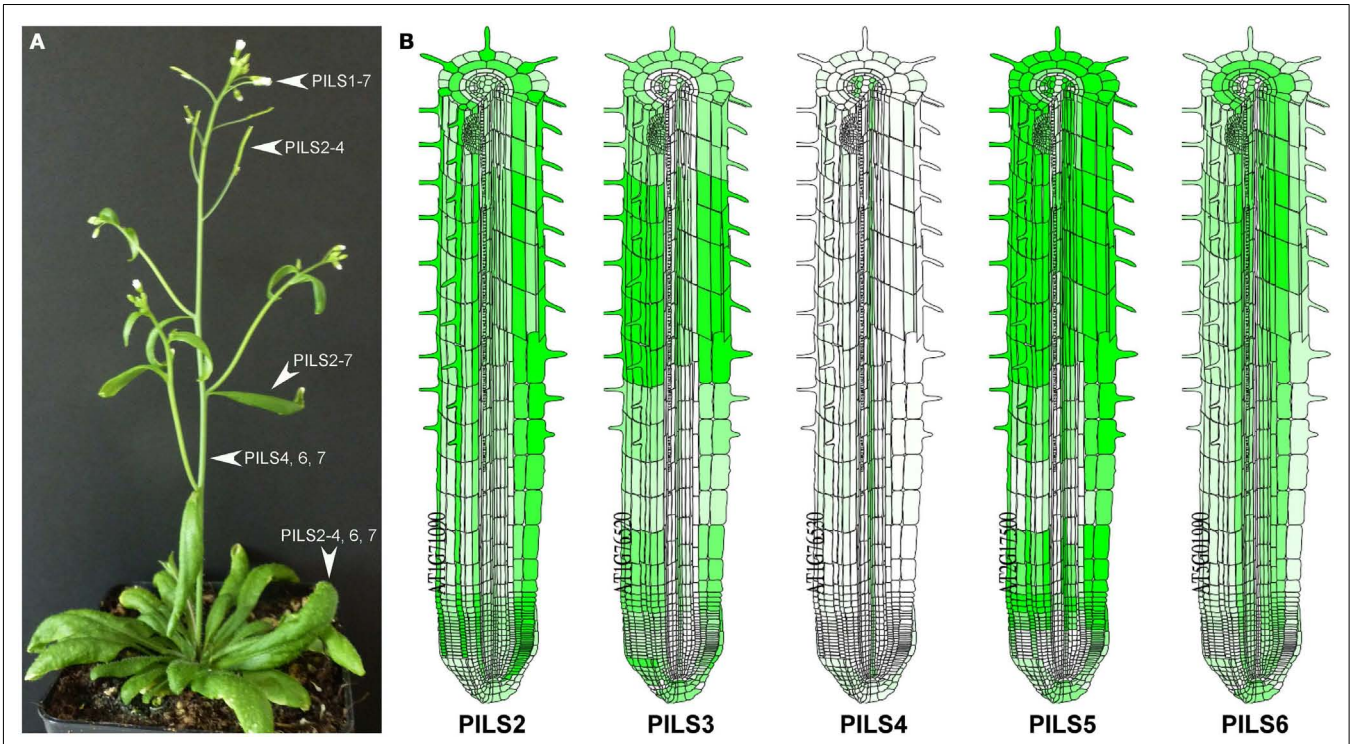

FIGURE 8 | Transcription pattern of *Arabidopsis thaliana PILS* genes. (A,B) Transcription of *PILS* genes in *A. thaliana* plant **(A)** and root **(B)**. Based on the RT-PCR data from individual organs published in Barbez et al. (2012). **(A)** As predicted by online server *Arabidopsis* eFP Browser (http://bar.utoronto.ca/efp/cgi-bin/efpWeb.cgi); **(B)**.

the putative carrier function, while the presumably cytosolic loop might have rather regulatory functions.

PILS and PIN proteins share only 10–18% sequence identity and belong to distinct protein families (**Figure 3**; Barbez et al., 2012). However, the predicted topology of PILS proteins is reminiscent to the predicted topology of PIN proteins (Krecek et al., 2009) and allowed the identification of this novel putative auxin carrier family (Barbez et al., 2012). Based on the hydrophilic loop size, PIN proteins are sub-grouped into two subfamilies. The subfamily of PIN1-type encompasses the PIN members with a long hydrophilic loop and PM localization (PIN1–PIN4, PIN7), while the subfamily of PIN5-type encompasses PIN5 and PIN8 that have very short hydrophilic loops and ER localization. Although PIN6 shows a reduction of the loop size, PIN6 is often included in the PIN1-type subfamily due to high sequence similarity in the transmembrane regions (Krecek et al., 2009). However, it is also localized to the ER in transient localization studies (Mravec et al., 2009).

Similarly to PIN proteins, PILS family members are characterized by the presence of the Interpro auxin carrier domain. This Interpro domain is relatively long and spans almost the whole length of the PILS protein and, hence, it is difficult to ascertain functional residues within the "domain".

Nothing is yet known about the post-translational modification of PILS proteins but generic phosphorylation sites (non-kinase-specific, such as serine, threonine, and tyrosine), kinase-specific phosphorylation sites and isoform variations could be predicted for PILS proteins by available online servers such as NetPhos (Blom et al., 1999) and NetPhosK (Blom et al., 2004). Interestingly, according with the number of the predicted serine, threonine, and tyrosine phosphorylation sites, PILS proteins can be grouped into three classes: (i) less than 10 (PILS5 and PILS7), (ii) between 10 and 15 (PILS2 and PILS6), and (iii) more than 15 (PILS1, PILS3, and PILS4). This finding may indicate the functional diversification among the PILS members and may suggest that different phosphorylation-based mechanisms are required for the regulation of PILS activity.

DISCUSSION

Auxin has pronounced importance for the plant development. Recent research shed light on a particular link between intracellular auxin transport processes and auxin metabolism (Mravec et al., 2009; Barbez et al., 2012; Bosco et al., 2012; Ding et al., 2012). Here, we report *in silico* analyses of PILS putative auxin flux facilitator sequences from *A. thaliana* and revealed certain features that might be functionally important for PILS activity.

The phylogenetic analysis of PILS sequences revealed that four *Physcomitrella* PILSes are found in Clade II, while only one is found in Clade III (**Figure 2**). Moreover, two *Selaginella* PILSes are found in each, Clade III and Clade II-PILS2 subclade, while four paralogs are found in the Clade II-PILS6 subclade (**Figure 2**). This, together with the distribution of the *Brachypodium, Oryza,* and *Arabidopsis* PILS sequences, indicates that the initial PILS divergence occurred in two separate clades already at the level of *Bryophytes*. We do not

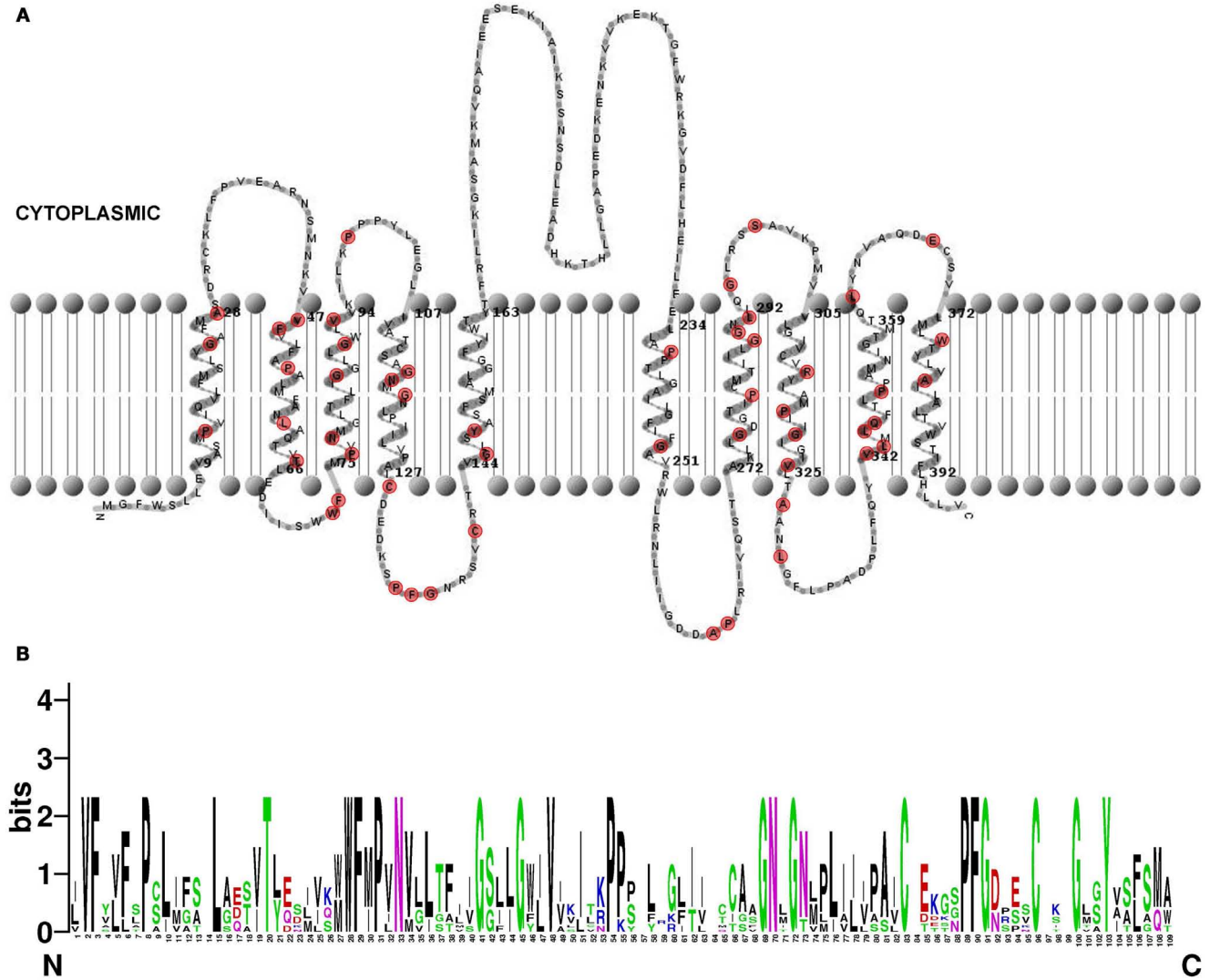

FIGURE 9 | Structure of *Arabidopsis thaliana* PILS proteins. (A) Predicted topology of *A. thaliana* PILS5 protein. The prediction was done by HMMTOP 2.0 (Tusnády and Simon, 1998, 2001) and visualized by TMRPres2D (Spyropoulos et al., 2004). Conserved amino acids in all seven PILS proteins are marked in red. **(B)** Sequence logos generated by WebLogo (Schneider and Stephens, 1990) representing a ClustalW multiple sequence alignment (Larkin et al., 2007) of 109 amino acids from N-terminal region of *A. thaliana* PILS proteins (exons 2–4). Note the PILS sequence conservation at the highest, single symbol positions.

know if PILSes are present in the genome of Rhodophytes, but we can speculate that Clade II- and Clade III-PILSes may have originated before land plant evolution at the level of Streptophytes, as these algae are direct ancestors of land plants. Moreover, Clade II presumably diverged before or during the origin of Embryophytes, because this clade is already diversified in PILS2- and PILS6-like subclades in mosses (**Figure 2**). Clade III particularly expanded during higher plant evolution (**Figure 2**; Figure S1 in Supplementary Material). This clade is divided in PILS1/PILS3/PILS4 and PILS5/PILS7 subclades (**Figure 2**; Figure S1 in Supplementary Material). We could not estimate when these subclades emerged because PILS sequences from conifers and ferns are either incomplete (only ESTs available) or not available. More than 30000 ESTs derived from gametophyte of fern *Adiantum* can be found on NCBI but we could not identify any PILS sequence which indicates that PILSes might be not transcribed in gametophyte.

Combining the gene and protein analyses, *AtPILS4* is likely to be a recent duplication of *AtPILS3*, because they show very high amino acid identity (**Table 2**), strong gene collinearity (**Figure 5A**), and no particular *PILS4* orthologs could be identified in the genomes of the other sequenced species. *PILS3/PILS4* seem to be originally derived from *PILS1* (69% amino acid identity; **Table 2**). Accordingly, by analyzing the amino acid sequence similarities and the PILS phylogeny, we can conclude that from seven *PILSes* in *A. thaliana* genome, six in *Oryza sativa* ssp *japonica* and eight in *Brachypodium distachyon* genome only four are true orthologs.

The other *PILS* members presumably represent lineage-specific duplications that occurred after the separation of the dicots and monocots about 200–250 *Mya*.

The existence of *PILS2* as a single-exon gene in most species is intriguing since single-exon genes are rather typical for prokaryotes. However, single-exon or intronless genes are present in eukaryotic genomes (Sakharkar et al., 2004) and can have many origins, but could pinpoint the relatedness to a prokaryotic gene (Zou et al., 2011). However, moss PILS2 orthologs display intronexon structure (**Figure 7**) and might suggest that *PILS2* genes lost the intron structure during evolution.

Our findings might highlight certain functional diversifications among PILS proteins. Notably, PILS2 and PILS5 have only 29% amino acid sequence identities (**Table 2**), display very diverged gene organization (**Figure 6**), and belong to diverse evolutionary sub clades (**Figure 2**). However, their gene regulation and function seem to be highly similar in *Arabidopsis*, because *PILS2* and *PILS5* have overlapping expression pattern in the root transition zone and redundantly control seedling growth and development (Barbez et al., 2012). Therefore, defined research is needed to evaluate the functional importance of the distinct features of the respective *PILS* genes and PILS proteins.

ACKNOWLEDGMENTS

We are indebted to the Vienna Science and Technology Fund (WWTF; to Elena Feraru, Mugurel I. Feraru, Jürgen Kleine-Vehn), Czech Science Foundation Grant GAP305/11/2476 (to Jan Petrášek) and Charles University in Prague, SVV 265203/2012 (to Jan Petrášek and Stanislav Vosolsobě). We thank Elke Barbez for helpful discussions.

SUPPLEMENTARY MATERIAL

The Supplementary Material for this article can be found online at http://www.frontiersin.org/Plant_Traffic_and_Transport/10.3389/fpls.2012.00227/abstract

Figure S1 | Molecular phylogenetic analysis of PILS proteins. The diagram shows an extended phylogentic tree of PILS proteins with collapsed branches for algae, *Physcomitrella*, and *Selaginella*. Note the high diversification of PILSes in *Medicago* and *Populus*. Because of incomplete sequences some of the PILSes were eliminated. The evolutionary history was inferred by using the Maximum Likelihood method based on the Data specific model (Nei and Kumar, 2000). The tree with the highest log likelihood (−55875.7936) is shown. The percentage of trees in which the associated taxa clustered together is shown above the branches. Initial tree(s) for the heuristic search were obtained automatically as follows. When the number of common sites was <100 or less than one fourth of the total number of sites, the maximum parsimony method was used; otherwise BIONJ method with MCL distance matrix was used. A discrete Gamma distribution was used to model evolutionary rate differences among sites [five categories (+*G*, parameter = 2.6899)]. The rate variation model allowed for some sites to be evolutionarily invariable ([+I], 3.7299% sites). The tree is drawn to scale, with branch lengths measured in the number of substitutions per site. The analysis involved 75 nucleotide sequences. All positions with less than 0% site coverage were eliminated. That is, fewer than 100% alignment gaps, missing data, and ambiguous bases were allowed at any position. There were a total of 1113 positions in the final dataset. Evolutionary analyses were conducted in MEGA5 (Tamura et al., 2011).

Figure S2 | Alignment of PILS amino acid sequences. The multiple amino acid alignment of PILSes was generated by using Muscle in MEGA5 software (Tamura et al., 2011). This alignment was generated for the phylogenetic analysis presented in the Supplementary **Figure 1**. The alignment for the smaller tree presented in the **Figure 2** is similar but with less sequences.

Figure S3 | Alignment of PILS and PIN amino acid sequences. The multiple alignment was generated by using Muscle in MEGA5 software (Tamura et al., 2011).

Figure S4 | Alignment of *Arabidopsis thaliana* PILS amino acid sequences. A multiple sequence alignment generated by ClustalW server (Larkin et al., 2007) of the seven PILSes is shown. Amino acids are color coded: red (small, hydrophobic, aromatic, not Y), blue (acidic); magenta (basic), green (hydroxyl, amine, amide, basic), gray (others). "∗," Identical amino acids; ":," conserved substitutions (same color group); "." semi-conserved substitution (similar shapes).

Table S1 | Sequence information.

REFERENCES

Altschul, S. F., Madden, T. L., Schäffer, A. A., Zhang, J., Zhang, Z., Miller, W., et al. (1997). Gapped BLAST and PSI-BLAST: a new generation of protein database search programs. *Nucleic Acids Res.* 25, 3389–3402.

Barbez, E., Kubeš, M., Rolcík, J., Béziat, C., Pencík, A., Wang, B., et al. (2012). A novel putative auxin carrier family regulates intracellular auxin homeostasis in plants. *Nature* 485, 119–122.

Bennett, M. J., Marchant, A., Green, H. G., May, S. T., Ward, S. P., Millner, P. A., et al. (1996). Arabidopsis AUX1 gene: a permease-like regulator of root gravitropism. *Science* 273, 948–950.

Blom, N., Gammeltoft, S., and Brunak, S. (1999). Sequence- and structure-based prediction of eukaryotic protein phosphorylation sites. *J. Mol. Biol.* 294, 1351–1362.

Blom, N., Sicheritz-Ponten, T., Gupta, R., Gammeltoft, S., and Brunak, S. (2004). Prediction of post-translational glycosylation and phosphorylation of proteins from the amino acid sequence. *Proteomics* 4, 1633–1649.

Bosco, C. D., Dovzhenko, A., Liu, X., Woerner, N., Rensch, T., Eismann, M., et al. (2012). The endoplasmic reticulum localized PIN8 is a pollen specific auxin carrier involved in intracellular auxin homeostasis. *Plant J.* 71, 860–870.

Braun, N., Wyrzykowska, J., Muller, P., David, K., Couch, D., Perrot-Rechenmann, C., et al. (2008). Conditional repression of AUXIN BINDING PROTEIN1 reveals that it coordinates cell division and cell expansion during postembryonic shoot development in Arabidopsis and tobacco. *Plant Cell* 20, 2746–2762.

Chapman, E. J., and Estelle, M. (2009). Mechanism of auxin-regulated gene expression in plants. *Annu. Rev. Genet.* 43, 265–285.

Chen, R., Hilson, P., Sedbrook, J., Rosen, E., Caspar, T., and Masson, P. H. (1998). The Arabidopsis thaliana AGRAVITROPIC 1 gene encodes a component of the polar-auxin-transport efflux carrier. *Proc. Natl. Acad. Sci. U.S.A.* 95, 15112–15117.

De Smet, I., Voss, U., Lau, S., Wilson, M., Shao, N., Timme, R. E., et al. (2011). Unraveling the evolution of auxin signaling. *Plant Physiol.* 155, 209–221.

Ding, Z., Wang, B., Moreno, I., Dupláková, N., Simon, S., Carraro, N., et al. (2012). ER-localized auxin transporter PIN8 regulates auxin homeostasis and male gametophyte development in Arabidopsis. *Nat. Commun.* 3, 941.

Finet, C., and Jaillais, Y. (2012). AUXOLOGY: when auxin meets plant evo-devo. *Dev. Biol.* 369, 19–31.

Gälweiler, L., Guan, C., Müller, A., Wisman, E., Mendgen, K., Yephremov, A., et al. (1998). Regulation of polar auxin transport by AtPIN1 in Arabidopsis vascular tissue. *Science* 282, 2226–22230.

Geisler, M., Blakeslee, J. J., Bouchard, R., Lee, O. R., Vincenzetti, V., Bandyopadhyay, A., et al. (2005). Cellular efflux of auxincatalyzed by the Arabidopsis MDR/PGP transporter AtPGP1. *Plant J.* 44, 179–194.

Jones, A. M., and Venis, M. A. (1989). Photoaffinitylabeling of indole-3-acetic acid-binding proteins in maize. *Proc. Natl. Acad. Sci. U.S.A.* 86, 6153–6156.

Jurado, S., Abraham, Z., Manzano, C., López-Torrejón, G., Pacios, L. F., and Del Pozo, J. C. (2010). The Arabidopsis cell cycle F-box protein SKP2A binds to auxin. *Plant Cell* 22, 3891–3904.

Krecek, P., Skupa, P., Libus, J., Naramoto, S., Tejos, R., Friml, J., et al. (2009). The PIN-FORMED (PIN) protein family of auxin transporters. *Genome Biol.* 10, 249.

Larkin, M. A., Blackshields, G., Brown, N. P., Chenna, R., McGettigan, P. A., McWilliam, H., et al. (2007). ClustalW and clustalX version 2 (2007). *Bioinformatics* 23, 2947–2948.

Leyser, O. (2006). Dynamic integration of auxin transport and signalling. *Curr. Biol.* 16, R424-33.

Luschnig, C., Gaxiola, R. A., Grisafi, P., and Fink, G. R. (1998). EIR1, a root-specific protein involved in auxin transport, is required for gravitropism in Arabidopsis thaliana. *Genes Dev.* 12, 2175–2187.

Mravec, J., Skupa, P., Bailly, A., Hoyerová, K., Krecek, P., Bielach, A., et al. (2009). Subcellular homeostasis of phytohormone auxin is mediated by the ER-localized PIN5 transporter. *Nature* 459, 1136–1140.

Müller, A., Guan, C., Gälweiler, L., Tänzler, P., Huijser, P., Marchant, A., et al. (1998). AtPIN2 defines a locus of Arabidopsis for root gravitropism control. *EMBO J.* 17, 6903–6911.

Nei, M., and Kumar, S. (2000). *Molecular Evolution and Phylogenetics.* New York: Oxford University Press.

Petrásek, J., Mravec, J., Bouchard, R., Blakeslee, J. J., Abas, M., Seifertová, D., et al. (2006). PIN proteins perform a rate-limiting function in cellular auxin efflux. *Science* 312, 914–918.

Robert, S., Kleine-Vehn, J., Barbez, E., Sauer, M., Paciorek, T., Baster, P., et al. (2010). ABP1 mediates auxin inhibition of clathrin-dependent endocytosis in Arabidopsis. *Cell* 143, 111–121.

Ruiz Rosquete, M., Barbez, E., and Kleine-Vehn, J. (2012). Cellular auxin homeostasis: gatekeeping is housekeeping. *Mol. Plant* 5, 772–786.

Sakharkar, M. K., Chow, V. T. K., Chaturvedi, I., Mathura, V. S., Shapshak, P., and Kangueane, P. (2004). A report on single exon genes (seg) in eukaryotes. *Front. Biosci.* 9, 3262–3267.

Schneider, T. D., and Stephens, R. M. (1990). Sequence logos: a new way to display consensus sequences. *Nucleic Acids Res.* 18, 6097–6100.

Spyropoulos, I. C., Liakopoulos, T. D., Bagos, P. G., and Hamodrakas, S. J. (2004). TMRPres2D: high quality visual representation of transmembrane protein models. *Bioinformatics* 20, 3258–3260.

Tamura, K., Peterson, D., Peterson, N., Stecher, G., Nei, M., and Kumar, S. (2011). MEGA5: molecular evolutionary genetics analysis using maximum likelihood, evolutionary distance, and maximum parsimony methods. *Mol. Biol. Evol.* 28, 2731–2739.

Teale, W. D., Ditengou, F. A., Dovzhenko, A. D., Li, X., Molendijk, A. M., Ruperti, B., et al. (2008). Auxin as a model for the integration of hormonal signal processing and transduction. *Mol. Plant* 1, 229–237.

Tromas, A., Braun, N., Muller, P., Khodus, T., Paponov, I. A., Palme, K., et al. (2009). The AUXIN BINDING PROTEIN 1 is required for differential auxin responses mediating root growth. *PLoS ONE* 4, e6648. doi:10.1371/journal.pone.0006648

Tusnády, G. E., and Simon, I. (1998). Principles governing amino acid composition of integral membrane proteins: applications to topology prediction. *J. Mol. Biol.* 283, 489–506.

Tusnády, G. E., and Simon, I. (2001). The HMMTOP transmembrane topology prediction server. *Bioinformatics* 17, 849–850.

Utsuno, K., Shikanai, T., Yamada, Y., and Hashimoto, T. (1998). Agr, an agravitropic locus of Arabidopsis thaliana, encodes a novel membrane-protein family member. *Plant Cell Physiol.* 39, 1111–1118.

Van Bel, M., Proost, S., Wischnitzki, E., Movahedi, S., Scheerlinck, C., Van de Peer, Y., et al. (2012). Dissecting plant genomes with the PLAZA comparative genomics platform. *Plant Physiol.* 158, 590–600.

Vanneste, S., and Friml, J. (2009). Auxin: a trigger for change in plant development. *Cell* 136, 1005–1016.

Whelan, S., and Goldman, N. (2001). A general empirical model of protein evolution derived from multiple protein families using a maximum-likelihood approach. *Mol. Biol. Evol.* 18, 691–699.

Wisniewska, J., Xu, J., Seifertová, D., Brewer, P. B., Ruzicka, K., Blilou, I., et al. (2006). Polar PIN localization directs auxin flow in plants. *Science* 312, 883.

Woodward, A. W., and Bartel, B. (2005). A receptor for auxin. *Plant Cell* 17, 2425–2429.

Xu, T., Wen, M., Nagawa, S., Fu, Y., Chen, J.-G., Wu, M.-J., et al. (2010). Cell surface- and rho GTPase-based auxin signaling controls cellular interdigitation in Arabidopsis. *Cell* 143, 99–110.

Yogeeswaran, K., Frary, A., York, T. L., Amenta, A., Lesser, A. H., Nasrallah, J. B., et al. (2005). Comparative genome analyses of Arabidopsis spp.: inferring chromosomal rearrangement events in the evolutionary history of A. thaliana. *Genome Res.* 15, 505–515.

Zazímalová, E., Murphy, A. S., Yang, H., Hoyerová, K., and Hosek, P. (2010). Auxin transporters – why so many? *Cold Spring Harb. Perspect. Biol.* 2, a001552.

Zhao, Y. (2012). Auxin biosynthesis: a simple two-step pathway converts tryptophan to indole-3-acetic acid in plants. *Mol. Plant* 5, 334–338.

Zou, M., Guo, B., and He, S. (2011). The roles and evolutionary patterns of intronless genes in deuterostomes. *Comp. Funct. Genomics* 2011, 1–8.

Conflict of Interest Statement: The authors declare that the research was conducted in the absence of any commercial or financial relationships that could be construed as a potential conflict of interest.

Received: 12 September 2012; accepted: 21 September 2012; published online: 12 October 2012.

*Citation: Feraru E, Vosolsobě S, Feraru MI, Petrášek J and Kleine-Vehn J (2012) Evolution and structural diversification of PILS putative auxin carriers in plants. Front. Plant Sci. **3**:227. doi: 10.3389/fpls.2012.00227*

This article was submitted to Frontiers in Plant Traffic and Transport, a specialty of Frontiers in Plant Science.

frontiers in
PLANT SCIENCE

REVIEW ARTICLE
published: 18 October 2012
doi: 10.3389/fpls.2012.00225

AUX/LAX family of auxin influx carriers—an overview

Ranjan Swarup*[1] *and* ***Benjamin Péret*[2]**

[1] *School of Biosciences and Centre for Plant Integrative Biology, University of Nottingham, Loughborough, UK*
[2] *Laboratory of Plant Development Biology, SBVME/Institute for Biotechnology and Environmental Biology, CEA Cadarache, St. Paul lez Durance, France*

Edited by:
Markus Geisler, University of Fribourg, Switzerland

Reviewed by:
Christian Luschnig, University of Natural Resources and Life Sciences, Austria
Eva Zazimalova, Institute of Experimental Botany of the Academy of Sciences of the Czech Republic, Czech Republic

****Correspondence:***
Ranjan Swarup, School of Biosciences and Centre for Plant Integrative Biology, University of Nottingham, Sutton Bonington Campus, Loughborough, LE12 5RD, UK.
e-mail: ranjan.swarup@nottingham.ac.uk

Auxin regulates several aspects of plant growth and development. Auxin is unique among plant hormones for exhibiting polar transport. Indole-3-acetic acid (IAA), the major form of auxin in higher plants, is a weak acid and its intercellular movement is facilitated by auxin influx and efflux carriers. Polarity of auxin movement is provided by asymmetric localization of auxin carriers (mainly PIN efflux carriers). PIN-FORMED (PIN) and P-GLYCOPROTEIN (PGP) family of proteins are major auxin efflux carriers whereas AUXIN1/LIKE-AUX1 (AUX/LAX) are major auxin influx carriers. Genetic and biochemical evidence show that each member of the AUX/LAX family is a functional auxin influx carrier and mediate auxin related developmental programmes in different organs and tissues. Of the four *AUX/LAX* genes, AUX1 regulates root gravitropism, root hair development and leaf phyllotaxy whereas LAX2 regulates vascular development in cotyledons. Both AUX1 and LAX3 have been implicated in lateral root (LR) development as well as apical hook formation whereas both AUX1 and LAX1 and possibly LAX2 are required for leaf phyllotactic patterning.

Keywords: AUXLAX, auxin transport, auxin, AUX1, LAX1, LAX2, LAX3, influx carriers

INTRODUCTION

Genetic, molecular and pharmacological approaches have elegantly demonstrated that auxin regulates several aspects of plant growth and development including embryo (Steinmann et al., 1999; Wolters et al., 2011), root (Swarup et al., 2001, 2004, 2005), lateral root (LR) (Swarup et al., 2008; Péret et al., 2009a,b), leaf (Bainbridge et al., 2008; Guenot et al., 2012) and flower development. Auxin also plays a key role in plant tropic responses (Swarup et al., 2001, 2004, 2005), vascular development (Sieburth and Deyholos, 2006; Péret et al., 2012) and regulation of apical dominance (Aloni et al., 2006; Prusinkiewicz et al., 2009). At cellular level, auxin regulates cell division, cell elongation and cell differentiation (Petrásek and Friml, 2009; Vanneste and Friml, 2009).

Indole-3-acetic acid (IAA) is the major form of auxin in higher plants and was the first plant hormone to be discovered (Went, 1926). Besides, there are a few other naturally occurring auxins. Auxins are organic compounds composed of an indole ring covalently linked to a carboxylic acid group (or a benzene ring in the case of phenylacetic acid—PAA). In addition, several synthetic compounds with auxin like activities have also been identified. Of them 2,4-dichlorophenoxyacetic acid (2,4-D) is one of the most widely used in auxin research.

Auxin is unique among all plant hormones for exhibiting polar transport. It is primarily synthesized in the shoot apex and developing leaf primordia and is then transported either through the bulk flow in the phloem in a non-polar fashion or actively in a polar manner to distal target tissues (Swarup and Bennett, 2003).

AUXIN DISTRIBUTION: SIMPLY COMPLEX

Use of auxin response reporters for example DR5 (Ulmasov et al., 1997) and IAA2 (Abel et al., 1994) and auxin sensors DII 28 (Brunoud et al., 2012) have provided great insight into auxin accumulation and distribution in plant tissues. These studies show that auxin gradients are crucial for several aspects of plant development including tropic responses, organ development and meristem size. For example, several studies show that differential accumulation of auxin between lower and upper side of a gravistimulated root regulate root bending (Ottenschläger et al., 2003; Swarup et al., 2005); auxin maxima are known to regulate organ development (Sabatini et al., 1999; Benková et al., 2003; Blilou et al., 2005; Grieneisen et al., 2007) and even auxin minimum has been implicated in regulating seed dispersal in *Arabidopsis* (Sorefan et al., 2009). Genetic and pharmacological studies show that auxin transport is crucial for establishment of auxin gradients and disruption of these gradients result in several auxin related developmental defects. Besides auxin transport, local auxin biosynthesis, metabolism, conjugation/deconjugation of active auxins to/from their inactive conjugated forms and intracellular auxin movement can also control and fine tune auxin accumulation in specific cell or tissues types (Chandler, 2009; Ikeda et al., 2009; Petrásek and Friml, 2009; Vanneste and Friml, 2009).

AUXIN TRANSPORTERS: PROVIDING DIRECTION

As per chemiosmotic polar diffusion hypothesis, the term first coined by Goldsmith (1977) based on the famous work of Rubery and Sheldrake (1974) and Raven (1975) cellular IAA movement is

facilitated by combined activities of auxin influx and efflux carriers. IAA is a weak acid (pKa 4.75) and at mildly acidic apoplastic pH, only a small portion of IAA (IAAH ∼15%) is able to passively diffuse inside the cell but the majority (85%) of IAA remains in its dissociated form (IAA^-) and would require a carrier for its active uptake across the cell (**Figure 1A**). Inside the cell, at pH 7.0, all IAA remains in its polar IAA^- form and would require auxin efflux carriers (Zazímalová et al., 2010). Chemiosmotic hypothesis also predicted that the polarity of auxin movement is provided by asymmetric localization of auxin carriers.

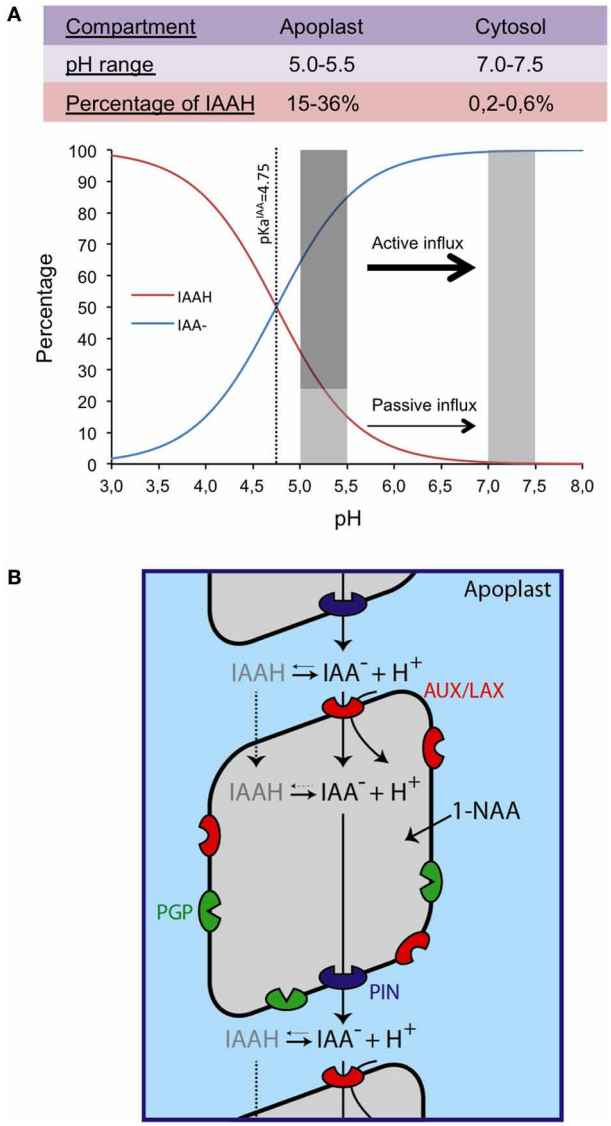

FIGURE 1 | Auxin chemical properties and chemioosmotic hypothesis of auxin transport. The percentages of the anionic and protonated forms of IAA (indole acetic acid) are given as a funtion of pH with an emphasis on the apoplastic and cytosolic pH ranges **(A)**. Chemiosmotic auxin transport model showing the different families of transporters: AUX/LAX, PIN, and PGP. The artificial form of auxin 1-NAA (1-Naphthalene acetic acid) is lipophilic and diffuses freely inside the cell **(B)**.

In *Arabidopsis*, evidence has been provided that AUXIN1/LIKE-AUX1 (AUX/LAX) family of auxin transporters are major influx carriers whereas PIN-FORMED (PIN) and P-GLYCOPROTEIN (PGP) family members are major auxin efflux carriers (**Figure 1B**). Among the efflux carriers, PIN family is most well studied and PIN homologs are found throughout the plant kingdom (Paponov et al., 2005; Pattison and Catalá, 2011; Wang et al., 2011; Carraro et al., 2012). In *Arabidopsis*, PINs are encoded by a small gene family comprising of eight members (Grunewald and Friml, 2010; Bosco et al., 2012). They have been shown to play crucial roles in several aspects of plant growth and development including root meristem patterning, LR development, vascular development and embryo development (Friml et al., 2002; Benková et al., 2003; Friml et al., 2003; Reinhardt, 2003; Blilou et al., 2005; Sieburth and Deyholos, 2006). PIN proteins are localized either on the plasma membrane (PIN1, 2, 3, 4, and 7) or in the ER (PIN5 and 8) and thus play a key part in both intercellular and intracellular auxin movement and regulation of auxin homeostasis (Mravec et al., 2009; Bosco et al., 2012). It is now well established that directionality of auxin movement is provided by asymmetric localization of PIN proteins. For example, PIN1 is localized on the basal rootward face of vascular cells (Gälweiler et al., 1998) facilitating rootward movement of auxin. In contrast, PIN2 is asymmetrically localized at the apical shootward face of LRC and epidermal cells and basal rootward face of cortical cells of the meristem thus creating an auxin reflux loop (Blilou et al., 2005; Wisniewska et al., 2006; Rahman et al., 2010). In response to gravity PIN3 is asymmetrically localized on the lateral face of the root to facilitate differential movement of auxin between upper and lower faces of a gravi-stimulated root (Friml et al., 2002).

In addition to PINs, a novel PIN like family of auxin transport facilitators termed PILS (PIN-LIKES) has recently been discovered by *in silico* studies and appears to be involved in the regulation of auxin homeostasis in *Arabidopsis* (Barbez et al., 2012).

Three members of the PGP class of ABC transporters PGP1, PGP4, and PGP19 have also been implicated in regulating auxin transport. Both PGP1 and PGP19 are involved in auxin efflux (Noh et al., 2003; Blakeslee et al., 2007), PGP4 has been demonstrated to participate in the shootward (basipetal) redirection of auxin from the root apex and there is some evidence to suggest that PGP4 functions as an auxin influx carrier (Terasaka et al., 2005; Kubeš et al., 2012). However, Cho et al. (2007) showed that PGP4 functions as an auxin efflux carrier. Direct auxin measurement experiment in heterologous expression system suggests that PGP4 can indeed function both as an efflux and influx carrier (Yang and Murphy, 2009).

Recently, a role for the nitrate transporter NRT1.1 in auxin influx has been demonstrated in heterologous system, providing an explanation for its ability to alter LR formation depending on the nitrogen status of the plant (Krouk et al., 2010). Interestingly, NRT1.1 acts as a transceptor as it is also involved in the perception/transduction of the nitrate signal (Ho et al., 2009). Further understanding of the auxin transport function of NRT1.1 is of great interest as this provides a direct mechanism for

developmental effects of auxin in response to nutrient status of the soil.

THE AUX/LAX FAMILY OF AUXIN INFLUX CARRIERS: HISTORICAL PERSPECTIVE

The existence of auxin influx carriers was first suggested by (Rubery and Sheldrake, 1974) when they showed a saturable component for auxin uptake in *Parthenocissus tricuspidata* crown gall suspension cells. Using sealed zucchini membrane vesicles, Lomax et al. (1985) provided further evidence that IAA uptake is an active process and is driven by proton motive force. They also proposed that auxin influx carrier acts as a proton symporter that was later confirmed by Sabater and Rubery (1987). In 1996, Delbarre et al. showed that the synthetic auxin 2, 4-D was a substrate for auxin influx carrier but not the lipophilic auxin 1-naphthalene acetic acid (1-NAA) that is able to diffuse freely into the cells (**Figure 1B**). They also showed that almost 75% of 2,4-D uptake was carrier mediated thus underlining the importance of auxin influx carriers in auxin uptake.

In the same year Bennett et al. (1996) cloned the *AUX1* gene. *aux1* mutants are agravitropic and were first identified in an screen for auxin (2,4-D) resistance (Maher and Martindale, 1980). *AUX1* gene showed similarity to amino acid transporters and the fact that IAA is structurally similar to tryptophan led Bennett et al. to propose that *AUX1* encodes a putative auxin influx permease. Detailed characterization of *aux1* mutants revealed that they show selective resistance to various auxins and root agravitropic defect of *aux1* can be rescued by application of lipophilic auxin 1-NAA (Yamamoto and Yamamoto, 1998; Marchant et al., 1999). Swarup et al. (2001) later showed that in *Arabidopsis* roots, besides in protophloem, *AUX1* is expressed in tissues that are involved in gravity perception (columella), signal transmission (LRC) and response (epidermis). They also were able to provide a molecular basis of *aux1* root gravitropic phenotype when they showed that *aux1* mutants were defective in basipetal auxin transport. The first direct evidence to show that AUX1 is an auxin permease came from Erik Nielsen's group when they expressed AUX1 in *Xenopus laevis* oocytes and showed a saturable, pH dependent increase in IAA uptake (Yang et al., 2006). Their experiments provided the first direct evidence that AUX1 is a high affinity auxin transporter. Later Carrier et al. (2008) provided first direct evidence of the affinity of an auxin influx carrier for its cognate ligand. They provided evidence that IAA binds to AUX1 in a pH dependent fashion with maximal binding taking place between pH5 and 6.

THE AUX/LAX FAMILY: A CASE FOR SUBFUNCTIONALIZATION

AUX/LAX homologs have been reported to be present throughout the plant kingdom (Hochholdinger et al., 2000; de Billy et al., 2001; Kamada et al., 2003; Schrader et al., 2003; Schnabel and Frugoli, 2004; Péret et al., 2007; Hoyerová et al., 2008; Oliveros-Valenzuela et al., 2008; Shen et al., 2010; Pattison and Catalá, 2011; Carraro et al., 2012) and may have evolved before the evolution of land plants as *AUX/LAX* like sequences have been reported to be present in several single-celled and colony-forming Chlorophyta species (De Smet et al., 2011).

In *Arabidopsis*, *AUX1* belongs to a small gene family comprising of four highly conserved genes, *AUX1* and *LIKE-AUX1* (*LAX*) genes, *LAX1*, *LAX2,* and *LAX3* and form a plant- specific subclass within the amino acid/auxin permease (AAAP) super family (Young et al., 1999; Péret et al., 2012) (**Figure 2**). These genes encode multi membrane spanning transmembrane proteins. In a very elegant study, Swarup et al. (2004) using a pH sensitive YFP as a probe to determine the topology of AUX1 showed that AUX1 has 11 transmembrane segments with N terminal residing inside the cell and C-terminal outside. *AUX/LAX* genes share extensive sequence similarity (Péret et al., 2012). There is ample evidence to suggest that these genes have originated from a common ancestor through gene duplication. For example, AUX1 shares 82, 78, and 76% identity with LAX1, LAX2, and LAX3, respectively, and they also show well conserved gene structure (Péret et al., 2012) (**Figure 2**), At functional level evidence has been provided that these genes encode functional auxin influx carriers (Yang et al., 2006; Swarup et al., 2008; Péret et al., 2012) and mutations in these genes result in auxin related developmental defects (**Figure 3**; Bennett et al., 1996; Swarup et al., 2001, 2004, 2005, 2007, 2008; Bainbridge et al., 2008; Péret et al., 2012). Despite the conservation of biochemical function, these genes show mostly non-redundant expression and during the course of evolution have subfunctionalized to facilitate auxin related developmental programmes in different plant organs and tissues as reviewed below.

ROOT GRAVITROPISM: AUX1 AT THE HELM

The founder member of the AUX/LAX family, AUX1 is well documented to play a key role in root gravitropic response. *AUX1* is expressed in tissues that are involved in gravity perception,

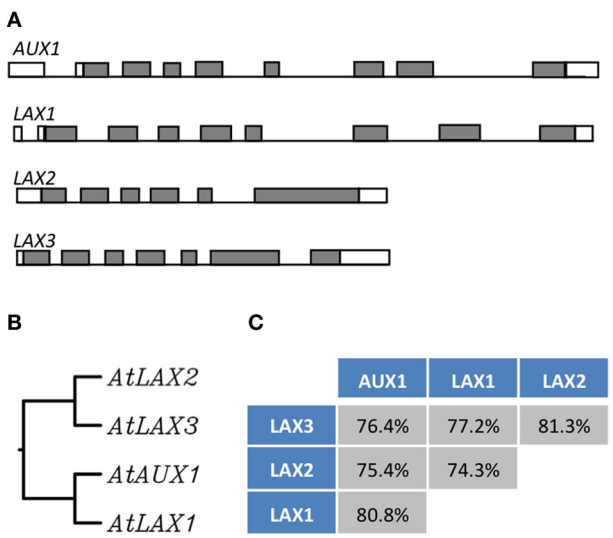

	AUX1	LAX1	LAX2
LAX3	76.4%	77.2%	81.3%
LAX2	75.4%	74.3%	
LAX1	80.8%		

FIGURE 2 | The AUX/LAX family of auxin influx transporters. Genetic organization of the *AUX/LAX* genes sequences showing exons (gray boxes) and introns (bars) (Péret et al., 2012) **(A).** Phylogenetic tree of the AUX/LAX protein sequences generated from a ClustalW alignment **(B)**. Percentage of identity between the members of the AUX/LAX family (identity is given a the score returned upon the ClustalW alignment) **(C)**.

FIGURE 3 | Mutations in *AUX/LAX* genes result in auxin related developmental defects. AUX1 regulates root gravitropism (Swarup et al., 2001, 2004, 2005). *AUX1* is expressed in tissues that are involved in gravity perception, signal transmission, and response and mutation in *aux1* cause agravitropic roots **(A)**. Both AUX1 and LAX3 regulate lateral root development (Swarup et al., 2008). *AUX1* is expressed in lateral root primordia whereas *LAX3* in the cortical and epidermal cells in contact with the primordia and *aux1 lax3* double mutants have severely delayed lateral root emergence **(B)**. LAX2 regulates vascular patterning in cotyledons (Péret et al., 2012). *LAX2* is expressed in the vascular tissues during embryo development and *lax2* mutants show vascular breaks in the cotyledons **(C)**. (Scale bars 20 μm).

signal transmission and response (**Figure 3A**). Mutation in *AUX1* results in severely agravitropic roots. Using an auxin responsive *IAA2:GUS* reporter, Swarup et al. (2001) showed that *aux1* mutants had defects in auxin movement from the root apex to the distal elongation zone. Later using a transactivation based approach, Swarup et al. (2005) mapped the auxin transport route during a gravitropic response and provided evidence that AUX1 was important for facilitating movement of auxin from the site of gravi-perception to gravi-response. Computer simulations of auxin fluxes through elongation zone tissues suggest that expression of auxin influx carrier *AUX1* and efflux carrier *PIN2* in the epidermis minimize the effect of radial diffusion while facilitating basipetal auxin transport (Swarup et al., 2005). Thus while PIN2 provides directionality of auxin movement, AUX1 appears essential for the efficient auxin uptake by expanding epidermal cells. More recently, Monshausen et al. (2011) have provided further insight into the importance of AUX1 in root gravitropism. Using confocal microscopy and fluorescent pH sensors, they show that there is an increase in the surface pH on the lower side of a gravistimulated wildtype but not *aux1* roots. One important implication of this finding is that increase in the root apoplastic pH will result in more IAA in its ionic IAA^- form. IAA^- is not membrane permeable and will require a carrier (AUX1) mediated uptake. This work helps to clarify a common misconception that because protonated IAA is membrane permeable, influx carriers play only a supplemental role and backs up computer simulation studies that estimate that carrier mediated IAA uptake is 15 times greater than the diffusion when *AUX1* is expressed in the root epidermal cells (Swarup et al., 2005; Kramer and Bennett, 2006).

Except AUX1, no other member of the AUX/LAX family plays a role in root gravitropic response (Péret et al., 2012). Apart from some expression of *LAX2* and *LAX3* in the columella cells, none of them are expressed in the tissues that are involved in gravity signal transmission (LRC) or response (epidermis). Also both *lax2* and *lax3* single mutants do not show any root gravitropic defect and *lax2 aux1* double mutants are no more severe than *aux1* (Péret et al., 2012).

LATERAL ROOT DEVELOPMENT: THE EMERGING STORY

LRs originate from the pericycle cells that divide and self organize to create a new primordium (Dubrovsky et al., 2000, 2001). As the LR formation process occurs deep inside the primary root tissues (**Figure 4A**), the newly formed organ has to penetrate through several layers of cells ranging from 3 in *Arabidopsis* (Swarup et al., 2008; Péret et al., 2009a,b) to as many as 15 in rice (Rebouillat et al., 2008). Several lines of evidences implicate auxin in LR initiation and development (Péret et al., 2009a,b).

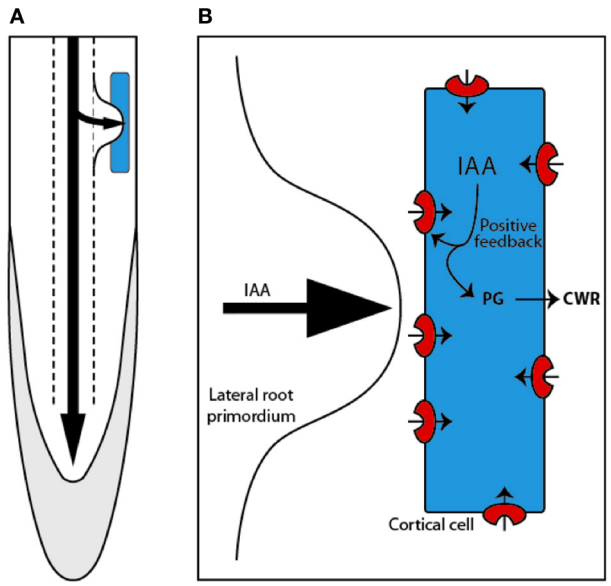

FIGURE 4 | Lateral root are formed within the pericycle deep inside the primary root and have to emerge through the outer tissue, passing through the endodermal, cortical (blue), and epidermal cells (A). Mechanism proposed by Swarup et al. (2008) describing how auxin (IAA) entering the cortical cell induces the expression of *LAX3*. This generates the establishment of a positive feedback loop that triggers high auxin levels and subsequent induction of cell wall remodeling (CWR) genes, such as the *polygalacturonase (PG)* **(B)**.

The initiation phase starts when two adjacent pericycle cells start to divide asymmetrically and create a LR primordium (Péret et al., 2009a,b). This process is associated with the creation of an auxin maximum in the pericycle founder cells (Benková et al., 2003; De Smet et al., 2007). Auxin influx carriers have been implicated in regulating LR development (Marchant et al., 2002; De Smet et al., 2007; Swarup et al., 2008) Marchant et al. (2002) demonstrated that *AUX1* is expressed in the pericycle cells before the first periclinal division and the *aux1* mutant displays a 50% reduction in the number of LRs (Hobbie and Estelle, 1995). Analysis of the auxin response reporter *IAA2:GUS* revealed that auxin content and distribution is altered in the *aux1* mutant that led Marchant et al. (2002) to conclude that AUX1 facilitates IAA loading into the vascular transport system.

Working on *LAX3*, Swarup et al. (2008) provided evidence that auxin influx carriers also regulate LR emergence (Swarup et al., 2008). They discovered that mutations in auxin influx carrier *LAX3* resulted in reduced number of emerged LR. Interestingly they found that the total number of initiation events was increased in *lax3* and this led them to suggest that initiation and emergence compete for the same source of auxin (Lucas et al., 2008a,b).

Molecular characterization of *LAX3* by Swarup et al. (2008) revealed that *LAX3* is expressed in the cortical and epidermal cells specifically situated in front of the LR primordia (**Figure 3B**). From Benková et al. (2003) work, they knew that auxin maxima is localized in the LR primordia and this led them to test the tantalising possibility that auxin itself could be the signal for *LAX3* expression in front of the primordia. Indeed, *LAX3* turned out to be auxin inducible. But how does LAX3 facilitate emergence? To find answer, Swarup et al. (2008) used a substractive transcriptomics approach to identify genes that are co expressed with *LAX3* in outer tissues and discovered that several cell wall remodeling genes were expressed in these cells in *LAX3* dependent fashion. Progression of the primordium inside the root tissues has long been associated with production of cell wall remodeling enzymes (Cosgrove, 2000, 2005) and this led Swarup et al. (2008) to propose that auxin from the LR primordia enters the cortical cells and induces *LAX3* expression (**Figure 4**). The activity of LAX3 at the plasma membrane is then proposed to facilitate auxin uptake in the same cell and would reinforce *LAX3* expression. As a result more and more auxin would accumulate in the cortical cells that will result in the induction of cell wall remodeling enzymes that is then proposed to facilitat smooth passage of the primordium through the cortex. The similar mechanism can then allow primordia passage through the epidermis. Therefore, as per this hypothesis, LAX3 participates in the creation of an auxin sink in a few cells and its expression in the outer tissues is dependent on its position compared to the source of auxin (the LR primordium) resulting in a typical "all or nothing" response.

ROOT HAIR DEVELOPMENT: BACK SEAT DRIVING

As the roots grow, old cells are continuously being pushed upwards and they pass through zones of elongation and differentiation. Root hairs are produced from a subset of epidermal cells in the differentiation zone. Auxin plays a key role in several aspects of root development including maintenance of the root apical meristem (Blilou et al., 2005); epidermal cell development (Sabatini et al., 1999; Grieneisen et al., 2007) and initiation and continued growth of root hairs (Pitts et al., 1998; Grebe et al., 2002; Rahman et al., 2002; Knox et al., 2003; Fischer et al., 2006). Interestingly, despite the importance of auxin in root hair development, no auxin influx carrier is expressed in the root hair cells. Jones et al. (2009) discovered that *AUX1* is expressed in the neighboring non-hair cells. In contrast to *AUX1*, auxin efflux carrier *PIN2* is expressed in both hair and non-root hair cells. Despite no *AUX1* being expressed in the hair cells, root hair length in the *aux1* mutant was shorter but can be restored to wildtype levels by treatment with exogenous auxin clearly implicating AUX1 in root hair growth. Furthermore, epidermal expression of *AUX1* was not detected in *werewolf/myb23* mutants that lack non-hair cells. These mutants have shorter root hairs but can be restored to wildtype levels by auxin treatment. This led Jones et al. (2009) to conclude that non-hair cells affect auxin abundance in hair cells. Computer simulation studies indicate that expression of *AUX1* in the non-hair cells result in over 10 fold accumulation of auxin in these cells compared to the adjacent hair cells. Due to the PIN2 activity, auxin can be effluxed out of the non-hair cells and into the apoplast and despite the lack of AUX1 in the hair cells, high auxin concentration can still be maintained in the hair cells in the differentiation zone up to 500 μm from the root apex. In contrast, in the *aux1* mutants, there will be significantly less accumulation of auxin in the root hair cells as due to the slow rate of diffusion, most of the auxin will either be recycled to the vascular tissues or will be lost through the epidermis before

it reaches the differentiation zone (Jones et al., 2009). Thus their work suggests that AUX1 helps to maintain high auxin levels in the differentiation zone and facilitates root hair growth.

AUX1 has also been implicated in maintenance of hair cell polarity (Grebe et al., 2002). Root hairs are formed on the basal side of the hair cells but they initiate from a more basal position in presence of auxin. Mutation in *aux1* results in apical shifting of the root hairs. *aux1* mutants also had 30 times higher frequency of double hair formation compared to wildtype. These results provided a clear link between auxin transport and the establishment of apical-basal epidermal polarity in *Arabidopsis*.

EMBRYONIC ROOT CELL ORGANIZATION: SIZE MATTERS

Arabidopsis root meristem is highly organized and a combination of apical basal and radial patterning inputs establish the positioning of the stem cell niche (Scheres, 2007). Both genetic and pharmacological approaches show that auxin transport plays a key role in this process. Working in *Arabidopsis* embryo, Ugartechea-Chirino et al. (2010) provided first evidence for the role of auxin influx carriers in patterning of the embryonic root. They showed that the quadruple *aux/lax* mutants had severely disorganized radicle apex and had significant increase in the root-cap cell number, average cell size, or both.

VASCULAR DEVELOPMENT: A ROLE FOR LAX2

Genetic and pharmacological studies have clearly shown that auxin regulates vascular development (Reinhardt, 2003; Petrásek and Friml, 2009). Recently, Péret et al. (2012) provided evidence that LAX2 is important for vascular development in cotyledons (**Figure 3C**). Using a *promoter:GUS* approach they show that *LAX2* is expressed in procambial and vascular tissues during embryogenesis. Examination of the *lax2* mutants revealed that they had higher propensity of discontinuity in vascular strands in the cotyledons. Though *LAX2* expression is also detected very early in developing leaves at the sites of initiating veins surprisingly, Péret et al. (2012) did not find any apparent defect in vascular patterning in *lax2* leaves. *AUX1* is also expressed in developing leaves and it will be interesting to see if *lax2 aux1* and quadruple *aux/lax* mutants show any defect in vascular patterning in leaves.

APICAL HOOK DEVELOPMENT: CROSS TALK AT ITS BEST

In dicotyledonous seedlings, apical hook protects the meristem when seedlings emerge from the soil. In the light, apical hooks opens, cotyledons expand and the photosynthesis begins (Chen and Chory, 2011). Besides light, plant hormones auxin, ethylene, gibberellins, and brassinosteroids are crucial for the maintenance and development of apical hook. Using a very elegant transactivation based approach Vandenbussche et al. (2010) showed that the auxin response maximum on the concave side is essential for correct hook development. The first evidence to implicate auxin influx carriers in apical hook development was provided by Roman et al. (1995) when they showed that *aux1* mutants are defective in hook development, a finding later confirmed by Stepanova et al. (2007). More recently, Vandenbussche et al. (2010) have provided evidence that LAX3 is also involved in apical hook development. Using single and multiple *aux/lax* mutant combinations, they showed that *lax3* mutants had partial hookless phenotype. They also showed that upon treatment with ethylene, both *aux1* and *lax3* had less exaggerated apical hook and *aux1 lax3* double mutants apical hook defect was as severe as seen when treated with auxin influx inhibitor 1-NOA (1-naphthoxyacetic acid). More detailed characterization including kinetics of hook development led Vandenbussche et al. (2010) to conclude that LAX3 is the major auxin influx carrier in hook development assisted by AUX1 and AUX1 appears to play a major role in ethylene-mediated hook exaggeration.

PHYLLOTACTIC PATTERNING: TEAM WORK

Phyllotaxy is the arrangement of organ primordia on a plant stem. Spiral phyllotaxy is the most common phyllotactic patterns in nature where new organ primorida initiates roughly at an angle of 137.5° and has intrigued biologists for generations (Fleming, 2005). Auxin transport appears to be crucial for the development of phyllotactic patterns. Auxin response reporter DR5 based studies in *Arabidopsis* show that auxin maxima is localized at the site where new primordia originate (Benková et al., 2003; Heisler et al., 2005; Smith et al., 2006). Reinhardt et al. (2003) showed that asymmetric localization of auxin efflux carrier PIN1 is important for the establishment of this auxin maxima that provides instructive signal for the formation of primordia. Stieger et al. (2002) provided evidence for a role for auxin influx carriers in phylltactic patterning. Using inhibitors of auxin influx carrier (Parry et al., 2001; Lankova et al., 2010), they revealed that auxin influx carriers were required for proper localization of leaf primordia. Further proof for the involvement of auxin influx carriers in phyllotactic patterning was provided by Reinhardt et al. (2003) and Bainbridge et al. (2008). Working on *pin1* mutants, Reinhardt et al. (2003) showed that localized auxin application on *pin1* meristem can restore primordia formation but such localized auxin application on *aux1 pin1* double mutants resulted in wider primordia formation. Using single and multiple *aux lax* mutants and their combinations Bainbridge et al. (2008) then showed that *AUX/LAX* genes act redundantly to regulate phyllotactic patterning in *Arabidopsis*. They revealed that in the *aux/lax* quadruple mutant, primordia formed at irregular angles (as compared to 137.5° in controls) and unusually often showed primordia clusters. Study of the multiple *aux/lax* mutant combinations revealed that besides quadruple, *aux1 lax1 lax2*, *aux1 lax1 lax3,* and *aux1 lax1* combinations had defect in phyllotactic patterning. They also reported that patterning in inflorescence meristem was also defective in the same mutant combinations. This led them to conclude that AUX1 and LAX1 act redundantly to regulate phyllotactic patterning in *Arabidopsis*. They also discovered that the phyllotactic defect in quadruple and *aux1 lax1 lax2* mutants was more severe compared to *aux1 lax1 lax3* and *aux1 lax1* mutants combination. On this basis they conclude that LAX2 may have a redundant function in regulating phyllotactic patterning. Interestingly *LAX2* is expressed in the vasculature but not expressed in the shoot apical meristem itself and to account for its involvement in phyllotactic patterning, Bainbridge et al. (2008) propose that LAX2 may increase the sink strength by pulling auxin out of the L1 layer and thus inhibiting primordium formation in this region.

ROLE OF AUX-LAX GENES IN BIOTIC INTERACTIONS

Many plant-associated bacteria are known to synthesize auxins, including IAA, which leads to diverse outcomes for the plant ranging from simple growth stimulation to promoting symbiotic interactions and even pathogenesis (Spaepen et al., 2007). Sequencing of several bacterial genomes has revealed the existence of different auxin synthesis pathways with a high degree of similarity with plant pathways (Spaepen et al., 2007). For example, in actinobacterium *Frankia*, at least two auxin synthesis pathways have been identified correlating with the production of two naturally occurring auxins: IAA and PAA. Interestingly, production of both these auxins is increased in nitrogen-deprived medium (Perrine-Walker et al., 2010). Furthermore, nitrogen deprivation promotes nitrogen-fixing symbiosis demonstrating that the establishment of this symbiotic interaction can be modulated by environmental (and genetic) factors. On the other hand, manipulation of auxin perception in the plant hosts appears to be a common mechanism during plant-microbe interactions. For instance, a plant miRNA induced by *Pseudomonas syringae* flagellin-derived peptide reduces the expression of the auxin receptor *TIR1* and its homologs *AFB2* and *AFB3* (Navarro et al., 2006). In recent years evidence is emerging that auxin transport may also play a key role in both symbiotic and pathogenic plant microbe interactions affecting penetration of auxin in the host plant cell.

In actinorhizal plant *Casuarina glauca*, a symbiotic interaction with soil actinobacteria from the *Frankia* species leads to infection of the host plant cell and subsequent development of a new organ "the actinorhizal nodule" the site of bacterial nitrogen fixation. Nodule formation in *Casuarina glauca,* can be severely impaired by treatment with auxin influx inhibitor 2-NOA suggesting that auxin influx activity is associated with nodule formation (Péret et al., 2007). This is further supported by molecular studies that show that a homolog of *Arabidopsis AUX1* "Cg*AUX1*" is expressed in all the infected cells, underlining its importance in the infection process (**Figure 5A**).

Auxin transport has also been implicated in plant pathogen interactions. The cyst nematode is a sedentary endoparasite of plant roots that penetrate the root and migrate toward a cell located near the vasculature to initiate feeding. The nematode then secretes effector proteins in the host cell, leading to genetic reprogramming into a feeding site called a syncytium (Davis et al., 2008). One of these effector proteins (19C07) identified in *Heterodera schachtii* was found to interact with *Arabidopsis* LAX3

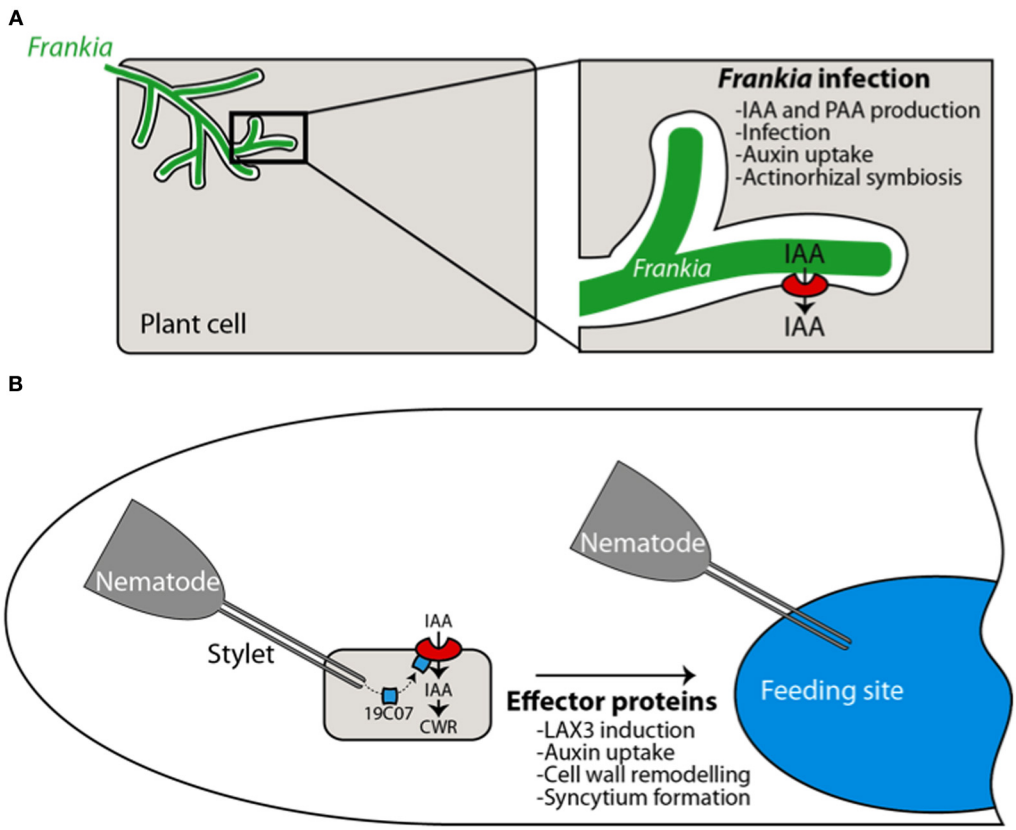

FIGURE 5 | Auxin influx transporters are involved in biotic interactions. During the actinorhizal symbiosis, Frankia infects the plant cell and triggers the expression of *CgAUX1,* resulting in auxin (IAA) uptake by the plant. Auxin is presumably synthesized by the actinobacteria (Péret et al., 2007) **(A)**. During cyst nematode infection, effector proteins are released in the plant cell. The 19C07 protein has been shown to directly interact with LAX3. High expression levels of LAX3 in the feeding site and adjacent cells participates in the incorporation of these cells in the feeding sites by promoting cell wall remodeling (CWR) (Lee et al., 2011) **(B)**.

auxin transporter in a yeast two-hybrid assay (Lee et al., 2011). The auxin transporter is strongly expressed in the syncytium, together with the auxin inducible cell wall related gene polygalacturonase that is likely to be involved in cell wall loosening. Auxin accumulation in the cells near the syncytium and subsequent cell wall modification would prime the cells for incorporation into the syncytium (**Figure 5B**). This suggests that the nematode manipulates auxin flow to promote formation of its own feeding site. This is supported by the fact that nematode infectivity is reduced in the *aux1 lax3* double mutant (Lee et al., 2011).

Among the myriad of biotic interactions—both pathogenic and symbiotic, it can be expected that auxin import is involved in a vast number of mechanisms underlying plant interactions with other organisms. A comprehensive study of *AUX-LAX* genes expression during these interactions associated with their functional role both in the model plant *Arabidopsis* and other non-model organisms would greatly improve our understanding of these mechanisms.

MODELING AUXIN TRANSPORT

Modeling studies have provided greater insight into the role of auxin transport in auxin related developmental programmes (Swarup et al., 2005; Kramer and Bennett, 2006; Kramer, 2008; Laskowski et al., 2008; Jones et al., 2009; Prusinkiewicz et al., 2009; Mironova et al., 2010; Szymanowska-Pułka and Nakielski, 2010; Vernoux et al., 2011; Bridge et al., 2012). Modeling auxin fluxes help us to understand how these fluxes are established and maintained, as well as their effect on growth and development. For example, recently, a computational approach studied the dynamics of auxin transport by taking into account pH modifications (Steinacher et al., 2012). The model predicts that auxin-induced acidification of cell wall compartments increases the rate of both auxin influx and efflux. This study also emphasizes the role of proton fluxes, an aspect of the auxin transport machinery that has been poorly studied. Modeling studies have already provided unparalleled insight into the role of AUX1 in establishing and maintaining auxin gradients during root gravitropism (Swarup et al., 2005) and root hair development (Jones et al., 2009). Modeling studies also suggest that AUX1-dependent transport in the root epidermis is necessary for gravitropic response but not for LR initiation. LR formation occurs preferentially at the convex side of roots. Lucas et al. (2008a,b) showed that the LR formation can also be induced by forcing root gravitropic response and proposed a mechanistic model based on an auxin budget system to describe auxin consumption by LR initiation and gravitropic response. Thus, modeling approaches are providing greater insight into the dynamics of auxin distribution and are likely to be at the forefront in the prediction of testable hypothesis of how auxin fluxes control plant development.

CONCLUSION AND PERSPECTIVES

In the last decade, genetic and cell biology approaches have resulted in greater understanding of molecular basis of cellular auxin transport. Auxin concentration in plant is affected by either changes in its metabolism or transport, both of which are altered to control plant development (Petrásek and Friml, 2009; Vanneste and Friml, 2009). Auxin influx carriers play a key role in regulating auxin homeostasis. It has been shown that their targeting is cell type specific (Péret et al., 2012) and this adds another level of regulation at tissue level. Identification of proteins that regulate their targeting will provide further insight into their localization and how this affects auxin distribution. Modeling studies have also been crucial in highlighting the role of auxin influx carriers in establishing and maintaining auxin gradients during root gravitropism (Swarup et al., 2005) and root hair development (Jones et al., 2009). Further refinement of the models taking into account all auxin transporters including AUX/LAX, PIN, PGP, and PILS promise to provide further understanding of the role of auxin transporters in auxin distribution.

ACKNOWLEDGMENTS

Authors acknowledge the support of the Biotechnology and Biological Sciences Research Council (BBSRC) and Engineering and Physical Sciences Research Council (EPSRC) funding to the Centre for Plant Integrative Biology (CPIB); Marie Curie Intra-European Fellowship within the 7th European Community Framework Programme PIEF-GA-2008-220506 (Benjamin Péret) and a grant from the Agence Nationale de la Recherche "Retour post-doctorants" 2011 EmPhos to Benjamin Péret.

REFERENCES

Abel, S., Oeller, P. W., and Theologis, A. (1994). Early auxin-induced genes encode short-lived nuclear proteins. *Proc. Natl. Acad. Sci. U.S.A.* 91, 326–330.

Aloni, R., Aloni, E., Langhans, M., and Ullrich, C. I. (2006). Role of cytokinin and auxin in shaping root architecture: regulating vascular differentiation, lateral root initiation, root apical dominance and root gravitropism. *Ann. Bot.* 97, 883–893.

Bainbridge, K., Guyomarc'h, S., Bayer, E., Swarup, R., Bennett, M., Mandel, T., et al. (2008). Auxin influx carriers stabilize phyllotactic patterning. *Genes Dev.* 22, 810–823.

Barbez, E., Kubeš, M., Rolčík, J., Béziat, C., Pěnčík, A., Wang, B., et al. (2012). A novel putative auxin carrier family regulates intracellular auxin homeostasis in plants. *Nature* 485, 119–122.

Benková, E., Michniewicz, M., Sauer, M., Teichmann, T., Seifertová, D., Jürgens, G., et al. (2003). Local, efflux-dependent auxin gradients as a common module for plant organ formation. *Cell* 115, 591–602.

Bennett, M. J., Marchant, A., Green, H. G., May, S. T., Ward, S. P., Millner, P. A., et al. (1996). *Arabidopsis AUX1* gene: a permease-like regulator of root gravitropism. *Science* 273, 948–950.

Blakeslee, J. J., Bandyopadhyay, A., Lee, O. R., Mravec, J., Titapiwatanakun, B., Sauer, M., et al. (2007). Interactions among PIN-FORMED and P-glycoprotein auxin transporters in *Arabidopsis*. *Plant Cell* 19, 131–147.

Blilou, I., Xu, J., Wildwater, M., Willemsen, V., Paponov, I., Friml, J., et al. (2005). The PIN auxin efflux facilitator network controls growth and patterning in *Arabidopsis* roots. *Nature* 433, 39–44.

Bosco, C. D., Dovzhenko, A., Liu, X., Woerner, N., Rensch, T., Eismann, M., et al. (2012). The endoplasmic reticulum localized PIN8 is a pollen specific auxin carrier involved in intracellular auxin homeostasis. *Plant J.* 71, 860–870.

Bridge, L. J., Mirams, G. R., Kieffer, M. L., King, J. R., and Kepinski, S. (2012). Distinguishing possible mechanisms for auxin-mediated developmental control in *Arabidopsis*: models with two Aux/IAA and ARF proteins, and two target gene-sets. *Math. Biosci.* 235, 32–44.

Brunoud, G., Wells, D. M., Oliva, M., Larrieu, A., Mirabet, V., Burrow, A. H., et al. (2012). A novel sensor to map auxin response and distribution at high spatio-temporal resolution. *Nature* 482, 103–106.

Carraro, N., Tisdale-Orr, T. E., Clouse, R. M., Knöller, A. S., and Spicer, R. (2012). Diversification and expression of the PIN, *AUX/LAX*, and ABCB families of putative auxin transporters in Populus. *Front. Plant Sci.* 3:17. doi: 10.3389/fpls.2012.00017

Carrier, D., Abu Bakar, N., Swarup, R., Callaghan, R., Napier, R., Bennett, M. J., et al. (2008). The binding of auxin to the *Arabidopsis* auxin influx transporter AUX1. *Plant Physiol.* 148, 529–535.

Chandler, J. W. (2009). Local auxin production: a small contribution to a big field. *Bioessays* 31, 60–70.

Chen, M., and Chory, J. (2011). Phytochrome signaling mechanisms and the control of plant development. *Trends Cell Biol.* 21, 664–671.

Cho, M., Lee, S. H., and Cho, H. T. (2007). P-glycoprotein4 displays auxin efflux transporter-like action in *Arabidopsis* root hair cells and tobacco cells. *Plant Cell* 19, 3930–3943.

Cosgrove, D. J. (2000). Loosening of plant cell walls by expansins. *Nature* 407, 321–326.

Cosgrove, D. J. (2005). Growth of the plant cell wall. *Nat. Rev. Mol. Cell Biol.* 6, 850–861.

Davis, E. L., Hussey, R. S., Mitchum, M. G., and Baum, T. J. (2008). Parasitism proteins in nematode-plant interactions. *Curr. Opin. Plant Biol.* 11, 360–366.

de Billy, F., Grosjean, C., May, S., Bennett, M., and Cullimore, J. V. (2001). Expression studies on *AUX1*-like genes in *Medicago truncatula* suggest that auxin is required at two steps in early nodule development. *Mol. Plant Microbe Interact.* 14, 267–277.

Delbarre, A., Muller, P., Imhoff, V., and Guern, J. (1996). Comparison of mechanisms controlling uptake and accumulation of 2, 4-dichlorophenoxy acetic acid, naphthalene-1-acetic acid, and indole-3-acetic acid in suspension-cultured tobacco cells. *Planta* 198, 532–541.

De Smet, I., Tetsumura, T., De Rybel, B., Frey, N. F., Laplaze, L., Casimiro, I., et al. (2007). Auxin-dependent regulation of lateral root positioning in the basal meristem of *Arabidopsis*. *Development* 134, 681–690.

De Smet, I., Voß, U., Lau, S., Wilson, M., Shao, N., Timme, R., et al. (2011). Unraveling the evolution of auxin signaling. *Plant Physiol.* 155, 209–221.

Dubrovsky, J. G., Doerner, P. W., Colón-Carmona, A., and Rost, T. L. (2000). Pericycle cell proliferation and lateral root initiation in *Arabidopsis*. *Plant Physiol.* 124, 1648–1657.

Dubrovsky, J. G., Rost, T. L., Colón-Carmona, A., and Doerner, P. (2001). Early primordium morphogenesis during lateral root initiation in *Arabidopsis thaliana*. *Planta* 214, 30–36.

Fischer, U., Ikeda, Y., Ljung, K., Serralbo, O., Singh, M., Heidstra, R., et al. (2006). Vectorial information for *Arabidopsis* planar polarity is mediated by combined AUX1, EIN2, and GNOM activity. *Curr. Biol.* 16, 2143–2149.

Fleming, A. J. (2005). Formation of primordia and phyllotaxy. *Curr. Opin. Plant Biol.* 8, 53–58.

Friml, J., Vieten, A., Sauer, M., Weijers, D., Schwarz, H., Hamann, T., et al. (2003). Efflux-dependent auxin gradients establish the apical-basal axis of *Arabidopsis*. *Nature* 426, 147–153.

Friml, J., Wiśniewska, J., Benková, E., Mendgen, K., and Palme, K. (2002). Lateral relocation of auxin efflux regulator PIN3 mediates tropism in *Arabidopsis*. *Nature* 415, 806–809.

Gälweiler, L., Guan, C., Müller, A., Wisman, E., Mendgen, K., Yephremov, A., et al. (1998). Regulation of polar auxin transport by AtPIN1 in *Arabidopsis* vascular tissue. *Science* 282, 2226–2230.

Goldsmith, M. H. (1977). The polar transport of auxin. *Ann. Rev. Plant Physiol.* 28, 439–478.

Grebe, M., Friml, J., Swarup, R., Ljung, K., Sandberg, G., Terlou, M., et al. (2002). Cell polarity signaling in *Arabidopsis* involves a BFA-sensitive auxin influx pathway. *Curr. Biol.* 12, 329–334.

Grieneisen, V. A., Xu, J., Marée, A. F., Hogeweg, P., and Scheres, B. (2007). Auxin transport is sufficient to generate a maximum and gradient guiding root growth. *Nature* 449, 1008–1013.

Grunewald, W., and Friml, J. (2010). The march of the PINs: developmental plasticity by dynamic polar targeting in plant cells. *EMBO J.* 29, 2700–2714.

Guenot, B., Bayer, E., Kierzkowski, D., Smith, R. S., Mandel, T., Zadnikova, P., et al. (2012). PIN1- leaf initiation in *Arabidopsis thaliana*. *Plant Physiol.* 159, 1501–1510.

Heisler, M. G., Ohno, C., Das, P., Sieber, P., Reddy, G. V., Long, J. A., et al. (2005). Patterns of auxin transport and gene expression during primordium development revealed by live imaging of the *Arabidopsis* inflorescence meristem. *Curr. Biol.* 15, 1899–1911.

Ho, C. H., Lin, S. H., Hu, H. C., and Tsay, Y. F. (2009). CHL1 functions as a nitrate sensor in plants. *Cell* 138, 1184–1194.

Hobbie, L., and Estelle, M. (1995). The axr4 auxin-resistant mutants of *Arabidopsis thaliana* define a gene important for root gravitropism and lateral root initiation. *Plant J.* 7, 211–220.

Jones, A. R., Kramer, E. M., Knox, K., Swarup, R., Bennett, M. J., Lazarus, C. M., et al. (2009). Auxin transport through non-hair cells sustains root-hair development. *Nat. Cell Biol.* 11, 78–84.

Hochholdinger, F., Wulff, D., Reuter, K., Park, W., and Feix, G. (2000). Tissue-specific expression of AUX1 in maize roots. *J. Plant Physiol.* 157, 315–319.

Hoyerová, K., Perry, L., Hand, P., Lanková, M., Kocábek, T., May, S., et al. (2008). Functional characterization of PaLAX1, a putative auxin permease, in heterologous plant systems. *Plant Physiol.* 146, 1128–1141.

Ikeda, Y., Men, S., Fischer, U., Stepanova, A., Alonso, J., Ljung, K., et al. (2009). Local auxin biosynthesis modulates gradient-directed planar polarity in *Arabidopsis*. *Nat. Cell Biol.* 11, 731–738.

Kamada, M., Yamasaki, S., Fujii, N., Higashitani, A., and Takahashi, H. (2003). Gravity-induced modification of auxin transport and distribution for peg formation in cucumber seedlings: possible roles for CS-AUX1 and CS-PIN1. *Planta* 218, 15–26.

Knox, K., Grierson, C. S., and Leyser, O. (2003). AXR3 and SHY2 interact to regulate root hair development. *Development* 130, 5769–5777.

Kramer, E. (2008). Computer models of auxin transport: a review and commentary. *J. Exp. Bot.* 59, 45–53.

Kramer, E. M., and Bennett, M. J. (2006). Auxin transport: a field in flux. *Trends Plant Sci.* 11, 382–386.

Krouk, G., Lacombe, B., Bielach, A., Perrine-Walker, F., Malinska, K., Mounier, E., et al. (2010). Nitrate-regulated auxin transport by NRT1.1 defines a mechanism for nutrient sensing in plants. *Dev. Cell* 18, 927–937.

Kubeš, M., Yang, H., Richter, G. L., Cheng, Y., Młodzińska, E., Wang, X., et al. (2012). The Arabidopsis concentration-dependent influx/efflux transporter ABCB4 regulates cellular auxin levels in the root epidermis. *Plant J.* 69, 640–654.

Lankova, M., Smith, R., Pesek, B., Kubes, M., Zazimalova, E., Petrasek, J., et al. (2010). Auxin influx inhibitors 1-NOA, 2-NOA and CHPAA interfere with membrane dynamics in tobacco cells. *J. Exp. Bot.* 61, 3589–3598.

Laskowski, M., Grieneisen, V. A., Hofhuis, H., Hove, C. A., Hogeweg, P., Marée, A. F., et al. (2008). Root system architecture from coupling cell shape to auxin transport. *PLoS Biol.* 6:e307. doi: 10.1371/journal.pbio.0060307

Lee, C., Chronis, D., Kenning, C., Péret, B., Hewezi, T., Davis, E. L., et al. (2011). The novel cyst nematode effector protein 19C07 interacts with the *Arabidopsis* auxin influx transporter LAX3 to control feeding site development. *Plant Physiol.* 155, 866–880.

Lomax, T. L., Mehlhorn, R. J., and Briggs, W. R. (1985). Active auxin uptake by zucchini membrane vesicles: quantitation using ESR volume and delta pH determinations. *Proc. Natl. Acad. Sci. U.S.A.* 82, 6541–6545.

Lucas, M., Godin, C., Jay-Allemand, C., and Laplaze, L. (2008a). Auxin fluxes in the root apex co-regulate gravitropism and lateral root initiation. *J. Exp. Bot.* 59, 55–66.

Lucas, M., Guédon, Y., Jay-Allemand, C., Godin, C., and Laplaze, L. (2008b). An auxin transport-based model of root branching in *Arabidopsis thaliana*. *PLoS ONE* 3:e3673. doi: 10.1371/journal.pone.0003673

Maher, E. P., and Martindale, S. J. (1980). Mutants of *Arabidopsis thaliana* with altered responses to auxins and gravity. *Biochem. Genet.* 18, 1041–1053.

Marchant, A., Bhalerao, R., Casimiro, I., Eklöf, J., Casero, P. J., Bennett, M., et al. (2002). AUX1 promotes lateral root formation by facilitating indole-3-acetic acid distribution between sink and source tissues in the *Arabidopsis* seedling. *Plant Cell* 14, 589–597.

Marchant, A., Kargul, J., May, S., Muller, P., Delbarre, A., Perrot-Rechenmann, C., et al. (1999). AUX1 regulates root gravitropism in Arabidopsis by facilitating auxin uptake within root apical tissues. *EMBO J.* 18, 2066–2073.

Mironova, V. V., Omelyanchuk, N. A., Yosiphon, G., Fadeev, S. I., Kolchanov, N. A., Mjolsness, E., et al. (2010). A plausible mechanism for auxin patterning along the developing root. *BMC Syst. Biol.* 4:98. doi: 10.1186/1752-0509-4-98

Monshausen, G. B., Miller, N. D., Murphy, A. S., and Gilroy, S. (2011). Dynamics of auxin-dependent Ca2+ and pH signaling in root growth revealed by integrating high-resolution imaging with automated computer vision-based analysis. *Plant J.* 65, 309–318.

Mravec, J., Skůpa, P., Bailly, A., Hoyerová, K., Krecek, P., Bielach, A., et al. (2009). Subcellular homeostasis of phytohormone auxin is mediated by the ER-localized PIN5 transporter. *Nature* 459, 1136–1140.

Navarro, L., Dunoyer, P., Jay, F., Arnold, B., Dharmasiri, N., Estelle, M., et al. (2006). A plant miRNA contributes to antibacterial resistance by repressing auxin signaling. *Science* 312, 436–439.

Noh, B., Bandyopadhyay, A., Peer, W. A., Spalding, E. P., and Murphy, A. S. (2003). Enhanced gravi- and phototropism in plant mdr mutants mislocalizing the auxin efflux protein PIN1. *Nature* 423, 999–1002.

Oliveros-Valenzuela, M., Reyes, D., Sanchez-Bravo, J., Acosta, M., and Nicolas, C. (2008). Isolation and characterization of a cDNA clone encoding an auxin influx carrier in carnation cuttings. Expression in different organs and cultivars and its relationship with cold storage. *Plant Phys. Biochem.* 46, 1071–1076.

Ottenschläger, I., Wolff, P., Wolverton, C., Bhalerao, R. P., Sandberg, G., Ishikawa, H., et al. (2003). Gravity-regulated differential auxin transport from columella to lateral root cap cells. *Proc. Natl. Acad. Sci. U.S.A.* 100, 2987–2991.

Paponov, I. A., Teale, W. D., Trebar, M., Blilou, I., and Palme, K. (2005). The PIN auxin efflux facilitators: evolutionary and functional perspectives. *Trends Plant Sci.* 10, 170–177.

Parry, G., Delbarre, A., Marchant, A., Swarup, R., Perrot-Rechenmann, C., and Bennett, M. (2001). Physiological characterization of a novel class of auxin influx carrier inhibitors. *Plant J.* 25, 399–406.

Pattison, R. J., and Catalá, C. (2011). Evaluating auxin distribution in tomato (*Solanum lycopersicum*) through an analysis of the PIN and *AUX/LAX* gene families. *Plant J.* 70, 585–598.

Perrine-Walker, F., Doumas, P., Lucas, M., Vaissayre, V., Beauchemin, N. J., Band, L. R., et al. (2010). Auxin carriers localization drives auxin accumulation in plant cells infected by Frankia in *Casuarina glauca* actinorhizal nodules. *Plant Physiol.* 154, 1372–1380.

Petrásek, J., and Friml, J. (2009). Auxin transport routes in plant development. *Development* 136, 2675–2688.

Péret, B., De Rybel, B., Casimiro, I., Benková, E., Swarup, R., Laplaze, L., et al. (2009a). *Arabidopsis* lateral root development: an emerging story. *Trends Plant Sci.* 14, 399–408.

Péret, B., Larrieu, A., and Bennett, M. J. (2009b). Lateral root emergence: a difficult birth. *J. Exp. Bot.* 60, 3637–3643.

Péret, B., Swarup, K., Ferguson, A., Seth, M., Yang, Y., Dhondt, S., et al. (2012). *AUX/LAX* genes encode a family of auxin influx transporters that perform distinct functions during *Arabidopsis* development. *Plant Cell* 24, 1–12.

Péret, B., Swarup, R., Jansen, L., Devos, G., Auguy, F., Collin, M., et al. (2007). Auxin influx activity is associated with Frankia infection during actinorhizal nodule formation in *Casuarina glauca*. *Plant Physiol.* 144, 1852–1862.

Pitts, R. J., Cernac, A., and Estelle, M. (1998). Auxin and ethylene promote root hair elongation in *Arabidopsis*. *Plant J.* 16, 553–560.

Prusinkiewicz, P., Crawford, S., Smith, R. S., Ljung, K., Bennett, T., Ongaro, V., et al. (2009). Control of bud activation by an auxin transport switch. *Proc. Natl. Acad. Sci. U.S.A.* 106, 17431–17436.

Rahman, A., Hosokawa, S., Oono, Y., Amakawa, T., Goto, N., and Tsurumi, S. (2002). Auxin and ethylene response interactions during *Arabidopsis* root hair development dissected by auxin influx modulators. *Plant Physiol.* 130, 1908–1917.

Rahman, A., Takahashi, M., Shibasaki, K., Wu, S., Inaba, T., Tsurumi, S., et al. (2010). Gravitropism of *Arabidopsis* thaliana roots requires the polarization of PIN2 toward the root tip in meristematic cortical cells. *Plant Cell* 22, 1762–1776.

Raven, J. A. (1975). Transport of indoleacetic acid in plant cells in relation to pH and electrical potential gradients, and its significance for polar IAA transport. *New Phytol.* 74, 163–172.

Rebouillat, J., Dievart, A., Verdeil, J. A., Escoute, J., Giese, G., Breitler, J. C., et al. (2008). Molecular genetics of rice root development. *Rice* 2, 15–34.

Reinhardt, D. (2003). Vascular patterning: more than just auxin? *Curr. Biol.* 13, R485–R487.

Reinhardt, D., Pesce, E., Stieger, P., Mandel, T., Baltensperger, K., Bennett, M., et al. (2003). Regulation of phyllotaxy by polar auxin transport. *Nature* 426, 255–260.

Roman, G., Lubarsky, B., Kieber, J. J., Rothenberg, M., and Ecker, J. R. (1995). Genetic analysis of ethylene signal transduction in *Arabidopsis thaliana*: five novel mutant loci integrated into a stress response pathway. *Genetics* 139, 1393–1409.

Rubery, P. H., and Sheldrake, A. R. (1974). Carrier-mediated auxin transport *Planta* 118, 101–121.

Sabater, M., and Rubery, P. H. (1987). Auxin carriers in Cucurbita vesicles. 1. Imposed perturbations of transmembrane pH and electrical potential gradients characterized by radioactive probes. *Planta* 171, 501–506.

Sabatini, S., Beis, D., Wolkenfelt, H., Murfett, J., Guilfoyle, T., Malamy, J., et al. (1999). An auxin-dependent distal organizer of pattern and polarity in the *Arabidopsis* root. *Cell* 99, 463–472.

Scheres, B. (2007). Stem-cell niches: nursery rhymes across kingdoms. *Nat. Rev. Mol. Cell Biol.* 8, 345–354.

Schnabel, E., and Frugoli, J. (2004). The PIN and LAX families of auxin transport genes in *Medicago truncatula*. *Mol. Genet. Genomics* 272, 420–432.

Schrader, J., Baba, K., May, S., Palme, K., Bennett, M., Bhalerao, R., et al. (2003). Polar auxin transport in the wood-forming tissues of hybrid aspen is under simultaneous control of developmental and environmental signals. *Proc. Natl. Acad. Sci. U.S.A.* 100, 10096–10101.

Shen, C., Bai, Y., Wang, S., Zhang, S., Wu, Y., Chen, M., et al. (2010). Expression profile of PIN, AUX/LAX and PGP auxin transporter gene families in *Sorghum bicolor* under phytohormone and abiotic stress. *FEBS J.* 277, 2954–2969.

Sieburth, L. E., and Deyholos, M. K. (2006). Vascular development: the long and winding road *Curr. Opin. Plant Biol.* 9, 48–54.

Smith, R. S., Guyomarc'h, S., Mandel, T., Reinhardt, D., Kuhlemeier, C., and Prusinkiewicz, P. (2006). A plausible model of phyllotaxis. *Proc. Natl. Acad. Sci. U.S.A.* 103, 1301–1306.

Sorefan, K., Girin, T., Liljegren, S. J., Ljung, K., Robles, P., Galván-Ampudia, C. S., et al. (2009). A regulated auxin minimum is required for seed dispersal in *Arabidopsis*. *Nature* 459, 583–586.

Spaepen, S., Vanderleyden, J., and Remans, R. (2007). Indole-3-acetic acid in microbial and microorganism-plant signaling. *FEMS Microbiol. Rev.* 31, 425–448.

Steinmann, T., Geldner, N., Grebe, M., Mangold, S., Jackson, C. L., Paris, S., et al. (1999). Coordinated polar localization of auxin efflux carrier PIN1 by GNOM ARF GEF. *Science* 286, 316–318.

Steinacher, A., Leyser, O., and Clayton, R. H. (2012). A computational model of auxin and pH dynamics in a single plant cell. *J. Theor. Biol.* 296, 84–94.

Stepanova, A. N., Yun, J., Likhacheva, A. V., and Alonso, J. M. (2007). Multilevel interactions between ethylene and auxin in *Arabidopsis* roots. *Plant Cell* 19, 2169–2185.

Stieger, P., Reinhardt, D., and Kuhlemeier, C. (2002). The auxin influx carrier is essential for correct leaf positioning. *Plant J.* 32, 509–517.

Swarup, K., Benková, E., Swarup, R., Casimiro, I., Péret, B., Yang, Y., et al. (2008). The auxin influx carrier LAX3 promotes lateral root emergence. *Nat. Cell Biol.* 10, 946–954.

Swarup, R., and Bennett, M. (2003). Auxin transport: the fountain of life in plants? *Dev. Cell* 5, 824–826.

Swarup, R., Friml, J., Marchant, A., Ljung, K., Sandberg, G., Palme, K., et al. (2001). Localization of the auxin permease AUX1 suggests two functionally distinct hormone transport pathways operate in the *Arabidopsis* root apex. *Genes Dev.* 15, 2648–2653.

Swarup, R., Kargul, J., Marchant, A., Zadik, D., Rahman, A., Mills, R., et al. (2004). Structure-function analysis of the presumptive *Arabidopsis* auxin permease AUX1. *Plant Cell* 16, 3069–3083.

Swarup, R., Kramer, E. M., Perry, P., Knox, K., Leyser, H. M., Haseloff, J., et al. (2005). Root gravitropism requires lateral root cap and epidermal cells for transport and response to a mobile auxin signal. *Nat. Cell Biol.* 7, 1057–1065.

Swarup, R., Perry, P., Hagenbeek, D., Van Der Straeten, D., Beemster, G. T., Sandberg, G., et al. (2007). Ethylene upregulates auxin biosynthesis in *Arabidopsis* seedlings to enhance inhibition of root cell elongation. *Plant Cell* 19, 2186–2196.

Szymanowska-Pułka, J., and Nakielski, J. (2010). The tensor-based model for growth and cell divisions of the

root apex. II. Lateral root formation. *Planta* 232, 1207–1218.

Terasaka, K., Blakeslee, J. J., Titapiwatanakun, B., Peer, W. A., Bandyopadhyay, A., Makam, S. N., et al. (2005). PGP4, an ATP binding cassette P-glycoprotein, catalyzes auxin transport in *Arabidopsis thaliana* roots. *Plant Cell* 17, 2922–2939.

Ugartechea-Chirino, Y., Swarup, R., Swarup, K., Péret, B., Whitworth, M., Bennett, M., et al. (2010). The AUX1 LAX family of auxin influx carriers is required for the establishment of embryonic root cell organization in *Arabidopsis thaliana*. *Ann. Bot.* 105, 277–289.

Ulmasov, T., Murfett, J., Hagen, G., and Guilfoyle, T. J. (1997). Aux/IAA proteins repress expression of reporter genes containing natural and highly active synthetic auxin response elements. *Plant Cell* 9, 1963–1971.

Vandenbussche, F., Petrásek, J., Zádníková, P., Hoyerová, K., Pesek, B., Raz, V., et al. (2010). The auxin influx carriers AUX1 and LAX3 are involved in auxin-ethylene interactions during apical hook development in *Arabidopsis thaliana* seedlings. *Development* 137, 597–606.

Vanneste, S., and Friml, J. (2009). Auxin: a trigger for change in plant development. *Cell* 136, 1005–1016.

Vernoux, T., Brunoud, G., Farcot, E., Morin, V., Van den Daele, H., Legrand, J., et al. (2011). The auxin signalling network translates dynamic input into robust patterning at the shoot apex. *Mol. Syst. Biol.* 7, 508.

Wang, L., Li, Z., Qian, W., Guo, W., Gao, X., Huang, L., et al. (2011). The *Arabidopsis* purple acid phosphatase AtPAP10 is predominantly associated with the root surface and plays an important role in plant tolerance to phosphate limitation. *Plant Physiol.* 157, 1283–1299.

Went, F. W. (1926). On growth accelerating substances in the coleoptile of *Avena sativa*. *Proc. Kon. Ned. Akad. Weten.* 30, 1019.

Wisniewska, J., Xu, J., Seifertová, D., Brewer, P. B., Ruzicka, K., Blilou, I., et al. (2006). Polar PIN localization directs auxin flow in plants. *Science* 312, 883.

Wolters, H., Anders, N., Geldner, N., Gavidia, R., and Jürgens, G. (2011). Coordination of apical and basal embryo development revealed by tissue-specific GNOM functions. *Development* 138, 117–126.

Yamamoto, M., and Yamamoto, K. (1998). Differential effects of 1-naphthaleneacetic acid, indole-3-acetic acid and 2, 4-dichlorophenoxyacetic acid on the gravitropic response of roots in an auxin-resistant mutant of Arabidopsis, *aux1*. *Plant Cell Physiol.* 39, 660–664.

Yang, H., and Murphy, A. S. (2009). Functional expression and characterization of Arabidopsis ABCB, AUX 1 and PIN auxin transporters in *Schizosaccharomyces pombe*. *Plant J.* 59, 179–191.

Yang, Y., Hammes, U. Z., Taylor, C. G., Schachtman, D. P., and Nielsen, E. (2006). High-affinity auxin transport by the AUX1 influx carrier protein. *Curr. Biol.* 16, 1123–1127.

Young, G. B., Jack, D. L., Smith, D. W., and Saier, M. H. (1999). The amino acid/auxin:proton symport permease family. *Biochim. Biophys. Acta* 1415, 306–322.

Zazímalová, E., Murphy, A. S., Yang, H., Hoyerová, K., and Hosek, P. (2010). Auxin transporters-why so many? *Cold Spring Harb. Perspect. Biol.* 2, a001552.

Conflict of Interest Statement: The authors declare that the research was conducted in the absence of any commercial or financial relationships that could be construed as a potential conflict of interest.

Received: 01 July 2012; accepted: 20 September 2012; published online: 18 October 2012.

*Citation: Swarup R and Péret B (2012) AUX/LAX family of auxin influx carriers—an overview. Front. Plant Sci. **3**:225. doi: 10.3389/fpls.2012.00225*

This article was submitted to Frontiers in Plant Traffic and Transport, a specialty of Frontiers in Plant Science.

frontiers in
PLANT SCIENCE

ORIGINAL RESEARCH ARTICLE
published: 12 November 2012
doi: 10.3389/fpls.2012.00251

The putative K^+ channel subunit AtKCO3 forms stable dimers in *Arabidopsis*

Alessandra Rocchetti[1†], Tripti Sharma[2†], Camilla Wulfetange[2], Joachim Scholz-Starke[3], Alexandra Grippa[1], Armando Carpaneto[3], Ingo Dreyer[2,4], Alessandro Vitale[1], Katrin Czempinski[2] and Emanuela Pedrazzini[1]*

[1] Istituto di Biologia e Biotecnologia Agraria, Consiglio Nazionale delle Ricerche, Milano, Italy
[2] Institute of Biochemistry and Biology, University of Potsdam, Potsdam-Golm, Germany
[3] Istituto di Biofisica, Consiglio Nazionale delle Ricerche, Genova, Italy
[4] Centro de Biotecnología y Genómica de Plantas, Universidad Politécnica de Madrid, Madrid, Spain

Edited by:
Markus Geisler, University of Fribourg, Switzerland

Reviewed by:
Jianhua Zhu, University of Maryland, USA
Gerhard Obermeyer, University Salzburg, Austria

***Correspondence:**
Emanuela Pedrazzini, Istituto di Biologia e Biotecnologia Agraria, Consiglio Nazionale delle Ricerche, via Bassini 15, 20133 Milano, Italy.
e-mail: pedrazzini@ibba.cnr.it

†*Alessandra Rocchetti and Tripti Sharma have contributed equally to the work.*

The permeation pore of K^+ channels is formed by four copies of the pore domain. AtKCO3 is the only putative voltage-independent K^+ channel subunit of *Arabidopsis thaliana* with a single pore domain. KCO3-like proteins recently emerged in evolution and, to date, have been found only in the genus *Arabidopsis* (*A. thaliana* and *A. lyrata*). We show that the absence of KCO3 does not cause marked changes in growth under various conditions. Only under osmotic stress we observed reduced root growth of the *kco3-1* null-allele line. This phenotype was complemented by expressing a KCO3 mutant with an inactive pore, indicating that the function of KCO3 under osmotic stress does not depend on its direct ability to transport ions. Constitutively overexpressed AtKCO3 or AtKCO3::GFP are efficiently sorted to the tonoplast indicating that the protein is approved by the endoplasmic reticulum quality control. However, vacuoles isolated from transgenic plants do not have significant alterations in current density. Consistently, both AtKCO3 and AtKCO3::GFP are detected as homodimers upon velocity gradient centrifugation, an assembly state that would not allow for activity. We conclude that if AtKCO3 ever functions as a K^+ channel, active tetramers are held by particularly weak interactions, are formed only in unknown specific conditions and may require partner proteins.

Keywords: *Arabidopsis*, membrane proteins, potassium channels, protein assembly, tonoplast

INTRODUCTION

Homeostasis of potassium, the most abundant cation of plants, is maintained by the activity of transporters and channels of the plasma membrane and the tonoplast (Dreyer and Uozumi, 2011). *Arabidopsis thaliana* contains 15 genes encoding K^+ channel subunits. Among these are the five members (*At*TPK1–5) of the voltage-independent, tandem-pore family (Voelker et al., 2010). The key signature of K^+ channels is the pore (P) domain which must be present in four copies in an active channel complex. Tandem-pore channels are therefore expected to be dimers. Consistently, fluorescence resonance energy transfer (FRET) and bimolecular fluorescence complementation (BiFC) experiments conducted on *At*TPK1 or *At*TPK5 in transiently transformed plant cells strongly support the existence of homodimers (Voelker et al., 2006). Stable heteromeric interactions between different *At*TPK members were instead not detected (Voelker et al., 2006). The assembly of *At*TPK1 into stable dimers has been directly confirmed in transgenic *Arabidopsis* constitutively expressing an AtTPK1::GFP fusion (Maîtrejean et al., 2011). An additional polypeptide with one pore domain only, *At*KCO3 (locus AT5G46360), is most closely related to *At*TPK2 and believed to have originated from gene duplication followed by a partial deletion event (Marcel et al., 2010; Voelker et al., 2010). KCO3-like proteins have only been identified in the genus *Arabidopsis* (*A. thaliana* and *A. lyrata*), so far. They were not found in other known plant genomes (Gomez-Porras et al., 2012). Upon transient expression in protoplasts from *Arabidopsis* cell cultures, *At*KCO3::GFP localizes at the tonoplast, like similar fusions of *At*TPK1, 2, 3, and 5 (Voelker et al., 2006). Homomeric *At*KCO3 interactions have been detected by FRET and BiFC (Voelker et al., 2006) but it is not known whether the polypeptide forms tetramers, a prerequisite for activity in the case of this one-pore subunit. Here we have applied a number of experimental approaches in order to get insights on the assembly state and possible function of *At*KCO3.

MATERIALS AND METHODS

PLANT GENOTYPING AND ANALYSIS

The *A. thaliana* knock-out mutant *kco3-1* (Salk_096038) was ordered from the Salk Institute. Genomic DNA was extracted from frozen leaves with 1 ml of CTAB extraction buffer (0.8% CTAB, 0.14 M sorbitol, 0.22 mM Tris–HCl, pH 6, 0.022 mM EDTA, 0.8 M NaCl, 1% *N*-Lauroylsarcosine). Confirmation of the T-DNA insertion in *kco3-1* was done using the following primers: 5′GCGTGGACCGCTTGCTGCAACT3′ (T-DNA-LB), 5′CACGATTTCTATGCCAATGACTCCATCGG3′ (KCO3-fwd), 5′AAAAAGAGCTCTTAAACTGGTTCAACTATATCC3′ (KCO3-rev).

For phenotypic analysis, seeds were plated on MS media supplemented with 3% sucrose in axenic condition. One-week-old seedlings were transferred to media containing the appropriate solute for the growth test in different abiotic stress conditions and were vertically grown in 16 h day/8 h night conditions. Different potassium concentration: seedlings were transferred on K^+ deficient medium [2.5 mM $NaNO_3$, 2.5 mM $Ca(NO_3)_2$, 2 mM $NH_4(H_2PO_4)$, 2 mM $MgSO_4$, 0.1 mM FeNaEDTA, 25 μM $CaCl_2$, 25 μM H_3BO_3, 2 μM $ZnSO_4$, 2 μM $MnSO_4$, 0.5 μM $CuSO_4$, 0.2 μM Na_2MoO_4, 0.01 μM $CoCl_2$, 1% sucrose, pH 5.7; jellified with 0.8% Phytagel (Sigma Aldrich)] supplemented with low (100 μM) or high (2.5 mM) K^+; salt stress: 75 mM NaCl; osmotic stress: 100 mM mannitol. Oxidative stress: 15 days after sowing the seedlings were moved to liquid MS media with 10 mM H_2O_2. For mock treatment, plants were transferred to liquid MS media. Plants were grown on a shaker for 5 days, with daily change of media.

GENERATION OF TRANSGENIC PLANTS

Plasmid DNA required for sequencing purposes was prepared using Qiagen columns (Qiagen, Hilden, Germany). Sequence determinations were performed by MWG-Biotech (Ebersberg, Germany) and Replicon (Berlin, Germany). For sequence analysis the BLAST server at the National Center of Biological Information (NCBI, Bethesda, USA), or the University of Wisconsin GCG software package, version 8 (Devereux et al., 1984) were used. Either Pfu polymerase (Stratagene, Heidelberg, Germany) or Taq polymerase (Gibco BRL, Eggenstein, Germany) was employed for PCR. All PCR-derived fragments were sequenced to ensure the absence of amplification errors.

To produce *dnKCO3* transgenic plants, site directed mutagenesis was performed on the *KCO3* gene to insert dominant negative mutation F141R. PCR product was digested with *Sal*I–*Sac*I and inserted in *Sal*I–*Sac*I digested pBS generating pBS-dnKCO3. To generate pBIBhygro-dnKCO3, amplification was done on pBS-dnKCO3 with pKCO3-fwd (5′ATTTAGTCGACACACATCACAACATGATTGAAGATGACAATG3′) and KCO3-rev primers (**Figure 1B**). Amplification product was double digested with *Sal*I–*Sac*I and cloned in *Sal*I–*Sac*I digested pBibHygro. Positive clones were further confirmed by sequencing and transformed in *Agrobacterium tumefaciens* strain GV1301. The positive *Agrobacterium* clones were detected through PCR with gene-specific primers on mini preparation of DNA from *Agrobacterium*. Overnight grown culture of *Agrobacterium* was infiltrated in Col-0 wild-type plants through floral dip method. Seeds from infiltrated plants were screened on hygromycin-containing medium to select transgenic plants. Seedlings surviving on hygromycin-containing medium were used for genotyping to detect the presence of transformed transgene.

To generate *kco3-1* × *dnKCO3* transgenic plants, homozygous lines of *dnKCO3* were crossed with *kco3-1* null-allele (Salk_96038) mutant. The seeds obtained from the crossed plants were then screened to procure dominant-negative knockout mutant plants of KCO3. These *kco3-1* × *dnKCO3* were grown again in the next generation under self-fertilization condition. Seeds thus inherited after self-cross were screened by performing PCR reactions to obtain homozygous *kco3-1* × *dnKCO3*.

AtKCO3 cDNA clones were isolated from cDNA preparations of *A. thaliana* seedlings (C24 ecotype) using primers 5′CAACAACAAGGACCCATTACACC3′ (KCO3.seq) and 5′CCACTGCCATCTTCAATCATG3′ (KCO3.rev). Fragments corresponding to the *AtKCO3* cDNA were subcloned into pPCRII (Stratagene, Heidelberg, Germany) giving rise to the plasmid pCRII-*KCO3*. Sequence determination was done for three clones

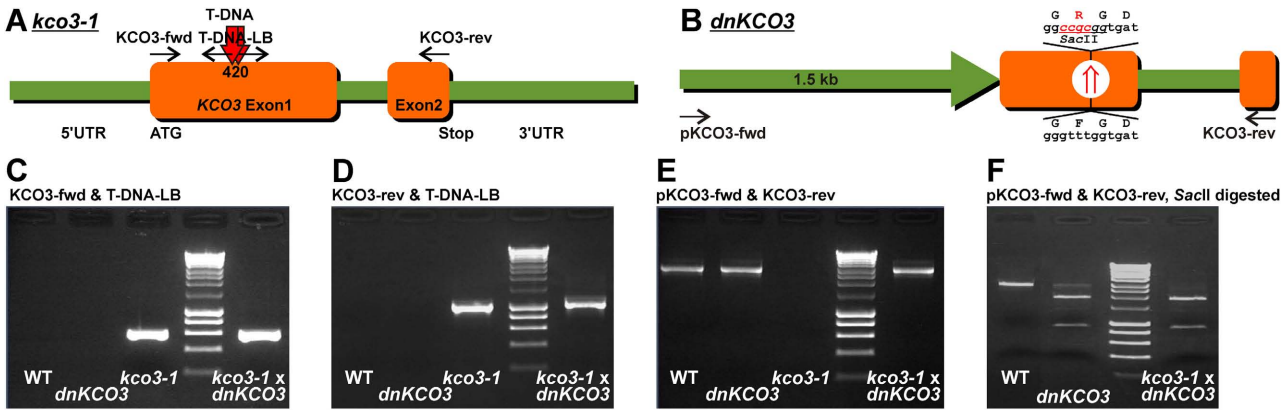

FIGURE 1 | Genotyping of *kco3-1* null-allele, *dnKCO3* and *kco3-1* × *dnKCO3* mutant plants. (A) Schematic representation of the Salk_96038 T-DNA insertion line that contains two head to head T-DNA insertions at position 420 in the first exon of the KCO3 gene. **(B)** Schematic representation of *dnKCO3* mutant, where, in the first exon of the *KCO3* gene, a dominant negative mutation has been created by mutating the GFGD motif to GRGD. Additionally, a recognition site of the restriction enzyme *Sac*II has been inserted. **(C,D)** PCR was performed on genomic DNA with the indicated primer sets specific for T-DNA amplification. Amplification was attained in case of *kco3-1* and *kco3-1* × *dnKCO3* while the wild-type and *dnKCO3* does not show any amplification product with the T-DNA primer sets. **(E)** PCR was performed with the indicated gene specific primer pair. Amplification can be observed in Col-0 wild-type, *dnKCO3* and *kco3-1* × *dnKCO3*. No amplification product is detectable in the homozygous T-DNA insertion line (*kco3-1*). **(F)** *Sac*II restriction digestion of the PCR products obtained by amplification with the gene specific primer pair. PCR product from Col-0 wild-type was not digested. The amplification product from the *dnKCO3* mutant was digested but some undigested product can also be seen. The PCR product from *kco3-1* × *dnKCO3* shows complete digestion.

as described above. Plasmid p35S-*KCO3* was generated by inserting the At*KCO3* cDNA (KpnI/blunt/EcoRV pCRII-*KCO3*) into SmaI site of pBinAR-Kan (Höfgen and Willmitzer, 1988). A C-terminal *GFP*-fusion construct was created using pBI-35S-10H-GFP-JFH1 (Hong et al., 1999). The *At*KCO3 cDNA was amplified using the primers 5′CGCGTCGACATGCCAATGACTCCATCGG3′ (KCO3-FSI.seq) and 5′ATCACTAGTACAGAAGTTGCGGTGGTTAAATCCAA3′ (KCO3-FSII.rev) and fused to *GFP* coding sequence via *Sal*I/*Xho*I/*Spe*I sites to generate p35S-*KCO3::GFP*.

Transgenic *Arabidopsis* plants expressing KCO3 or KCO3::GFP were generated by vacuum infiltration with *Agrobacterium tumefaciens* strain GV3101 transformed with the constructs p35S-*KCO3* or 35S-*KCO3::GFP*. Kanamycin-resistant plants (T0) were identified. Experiments were conducted using T3 or T4 plants.

ANTIBODIES

The following antibodies were used in this study: rabbit polyclonal anti-GFP (1:1000 dilution, Invitrogen), rabbit polyclonal anti-endoplasmin/GRP94 (1:1,000 dilution; Klein et al., 2006), rabbit polyclonal anti-PiP2 (1:10,000 dilution; Santoni et al., 2003), or chicken polyclonal anti-γTIP raised against a synthetic peptide corresponding to the C-terminal nine amino acids of *Arabidopsis* γTIP (1:1,000 dilution, a gift from N. V. Raikhel).

An anti-KCO3 antiserum was raised against a synthetic peptide (NH_2-SEFKNRLLFGSLPRC-COOH) located at the N-terminus of AtKCO3 and provided by Covalab (Villeurbanne, France). The total IgG fraction from immunized rabbit was then purified using protein A bead column. The affinity-purified antibodies were then subjected to immuno-affinity purification, passing through a resin-column containing the antigenic peptide. This affinity-purified rabbit polyclonal anti-KCO3 was used at 1:2,000 dilution.

VACUOLE ISOLATION, PATCH-CLAMP RECORDINGS, AND DATA ANALYSIS

Mesophyll tissue of *Arabidopsis* plants was enzymatically digested for 30 min at 30°C. The enzyme solution contained 0.3% (w/v) cellulase R-10, 0.03% (w/v) pectolyase Y-23, 1 mM $CaCl_2$, 500 mM sorbitol, 10 mM 2-(*N*-morpholino)ethanesulfonic acid (MES), pH 5.3. Protoplasts were washed twice and maintained in W5 solution (125 mM $CaCl_2$, 154 mM NaCl, 5 mM KCl, 2 mM MES-KOH, pH 5.6; Yoo et al., 2007). Vacuoles were released by the addition of 10 volumes of a solution containing 100 mM malic acid, 160 mM 1,3-bis(tris(hydroxymethyl)methylamino)propane (BTP), 5 mM ethylene glycol-bis(2-aminoethylether)-*N*,*N*,*N*′,*N*′-tetraacetic acid (EGTA), 3 mM $MgCl_2$, pH 7.5, adjusted to 450 mOsm with D-sorbitol. After settling of the vacuoles, the recording chamber was carefully perfused with fresh bath solution. Membrane currents of isolated vacuoles were recorded using the patch-clamp technique, as described elsewhere (Scholz-Starke et al., 2006; Gradogna et al., 2009). Trans-membrane voltages and ionic currents were controlled and monitored with an Axon 200-A current-voltage amplifier interfaced with a 16 bit AD/DA board (ITC-16 Instrutech, Elmont, NY, USA). A Macintosh personal computer running the Pulse program (Heka Electronic, Lambrecht, Germany) was used to generate the stimulation protocol and to acquire the current records. Current records were low-pass filtered at 200 Hz with a 4-pole Bessel filter Kemo VBF8 (Kemo, Beckenham, UK) and sampled at a frequency of 1 kHz. All patches with seal resistance lower than 3 GOhm were systematically discarded. Membrane capacitance (C_m) and access resistance (R_a) were estimated by using the compensation circuit of the amplifier; R_a varied from 6 to 10 MOhm and was not corrected, since the resulting voltage error did not exceed 5 mV. C_m and R_a were monitored throughout the experiment. No leak current subtraction procedure was applied. Patch pipettes had resistance values of 3.5–4 MOhm, when filled with pipette solution (vacuolar side) containing 200 mM KCl, 2 mM $CaCl_2$, 2 mM $MgCl_2$, 10 mM MES-KOH, pH 5.5. All bath solutions contained 100 mM KCl, 1 mM dithiothreitol (DTT), 5 mM Tris and additionally 1 mM EGTA for low-calcium conditions or 100 μM $CaCl_2$ for high-calcium conditions. The pH value of the bath solutions was set either to pH 7.5 (by addition of HEPES) or to pH 6.5 (by addition of MES). The osmolarity of the pipette and bath solutions was adjusted to 500 and 540 mOsm, respectively, by the addition of D-sorbitol. Liquid junction voltages in our experimental conditions were smaller than 1 mV.

Immediately after the establishment of the whole-vacuole configuration, current recordings reproducibly displayed background currents with negative reversal potentials (**Figure A1A**). These currents gradually decreased at all membrane potentials and finally stabilized at a slightly positive reversal potential after 15–30 min in the whole-vacuole configuration (**Figure A1B**), depending on the vacuole size. Only vacuoles which reached this point were considered for data analysis and successively exposed to other bath solutions by means of a gravity-driven perfusion system coupled to a peristaltic pump. Steady-state current amplitudes were normalized to the vacuolar membrane capacitance, which was on average 30 ± 3 pS ($n = 22$). Data are represented as mean values ± SEM (for the number n of vacuoles).

TOTAL PROTEIN ANALYSIS

Arabidopsis wild-type or transgenic plants were grown in sterile conditions on half-concentrated MS media (Duchefa Biochemie) supplemented with 10 g/l sucrose and 0.8% (w/v) phyto agar (Duchefa Biochemie) at 23°C under a 16/8 h light/dark cycle. 3–6 weeks old leaves were homogenized in ice-cold homogenization buffer [200 mM NaCl, 1 mM EDTA, 0.2% Triton X-100, 2% 2-mercaptoethanol, 100 mM Tris–Cl pH 7.8, supplemented with Complete protease inhibitor cocktail (Roche)]. After centrifugation at 5,000 × *g* for 10 min at 4°C, the resulting supernatant was considered as the total protein extract and analyzed by SDS-PAGE followed by western blot, as follows. Samples were adjusted to 1% SDS, 0.3% 2-mercaptoethanol, 8.3% glycerol, 20 mM Tris–Cl, pH 8.6 and denatured by heating at 95°C for 4 min. SDS-PAGE was performed in 15% acrylamide gels using a Tris-glycine running buffer. After electrophoresis, proteins were transferred to nitrocellulose membrane (Protran, Whatman) using a Tris/glycine/methanol (25 mM/192 mM/ 20%, respectively) buffer in a wet electroblotting system (Trans-Blot® Cell, Bio-Rad). We verified that even protein polymers larger than 600 kDa are efficiently transferred using this protocol. Molecular weight markers (Fermentas) were used as molecular mass markers.

SUBCELLULAR FRACTIONATION

Total microsomes were prepared as follows: leaf tissues were homogenized in a medium containing 50 mM Tris-acetate (pH 7.5), 250 mM sorbitol, 2 mM EGTA, 2 mM $MgCl_2$, 2 mM DTT supplemented with Complete. The homogenate was filtered and centrifuged at 10,000 × *g* for 10 min at 4°C. The supernatant was further centrifuged at 100,000 × *g* (r_{av}) in a Beckman SW55Ti rotor (Beckman Instruments) for 30 min at 4°C. The resulting pellet, containing total microsomes, was resuspended in 10 mM Tricine-KOH (pH 7.5), 1 mM EGTA, 2 mM $MgCl_2$, 5% (w/w) sucrose, and was loaded on a sucrose-density gradient (10.4 ml, 15–45% w/w sucrose in 10 mM Tricine-KOH (pH 7.5), 1 mM EGTA and 2 mM $MgCl_2$), centrifuged at 77,000 × *g* (r_{av}) for 19 h in a Beckman SW40 rotor and collected in 0.6-ml fractions. Equal volumes of each fraction were analyzed by SDS-PAGE followed by western blot with the appropriate antibody.

VELOCITY SUCROSE GRADIENT CENTRIFUGATION

Arabidopsis leaves (3–6 weeks old) were homogenized in ice-cold buffer containing 40 mM KCl or 200 mM NaCl, 0.2% Triton X-100, 50 mM Tris–Cl pH 7.8 (2 ml/g of leaf tissue), supplemented with Complete. Lysate was cleared by centrifugation at 700 × *g* for 10 min, loaded on a linear 5–25% (w/v) sucrose gradient (20 mM KCl or 150 mM NaCl, 0.1% Triton X-100, 25 mM Tris–Cl, pH 7.5) and centrifuged at 200,000 × *g* (r_{av}) for 25 h at 4°C in a Beckman SW40 rotor. An additional gradient was loaded with a mixture of molecular mass markers containing 200 μg each of cytochrome *c* (12.4 kDa), ovalbumin (43 kDa), bovine serum albumin (67 kDa), aldolase (161 kDa), and catalase (232 kDa). Equal volumes of each fraction were analyzed by SDS-PAGE followed by western blot with the appropriate antibody.

MICROSCOPY

Epifluorescence microscopy on plant tissues was performed using a Zeiss Axiovert 200 microscope (Carl Zeiss) equipped for epifluorescence, followed by the collection of optical sections using Zeiss Apotome and Axiovision 4.1 software. Figures were assembled with Adobe Photoshop 10.0.

RESULTS

THE ABSENCE OF KCO3 CAUSES SLIGHT GROWTH DEFECTS UNDER OSMOTIC STRESS

Inactivation of the KCO3 gene could provide insights on the function of the protein. The Salk_96038 T-DNA insertion mutant was analyzed using T-DNA left border primer and *KCO3*-specific forward and reverse primers. Amplification was obtained with both primer sets and showed two head-to-head T-DNA insertions at position 420 bp within *KCO3* exon 1, as shown schematically in **Figure 1**. End-point PCR, with a couple of *KCO3*-specific primers, performed on genomic DNA from *Arabidopsis* T-DNA insertion line did not give rise to any product (**Figure 1E**, *kco3-1*), while a fragment of the correct length was obtained from wild-type plant DNA (**Figure 1E**, wt). The insertion line is therefore a full loss of function mutant and was termed *kco3-1*. Col-0 and *kco3-1* seeds were sown on MS medium with 3% sucrose. Seven days after sowing, the seedlings were grown for 15 days on MS medium under long day conditions. No significant (Student's *t*-test) differences were observed in root development, leaf number, and leaf size (**Figure 2A**). The response to osmotic stress or salt stress was tested by supplementing the MS medium with 100 mM mannitol or 75 mM NaCl. Mannitol caused a small but significant decrease of root growth in *kco3-1* plantlets with respect to Col-0 (**Figure 2B**). This phenotype could be complemented by expressing a dominant-negative KCO3-mutant under control of the AtKCO3 promoter in the *kco3-1* background (**Figure 2B**; *dnKCO3* × *kco3-1*). Expressing the dominant-negative mutant in the wild-type background had no beneficial effect for the plant (**Figure 2B**; *dnKCO3*). Upon NaCl treatment no difference was observed (**Figure 2C**). The effect of oxidative stress was tested by growing plantlets for 5 days in the presence of 10 mM H_2O_2. Both Col-0 and *kco3-1* showed similar symptoms of bleaching and plant decay (**Figure 2D**). Finally, growth in medium supplemented with 100 μM K^+ (K^+ deficient) or 2.5 mM K^+ (K^+ sufficient) was analyzed (**Figure 2E**). No significant differences were observed in the mean values for increase in root length.

Altogether, these analyses indicate that the absence of KCO3 causes small defects in the early stages of plant growth under osmotic stress. These defects could be complemented by a dominant-negative mutant of KCO3.

KCO3 AND KCO3::GFP CONSTITUTIVELY EXPRESSED IN *ARABIDOPSIS* TRANSGENIC PLANTS LOCALIZE AT THE TONOPLAST

Endogenous expression levels of KCO3 are very low (Schönknecht et al., 2002, and see eFP developmental map: http://bbc.botany.utoronto.ca/efp/cgi-bin/efpWeb.cgi), hampering biochemical and cell biology studies. *Arabidopsis* transgenic plants expressing KCO3::GFP under the constitutive CaMV 35S promoter were therefore produced. Transgenic lines, selected on the basis of their kanamycin resistance, were tested for KCO3::GFP accumulation by western blot analysis of leaf extracts using anti-GFP antiserum (**Figure 3A**). Extracts from wild-type plants (**Figure 3A**, Co) did not react with the antiserum. A polypeptide with apparent molecular mass around 60 kDa was specifically detected in the kanamycin-resistant plants. This is in good agreement with the predicted mass of the fusion between KCO3 (29 kDa) and GFP (27 kDa), indicating that the 60 kDa polypeptide is intact or nearly intact KCO3::GFP (**Figure 3A**, KCO3::GFP). An additional polypeptide around 25 kDa was also detected in some of the transgenic plants, often when accumulation of KCO3::GFP was higher. Its molecular mass suggests that it corresponds to the entire or nearly entire GFP sequence, released from fusion protein (**Figure 3A**, plants 1, 2, 4, 11 – free GFP). Accumulation of KCO3::GFP in T1 and T2 generations was highly variable but it became stable in a number of T3 plants and generations. These plants did not show evident morphological and developmental differences compared to the wild-type. We reasoned that the detection of KCO3::GFP using the anti-GFP antiserum could limit our studies, because this does not allow to follow the destiny of KCO3 once GFP has been released. We therefore produced a specific antiserum against KCO3 (anti-KCO3), using as antigen 15 amino acids near the N-terminal end (residues 6–20). To test the specificity of this antiserum, equal amounts of total leaf homogenate from KCO3::GFP transgenic

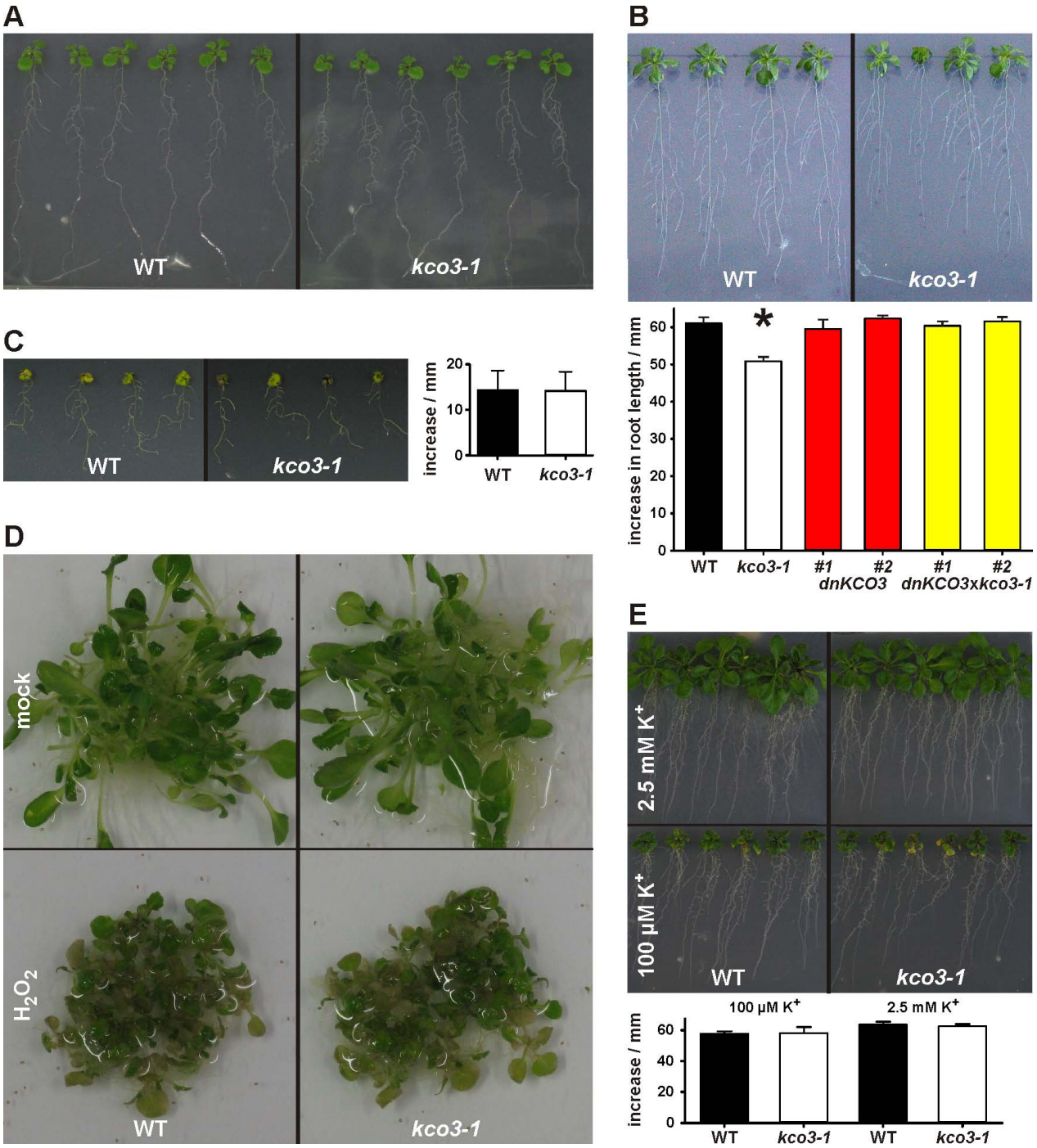

FIGURE 2 | Phenotypic analysis of kco3-1. (A) Growth on MS medium supplemented with 3% sucrose. The wild-type and the *kco3-1* knock-out mutant do not show significant differences in shoot development and root length. Figure is representative of three independent experiments. **(B)** Osmotic stress. The figure is representative of three independent experiments. Lower panel: increase in root length after 15 days. The values shown are mean of six repeats ± SD (indicated by error bars). Data were analyzed using Student's *t*-test. The values obtained for *kco3-1* are significantly different from those of the WT control, *dnKCO3* and *kco3-1* × *dnKCO3* plants ($P < 0.001$). **(C)** Salt stress. Growth of Col-0 and *kco3-1* plants was severely hampered by the presence of NaCl. The figure is representative for three independent experiments. Right panel: increase in root length after 15 days. The values shown are mean of six repeats ± SD (indicated by error bars). Student's *t*-test revealed that Col-0 and *kco3-1* are not significantly different ($P > 0.1$). **(D)** Oxidative stress. After five days of H_2O_2 stress, Col-0 and *kco3-1* plants showed symptoms such as bleaching of leaves and plant decay. The figure is representative for two independent experiments. **(E)** K^+ deficient and K^+ sufficient medium. Lower panel: increase in root length after 15 days was plotted as means ± SD (indicated by error bars) of six repeats. Student's *t*-test did not reveal any significant difference between Col-0 and *kco3-1* ($P > 0.1$).

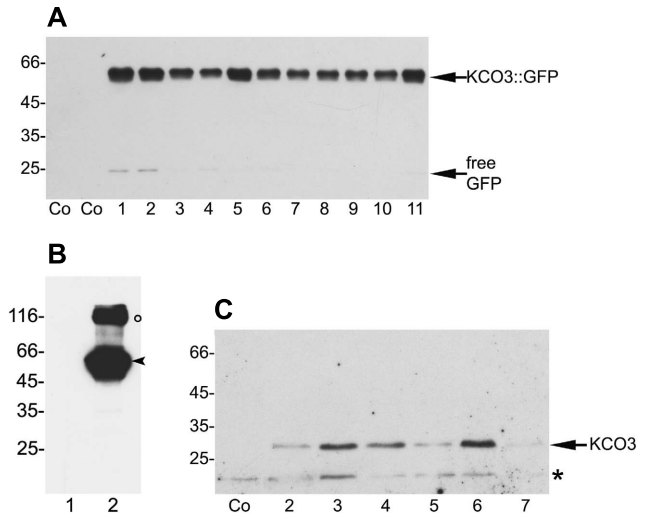

FIGURE 3 | Selection of *Arabidopsis* plants overexpressing KCO3::GFP and KCO3. (A) Equal amounts of leaf extracts (50 μg of total protein) from wild-type plants (Co) and independent transgenic *Arabidopsis* plants expressing KCO3::GFP (plants 1–11) were subjected to SDS-PAGE and western blot analysis with anti-GFP antiserum. The positions of the entire fusion protein and of free GFP are indicated. **(B)** Leaf extracts from one wild-type plant (lane 1) and transgenic plant *n*° 6 of panel A (lane 2) were analyzed by western blot using anti-KCO3 antibodies. The positions of monomers (arrowhead) and putative dimers (circle) are indicated. **(C)** Equal amounts (50 μg of total protein) of leaf extracts from wild-type (Co) or independent transgenic *Arabidopsis* plants overexpressing KCO3 (plants 2–7) were analyzed by western blot with anti-KCO3 antiserum. The positions of KCO3 (arrow) and an unspecific, cross-reacting polypeptide (asterisk) are indicated. In each panel, numbers on the left indicate the position and size (in kDa) of molecular mass markers.

or control plants were subjected to SDS-PAGE and western blot with anti-GFP or the immuno-affinity purified anti-KCO3 antiserum (**Figure 3B**). No bands were visible in the control sample, consistent with the known very low endogenous expression level of KCO3. In the transgenic extract the anti-KCO3 antiserum specifically recognized two polypeptides around 60 and 120 kDa (**Figure 3B**, lane 4, arrowhead and empty circle, respectively) and, as expected, did not recognize the 25 kDa fragment. The 60 kDa polypeptide corresponds to the entire KCO3::GFP fusion also detected by anti-GFP. At this stage of investigation the 120 kDa polypeptide was tentatively identified as a minor proportion of KCO3 polypeptides not completely denatured and still assembled into dimers. The ratio between these putative dimers and monomers was variable in different experiments. We tested different extraction and denaturation procedures, but we were unable to determine conditions in which such a variability could be avoided.

Having confirmed the ability of the antiserum to detect KCO3, transgenic *Arabidopsis* overexpressing KCO3 under the CaMV 35S promoter were prepared. Leaf homogenates were analyzed by SDS-PAGE and western blot with the anti-KCO3 antiserum. A polypeptide with apparent molecular mass around 30 kDa, consistent with the 29 kDa calculated mass of KCO3, was detected in the transgenic lines but not in control plants (**Figure 3C**, plants 2–7 and Co, respectively). A polypeptide around 20 kDa was also detected in both control and KCO3 plants (**Figure 3C**, asterisk); however, this was not related to KCO3, because it was also recognized by the pre-immune serum (not shown). We propagated line 6 from T3 generation, but also in T4 the accumulation levels of KCO3 were variable. We were unable to obtain a line giving constant KCO3 levels in the progeny, possibly because of transgene silencing.

The subcellular localization of KCO3::GFP was analyzed by epifluorescence microscopy in leaf and hypocotyl tissues (**Figure 4**). In leaf epidermal cells, GFP fluorescence was clearly detected on the tonoplast (**Figures 4A–C**). In different cells, the GFP fluorescence appeared either continuous or irregularly distributed on the tonoplast, with several highly fluorescent "spots." No colocalization with the plasma membrane was observed when the GFP and the brightfield images were superimposed (**Figures 4G–I**). The tonoplast localization was also observed in hypocotyl cells (**Figures 4D–F**). The results were confirmed by subcellular fractionation followed by western blot. Total microsomes were prepared from KCO3::GFP or KCO3 leaf homogenates, loaded onto a continuous sucrose gradient and subjected to isopycnic ultracentrifugation (**Figure 5**). The distributions of KCO3::GFP, KCO3, and the tonoplast aquaporin γTIP were similar and they markedly differed from those of the plasma membrane aquaporin PIP2 or the endoplasmic reticulum marker endoplasmin/GRP94. γTIP monomers have a calculated molecular mass around 20 kDa, but a relevant proportion of the protein is detected as oligomers, most probably corresponding to dimers; incomplete denaturation, resulting in the detection of dimers and tetramers upon SDS-PAGE is a common characteristic of aquaporins (Kammerloher et al., 1994; Karlsson et al., 2000). It can be concluded that both KCO3::GFP and KCO3 localize at the tonoplast when overexpressed in *Arabidopsis* transgenic plants.

VACUOLES FROM WILD-TYPE AND KCO3-OVEREXPRESSING PLANTS DO NOT SHOW SIGNIFICANTLY DIFFERENT CURRENT DENSITIES

In order to investigate the functional properties of KCO3, we performed patch-clamp recordings on whole-vacuoles isolated from leaves of KCO3-overexpressing plants. Experiments were designed in a way to minimize background currents. The activity of the major cationic ion channels at resting and elevated cytosolic $[Ca^{2+}]$ – the Fast Vacuolar (FV) and the Slow Vacuolar (SV) channel, respectively (Hedrich and Neher, 1987; Allen and Sanders, 1996) – was greatly reduced by divalent cations, i.e., calcium (Tikhonova et al., 1997; Dadacz-Narloch et al., 2011) and magnesium (Pei et al., 1999; Pottosin et al., 2004), which were present in the pipette solution at 2 mM concentration. Preliminary experiments had revealed normal FV- and SV-type currents in vacuoles from *kco3-1* mutant plants (data not shown). These data, together with the presence of a K^+ channel signature within the KCO3 protein sequence, argue against a possible participation of KCO3 in the pore formation of these non-selective cation channels.

The K^+ channel signature in the pore loop and two calcium-binding EF hand motifs present in the KCO3 sequence are features shared by TPK1, which has been previously shown to encode a Ca^{2+}-activated K^+-selective conductance in the vacuolar

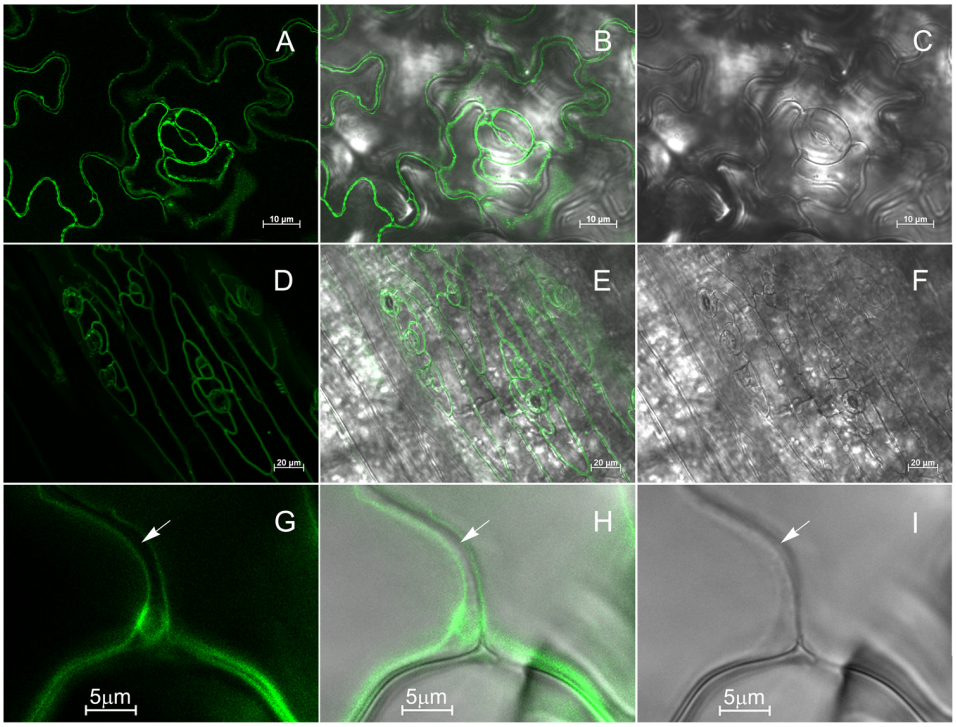

FIGURE 4 | KCO3::GFP is located at the tonoplast. Leaf epidermis **(A–C, G–I)** or hypocotyl **(D–F)** from KCO3::GFP transgenic plant were analyzed by epifluorescence microscopy. **(A,D,G)**: GFP fluorescence; **(C,F,I)**: brightfield; **(B,E,H)**: Merge of fluorescence and brightfield. The arrow indicates the cell surface.

membrane (VK channel; Gobert et al., 2007; Latz et al., 2007). Furthermore, the activity of VK channels is stimulated by acidic cytosolic pH (Allen et al., 1998; Gobert et al., 2007). Consequently, we probed KCO3 activity by recording membrane currents from isolated vacuoles successively exposed to four different experimental conditions, varying the cytosolic Ca^{2+} concentration (low versus high Ca^{2+}) at two cytosolic pH values (pH_{cyt} 7.5 and pH_{cyt} 6.5). As summarized in **Figure 6**, the current densities of KCO3-overexpressing vacuoles were almost identical to those determined for wild-type vacuoles at either pH_{cyt}. Increases of cytosolic $[Ca^{2+}]$ generally caused only minor changes in the current amplitudes: the slight decrease at pH_{cyt} 7.5 (**Figure 6C**) was possibly due to a further reduction of residual FV channel activity, while the small increase at pH_{cyt} 6.5 (**Figure 6F**) may correspond to the activation of a small population of VK channels.

In summary, these data strongly suggest that KCO3, present in the vacuolar membrane of overexpressing plants, does not constitute a functional ion channel in our experimental conditions.

KCO3 AND KCO3::GFP ARE DETECTED AS DIMERS

The formation of a tetrameric complex is a prerequisite for ion channel activity in the case of the one-P subunit KCO3. We therefore investigated on the oligomerization state of KCO3 and KCO3::GFP. Total leaf homogenate from KCO3::GFP plants was fractionated by velocity sucrose gradient centrifugations in the presence of non-ionic detergent. Using this assay, we have previously confirmed that TPK1::GFP is a dimer, as expected (Maîtrejean et al., 2011). Equal volumes of fractions were analyzed by western blot with anti-GFP (**Figure 7A**) or anti-KCO3 (**Figure 7B**) antisera. KCO3::GFP sedimented slightly slower than the 150 kDa marker, indicating a dimer of the 60 kDa polypeptide. Each gradient fraction contains a similar ratio between polypeptides that are fully denatured upon SDS-PAGE and polypeptides that remain assembled into putative dimers (**Figures 7A,B**, fractions 9–12). The co-migration of the two forms along the gradient strongly suggests that the component around 120 kDa really represents dimers. No polypeptides recognized by anti-GFP or anti-KCO3 antisera peaked in the expected position of putative tetramers (their migration should be slightly faster than the 232 kDa marker). Free GFP released from the fusion protein migrated as a monomer and was recognized by the anti-GFP antiserum (**Figure 7**, compare **Figure 7A** and **Figure 7B**, fractions 4–5). This strongly suggests that the GFP moiety does not have a role in the dimerization of KCO3::GFP. The same behavior had been observed for free GFP released from TPK1::GFP (Maîtrejean et al., 2011). Partial proteolysis also seems to occur, as indicated by the additional bands detected below the major 66 kDa band.

To exclude that GFP appended at the C-terminal end of KCO3 impaired tetramerization, velocity gradient centrifugation analysis was performed on leaf extracts from KCO3 transgenic plants. Fractions were analyzed by western blot with anti-KCO3 antiserum. KCO3 sedimented slightly slower than the 67 kDa marker (**Figure 7C**, fractions 7–9), indicating that also the wild-type protein is a dimer in the conditions used in our analysis. We then tested whether the assembly grade of another

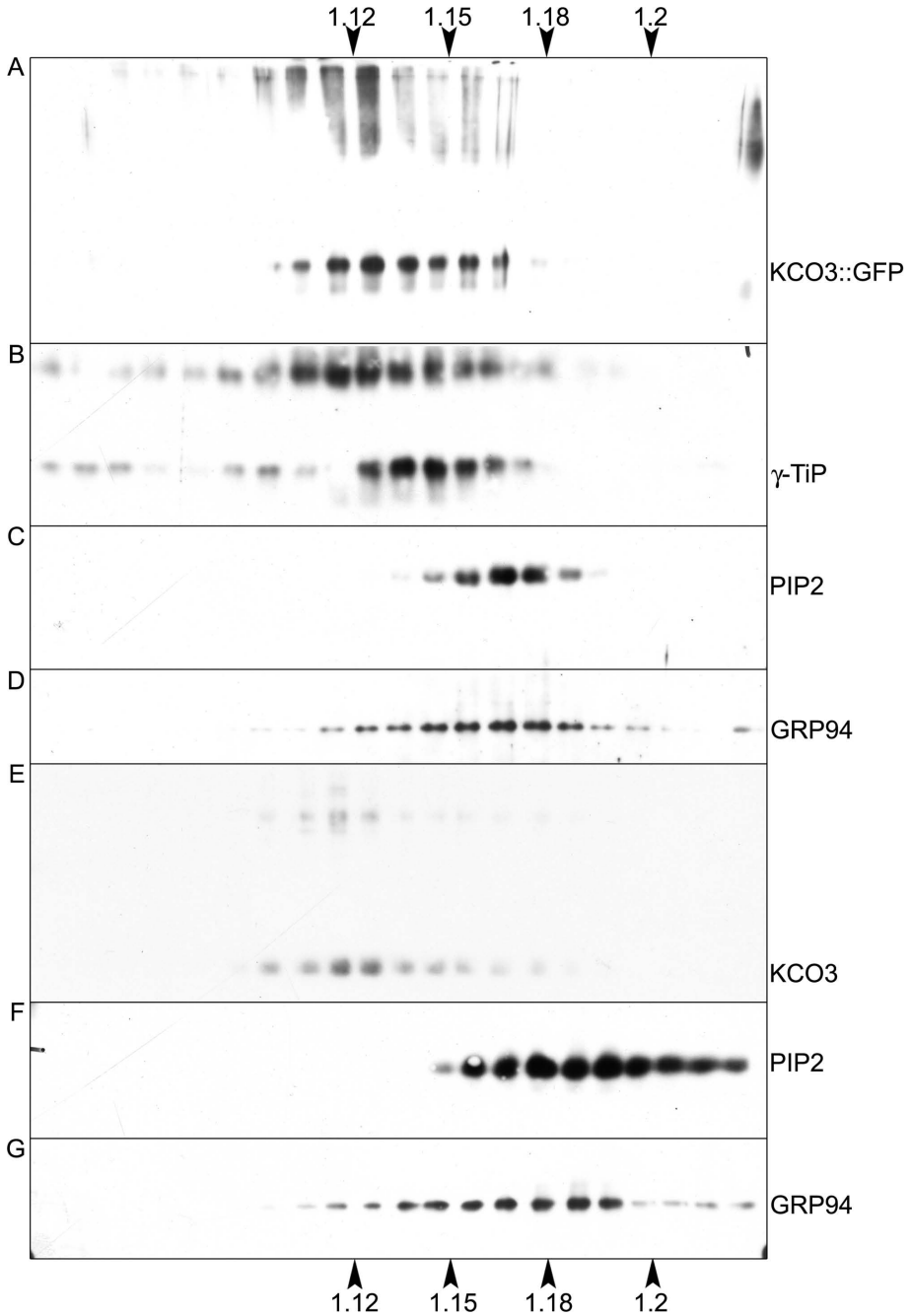

FIGURE 5 | KCO3::GFP and KCO3 co-fractionate with a tonoplast marker in isopycnic gradients. Young leaves from transgenic *Arabidopsis* plants expressing KCO3::GFP **(A–D)** or KCO3 **(E–G)** were homogenized in the presence of sucrose and the absence of detergent. Microsomes were pelleted and further separated by centrifugation on isopycnic sucrose gradient. Proteins in each fraction (1/10 of fraction volume) were analyzed by SDS-PAGE and western blot with antibodies against KCO3 (to detect KCO3::GFP or KCO3), γTIP (tonoplast marker), PIP2 (plasma membrane marker) or endoplasmin (GRP94, endoplasmic reticulum marker), as indicated at the right of each panel. Top of each gradient is at left; numbers on top or bottom of the figure indicate fraction density (g/ml).

multispanning tonoplast protein was preserved in our assay. Western blots of gradient fractions were therefore visualized with anti-γTIP antiserum: γTIP, which is a tetramer, peaked as expected between the 67 and 150 kDa markers (**Figure 7D**, fractions 9–10). We conclude that our experimental conditions preserve the correct assembly of another multispanning tonoplast protein.

It has been previously reported that tetramerization of the viral K^+ channel Kcv was perturbed in the presence of a high concentration of sodium ions, but was maintained if 40 mM

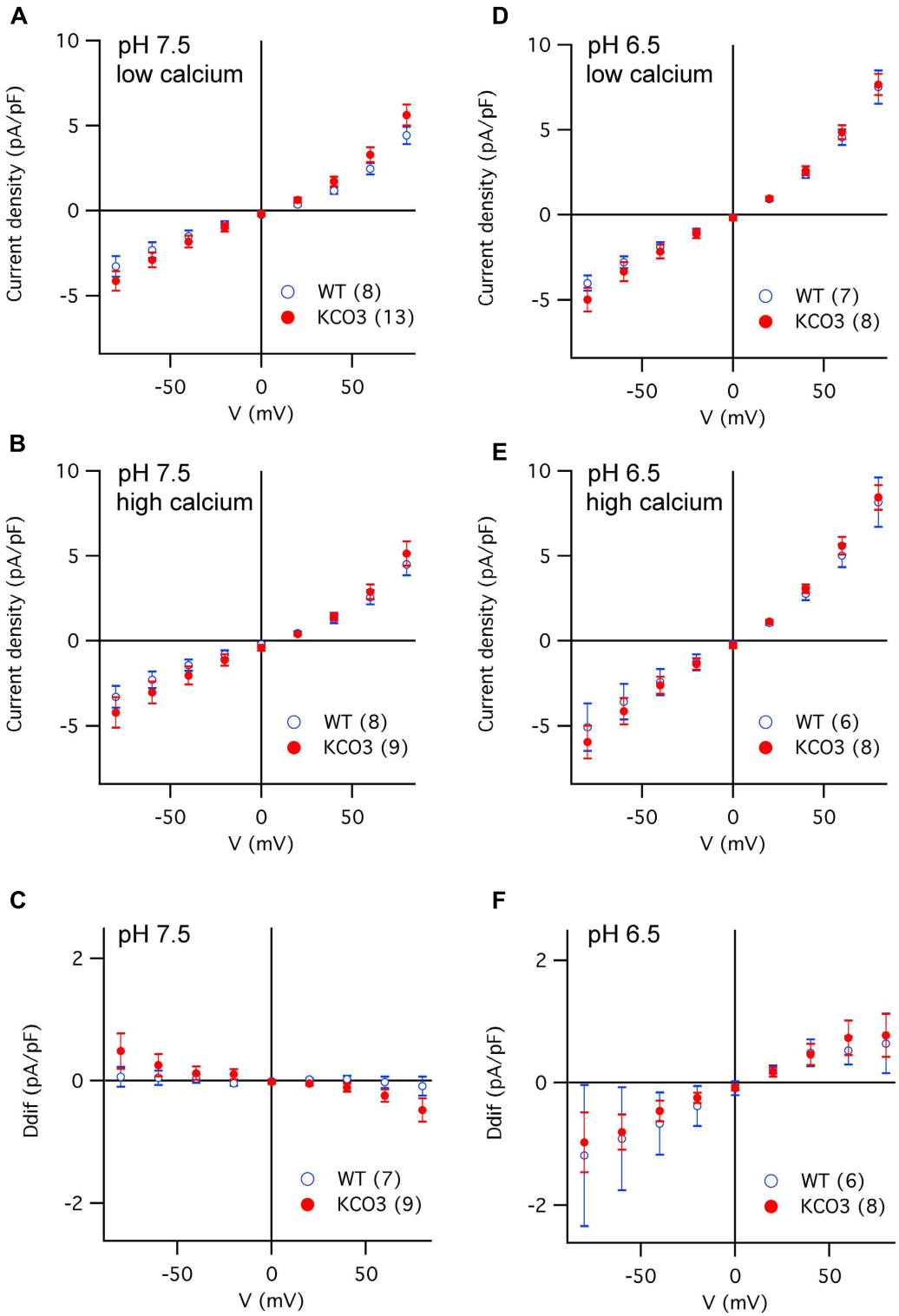

FIGURE 6 | Current density versus voltage characteristics recorded in different experimental conditions from vacuoles of *Arabidopsis* wild-type and KCO3-overexpressing plants. (A–C) Current density–voltage relationships recorded in the whole-vacuole configuration (see **Figure A1**) from vacuoles of *Arabidopsis* wild-type (open blue symbols) and KCO3-overexpressing plants (filled red symbols). Bath solutions of pH 7.5 contained either low calcium **(A)** or high calcium **(B)**. The current density difference (Ddif) between high and low calcium conditions was calculated for individual vacuoles and averaged **(C)**. **(D,F)** As in **(A–C)**, but in bath solutions of pH 6.5, in low calcium **(D)**, in high calcium **(E)**, difference (**F**; Ddif). In each panel, the number of WT or KCO3 vacuoles analyzed is given in brackets.

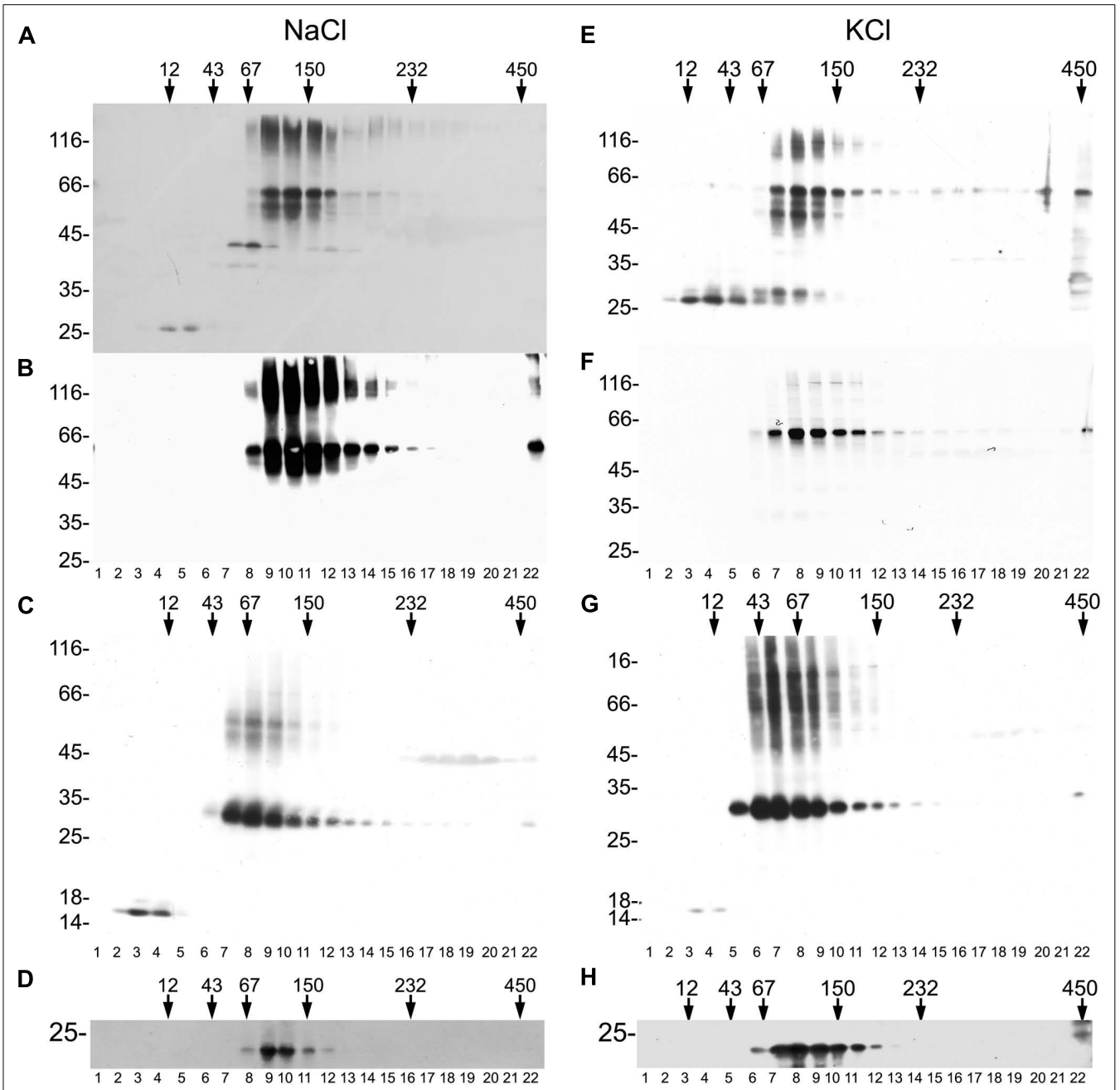

FIGURE 7 | KCO3::GFP and KCO3 are dimers. Leaves from KCO3::GFP **(A,B,D–F,H)** or KCO3 **(C,G)** transgenic *Arabidopsis* plants were homogenized in the presence of non-ionic detergent and either 200 mM NaCl **(A–D)** or 40 mM KCl **(E–H)**. The homogenates were then subjected to sedimentation velocity centrifugation on a continuous 5–25% (w/v) sucrose gradient. One-tenth of the total volume of each gradient fraction were analyzed by SDS-PAGE and western blot using anti-GFP antiserum to detect KCO3::GFP **(A,E)**, anti-KCO3 antiserum to detect KCO3::GFP **(B,F)** or KCO3 **(C,G)**, anti-γTIP **(D,H)**. Top of each gradient is at left. Numbers on top indicate the position along the gradient and the molecular mass (in kDa) of sedimentation markers. Numbers at left indicate the positions of SDS-PAGE molecular mass markers.

KCl was used instead of 200 mM NaCl (Pagliuca et al., 2007). We therefore analyzed the assembly state substituting NaCl with KCl in the homogenization and gradient buffers. Neither tetramers or monomers of KCO3::GFP and KCO3 could be detected, and the assembly state of γTIP was not altered as well (**Figures 7E–H**).

Therefore, stable KCO3 or KCO3::GFP homodimers are detected in experimental conditions in which the related TPK1 protein and the other multispanning tonoplast protein γTIP maintain their correct assembly properties. This indicates that KCO3 tetramers are either held together by weaker or very transient interactions, or are never formed.

DISCUSSION

In this study, we applied different experimental approaches with the aim to shed light on the functional properties and physiological roles of AtKCO3, a putative potassium channel subunit in *A. thaliana*, which has remained enigmatic until now.

The features of the *kco3-1* null-allele mutant observed in the presence of mannitol indicate that under certain conditions KCO3 exhibits a small effect on root elongation. The absence of KCO3 could be compensated by a dominant-negative version of this subunit. This indicates that, whatever the function of KCO3, it does not depend on putative direct ability to transport ions. It is however clear that in most conditions no significant alteration in growth was detected.

Using transgenic plants expressing the *KCO3* gene or a *KCO3::GFP* fusion construct under the control of the constitutive CaMV 35S promoter, we confirmed and extended to stable transgenic *Arabidopsis* previous results from transient expression experiments (Voelker et al., 2006) on the tonoplast localization of KCO3. Patch-clamp recordings were therefore performed on vacuoles isolated from KCO3-overexpressing plants, in order to provide evidence of ion channel activity. In the design of these experiments, we started from the idea that KCO3 activity may be regulated, either positively or negatively, by cytosolic calcium via the canonical EF-hand motifs in the protein's C-terminal domain. Previous studies have unequivocally established that AtTPK1, a well-characterized member of the tandem-pore family in *Arabidopsis*, encodes a Ca^{2+}-activated K^+-selective conductance in the vacuolar membrane, the so-called VK channel (Gobert et al., 2007; Latz et al., 2007). Conversely, our data set on KCO3-containing vacuoles did not reveal significant differences compared to background currents recorded from wild-type vacuoles. In similar working conditions, TPK1 activity was detected both in transformed yeast cells (Latz et al., 2007) and overexpressing *Arabidopsis* plants (Gobert et al., 2007).

The failure to obtain evidence for changes in current in the overexpressing plants prompted us to investigate on the KCO3 assembly status. To be active as a cation channel, KCO3 must either form homotetramers or contribute to the formation of a hetero-oligomer with four P-domains in total. However, we have only been able to detect homodimers of KCO3 or KCO3::GFP, in line with its evolutionary origin from dimeric TPK channels. The fact that both recombinant proteins, which have quite different molecular masses, migrate along velocity gradients at the positions expected for the corresponding homodimers rules out the possibility that the forms we detect are hetero-oligomers containing other unknown polypeptides. We have previously used this velocity centrifugation assay to study the assembly state of wild-type or different mutated forms of TPK1 fused to GFP (Maîtrejean et al., 2011). Constructs unable to traffic along the secretory pathway, and therefore with incorrect subunit interactions, could be distinguished by the assay from correctly assembled dimeric TPK1::GFP (Maîtrejean et al., 2011). This indicated that wrongly assembled forms of a tandem-pore channel are unable to traffic and that the incorrect interactions can be detected by the velocity centrifugation assay. The tonoplast localization of KCO3 and KCO3::GFP in transgenic *Arabidopsis* instead indicates that these proteins traffic along the secretory pathway and therefore are not recognized as defective proteins by the endoplasmic reticulum quality control.

The stable assembly of a dimeric form of a cation channel subunit with one P-domain is thus compatible with traffic, but it is clearly incompatible with activity. KCO3 is not the only *Arabidopsis* K^+ channel that does not show activity. AtKC1, which belongs to the Shaker-like family is also inactive, but, unlike KCO3, remains located in the endoplasmic reticulum when overexpressed alone (Dreyer et al., 1997; Duby et al., 2008). Interaction of AtKC1 with other Shaker-like subunits allows the formation of traffic-competent, active heterotetramers with differences in activity compared to the respective homotetramers. AtKC1 thus acts as a modulator of channel activity. Furthermore, it has been shown that these heteromers can be further regulated by interaction with the SNARE protein SYP121 at the plasma membrane (Honsbein et al., 2009). KCO3 could in theory have a regulatory function by interacting with TPK subunits. Such an interaction could escape our assembly assay because of its transient or weak nature. Possibly, the formation of heteromers with KCO3 would prevent these TPK subunits from proper assembly into functional channels and expression of KCO3 would then have a modulatory function on certain tandem-pore channels. Although such a regulation does not appear to be very efficient, it might nevertheless be useful in fine-tuning the permeability of the tonoplast for K^+ ions and would be consistent with the minor but detectable growth phenotype of the null allele that was complemented by a dominant-negative version of KCO3. However, it should be taken into consideration that, unlike AtKC1, overexpressed KCO3 traffics along the secretory pathway also in the absence of co-expressed putative partner subunits. Its tissue expression overlaps mostly with that of TPK5, but fluorescence transfer and bimolecular fluorescence complementation experiments failed to detect heteromeric interactions between KCO3 and TPK1 or TPK5 (Voelker et al., 2006). Heteromeric interactions seem therefore very unlikely, even if our results do not exclude that KCO3 actually forms a homotetramer by interactions that are not preserved in our conditions. Indeed, tetramers of Kcv, a viral K^+ channel with one pore domain per subunit, are disrupted when K^+ is substituted by Na^+ or Li^+ in the assay buffer. This disruption results in full Kcv disassembly into monomers, without the production of detectable dimers (Pagliuca et al., 2007). This supports the hypothesis that KCO3 dimers detected in the present study are stable, natural forms of this one P-subunit.

Recent fluorescence fluctuation analysis in transfected CHO cells suggested that human vanilloid receptor 1 (TRPV1), which belongs to the superfamily of cation channels with six transmembrane segments and one P-region, exists in two oligomerization states: dimeric in basal conditions and tetrameric upon activation (Storti et al., 2012). Similarly, it is possible that KCO3 dimers further assemble very transiently and reversibly or only upon certain physiological conditions: if only a very minor proportion of polypeptides were involved in this process at a given time, this could be below our detection limit. The process of further assembly could also require the presence of an additional factor. 14-3-3 proteins are among the candidates, since physical interaction and activity stimulation has also been shown for TPK1 (Latz et al., 2007).

In any case, our results indicate that KCO3 homodimers are as stable as TPK1 homodimers in the extraction and analysis conditions used here. If further assembly ever produces tetrameric KCO3 channels, at least part of the interactions involved must be different from those that hold together dimers. The search for such putative interactions would need further experimental approaches.

ACKNOWLEDGMENTS

We thank Christophe Maurel and Natasha Raikhel for the gift of anti-PIP and anti-γTIP antisera. We are grateful to Marie Maîtrejean for the useful discussions and suggestions. Study supported by the EU Marie Curie Research Training Network "Vacuolar Transport Equipment for Growth Regulation in Plants" (MRTN-CT-2006–035833) and by the 2008 "Progetti di Ricerca di Interesse Nazionale" to Armando Carpaneto. Tripti Sharma was member of the Max-Planck Research School "Primary Metabolism and Plant Growth" at the University of Potsdam and the Max-Planck Institute of Molecular Plant Physiology (Potsdam-Golm) and received a fellowship of the German Academic Exchange Service (DAAD). Ingo Dreyer is supported by a Marie Curie Career Integration Grant (FP7-PEOPLE-2011-CIG No. 303674 – Regopoc) of the EU.

REFERENCES

Allen, G. J., Amtmann, A., and Sanders, D. (1998). Calcium-dependent and calcium-independent K^+ mobilization channels in *Vicia faba* guard cell vacuoles. *J. Exp. Bot.* 49, 305–318.

Allen, G. J., and Sanders, D. (1996). Control of ionic currents in guard cell vacuoles by cytosolic and luminal calcium. *Plant J.* 10, 1055–1069.

Dadacz-Narloch, B., Beyhl, D., Larisch, C., Lopez-Sanjurjo, E. J., Reski, R., Kuchitsu, K., et al. (2011). A novel calcium binding site in the slow vacuolar cation channel TPC1 senses luminal calcium levels. *Plant Cell* 23, 2696–2707.

Devereux, J., Haeberli, P., and Smithies, O. (1984). A comprehensive set of sequence analysis programs for the VAX. *Nucleic Acids Res.*12, 387–395.

Dreyer, I., Antunes, S., Hoshi, T., Müller-Röber, B., Palme, K., Pongs, O., et al. (1997). Plant K^+ channel α-subunits assemble indiscriminately. *Biophys. J.* 72, 2143–2150.

Dreyer, I., and Uozumi, N. (2011). Potassium channels in plant cells. *FEBS J.* 278, 4293–4303.

Duby, G., Hosy, E., Fizames, C., Alcon, C., Costa, A., Sentenac, H., et al. (2008). AtKC1, a conditionally targeted Shakertype subunit, regulates the activity of plant K^+ channels. *Plant J.* 53, 115–123.

Gobert, A., Isayenkov, S., Voelker, C., Czempinski, K., and Maathuis, F. J. M. (2007). The two-pore channel TPK1 gene encodes the vacuolar K^+ conductance and plays a role in K^+ homeostasis. *Proc. Natl. Acad. Sci. U.S.A.* 104, 10726–10731.

Gomez-Porras, J. L., Riaño-Pachón, D. M., Benito, B., Haro, R., Sklodowski, K., Rodriguez-Navarro, A., et al. (2012). Phylogenetic analysis of K^+ transporters in bryophytes, lycophytes, and flowering plants indicates a specialization of vascular plants. *Front. Plant Sci.* 3:167. doi: 10.3389/fpls.2012.00167

Gradogna, A., Scholz-Starke, J., Gutla, P. V., and Carpaneto, A. (2009). Fluorescence combined with excised patch: measuring calcium currents in plant cation channels. *Plant J.* 58, 175–182.

Hedrich, R., and Neher, E. (1987). Cytoplasmic calcium regulates voltage-dependent ion channels in plant vacuoles. *Nature* 329, 833–835.

Hong, B., Ichida, A., Wang, Y., Gens, J. S., Pickard, B. G., and Harper, J. F. (1999). Identification of a calmodulin-regulated Ca^{2+}-ATPase in the endoplasmic reticulum. *Plant Physiol.* 119, 1165–1175.

Honsbein, A., Sokolovski, S., Grefen, C., Campanoni, P., Pratelli, R., Paneque, M., et al. (2009). A tripartite SNARE-K^+ channel complex mediates in channel-dependent K^+ nutrition in *Arabidopsis*. *Plant Cell* 21, 2859–2877.

Höfgen, R., and Willmitzer, L. (1988). Storage of competent cells for Agrobacterium transformation. *Nucleic Acids Res.* 16, 9877.

Kammerloher, W., Fischer, U., Piechottka, G. P., and Schäffner, A. R. (1994). Water channels in the plant plasma membrane cloned by immunoselection from a mammalian expression system. *Plant J.* 6, 187–199.

Karlsson, M., Johansson, I., Bush, M., McCann, M. C., Maurel, C., Larsson, C., et al. (2000). An abundant TIP expressed in mature highly vacuolated cells. *Plant J.* 21, 83–90.

Klein, E. M., Mascheroni, L., Pompa, A., Ragni, L., Weimar, T., Lilley, K. S., et al. (2006). Plant endoplasmin supports the protein secretory pathway and has a role in proliferating tissues. *Plant J.* 48, 657–673.

Latz, A., Becker, D., Hekman, M., Mueller, T., Beyhl, D., Marten, I., et al. (2007). TPK1, a Ca^{2+}-regulated *Arabidopsis* vacuole two-pore K^+ channel is activated by 14-3-3 proteins. *Plant J.* 52, 449–459.

Maîtrejean, M., Wudick, M. M., Voelker, C., Prinsi, B., Mueller-Roeber, B., Czempinski, K., et al. (2011). Assembly and sorting of the tonoplast potassium channel AtTPK1 and its turnover by internalization into the vacuole. *Plant Physiol.* 156, 1783–1796.

Marcel, D., Müller, T., Hedrich, R., and Geiger, D. (2010). K^+ transport characteristics of the plasma membrane tandem-pore channel TPK4 and pore chimeras with its vacuolar homologs. *FEBS Lett.* 584, 2433–2439.

Pagliuca, C., Goetze, T. A., Wagner, R., Thiel, G., Moroni, A., and Parcej, D. (2007). Molecular properties of Kcv, a virus encoded K^+ channel. *Biochemistry* 46, 1079–1090.

Pei, Z. M., Ward, J. M., and Schroeder, J. I. (1999). Magnesium sensitizes slow vacuolar channels to physiological cytosolic calcium and inhibits fast vacuolar channels in fava bean guard cell vacuoles. *Plant Physiol.* 121, 977–986.

Pottosin, I., Martinez-Estevez, M., Dobrovinskaya, O. R., Muniz, J., and Schonknecht, G. (2004). Mechanism of luminal Ca^{2+} and Mg^{2+} action on the vacuolar slowly activating channels. *Planta* 219, 1057–1070.

Santoni, V., Vinh, J., Pflieger, D., Sommerer, N., and Maurel, C. (2003). A proteomic study reveals novel insights into the diversity of aquaporin forms expressed in the plasma membrane of plant roots. *Biochem. J.* 373, 289–296.

Scholz-Starke, J., Carpaneto, A., and Gambale, F. (2006). On the interaction of neomycin with the slow vacuolar channel of *Arabidopsis thaliana*. *J. Gen. Physiol.* 127, 329–340.

Schönknecht, G., Spoormaker, P., Steinmeyer, R., Brüggeman, L., Ache, P., Dutta, R., et al. (2002). KCO1 is a component of the slow-vacuolar (SV) ion channel. *FEBS Lett.* 511, 28–32.

Storti, B., Bizzarri, R., Cardarelli, F., and Beltram, F. (2012). Intact microtubules preserve transient receptor potential vanilloid 1 (TRPV1) functionality through receptor binding. *J. Biol. Chem.* 287, 7803–7811.

Tikhonova, L. I., Pottosin, I., Dietz, K. J., and Schönknecht, G. (1997). Fast-activating cation channel in barley mesophyll vacuoles. Inhibition by calcium. *Plant J.* 11, 1059–1070.

Voelker, C., Gomez-Porras, J. L., Becker, D., Hamamoto, S., Uozumi, N., Gambale, F., et al. (2010). Roles of tandem-pore K^+ channels in plants – a puzzle still to be solved. *Plant Biol.* 12, 56–63.

Voelker, C., Schmidt, D., Mueller-Roeber, B., and Czempinski, K. (2006). Members of the *Arabidopsis* AtTPK/KCO family form homomeric vacuolar channels in planta. *Plant J.* 48, 296–306.

Yoo, S. D., Cho, Y. H., and Sheen, J. (2007). *Arabidopsis* mesophyll protoplasts: a versatile cell system for transient gene expression analysis. *Nat. Protoc.* 2, 1565–1572.

Conflict of Interest Statement: The authors declare that the research was conducted in the absence of any commercial or financial relationships that could be construed as a potential conflict of interest.

Received: 08 June 2012; accepted: 22 October 2012; published online: 12 November 2012.

Citation: Rocchetti A, Sharma T, Wulfetange C, Scholz-Starke J, Grippa A, Carpaneto A, Dreyer I, Vitale A, Czempinski K and Pedrazzini E (2012) The putative K^+ channel subunit AtKCO3 forms stable dimers in Arabidopsis. Front. Plant Sci. ***3****:251. doi: 10.3389/fpls.2012.00251*

This article was submitted to Frontiers in Plant Traffic and Transport, a specialty of Frontiers in Plant Science.

APPENDIX

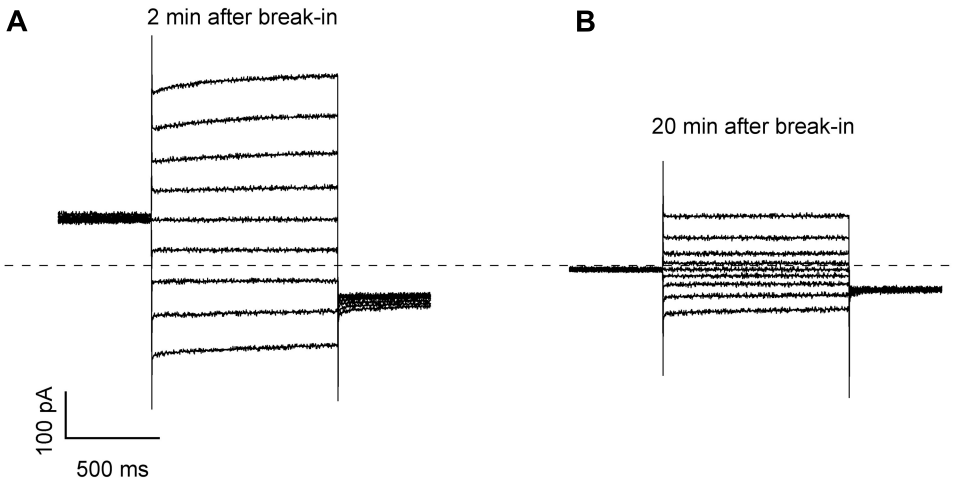

FIGURE A1 | Current traces recorded in whole-vacuole mode in vacuoles isolated from *Arabidopsis* mesophyll cells. (A) Current traces recorded 2 min after achieving the whole-vacuole configuration in response to voltage steps from +80 to −80 mV, step −20 mV. The holding and tail voltages were 0 and −50 mV, respectively. The vacuole had a capacitance of 34 pF and derived from an *Arabidopsis* wild-type plant. **(B)** Current traces recorded from the same vacuole as in A, 20 min after the break-in.

frontiers in
PLANT SCIENCE

HYPOTHESIS AND THEORY ARTICLE
published: 29 November 2012
doi: 10.3389/fpls.2012.00263

Molecular evolution of slow and quick anion channels (SLACs and QUACs/ALMTs)

Ingo Dreyer[1]*, Judith Lucia Gomez-Porras[2], Diego Mauricio Riaño-Pachón[3], Rainer Hedrich[4] and Dietmar Geiger[4]

[1] *Plant Biophysics, Centro de Biotecnología y Genómica de Plantas, Universidad Politécnica de Madrid, Madrid, Spain*
[2] *Molecular Biology of Winter Dormancy and Cold Acclimation in Woody Plants, Centro de Biotecnología y Genómica de Plantas, Universidad Politécnica de Madrid, Madrid, Spain*
[3] *Grupo de Biología Computacional y Evolutiva, Departamento de Ciencias Biológicas, Universidad de los Andes, Bogotá DC, Colombia*
[4] *Julius-von-Sachs Institute for Biosciences, Molecular Plant Physiology and Biophysics, Universität Würzburg, Würzburg, Germany*

Edited by:
Markus Geisler, University of Fribourg, Switzerland

Reviewed by:
Sebastien Thomine, Centre National de la Recherche Scientifique, France
Enrico Martinoia, University of Zurich, Switzerland

****Correspondence:***
Ingo Dreyer, Plant Biophysics, Centro de Biotecnología y Genómica de Plantas, Universidad Politécnica de Madrid, Campus de Montegancedo, Carretera M-40, km 37.7, Pozuelo de Alarcón, Madrid E-28223, Spain.
e-mail: ingo.dreyer@upm.es

Electrophysiological analyses conducted about 25 years ago detected two types of anion channels in the plasma membrane of guard cells. One type of channel responds slowly to changes in membrane voltage while the other responds quickly. Consequently, they were named SLAC, for SLow Anion Channel, and QUAC, for QUick Anion Channel. Recently, genes *SLAC1* and *QUAC1/ALMT12*, underlying the two different anion current components, could be identified in the model plant *Arabidopsis thaliana*. Expression of the gene products in *Xenopus* oocytes confirmed the quick and slow current kinetics. In this study we provide an overview on our current knowledge on slow and quick anion channels in plants and analyze the molecular evolution of ALMT/QUAC-like and SLAC-like channels. We discovered fingerprints that allow screening databases for these channel types and were able to identify 192 (177 non-redundant) SLAC-like and 422 (402 non-redundant) ALMT/QUAC-like proteins in the fully sequenced genomes of 32 plant species. Phylogenetic analyses provided new insights into the molecular evolution of these channel types. We also combined sequence alignment and clustering with predictions of protein features, leading to the identification of known conserved phosphorylation sites in SLAC1-like channels along with potential sites that have not been yet experimentally confirmed. Using a similar strategy to analyze the hydropathicity of ALMT/QUAC-like channels, we propose a modified topology with additional transmembrane regions that integrates structure and function of these membrane proteins. Our results suggest that cross-referencing phylogenetic analyses with position-specific protein properties and functional data could be a very powerful tool for genome research approaches in general.

Keywords: anion channel, evolution, SLAC/SLAH, ALMT, QUAC, voltage dependent, topology, phosphorylation

INTRODUCTION

Patch-clamp studies with guard cells in the late 1980s and early 1990s showed that the guard cell plasma membranes harbor at least two types of anion channels (Schroeder and Hagiwara, 1989; Hedrich et al., 1990; Linder and Raschke, 1992; Schroeder and Keller, 1992). Based on the activation kinetics of the anion channel currents in response to voltage pulses, these were designated R(rapid) and S(slow)-type. Whereas the activation of R-type channels is in the low millisecond range, the transition of S-type channels to the open state takes several seconds (Linder and Raschke, 1992; Kolb et al., 1995). Furthermore, R-type channels display a pronounced voltage dependence. They are inactive at hyperpolarized membrane potentials but progressively activate upon depolarization (Hedrich and Marten, 1993; Kolb et al., 1995). In contrast, S-type channels are only weakly voltage dependent. The voltage dependent gating of both anion channel types is strongly modulated by the external anion activity (Hedrich and Marten, 1993; Hedrich et al., 1994; Lohse and Hedrich, 1995; Dietrich and Hedrich, 1998). Thus, the anion species and its concentration determine permeation and gating of these channels. It was shown, for instance, that malate represents not just a major substrate for R-type channels but also a gating modifier. This organic anion shifts the voltage dependent open probability of R-type channels to more negative voltages as it modifies the resting potential window of guard cells (Raschke, 2003). S-type currents are predominantly carried by chloride and nitrate ions instead (Schmidt and Schroeder, 1994). Similar to the situation with R-type channels, it has recently been shown that S-type channel gating is also modulated by permeating anions (Geiger et al., 2009, 2011).

Following the discovery of anion channel currents in plants, it took almost two decades to identify the underlying genes encoding S and R-type anion channels. In 2008, the molecular nature of the guard cell slow anion channel from *A. thaliana* was uncovered using two independent screens: one for ozone-insensitive open-stomata mutants and the other for mutants impaired in CO_2-dependent leaf temperature change (*oz* and *cdi3*, respectively;

Negi et al., 2008; Saji et al., 2008; Vahisalu et al., 2008). When it became clear that the defect in the *cdi3/oz* gene affected distinctive properties of S-type channels in guard cells, the gene was (re)named *SLAC1* (slow anion channel) according to the nomenclature proposed by Klaus Raschke (Linder and Raschke, 1992). SLAC1 shares homology to the tellurite-resistance/C(4)-dicarboxylate transporters expressed in bacteria, archaea, and fungi. Recently, the crystal structure of one member of this family, HiTehA from *Haemophilus influenza*, was obtained (Chen et al., 2010). Using this structure as a template, a molecular model of SLAC1 was calculated. According to the structure of HiTehA, these channels are trimers composed of quasi-symmetrical subunits (**Figure 1**). Each subunit has 10 transmembrane helices arranged from helical hairpin pairs to form an inner five-helix transmembrane pore with a central conserved phenylalanine residue (*A. thaliana* SLAC1-F450) that could represent the anion gate. Indeed, mutation of the pore phenylalanine led to open anion conductance in both HiTehA and the flowering plant homolog SLAC1 (Chen et al., 2010). Besides the founding member SLAC1, that is exclusively expressed in guard cells, four SLAC1 Homologs were recognized in *A. thaliana* (SLAH1–4; Negi et al., 2008). Apart from SLAC1, SLAH3 is the only other S-type channel functionally characterized so far (Geiger et al., 2011); both channels differ significantly in their biophysical properties. In comparison to SLAC1, SLAH3 exhibits a higher preference for nitrate. In fact, for priming SLAH3 requires the presence of nitrate at its extracellular face. Nitrate thus functions as a substrate as well as a gate opener of SLAH3. SLAC1 and SLAH3 co-localize in the plasma membrane of guard cells, suggesting that upon stomatal closure they release chloride and nitrate in a concerted action (Negi et al., 2008; Vahisalu et al., 2008; Geiger et al., 2011). Lack of SLAC1 in Arabidopsis and rice was shown to result in stomata that appear not to close properly in response to high atmospheric CO_2 levels, low relative humidity, and darkness (Negi et al., 2008; Vahisalu et al., 2008; Kusumi et al., 2012). Under the conditions tested so far, *Slah3* knockout plants did not show any stomatal phenotype. Patch-clamp studies, however, revealed that in *slac1* knockout plants S-type anion channels are active in nitrate-based buffers, whereas they are absent in guard cells of *slah3* loss-of-function plants (Geiger et al., 2011).

SLAC1 and SLAH3 both require interacting partners for opening. This may explain why initial attempts to express SLAC1 heterologously in *Xenopus* oocytes, for instance, did not result in the expected S-type anion conductance (Negi et al., 2008; Vahisalu et al., 2008). BiFC-based screens for interacting protein partners in oocytes followed by electrophysiological studies finally revealed the expected S-type activity. Both anion channels SLAC1 and SLAH3 interact with protein kinase-phosphatase pairs associated with abscisic acid (ABA) signaling (Geiger et al., 2009, 2010, 2011). In guard cells, and most likely all other plant cell types, increasing levels of the water stress hormone ABA as produced upon drought periods - is perceived in the cytosol (Levchenko et al., 2005) by members of the ABA receptor PYR/PYL/RCAR family (Ma et al., 2009; Park et al., 2009). Upon perception of ABA, the ABA receptor interacts with protein phosphatases of the PP2C family (ABI1) and suppresses their enzymatic activity. Phosphatase inhibition in turn

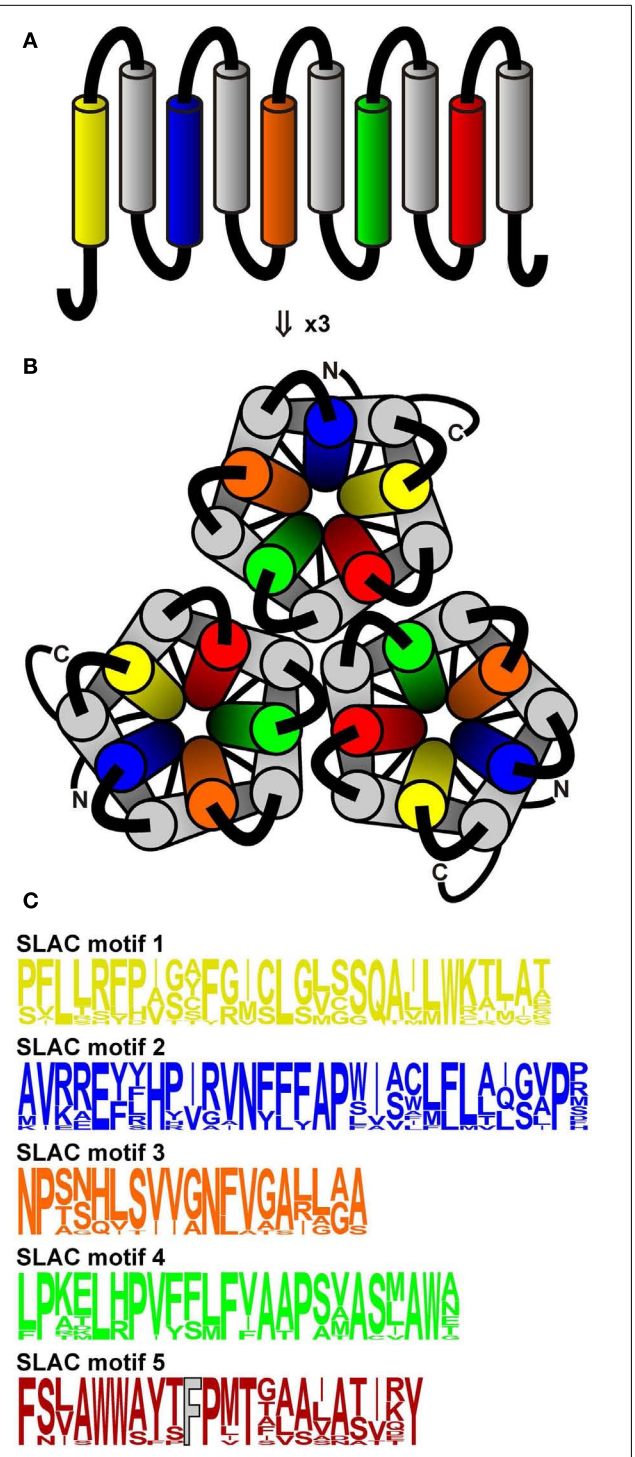

FIGURE 1 | Topology of SLAC-like channels. (A) SLAC-like channels show a topology of ten transmembrane regions and cytosolic N- and C-termini. **(B)** Three channel modules assemble into a trimeric structure. The pore-forming transmembrane regions (yellow, blue, orange, green, red) were used to generate Hidden Markov Models (HMMs) to screen for SLAC-like channels in plant genomes. **(C)** Sequence logos of the HMMs of the regions shown in **(A)** and **(B)**. The crucial phenylalanine residue in the motif 5 (corresponding to Aratha-SLAC1-F450) is displayed in gray.

enables activation of distinct SnRK- and/or CPK protein kinases. Among them, the SnR kinase OST1 and the CPK kinases 3, 6, 21, and 23 activated SLAC1, while SLAH3 was shown to be stimulated by CPK3, 6, 21, and 23 but not by OST1 (Geiger et al., 2009, 2010, 2011; Brandt et al., 2012; Scherzer et al., 2012). Following phosphorylation of the cytosolic N-terminal moieties of SLAC1 and SLAH3, the channels open very likely by a conformational change involving the phenylalanine gate. As a consequence, chloride and nitrate is released from guard cells and the membrane potential depolarizes. Depolarization activates Guard cell Outward Rectifying K^+ channels (GORK, Ache et al., 2000; Hosy et al., 2003), leading to the release of potassium, thereby decreasing the osmotic potential and thus driving water out of the cell. The loss of guard cell turgor finally leads to stomatal closure.

Lately, ALMT12 from *A. thaliana* was identified as the guard cell quick anion channel or a prominent part of it. ALMT12 represents a member of the Aluminum activated malate transporters (ALMTs) family (Meyer et al., 2010; Sasaki et al., 2010). ALMT12 loss-of-function plants appeared impaired in malate-induced R-type anion currents in guard cells (Meyer et al., 2010) as well as in stimulus-induced stomatal closure (Meyer et al., 2010; Sasaki et al., 2010) indicating that the gene product of *ALMT12* is part of a channel complex that is involved in the release of anions from guard cells.

Al^{3+}-activated malate transporters within this family were initially identified in wheat (*Triticum aestivum*; TaALMT1), rapeseed (*Brassica napus*), and *A. thaliana* (Sasaki et al., 2004; Hoekenga et al., 2006; Ligaba et al., 2006). ALMTs were shown to be involved in the detoxification of soil-borne Al^{3+}, mediated by the release of malate that chelates the toxic cation (Ryan et al., 1997; Kollmeier et al., 2001; Ligaba et al., 2006; Delhaize et al., 2007). ALMT-expressing *Xenopus* oocytes were found to conduct Al^{3+}-enhanced malate currents, in line with the physiological function of ALMT (Sasaki et al., 2004). Pre-incubation of oocytes with the protein kinase inhibitors K252 and staurosporine prevented Al^{3+}-induced TaALMT1-derived currents (Ligaba et al., 2009), with Ser384 in the C-terminus of TaALMT1 identified as the key residue. In contrast to the well-known R-type features known from guard cells, the current response of TaALMT1 and homologs thereof did not show strong voltage sensitivity (Ryan et al., 1997; Kollmeier et al., 2001; Pineros and Kochian, 2001). In contrast, when expressed in *Xenopus* oocytes, ALMT12 reflected the hallmark electrical properties of R-type anion channels of Arabidopsis guard cell plasma membranes (Meyer et al., 2010). According to the nomenclature proposed by Klaus Raschke (Linder and Raschke, 1992), ALMT12 was renamed QUAC1 (QUick Anion Channel 1). This name better suits the function of the *ALMT12* gene product in guard cells, because QUAC1 is evidentially not activated by Al^{3+} as the initially identified, eponymous ALMT family members, and moreover, QUAC1 operates as channel rather than transporter. Note, however, that both the QUAC1 channel and TaALMT1-type transporters share malate as a permeating ion.

Recently, two members of the Arabidopsis ALMT family have been shown to reside in the vacuolar membrane (Kovermann et al., 2007; Meyer et al., 2011). Patch-clamp experiments on vacuoles overexpressing ALMT6 revealed large channel-mediated inward-rectifying malate currents that appeared to be modulated by the vacuolar pH and the cytosolic malate concentration. Conversely, ALMT6 loss-of-function plants carry reduced malate currents (Meyer et al., 2011). ALMT9 shares its hallmark properties with ALMT6, but in contrast to the guard cell specific expression of ALMT6, ALMT9 was found to be expressed ubiquitously (Kovermann et al., 2007).

In contrast to the SLAC1 anion channel family, not even gross structural information for ALMT channels is available. From hydrophobicity considerations and subsequent immunocytochemical experiments, an initial topology model of TaALMT1 with six transmembrane helices and a long C-terminal domain was deduced (**Figure 2A**; Motoda et al., 2007). This model predicts the N- and C-termini to face the apoplast, which would put the key

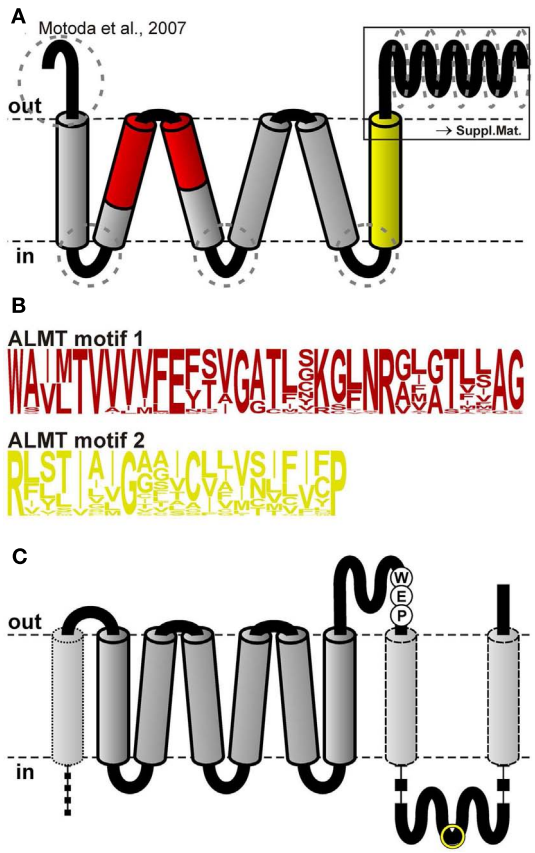

FIGURE 2 | Topology of ALMT/QUAC-like channels. (A) Topology model developed by Motoda et al. (2007) for the channel TaALMT1. The red and the yellow regions were used to generate Hidden Markov Models (HMMs) to screen for ALMT/QUAC-like channels in plant genomes. Dotted ellipses indicate regions that differ most between the different clades of the ALMT/QUAC protein family. A detailed analysis of the C-terminal half is shown in Presentation S1 in Supplementary Material. **(B)** Sequence logos of the HMMs of the regions shown in **(A)**. **(C)** Proposed modified topology for ALMT/QUAC-like channels. In addition to the model of Motoda et al. (2007), the C-terminal half is spanning twice the membrane resulting in extracellular and intracellular C-terminal regions. Furthermore, the larger N-terminal extension may contain another membrane spanning region (dotted). The positions of the highly conserved WEP-motif as well as the position of the phosphorylation site TaALMT1-S384 (yellow circle) are indicated.

phosphorylation site Ser384 of TaALMT1 at the extracellular side, contrary to expectations, as it would not be accessible to protein kinases of the types known to control ion channel function in plants (Ligaba et al., 2009).

The comprehensive introduction presented so far summarized our current knowledge on slow and quick anion channels in plants in order to provide an overview also to readers who are not familiar with the field. In the following of this study we took the next step in gaining further detailed insights into the physiological role of SLAC and QUAC/ALMT proteins and their regulation. We investigated the molecular functional evolution of the two gene families by mining the available plant genomics data for valuable information on evolutionary conserved, potential functional domains in these proteins. The combination of phylogenetic analyses with predictions of protein features allowed to prognosticate putative phosphorylation sites in SLAC-like channels and to propose a new topology of QUAC/ALMT-like channels that reconciles the apparently contradicting experimental findings. Analyses of this type are intended to foster future structure-function studies on SLAC- and QUAC/ALMT-like channels, which, in the case of voltage-gated K^+ channels, for instance, proved to be very successful for unveiling mechanisms of physiologically important regulations (Dreyer and Blatt, 2009; Dreyer and Uozumi, 2011).

RESULTS AND DISCUSSION

The protein classes of slow and quick anion channels show several characteristic sequence fingerprints. We used some of these sequence motifs (colored regions in **Figures 1** and **2**) and build Hidden Markov Models (HMMs) for these based on the known families of SLAC-like and ALMT/QUAC-like channels from a few model species. The HMMs (**Figures 1C** and **2B**) were then employed to screen the deduced proteomes of two chlorophytes[1], one bryophyte[2], one lycophyte[3], five Poaceae[4], five Brassicaceae[5], three Fabaceae[6], two Euphorbiaceae[7], two Rosaceae[8], two Rutaceae[9], one Salicaceae[10], one Linaceae[11], one Cucurbitaceae[12], one Caricaceae[13], one Myrtaceae[14], one Vitaceae[15], one Solanaceae[16], one Scrophulariaceae[17], and one Ranunculaceae[18]. In this process, duplicated database entries and a few false positives were removed from the data sets.

[1] *Chlamydomonas reinhardtii* and *Volvox carteri*
[2] *Physcomitrella patens*
[3] *Selaginella moellendorffii*
[4] *Sorghum bicolor*, *Zea mays*, *Setaria italica*, *Oryza sativa*, and *Brachypodium distachyon*
[5] *Arabidopsis thaliana*, *Arabidopsis lyrata*, *Capsella rubella*, *Brassica rapa*, and *Thellungiella halophila*
[6] *Medicago truncatula*, *Phaseolus vulgaris*, and *Glycine max*
[7] *Manihot esculenta* and *Ricinus communis*
[8] *Prunus persica* and *Malus domestica*
[9] *Citrus sinensis* and *Citrus clementina*
[10] *Populus trichocarpa*
[11] *Linum usitatissimum*
[12] *Cucumis sativus*
[13] *Carica papaya*
[14] *Eucalyptus grandis*
[15] *Vitis vinifera*
[16] *Solanum lycopersicum*
[17] *Mimulus guttatus*
[18] *Aquilegia caerulea*

THE FAMILY OF ALMT/QUAC-LIKE PROTEINS

In the model plant *A. thaliana*, the family of aluminum tolerance associated transporters (ALMTs) together with QUAC-like channels comprises 13 members (Hoekenga et al., 2006). Using BLAST with these as target sequences we identified 9 and 22 homologous channels/transporters in the genomes of *O. sativa* and *P. trichocarpa*, respectively. Based on this initial dataset we identified two regions as suitable for building HMMs for database searches. Motif 1 reaches from the middle of the second to the middle of the third transmembrane region (**Figure 2**, red) and motif 2 comprises the sixth predicted transmembrane region (**Figure 2**, yellow). Genome-wide screens spotted 400 non-redundant ALMT/QUAC-like proteins in 30 embryophyte species and two in two chlorophytes (Table S1 in Supplementary Material). Phylogenetic analyses assigned all of them to a single group of orthologs, indicating that the most recent common ancestor of all green plants comprised a single protein of the ALMT/QUAC type. Additionally, we realized that the basic structure of the phylogenetic tree can be inferred already by selecting ALMT/QUAC-like proteins of a few representative species. For better visualization of our conclusions we selected a set of 62 ALMT/QUAC-like proteins from *P. trichocarpa*, *P. patens*, and *S. moellendorffii* as well as *A. thaliana* (representing the Brassicaceae), *O. sativa* (for the Poaceae), and *M. truncatula* (for the Fabaceae).

Previous phylogenetic analyses of ALMT/QUAC-like proteins from *A. thaliana*, *O. sativa*, and *P. trichocarpa* allowed subdividing this family into five clades (Barbier-Brygoo et al., 2011). Our analysis indicated that this classification is well suited to categorize these transporters from angiosperms. However, ALMT/QUAC-like channels from Bryophyta and Lycophyta cannot be grouped as such (**Figure 3**). Instead, proteins from *S. moellendorffii* and *P. patens* form separate groups of species-specific gene family amplifications.

Species tree vs. gene tree reconciliation analyses revealed that the functional and structural diversity of the class of ALMT/QUAC-like proteins derived from several gene duplication events in different lineages (**Figure 3**). An early duplication event before the emergence of lycophytes separated the groups 2/5 from 1/3/4, followed by the split of clade 3 by another duplication event after the emergence of lycophytes. Groups 1 and 4, and 2 and 5 divided thereafter. The separation of the groups is apparently combined by functional diversification. For instance, the proteins *A. thaliana* Aratha-ALMT6 and Aratha-ALMT9 (clade 2) are vacuolar malate-permeable channels (Kovermann et al., 2007; Meyer et al., 2011) whereas Aratha-ALMT1 (clade 1) and QUAC1 (=Aratha-ALMT12, clade 3) are located in the plasma membrane. Here, Aratha-ALMT1 mediates Al^{3+}-induced malate extrusion (Hoekenga et al., 2006), while QUAC1 is an Al^{3+}-insensitive voltage-gated anion channel (Meyer et al., 2010).

STRUCTURAL SIMILARITIES AND DIFFERENCES AMONG QUAC/ALMT PROTEINS

The available robust sequence information allowed spotting regions that might imply functional differences of the channels/transporters from the different clades in angiosperms. For analyses we used more than 300 putatively full-length QUAC/ALMT channel sequences of the five clades that did not

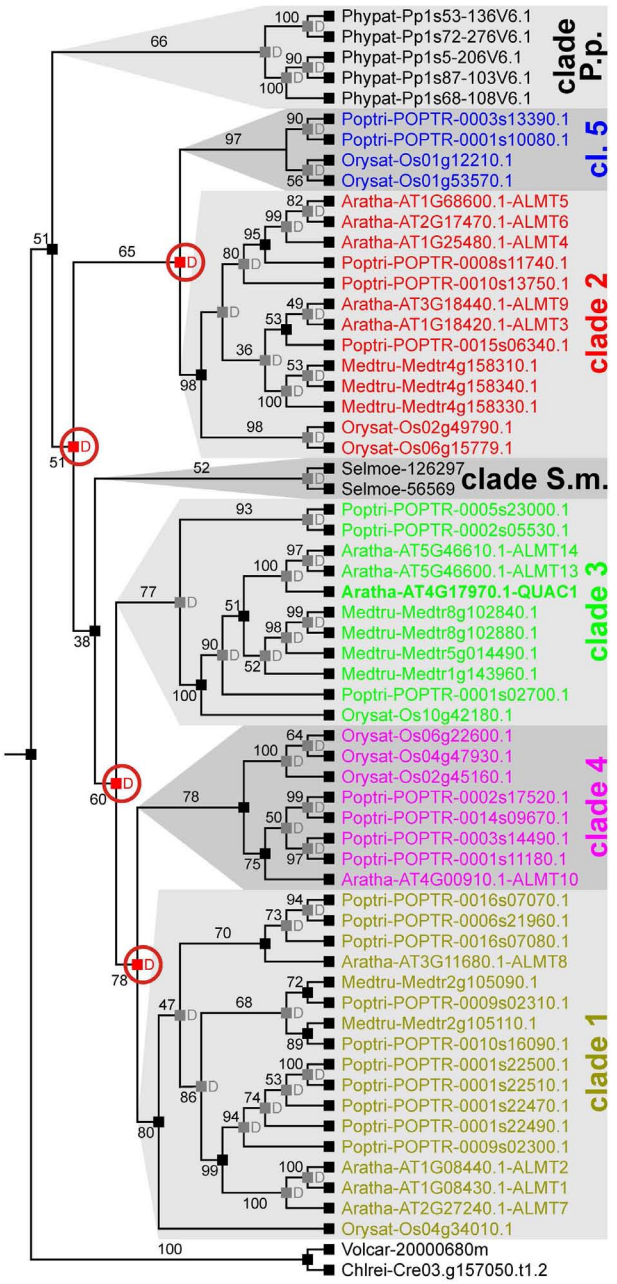

FIGURE 3 | Evolutionary relationships among ALMT/QUAC-like channels in land plants. There are seven clearly distinguished clades of ALMT/QUAC-like channels in extant land plants, i.e., clades 1, 2, 3, 4, 5, clade S.m. (*S. moellendorffii* specific) and clade P.p. (*P. patens*-specific). Each clade represents an independent group of orthologs. To elaborate the evolutionary relationship, reconciliation analyses have been carried out. The last recent common ancestor of all embryophytes had a single ALMT/QUAC-like channel. Several duplications resulted in the diversity observed today in angiosperms. A *P. patens*-specific group separated relatively early. Right after, gene duplication separated clades 2/5 from the others. A second duplication separated clade 3 (comprising QUAC1/ALMT12) from clades 1/4 followed by a third duplication that then separated clade 1 from clade 4. In comparison quite recently, another duplication event led to the separation of clades 2 and 5. Red "D"s at branching points indicate predicted gene duplications, numbers designate bootstrap values. For clarity, predicted events of gene losses are not shown.

show apparent deletions or potentially wrongly predicted splicing events.

The sequence alignment indicated several highly conserved regions, such as the six predicted transmembrane domains and certain areas in the C-terminal extension. Most divergent regions were found at the N-terminus before the first transmembrane domain, in the cytosolic linkers between the transmembrane domains 1 and 2, 3 and 4, and 5 and 6, and within the C-terminal half of the proteins (**Figure 2A**, dotted circles). Especially, the latter region appears to be more structured than hitherto reported. Our alignment identified 10 separable zones of variable length with alternating higher and lower levels of conservation (29–50 vs. 17–28% identity; Presentation S1 in the Supplementary Material). Remarkable as fingerprints are the WEP-motif in the third zone, consisting of the highly conserved amino acid triplet Trp-Glu-Pro, and the conserved agglomeration of hydrophobic residues in the ninth zone. To evaluate whether the C-terminal halves of QUAC/ALMT proteins might contain overlooked transmembrane regions we combined our alignment with the hydropathicity scores of the single proteins. At each position average values were calculated for every clade and for all sequences. For further display only those positions were considered, where less than 25% of the sequences showed gaps. This analysis revealed that – besides the six known transmembrane domains in the first part of the proteins – two additional, conserved hydrophobic regions appeared in the C-terminal half (**Figure 4**): one is located right after the WEP-motif and the other coincides with the cluster of hydrophobic residues in the ninth zone. Based on these results we propose a modified topology for QUAC/ALMT channels, with the C-terminal half of the protein being partially extracellular and partially cytosolic (**Figure 2C**). This topology would be in line with all immunocytochemical results of Motoda et al. (2007) and would explain how the glutamate in the WEP-motif can be involved in external Al^{3+}-activation of Aratha-ALMT1 and TaALMT1 (Furuichi et al., 2010) while TaALMT1-S384 (in the seventh zone) is a key residue for cytosolic phosphorylation processes (Ligaba et al., 2009). In the current model with the C-terminal half being exclusively extracellular these experimental findings are apparently contradictory. Future studies will have to provide further experimental evidence to distinguish between the different suggested topology models. They will also need to clarify whether the larger N-terminal extension is extracellular for all QUACs/ALMTs, as proposed for TaALMT1 (Motoda et al., 2007), or whether in this case there is also an additional transmembrane domain, at least in some channels/transporters (**Figure 2C**, dotted). In this context, it should be mentioned that so far no clear signal sequence for an extracellular localization of the N-terminal end of ALMT/QUAC channel proteins has been identified.

THE FAMILY OF SLAC-LIKE PROTEINS

Earlier studies have identified SLAC1 homologs in Arabidopsis (*A. thaliana*), rice (*O. sativa*), grapevine (*V. vinifera*), and poplar (*P. trichocarpa*; Negi et al., 2008; Chen et al., 2010; Barbier-Brygoo et al., 2011). From these seed data sets we realized that SLAC-like proteins can be pinpointed by the presence of several conserved consensus motifs, which in turn might be exploited in genome-wide screenings. On the basis of the structural homology model of SLAC1 (Chen et al., 2010) we therefore generated Hidden Markov

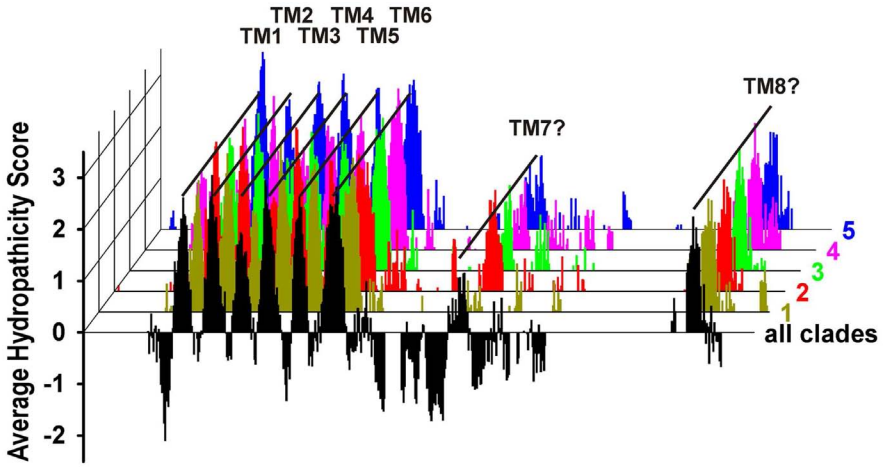

FIGURE 4 | Averaged Kyte and Doolittle plot of ALMT/QUAC-like channels. The hydropathicity score was determined separately for each channel and then assigned to the respective position in the global sequence alignment. Subsequently, for each clade and for all channels the average values at each position were determined. The plot identified clearly the known six transmembrane domains TM1-TM6 and, additionally, two further potential transmembrane domains in the C-terminal halves of the proteins (TM7 and TM8). For clarity, negative values were only displayed for the average over all clades.

Models (HMMs) of the five transmembrane regions spanning the permeation pathway (**Figure 1**, colored). These HMMs allowed us to identify in total 176 non-redundant SLAC-like proteins in 29 species (Table S2 in Supplementary Material). However, this data set was not well suited for phylogenetic approaches because bootstrap analyses resulted – in part – in very low values, i.e., low statistical support of the tree structure. We therefore chose an alternative multi-step approach to fathom out the evolutionary relationship within this protein family. First, we identified the transmembrane segments and potential regulatory domains located in the cytosolic N-termini of the channels and extracted these regions for further analyses. For the channels of the model plant *A. thaliana* this corresponds to the amino acid stretches Aratha-SLAC1-K103_K516 (414 residues), Aratha-SLAH1-L26_K373 (348 residues), Aratha-SLAH2-D67_Q468 (402 residues), Aratha-SLAH3-D179_P583 (405 residues), and Aratha-SLAH4-L26_K365 (340 residues). Secondly, we determined by pairwise comparisons whether the respective sequences were complete. The gold standard in this context was provided by the five SLAC-like channels from *A. thaliana*. Potential deletions in the amino acid sequence might result from wrongly predicted splicing sites due to premature gene annotation, for instance. From the 176 SLAC-like channels, 135 appear to be complete in the selected sequence range. The sequences were then hierarchically clustered based on pairwise identities using UPGMA (Unweighted Pair Group Method with Arithmetic Mean). This clustering already provided us with a first picture of the phylogenetic structure of the SLAC-like channel protein family. Whereas channels from *S. moellendorffii* and *P. patens* take some intermediate position, channels of angiosperms could be clearly classified into three different similarity groups (**Figure 5A**): the SLAH1/4-group (green) contains Aratha-SLAH1 and Aratha-SLAH4; the SLAH2/3-group (red) with Aratha-SLAH2 and Aratha-SLAH3 and the SLAC1-group (blue) harboring Aratha-SLAC1, the funding member of the SLAC/SLAH family. Within these groups, channel identities are highly conserved ranging from ∼58% in the SLAH1/4-group, ∼69% in the SLAH2/3-group to ∼78% in the SLAC1-group (**Figure 5B**). In contrast, inter-group identities with ∼35% (SLAH1/4- vs. SLAH2/3-group), ∼36% (SLAH1/4- vs. SLAC1-group), and ∼52% (SLAH2/3- vs. SLAC1-group) are lower. Assuming that dispersion of identities is a measure for the age of a group, we may conclude the SLAC1-group to be the youngest and the SLAH1/4-group to be the oldest group of this protein family. This conclusion was further supported by reconciliation analysis of the data set (**Figure 5C**). The SLAH1/4-group apparently separated from the others already in a very early event before the appearances of bryophytes. From the available data it cannot be judged whether this process took place with the emergence of terrestrial plants or developed in the aquatic environment before colonizing the land. It is clear, however, that separation of the SLAH2/3-group from the SLAC1-group took place in a subsequent event on land after the appearance of bryophytes but before the occurrence of lycophytes. To further corroborate this hypothesis, we carried out detailed phylogenetic analyses with a condensed data set comprising SLAC-like channels from *P. patens* and one representative each from the SLAC1-group (Aratha-SLAC1), the SLAH2/3-group (Aratha-SLAH2), and the SLAH1/4-group (Aratha-SLAH1). Despite slight variations in the precise assignment of one channel from *P. patens*, the global tree structure and thus our picture on the evolutionary history of SLAC-like channels was confirmed (**Figures 5D,E**).

STRUCTURAL SIMILARITIES AND DIFFERENCES AMONG SLAC-LIKE PROTEINS

As in the case of QUAC/ALMT channels we also used the robust sequence information of SLAC-like channels to pinpoint regions and/or positions that might underlie functional variations between the groups. Most prominent differences between channels of the SLAH1/4-group and those of the other groups are (i) a

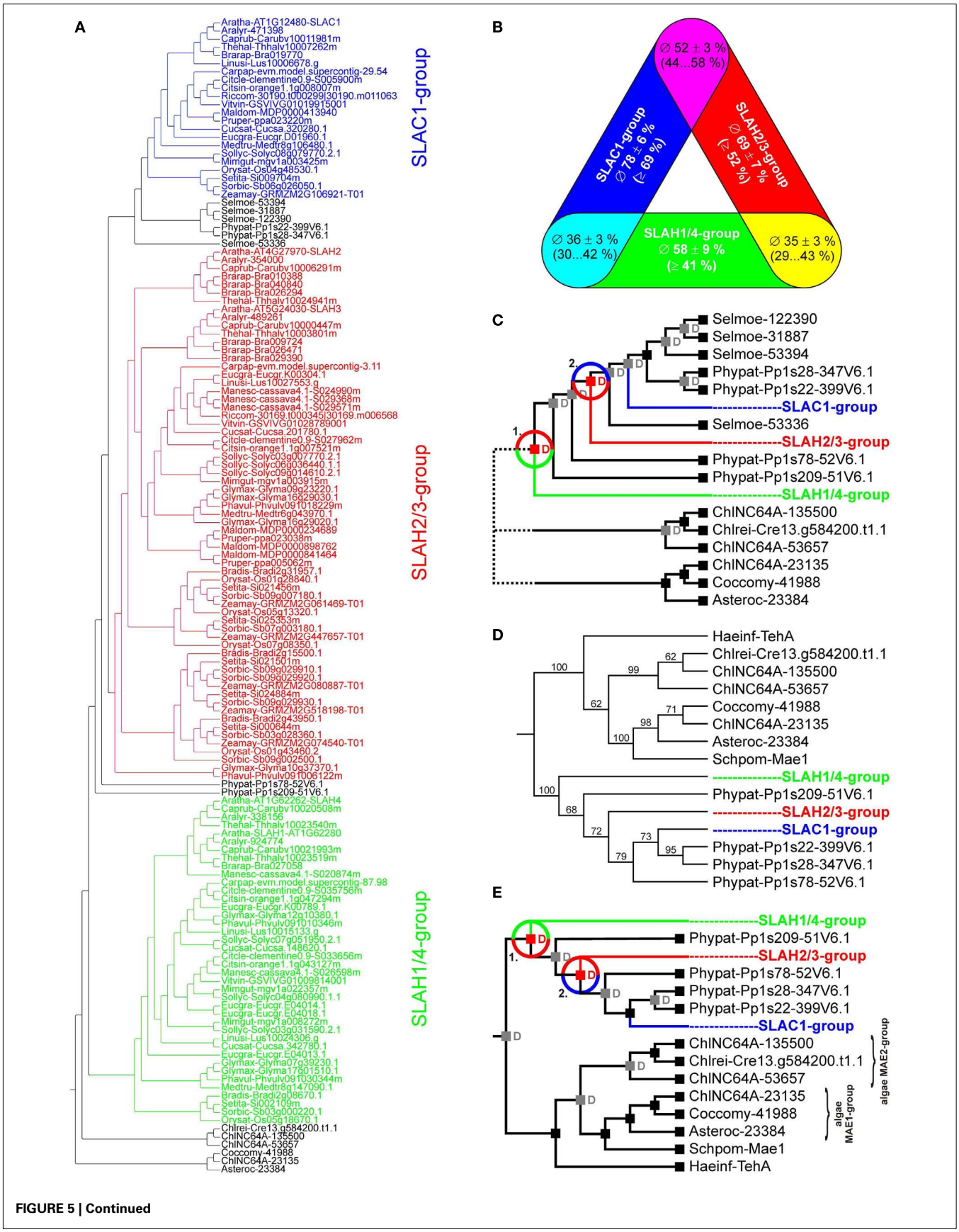

FIGURE 5 | Continued

FIGURE 5 | Evolutionary relationships among SLAC-like channels in land plants. (A) Phylogenetic tree resulting from UPGMA analyses of 135 SLAC-like channels that did not show apparent deletions or wrong predictions of splicing sites. SLAC-like channels of angiosperms could be grouped into three-groups: SLAC1-group (blue), SLAH2/3-group (red) and SLAH1/4-group (green). **(B)** Summary of pairwise identities of proteins within the three different groups and between the groups. Data are mean ± SD. In brackets the value range is specified. **(C)** Reconciliation analysis of early duplication events in SLAC-like proteins. SLAC-like channels diversified into the three groups by two duplication events (red "D"s and circles). For clarity, predicted events of gene losses are not shown. **(D)** Phylogenetic analysis of representative SLAC-like and algae-Mae-like channels. Aratha-SLAH1 represents the SLAH1/4-group, Aratha-SLAH2 the SLAH2/3-group and Aratha-SLAC1 the SLAC1-group. For comparison the tellurite-resistance/C(4)-dicarboxylate transporter Haeinf-TehA from *Haemophilus influenzae* and the malic acid transport protein Mae1 from *Schizosaccharomyces pombe* were included in the analysis. **(E)** Reconciliation analysis of the tree in **(D)** confirmed the results already obtained with the UPGMA data set. For clarity, predicted events of gene losses are not shown.

shorter cytosolic C-terminus, (ii) a different initial stretch within the first transmembrane region TM1, and (iii) a much shorter cytosolic N-terminus. Especially the latter region was shown in Aratha-SLAC1 and Aratha-SLAH3 to contain important targets of kinases that regulate channel activity (Geiger et al., 2009, 2011; Vahisalu et al., 2010). This prompted us to exemplarily investigate the positional conservation of potential phosphorylation sites. We generated an alignment of the full-length sequences of the 135 SLAC-like channels mentioned above, combined this with the structure-based prediction of protein phosphorylation sites provided by Netphos 2.0, and obtained for each of the 12,155 Thr, Ser, or Tyr residues in the matrix an individual score. Further analyses were then limited to those residues that fulfilled all of the three following conditions: (i) >90% conservation of the potential phosphorylation site among all channels of one group, (ii) score >0.6 for at least one of these residues, and (iii) the average score >0.2 within a channel group. This screen for potential group-specific, conserved targets for kinases did not identify any tyrosine residue, but nine serine/threonine residues in channels of the SLAC1-group, six in the SLAH2/3-group and one in the SLAH1/4-group (**Figure 6**). Three SLAC1-group-specific potential phosphoserine residues were located in the first part of the cytosolic N-terminal region (S59, S83, and S86 in the model channel Aratha-SLAC1; **Figures 6B,C**). Interestingly, both regions of Aratha-SLAC1 have already been shown experimentally to be phosphorylated by the protein kinase OST1 (Geiger et al., 2009; S59 and S86, Vahisalu et al., 2010) and CPK6 (S59, Brandt et al., 2012). Another cytosolic region, short before the first transmembrane domain, contains several predicted, highly conserved phosphorylation sites in the two SLAC1- and SLAH2/3-groups (in Aratha-SLAC1: S107, S113, S116, and S120; in Aratha-SLAH3: T187, S189, T197; **Figure 6D**). Also, these regions had been experimentally proven to be phosphorylated by OST1 (Aratha-SLAC1, S120) and CPK21 (Aratha-SLAH3, T187), respectively (Geiger et al., 2009, 2011; Vahisalu et al., 2010). Besides these N-terminal regions, our screen also predicted a highly conserved phosphorylation site in the cytosolic C-terminus right after the last transmembrane domain of SLAC1- and SLAH2/3-like channels (Aratha-SLAC1-T513 and Aratha-SLAH3-S580; **Figure 6G**). In Aratha-SLAC1, this region was already identified as target of the kinase OST1 (Geiger et al., 2009). Thus, our unbiased prediction of group-specifically conserved phosphorylation sites matched perfectly the experimental findings obtained so far on the model channels Aratha-SLAC1 and Aratha-SLAH3. In addition, the screen predicts two further sites in the cytosolic linkers between the fourth and fifth and between the eighth and ninth transmembrane domains of SLAH1/4- and SLAH2/3-like (**Figure 6E**) and SLAC1- and SLAH2/3-like channels (**Figure 6F**), respectively. These data provide a valuable source of information for future studies that will focus *in vitro*, in oocytes, and *in planta* on single as well multiple phoshorylation site mutants in order to understand role and mechanism of the different SLAC/SLAH kinases.

EVOLUTIONARY ORIGIN OF SLACs AND ALMTs/QUACs

Our analysis indicated that ALMT/QUAC-like channels have diversified from a single gene in the most recent common ancestor of green plants. The fact that one ALMT/QUAC ortholog each was identified in the chlorophytes *C. reinhardtii* and *V. carteri* adds substance to such an explanation (**Figure 3**, Table S1 in Supplementary Material). The analysis of homologs in higher plants is consistent with processes that involved several successive gene duplications since the colonization of the land environment. Interestingly, clades 2/5 split from the other three with or before the appearance of vascular plants. Clade 2 contains Aratha-ALMT6 and Aratha-ALMT9, both of which have been previously characterized at the functional level. Both ALMTs were localized in the tonoplast and typified as vacuolar malate channels rather than transporters (Kovermann et al., 2007; Meyer et al., 2011). Following clade 2/5, clade 3 (containing QUAC1) separated from clades 1 (containing ALMT1) and 4. Since ALMT1 is activated by Al^{3+} but QUAC1 is not, it remains an open question whether Al^{3+}-activation in channels of the ALMT/QUAC-like protein family was lost at some point or developed later during evolutionary specialization.

The evolutionary path of SLAC-like channels is not as straight as it appears for the ALMT/QUAC-like proteins. In algae we identified two distinct groups of the Tellurite-resistance/Dicarboxylate Transporter (TDT) family (**Figures 5A,D,E**; Table S2 in Supplementary Material). None of those is a clade of SLAC-like orthologs but show closer similarity to the malate permease Mae1 from *Schizosaccharomyces pombe*. In some species, e.g., *Coccomyxasubellipsoidea* C-169, *Chlorella variabilis*, and *Asterochloris* sp., we identified only proteins of one group, in other species, e.g., *C. reinhardtii*, only members of the other. Interestingly, *Chlorella* NC64A comprises both groups in parallel, indicating that algae may exhibit a larger variability of TDTs. Thus, SLAC-like channels might have originated from another clade of this protein family still waiting to be identified in Chlorophyta. The diversity of TDT proteins in algae very likely collapsed with the transition of plants from an aqueous environment to one where water was often limiting. Functional diversification of SLAC-like channels in higher plants appears to have

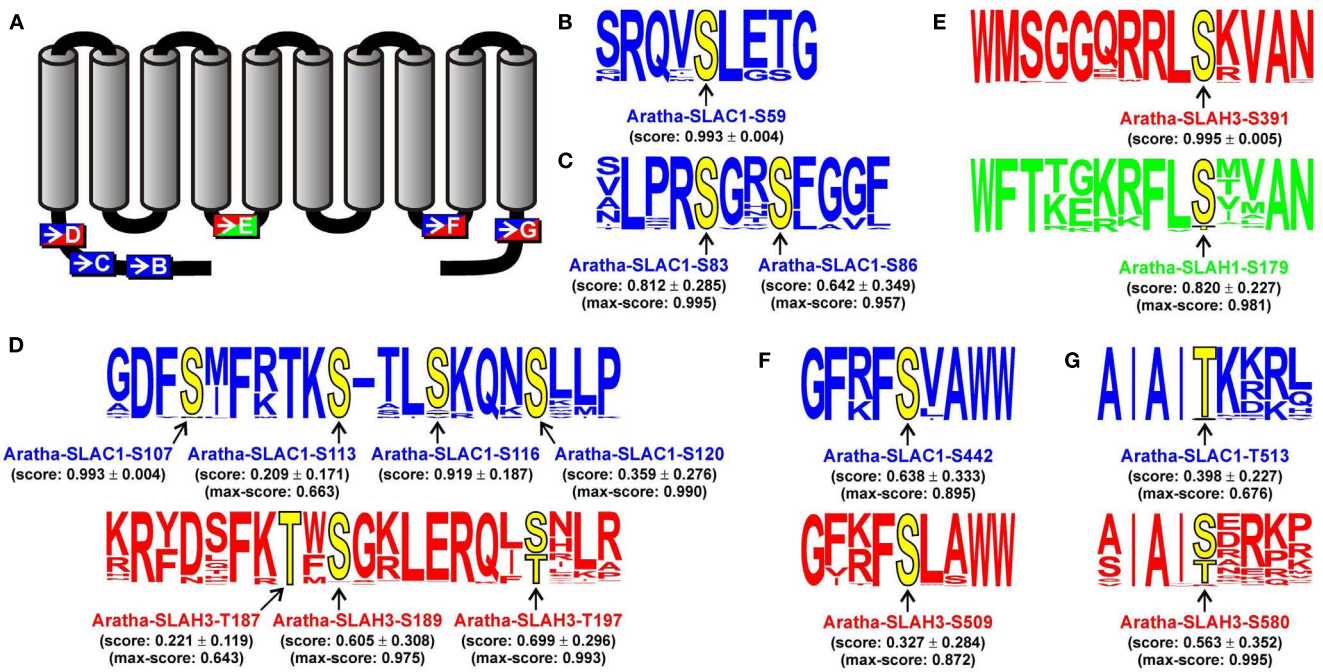

FIGURE 6 | Prediction of group-specifically conserved phosphorylation sites in SLAC-like channels. The Netphos 2.0 score for S, T, and Y residues was determined separately for each channel and then assigned to the respective position in the global sequence alignment. Subsequently, the average values at each position were determined for each clade. Conserved positions were identified using the following criteria: (i) conservation of >90% of the potential phosphorylation site within one group, (ii) minimum score of 0.6 for at least one of these residues, and (iii) minimum average score of 0.2 within one channel group. **(A)** Illustration of the localization of the identified conserved phosphorylation sites. Letters refer to detailed information in **(B–G)**. **(B–G)** Sequence logos of the closer environment of the conserved putative phosphorylation sites (yellow). The positional information of the model channels Aratha-SLAC1, Aratha-SLAH3, and Aratha-SLAH1 is displayed explicitly. Values indicate mean ± SD of the score values. In case the mean score value was below 0.9, also the maximal value obtained for a single sequence is indicated. The displayed information is color coded (blue: SLAC1-group, red: SLAH2/3-group, green: SLAH1/4-group).

originated from only one group that survived the land transition (**Figure 7**). A similar bottleneck scenario was recently proposed for voltage-gated K^+ channels (Gomez-Porras et al., 2012). This concept was challenged by screening databases of embryophytes for the presence of *S. pombe* Mae1-like proteins. As a matter of fact, we identified ESTs coding for such proteins also from higher plants, e.g., from clementine (*C. clementine*), apple (*M. domestica*), Japanese cedar (*Cryptomeria japonica*), the perennial grass *Cleistogenes songorica*, and common hop (*Humulus lupulus*). Closer inspection, however, revealed that the encoded proteins show best hits with very high sequence identities (50–90%) to annotated C4-dicarboxylate transporter/malic acid transporters from plant pathogens. Therefore we conclude that the few found ESTs originate from contaminations rather than from the host species themselves. Thus apart from SLAC-like channels, unequivocal evidence for the existence of other classes of the Tellurite-resistance/Dicarboxylate Transporter (TDT) family in embryophytes is apparently lacking.

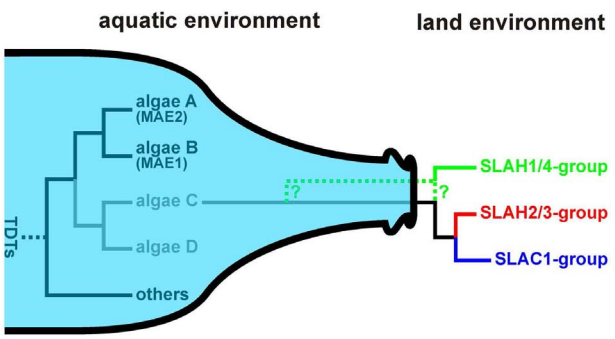

FIGURE 7 | Bottleneck model for the evolution of SLAC-like channels. In the aquatic environment Tellurite-resistance/Dicarboxylate Transporters (TDTs) evolved into a huge variability. In algae transporters were identified that share features with malic acid transport proteins (MAEs). Closer relatives of the common ancestor of SLAC-like channels still need to be identified in Chlorophyta (algae C, algae D). Only one of these protein classes survived the transition from the aquatic to the land environment setting the starting point for the further evolution of SLAC-like channels.

SUMMARY

Slow and quick anion channels are essential for proper guard cell function (Kollist et al., 2011; Hedrich, 2012; Roelfsema et al., 2012). Both SLAC- and ALMT/QUAC-like proteins belong to larger protein families and each evolved from a common ancestor. Despite these parallels it is evident that SLAC-like channels show a higher degree of conservation than ALMTs/QUACs. Whereas SLAC-like proteins diversified via two duplication events, ALMT/QUAC-like

proteins expanded by a rather early split followed closely by two subsequent events and a more recent final one.

Based on these phylogenetic analyses we hypothesize that group-specific evolution and conservation of structural and regulatory sites laid the ground for the development of unique properties associated with each channel type. The strategy of combining sequence alignment and clustering with predictions of local protein properties allowed us pinpointing potential phosphorylation sites in SLAC1-like channels in an unbiased manner. Several residues have been verified by site-directed approaches before. Experimental analysis of the remaining population of likely phosphorylation sites will help further understand multi-kinase activation of SLAC/SLAH channels (Scherzer et al., 2012). Using a similar strategy as with SLAC/SLAHs, we generated a modified topology model for ALMT/QUAC-like channels, which could serve as a valuable source for comparative physiological approaches and structure-function studies.

We are optimistic that cross-referencing phylogenetic analyses with position-specific protein properties together with subsequent experimental functional testing *in vitro*, in oocytes and finally *in planta*, will foster genome research approaches on plant ion channels and very likely on transporters and pumps as well.

MATERIALS AND METHODS

GENOME-WIDE SEARCH FOR SLAC- AND ALMT/QUAC-LIKE PROTEINS

Putative ALMT/QUACs and SLACs were identified using the conceptual proteomes of *A. caerulea*, *A. lyrata*, *A. thaliana*, *B. distachyon*, *B. rapa*, *C. rubella*, *C. papaya*, *C. reinhardtii*, *C. clementina*, *C. sinensis*, *C. sativus*, *E. grandis*, *G. max*, *L. usitatissimum*, *M. domestica*, *M. esculenta*, *M. truncatula*, *M. guttatus*, *O. sativa*, *P. vulgaris*, *P. patens*, *P. trichocarpa*, *P. persica*, *R. communis*, *S. moellendorffii*, *S. italica*, *S. bicolor*, *T. halophila*, *V. vinifera*, *V. carteri*, and *Z. mays* (Phytozome v8.0), and the proteome of *S. lycopersicum* (SOL Genomics). Initially, we identified a starting data set obtained by BLAST searches in the genomes using known channels from *A. thaliana* as templates. Then, for each of the transmembrane domains 1, 3, 5, 7, and 9 of SLAC-like channels (**Figure 1**, colored) and of the two selected regions of ALMT/QUAC-like proteins (**Figure 2**, colored) a multiple alignment was created and an HMM built using the HMMER[19] v3.0 package suite (**Figures 1C** and **2B**). Thereafter, the HMMs were used to screen the deduced proteomes of the species under study. The criterion for inclusion was that at least one of the motifs must be present in the protein with a score >0.001. The entire protein sequence was then extracted. Retrieved proteins were curated in a semi-automatic way in order to eliminate false positives: the n protein sequences of each channel type of each species were pairwise aligned using Clustall W2[20]. From the resulting $n(n\text{-}1)/2$ pairs those with a score of <20 and of >97 (identical sequences) were removed. The residual pairs fragmented the sequences into distinct groups. That group with the highest similarity to the corresponding *Arabidopsis* channels was selected for further analyses. Proteins of the TDT family from algae were identified by blastp searches in the proteomes of *Asterochloris* sp. *Cgr/DA1pho*[21], *Chlorella variabilis* NC64A[22], and *Coccomyxasubellipsoidea* C-169[23] using the malic acid transport protein Mae1 from *Schizosaccharomyces pombe* (NP_594777.1) as template. The NCBI accession number of Haeinf-TehA is NP_438669.

PHYLOGENETIC ANALYSES

Sequences were aligned using the auto setting in MAFFT[24] (Multiple Alignment with Fast Fourier Transform; Katoh and Toh, 2010) and the resulting alignments were analyzed by GBlocks (Talavera and Castresana, 2007), in order to keep robust regions for the phylogenetic inference. For the analysis presented in **Figure 3**, these were localized in the predicted transmembrane areas and in the zones 1 and 3 in the C-terminal part of the proteins (Presentation S1 in Supplementary Material). For the analysis presented in **Figure 5D**, these regions were localized in the transmembrane areas of SLAC-like and MAE-like channels. Sequence alignments are provided in DataSheet S1.FASTA and DataSheet S2.FASTA in the Supplementary Material. Evolutionary relationships were inferred by Maximum Likelihood using RAxML and 1000 bootstrap replicates (Stamatakis, 2006). The evolutionary model used for phylogenetic analyses was inferred using ProtTest (Darriba et al., 2011). In both cases, ALMTs/QUACs and SLACs, the evolutionary model determined by ProtTest was JTT + Γ. In order to root and resolve the gene trees, we performed a gene tree-species tree reconciliation analysis using the species tree from from Phytozome v8.0[25] and the Tree Of Life[26]. Reconciliation analysis was carried out in Notung 2.6 (Chen et al., 2000; Vernot et al., 2007). Events of gene losses were not shown. UPGMA (Unweighted Pair Group Method with Arithmetic Mean) analyses were carried out in MAFFT.

ANALYSES OF PROTEIN FEATURES

Protein hydropathicity at the amino acid scale were analyzed for each protein sequence separately with the web-based tool ProtScale[27] using the "Kyte and Doolittle (1982)" option. The obtained values were then integrated into the global sequence alignment. If at a specific position of the alignment less than 25% of the sequences showed gaps, average hydropathicity scores were calculated. Results were qualitatively not different when – instead of 25% – any threshold between 1 and 95% was chosen.

The probability of an S/T or Y residue in SLAC1-like channels to be a protein kinase target was estimated with the web-based tool Netphos 2.0[28]. The obtained values were then integrated into the global sequence alignment and analyzed for group-specifically conserved phosphorylation sites as outlined in the text. Sequence

[19] http://hmmer.org
[20] http://www.ebi.ac.uk/Tools/services/web/toolform.ebi?tool=clustalw2
[21] http://genome.jgi-psf.org/Astpho1/Astpho1.home.html
[22] http://genome.jgi-psf.org/ChlNC64A_1/ChlNC64A_1.home.html
[23] http://genome.jgi.doe.gov/Coc_C169_1/Coc_C169_1.home.html
[24] http://mafft.cbrc.jp/alignment/software/
[25] http://www.phytozome.net/
[26] http://tolweb.org/tree/
[27] http://web.expasy.org/protscale/
[28] http://www.cbs.dtu.dk/services/NetPhos/

logos of identified sites were generated with the web-based tool WebLogo[29].

ACKNOWLEDGMENTS

This work was supported by grants from the Spanish Ministerio de Economía y Competitividad to Ingo Dreyer (BFU2011-28815), a Marie-Curie Career Integration Grant to Ingo Dreyer (FP7-PEOPLE-2011-CIG No. 303674 – Regopoc), a Marie-Curie Cofund fellowship to Judith Lucia Gomez-Porras and by grants of the Deutsche Forschungsgemeinschaft (DFG) within GK1342 to Rainer Hedrich and Dietmar Geiger, and within the grant HE1640/28-1 to Rainer Hedrich. Rainer Hedrich and Dietmar Geiger were supported by grants of the Strategic Technologies Program–National Science, Technology and Innovation Plan, Saudi Arabia project No. 10-ENV1181–02. Thanks to Khaled A. S. Al-Rasheid for helpful discussion on anion physiology in animals. We are grateful to Jorge E. Mayer, Canberra/Australia, and three reviewers for helpful comments on the manuscript. Diego Mauricio Riaño-Pachón acknowledges support from the program "Proyecto de ProfesorAsistente" from the Faculty of Sciences of the Universidad de los Andes, Bogotá, Colombia.

[29]http://weblogo.berkeley.edu/logo.cgi

SUPPLEMENTARY MATERIAL

The Supplementary Material for this article can be found online at http://www.frontiersin.org/Plant_Traffic_and_Transport/10.3389/fpls.2012.00263/abstract

Presentation S1 | Alignment of the C-terminal regions of ALMT-like proteins. Based on the grade of conservation, the C-terminal regions of ALMT-like proteins can be divided into 10 zones. Zone 3 contains the highly conserved fingerprint amino acid triplet Trp-Glu-Pro (WEP-motif) and zone 7 contains the residue TaALMT1-S384 that was shown to be involved in phosphoregulation of this transporter. The two additional putative transmembrane regions that were identified in this study are indicated (TM7 and TM8).

DataSheet S1.FASTA | Alignment of the sequence blocks used to generate the phylogenetic analysis shown in Figure 3.

DataSheet S2.FASTA | Alignment of the sequence blocks used to generate the phylogenetic analysis shown in Figure 5D.

DataSheet S3.XLSX |

Table S1 | ALMT/QUAC-like channels presented in this study. Channels were categorized according to **Figure 3**.

Table S2 | SLAC-like channels presented in this study. Channels were categorized according to **Figure 5**.

REFERENCES

Ache, P., Becker, D., Ivashikina, N., Dietrich, P., Roelfsema, M. R., and Hedrich, R. (2000). GORK, a delayed outward rectifier expressed in guard cells of *Arabidopsis thaliana*, is a K+-selective, K+-sensing ion channel. *FEBS Lett.* 486, 93–98.

Barbier-Brygoo, H., De, A. A., Filleur, S., Frachisse, J. M., Gambale, F., Thomine, S., et al. (2011). Anion channels/transporters in plants: from molecular bases to regulatory networks. *Annu. Rev. Plant Biol.* 62, 25–51.

Brandt, B., Brodsky, D. E., Xue, S., Negi, J., Iba, K., Kangasjarvi, J., et al. (2012). Reconstitution of abscisic acid activation of SLAC1 anion channel by CPK6 and OST1 kinases and branched ABI1 PP2C phosphatase action. *Proc. Natl. Acad. Sci. U.S.A.* 109, 10593–10598.

Chen, K., Durand, D., and Farach-Colton, M. (2000). NOTUNG: a program for dating gene duplications and optimizing gene family trees. *J. Comput. Biol.* 7, 429–447.

Chen, Y. H., Hu, L., Punta, M., Bruni, R., Hillerich, B., Kloss, B., et al. (2010). Homologue structure of the SLAC1 anion channel for closing stomata in leaves. *Nature* 467, 1074–1080.

Darriba, D., Taboada, G. L., Doallo, R., and Posada, D. (2011). ProtTest 3: fast selection of best-fit models of protein evolution. *Bioinformatics* 27, 1164–1165.

Delhaize, E., Gruber, B. D., and Ryan, P. R. (2007). The roles of organic anion permeases in aluminium resistance and mineral nutrition. *FEBS Lett.* 581, 2255–2262.

Dietrich, P., and Hedrich, R. (1998). Anions permeate and gate GCAC1, a guard cell anion channel. *Plant J.* 15, 479–487.

Dreyer, I., and Blatt, M. R. (2009). What makes a gate? The ins and outs of Kv-like K+ channels in plants. *Trends Plant Sci.* 14, 383–390.

Dreyer, I., and Uozumi, N. (2011). Potassium channels in plant cells. *FEBS J.* 278, 4293–4303.

Furuichi, T., Sasaki, T., Tsuchiya, Y., Ryan, P. R., Delhaize, E., and Yamamoto, Y. (2010). An extracellular hydrophilic carboxy-terminal domain regulates the activity of TaALMT1, the aluminum-activated malate transport protein of wheat. *Plant J.* 64, 47–55.

Geiger, D., Maierhofer, T., Al-Rasheid, K. A., Scherzer, S., Mumm, P., Liese, A., et al. (2011). Stomatal closure by fast abscisic acid signaling is mediated by the guard cell anion channel SLAH3 and the receptor RCAR1. *Sci. Signal.* 4, ra32.

Geiger, D., Scherzer, S., Mumm, P., Marten, I., Ache, P., Matschi, S., et al. (2010). Guard cell anion channel SLAC1 is regulated by CDPK protein kinases with distinct Ca2+ affinities. *Proc. Natl. Acad. Sci. U.S.A.* 107, 8023–8028.

Geiger, D., Scherzer, S., Mumm, P., Stange, A., Marten, I., Bauer, H., et al. (2009). Activity of guard cell anion channel SLAC1 is controlled by drought-stress signaling kinase-phosphatase pair. *Proc. Natl. Acad. Sci. U.S.A.* 106, 21425–21430.

Gomez-Porras, J. L., Riaño-Pachón, D. M., Benito, B., Haro, R., Sklodowski, K., Rodriguez-Navarro, A., et al. (2012). Phylogenetic analysis of K+ transporters in bryophytes, lycophytes, and flowering plants indicates a specialization of vascular plants. *Front. Plant Sci.* 3:167. doi:10.3389/fpls.2012.00167

Hedrich, R. (2012). Ion channels in plants. *Physiol. Rev.* 92, 1777–1811.

Hedrich, R., Busch, H., and Raschke, K. (1990). Ca2+ and nucleotide dependent regulation of voltage dependent anion channels in the plasma membrane of guard cells. *EMBO J.* 9, 3889–3892.

Hedrich, R., and Marten, I. (1993). Malate-induced feedback regulation of plasma membrane anion channels could provide a CO2 sensor to guard cells. *EMBO J.* 12, 897–901.

Hedrich, R., Marten, I., Lohse, G., Dietrich, P., Winter, H., Lohaus, G., et al. (1994). Malate-sensitive anion channels enable guard cells to sense changes in the ambient CO2 concentration. *Plant J.* 6, 741–748.

Hoekenga, O. A., Maron, L. G., Pineros, M. A., Cancado, G. M., Shaff, J., Kobayashi, Y., et al. (2006). AtALMT1, which encodes a malate transporter, is identified as one of several genes critical for aluminum tolerance in Arabidopsis. *Proc. Natl. Acad. Sci. U.S.A.* 103, 9738–9743.

Hosy, E., Vavasseur, A., Mouline, K., Dreyer, I., Gaymard, F., Porée, F., et al. (2003). The *Arabidopsis* outward K+ channel GORK is involved in regulation of stomatal movements and plant transpiration. *Proc. Natl. Acad. Sci. U.S.A.* 100, 5549–5554.

Katoh, K., and Toh, H. (2010). Parallelization of the MAFFT multiple sequence alignment program. *Bioinformatics* 26, 1899–1900.

Kolb, H. A., Marten, I., and Hedrich, R. (1995). Hodgkin-Huxley analysis of a GCAC1 anion channel in the plasma membrane of guard cells. *J. Membr. Biol.* 146, 273–282.

Kollist, H., Jossier, M., Laanemets, K., and Thomine, S. (2011). Anion channels in plant cells. *FEBS J.* 278, 4277–4292.

Kollmeier, M., Dietrich, P., Bauer, C. S., Horst, W. J., and Hedrich, R. (2001). Aluminum activates a citrate-permeable anion channel in the aluminum-sensitive zone of the maize root apex. A comparison between an aluminum-sensitive and an aluminum-resistant cultivar. *Plant Physiol.* 126, 397–410.

Kovermann, P., Meyer, S., Hortensteiner, S., Picco, C., Scholz-Starke, J., Ravera, S., et al. (2007). The *Arabidopsis* vacuolar malate channel is a member of the ALMT family. *Plant J.* 52, 1169–1180.

Kusumi, K., Hirotsuka, S., Kumamaru, T., and Iba, K. (2012). Increased leaf photosynthesis caused by elevated stomatal conductance in a rice mutant deficient in SLAC1, a guard cell anion channel protein. *J. Exp. Bot.* 63, 5635–5644.

Kyte, J., and Doolittle, R. F. (1982). A simple method for displaying the hydropathic character of a protein. *J. Mol. Biol.* 157, 105–132.

Levchenko, V., Konrad, K. R., Dietrich, P., Roelfsema, M. R., and Hedrich, R. (2005). Cytosolic abscisic acid activates guard cell anion channels without preceding Ca2+ signals. *Proc. Natl. Acad. Sci. U.S.A.* 102, 4203–4208.

Ligaba, A., Katsuhara, M., Ryan, P. R., Shibasaka, M., and Matsumoto, H. (2006). The BnALMT1 and BnALMT2 genes from rape encode aluminum-activated malate transporters that enhance the aluminum resistance of plant cells. *Plant Physiol.* 142, 1294–1303.

Ligaba, A., Kochian, L., and Pineros, M. (2009). Phosphorylation at S384 regulates the activity of the TaALMT1 malate transporter that underlies aluminum resistance in wheat. *Plant J.* 60, 411–423.

Linder, B., and Raschke, K. (1992). A slow anion channel in guard-cells, activating at large hyperpolarization, may be principal for stomatal closing. *FEBS Lett.* 313, 27–30.

Lohse, G., and Hedrich, R. (1995). Anions modify the response of guard-cell anion channels to auxin. *Planta* 197, 546–552.

Ma, Y., Szostkiewicz, I., Korte, A., Moes, D., Yang, Y., Christmann, A., et al. (2009). Regulators of PP2C phosphatase activity function as abscisic acid sensors. *Science* 324, 1064–1068.

Meyer, S., Mumm, P., Imes, D., Endler, A., Weder, B., Al-Rasheid, K. A., et al. (2010). AtALMT12 represents an R-type anion channel required for stomatal movement in Arabidopsis guard cells. *Plant J.* 63, 1054–1062.

Meyer, S., Scholz-Starke, J., De, A. A., Kovermann, P., Burla, B., Gambale, F., et al. (2011). Malate transport by the vacuolar AtALMT6 channel in guard cells is subject to multiple regulation. *Plant J.* 67, 247–257.

Motoda, H., Sasaki, T., Kano, Y., Ryan, P. R., Delhaize, E., Matsumoto, H., et al. (2007). The membrane topology of ALMT1, an aluminum-activated malate transport protein in wheat (*Triticum aestivum*). *Plant Signal. Behav.* 2, 467–472.

Negi, J., Matsuda, O., Nagasawa, T., Oba, Y., Takahashi, H., Kawai-Yamada, M., et al. (2008). CO_2 regulator SLAC1 and its homologues are essential for anion homeostasis in plant cells. *Nature* 452, 483–486.

Park, S. Y., Fung, P., Nishimura, N., Jensen, D. R., Fujii, H., Zhao, Y., et al. (2009). Abscisic acid inhibits type 2C protein phosphatases via the PYR/PYL family of START proteins. *Science* 324, 1068–1071.

Pineros, M. A., and Kochian, L. V. (2001). A patch-clamp study on the physiology of aluminum toxicity and aluminum tolerance in maize. Identification and characterization of Al(3+)-induced anion channels. *Plant Physiol.* 125, 292–305.

Raschke, K. (2003). Alternation of the slow with the quick anion conductance in whole guard cells effected by external malate. *Planta* 217, 651–657.

Roelfsema, M. R., Hedrich, R., and Geiger, D. (2012). Anion channels: master switches of stress responses. *Trends Plant Sci.* 17, 221–229.

Ryan, P. R., Skerrett, M., Findlay, G. P., Delhaize, E., and Tyerman, S. D. (1997). Aluminum activates an anion channel in the apical cells of wheat roots. *Proc. Natl. Acad. Sci. U.S.A.* 94, 6547–6552.

Saji, S., Bathula, S., Kubo, A., Tamaoki, M., Kanna, M., Aono, M., et al. (2008). Disruption of a gene encoding C4-dicarboxylate transporter-like protein increases ozone sensitivity through deregulation of the stomatal response in *Arabidopsis thaliana*. *Plant Cell Physiol.* 49, 2–10.

Sasaki, T., Mori, I. C., Furuichi, T., Munemasa, S., Toyooka, K., Matsuoka, K., et al. (2010). Closing plant stomata requires a homolog of an aluminum-activated malate transporter. *Plant Cell Physiol.* 51, 354–365.

Sasaki, T., Yamamoto, Y., Ezaki, B., Katsuhara, M., Ahn, S. J., Ryan, P. R., et al. (2004). A wheat gene encoding an aluminum-activated malate transporter. *Plant J.* 37, 645–653.

Scherzer, S., Maierhofer, T., Al-Rasheid, K. A., Geiger, D., and Hedrich, R. (2012). Multiple calcium-dependent kinases modulate ABA-activated guard cell anion channels. *Mol. Plant.* doi:10.1093/mp/sss084

Schmidt, C., and Schroeder, J. I. (1994). Anion selectivity of slow anion channels in the plasma membrane of guard cells (large nitrate permeability). *Plant Physiol.* 106, 383–391.

Schroeder, J. I., and Hagiwara, S. (1989). Cytosolic calcium regulates ion channels in the plasma membrane of Vicia faba guard cells. *Nature* 338, 427–430.

Schroeder, J. I., and Keller, B. U. (1992). Two types of anion channel currents in guard cells with distinct voltage regulation. *Proc. Natl. Acad. Sci. U.S.A.* 89, 5025–5029.

Stamatakis, A. (2006). RAxML-VI-HPC: maximum likelihood-based phylogenetic analyses with thousands of taxa and mixed models. *Bioinformatics* 22, 2688–2690.

Talavera, G., and Castresana, J. (2007). Improvement of phylogenies after removing divergent and ambiguously aligned blocks from protein sequence alignments. *Syst. Biol.* 56, 564–577.

Vahisalu, T., Kollist, H., Wang, Y. F., Nishimura, N., Chan, W. Y., Valerio, G., et al. (2008). SLAC1 is required for plant guard cell S-type anion channel function in stomatal signalling. *Nature* 452, 487–491.

Vahisalu, T., Puzorjova, I., Brosche, M., Valk, E., Lepiku, M., Moldau, H., et al. (2010). Ozone-triggered rapid stomatal response involves the production of reactive oxygen species, and is controlled by SLAC1 and OST1. *Plant J.* 62, 442–453.

Vernot, B., Stolzer, M., Goldman, A., and Durand, D. (2007). Reconciliation with non-binary species trees. *Comput. Syst. Bioinformatics Conf.* 6, 441–452.

Conflict of Interest Statement: The authors declare that the research was conducted in the absence of any commercial or financial relationships that could be construed as a potential conflict of interest.

Received: 17 June 2012; accepted: 12 November 2012; published online: 29 November 2012.

*Citation: Dreyer I, Gomez-Porras JL, Riaño-Pachón DM, Hedrich R and Geiger D (2012) Molecular evolution of slow and quick anion channels (SLACs and QUACs/ALMTs). Front. Plant Sci. **3**:263. doi: 10.3389/fpls.2012.00263*

This article was submitted to Frontiers in Plant Traffic and Transport, a specialty of Frontiers in Plant Science.

frontiers in
PLANT SCIENCE

REVIEW ARTICLE
published: 30 October 2012
doi: 10.3389/fpls.2012.00235

Glutamate receptor homologs in plants: functions and evolutionary origins

Michelle Beth Price, John Jelesko and Sakiko Okumoto*

Department of Plant Pathology, Physiology and Weed Science, Virginia Tech, Blacksburg, VA, USA

Edited by:
Heven Sze, University of Maryland, USA

Reviewed by:
Rashid Ali, University of Connecticut, USA
Sebastien Thomine, Centre National de la Recherche Scientifique, France
Heng-Cheng Hu, University of Maryland, USA

****Correspondence:***
Sakiko Okumoto, Department of Plant Pathology, Physiology and Weed Science, Virginia Tech, 549 Latham Hall, Blacksburg, VA 24060, USA.
e-mail: sokumoto@vt.edu

The plant glutamate-like receptor homologs (GLRs) are homologs of mammalian ionotropic glutamate receptors (iGluRs) which were discovered more than 10 years ago, and are hypothesized to be potential amino acid sensors in plants. Although initial progress on this gene family has been hampered by gene redundancy and technical issues such as gene toxicity; genetic, pharmacological, and electrophysiological approaches are starting to uncover the functions of this protein family. In parallel, there has been tremendous progress in elucidating the structure of animal glutamate receptors (iGluRs), which in turn will help understanding of the molecular mechanisms of plant GLR functions. In this review, we will summarize recent progress on the plant GLRs. Emerging evidence implicates plant GLRs in various biological processes in and beyond N sensing, and implies that there is some overlap in the signaling mechanisms of amino acids between plants and animals. Phylogenetic analysis using iGluRs from metazoans, plants, and bacteria showed that the plant GLRs are no more closely related to metazoan iGluRs as they are to bacterial iGluRs, indicating the separation of plant, other eukaryotic, and bacterial GLRs might have happened as early on as the last universal common ancestor. Structural similarities and differences with animal iGluRs, and the implication thereof, are also discussed.

Keywords: ligand-gated channel, calcium ion, membrane protein, glutamate, amino acids

INTRODUCTION

Nitrogen (N) is quantitatively the most important mineral nutrient, and often the limiting factor for plant growth in the field. The availability of N has a profound short- and long-term effect on plant physiology, which involves developmental reprogramming to maximize N use efficiency. Without a doubt, nitrogen-sensing mechanisms that allow such adjustments are essential for the fitness of plants.

Genome-wide studies on plant responses to amino acids have revealed that a large fraction of N-regulated genes (∼81%) require the incorporation of inorganic nitrogen to organic nitrogen, strongly suggesting that plants possess sensory mechanisms for organic N (Gutierrez et al., 2008). Amino acids, formed as the result of the assimilation of inorganic N, serve as N signaling molecules in other organisms, and are considered the prime candidate for organic N signals in plants. Ample evidence demonstrates that amino acid levels affect the activities of key players in nitrogen assimilation pathway through transcriptional and post-transcriptional processes. For example, gene expression of both cytosolic and plastidic glutamine synthetases, GLN1 and GLN2, are regulated by the levels of amino acids in *Arabidopsis* and tobacco (Vincentz et al., 1993; Oliveira et al., 2001; Fritz et al., 2006; Sulieman et al., 2010). The non-protein amino acid GABA (γ-amino-butyric acid), when supplied to plant growth medium, is capable of modulating not only the activity of key enzymes in nitrogen assimilation, but also the uptake of nitrate itself (Barbosa et al., 2010). Furthermore, amino acids are capable of modulating uptake of inorganic and organic nitrogen (Rawat et al., 1999; Nazoa et al., 2003; Hirner et al., 2006). In addition to gene regulation at the transcriptional level, amino acids have been shown to trigger rapid responses when supplied externally to plant cells. For example, exogenous application of amino acids to plants causes a transient cytosolic calcium increase and membrane depolarization (Dennison and Spalding, 2000; Dubos et al., 2003; Demidchik et al., 2004; Qi et al., 2006; Stephens et al., 2008). Further, GABA and D-Ser, have been shown to trigger transient changes in cytosolic $[Ca^{2+}]$ in pollen grains (Yu et al., 2006; Michard et al., 2011). These studies suggest that plants have endogenous mechanisms of monitoring the concentration of amino acid levels, enabling modulation of nitrogen metabolism.

Some mechanisms of amino acid sensing have been documented in bacteria, yeast, and mammals. For example, PII proteins found in bacteria and archaea play a pivotal role as master regulators of carbon/nitrogen homeostasis. The conformations of PII proteins are reciprocally regulated by 2-oxoglutarate and glutamine, which signal for carbon and nitrogen abundance, respectively (Leigh and Dodsworth, 2007). In yeast, multiple sensory systems for amino acids have been discovered, namely amino acid permeases such as SSY1 and GAP1 which sense extracellular amino acids (Didion et al., 1998; Wipf et al., 2002; Hundal and Taylor, 2009) and the amino acid-regulated protein kinase that responds to intracellular amino acids (reviewed in (Hinnebusch, 2005). Perception of amino acids by these sensors initiates multiple signaling cascades in which the target of rapamycin (TOR) pathway plays a central role (Zuo et al., 1997; Jacinto and Hall, 2003; Kang et al., 2006). Perception of extracellular amino acids through membrane

transport and control of the TOR pathway have also been reported in *Drosophila* (PATH and Slimfast) and mammals (SNAT2; Hundal and Taylor, 2009).

Aside from their roles as nutritional cues, extracellular amino acids play fundamental roles in the signal transduction in the central nervous system of animals. In these tissues, amino acids released from the presynaptic terminal are recognized by membrane receptors on the postsynaptic membrane. Binding of amino acids to these receptors induces opening of amino acid-gated channels or activates G-protein coupled receptors (Kandel et al., 2000).

The mechanisms of amino acid and internal nitrogen level sensing utilized by plants are largely unknown. Sequencing of the model plant *Arabidopsis* genome allowed for identification of proteins that are homologous to the ones involved in amino acid sensing in other organisms. For example, the *Arabidopsis* PII protein homolog GLB1 interacts with and regulates the activity of two enzymes (*N*-acetyl glutamate kinase and acetyl-CoA carboxylase) involved in the regulation of C/N metabolism (Karakas et al., 2011; Kumar et al., 2011). Although GLB1 is unlikely to be the "master regulator" of growth as is its bacterial counterpart, it does seem to be responsible for a sub-network of nitrogen-sensing. It was also found that *Arabidopsis* (and probably other plants) carry genes required for the operation of the TOR pathway (Deprost et al., 2007; Sobolevsky et al., 2009). The depletion of protein phosphatase 2A activity that functions downstream of TOR leads to autophagy and N remobilization, suggesting that the TOR pathway is involved in nutrient signaling in plants (Li et al., 2006). In addition, the possibility of amino acid transporters functioning as amino acid sensors, as is the case with yeast proteins SSY1 and GAP1, has also been suggested although no experimental evidence so far has supported such a role (Tegeder, 2012).

While these pathways are involved in some aspects of N sensing in plants, it is likely that there are additional mechanisms for amino acid sensing. In particular, the mechanism through which amino acids induce rapid signal transduction events such as Ca^{2+} transient and membrane depolarization is largely unknown. Genome sequencing projects of *Arabidopsis* and other plants, including basic land plants such as Bryophytes and Lycophytes, revealed that plants have glutamate-like receptor homologs (GLRs) of mammalian ionotropic glutamate receptors (iGluRs), which are involved in neurotransmission.

Previous studies indicated the involvement of GLRs in various biological processes, such as C/N balance (Kang and Turano, 2003), photosynthesis (Teardo et al., 2010, 2011), responses to abiotic stress (Kang et al., 2004; Meyerhoff et al., 2005), root morphogenesis (Li et al., 2006; Miller et al., 2010), plant-pathogen interaction (Kang et al., 2006; Kwaaitaal et al., 2011), regulation of cellular Ca^{2+} kinetics (Kim et al., 2001; Dubos et al., 2003; Kang et al., 2006; Qi et al., 2006; Cho et al., 2009; Vincill et al., 2012), and pollen tube growth (Michard et al., 2011). While these studies used genetic and pharmacological approaches to study the functions of plant GLRs, the evidence that the plant GLRs function in a similar manner as the mammalian counterpart had been lacking. In particular, ligand-gated activity of plant GLRs had not been demonstrated. Recent work by the Spalding group has, for the first time, demonstrated that at least one plant GLR (AtGLR3.4) is indeed an amino acid-gated channel capable of inducing cytosolic calcium peaks (Vincill et al., 2012). This finding implies that GLRs are indeed capable of perceiving and transducing amino acid signals. During the same period, the structures of animal iGluR have been well characterized. Now we know the structural basis of ligand binding, the interaction between amino terminal domains (ATD), and the molecular structure of the channel domain for animal iGluRs (Mayer, 2011). Since the domain structures of GLRs seem to be well conserved, such structural information is expected to guide the research of plant GLRs.

In this review, we will summarize the recent progress in understanding the function of plant GLRs. Although the picture is far from being complete, critical channel properties of GLRs are starting to be elucidated. Information gained about structural components on animal iGluRs and the implications to plant GLRs are summarized. In addition, phylogenetic relationships between plant GLRs and iGluRs from other organisms have also been discussed.

THE STRUCTURES OF GLUTAMATE RECEPTORS

SECONDARY AND TERTIARY STRUCTURES OF GLUTAMATE RECEPTORS

Mammalian ionotropic GluRs are classified into four classes based on their pharmacological response to agonists and antagonists: α-amino-3-hydroxy-5-methyl-4-isoxazole propionate (AMPA), kainate (KA), and *N*-methyl-D-aspartate (NMDA) and δ (no known ligands; Mayer, 2005; Connaughton, 2007). These classifications are not rigid however, as a result of sequence similarity and cross-reactivity between classes, often resulting in functional grouping of AMPA, δ, and KA together as the non-NMDA receptors (Kandel et al., 2000; Connaughton, 2007). Paralogs of iGluRs can be found in bacteria, metazoans, and plants. They share the basic structure of domains constituting the ligand binding site and trans-membrane domains, but there is a significant difference in the structures that may have implications in the function of these channels.

The minimal structure of an ionotropic glutamate receptor consists of a ligand binding domain (LBD) and a channel-forming domain (**Figure 1**). A LBD consists of two subdomains, GlnH1/S1, and GlnH2/S2, which are considered to have evolved from periplasmic binding proteins of bacteria because of significant primary sequence similarity (Nakanishi et al., 1990). Indeed, crystal structures of LBDs of all iGluRs analyzed so far has revealed striking structural similarities between the LBDs and bacterial glutamine binding protein (Armstrong et al., 1998; Armstrong and Gouaux, 2000; Naur et al., 2005). The channel-forming domain consists of two or three complete trans-membrane domains (M1 and M3 in prokaryotic channels; M1, M3, and M4 in eukaryotic channels) and one partial trans-membrane domain (M2) that forms a pore-loop (P-loop) structure (Kandel et al., 2000). The structure formed by the M1, M3, and P-loop resembles the structure of tetrameric potassium channels such as KcsA, with inverted topology (MacKinnon, 2003). Due to these structural similarities, prokaryotic iGluRs are considered to be the result of a fusion between bacterial periplasmic binding proteins (PBP) and potassium channels.

While bacterial iGluRs consist only of the LBD and the channel-forming domain (Chen et al., 1999), eukaryotic iGluRs possess

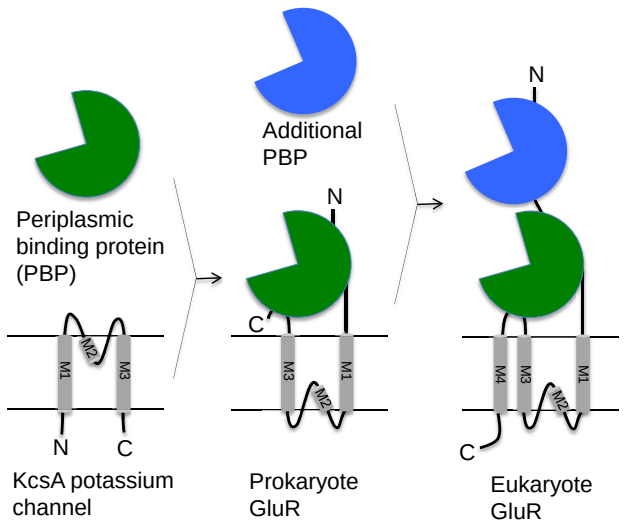

FIGURE 1 | Schematic representations of prokaryote and eukaryote glutamate receptors. The proposed origins of ligand binding domain (LBD, green) and amino terminal domain (ATD, blue), and the channel domain. Bacterial periplasmic binding protein and potassium channel are shown for comparison. Proposed gene fusion events that gave rise to the eukaryotic glutamate receptors are represented by arrows.

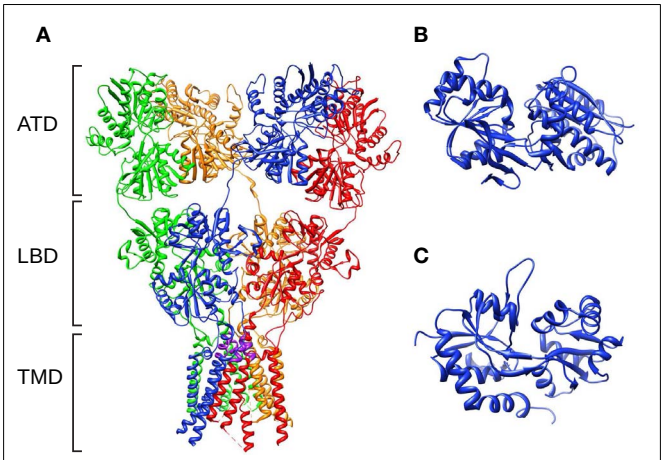

FIGURE 2 | The crystal structure of the rat glutamate receptor, GluA2. **(A)** Structure of the intact channel (3KG2; Sobolevsky et al., 2009). Four subunits are shown in different colors. The "SYTANLAA" motif, which consists of the narrowest part of the channel in each subunit, is marked in purple. **(B,C)** The structures of isolated ATD (3H5V; Jin et al., 2009) and LBD (2UXA; Greger et al., 2006), respectively. Note the "venus-flytrap" like structure in both domains.

an additional ATD. Similar to LBD, ATD share sequence and structural similarity with bacterial periplasmic binding proteins, presumably incorporated through another fusion event (**Figure 2**). The ATDs are responsible for the interaction between the subunits (see Structure and Subunit Compositions of Glutamate Receptors), which in turn contributes to determining the subunit composition of the channel (Jin et al., 2009). Further, the ATD of NMDA receptors can bind a wide range of molecules and ions that work as modulators of the channel activities (Lipton et al., 1997).

Plant iGluRs share the signature "three plus one" transmembrane domains M1 to M4 as well as the putative LBDs GlnH1 and GlnH2, which show high amino acid sequence identity (63–16%), particularly with the M3 domain (63%) with animal NMDA receptor iGluRs (Lam et al., 1998; Chiu et al., 1999). In addition, the predicted membrane topology and orientation of the protein, with the LBDs exposed to the external side of the membrane, are considered to be conserved (Lam et al., 1998; Dubos et al., 2003, 2005; Furukawa et al., 2005).

STRUCTURE AND SUBUNIT COMPOSITIONS OF GLUTAMATE RECEPTORS

Early evidence favored a pentameric structure for iGluRs based on the sizes of chemically cross-linked proteins and the number of distinct channel activities produced by the mixture of two subunits (Dingledine et al., 1999). However, an overwhelming number of studies analyzing structures, desensitization properties and cross-linking between subunits through cysteines now suggest that mammalian iGluRs assemble as tetramers (reviewed in Mayer, 2006; Traynelis et al., 2010). In mammals, functional ligand-gated channels can be formed from either homo- or heteromers of four subunits within the same agonist class (Rosenmund et al., 1998). NMDA receptors form obligatory hetero-tetramers consisting of two glycine-binding subunits and glutamate-binding subunits (Monyer et al., 1992), whereas some AMPA and kainate receptors can form functional homo-tetramers (Mano and Teichberg, 1998). The subunit composition dictates the functional properties of the channel, resulting in a large number of receptor types which function differently *in vivo* (Mayer, 2005). In addition, alternative splicing and RNA editing of iGluRs further increases the diversity of the receptor complexes (Egebjerg and Heinemann, 1993; Gereau and Swanson, 2008).

In 2009, the crystal structure of the homo-tetrameric AMPA receptor, rat GluA2 was resolved, shedding light onto the assembly of the entire channel (Sobolevsky et al., 2009). The resolved crystal structure has a "Y"-shape, where the ATD and LBD spread outward from the more compact channel-forming domains (**Figure 2**). The tetramer is formed as "dimer of dimers," and the ATD and LBD exhibits approximate overall twofold molecular symmetry to the axis perpendicular to the membrane. The trans-membrane domain, on the other hand, assumes a fourfold rotational symmetry that is remarkably similar to the bacterial potassium channel KcsA (Doyle et al., 1998).

The structure revealed extensive inter-subunit interaction through ATDs (interface ~330 Å^2), which was essentially identical to what was observed in the crystal structures of isolated ATDs (Sobolevsky et al., 2009; Mayer, 2011). On the other hand, the inter-subunit interaction in LBDs is much smaller (interface ~224 Å^2), hence the role of LBD in the subunit assembly is considered to be minimal. This result corroborates the previous studies using isolated ATD domains: ATDs of two interacting subunits exhibit very high affinity (e.g., 11 nM for GluR6 and KA2 heterodimer, 0.7 μM for NR1 and NR2 heterodimer) to each other compared to the affinity for itself (Karakas et al., 2011; Kumar et al., 2011). Therefore, while ATD might not be the only domain

that dictates the interaction partners (Pasternack et al., 2002), it is considered to play an important role in the correct assembly of subunits.

The subunit compositions of plant iGluRs are unknown. Co-expression analysis using single-cell sampling revealed that, at least in *Arabidopsis* leaf epidermal and mesophyll cells, there are five to six GLRs co-expressed on average, therefore hetero-tetramer formation is quite likely (Roy et al., 2008). In studies using T-DNA insertion mutants of AtGLR3.3 and 3.4, it was shown that the response to all six amino acids that can induce membrane depolarization (Ala, Cys, Asn, Glu, Ser, Gly) were affected in *glr3.3* mutants, while in *glr3.4* mutants responses were affected in only a subset of amino acids (Stephens et al., 2008). These results support a model where GLR3.3 is included in all receptor complexes in the cell type tested (hypocotyl) whereas a sub-fraction of complexes include at least GLR3.3 and 3.4. To date, heterologous expression in mammalian cells proved that AtGLR3.4 can form a homo-meric channel (Vincill et al., 2012). Further investigations are necessary to understand the subunit compositions of GLRs *in vivo*.

EVOLUTIONARY ORIGIN OF PLANT GLUTAMATE RECEPTORS

The 20 *At*GLRs have been divided into three distinct phylogenetic clades on the basis of parsimony analysis with bacterial amino acid binding proteins as out-groups (Chiu et al., 1999). Examination of amino acid sequence similarity between GLRs and various kinds of ion channels such as animal iGluRs, potassium channels, acetylcholine receptors, and $GABA_A$ receptors suggested that the plant GLRs are most closely related to animal iGluRs (Chiu et al., 1999). Phylogenetic analyses using both parsimony and neighbor joining suggests that plant and animal iGluRs diverged from a common ancestor as opposed to convergent evolution of genes with similar structure and function (Chiu et al., 1999).

The deep phylogenetic relationships between plants, metazoans, and bacteria GLRs were investigated using statistically oriented phylogenetic methods that are amenable to formal hypothesis testing of alternative molecular evolution models. GLR homologs were identified using the AtGLR1.1 and the human NMDA receptor NR1-3 sequences as queries using a sensitive similarity search algorithm (SSEARCH) enforcing a criteria for establishing homology (i.e., common ancestry) that combined both a maximum expectation value of e^{-4} and mutual hits by both query sequences. A bootstrap Maximum Likelihood (ML) phylogenetic analysis indicated a tripartite basal split between bacterial, plant, and other eukaryotic GLR homologs (**Figure 3**). This topology had good bootstrap support and was generally consistent with the separation of bacteria from eukaryotes in the tree of life (ToL), in agreement with previously published results (Janovjak et al., 2011). Cyanobacterial iGluRs clustered tightly with other bacterial homologs, suggesting against the possibility that the plant iGluRs have a cyanobacterial origin. The hypothesis of a cyanobacterial origin of plant GLRs was also statistically rejected by likelihood ratio testing of phylogenetic analyses using alternatively constrained topologies (Table S1 in Supplemental Material).

The basal positioning of the plant GLR homologs relative to other eukaryotic GLR homologs was also consistent with a very ancient separation of plant GLRs from other eukaryotic GLRs. Indeed, likelihood ratio testing indicated that a model of monophyletic plant-eukaryotic association was not a statistically significant better fit to the data than either monophyletic plant-bacteria association or monophyletic eukaryotic-bacteria association models (Table S1 in Supplemental Material). Thus, plant GLRs were no more closely related to eukaryotic GLR homologs than either plant or eukaryotic GLRs were to the bacterial GLRs. These results indicate a very ancient separation of plant, eukaryotic, and bacterial GLRs that dates back to perhaps as far as the separation of the last universal common ancestor (LUCA) in the ToL, or to the very early evolution of the Eukaryotic domain. This GLR molecular evolutionary model is consistent with the current placement of the Plantae (Archaeplastida) as one of the five supergroups of eukaryote taxonomy (Simpson and Roger, 2002; Adl et al., 2005; Keeling et al., 2005). Thus, the plant GLR homologs should be considered as phylogenetically distinct from metazoan GLRs as they are from the bacterial GLRs.

PROPERTIES OF PLANT GLUTAMATE RECEPTORS

LIGANDS TO THE GLUTAMATE RECEPTORS

Mammalian glutamate receptor subunits bind to a number of endogenous substrates, including glutamate, aspartate, glycine, L- and D-serine, and homocysteine (Lipton et al., 1997; Kandel et al., 2000; Schwartz, 2000; Wolosker, 2006). To date, more than 150 high-resolution crystal structures have been obtained for multiple iGluR subtypes. These studies unequivocally showed that the LBD undergoes "venus-flytrap"-like movement when the ligand binds to the cleft between the two lobes. Although the structure of an intact iGluR in the ligand-bound, open state is not available, it is assumed that such conformational change induces opening of the channel. In fact, the potency of an agonist for an iGluR is very well correlated with the degree of domain closure induced by the compound (Pohlsgaard et al., 2011).

For more than a decade, the ligands for plant GLRs were not known. Initial sequence analysis revealed that plant iGluRs carry a mutation in the pore-forming M3 region which is known to render the mammalian δ2 receptor constitutively active (Zuo et al., 1997; Chiu et al., 1999; **Figure 4**), suggesting the possibility that plant iGluRs might not function as ligand-gated channels. On the other hand, glutamate and other amino acids are able to induce membrane depolarization and Ca^{2+} conductance in plants, suggesting that there are amino acid-gated calcium channels in plants (Dennison and Spalding, 2000; Dubos et al., 2003; Qi et al., 2006; Stephens et al., 2008). In addition, various studies using agonists and antagonists of mammalian iGluRs indicated that agonists and antagonists that bind to the LBD of animal iGluR are also pharmacologically active in plants (see Properties of Plant Glutamate Receptors).

In a recent study, *At*GLR3.4 was shown to be gated by Asn, Ser, and Gly when expressed in mammalian cells, demonstrating that at least one plant GLRs is capable of forming an amino acid-gated channel (Vincill et al., 2012). This result corroborates with previous work using a structural modeling approach, which indicated Gly could be a more likely agonist than Glu for the majority of GLRs including AtGLR3.4 (Dubos et al., 2003). Although the LBD structures of plant GLRs are not known, it is highly likely that the binding of these amino acids to the LBD of AtGLR3.4 causes opening of the channel. If this is the case, LBDs of plant GLRs

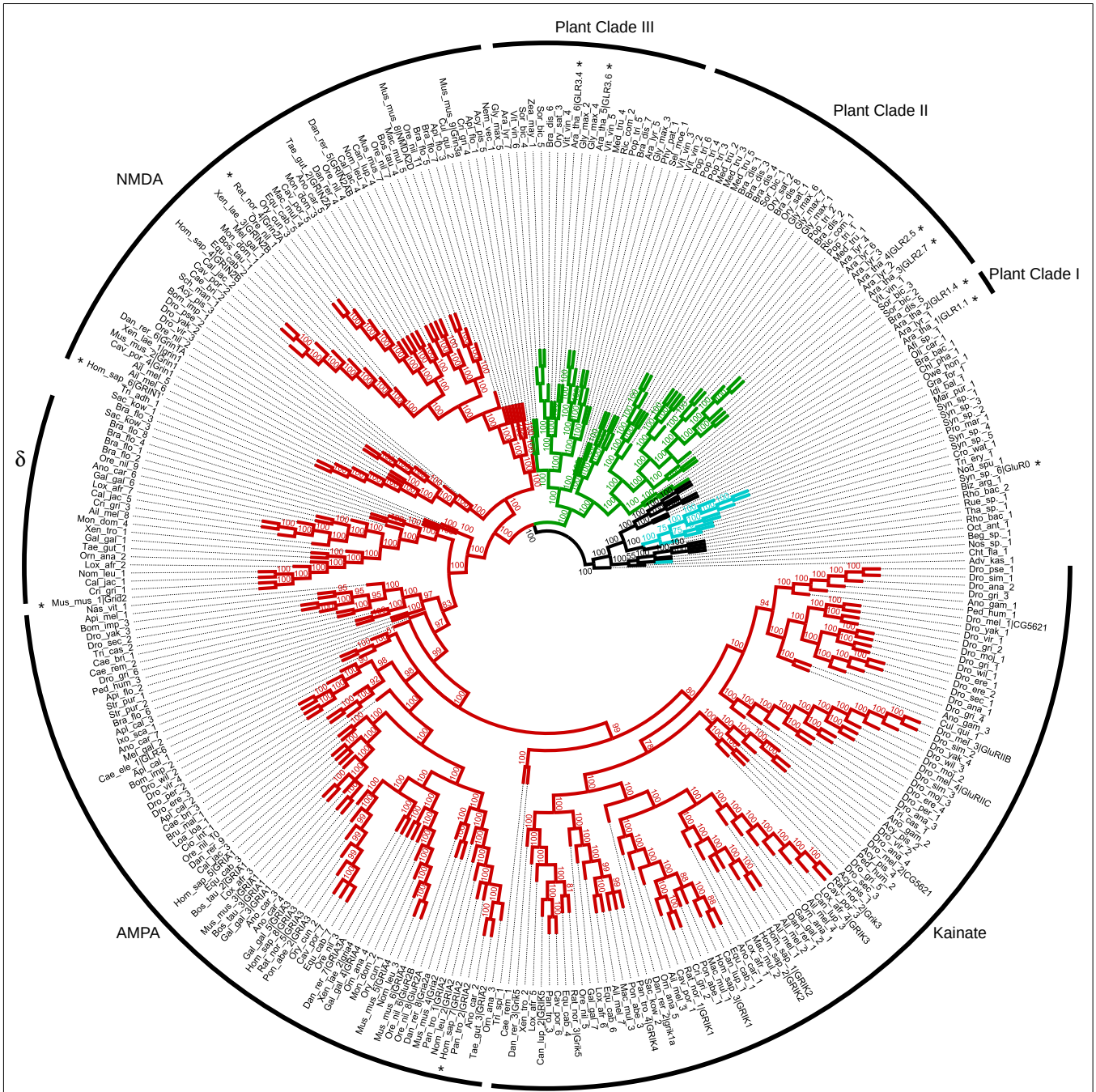

FIGURE 3 | Phylogenetic tree of plant, animal, and bacterial glutamate receptors. Metazoan, bacteria, cyanobacteria, plant proteins are marked in red, black, cyan, and green, respectively. NMDA, AMPA, and Kainate subfamilies of mammalian receptors are also indicated. Accession numbers of proteins included in the tree are provided in the Table S2 in Supplemental Material. Sequences represented in **Figure 4** are marked with asterisks.

have much broader specificity to ligands compared to their animal counterparts. To examine whether the LBD functions in a similar manner as its mammalian counterpart, ligand binding needs to be proven. The molecular structure of AtGLR3.4 in combination with the proposed ligands will help in understanding the basis of ligand gating mechanisms. Ligand specificity of other plant GLRs remains to be investigated.

CHANNEL SELECTIVITY

Mammalian iGluRs are non-selective cation channels (NSCCs) that function to conduct Na^+, K^+, and Ca^{2+} cations in the presence of glutamate (Kandel et al., 2000; Davenport, 2002; Furukawa et al., 2005). The selectivity for cations is determined by residues in the M2 and M3 regions that line the pore (Panchenko et al., 2001). For example, conversion of a glutamine residue into arginine through

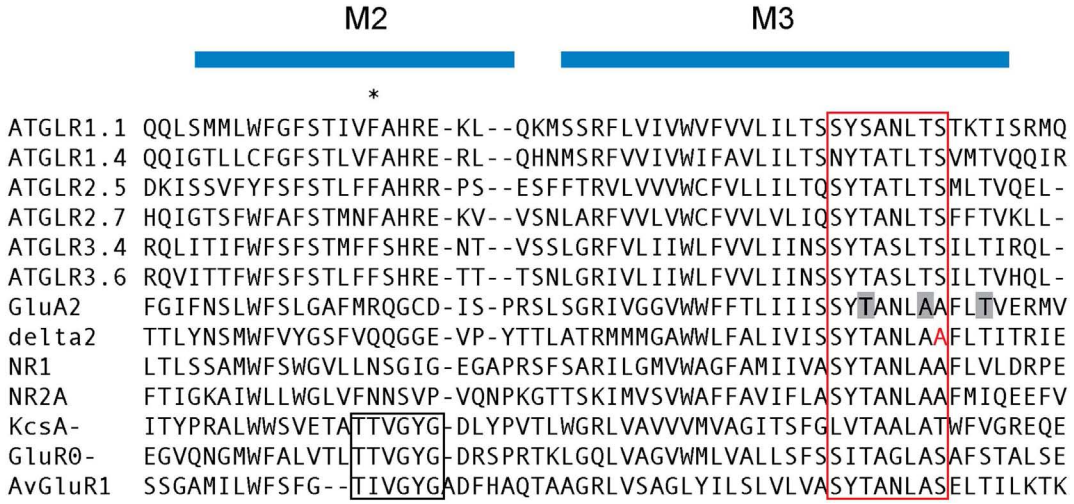

FIGURE 4 | An alignment of the regions consisting of the selectivity filter and the constrictive domain [the end of M2 (P-loop) and M3 region, respectively]. The Q/R/N site of mammalian glutamate receptors is marked with an asterisk. The SYTANLAA motif conserved among glutamate receptors is marked in red box. Residues that form the constrictive portion of GluA2 channel is marked with gray. The "lurcher" residue in δ2 is marked in red. The TXVGYG motif in the potassium channel KcsA, GluR0, and AvGluR1 is also marked by a box. AGI and Genbank accession numbers: ATGLR1.1, at3g04110; ATGLR1.4, at3g07520; ATGLR2.5, at5g11210; ATGLR2.7, at2g29120; ATGLR3.4, at1g05200; ATGLR3.6, at3G51480; GluA2 (*Rattus norvegicus*), NP_000817.2; delta2 (*Mus musculus*), *NP_032193.1*; NR1 (*Homo sapiens*), NP_015566.1; NR2A (*Rattus norvegicus*), NP_036705.3; KcsA (*Streptomyces lividans*), P0A334.1; GluR0 (*Synechocystis* sp. *PCC 6803*), ZP_06526299.1; AvGluR1 (*Adineta vaga*), ADW94593.1.

RNA editing in GluA2 results in a reduced permeability to Ca^{2+} (Egebjerg and Heinemann, 1993). This so-called Q/R/N site topologically overlaps with the selectivity filter of the potassium channel KcsA and the bacterial glutamate receptor GluR0, reinforcing the role of this domain in the determination of ion permeability. The recently resolved GluA2 structure revealed remarkable similarity between the overall topology between GluA2 and KcsA ion channel domains. The M3 domains of four subunits cross each other at the "SYTANLAA" motif, which is highly conserved in iGluRs, and form the narrowest portion of the channel (**Figures 2** and **4**; Sobolevsky et al., 2009).

While the "SYTANLAA" motif is also conserved in plant GLRs, primary sequence of the remainder of the M2 and M3 regions, which determines the selectivity of the channel, are completely different from animal iGluRs, hence it is reasonable to expect that the channel specificities would be different (**Figure 4**; Davenport, 2002). In fact, predicting the selectivity of the channel solely by the primary sequence is not possible, highlighted by a recent discovery of a glutamate receptor channel from *Adineta vaga*, which possesses a potassium selective "TXVGYG" motif, yet is permeable to Na^+ (Janovjak et al., 2011). Studies conducted thus far suggest that plant GLRs are NSCCs. *Arabidopsis* plants over-expressing the *At*GLR3.2 gene exhibited a phenotype consistent with Ca^{2+} deficiency that was reversed when supplemented with exogenous Ca^{2+} (Kim et al., 2001). These plants also exhibited an increased sensitivity to K^+, Na^+, and Mg^{2+}cations, consistent with their putative roles as NSCCs (Kim et al., 2001). Additionally, expression of *At*GLR3.7 in *Xenopus* oocytes enhanced plasma membrane conductance of Ba^{2+}, Ca^{2+}, and Na^+ ions, providing further evidence that plant GLRs function as NSCCs (Roy et al., 2008). Transplantation of the pore domains of *At*GLR1.1 and 1.4 into rat GluR1 and GluR6 chimeras produced functional K^+, Na^+, and Ca^{2+} channels, suggesting that *At*GLR1.1 and 1.4 function as NSCC (Tapken and Hollmann, 2008). One notable exception is *At*GLR3.4, which was shown to be highly selective to Ca^{2+} by whole-cell patch clamp of HEK293 cells expressing *At*GLR3.4 (Vincill et al., 2012).

PHARMACOLOGICAL PROPERTIES OF PLANT GLRs

Glutamate-like receptor homologs form a large family in plants, presenting a challenge for genetic approaches due to the potential for functional redundancy. To circumvent this, the utilization of pharmacology to act on multiple members of the family is a common strategy. As discussed previously, the LBD of plant GLRs shares homology at the amino acid level with mammalian iGluRs. Thus, several groups have investigated whether plant GLRs are influenced similarly to their mammalian counterparts in response to known iGluR agonists and antagonists (Lam et al., 1998; Brenner et al., 2000).

The possible *in vivo* function of plant GLRs was first examined by investigating the responses of plants to the known competitive antagonist 6,7-dinitroquinoxaline-2,3-(1*H*,4*H*)-dione (DNQX; Lam et al., 1998). When *Arabidopsis* seedlings were treated with DNQX, plants grown in light exhibited a dose- and light-dependent increase in hypocotyl elongation and reduced light-induced chlorophyll synthesis (Lam et al., 1998). Likewise, when light grown *Arabidopsis* seedlings were treated with *S*(+)-β-methyl-α,β-diaminopropionic acid (BMAA), an agonist of AMPA-kainate iGluRs, and a glutamate analog, hypocotyl elongation was increased while cotyledon opening was impaired (Brenner et al., 2000). BMAA-induced hypocotyl responses are alleviated when exogenous glutamate is applied, suggesting that there may be a conserved mechanism for the activity of BMAA between mammalian

and plant iGluRs (Brenner et al., 2000). In addition, the fact that two different compounds capable of interacting with mammalian iGluRs, DNQX, and BMAA, each induce hypocotyl elongation in light grown seedlings suggests a role for *At*GLRs in photomorphogenic development (Brenner et al., 2000). DNQX, along with AP-5 and 6-cyano-7-nitroquinoxaline-2,3-dione (CNQX), was also recently found to suppress pollen tube growth in tobacco (Michard et al., 2011).

In another study, it was revealed that Ca^{2+} conductance induced by microbe-associated molecular patterns (MAMPs) are inhibited specifically by mammalian glutamate receptor agonists (glutamate, aspartate) and antagonists (AP-5, AP7, and kynurenic acid; Kwaaitaal et al., 2011). In this study, DNQX, which had a pharmacological effect on the hypocotyl elongation, was not effective in inducing Ca^{2+} influx, suggesting that a different molecular target (e.g., a different subfamily of GLRs) are responsible for the influx of calcium compared to the situation in the hypocotyl. Direct evidence showing that mammalian glutamate receptor agonists and antagonists do bind plant GLRs, or discovery of more agonists and antagonists of plant GLRs, would accelerate the research tremendously.

SUBCELLULAR LOCALIZATION OF PLANT GLRs

Localization of iGluRs from metazoans is highly dynamic, continuously cycling between endosomal compartments and the "site of action," the postsynaptic membrane (Moss and Henley, 2002). So far, only two plant GLRs have been characterized for their subcellular localizations. AtGLR3.4 was shown to localize to the plasma membrane (Meyerhoff et al., 2005; Teardo et al., 2010, 2011; Vincill et al., 2012). Likewise, a GFP-fusion of a GLR from small radish (RsGluR) localized to the plasma membrane (Kang et al., 2006). Interestingly though, biochemical analysis using antibodies detected the presence of AtGLR3.4 in the chloroplast in addition to the plasma membrane (Teardo et al., 2011), and similar result was obtained in spinach (Teardo et al., 2010). Whether such dual-localization is common to other members of plant GLRs remains to be investigated.

PHYSIOLOGICAL ROLES OF PLANT GLRs

Now that ligand-gated calcium conductance of *At*GLR3.4 has been shown in the heterologous expression system, it seems that there is little doubt about at least one, probably more, of plant GLRs being amino acid-activated channels (Vincill et al., 2012). Although there is no experimental evidence showing that the topology of plant GLRs are identical to the animal GLRs, homology to the well characterized iGluRs from other organisms make such a scenario quite likely. Thus, one function of GLRs would be to sense amino acids at the exterior of the membrane in which the GLRs are localized.

A number of studies suggest that amino acid content in the apoplast is influenced by factors such as carbon and nitrogen supplies and stress. Microarray analysis using an inhibitor of glutamine biosynthesis suggested that a significant fraction of N-responsive genes (126/834) respond to the extracellular glutamate/glutamine, indicating a sensory mechanism for apoplasmic amino acids (Gutierrez et al., 2008). GLRs expressed at the plasma membrane function as sensory mechanisms for apoplasmic amino acids. Antisense plants for *At*GLR1.1 show altered transcript abundance in carbon and nitrogen metabolic enzymes such as cytosolic glutamine synthase (GS1), cytosolic aspartate aminotransferase (AAT2), nitrate reductase (NR1), nitrite reductase (NiR), nitrate transporter (CHL1), and hexokinase (HXK1; Kang and Turano, 2003). These results suggest a role for GLR1.1 in regulation of carbon and nitrogen metabolism (Kang and Turano, 2003; Kang et al., 2004).

In addition to the local nitrogen status, plants have intricate mechanism of communicating nitrogen availability in the rhizosphere to the above-ground organs (Ruffel et al., 2008, 2011). Although molecular mechanisms for such long-distance communication are not completely understood, it is well documented that the feeding of amino acids through the xylem induces transcriptional and post-transcriptional changes in key enzymes of the nitrogen assimilation pathway (Vincentz et al., 1993; Fritz et al., 2006; Sulieman et al., 2010). The amino acid profile in xylem sap, which is a continuum of the apoplasmic space, is influenced by many factors such as nitrogen supply, light cycle, and stress (Rosnitschek-Schimmel, 1985; Lam et al., 1995; Mayer, 2011). It is tempting to speculate that GLRs could be involved in amino acid sensing in the xylem. The expression patterns of GLRs suggest that at least some of them are expressed in the vasculature (Kim et al., 2001; Chiu et al., 2002; Meyerhoff et al., 2005; Cho et al., 2009). Perhaps GLRs play roles in the communication of C/N status in the apoplasm to the cells surrounding vascular tissue, in the form of Ca^{2+} signaling.

Recent studies reporting the localization of GLRs in chloroplasts indicate an additional role of GLRs in this organ. Indeed, plants carrying T-DNA insertions in AtGLR3.4 showed weak photosynthetic phenotypes (Teardo et al., 2010, 2011). The exact roles of GLRs in chloroplasts awaits further investigation.

Amino acids are also involved in host-pathogen interactions. Changes in the amino acid profile in the apoplasm upon pathogen infection have been documented in multiple host-pathogen combinations (Solomon and Oliver, 2001). Recent findings show that the availability of apoplasmic GABA is important for colonization of tomato by *Pseudomonas syringae*, yet a relatively high concentration of GABA enhances the defense response of plants (Park et al., 2010). GABA is also involved in quorum sensing in *Agrobacterium*, which is counteracted by another amino acid, proline (Chevrot et al., 2006; Haudecoeur et al., 2009). Further, it is interesting that the NMDA receptor agonists applied to *Arabidopsis* seedlings inhibit the cytosolic calcium peaks induced by MAMPs (Kwaaitaal et al., 2011). Whether GLRs play a role in sensing changes in amino acids induced by plant-pathogen interaction remains to be seen.

Interestingly, pharmacological and genetic approaches to understand the functions of GLR revealed their roles in biological processes that were previously not linked to extracellular amino acids. Recently it was demonstrated that gene insertions in *At*GLR1.2 and 3.7 result in a pollen tube phenotype, and that the Ca^{2+} signature was altered in a *glr1.2* mutant. Moreover, D-Ser, an agonist to animal iGluR, is capable of inducing calcium peaks in the growing pollen tube, and pollen tube growth is disturbed in a knock-out mutant of serine-racemase (SR1). These results suggested a possible involvement of D-Ser and GLRs in male gametophyte-pistil communication (Michard et al., 2011). Interestingly, a concentration gradient of another amino acid, GABA

was shown to be important in the guidance of the pollen tube (Palanivelu et al., 2003). It is possible that more members of the GLR family are involved in such cell-to-cell communication in plants. Likewise, it was shown that *At*GLR3.1 is expressed preferentially in guard cells, and over-expression of *At*GLR3.1 has been shown to lead to the impairment of stomatal closure that is induced by external Ca^{2+} (Cho et al., 2009). Since amino acid-gated channel activity is not reported for *At*GLR3.1, whether the channel conductivity is influenced by apoplasmic amino acid remain to be seen.

FUTURE PERSPECTIVES

After 14 years of research, we are now beginning to understand the diverse functions of plant GLRs. However, our understanding of their molecular mechanisms is still in its infancy. For example, conductivity and ligand spectrum for more subunits need to be elucidated in order to understand their *in vivo* function. Successful expression in heterologous systems such as mammalian cell culture and *Xenopus* oocyte would be a key step. It has previously been reported that plant GLRs do not localize to the membrane when expressed in heterologous systems (Li et al., 2006). Analogous to some of the obligatory heteromers in animal systems, correct formation of heteromer might be necessary for the trafficking of receptor complexes to the plasma membrane (Qiu et al., 2009). Co-expression analysis at a higher resolution, as well as protein–protein interaction studies in a heterologous system such as yeast (Lalonde et al., 2010) will help in identifying the necessary components of functional channels.

Another open area is the post-translational regulation of plant GLRs. The C-termini of animal GLRs contain multiple sites for phosphorylation and protein–protein interaction, which in turn determine the localization and surface expression of the receptor (Chen and Roche, 2007; Bard and Groc, 2011). Interestingly, multiple GLRs (1.2, 2.1, 2.9, 3.4, 3.7) were identified as potential 14-3-3 client proteins in a proteomics study (Chang et al., 2009). The effect of such interactions on channel properties would be an interesting subject.

SUPPLEMENTARY MATERIAL

The Supplementary Material for this article can be found online at: http://www.frontiersin.org/Plant_Traffic_and_Transport/10.3389/fpls.2012.00235/abstract

REFERENCES

Adl, S. M., Simpson, A. G., Farmer, M. A., Andersen, R. A., Anderson, O. R., Barta, J. R., et al. (2005). The new higher level classification of eukaryotes with emphasis on the taxonomy of protists. *J. Eukaryot. Microbiol.* 52, 399–451.

Armstrong, N., and Gouaux, E. (2000). Mechanisms for activation and antagonism of an AMPA-sensitive glutamate receptor: crystal structures of the GluR2 ligand binding core. *Neuron* 28, 165–181.

Armstrong, N., Sun, Y., Chen, G. Q., and Gouaux, E. (1998). Structure of a glutamate-receptor ligand-binding core in complex with kainate. *Nature* 395, 913–917.

Barbosa, J. M., Singh, N. K., Cherry, J. H., and Locy, R. D. (2010). Nitrate uptake and utilization is modulated by exogenous gamma-aminobutyric acid in Arabidopsis thaliana seedlings. *Plant Physiol. Biochem.* 48, 443–450.

Bard, L., and Groc, L. (2011). Glutamate receptor dynamics and protein interaction: lessons from the NMDA receptor. *Mol. Cell. Neurosci.* 48, 298–307.

Brenner, E. D., Martinez-Barboza, N., Clark, A. P., Liang, Q. S., Stevenson, D. W., and Coruzzi, G. M. (2000). Arabidopsis mutants resistant to S(+)-beta-methyl-alpha, beta-diaminopropionic acid, a cycad-derived glutamate receptor agonist. *Plant Physiol.* 124, 1615–1624.

Chang, I. F., Curran, A., Woolsey, R., Quilici, D., Cushman, J. C., Mittler, R., et al. (2009). Proteomic profiling of tandem affinity purified 14-3-3 protein complexes in Arabidopsis thaliana. *Proteomics* 9, 2967–2985.

Chen, B. S., and Roche, K. W. (2007). Regulation of NMDA receptors by phosphorylation. *Neuropharmacology* 53, 362–368.

Chen, G. Q., Cui, C., Mayer, M. L., and Gouaux, E. (1999). Functional characterization of a potassium-selective prokaryotic glutamate receptor. *Nature* 402, 817–821.

Chevrot, R., Rosen, R., Haudecoeur, E., Cirou, A., Shelp, B. J., Ron, E., et al. (2006). GABA controls the level of quorum-sensing signal in *Agrobacterium tumefaciens*. *Proc. Natl. Acad. Sci. U.S.A.* 103, 7460–7464.

Chiu, J., Desalle, R., Lam, H. M., Meisel, L., and Coruzzi, G. (1999). Molecular evolution of glutamate receptors: a primitive signaling mechanism that existed before plants and animals diverged. *Mol. Biol. Evol.* 16, 826–838.

Chiu, J. C., Brenner, E. D., Desalle, R., Nitabach, M. N., Holmes, T. C., and Coruzzi, G. M. (2002). Phylogenetic and expression analysis of the glutamate-receptor-like gene family in Arabidopsis thaliana. *Mol. Biol. Evol.* 19, 1066–1082.

Cho, D., Kim, S. A., Murata, Y., Lee, S., Jae, S. K., Nam, H. G., et al. (2009). De-regulated expression of the plant glutamate receptor homolog AtGLR3.1 impairs long-term Ca2+-programmed stomatal closure. *Plant J.* 58, 437–449.

Connaughton, V. (2007). "Glutamate and glutamate receptors in the vertebrate retina," in *Webvision: The Organization of the Retina and Visual System*, eds H. Kolb, E. Fernandez, and R. Nelson (Salt Lake City: University of Utah Health Sciences Center).

Davenport, R. (2002). Glutamate receptors in plants. *Ann. Bot.* 90, 549–557.

Demidchik, V., Essah, P. A., and Tester, M. (2004). Glutamate activates cation currents in the plasma membrane of Arabidopsis root cells. *Planta* 219, 167–175.

Dennison, K. L., and Spalding, E. P. (2000). Glutamate-gated calcium fluxes in Arabidopsis. *Plant Physiol.* 124, 1511–1514.

Deprost, D., Yao, L., Sormani, R., Moreau, M., Leterreux, G., Nicolai, M., et al. (2007). The Arabidopsis TOR kinase links plant growth, yield, stress resistance and mRNA translation. *EMBO Rep.* 8, 864–870.

Didion, T., Regenberg, B., Jorgensen, M. U., Kielland-Brandt, M. C., and Andersen, H. A. (1998). The permease homologue Ssy1p controls the expression of amino acid and peptide transporter genes in Saccharomyces cerevisiae. *Mol. Microbiol.* 27, 643–650.

Dingledine, R., Borges, K., Bowie, D., and Traynelis, S. F. (1999). The glutamate receptor ion channels. *Pharmacol. Rev.* 51, 7–61.

Doyle, D. A., Morais Cabral, J., Pfuetzner, R. A., Kuo, A., Gulbis, J. M., Cohen, S. L., et al. (1998). The structure of the potassium channel: molecular basis of K+ conduction and selectivity. *Science* 280, 69–77.

Dubos, C., Huggins, D., Grant, G. H., Knight, M. R., and Campbell, M. M. (2003). A role for glycine in the gating of plant NMDA-like receptors. *Plant J.* 35, 800–810.

Dubos, C., Willment, J., Huggins, D., Grant, G. H., and Campbell, M. M. (2005). Kanamycin reveals the role played by glutamate receptors in shaping plant resource allocation. *Plant J.* 43, 348–355.

Egebjerg, J., and Heinemann, S. F. (1993). Ca2+ permeability of unedited and edited versions of the kainate selective glutamate receptor GluR6. *Proc. Natl. Acad. Sci. U.S.A.* 90, 755–759.

Fritz, C., Mueller, C., Matt, P., Feil, R., and Stitt, M. (2006). Impact of the C-N status on the amino acid profile in tobacco source leaves. *Plant Cell Environ.* 29, 2055–2076.

Furukawa, H., Singh, S. K., Mancusso, R., and Gouaux, E. (2005). Subunit arrangement and function in NMDA receptors. *Nature* 438, 185–192.

Gereau, R. W., and Swanson, G. (2008). *The Glutamate Receptors*. New York: Humana Press.

Greger, I. H., Akamine, P., Khatri, L., and Ziff, E. B. (2006). Developmentally regulated, combinatorial RNA processing modulates AMPA receptor biogenesis. *Neuron* 51, 85–97.

Gutierrez, R. A., Stokes, T. L., Thum, K., Xu, X., Obertello, M., Katari, M. S., et al. (2008). Systems approach identifies an organic nitrogen-responsive gene network that is regulated by the master clock control gene CCA1. *Proc. Natl. Acad. Sci. U.S.A.* 105, 4939–4944.

Haudecoeur, E., Planamente, S., Cirou, A., Tannieres, M., Shelp, B. J., Morera, S., et al. (2009). Proline antagonizes GABA-induced quenching of quorum-sensing in Agrobacterium tumefaciens. *Proc. Natl. Acad. Sci. U.S.A.* 106, 14587–14592.

Hinnebusch, A. G. (2005). Translational regulation of GCN4 and the general amino acid control of yeast. *Annu. Rev. Microbiol.* 59, 407–450.

Hirner, A., Ladwig, F., Stransky, H., Okumoto, S., Keinath, M., Harms, A., et al. (2006). Arabidopsis LHT1 is a high-affinity transporter for cellular amino acid uptake in both root epidermis and leaf mesophyll. *Plant Cell* 18, 1931–1946.

Hundal, H. S., and Taylor, P. M. (2009). Amino acid transceptors: gate keepers of nutrient exchange and regulators of nutrient signaling. *Am. J. Physiol. Endocrinol. Metab.* 296, E603–E613.

Jacinto, E., and Hall, M. N. (2003). Tor signalling in bugs, brain and brawn. *Nat. Rev. Mol. Cell Biol.* 4, 117–126.

Janovjak, H., Sandoz, G., and Isacoff, E. Y. (2011). A modern ionotropic glutamate receptor with a K(+) selectivity signature sequence. *Nat. Commun.* 2, 232.

Jin, R., Singh, S. K., Gu, S., Furukawa, H., Sobolevsky, A. I., Zhou, J., et al. (2009). Crystal structure and association behaviour of the GluR2 amino-terminal domain. *EMBO J.* 28, 1812–1823.

Kandel, E. R., Schwartz, J. H., and Jessell, T. M. (2000). *Principles of Neural Science.* New York: McGraw-Hill.

Kang, J., Mehta, S., and Turano, F. J. (2004). The putative glutamate receptor 1.1 (AtGLR1.1) in Arabidopsis thaliana regulates abscisic acid biosynthesis and signaling to control development and water loss. *Plant Cell Physiol.* 45, 1380–1389.

Kang, J., and Turano, F. J. (2003). The putative glutamate receptor 1.1 (AtGLR1.1) functions as a regulator of carbon and nitrogen metabolism in Arabidopsis thaliana. *Proc. Natl. Acad. Sci. U.S.A.* 100, 6872–6877.

Kang, S., Kim, H. B., Lee, H., Choi, J. Y., Heu, S., Oh, C. J., et al. (2006). Overexpression in Arabidopsis of a plasma membrane-targeting glutamate receptor from small radish increases glutamate-mediated Ca2+ influx and delays fungal infection. *Mol. Cells* 21, 418–427.

Karakas, E., Simorowski, N., and Furukawa, H. (2011). Subunit arrangement and phenylethanolamine binding in GluN1/GluN2B NMDA receptors. *Nature* 475, 249–253.

Keeling, P. J., Burger, G., Durnford, D. G., Lang, B. F., Lee, R. W., Pearlman, R. E., et al. (2005). The tree of eukaryotes. *Trends Ecol. Evol. (Amst.)* 20, 670–676.

Kim, S. A., Kwak, J. M., Jae, S. K., Wang, M. H., and Nam, H. G. (2001). Overexpression of the AtGluR2 gene encoding an Arabidopsis homolog of mammalian glutamate receptors impairs calcium utilization and sensitivity to ionic stress in transgenic plants. *Plant Cell Physiol.* 42, 74–84.

Kumar, J., Schuck, P., and Mayer, M. L. (2011). Structure and assembly mechanism for heteromeric kainate receptors. *Neuron* 71, 319–331.

Kwaaitaal, M., Huisman, R., Maintz, J., Reinstadler, A., and Panstruga, R. (2011). Ionotropic glutamate receptor (iGluR)-like channels mediate MAMP-induced calcium influx in Arabidopsis thaliana. *Biochem. J.* 440, 355–365.

Lalonde, S., Sero, A., Pratelli, R., Pilot, G., Chen, J., Sardi, M. I., et al. (2010). A membrane protein/signaling protein interaction network for Arabidopsis version AMPv2. *Front. Physiol.* 1:24. doi:10.3389/fphys.2010.00024

Lam, H. M., Chiu, J., Hsieh, M. H., Meisel, L., Oliveira, I. C., Shin, M., et al. (1998). Glutamate-receptor genes in plants. *Nature* 396, 125–126.

Lam, H. M., Coschigano, K., Schultz, C., Melo-Oliveira, R., Tjaden, G., Oliveira, I., et al. (1995). Use of Arabidopsis mutants and genes to study amide amino acid biosynthesis. *Plant Cell* 7, 887–898.

Leigh, J. A., and Dodsworth, J. A. (2007). Nitrogen regulation in bacteria and archaea. *Annu. Rev. Microbiol.* 61, 349–377.

Li, J., Zhu, S., Song, X., Shen, Y., Chen, H., Yu, J., et al. (2006). A rice glutamate receptor-like gene is critical for the division and survival of individual cells in the root apical meristem. *Plant Cell* 18, 340–349.

Lipton, S. A., Kim, W. K., Choi, Y. B., Kumar, S., D'Emilia, D. M., Rayudu, P. V., et al. (1997). Neurotoxicity associated with dual actions of homocysteine at the N-methyl-D-aspartate receptor. *Proc. Natl. Acad. Sci. U.S.A.* 94, 5923–5928.

MacKinnon, R. (2003). Potassium channels. *FEBS Lett.* 555, 62–65.

Mano, I., and Teichberg, V. I. (1998). A tetrameric subunit stoichiometry for a glutamate receptor-channel complex. *Neuroreport* 9, 327–331.

Mayer, M. L. (2005). Glutamate receptor ion channels. *Curr. Opin. Neurobiol.* 15, 282–288.

Mayer, M. L. (2006). Glutamate receptors at atomic resolution. *Nature* 440, 456–462.

Mayer, M. L. (2011). Emerging models of glutamate receptor ion channel structure and function. *Structure* 19, 1370–1380.

Meyerhoff, O., Muller, K., Roelfsema, M. R., Latz, A., Lacombe, B., Hedrich, R., et al. (2005). AtGLR3.4, a glutamate receptor channel-like gene is sensitive to touch and cold. *Planta* 222, 418–427.

Michard, E., Lima, P. T., Borges, F., Silva, A. C., Portes, M. T., Carvalho, J. E., et al. (2011). Glutamate receptor-like genes form Ca2+ channels in pollen tubes and are regulated by pistil D-serine. *Science* 332, 434–437.

Miller, N. D., Durham Brooks, T. L., Assadi, A. H., and Spalding, E. P. (2010). Detection of a gravitropism phenotype in glutamate receptor-like 3.3 mutants of Arabidopsis thaliana using machine vision and computation. *Genetics* 186, 585–593.

Monyer, H., Sprengel, R., Schoepfer, R., Herb, A., Higuchi, M., Lomeli, H., et al. (1992). Heteromeric NMDA receptors: molecular and functional distinction of subtypes. *Science* 256, 1217–1221.

Moss, S. J., and Henley, J. (2002). *Receptor and Ion-Channel Trafficking: Cell Biology of Ligand-Gated and Voltage-Sensitive Ion Channels.* New York: Oxford University Press.

Nakanishi, N., Shneider, N. A., and Axel, R. (1990). A family of glutamate receptor genes: evidence for the formation of heteromultimeric receptors with distinct channel properties. *Neuron* 5, 569–581.

Naur, P., Vestergaard, B., Skov, L. K., Egebjerg, J., Gajhede, M., and Kastrup, J. S. (2005). Crystal structure of the kainate receptor GluR5 ligand-binding core in complex with (S)-glutamate. *FEBS Lett.* 579, 1154–1160.

Nazoa, P., Vidmar, J. J., Tranbarger, T. J., Mouline, K., Damiani, I., Tillard, P., et al. (2003). Regulation of the nitrate transporter gene AtNRT2.1 in Arabidopsis thaliana: responses to nitrate, amino acids and developmental stage. *Plant Mol. Biol.* 52, 689–703.

Oliveira, I. C., Brenner, E., Chiu, J., Hsieh, M. H., Kouranov, A., Lam, H. M., et al. (2001). Metabolite and light regulation of metabolism in plants: lessons from the study of a single biochemical pathway. *Braz. J. Med. Biol. Res.* 34, 567–575.

Palanivelu, R., Brass, L., Edlund, A. F., and Preuss, D. (2003). Pollen tube growth and guidance is regulated by POP2, an Arabidopsis gene that controls GABA levels. *Cell* 114, 47–59.

Panchenko, V. A., Glasser, C. R., and Mayer, M. L. (2001). Structural similarities between glutamate receptor channels and K(+) channels examined by scanning mutagenesis. *J. Gen. Physiol.* 117, 345–360.

Park, D. H., Mirabella, R., Bronstein, P. A., Preston, G. M., Haring, M. A., Lim, C. K., et al. (2010). Mutations in gamma-aminobutyric acid (GABA) transaminase genes in plants or Pseudomonas syringae reduce bacterial virulence. *Plant J.* 64, 318–330.

Pasternack, A., Coleman, S. K., Jouppila, A., Mottershead, D. G., Lindfors, M., Pasternack, M., et al. (2002). Alpha-amino-3-hydroxy-5-methyl-4-isoxazolepropionic acid (AMPA) receptor channels lacking the N-terminal domain. *J. Biol. Chem.* 277, 49662–49667.

Pohlsgaard, J., Frydenvang, K., Madsen, U., and Kastrup, J. S. (2011). Lessons from more than 80 structures of the GluA2 ligand-binding domain in complex with agonists, antagonists and allosteric modulators. *Neuropharmacology* 60, 135–150.

Qi, Z., Stephens, N. R., and Spalding, E. P. (2006). Calcium entry mediated by GLR3.3, an Arabidopsis glutamate receptor with a broad agonist profile. *Plant Physiol.* 142, 963–971.

Qiu, S., Zhang, X. M., Cao, J. Y., Yang, W., Yan, Y. G., Shan, L., et al. (2009). An endoplasmic reticulum retention signal located in the extracellular amino-terminal domain of the NR2A subunit of N-Methyl-D-aspartate receptors. *J. Biol. Chem.* 284, 20285–20298.

Rawat, S. R., Silim, S. N., Kronzucker, H. J., Siddiqi, M. Y., and Glass, A. D. (1999). AtAMT1 gene expression and NH4+ uptake in roots of Arabidopsis thaliana: evidence for regulation by root glutamine levels. *Plant J.* 19, 143–152.

Rosenmund, C., Stern-Bach, Y., and Stevens, C. F. (1998). The tetrameric structure of a glutamate receptor channel. *Science* 280, 1596–1599.

Rosnitschek-Schimmel, I. (1985). The influence of nitrogen nutrition on the accumulation of free amino acids in root tissue of Urtica dioica [Urticaceae] and their apical

transport in xylem sap. *Plant Cell Physiol.* 26, 215–219.

Roy, S. J., Gilliham, M., Berger, B., Essah, P. A., Cheffings, C., Miller, A. J., et al. (2008). Investigating glutamate receptor-like gene co-expression in Arabidopsis thaliana. *Plant Cell Environ.* 31, 861–871.

Ruffel, S., Freixes, S., Balzergue, S., Tillard, P., Jeudy, C., Martin-Magniette, M. L., et al. (2008). Systemic signaling of the plant nitrogen status triggers specific transcriptome responses depending on the nitrogen source in Medicago truncatula. *Plant Physiol.* 146, 2020–2035.

Ruffel, S., Krouk, G., Ristova, D., Shasha, D., Birnbaum, K. D., and Coruzzi, G. M. (2011). Nitrogen economics of root foraging: transitive closure of the nitrate-cytokinin relay and distinct systemic signaling for N supply vs. demand. *Proc. Natl. Acad. Sci. U.S.A.* 108, 18524–18529.

Schwartz, J. H. (2000). "Many neuroactive peptides serve as neuotransmitters," in *Principles of Neural Science*, eds E. R. Kandel, J. H. Schwartz, and T. M. Jessell (New York: McGraw-Hill), 286–290.

Simpson, A. G., and Roger, A. J. (2002). Eukaryotic evolution: getting to the root of the problem. *Curr. Biol.* 12, R691–R693.

Sobolevsky, A. I., Rosconi, M. P., and Gouaux, E. (2009). X-ray structure, symmetry and mechanism of an AMPA-subtype glutamate receptor. *Nature* 462, 745–756.

Solomon, P. S., and Oliver, R. P. (2001). The nitrogen content of the tomato leaf apoplast increases during infection by Cladosporium fulvum. *Planta* 213, 241–249.

Stephens, N. R., Qi, Z., and Spalding, E. P. (2008). Glutamate receptor subtypes evidenced by differences in desensitization and dependence on the GLR3.3 and GLR3.4 genes. *Plant Physiol.* 146, 529–538.

Sulieman, S., Fischinger, S. A., Gresshoff, P. M., and Schulze, J. (2010). Asparagine as a major factor in the N-feedback regulation of N2 fixation in Medicago truncatula. *Physiol. Plant* 140, 21–31.

Tapken, D., and Hollmann, M. (2008). Arabidopsis thaliana glutamate receptor ion channel function demonstrated by ion pore transplantation. *J. Mol. Biol.* 383, 36–48.

Teardo, E., Formentin, E., Segalla, A., Giacometti, G. M., Marin, O., Zanetti, M., et al. (2011). Dual localization of plant glutamate receptor AtGLR3.4 to plastids and plasmamembrane. *Biochim. Biophys. Acta* 1807, 359–367.

Teardo, E., Segalla, A., Formentin, E., Zanetti, M., Marin, O., Giacometti, G. M., et al. (2010). Characterization of a plant glutamate receptor activity. *Cell. Physiol. Biochem.* 26, 253–262.

Tegeder, M. (2012). Transporters for amino acids in plant cells: some functions and many unknowns. *Curr. Opin. Plant Biol.* 15, 315–321.

Traynelis, S. F., Wollmuth, L. P., Mcbain, C. J., Menniti, F. S., Vance, K. M., Ogden, K. K., et al. (2010). Glutamate receptor ion channels: structure, regulation, and function. *Pharmacol. Rev.* 62, 405–496.

Vincentz, M., Moureaux, T., Leydecker, M. T., Vaucheret, H., and Caboche, M. (1993). Regulation of nitrate and nitrite reductase expression in Nicotiana-plumbaginifolia leaves by nitrogen and carbon metabolites. *Plant J.* 3, 315–324.

Vincill, E. D., Bieck, A. M., and Spalding, E. P. (2012). Ca2+ conduction by an amino acid-gated ion channel related to glutamate receptors. *Plant Physiol.* 159, 40–46.

Wipf, D., Ludewig, U., Tegeder, M., Rentsch, D., Koch, W., and Frommer, W. B. (2002). Conservation of amino acid transporters in fungi, plants and animals. *Trends Biochem. Sci.* 27, 139–147.

Wolosker, H. (2006). D-serine regulation of NMDA receptor activity. *Sci. STKE* 2006, pe41.

Yu, G., Liang, J., He, Z., and Sun, M. (2006). Quantum dot-mediated detection of gamma-aminobutyric acid binding sites on the surface of living pollen protoplasts in tobacco. *Chem. Biol.* 13, 723–731.

Zuo, J., De Jager, P. L., Takahashi, K. A., Jiang, W., Linden, D. J., and Heintz, N. (1997). Neurodegeneration in Lurcher mice caused by mutation in delta2 glutamate receptor gene. *Nature* 388, 769–773.

Conflict of Interest Statement: The authors declare that the research was conducted in the absence of any commercial or financial relationships that could be construed as a potential conflict of interest.

Received: 11 July 2012; paper pending published: 19 August 2012; accepted: 02 October 2012; published online: 30 October 2012.

Citation: Price MB, Jelesko J and Okumoto S (2012) Glutamate receptor homologs in plants: functions and evolutionary origins. Front. Plant Sci. ***3****:235. doi: 10.3389/fpls.2012.00235*

This article was submitted to Frontiers in Plant Traffic and Transport, a specialty of Frontiers in Plant Science.

frontiers in
PLANT SCIENCE

REVIEW ARTICLE
published: 05 October 2012
doi: 10.3389/fpls.2012.00223

How membranes shape plant symbioses: signaling and transport in nodulation and arbuscular mycorrhiza

Laure Bapaume and Didier Reinhardt*

Department of Biology, University of Fribourg, Fribourg, Switzerland

Edited by:
Markus Geisler, University of Fribourg, Switzerland

Reviewed by:
Daniel Wipf, Burgundy University, France
Soizic Rochange, Toulouse University, France

****Correspondence:***
Didier Reinhardt, Department of Biology, University of Fribourg, Rte Albert Gockel 3, CH-1700 Fribourg, Switzerland.
e-mail: didier.reinhardt@unifr.ch

As sessile organisms that cannot evade adverse environmental conditions, plants have evolved various adaptive strategies to cope with environmental stresses. One of the most successful adaptations is the formation of symbiotic associations with beneficial microbes. In these mutualistic interactions the partners exchange essential nutrients and improve their resistance to biotic and abiotic stresses. In arbuscular mycorrhiza (AM) and in root nodule symbiosis (RNS), AM fungi and rhizobia, respectively, penetrate roots and accommodate within the cells of the plant host. In these endosymbiotic associations, both partners keep their plasma membranes intact and use them to control the bidirectional exchange of signaling molecules and nutrients. Intracellular accommodation requires the exchange of symbiotic signals and the reprogramming of both interacting partners. This involves fundamental changes at the level of gene expression and of the cytoskeleton, as well as of organelles such as plastids, endoplasmic reticulum (ER), and the central vacuole. Symbiotic cells are highly compartmentalized and have a complex membrane system specialized for the diverse functions in molecular communication and nutrient exchange. Here, we discuss the roles of the different cellular membrane systems and their symbiosis-related proteins in AM and RNS, and we review recent progress in the analysis of membrane proteins involved in endosymbiosis.

Keywords: symbiosis, arbuscule, mycorrhiza, LysM receptor, SYMRK, VAPYRIN, root nodules, rhizobium

INTRODUCTION

In nature, the majority of plants live in association with fungal and/or bacterial symbionts. The most widespread symbiosis in all taxa of extant land plants is arbuscular mycorrhiza (AM). The fossil record and phylogenetic analysis suggest an early origin of AM before the Devonian period, approximately 450 Ma ago (Redecker et al., 2000; Heckman et al., 2001; Kistner and Parniske, 2002). AM occurs between fungi of the phylum *Glomeromycota*, also referred to as AM fungi, and the majority of land plants in almost all ecological niches (Wang and Qiu, 2006), and is thought to be essential for plant survival in harsh environments such as deserts and hot springs (Bunn et al., 2009; Al-Yahya'ei et al., 2011). Whereas AM fungi can colonize the majority of land plants, root nodule symbiosis (RNS) with bacteria (rhizobia), which has evolved considerably later than AM (Kistner and Parniske, 2002), involves almost exclusively legumes (*Fabaceae*).

Abbreviations: AM, Arbuscular mycorrhiza; CCaMK, Calcium and calmodulin-dependent protein kinase; DMI, Does not make infections; ER, Endoplasmic reticulum; IT, Infection thread; LCO, Lipochitooligosaccharide; LRR, Leucine-rich repeat; LYK, LysM-containing receptor-like kinase; LYM, LysM-containing protein; LysM, Lysin motif; MAPK, Mitogen-activated protein kinase; MF, Myc factor, mycorrhization factor; MFR, Myc factor receptor; NCR, Nodule-specific cysteine-rich; NF, Nod factor, nodulation factor; NFR, Nod factor receptor; NPC, Nuclear pore complex; PAM, Periarbuscular membrane; PIT, Pre-infection thread; PPA, Prepenetration apparatus; PT, Phosphate transporter; RNS, Root nodule symbiosis; SNARE, soluble *N*-ethylmaleimide-sensitive factor attachment protein receptor; SPC, Signal peptidase complex; SYMRK, Symbiosis receptor kinase; SYP, Syntaxin of plants; VAMP, Vesicle-associated membrane protein.

AM and RNS are both regulated by a common set of genes that define the common SYM pathway. They encode a receptor kinase localized to the plasma membrane, components of signal transduction to the nucleus, and a nuclear CCaMK (calcium and calmodulin-dependent protein kinase; Parniske, 2008; Oldroyd et al., 2011; Singh and Parniske, 2012).

Upon detection of AM fungal hyphopodia, epidermal cells generate an infection structure, the prepenetration apparatus (PPA) that is essential for infection of epidermal cells (Genre et al., 2005, 2008). At later stages of AM, finely branched hyphal structures, the arbuscules, are formed by AM fungi which serve to increase the surface area for nutrient exchange. In RNS, root hair cells form a curl in which bacteria are entrapped and subsequently guided through an infection thread (IT) toward the root cortex (Fournier et al., 2008). Cortical cells prepare for infection with a pre-infection thread (PIT) before they come into contact with the rhizobia (Van Brussel et al., 1992). Ultimately, in the mature nodules, bacteria differentiate into bacteroids inside the cytoplasm of the host (Jones et al., 2007; Oldroyd et al., 2011).

The arbuscules and bacteroids are contained within host-derived membranes that represent specialized symbiotic interfaces dedicated to nutrient exchange (Spaink, 1995; Limpens et al., 2005; Parniske, 2008). As a consequence of the large contact area between the host and the endosymbiont, the membrane surface area of host cells (comprising plasma membrane and the membrane around the endosymbiont) increases several-fold during arbuscule formation (Cox and Sanders, 1974), and up to

20-fold in the case of nodule cells filled with nitrogen-fixing bacteria (Verma et al., 1978). Similarly, the endomembrane system undergoes a general expansion since the amount of organelles such as ER, plastids, and mitochondria is amplified (Genre et al., 2005; Lohse et al., 2005; Fournier et al., 2008; Genre et al., 2008; **Figures 1** and **2**). These adaptations during the transition of a cortical cell to an active symbiotic machinery requires the production of large amounts of new membrane material in the host, and of specialized membrane proteins for symbiotic communication and nutrient exchange.

While the components involved in recognition and signal transduction are expressed constitutively, the machinery required for the functioning of endosymbioses is induced as a consequence of the transcriptional reprogramming of the symbiotic host cells. Many of these genes, which encode among others transporters of various mineral nutrients, are expressed only in symbiotic cells and are therefore likely to play symbiosis-specific roles. In the case of AM, the plant receives nutrients such as phosphorus (P), nitrogen (N), sulfur (S), zinc (Zn), and copper (Cu), which are taken up by the periarbuscular membrane (PAM) in arbuscule-containing cells (Clark and Zeto, 2000; Karandashov and Bucher, 2005; Allen and Shachar-Hill, 2009; Tian et al., 2010; Smith and Smith, 2011), whereas in RNS, the plant is provided with N only (Prell and Poole, 2006). In exchange plants provide carbohydrates (C) to their symbionts (Prell and Poole, 2006; Smith and Smith, 2011). Consistent with a central role of membranes in symbiosis, a large part of the symbiosis-related proteins are localized to membranes. Here, we discuss the different roles of membrane systems in endosymbiosis and we review recent progress in the analysis of symbiosis-related proteins on membranes and their roles in signaling, intracellular accommodation, and nutrient transport.

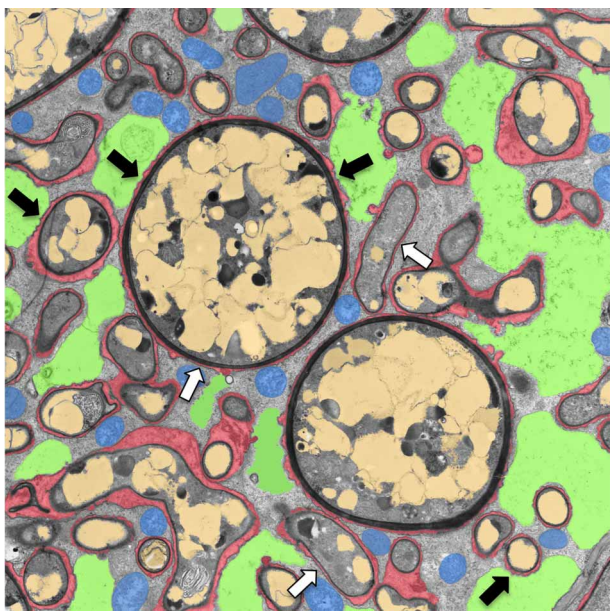

FIGURE 1 | Transmission electron micrograph of a cortical cell of *P. hybrida* colonized by *G. intraradices* (*Rhizophagus irregularis*). For clarity, cellular components are pseudocolored as follows: green, fragmented plant vacuole; blue, plant mitochondria and plastids; light brown, fungal vacuoles; red, symbiotic interface. Note the very close contact of the periarbuscular membrane (PAM) with fungal hyphae (white arrows), and the proximity of the tonoplast with the PAM (black arrows).

SYMBIOTIC SIGNALING

FLAVONOIDS, STRIGOLACTONES, NOD FACTORS, AND MYC FACTORS

The rhizosphere is a habitat for a plethora of microbes (Pini et al., 2012). Most of them are neutral commensalists, but some are relevant for plants, either as pathogens or as mutualists. Since it is vital for the plant to react early and adequately, communication in the rhizosphere is crucial for plant survival. Most plant species constitutively release from their roots diffusible signal molecules, strigolactones that stimulate hyphal branching in AM fungi (Akiyama et al., 2005; Besserer et al., 2006), as well as in fungal pathogens (Dor et al., 2011). However, whereas AM fungal metabolism is stimulated by strigolactones (Besserer et al., 2006), the growth of fungal pathogens is inhibited (Dor et al., 2011).

Strigolactone is secreted from roots of petunia (*Petunia hybrida*) by the ATP-binding cassette subtype G (ABCG) transporter PDR1 (Kretzschmar et al., 2012; **Figure 3**). *PDR1* is expressed preferentially during P starvation, a condition that favors AM. PDR1 is localized to the plasma membrane of the subepidermal passage cells, which are the preferred entry point for AM fungi (Sharda and Koide, 2008). Hence, PDR1 may play a role in establishing strigolactone gradients that direct AM fungal hyphae toward suitable points for root penetration (Kretzschmar et al., 2012).

The roots of legumes secrete flavonoids that are perceived as diffusible attractants by rhizobia and that activate them to produce a specific symbiotic signal, the nod factor (NF; Hassan

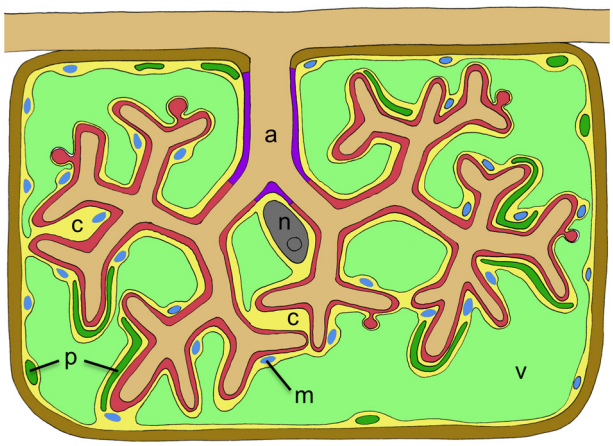

FIGURE 2 | Schematic representation of a cortex cell with an arbuscule. The arbuscule takes most of the space that is normally occupied by the central vacuole. Cellular compartments are colored in light green (plant vacuole), dark green (plant plastids), blue (plant mitochondria), yellow (plant cytoplasm), gray (nucleus), red (symbiotic interface), purple (trunc portion of the symbiotic interface), and brown (plant cell wall). The cellular constituents of the host are marked with letters as follows: c, cytoplasm; m, mitochondria; n, nucleus; p, plastids; v, vacuole. The fungal arbuscule is marked as well (a).

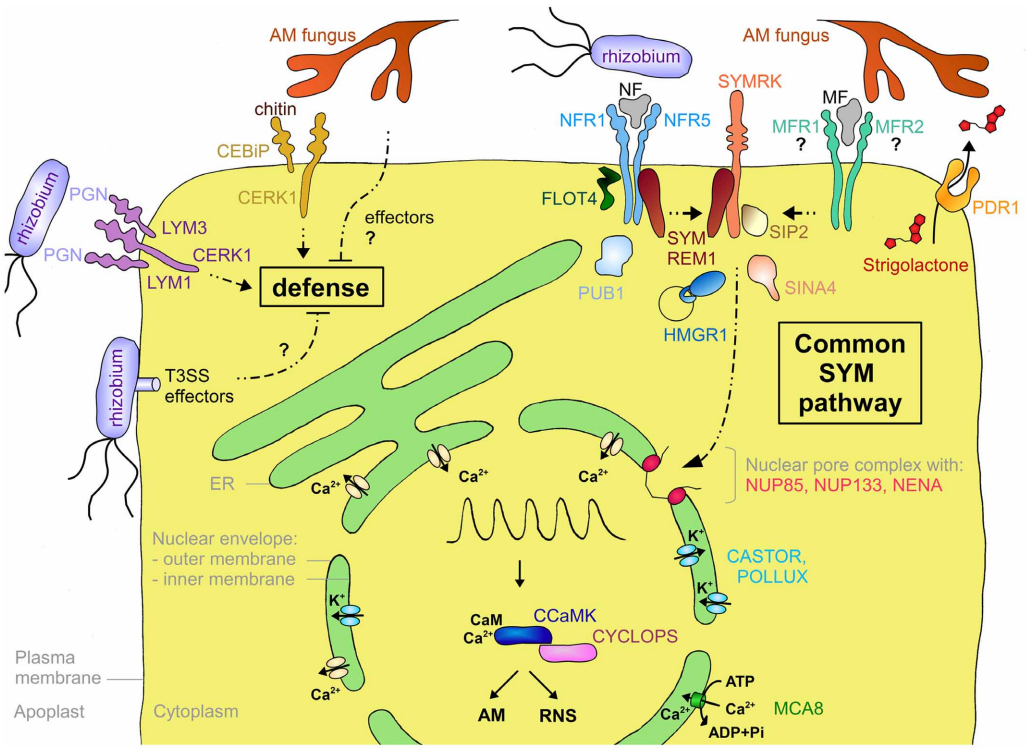

FIGURE 3 | Schematic representation of a plant cell with the major components involved in symbiotic signaling and defense signaling. The central vacuole has been omitted for clarity. Solid arrows indicate transport fluxes whereas dashed arrows represent signaling pathways. Receptor complexes involving LysM proteins originate from different plant species. Perception of bacterial peptidoglycan (PGN) is represented by CERK1, LYM1, and LYM3 of *Arabidopsis*. Chitin perception is represented by rice proteins CERK1 and CEBiP. The nod factor receptors (NFR1 and NFR5) are from *L. japonicus*, whereas the elusive nature of the myc factor receptors (MFR1 and MFR2) is shown with question marks. The common SYM pathway is represented by SYMRK, NENA, NUP85, NUP133, CASTOR, POLLUX, CCAMK, and CYCLOPS from *L. japonicus*. The remaining components (MCA8, SIP2, FLOT4, PUB1, SYMREM1, SINA4, and HMGR1) were described in *M. truncatula* or *L. japonicus*, except for PDR1 that was discovered in petunia. See **Table A1** and the main text for more information on the respective genes and their function in symbiosis.

and Mathesius, 2012). NFs are lipochitooligosaccharides (LCOs) that induce early plant responses such as root hair curling (Gough and Cullimore, 2011) and nodule organogenesis.

Only recently, LCO signal molecules similar to NFs were isolated from AM fungi, referred to as myc factors (MF; Maillet et al., 2011), indicating that AM and RNS involve similar symbiotic signals. In view of the obvious similarities in signaling between AM and RNS, it is still a mystery why RNS is characterized by a distinct host-specificity and very narrow host ranges (Wang et al., 2012), whereas AM exhibit a very low degree of specificity, resulting in extremely large host ranges (Smith and Read, 2008).

LysM RECEPTORS

Legumes have dedicated NF receptors (NFRs) that are localized to the plasma membrane and consist of an extracellular domain with two to three lysin motif (LysM) repeats and an intracellular kinase domain (Madsen et al., 2003; Radutoiu et al., 2003; Arrighi et al., 2006; Lohmann et al., 2010). LysM repeats were first identified in bacterial enzymes where they are involved in the binding of peptidoglycans (Buist et al., 2008). LysM-containing receptor-like kinases (LYKs) are plant-specific and occur as families of 5–21 members per species (Zhang et al., 2009). NF perception requires two LysM-containing proteins, which may function as dimers like many eukaryotic receptor systems (Gough and Cullimore, 2011; Gust et al., 2012; **Figure 3**). In *Lotus japonicus* they are referred to as Nod factor receptor1 (NFR1) and NFR5 (Madsen et al., 2003; Radutoiu et al., 2003), whereas in *Medicago truncatula* they are referred to as LYK3 and Nod factor perception (NFP), respectively (Ben Amor et al., 2003; Smit et al., 2007). Interestingly, the members of one of the subfamilies (including NFR5 and NFP) have a non-functional kinase domain, consistent with the idea that they may form a signaling complex with a second receptor that contains a functional kinase domain (Madsen et al., 2011). Domain swapping experiments between different NFRs and mutation analysis of the extracellular LysM domain support the idea that this part of the receptor (in particular LysM repeat 2) may be involved in the recognition of NFs (Radutoiu et al., 2007; Bensmihen et al., 2011). Indeed, NFR1 and NFR5 were recently shown to bind NF, presumably with their glycosylated extracellular LysM domain (Broghammer et al., 2012).

LCOs have an *N*-acetylglucosamine backbone (Dénarié et al., 1996) that they share with chitin and peptidoglycan (Lovering et al., 2012), the major components of fungal and bacterial cell walls, respectively. Plants have very sensitive receptors for

chitin and peptidoglycan oligomers that are structurally related to NFRs (**Figure 3**). In rice (*Oryza sativa*), two LysM-containing proteins, CEBiP (chitin oligosaccharide elicitor-binding protein) and CERK1 (chitin elicitor receptor kinase1), interact to form a chitin receptor at the plasma membrane (Kaku et al., 2006; Shimizu et al., 2010). In *Arabidopsis*, CERK1 which contributes to resistance against fungal pathogens, and LYM2 (LysM-containing protein2), a close homolog of CEBiP, can bind chitin (Miya et al., 2007; Wan et al., 2008; Petutschnig et al., 2010). However, recent mutant analysis suggests that despite its chitin-binding activity LYM2 is dispensable for chitin signaling (Shinya et al., 2012). Indeed, CERK1 alone, in particular its LysM repeat 2, can bind chitin oligomers and dimerize to form a functional receptor (Liu et al., 2012). Nevertheless, another LysM protein, LYK4, contributes to chitin signaling (Wan et al., 2012). Interestingly, CERK1 of *Arabidopsis* could also form a trimeric receptor complex with LYM1 and LYM3 that recognizes bacterial peptidoglycan. The binding activity is attributed to LYM1 and LYM3, whereas CERK1 appears to be responsible for subsequent defense signaling (Gimenez-Ibanez et al., 2009; Willmann et al., 2011). These results suggest that in general LysM-containing receptors may be formed by combinatorial oligomerization of different LYKs and LYMs (**Figure 3**). Notably, despite its inability to engage in symbiosis, *Arabidopsis* can perceive NFs at nanomolar concentrations (Khan et al., 2011), indicating that chitin or peptidoglycan receptors may have an affinity for LCOs. The fact that AM-competent plants such as rice (see above), and *M. truncatula* (Fliegmann et al., 2011) have chitin receptors raises the question how AM fungi escape defense response (see below).

While the NFRs of legumes recognize only one or few NFs, thereby limiting the host range in RNS (Wang et al., 2012), an NFP homolog of the non-legume *Parasponia andersonii* (*Cannabaceae*) serves as a common receptor in AM and RNS (Op Den Camp et al., 2011), suggesting that in this case the receptor can recognize different NFs and MFs. These results indicate that AM and RNS may have originally depended on the same receptor(s), which later diversified to produce functionally separate receptors for MFs and NFs in legumes. The functional characterization of further MF receptors (MFRs) from non-legume species will help understand the evolution and function of the LYKs.

SYMRK

A central component of symbiotic signaling is the symbiosis receptor-like kinase SYMRK that is essential for both AM and RNS (**Figure 3**). *SYMRK* was initially identified in *Medicago sativa* and *L. japonicus* (Endre et al., 2002; Stracke et al., 2002) but later was found to be conserved in most angiosperms. *SYMRKs* from different symbiosis-competent species in different families can complement each other indicating that SYMRK is functionally conserved and does not contribute to host specificity in RNS (Gherbi et al., 2008; Markmann et al., 2008). Indeed, SYMRK is considered to be the first component of the common SYM pathway which presumably integrates intermediary signals resulting from perception of MF and NF at the plasma membrane (Parniske, 2008).

In addition to its role in AM and in RNS of legumes, SYMRK is also involved in the actinorrhizal nodule symbiosis of *Casuarina glauca* (Fagales) and *Datisca glomerata* (Cucurbitales) with actinobacteria of the genus *Frankia* (Gherbi et al., 2008; Markmann et al., 2008). Hence, SYMRK can be considered the central symbiotic entry point of endosymbioses in plants. Interestingly, SYMRK occurs in different forms, which define its symbiotic potential. All nodulating species, including legumes, *D. glomerata*, alder (*Alnus glutinosa*), as well as the non-nodulating species poplar (*Populus trichocarpa*) and *Tropaeolum majus*, have a long version of SYMRK with a long N-terminal extracellular region (NEC domain) and three leucine-rich repeat (LRR) motifs (Markmann et al., 2008). Non-nodulating species such as tomato (*Solanum lycopersicum*) and poppy (*Papaver rhoeas*), have a slightly shorter version with only two LRR motifs, while in the monocots, SYMRK lacks the entire NEC domain and has two LRR motifs (Markmann et al., 2008). Interestingly, only the full length SYMRK of nodulating plant species among the eurosids can fully complement nodulation in the *L. japonicus symrk* mutant, whereas the two shorter types of SYMRK complement only AM but not RNS. Surprisingly, full length SYMRK of the non-nodulating *Tropaeolum* was able to restore nodulation in *L. japonicus* (Markmann et al., 2008). This indicates that the longest version of SYMRK has gained the potential to induce bacterial accommodation in the AM-competent common ancestor of all nodulating plants, and that this ability led to the independent evolution of bacterial endosymbioses in several clades of the eurosids, whereas others (e.g., *Tropaeolum*), remained only AM-competent. Based on sequence comparison, the predisposition to bacterial symbiosis may be related to the third LRR motif in the full-length SYMRK.

PROTEINS ASSOCIATED WITH SYMBIOTIC SIGNALING COMPONENTS AT THE PLASMA MEMBRANE

In order to better understand the biochemical function of the receptors in symbiotic signaling, interacting protein partners have been searched for. A yeast two-hybrid screen with SYMRK yielded a MAPKK (mitogen-activated protein kinase kinase) termed SIP2, for SYMRK-interacting protein2 (Chen et al., 2012; **Figure 3**), which is conserved at least between *L. japonicus* and *M. truncatula* (Chen et al., 2012). MAPKKs are components of MAP kinase cascades, which are well known signal transduction pathways in plant-pathogen interactions (Tena et al., 2011). SIP2 is necessary for nodulation and may be subject to negative regulation from SYMRK in *L. japonicus* (Chen et al., 2012), indicating that fine-tuning of the MAPK cascade may be required for successful symbiosis.

Another interactor of SYMRK is the E3 ubiquitin ligase SINA4, Seven in absentia4 (Den Herder et al., 2012; **Figure 3**). SINA4 recruits SYMRK to small puncta at the plasma membrane that may represent microdomains dedicated to symbiotic signaling (see below). SINA4 negatively regulates SYMRK abundance and consequently modulates symbiosis signaling. In agreement with this notion, overexpression of *SINA4* leads to defects in rhizobial infection (Den Herder et al., 2012). The NFR of *M. truncatula* LYK3 interacts with PUB1 (Plant U-box E3 ubiquitin ligase1), another type of E3 ligase induced during RNS (Mbengue et al., 2010; **Figure 3**). LYK3, which is involved in NF selectivity (Smit

et al., 2007), can phosphorylate PUB1, which in turn acts as a negative regulator of LYK3 function in infection and nodulation (Mbengue et al., 2010). Hence, PUB1 may indirectly modulate symbiosis signaling.

Interaction with several symbiosis-related receptor kinases was recently shown for remorins, a plant-specific gene family, of which at least one member, SYMREM1, is involved in nodulation (Jarsch and Ott, 2011). SYMREM1 interacts with the symbiosis receptor kinases NFP, LYK3, and DMI2 (Does not make infections2) in *M. truncatula* (Lefebvre et al., 2010), and with their respective orthologs in *L. japonicus* NFR5, NFR1, and SYMRK (Toth et al., 2012) (**Figure 3**). SYMREM1 is strongly and specifically upregulated in nodules and localizes to ITs, in particular at their tips where unwalled infection droplets form, and in symbiosomes (Lefebvre et al., 2010; Toth et al., 2012).

In *M. truncatula* an isoform of the isoprenoid biosynthetic enzyme HMGR (3-hydroxy-3-methylglutaryl coenzyme A reductase) was identified as an interactor of SYMRK (Kevei et al., 2007; **Figure 3**). Only one member of the HMGR gene family (HMGR1) interacted with SYMRK, demonstrating the specificity of the interaction. Reduction of HMGR1 activity, either by RNA interference or pharmacological inhibition of the enzyme, resulted in a strong reduction of nodulation. HMGR activity is involved in the biosynthesis of sterols, terpenoids, and in particular cytokinin, which plays an important role in RNS (Oldroyd et al., 2011). HMGR1 has two membrane-spanning domains and it localizes to small intracellular compartments of unknown identity (Kevei et al., 2007). It remains to be shown how HMGR1 interacts with SYMRK, which is localized to the plasma membrane, and what its role in nodulation is.

MEMBRANE MICRODOMAINS AS SIGNALING PLATFORMS IN SYMBIOSIS?

The plasma membrane of eukaryotes has long been thought to consist of fluid lipid bilayers in which proteins freely diffuse laterally like soluble molecules in a two-dimensional solution (Singer and Nicolson, 1972). However, biophysical as well as cell biological studies revealed that the plasma membrane is not homogeneous, but instead contains microdomains with sizes in the range of 10–100 nm in diameter that are different in their lipid and protein composition from the surrounding membrane. These microdomains are rich in sphingolipids and sterols and form platforms that can move laterally along the plasma membrane, a feature for which they were termed "lipid rafts" (Simons and Ikonen, 1997). Lipid rafts contain proteins involved in cellular signaling and membrane trafficking, whereas other general plasma membrane proteins are excluded from them. A large part of the "lipid raft" literature is based on fractionation of detergent-resistant membrane material, a technique that has been criticized for its potential to produce artifactual results (Tanner et al., 2011). We therefore focus here on proteins of which the localization has been confirmed *in vivo* with fluorescent markers or with transmission electron microscopy using immunogold labeling and we use the more generic term "microdomain" instead of "lipid rafts."

One of the first microdomain protein markers identified in plants is remorin (Jarsch and Ott, 2011). Remorins lack a transmembrane domain or membrane anchor, hence their localization to IT and symbiosome membranes is likely to result from binding to integral membrane proteins such as LysM receptors and SYMRK (see above). The co-localization of SYMREM1 with these receptor kinases (Lefebvre et al., 2010; Toth et al., 2012) indicates that either SYMREM1 localization is a consequence of the receptors being concentrated in microdomains, or that it is involved in recruiting these receptors to microdomains, although such a mechanism has not been directly documented by fluorescently tagged proteins as in the case of SINA4 (Den Herder et al., 2012).

Recently, flotillins have been implicated in RNS (Haney and Long, 2010; Haney et al., 2011) (**Figure 3**). Flotillins are well conserved proteins in animals and plants (Banning et al., 2011), and like remorins, they have no membrane spanning domain, but they localize to the plasma membrane, and they are concentrated in microdomains. In *M. truncatula*, which has a flotillin gene family of seven members, *FLOT2* and *FLOT4* are required for RNS (Haney and Long, 2010). Inoculation of *M. truncatula* with rhizobia favors co-localization of FLOT4 with LYK3 in microdomains of root hairs (Haney et al., 2011). In analogy to their function in animal systems, plant flotillins may function by bringing together in microdomains components of NF signaling, thereby increasing the efficiency and perhaps the specificity of symbiosis signaling at the membrane.

Taken together, NFRs and SYMRK, together with SYMREM1, FLOT4, and SINA4, could occur primarily in membrane microdomains that serve as dedicated signaling platforms at the plasma membrane (Simon-Plas et al., 2011). The observation that down-regulation of the membrane steroid-binding protein MSBP1 in *M. truncatula* interferes with AM (Kuhn et al., 2010), indicates that regulation of sterol homeostasis may be important for AM. Given the fact that microdomains are enriched in sterols, MSBP1 could affect AM by interfering with microdomain assembly. Interestingly, signaling platforms on membrane microdomains are involved not only in symbiosis, but also in plant-pathogen interactions (Bhat et al., 2005; Keinath et al., 2010). In addition, recent evidence suggests that membrane microdomains are also involved in sugar transport (Doidy et al., 2012).

INTRACELLULAR CALCIUM SIGNALING AT PERINUCLEAR MEMBRANES

Besides the plasma membrane proteins involved in symbiont recognition and early signal transduction (see above), membrane proteins with essential functions in symbiosis are localized to the nuclear envelope and the ER (**Figure 3**). The central second messenger in symbiosis is a rhythmic calcium transient (calcium spiking) that triggers transcriptional reprogramming in host cells (Oldroyd and Downie, 2006). Calcium spiking occurs around the nucleus, suggesting that the responsible calcium channels are localized to the membrane of the nuclear envelope, and that the calcium derives from the nuclear envelope (Capoen et al., 2011). Several components of the nuclear pore complex (NPC) are required for symbiotic signaling (Parniske, 2008). Mutations in the nucleoporins (NUPs) NUP85, NUP133, and NENA lead to defective calcium spiking and aborted symbiosis (Kanamori

et al., 2006; Saito et al., 2007; Groth et al., 2010). Although their role in symbiosis remains elusive, one possibility is that NUPs are involved in the translocation of membrane proteins between the inner and the outer membrane of the nuclear envelope.

The common SYM pathway also involves cation channels, DMI1 in *M. truncatula* and its homologs in *L. japonicus*, CASTOR and POLLUX, which all localize to the nuclear envelope (Riely et al., 2007; Charpentier et al., 2008; Parniske, 2008). These cation channels are thought to mediate potassium fluxes to compensate the charge imbalance resulting from calcium fluxes (Peiter et al., 2007; Charpentier et al., 2008). While the calcium channels that release the calcium are elusive, a calcium ATPase of *M. truncatula* (MCA8) has recently been described as an essential component in calcium spiking, presumably involved in reloading the calcium into the lumen of the nuclear envelope (and the ER), thereby replenishing its stores and resetting the low resting concentration of calcium in the cytoplasm and nucleoplasm (Capoen et al., 2011).

The specific calcium signatures in AM (Kosuta et al., 2008; Chabaud et al., 2011) and RNS (Oldroyd and Downie, 2006) are thought to be decoded by CCaMK (Oldroyd and Downie, 2006; Singh and Parniske, 2012). Activation of downstream transcriptional programs requires interaction with, and phosphorylation of, the CCaMK substrate CYCLOPS (Yano et al., 2008; Horvath et al., 2011). The orthologue of *CYCLOPS*, *IPD3* (Interacting Protein of DMI3), is required for symbiosis in *M. truncatula*, rice and pea (*Pisum sativum*), respectively (Messinese et al., 2007; Chen et al., 2008; Horvath et al., 2011; Ovchinnikova et al., 2011).

EVOLUTION OF SYMBIOTIC SIGNALING

Based on the fossil record and on the widespread occurrence of AM among the majority of vascular plants, the origin of AM is likely to have predated the radiation of land plants (Kistner and Parniske, 2002). It is conceivable that AM may even have been a precondition for successful colonization of land (Brundrett, 2002), although AM may not have been the earliest mycorrhizal association of land plants (Bidartondo et al., 2011). The finding that the common *SYM* genes are functionally conserved among mono- and dicotyledonous plant species (Chen et al., 2007, 2008; Gutjahr et al., 2008, 2012), and that they occur in lower plants such as liverworts, hornworts, mosses, and lycophytes has proven their ancient origin (Wang et al., 2010a). Interestingly, non-mycorrhizal angiosperms such as *Arabidopsis* have lost most common *SYM* genes, whereas the moss *Physcomitrella patens* has retained homologs of all *SYM* genes analyzed (Wang et al., 2010a), despite its apparent inability to undergo endosymbiosis (Wang and Qiu, 2006; Ligrone et al., 2012). It remains to be seen whether the common SYM genes of mosses play a role in other fungal associations, or whether the SYM pathway may serve other functions in the life of mosses.

Based on the fact that a number of genes are commonly required for both, AM and RNS, and that RNS ooccurs only in few taxa of the angiosperms, it was concluded that RNS evolved less than 100 Ma ago in an angiosperm predecessor that was already competent to engage in AM (Kistner and Parniske, 2002). Considering the different nodulation types, it is interesting to note that the common SYM genes are conserved also in species that form actinorhizal symbiosis (e.g., *A. glutinosa*, *C. glauca*) (Hocher et al., 2011), supporting the view that actinorrhizal symbiosis may have evolved independently from RNS in legumes, but from a common ancestor that became predisposed for bacterial symbiosis (Soltis et al., 1995; Pawlowski and Demchenko, 2012), perhaps by the modification of the LRR domain of SYMRK (Markmann et al., 2008) (see above).

The similarities between NFs and MFs (Maillet et al., 2011), and their receptors (Op Den Camp et al., 2011), also argue for a common evolutionary root of AM and RNS. In addition, the close homology of NFRs with the chitin receptor CERK1 indicates that the recognition of symbionts and pathogens derive from a common ancestral perception mechanism (Zhang et al., 2009). Since chitin, peptidoglycans and NF/MF share a common basic structure, the *N*-acetylglucosamine backbone, and since they are all perceived by LysM receptors, it is conceivable that recognition of symbiotic signals has evolved from a recognition mechanisms for an unspecific microbial signal such as chitin. The diversification of symbiotic signaling may then have been fostered by coevolution of NFRs with NFs during the evolution of RNS (Aguilar et al., 2004; Martinez-Romero, 2009). Interestingly, NFR1 and CERK1 are still so close that a few amino acid substitutions in the kinase domain of CERK1 are sufficient to confer to it the ability to induce nodules, when fused to the extracellular NF-binding domain of NFR1 (Nakagawa et al., 2011).

HOW SYMBIONTS AND PATHOGENS INFLUENCE THEIR PERCEPTION IN PLANTS

An open question is still why infection by AM fungi does not elicit a defense response in roots. Symbiotic plants retain, besides their NFRs and MFRs, potent receptors for microbial cell wall constituents such as chitin and peptidoglycan oligomers, which can trigger defense responses (Shimizu et al., 2010; Willmann et al., 2011). Hence, given the fact that AM fungal cell walls consist mainly of chitin, the perception of chitin fragments by plants could be expected to trigger a defense response that could block symbiosis. Indeed, some defense markers show a small transient induction at early stages of AM (García-Garrido and Ocampo, 2002), indicating that general microbe-associated molecular patterns (MAMPs) from AM fungi are perceived and elicit a transient defense response, which later is suppressed. Suppression may result from symbiotic signaling downstream of NFRs and MFRs or from manipulation by the AM fungus.

In order to escape a defense response, many microbes, beneficial and pathogenic, have evolved tools to interfere with their recognition either by hiding or by interfering with the deployment of a defense response (Zamioudis and Pieterse, 2012). The fungal pathogen *Cladosporium fulvum* has found a particularly elegant way to use the chitin-binding LysM motif to avoid its recognition: it secretes large amounts of a LysM-containing protein (Ecp6) that binds to soluble chitin fragments, thereby sequestering them from detection by the chitin receptors of the plant (Bolton et al., 2008; De Jonge et al., 2010). Hence Ecp6 is an effector protein that prevents detection of the pathogen by the host, and therefore contributes to virulence of the pathogen. Recently, an effector of an AM fungus has been described that is taken up by the host and functions through modification of defense-related

gene expression in the nucleus (Kloppholz et al., 2011). It remains to be seen whether AM fungi have also tools to directly interfere with the perception of MAMPs such as chitin. Bacterial pathogens produce their own effectors to interfere with LysM receptor function, thereby preventing their detection (Gimenez-Ibanez et al., 2009; Zeng et al., 2012). Bacterial effectors are in many cases delivered directly into the cytoplasm of the host by the type-three secretion system that also exists in rhizobia (Kambara et al., 2009). Interestingly, rhizobia contain homologs of pathogen effectors that influence infectivity and host range in RNS (Lewis et al., 2011; Soto et al., 2011).

INFECTION AND INTRACELLULAR ACCOMMODATION

INITIAL ACCOMMODATION: INFECTION THREAD AND PREPENETRATION APPARATUS

Intracellular accommodation of the microbial partner is the central unifying aspect of endosymbioses. In order to keep the invaded host cells intact, the microbial endosymbiont has to remain separated from the host cytoplasm by a host-derived membrane, which also has the role to control the environment of the microbe and to retrieve nutrients from it. Thus, endosymbioses require reorganization of the entire cell, in particular of the membrane system.

In order for rhizobia to invade root hair cells, the cell wall has to become locally softened and permeable. This implies a reduction in turgor pressure to avoid the plasma membrane of the host cell to rupture at the entry point. In addition, the invagination of the plasma membrane is likely to require a lowering of the turgor pressure, because the rhizobia cannot exert any inward force to promote invagination. On their way through the root hair cell, rhizobia are guided through the IT, a tubular hollow structure in which the bacteria remain confined and start to multiply. Toward the center of the root and below infected root hairs, files of cortical cells prepare for bacterial infection, before the rhizobia reach them, implying long distance transmission of a symbiotic signal (Oldroyd and Downie, 2008). Preparation of cortical cells involves migration of the nuclei to the cell center and formation of a cytoplasmic bridge through the central vacuole that traces the route for the formation of the IT, as in root hairs. This structure composed of cytoplasm and endomembranes has been termed the PIT (Van Brussel et al., 1992). On its centripetal path, the nucleus heads the PIT machinery which consists of large amounts of cytoplasm with ER thought to produce the elements of the IT (Fournier et al., 2008). Elements of the microtubular cytoskeleton are involved in the formation of the IT as well (Timmers et al., 1998). The absence of bacteria from the growing tip of the IT suggests that it is formed by the host without a direct contribution of rhizobia, although continuous signaling from the bacteria (e.g., trough NF) may influence IT development (Timmers et al., 1998; Fournier et al., 2008).

When epidermal cells are in contact with AM fungi, a similar process is triggered which consists of nuclear migration toward the contact point and assembly of an infection structure referred to as PPA. The PPA consists of dense cytoplasm with large amounts of ER cisternae, Golgi stacks, trans-Golgi network, and multivesicular bodies (Genre et al., 2005, 2008). These features of the PPA signify a strong biosynthetic activity, possibly associated with the invagination of the plasma membrane, in which the fungus inserts upon penetration of the cell wall. In *dmi2* and *dmi3* mutants, the nucleus of epidermal cells travels toward the fungal hyphopodium, but PPA formation does not occur (Genre et al., 2005), indicating that it is after nuclear migration and before PPA assembly that symbiotic signaling occurs.

GENERATION OF SYMBIOTIC MEMBRANE SYSTEMS

The generation of the host-derived membranes associated with PIT, IT, and PPA requires *de novo* synthesis of new membrane material and of membrane proteins with specific symbiosis-related functions in signaling and transport. Intense vesicular trafficking has indeed been observed at the growing tip of ITs (Robertson and Lyttleton, 1982). Likewise, infecting hyphae of AM fungi are surrounded by dense cytoplasm with ER, numerous Golgi stacks, vesicles, and other markers of exocytotic activity (Genre et al., 2008, 2012). Finally, the formation of the arbuscules in AM and the multiplication of the bacteroids in RNS, respectively, is associated with the massive expansion of the surfaces of the PAM and of the collective symbiosome membranes (**Box 1**). These observations demonstrate the need for intense membrane

Box 1 | What is the Identity of the Periarbuscular and the Symbiosome Membranes?

At the first intracellular stages of AM and RNS, the microbes are surrounded by the invaginated plasma membrane, and in the case of AM and some legume species that host the bacteria in fixation threads (Naisbitt et al., 1992), the PAM and the peribacteroid membrane remain continuous with the plasma membrane. The symbiosomes of most legumes, however, are isolated entities like organelles in the cytoplasm, and could therefore be compared topologically with vesicles or little vacuoles, rather than with the plasma membrane. Indeed, symbiosomes exhibit several common features with prevacuolar compartments that could turn into, or fuse with, lytic vacuoles to digest their content (Mellor, 1989). Interestingly, the analysis of membrane markers revealed an intermediate identity of the symbiosome membrane. The specific localization of the *M. truncatula* syntaxin MtSYP132 to symbiosome membranes signifies plasma membrane identity, indicating that the bacteroids reside in an "intracellular apoplastic domain" (Catalano et al., 2004, 2007; Limpens et al., 2009). Thereafter, the symbiosome membrane also carries Rab7, a marker for late endosomal/early vacuolar identity. This indicates that the symbiosome membrane goes through a phase of chimeric identity between plasma membrane and vacuolar identity (Limpens et al., 2009). At the onset of senescence, the appearance of the SNARE markers SYP22 and VTI11 signifies the identity of a lytic vacuole, in which the bacteroids are digested (Limpens et al., 2009). It is concluded that active symbiosomes are locked in a state of prevacuolar identity with contributions of plasmalemma identity. Considering the numerous symbiosis-specific features of symbiosome membrane and PAM, e.g., symbiosis-specific nutrient transporters (see main text), they may have a third, new identity which partially overlaps with plasma membrane and tonoplast identity. In addition, the PAM is subdivided into an arbuscule trunk region and the fine branches (**Figure 2**), which are characterized by different marker proteins (Pumplin and Harrison, 2009).

biosynthesis and trafficking during infection and endosymbiont accommodation.

Membrane trafficking proceeds through vesicles that are fused with target membranes by a highly conserved protein machinery (Pratelli et al., 2004; Jahn and Scheller, 2006). Central players in vesicular trafficking are the SNAREs (soluble *N*-ethylmaleimide-sensitive factor attachment protein receptors), of which there are two main types: R-SNAREs (also referred to as VAMP for vesicle-associated membrane proteins) on vesicle membranes and Q-SNAREs (some called syntaxins) on target membranes such as plasma membrane or tonoplast.

VESICLE TRAFFICKING TO HOST-DERIVED PERIMICROBIAL MEMBRANES

Intense cellular trafficking occurs in both mutualistic and pathogenic plant-microbe interactions (Wang and Dong, 2011; Yun and Kwon, 2012). It contributes to the local supply of new membrane material or to the delivery of cargo material (proteins or secondary metabolites) to the site of the interaction. A genetic screen in *Arabidopsis* identified PEN1/SYP121 (PENETRATION1/Syntaxin of plants121), a syntaxin with a specific role in plant immunity (Collins et al., 2003). PEN1 forms a SNARE complex with SNAP33 (Soluble *N*-ethylmaleimide-sensitive factor Adaptor Protein 33), VAMP721 and/or VAMP722, thereby providing an exocytotic delivery system for antifungal substances that contribute to full immunity in non-host resistance (Kwon et al., 2008). A related syntaxin of *Nicotiana benthamiana* (NbSYP132) plays a role in resistance against a bacterial pathogen, presumably by transporting antimicrobial proteins toward the site of bacterial infection (Kalde et al., 2007).

The symbiosome membranes of *M. truncatula* contain a syntaxin that is closely related to the aforementioned NbSYP132, namely MtSYP132 (Catalano et al., 2007). MtSYP132 may be involved in vesicle trafficking toward symbiosomes, however, the fact that it persists on the symbiosome membrane throughout its active period until senescence (Limpens et al., 2009) indicates that its function may reach beyond the generation of the symbiosome membrane, perhaps in the regulation of ion channels as it was shown for SYR1 (Syntaxin-related protein1) of *Nicotiana tabacum* (Leyman et al., 1999).

In *M. truncatula*, two vacuolar components of the quarternary SNARE complex, VAMP721d and VAMP721e, which are closely related to the PEN1 interactor VAMP721 of *Arabidopsis* (see above), play an essential role in intracellular accommodation of bacteroids and arbuscules (Ivanov et al., 2012). However, whether they interact with SYP132 on the symbiosome membrane, and what the cargo of the concerned vesicles might be, remains to be established. Taken together, these results show that in symbiosis as well as in pathogenesis of plants, a closely related machinery acts to either support intracellular accommodation of mutualistic microbes, or to fend off pathogens, respectively (Wang and Dong, 2011).

Recent evidence suggests that not all symbiosis-related factors delivered to the symbiotic interface through secretion rely on a symbiosis-specific trafficking pathway. Targeting of P transporters to the PAM may be independent of specific determinants of subcellular localization, and rather results from a general reorientation of protein trafficking from the plasma membrane toward the PAM (Pumplin et al., 2012). According to this scenario, localization to the PAM does not require specific targeting signals, but merely depends on the timing of gene expression.

SECRETION TOWARD DEVELOPING BACTEROIDS

Further evidence for a role of protein trafficking and secretion during RNS comes from the finding that the development of functional nodules requires the signal peptidase complex, SPC (Wang et al., 2010b). Secreted or integral membrane proteins have an N-terminal signal peptide that is recognized by a signal peptide recognition particle early during translation. The nascent protein together with the ribosome is then attached to the ER, so that the protein becomes inserted into the ER membrane or transported through it. Concomitantly, the signal peptide is removed by a signal peptidase, an essential step for further processing of the protein. The mutant *defective in nitrogen fixation1* (*dnf1*) carries a mutation in the subunit SPC22 of the SPC. Although it is not the catalytic subunit, its homolog in yeast is essential for signal peptidase activity and cell growth (Fang et al., 1997). Surprisingly, *dnf1* has no developmental phenotype (Starker et al., 2006), suggesting that the function of the SPC22 subunit in *M. truncatula* is symbiosis-specific. *Dnf1* mutants accumulate nodule-specific cysteine-rich (NCR) peptides in the ER, instead of secreting them into symbiosomes, where they cause the terminal differentiation of bacteroids, a prerequisite for determinate nodule development (Van De Velde et al., 2010).

Bacteroids can differentiate in two ways which differ in their degree of determinacy. In *L. japonicus*, the bacteroids retain their morphology and reproductive capacity, i.e., they remain indeterminate, whereas in *M. truncatula*, they terminally differentiate, involving a large size increase and the inability to divide. The fate of bacteroids is thought to depend on the plant, as some rhizobia can adopt both fates in function of their host (Mergaert et al., 2006). Indeed, expression of *M. truncatula* NCR peptides in *L. japonicus* causes rhizobia to terminally differentiate (Van De Velde et al., 2010). NCR247 peptide can trigger terminal differentiation of *Sinorhizobium meliloti* also *in vitro* (Van De Velde et al., 2010). Interestingly, high concentrations of NCR247 peptide interfere with bacterial membrane integrity, thereby exerting antimicrobial activity. This effect is particularly pronounced toward *bacA* mutants of *S. meliloti*, revealing a protective effect of BacA against NCR peptides (Haag et al., 2011). As BacA is predicted to encode a cytoplasmic subunit of an ABC transporter, this protein could be involved in either the uptake or efflux of NCR peptides in order to prevent plasma membrane damage (Haag et al., 2011). *BacA* mutants are protected in the *dnf1* mutant because NCRs are retained in the ER. These results show that RNS does not represent perfect harmony but rather a balance between cooperation and control.

ROLES OF ORGANELLES IN SYMBIOSIS

Cells with arbuscules and symbiosomes generally contain large amounts of organelles, indicative of intense metabolic activity (**Figures 1** and **2**). The plastids in mycorrhizal cells are of particular interest because they are closely associated with the arbuscules,

and they considerably change their shape to a network-like system, referred to as stromules (Lohse et al., 2005, 2006; Strack and Fester, 2006). The plastids of mycorrhizal roots are active in carotenoid and apocarotenoid metabolism, which may be significant for symbiosis due to their role in the biosynthesis of the hormones gibberellin, ABA and strigolactone (Walter et al., 2010). Furthermore, plastids serve as factories for fatty acid biosynthesis, which is a prerequisite for the expansion of the membrane systems in symbiotic cells.

During AM and RNS the large central vacuole of colonized cells fragments to yield room for the accommodation of the symbiont (Cox and Sanders, 1974; Bonfante-Fasolo, 1984; Van Brussel et al., 1992; Hause and Fester, 2005). The close association of the symbiosome membrane with the tonoplast in mycorrhizal cells (**Figure 1**) may indicate a role of vacuolar membranes or vacuolar constituents in symbiosis.

A NEW CELLULAR COMPARTMENT INVOLVED IN SYMBIOSIS?

In a genetic screen for mutants affected in intracellular accommodation of AM fungi in *P. hybrida*, the mutant *penetration and arbuscule morphogenesis1* (*pam1*), was isolated (Sekhara Reddy et al., 2007). *PAM1* encodes a novel plant-specific protein with an N-terminal major sperm protein (MSP) domain that is also found in the VAMP-associated proteins (VAPs) which are involved in vesicle trafficking (Lev et al., 2008; Feddermann et al., 2010). The C-terminus consists of 11 ankyrin repeats (Feddermann and Reinhardt, 2011), which are involved in protein–protein interactions in eukaryotes (Bennett and Baines, 2001; Mosavi et al., 2004). Due to this domain structure, the protein is referred to as VAPYRIN. VAPYRIN homologs were found in almost all plant species, including the non-symbiotic moss *P. patens*, but with the notable exception of *A. thaliana*. Functional conservation of VAPYRIN was shown in *M. truncatula*, where *vapyrin* mutants are defective in both AM and in RNS, indicating that intracellular accommodation, like the common SYM pathway, is shared between bacterial and fungal endosymbioses (Pumplin et al., 2010; Murray et al., 2011). The fact that calcium spiking is normal in *vapyrin* mutants shows that VAPYRIN acts downstream of the calcium signal and perhaps of the entire common SYM signaling pathway (Murray et al., 2011).

Petunia VAPYRIN localizes to the nucleus and the cytoplasm, with a conspicuous accumulation to mobile spherical structures that are associated with the tonoplast, and therefore termed tonospheres (Feddermann et al., 2010). In AM of petunia, tonospheres associate with fungal hyphae (Feddermann et al., 2010). In *M. truncatula*, mobile puncta with VAPYRIN-GFP protein that probably correspond to tonospheres, accumulate exclusively in colonized cells (Pumplin et al., 2010). VAPYRIN does not contain a signal peptide, nor any predicted transmembrane domain, indicating that the association with membranes is likely to result from protein–protein interaction with resident membrane proteins (Feddermann and Reinhardt, 2011).

MEMBRANE TRANSPORTERS IN SYMBIOSIS

The "raison d'être" of endosymbioses is the exchange of nutrients representing a mutual benefit to both symbiotic partners (**Box 2**). In RNS this involves primarily the transfer of N in the form of ammonium from bacteroids to the plant, and the reverse transfer of dicarboxylic acids such as malate, fumarate, or succinate to the bacteroids (Prell and Poole, 2006). In the case of AM, there is a range of nutrients that AM fungi can deliver to plants, with the most prominent examples of P, N, and S (Allen and Shachar-Hill, 2009; Smith and Smith, 2011). However, AM fungi can also

Box 2 | Are Nutritional Fluxes between Plants and AM Fungi Interrelated?

The ancient origin and the wide distribution of AM raises the question how mutualism has been stabilized over evolutionary time, but also during ontogenetic development. Mutualism requires a high degree of coordination and synchronization between the partners, and is prone to exploitation by one or the other, leading to a parasitic or pathogenic interaction. Indeed, heterotrophic (achlorophyllous) plants have in multiple independent cases turned into parasites of AM fungi (Merckx et al., 2012). In a less extreme converse scenario, an AM interaction can result in a negative growth effect on the plant reflecting a parasitic relationship where the costs of the interaction exceed the benefit for the plant (Li et al., 2008). However, in most cases, AM are mutualistic, and exploitation is the exception.

How is mutualism stabilized in AM? One possibility is that the partners prevent exploitation by imposing sanctions on their partner in case of reduced symbiotic service. There are indeed indications for such a scenario: for example, the flux of P_i toward the plant influences to which extent the fungus is allowed to proliferate in the root. If P_i delivery is blocked by a mutation in the PT of the plant, fungal colonization is reduced, and intracellular fungal structures are subject to premature senescence (Maeda et al., 2006; Javot et al., 2007). On the other end of the scale, high levels of P_i also repress AM fungal colonization (Breuillin et al., 2010). In both cases, the phenotype is different than in common *SYM* mutants, indicating that symbiosis is blocked at a rather late stage. However, high P_i supply is also known to impact on early signaling through the inhibition of strigolactone biosynthesis (Balzergue et al., 2011).

Direct insight into sanctions come from measurements of nutrient flux in monoxenic root cultures as a function of nutrient supply and environmental conditions. For example, plants can reduce C allocation to AM fungi, when they are supplied with optimal P_i levels through fertilization (Olsson et al., 2010). Conversely, when AM are supplied with limited C levels, P_i accumulates in the AM fungus instead of being transferred to the plant (Hammer et al., 2011). However, the question arises, whether in a more natural setting, when plants and AM fungi occur simultaneously in combinations with several potential partners, plants and AM fungi can selectively identify and reward better mutualists. This question was tested in an elegant approach, where isotope incorporation into newly synthesized fungal RNA allowed the separation of material from different AM fungi hosted by the same plant, allowing to estimate their relative consumption of sugar from the plant (Kiers et al., 2011). These experiments directly showed that plants colonized by two AM fungi preferentially reward the fungus that provides more P_i (Kiers et al., 2011). Conversely, AM fungi allocate P_i and N preferentially to roots that supply them with more C (Fellbaum et al., 2011; Kiers et al., 2011). These results document that AM involve a bidirectional rewarding system which can be considered a "biological market" and which is believed to help maintain mutualism within individual AM interactions and over evolutionary times.

acquire water and micronutrients from the soil and deliver them to the plant host in exchange for fixed C (Clark and Zeto, 2000).

WATER RELATIONS AND AQUAPORINS

AM fungi can increase the drought resistance of plants in several ways. Firstly, some AM fungi can considerably promote water uptake of mycorrhizal plants (Marulanda et al., 2003), and they can prevent leaf dehydration during drought and salt stress (Aroca et al., 2007). Furthermore, mycorrhizal plants have a lower and more stable root hydraulic conductance than non-mycorrhizal plants, leading to increased water use efficiency (WUE) that is higher amounts of photosynthate generated per volume of acquired water (Augé, 2001). Improved water relations may result from a generally improved nutritional status, but direct effects of AM fungi on water uptake and transport have also been reported (Marulanda et al., 2003; Egerton-Warburton et al., 2007).

In principle, water flux across membranes proceeds passively through osmosis along proteinaceous pores that facilitate water diffusion through the membrane (Zeuthen, 2010). Aquaporins facilitate water transfer through membranes along an osmotic gradient, but they cannot actively pump water against a water potential gradient. In plants, aquaporins occur as exceptionally large and diverse gene families, suggesting that they play important roles in various processes of plant life (Maurel et al., 2009; Anderberg et al., 2012). Aquaporins of higher plants are classified into five groups, according to their subcellular localization, expression pattern, and protein structure: plasma membrane intrinsic proteins (PIPs), tonoplast intrinsic proteins (TIPs), nodulin26-like intrinsic proteins (NIPs), small and basic intrinsic proteins (SIPs), and X intrinsic proteins (XIPs) (Danielson and Johanson, 2010).

Besides their function as water channels, aquaporins have been shown to facilitate the diffusion across membranes of low molecular weight neutral solutes such as glycerol, ammonia, and carbon dioxide (Dean et al., 1999; Uehlein et al., 2008; Hwang et al., 2010). Consistent with a role in endosymbiosis, several members of the PIP-, TIP-, and NIP-subfamilies are induced in both AM and RNS in rice, *M. truncatula*, *L. japonicus*, and petunia (Güimil et al., 2005; Hohnjec et al., 2005; Guether et al., 2009a; Breuillin et al., 2010). In particular the NIP NOD26, which can account for 10% of the total symbiosome membrane protein (Rivers et al., 1997; Catalano et al., 2004) is of considerable interest. With its ammonia transport activity, NOD26 would be well suited to allow for N transfer along the source to sink gradient between bacteroids and plant. The fact that *NOD26* is also induced in AM (Güimil et al., 2005; Hohnjec et al., 2005; Guether et al., 2009a; Breuillin et al., 2010) is in line with the finding that AM fungi, like rhizobia, release N to the plant host in the form of ammonia (Govindarajulu et al., 2005). However, it should be noted that in the acidic environment of the symbiotic interface around arbuscules and bacteroids, ammonia is almost completely protonated to the charged form ammonium (NH_4^+, pKb = 9.25), for which permeability in NOD26 has not been shown. Hence N uptake from the symbiotic interface into the host cytoplasm is more likely to be mediated by ammonium transporters (see below) than by NOD26.

In addition to their transport activity, aquaporins can mediate close interactions of juxtaposed membranes for example in the lens of mammals (Engel et al., 2008). Vacuolar subcompartments with multiple membrane layers and high contents of γ- and δ-TIP were observed in *Arabidopsis* cotyledons (Saito et al., 2002). These structures are highly mobile and move along the inner surface of the tonoplast to which they remain attached. Similar mobile structures were identified in mycorrhizal roots, where they contain the VAPYRIN protein (see above). Despite a number of reports about the involvement of aquaporins in AM and RNS, their exact biochemical function in symbiosis, as in many processes of plant development, remains to be established (Hill et al., 2004).

H^+-ATPases

In contrast to the aquaporins, mineral nutrient transporters require an active transport mechanism, since they often act against a concentration gradient. Most nutrient transporters in the plasma membrane use the energy of the proton electrochemical gradient generated by H^+-ATPases. In the direct (non-symbiotic) nutrient uptake pathway, plants acquire nutrients from the soil, whereas in the indirect mycorrhizal pathway, nutrients are taken up from the periarbuscular space over the PAM. In both cases, transport is energized by proton gradients. H^+-ATPases are induced in AM (Gianinazzi-Pearson et al., 2000; Krajinski et al., 2002) and are thought to contribute to the uptake of inorganic phosphate (P_i) and other nutrients from the symbiotic interface by proton symport (Karandashov and Bucher, 2005). Indeed, the periarbuscular space is acidified (Guttenberger, 2000), an observation which is compatible with the localization of an ATPase activity at the PAM (Marx et al., 1982). Hence, to energize nutrient uptake from the symbiotic interface, plants generate a proton gradient (Ferrol et al., 2002) to which the mycorrhizal fungus may also contribute (Requena et al., 2003; Breuninger and Requena, 2004; Balestrini and Lanfranco, 2007; Ramos et al., 2009). An activity analogous to the H^+-ATPase in the PAM was identified at the symbiosome membrane, which provides both the plant and the bacteroids with an electrochemical gradient for nutrient uptake from the peribacteroid space (Fedorova et al., 1999; Saalbach et al., 2002; Catalano et al., 2004).

PHOSPHATE TRANSPORT

The most thoroughly studied nutrient transport pathway in AM is the transport of P_i (Karandashov and Bucher, 2005) which is taken up from the soil by fungal P_i transporters (PTs) (Harrison and Van Buuren, 1995; Maldonado-Mendoza et al., 2001; Requena et al., 2003; Benedetto et al., 2005). Surprisingly, a PT of *Glomus mossae* (*GmosPT*) is expressed at similar levels in the extraradical and intraradical mycelium (Benedetto et al., 2005). Hence, the AM fungus could potentially control P_i flux toward the plant by partial re-uptake of P_i from the root (Benedetto et al., 2005; Balestrini et al., 2007). AM fungi store P_i as polyphosphate in tubular vacuoles (Uetake et al., 2002; Kuga et al., 2008; Olsson et al., 2011). Polyphosphate is a linear P_i polymer that can comprise thousands of P_i residues. Polyphosphate

as vacuolar storage form helps to keep P_i levels in a physiological range in the fungal cytoplasm, and prevents osmotic effects. Furthermore, the low cytoplasmic concentration of free P_i favors further P_i uptake from the soil. Polyphosphate is translocated in mobile vacuoles from the extraradical mycelium to the mycorrhizal roots (Maldonado-Mendoza et al., 2001; Hijikata et al., 2010), and released as free P_i into the periarbuscular space, where it is taken up by plant PTs.

The best-characterized symbiotic PT of plants is the *M. truncatula* AM-specific low-affinity transporter MtPT4, which is localized exclusively to the PAM (Harrison et al., 2002). MtPT4 activity is required not only for improved shoot P_i status, but also for sustained AM colonization of the root system (Javot et al., 2007). In *mtpt4* mutants, arbuscules accumulate polyphosphate, indicative of an impairment of P_i transfer, and they senesce prematurely. Thus plants can sense the quality of symbiotic service and sustain or terminate symbiosis, depending on the resulting benefit (Javot et al., 2007). *Solanaceae* such as tomato and petunia have three AM-responsive *PT* genes (*PT3*-*PT5*) among which *PT4* is the only AM-specific one (Wegmüller et al., 2008; Nagy et al., 2009). This redundancy complicates functional analysis compared to *M. truncatula*. In mycorrhizal tomato roots, high levels of *LePT3* and *LePT4* were detected in arbuscule-containing cells (Balestrini et al., 2007). In potato, the related *StPT3* gene is active in cells with arbuscules as with hyphal coils (Rausch et al., 2001; Karandashov et al., 2004), consistent with active P_i uptake in colonized cells of both *Arum*- and *Paris*-type AM. Expression of the AM-specific low-affinity rice PT *OsPT11* is correlated with the degree of *G. intraradices* colonization, as MtPT4 (Harrison et al., 2002; Paszkowski et al., 2002; Kobae and Hata, 2010). OsPT11, which was studied in both *Arum*-type and *Paris*-type mycorrhiza, localizes exclusively to the membrane around branched hyphae, but not at the plasma membrane neither around hyphal coils or hyphal trunks, a pattern similar to MtPT4 (Harrison et al., 2002; Pumplin and Harrison, 2009; Kobae and Hata, 2010). Hence, the expression pattern and the subcellular localization of AM-specific PTs in mono- and dicotyledonous plants reveals a conserved P_i uptake pathway in colonized cells of *Arum*- and *Paris*-type AM.

Interestingly, symbiosis-related PTs of monocots [e.g., OsPT11 of rice and ZmPT6 of maize (*Zea mais*)] and dicots (e.g., MtPT4 of *M. truncatula* and LePT4 of tomato) share a common phylogenetic root with the PT families of the lower land plants *P. patens* and *Selaginella moellendorffii*, documenting their common ancestral origin relative to the more derived members of the constitutive P_i uptake pathway in angiosperms (Paszkowski, pers. communication). A close evolutionary relationship among the symbiosis-specific PT is also documented by the conservation of their promoter sequences relative to related PTs that are induced by AM to a lesser degree, such as the PT3 lineage of the *Solanaceae* (Rausch et al., 2001; Chen et al., 2011).

NITROGEN TRANSPORT

AM fungi, like roots, can acquire N from the soil primarily as nitrate (NO_3^-) or as ammonium (NH_4^+) (Tian et al., 2010), although organic forms may also be involved (Cappellazzo et al., 2008). Two ammonium transporters, GintAMT1 and GinAMT2, were identified in *Glomus intraradices*. The high affinity transporter GintAMT1 is substrate-inducible and is expressed preferentially in the extraradical mycelium (Lopez-Pedrosa et al., 2006; Perez-Tienda et al., 2011), whereas GintAMT2 is preferentially expressed in the intraradical mycelium and is not substrate-regulated (Perez-Tienda et al., 2011). Interestingly, GintAMT1 and GintAMT2 are both expressed in arbuscule-containing cells (Perez-Tienda et al., 2011), indicating that they may modulate the amount of delivered N by reuptake, as it has been proposed for P_i transport (see above).

Once in the extraradical mycelium, N is thought to be translocated in the form of arginine which carries four N atoms per molecule and therefore represents a concentrated transport form of N (Govindarajulu et al., 2005). The fate of N from the soil to the plant through the AM fungus has been well described through the analysis of the enzymatic steps of ammonium assimilation, arginin biosynthesis in the extraradical hyphae, and arginine catabolism in intraradical hyphae (Govindarajulu et al., 2005; Tian et al., 2010). N is then thought to be transferred to the periarbuscular space in an inorganic form probably as ammonium, which can be taken up by the PAM via ammonium transporters such as LjAMT2.2 in *L. japonicus* (Guether et al., 2009b), GmAMT4.1 in soybean (*Glycine max*) (Kobae et al., 2010), and their homologs in *M. truncatula* (Gomez et al., 2009; Gaude et al., 2012).

Like AM fungi, the bacteroids in nodules release fixed N in the form of ammonia which is taken up by ammonium transporters in the symbiosome membrane (Kaiser et al., 1998; Rogato et al., 2008). Whether the ammonia-permeable aquaporin NOD26 plays a prominent role in N uptake of plants, as suggested by Hwang et al. (2010) is not clear (see above). However, patch clamp experiments have revealed a channel-like activity through which ammonium from the peribacteroid space can be taken up into the cytoplasm of the host (Tyerman et al., 1995;Kaiser et al., 1998).

CARBOHYDRATE TRANSPORT

Recent progress has significantly advanced our understanding of sugar transport within plants and in the interaction with beneficial and pathogenic microbes (Doidy et al., 2012). For nutrition of endosymbiotic microbes, two sugar transport steps are required. First, symbiotic tissues such as nodules and mycorrhizal roots need to attract photosynthate in competition with other sinks, and they need to take up sugar either directly from the phloem, or from the surrounding apoplast. Secondly, symbiotic cells need to release an appropriate form of C to the microbe at the symbiotic interface. In plants, the mobile form of reduced C is primarily sucrose which is cleaved to hexoses (glucose and fructose) in sink tissues. Hence, sink tissues of plants can acquire carbohydrate either by sucrose transporters or by monosaccharide (hexose) transporters. Candidates for sink-related transporters in symbiosis are the AM-inducible hexose transporter Mtst1 in *M. truncatula* (Harrison, 1996), and the sucrose transporter *LjSUT4* induced during nodule development in *L. japonicus* (Flemetakis et al., 2003).

It has long been an open question how hexoses may be released from cells in general, and from AM colonized cortex cells in particular. Only recently, a family of plant hexose transporters has been identified (SWEET) that can serve for hexose export from cells (Chen et al., 2010). SWEETs are uniporters that can transfer

hexoses in both directions, depending on the sugar gradient over the plasma membrane. In animals, SWEETs release hexoses to extracellular compartments such as the blood (Chen et al., 2010). *A. thaliana* has 17 SWEETs, suggesting that they play diverse roles in plant life. SWEETs can be exploited by pathogens for their own nutrition (Chen et al., 2010). Interestingly, the nodule-specific MtN3 is a member of the *M. truncatula* SWEET family, and may therefore be involved in the nutrition of the bacteroids in nodules. Whether members of the SWEET family indeed play a role in AM or RNS remains to be shown.

Hexoses are the likely transfer form to supply the heterotrophic AM fungus with fixed C (Pfeffer et al., 1999). AM fungi have a hexose transporter, MST2, that can take up glucose, galactose, mannose and the oxidized sugars glucuronic and galacturonic acid (Helber et al., 2011). MST2 is required for fungal proliferation in roots, indicating that it is involved in nutrition of the fungus during symbiosis (Helber et al., 2011).

The C source provided to bacteroids in nodules consists of dicarboxylic acids (Long, 1989). Indeed, *S. meliloti* possesses a dicarboxylate transporter, DctA, which is suggested to transport several compounds, mainly malate and fumarate (Yurgel and Kahn, 2005). DctA is required for RNS, in particular for the energy-demanding N fixation by bacteroids, since *dctA* mutants are impaired in N fixation.

OTHER TRANSPORTERS WITH POTENTIAL ROLES IN SYMBIOSIS

Some proteins are required for the establishment of a functional endosymbiosis, but their cellular and biochemical function remains elusive. For instance the *L. japonicus* mutant *sen1* can form nodules when colonized with *Mesorhizobium loti*, but the nodules remain pale and small, and N fixation is abolished (Hakoyama et al., 2012). SEN1, which is expressed specifically in the infected cells of nodules, is homologous to vacuolar cation transporters for iron and manganese. It is conceivable that a depletion in iron or manganese may hamper N fixation in bacteroids since iron is required for the nitrogenase complex, apart from general bacteroid metabolism (Hakoyama et al., 2012).

In AM, a likely candidate for a sulfate transporter was recently identified in *M. truncatula* (Casieri et al., 2012), however, its functional relevance in symbiosis, as well as its subcellular localization remain to be established. Two half-size ABC transporters of the same species, STUNTED ARBUSCULE (MtSTR) and MtSTR2 are essential for functional arbuscules (Zhang et al., 2010). *MtSTR* and *MtSTR2* are expressed specifically in arbuscule-containing cells, where they localize to the PAM. MtSTR and MtSTR2 were found to heterodimerize creating a full-size transporter that is localized to the PAM around young and mature arbuscules, but not around the hyphal trunk. Homologs of MtSTR and MtSTR2 were found in rice (*OsSTR1* and *OsSTR2*; Gutjahr et al., 2012), but not in the non-symbiotic model species *A. thaliana*, consistent with a specific role in symbiosis. However, their function in symbiosis remains elusive since their substrates are unknown.

CONCLUSIONS

Membranes are a central feature of life, since they allow the interior of cells to establish controlled conditions separated from the environment to provide optimal conditions for biochemical processes. In endosymbiosis, this aspect is accentuated, since two organisms cooperate in such close proximity that not much more than a membrane, a thin cell wall, and some interstitial material separates their cytoplasms. Therefore, highly organized membrane systems are at the core of endosymbioses. They are involved at all levels from initial recognition over intracellular accommodation to the establishment of the symbiotic interface, over which nutrients are exchanged. A topic that will attract increasing interest in coming years is the compartmentalization of the plasma membrane and the peri-microbial membranes (PAM and symbiosome membrane). An emerging scenario is that plants—like animals—have membrane microdomains that serve as signaling platforms in symbiosis and in plant-pathogen interactions. These membrane microdomains contain receptors and signaling components that are subject to dynamic regulation in space and time. Also, the emerging notion that the recognition of microbial pathogens and symbionts by LysM-containing receptors may share a common origin from non-self recognition mechanisms line out exciting new avenues for future research. Comparison of the molecular basis of symbiotic signaling and development in different taxa will help elucidate the evolution of AM in the ancestors of vascular plants, and the multiple emergence of RNS in a predisposed monophyletic clade within the angiosperms.

ACKNOWLEDGMENTS

We thank Eva Nouri for helpful discussion and support in the preparation of the manuscript. Our work is supported by the Swiss National Science Foundation (No. 31003A_135778/1) and by the National Centre of Competence in Research (NCCR) "Plant Survival."

REFERENCES

Aguilar, O. M., Rival, O., and Peltzer, E. (2004). Analysis of *Rhizobium etli* and of its symbiosis with wild *Phaseolus vulgaris* supports coevolution in centers of host diversification. *Proc. Natl. Acad. Sci. U.S.A.* 101, 13548–13553.

Akiyama, K., Matsuzaki, K., and Hayashi, H. (2005). Plant sesquiterpenes induce hyphal branching in arbuscular mycorrhizal fungi. *Nature* 435, 824–827.

Allen, J. W., and Shachar-Hill, Y. (2009). Sulfur transfer through an arbuscular mycorrhiza. *Plant Physiol.* 149, 549–560.

Al-Yahya'ei, M., Oehl, F., Vallino, M., Lumini, E., Redecker, D., Wiemken, A., et al. (2011). Unique arbuscular mycorrhizal fungal communities uncovered in date palm plantations and surrounding desert habitats of Southern Arabia. *Mycorrhiza* 21, 195–209.

Anderberg, H. I., Kjellbom, P., and Johanson, U. (2012). Annotation of *Selaginella moellendorffii* major intrinsic protein and the evolution of the protein family in terrestrial plants. *Front. Plant Sci.* 3, 1–14.

Aroca, R., Porcel, R., and Ruiz-Lozano, J. M. (2007). How does arbuscular mycorrhizal symbiosis regulate root hydraulic properties and plasma membrane aquaporins in Phaseolus vulgaris under drought, cold or salinity stresses? *New Phytol.* 173, 808–816.

Arrighi, J. F., Barre, A., Ben Amor, B., Bersoult, A., Soriano, L. C., Mirabella, R., et al. (2006). The *Medicago truncatula* lysine motif-receptor-like kinase gene family includes NFP and new nodule-expressed genes. *Plant Physiol.* 142, 265–279.

Augé, R. M. (2001). Water relations, drought and vesicular-arbuscular mycorrhizal symbiosis. *Mycorrhiza* 11, 3–42.

Balestrini, R., Gomez-Ariza, J., Lanfranco, L., and Bonfante, P. (2007). Laser microdissection reveals that transcripts for five

plant and one fungal phosphate transporter genes are contemporaneously present in arbusculated cells. *Mol. Plant Microbe Interact.* 20, 1055–1062.

Balestrini, R., and Lanfranco, L. (2007). Fungal and plant gene expression in arbuscular mycorrhizal symbiosis (vol 16, pg 509, 2006). *Mycorrhiza* 17, 153.

Balzergue, C., Puech-Pagès, V., Bécard, G., and Rochange, S. F. (2011). The regulation of arbuscular mycorrhizal symbiosis by phosphate in pea involves early and systemic signalling events. *J. Exp. Bot.* 62, 1049–1060.

Banning, A., Tomasovic, A., and Tikkanen, R. (2011). Functional aspects of membrane association of Reggie/Flotillin proteins. *Curr. Protein Pept. Sci.* 12, 725–735.

Ben Amor, B., Shaw, S. L., Oldroyd, G. E. D., Maillet, F., Penmetsa, R. V., Cook, D., et al. (2003). The NFP locus of *Medicago truncatula* controls an early step of Nod factor signal transduction upstream of a rapid calcium flux and root hair deformation. *Plant J.* 34, 495–506.

Benedetto, A., Magurno, F., Bonfante, P., and Lanfranco, L. (2005). Expression profiles of a phosphate transporter gene (GmosPT) from the endomycorrhizal fungus *Glomus mosseae*. *Mycorrhiza* 15, 620–627.

Bennett, V., and Baines, A. J. (2001). Spectrin and ankyrin-based pathways: metazoan inventions for integrating cells into tissues. *Physiol. Rev.* 81, 1353–1392.

Bensmihen, S., De Billy, F., and Gough, C. (2011). Contribution of NFP LysM domains to the recognition of nod factors during the *Medicago truncatula*/*Sinorhizobium meliloti* symbiosis. *PLoS ONE* 6:e26114. doi: 10.1371/journal.pone.0026114

Besserer, A., Puech-Pagès, V., Kiefer, P., Gomez-Roldan, V., Jauneau, A., Roy, S., et al. (2006). Strigolactones stimulate arbuscular mycorrhizal fungi by activating mitochondria. *PLoS Biol.* 4:e226. doi: 10.1371/journal.pbio.0040226

Bhat, R. A., Miklis, M., Schmelzer, E., Schulze-Lefert, P., and Panstruga, R. (2005). Recruitment and interaction dynamics of plant penetration resistance components in a plasma membrane microdomain. *Proc. Natl. Acad. Sci. U.S.A.* 102, 3135–3140.

Bidartondo, M. I., Read, D. J., Trappe, J. M., Merckx, V., Ligrone, R., and Duckett, J. G. (2011). The dawn of symbiosis between plants and fungi. *Biol. Lett.* 7, 574–577.

Bolton, M. D., Van Esse, H. P., Vossen, J. H., De Jonge, R., Stergiopoulos, I., Stulemeijer, I. J. E., et al. (2008). The novel *Cladosporium fulvum* lysin motif effector Ecp6 is a virulence factor with orthologues in other fungal species. *Mol. Microbiol.* 69, 119–136.

Bonfante-Fasolo, P. (1984). "Anatomy and morphology of VA mycorrhizae," in *VA Mycorrhizae*, eds C. L. Powell and D. J. Bagyaraj (Boca Raton, FL, USA: CRC Press), 5–33.

Breuillin, F., Schramm, J., Hajirezaei, M., Ahkami, A., Favre, P., Druege, U., et al. (2010). Phosphate systemically inhibits development of arbuscular mycorrhiza in *Petunia hybrida* and represses genes involved in mycorrhizal functioning. *Plant J.* 64, 1002–1017.

Breuninger, M., and Requena, N. (2004). Recognition events in AM symbiosis: analysis of fungal gene expression at the early appressorium stage. *Fungal Genet. Biol.* 41, 794–804.

Broghammer, A., Krusell, L., Blaise, M., Sauer, J., Sullivan, J. T., Maolanon, N., et al. (2012). Legume receptors perceive the rhizobial lipochitin oligosaccharide signal molecules by direct binding. *Proc. Natl. Acad. Sci. U.S.A.* 109, 13859–13864.

Brundrett, M. C. (2002). Coevolution of roots and mycorrhizas of land plants. *New Phytol.* 154, 275–304.

Buist, G., Steen, A., Kok, J., and Kuipers, O. R. (2008). LysM, a widely distributed protein motif for binding to (peptido)glycans. *Mol. Microbiol.* 68, 838–847.

Bunn, R., Lekberg, Y., and Zabinski, C. (2009). Arbuscular mycorrhizal fungi ameliorate temperature stress in thermophilic plants. *Ecology* 90, 1378–1388.

Capoen, W., Sun, J., Wysham, D., Otegui, M. S., Venkateshwaran, M., Hirsch, S., et al. (2011). Nuclear membranes control symbiotic calcium signaling of legumes. *Proc. Natl. Acad. Sci. U.S.A.* 108, 14348–14353.

Cappellazzo, G., Lanfranco, L., Fitz, M., Wipf, D., and Bonfante, P. (2008). Characterization of an amino acid permease from the endomycorrhizal fungus Glomus mosseae. *Plant Physiol.* 147, 429–437.

Casieri, L., Gallardo, K., and Wipf, D. (2012). Transcriptional response of *Medicago truncatula* sulphate transporters to arbuscular mycorrhizal symbiosis with and without sulphur stress. *Planta* 235, 1431–1447.

Catalano, C. M., Czymmek, K. J., Gann, J. G., and Sherrier, D. J. (2007). *Medicago truncatula* syntaxin SYP132 defines the symbiosome membrane and infection droplet membrane in root nodules. *Planta* 225, 541–550.

Catalano, C. M., Lane, W. S., and Sherrier, D. J. (2004). Biochemical characterization of symbiosome membrane proteins from *Medicago truncatula* root nodules. *Electrophoresis* 25, 519–531.

Chabaud, M., Genre, A., Sieberer, B. J., Faccio, A., Fournier, J., Novero, M., et al. (2011). Arbuscular mycorrhizal hyphopodia and germinated spore exudates trigger Ca2+ spiking in the legume and nonlegume root epidermis. *New Phytol.* 189, 347–355.

Charpentier, M., Bredemeier, R., Wanner, G., Takeda, N., Schleiff, E., and Parniske, M. (2008). *Lotus japonicus* CASTOR and POLLUX are ion channels essential for perinuclear calcium spiking in legume Root endosymbiosis. *Plant Cell* 20, 3467–3479.

Chen, A., Gu, M., Sun, S., Zhu, L., Hong, S., and Xu, G. (2011). Identification of two conserved cis-acting elements, MYCS and P1BS, involved in the regulation of mycorrhiza-activated phosphate transporters in eudicot species. *New Phytol.* 189, 1157–1169.

Chen, C. Y., Ane, J. M., and Zhu, H. Y. (2008). OsIPD3, an ortholog of the *Medicago truncatula* DMI3 interacting protein IPD3, is required for mycorrhizal symbiosis in rice. *New Phytol.* 180, 311–315.

Chen, C. Y., Gao, M. Q., Liu, J. Y., and Zhu, H. Y. (2007). Fungal symbiosis in rice requires an ortholog of a legume common symbiosis gene encoding a Ca2+/calmodulin-dependent protein kinase(1[OA]). *Plant Physiol.* 145, 1619–1628.

Chen, L.-Q., Hou, B.-H., Lalonde, S., Takanaga, H., Hartung, M. L., Qu, X.-Q., et al. (2010). Sugar transporters for intercellular exchange and nutrition of pathogens. *Nature* 468, 527–532.

Chen, T., Zhu, H., Ke, D., Cai, K., Wang, C., Gou, H., et al. (2012). A MAP kinase kinase interacts with SymRK and regulates nodule organogenesis in *Lotus japonicus*. *Plant Cell* 24, 823–838.

Clark, R. B., and Zeto, S. K. (2000). Mineral acquisition by arbuscular mycorrhizal plants. *J. Plant Nutr.* 23, 867–902.

Collins, N. C., Thordal-Christensen, H., Lipka, V., Bau, S., Kombrink, E., Qiu, J. L., et al. (2003). SNARE-protein-mediated disease resistance at the plant cell wall. *Nature* 425, 973–977.

Cox, G., and Sanders, F. (1974). Ultrastructure of the host-fungus interface in a vesicular-arbuscular mycorrhiza. *New Phytol.* 73, 901–912.

Danielson, J. A. H., and Johanson, U. (2010). "Phylogeny of major intrinsic proteins," in *Mips and Their Role in the Exchange of Metalloids,* eds T. P. Jahn and G. P. Bienert (New York, NY: Springer), 19–32.

De Jonge, R., Van Esse, H. P., Kombrink, A., Shinya, T., Desaki, Y., Bours, R., et al. (2010). Conserved fungal LysM effector Ecp6 prevents chitin-triggered immunity in plants. *Science* 329, 953–955.

Dean, R. M., Rivers, R. L., Zeidel, M. L., and Roberts, D. M. (1999). Purification and functional reconstitution of soybean nodulin 26. An aquaporin with water and glycerol transport properties. *Biochemistry* 38, 347–353.

Den Herder, G., Yoshida, S., Antolin-Llovera, M., Ried, M. K., and Parniske, M. (2012). *Lotus japonicus* E3 ligase SEVEN IN ABSENTIA4 destabilizes the symbiosis receptor-like kinase SYMRK and negatively regulates rhizobial infection. *Plant cell* 24, 1691–1707.

Dénarié, J., Debellé, F., and Promé, J. C. (1996). Rhizobium lipo-chitooligosaccharide nodulation factors: signaling molecules mediating recognition and morphogenesis. *Annu. Rev. Biochem.* 65, 503–535.

Doidy, J., Grace, E., Kühn, C., Simon-Plas, F., Casieri, L., and Wipf, D. (2012). Sugar transporters in plants and in their interactions with fungi. *Trends Plant Sci.* 17, 413–422.

Dor, E., Joel, D. M., Kapulnik, Y., Koltai, H., and Hershenhorn, J. (2011). The synthetic strigolactone GR24 influences the growth pattern of phytopathogenic fungi. *Planta* 234, 419–427.

Egerton-Warburton, L. M., Querejeta, J. I., and Allen, M. F. (2007). Common mycorrhizal networks provide a potential pathway for the transfer of hydraulically lifted water between plants. *J. Exp. Bot.* 58, 1473–1483.

Endre, G., Kereszt, A., Kevei, Z., Mihacea, S., Kaló, P., and Kiss, G. B. (2002). A receptor kinase gene regulating symbiotic nodule development. *Nature* 417, 962–966.

Engel, A., Fujiyoshi, Y., Gonen, T., and Walz, T. (2008). Junction-forming aquaporins. *Curr. Opin. Struct. Biol.* 18, 229–235.

Fang, H., Mullins, C., and Green, N. (1997). In addition to SEC11, a newly identified gene, SPC3, is essential for signal peptidase activity in the yeast endoplasmic reticulum. *J. Biol. Chem.* 272, 13152–13158.

Feddermann, N., Duvvuru Muni, R. R., Zeier, T., Stuurman, J., Ercolin, F., Schorderet, M., et al. (2010). The *PAM1* gene of petunia, required for intracellular accommodation and morphogenesis of arbuscular mycorrhizal fungi, encodes a homologue of *VAPYRIN*. *Plant J.* 64, 470–481.

Feddermann, N., and Reinhardt, D. (2011). Conserved residues in the ankyrin domain of VAPYRIN indicate potential protein-protein interaction surfaces. *Plant Signal. Behav.* 6, 680–684.

Fedorova, E., Thomson, R., Whitehead, L. F., Maudoux, O., Udvardi, M. K., and Day, D. A. (1999). Localization of H+ -ATPase in soybean root nodules. *Planta* 209, 25–32.

Fellbaum, C. R., Gachomo, E. W., Beesetty, Y., Choudhari, S., Strahan, G. D., Pfeffer, P. E., et al. (2011). Carbon availability triggers fungal nitrogen uptake and transport in arbuscular mycorrhizal symbiosis. *Proc. Natl. Acad. Sci. U.S.A.* 109, 2666–2671.

Ferrol, N., Gianinazzi, S., and Gianinazzi-Person, V. (2002). "Arbuscular mycorrhiza induced ATPases and membrane nutrient transport mechanisms," in *Mycorrhizal Technology in Agriculture: from Genes to Bioproducts*, eds S. Gianinazzi, H. Schüepp, J. M. Barea, and K. Haselwandter (Basel: Birkhäuser), 113–122.

Flemetakis, E., Dimou, M., Cotzur, D., Efrose, R. C., Aivalakis, G., Colebatch, G., et al. (2003). A sucrose transporter, LjSUT4, is up-regulated during *Lotus japonicus* nodule development. *J. Exp. Bot.* 54, 1789–1791.

Fliegmann, J., Uhlenbroich, S., Shinya, T., Martinez, Y., Lefebvre, B., Shibuya, N., et al. (2011). Biochemical and phylogenetic analysis of CEBiP-like LysM domain-containing extracellular proteins in higher plants. *Plant Physiol. Biochem.* 49, 709–720.

Fournier, J., Timmers, A. C. J., Sieberer, B. J., Jauneau, A., Chabaud, M., and Barker, D. G. (2008). Mechanism of infection thread elongation in root hairs of *Medicago truncatula* and dynamic interplay with associated rhizobial colonization. *Plant Physiol.* 148, 1985–1995.

García-Garrido, J. M., and Ocampo, J. A. (2002). Regulation of the plant defence response in arbuscular mycorrhizal symbiosis. *J. Exp. Bot.* 53, 1377–1386.

Gaude, N., Bortfeld, S., Duensing, N., Lohse, M., and Krajinski, F. (2012). Arbuscule-containing and non-colonized cortical cells of mycorrhizal roots undergo extensive and specific reprogramming during arbuscular mycorrhizal development. *Plant J.* 69, 510–528.

Genre, A., Chabaud, M., Faccio, A., Barker, D. G., and Bonfante, P. (2008). Prepenetration apparatus assembly precedes and predicts the colonization patterns of arbuscular mycorrhizal fungi within the root cortex of both *Medicago truncatula* and *Daucus carota*. *Plant Cell* 20, 1407–1420.

Genre, A., Chabaud, M., Timmers, T., Bonfante, P., and Barker, D. G. (2005). Arbuscular mycorrhizal fungi elicit a novel intracellular apparatus in *Medicago truncatula* root epidermal cells before infection. *Plant Cell* 17, 3489–3499.

Genre, A., Ivanov, S., Fendrych, M., Faccio, A., Zarsky, V., Bisseling, T., et al. (2012). Multiple exocytotic markers accumulate at the sites of perifungal membrane biogenesis in arbuscular mycorrhizas. *Plant Cell Physiol.* 53, 244–255.

Gherbi, H., Markmann, K., Svistoonoff, S., Estevan, J., Autran, D., Giczey, G., et al. (2008). SymRK defines a common genetic basis for plant root endosymbioses with arbuscular mycorrhiza fungi, rhizobia, and Frankia bacteria. *Proc. Natl. Acad. Sci. U.S.A.* 105, 4928–4932.

Gianinazzi-Pearson, V., Arnould, C., Oufattole, M., Arango, M., and Gianinazzi, S. (2000). Differential activation of H+-ATPase genes by an arbuscular mycorrhizal fungus in root cells of transgenic tobacco. *Planta* 211, 609–613.

Gimenez-Ibanez, S., Hann, D. R., Ntoukakls, V., Petutschnig, E., Lipka, V., and Rathjen, J. P. (2009). AvrPtoB targets the LysM receptor kinase CERK1 to promote bacterial virulence on plants. *Curr. Biol.* 19, 423–429.

Gomez, S. K., Javot, H., Deewatthanawong, P., Torres-Jerez, I., Tang, Y. H., Blancaflor, E. B., et al. (2009). Medicago truncatula and Glomus intraradices gene expression in cortical cells harboring arbuscules in the arbuscular mycorrhizal symbiosis. *BMC Plant Biol.* 9. doi: 10.1186/1471-2229-9-10

Gough, C., and Cullimore, J. (2011). Lipo-chitooligosaccharide signaling in endosymbiotic plant-microbe interactions. *Mol. Plant Microbe Interact.* 24, 867–878.

Govindarajulu, M., Pfeffer, P. E., Jin, H. R., Abubaker, J., Douds, D. D., Allen, J. W., et al. (2005). Nitrogen transfer in the arbuscular mycorrhizal symbiosis. *Nature* 435, 819–823.

Groth, M., Takeda, N., Perry, J., Uchida, H., Draexl, S., Brachmann, A., et al. (2010). NENA, a *Lotus japonicus* homolog of Sec13, is required for rhizodermal infection by arbuscular mycorrhiza fungi and rhizobia but dispensable for cortical endosymbiotic development. *Plant Cell* 22, 2509–2526.

Guether, M., Balestrini, R., Hannah, M., He, J., Udvardi, M., and Bonfante, P. (2009a). Genome-wide reprogramming of regulatory networks, cell wall and membrane biogenesis during arbuscular-mycorrhizal symbiosis in *Lotus japonicus*. *New Phytologist* 182, 200–212.

Guether, M., Neuhauser, B., Balestrini, R., Dynowski, M., Ludewig, U., and Bonfante, P. (2009b). A mycorrhizal-specific ammonium transporter from *Lotus japonicus* acquires nitrogen released by arbuscular mycorrhizal fungi. *Plant Physiol.* 150, 73–83.

Güimil, S., Chang, H. S., Zhu, T., Sesma, A., Osbourn, A., Roux, C., et al. (2005). Comparative transcriptomics of rice reveals an ancient pattern of response to microbial colonization. *Proc. Natl. Acad. Sci. U.S.A.* 102, 8066–8070.

Gust, A. A., Willmann, R., Desaki, Y., Grabherr, H. M., and Nürnberger, T. (2012). Plant LysM proteins: modules mediating symbiosis and immunity. *Trends Plant Sci.* 17, 495–502.

Gutjahr, C., Banba, M., Croset, V., An, K., Miyao, A., An, G., et al. (2008). Arbuscular mycorrhiza-specific signaling in rice transcends the common symbiosis signaling pathway. *Plant Cell* 20, 2989–3005.

Gutjahr, C., Radovanovic, D., Geoffroy, J., Zhang, Q., Siegler, H., Chiapello, M., et al. (2012). The half-size ABC transporters STR1 and STR2 are indispensable for mycorrhizal arbuscule formation in rice. *Plant J.* 69, 906–920.

Guttenberger, M. (2000). Arbuscules of vesicular-arbuscular mycorrhizal fungi inhabit an acidic compartment within plant roots. *Planta* 211, 299–304.

Hakoyama, T., Niimi, K., Yamamoto, T., Isobe, S., Sato, S., Nakamura, Y., et al. (2012). The integral membrane protein SEN1 is required for symbiotic nitrogen fixation in *Lotus japonicus* nodules. *Plant Cell Physiol.* 53, 225–236.

Hammer, E. C., Pallon, J., Wallander, H., and Olsson, P. A. (2011). Tit for tat? A mycorrhizal fungus accumulates phosphorus under low plant carbon availability. *FEMS Microbiol. Ecol.* 76, 236–244.

Haney, C. H., and Long, S. R. (2010). Plant flotillins are required for infection by nitrogen-fixing bacteria. *Proc. Natl. Acad. Sci. U.S.A.* 107, 478–483.

Haney, C. H., Riely, B. K., Tricoli, D. M., Cook, D. R., Ehrhardt, D. W., and Long, S. R. (2011). Symbiotic rhizobia bacteria trigger a change in localization and dynamics of the *Medicago truncatula* receptor kinase LYK3. *Plant Cell* 23, 2774–2787.

Harrison, M. J. (1996). A sugar transporter from *Medicago truncatula*: altered expression pattern in roots during vesicular-arbuscular (VA) mycorrhizal associations. *Plant J.* 9, 491–503.

Harrison, M. J., Dewbre, G. R., and Liu, J. Y. (2002). A phosphate transporter from *Medicago truncatula* involved in the acquisiton of phosphate released by arbuscular mycorrhizal fungi. *Plant Cell* 14, 2413–2429.

Harrison, M. J., and Van Buuren, M. L. (1995). A phosphate transporter from the mycorrhizal fungus *Glomus versiforme*. *Nature* 378, 626–629.

Hassan, S., and Mathesius, U. (2012). The role of flavonoids in root-rhizosphere signalling: opportunities and challenges for improving plant-microbe interactions. *J. Exp. Bot.* 63, 3429–3444.

Hause, B., and Fester, T. (2005). Molecular and cell biology of arbuscular mycorrhizal symbiosis. *Planta* 221, 184–196.

Heckman, D. S., Geiser, D. M., Eidell, B. R., Stauffer, R. L., Kardos, N. L., and Hedges, S. B. (2001). Molecular evidence for the early colonization of land by fungi and plants. *Science* 293, 1129–1133.

Helber, N., Wippel, K., Sauer, N., Schaarschmidt, S., Hause, B., and Requena, N. (2011). A versatile monosaccharide transporter that operates in the arbuscular mycorrhizal fungus Glomus sp is crucial for the symbiotic relationship with plants. *Plant Cell* 23, 3812–3823.

Hijikata, N., Murase, M., Tani, C., Ohtomo, R., Osaki, M., and Ezawa, T. (2010). Polyphosphate has a central role in the rapid and massive

accumulation of phosphorus in extraradical mycelium of an arbuscular mycorrhizal fungus. *New Phytol.* 186, 285–289.

Hill, A. E., Shachar-Hill, B., and Shachar-Hill, Y. (2004). What are aquaporins for? *J. Membr. Biol.* 197, 1–32.

Hocher, V., Alloisio, N., Auguy, F., Fournier, P., Doumas, P., Pujic, P., et al. (2011). Transcriptomics of actinorhizal symbioses reveals homologs of the whole common symbiotic signaling cascade. *Plant Physiol.* 156, 700–711.

Hohnjec, N., Vieweg, M. E., Puhler, A., Becker, A., and Kuster, H. (2005). Overlaps in the transcriptional profiles of *Medicago truncatula* roots inoculated with two different Glomus fungi provide insights into the genetic program activated during arbuscular mycorrhiza. *Plant Physiol.* 137, 1283–1301.

Horvath, B., Yeun, L. H., Domonkos, A., Halasz, G., Gobbato, E., Ayaydin, F., et al. (2011). *Medicago truncatula* IPD3 Is a member of the common symbiotic signaling pathway required for rhizobial and mycorrhizal symbioses. *Mol. Plant Microbe Interact.* 24, 1345–1358.

Hwang, J. H., Ellingson, S. R., and Roberts, D. M. (2010). Ammonia permeability of the soybean nodulin 26 channel. *FEBS Lett.* 584, 4339–4343.

Ivanov, S., Fedorova, E. E., Limpens, E., De Mita, S., Genre, A., Bonfante, P., et al. (2012). Rhizobium-legume symbiosis shares an exocytotic pathway required for arbuscule formation. *Proc. Natl. Acad. Sci. U.S.A.* 109, 8316–8321.

Jahn, R., and Scheller, R. H. (2006). SNAREs - engines for membrane fusion. *Nat. Rev. Mol. Cell Biol.* 7, 631–643.

Jarsch, I. K., and Ott, T. (2011). Perspectives on remorin proteins, membrane rafts, and their role during plant-microbe interactions. *Mol. Plant Microbe Interact.* 24, 7–12.

Javot, H., Penmetsa, R. V., Terzaghi, N., Cook, D. R., and Harrison, M. J. (2007). A *Medicago truncatula* phosphate transporter indispensable for the arbuscular mycorrhizal symbiosis. *Proc. Natl. Acad. Sci. U.S.A.* 104, 1720–1725.

Jones, K. M., Kobayashi, H., Davies, B. W., Taga, M. E., and Walker, G. C. (2007). How rhizobial symbionts invade plants: the Sinorhizobium-Medicago model. *Nat. Rev. Microbiol.* 5, 619–633.

Kaiser, B. N., Finnegan, P. M., Tyerman, S. D., Whitehead, L. F., Bergersen, F. J., Day, D. A., et al. (1998). Characterization of an ammonium transport protein from the peribacteroid membrane of soybean nodules. *Science* 281, 1202–1206.

Kaku, H., Nishizawa, Y., Ishii-Minami, N., Akimoto-Tomiyama, C., Dohmae, N., Takio, K., et al. (2006). Plant cells recognize chitin fragments for defense signaling through a plasma membrane receptor. *Proc. Natl. Acad. Sci. U.S.A.* 103, 11086–11091.

Kalde, M., Nuhse, T. S., Findlay, K., and Peck, S. C. (2007). The syntaxin SYP132 contributes to plant resistance against bacteria and secretion of pathogenesis-related protein 1. *Proc. Natl. Acad. Sci. U.S.A.* 104, 11850–11855.

Kambara, K., Ardissone, S., Kobayashi, H., Saad, M. M., Schumpp, O., Broughton, W. J., et al. (2009). Rhizobia utilize pathogen-like effector proteins during symbiosis. *Mol. Microbiol.* 71, 92–106.

Kanamori, N., Madsen, L. H., Radutoiu, S., Frantescu, M., Quistgaard, E. M. H., Miwa, H., et al. (2006). A nucleoporin is required for induction of Ca2+ spiking in legume nodule development and essential for rhizobial and fungal symbiosis. *Proc. Natl. Acad. Sci. U.S.A.* 103, 359–364.

Karandashov, V., and Bucher, M. (2005). Symbiotic phosphate transport in arbuscular mycorrhizas. *Trends Plant Sci.* 10, 22–29.

Keinath, N. F., Kierszniowska, S., Lorek, J., Bourdais, G., Kessler, S. A., Shimosato-Asano, H., et al. (2010). PAMP (Pathogen-associated Molecular Pattern)-induced changes in plasma membrane compartmentalization reveal novel components of plant immunity. *J. Biol. Chem.* 285, 39140–39149.

Kevei, Z., Lougnon, G., Mergaert, P., Horvath, G. V., Kereszt, A., Jayaraman, D., et al. (2007). 3-hydroxy-3-methylglutaryl coenzyme A reductase1 interacts with NORK and is crucial for nodulation in *Medicago truncatula*. *Plant Cell* 19, 3974–3989.

Khan, W., Costa, C., Souleimanov, A., Prithiviraj, B., and Smith, D. L. (2011). Response of *Arabidopsis thaliana* roots to lipo-chitooligosaccharide from *Bradyrhizobium japonicum* and other chitin-like compounds. *Plant Growth Regul.* 63, 243–249.

Kiers, E. T., Duhamel, M., Beesetty, Y., Mensah, J. A., Franken, O., Verbruggen, E., et al. (2011). Reciprocal rewards stabilize cooperation in the mycorrhizal symbiosis. *Science* 333, 880–882.

Kistner, C., and Parniske, M. (2002). Evolution of signal transduction in intracellular symbiosis. *Trends Plant Sci.* 7, 511–518.

Kloppholz, S., Kuhn, H., and Requena, N. (2011). A secreted fungal effector of *Glomus intraradices* promotes symbiotic biotrophy. *Curr. Biol.* 21, 1204–1209.

Kobae, Y., and Hata, S. (2010). Dynamics of periarbuscular membranes visualized with a fluorescent phosphate transporter in arbuscular mycorrhizal roots of rice. *Plant Cell Physiol.* 51, 341–353.

Kobae, Y., Tamura, Y., Takai, S., Banba, M., and Hata, S. (2010). Localized expression of arbuscular mycorrhiza-inducible ammonium transporters in soybean. *Plant Cell Physiol.* 51, 1411–1415.

Kosuta, S., Hazledine, S., Sun, J., Miwa, H., Morris, R. J., Downie, J. A., et al. (2008). Differential and chaotic calcium signatures in the symbiosis signaling pathway of legumes. *Proc. Natl. Acad. Sci. U.S.A.* 105, 9823–9828.

Krajinski, F., Hause, B., Gianinazzi-Pearson, V., and Franken, P. (2002). Mtha1, a plasma membrane H+-ATPase gene from *Medicago truncatula*, shows arbuscule-specific induced expression in mycorrhizal tissue. *Plant Biol.* 4, 754–761.

Kretzschmar, T., Kohlen, W., Sasse, J., Borghi, L., Schlegel, M., Bachelier, J. B., et al. (2012). A petunia ABC protein controls strigolactone-dependent symbiotic signalling and branching. *Nature* 483, 341–346.

Kuga, Y., Saito, K., Nayuki, K., Peterson, R. L., and Saito, M. (2008). Ultrastructure of rapidly frozen and freeze-substituted germ tubes of an arbuscular mycorrhizal fungus and localization of polyphosphate. *New Phytol.* 178, 189–200.

Kuhn, H., Kuster, H., and Requena, N. (2010). Membrane steroid-binding protein 1 induced by a diffusible fungal signal is critical for mycorrhization in *Medicago truncatula*. *New Phytol.* 185, 716–733.

Kwon, C., Neu, C., Pajonk, S., Yun, H. S., Lipka, U., Humphry, M., et al. (2008). Co-option of a default secretory pathway for plant immune responses. *Nature* 451, 835–840.

Lefebvre, B., Timmers, T., Mbengue, M., Moreau, S., Herve, C., Toth, K., et al. (2010). A remorin protein interacts with symbiotic receptors and regulates bacterial infection. *Proc. Natl. Acad. Sci. U.S.A.* 107, 2343–2348.

Lev, S., Ben Halevy, D., Peretti, D., and Dahan, N. (2008). The VAP protein family: from cellular functions to motor neuron disease. *Trends Cell Biol.* 18, 282–290.

Lewis, J. D., Lee, A., Ma, W. B., Zhou, H. B., Guttman, D. S., and Desveaux, D. (2011). The YopJ superfamily in plant-associated bacteria. *Mol. Plant Pathol.* 12, 928–937.

Leyman, B., Geelen, D., Quintero, F. J., and Blatt, M. R. (1999). A tobacco syntaxin with a role in hormonal control of guard cell ion channels. *Science* 283, 537–540.

Li, H. Y., Smith, F. A., Dickson, S., Holloway, R. E., and Smith, S. E. (2008). Plant growth depressions in arbuscular mycorrhizal symbioses: not just caused by carbon drain? *New Phytol.* 178, 852–862.

Ligrone, R., Duckett, J. G., and Renzaglia, K. S. (2012). Major transitions in the evolution of early land plants: a bryological perspective. *Ann. Bot.* 109, 851–871.

Limpens, E., Ivanov, S., Van Esse, W., Voets, G., Fedorova, E., and Bisseling, T. (2009). Medicago N-2-fixing symbiosomes acquire the endocytic identity marker Rab7 but delay the acquisition of vacuolar identity. *Plant Cell* 21, 2811–2828.

Limpens, E., Mirabella, R., Fedorova, E., Franken, C., Franssen, H., Bisseling, T., et al. (2005). Formation of organelle-like N-2-fixing symbiosomes in legume root nodules is controlled by DMI2. *Proc. Natl. Acad. Sci. U.S.A.* 102, 10375–10380.

Liu, T. T., Liu, Z. X., Song, C. J., Hu, Y. F., Han, Z. F., She, J., et al. (2012). Chitin-induced dimerization activates a plant immune receptor. *Science* 336, 1160–1164.

Lohmann, G. V., Shimoda, Y., Nielsen, M. W., Jorgensen, F. G., Grossmann, C., Sandal, N., et al. (2010). Evolution and regulation of the *Lotus japonicus* LysM receptor gene family. *Mol. Plant Microbe Interact.* 23, 510–521.

Lohse, S., Hause, B., Hause, G., and Fester, T. (2006). FtsZ characterization and immunolocalization in the two phases of plastid reorganization in arbuscular mycorrhizal roots of *Medicago truncatula*. *Plant Cell Physiol.* 47, 1124–1134.

Lohse, S., Schliemann, W., Ammer, C., Kopka, J., Strack, D., and Fester, T. (2005). Organization and metabolism of plastids and mitochondria in arbuscular mycorrhizal roots of *Medicago truncatula*. *Plant Physiol.* 139, 329–340.

Long, S. R. (1989). Rhizobium-legume nodulation - life together in the underground. *Cell* 56, 203–214.

Lopez-Pedrosa, A., Gonzalez-Guerrero, M., Valderas, A., Azcon-Aguilar, C., and Ferrol, N. (2006). GintAMT1 encodes a functional high-affinity ammonium transporter that is expressed in the extraradical mycelium of *Glomus intraradices*. *Fungal Genet. Biol.* 43, 102–110.

Lovering, A. L., Safadi, S. S., and Strynadka, N. C. J. (2012). Structural perspective of peptidoglycan biosynthesis and assembly. *Annu. Rev. Biochem.* 81, 451–478.

Madsen, E. B., Antolı́N-Llovera, M., Grossmann, G., Ye, J., Vieweg, S., Broghammer, A., et al. (2011). Autophosphorylation is essential for the *in vivo* function of the *Lotus japonicus* Nod factor receptor 1 and receptor-mediated signalling in cooperation with Nod factor receptor 5. *Plant J.* 65, 404–417.

Madsen, E. B., Madsen, L. H., Radutoiu, S., Olbryt, M., Rakwalska, M., Szczyglowski, K., et al. (2003). A receptor kinase gene of the LysM type is involved in legume perception of rhizobial signals. *Nature* 425, 637–640.

Maeda, D., Ashida, K., Iguchi, K., Chechetka, S. A., Hijikata, A., Okusako, Y., et al. (2006). Knockdown of an arbuscular mycorrhiza-inducible phosphate transporter gene of *Lotus japonicus* suppresses mutualistic symbiosis. *Plant Cell Physiol.* 47, 807–817.

Maillet, F., Poinsot, V., André, O., Puech-Pagès, V., Haouy, A., Gueunier, M., et al. (2011). Fungal lipochitooligosaccharide symbiotic signals in arbuscular mycorrhiza. *Nature* 469, 58–64.

Maldonado-Mendoza, I. E., Dewbre, G. R., and Harrison, M. J. (2001). A phosphate transporter gene from the extra-radical mycelium of an arbuscular mycorrhizal fungus *Glomus intraradices* is regulated in response to phosphate in the environment. *Mol. Plant Microbe Interact.* 14, 1140–1148.

Markmann, K., Giczey, G., and Parniske, M. (2008). Functional adaptation of a plant receptor-kinase paved the way for the evolution of intracellular root symbioses with bacteria. *PLoS Biol.* 6:e68. doi: 10.1371/journal.pbio.0060068

Martinez-Romero, E. (2009). Coevolution in rhizobium-legume symbiosis? *DNA Cell Biol.* 28, 361–370.

Marulanda, A., Azcon, R., and Ruiz-Lozano, J. M. (2003). Contribution of six arbuscular mycorrhizal fungal isolates to water uptake by *Lactuca sativa* plants under drought stress. *Physiologia Plantarum* 119, 526–533.

Marx, C., Dexheimer, J., Gianinazzi-Pearson, V., and Gianinazzi, S. (1982). Enzymatic studies on the metabolism of vesicular-arbuscular mycorrhizas. 4. Ultracytoenzymological evidence (ATPase) for active transfer processes in the host-arbuscule interface. *New Phytol.* 90, 37–43.

Maurel, C., Santoni, V., Luu, D. T., Wudick, M. M., and Verdoucq, L. (2009). The cellular dynamics of plant aquaporin expression and functions. *Curr. Opin. Plant Biol.* 12, 690–698.

Mbengue, M., Camut, S., De Carvalho-Niebel, F., Deslandes, L., Froidure, S., Klaus-Heisen, D., et al. (2010). The *Medicago truncatula* E3 ubiquitin ligase PUB1 interacts with the LYK3 symbiotic receptor and negatively regulates infection and nodulation. *Plant Cell* 22, 3474–3488.

Mellor, R. B. (1989). Bacteroids in the Rhizobium-legume symbiosis inhabit a plant internal lytic compartment - implications for other microbial endosymbioses. *J. Exp. Bot.* 40, 831–839.

Merckx, V. S. F. T., Janssens, J. B., Hynson, N. A., Specht, C. D., Bruns, T. D., and Smets, E. F. (2012). Mycoheterotrophic interactions are not limited to a narrow phylogenetic range of arbuscular mycorrhizal fungi. *Mol. Ecol.* 21, 1524–1532.

Messinese, E., Mun, J. H., Yeun, L. H., Jayaraman, D., Rouge, P., Barre, A., et al. (2007). A novel nuclear protein interacts with the symbiotic DMI3 calcium- and calmodulin-dependent protein kinase of Medicago truncatula. *Mol. Plant Microbe Interact.* 20, 912–921.

Miya, A., Albert, P., Shinya, T., Desaki, Y., Ichimura, K., Shirasu, K., et al. (2007). CERK1, a LysM receptor kinase, is essential for chitin elicitor signaling in *Arabidopsis*. *Proc. Natl. Acad. Sci. U.S.A.* 104, 19613–19618.

Mosavi, L. K., Cammett, T. J., Desrosiers, D. C., and Peng, Z. Y. (2004). The ankyrin repeat as molecular architecture for protein recognition. *Protein Sci.* 13, 1435–1448.

Murray, J. D., Duvvuru Muni, R., Torres-Jerez, I., Tang, Y., Allen, S., Andriankaja, M., et al. (2011). *Vapyrin*, a gene essential for intracellular progression of arbuscular mycorrhizal symbiosis, is also essential for infection by rhizobia in the nodule symbiosis of *Medicago truncatula*. *Plant J.* 65, 244–252.

Nagy, R., Drissner, D., Amrhein, N., Jakobsen, I., and Bucher, M. (2009). Mycorrhizal phosphate uptake pathway in tomato is phosphorus-repressible and transcriptionally regulated. *New Phytol.* 181, 950–959.

Naisbitt, T., James, E. K., and Sprent, J. I. (1992). The evolutionary significance of the legume genus Chamaecrista, as determined by nodule structure. *New Phytol.* 122, 487–492.

Nakagawa, T., Kaku, H., Shimoda, Y., Sugiyama, A., Shimamura, M., Takanashi, K., et al. (2011). From defense to symbiosis: limited alterations in the kinase domain of LysM receptor-like kinases are crucial for evolution of legume-Rhizobium symbiosis. *Plant J.* 65, 169–180.

Oldroyd, G. E. D., and Downie, J. A. (2006). Nuclear calcium changes at the core of symbiosis signalling. *Curr. Opin. Plant Biol.* 9, 351–357.

Oldroyd, G. E. D., and Downie, J. A. (2008). Coordinating nodule morphogenesis with rhizobial infection in legumes. *Annu. Rev. Plant Biol.* 59, 519–546.

Oldroyd, G. E. D., Murray, J. D., Poole, P. S., and Downie, J. A. (2011). The rules of engagement in the legume-rhizobial symbiosis. *Ann. Rev. Genet.* 45, 119–144.

Olsson, P. A., Hammer, E. C., Pallon, J., Van Aarle, I. M., and Wallander, H. (2011). Elemental composition in vesicles of an arbuscular mycorrhizal fungus, as revealed by PIXE analysis. *Fungal Biol.* 115, 643–648.

Olsson, P. A., Rahm, J., and Aliasgharzad, N. (2010). Carbon dynamics in mycorrhizal symbioses is linked to carbon costs and phosphorus benefits. *FEMS Microbiol. Ecol.* 72, 123–131.

Op Den Camp, R., Streng, A., De Mita, S., Cao, Q., Polone, E., Liu, W., et al. (2011). LysM-type mycorrhizal receptor recruited for *Rhizobium* symbiosis in nonlegume *Parasponia*. *Science* 331, 909–912.

Ovchinnikova, E., Journet, E. P., Chabaud, M., Cosson, V., Ratet, P., Duc, G., et al. (2011). IPD3 controls the formation of nitrogen-fixing symbiosomes in pea and Medicago Spp. *Mol. Plant Microbe Interact.* 24, 1333–1344.

Parniske, M. (2008). Arbuscular mycorrhiza: the mother of plant root endosymbioses. *Nat. Rev. Microbiol.* 6, 763–775.

Paszkowski, U., Kroken, S., Roux, C., and Briggs, S. P. (2002). Rice phosphate transporters include an evolutionarily divergent gene specifically activated in arbuscular mycorrhizal symbiosis. *Proc. Natl. Acad. Sci. U.S.A.* 99, 13324–13329.

Pawlowski, K., and Demchenko, K. N. (2012). The diversity of actinorhizal symbiosis. *Protoplasma.* doi: 10.1007/s00709-012-0388-4. [Epub ahead of print].

Peiter, E., Sun, J., Heckmann, A. B., Venkateshwaran, M., Riely, B. K., Otegui, M. S., et al. (2007). The *Medicago truncatula* DMI1 protein modulates cytosolic calcium signaling. *Plant Physiol.* 145, 192–203.

Perez-Tienda, J., Testillano, P. S., Balestrini, R., Fiorilli, V., Azcon-Aguilar, C., and Ferrol, N. (2011). GintAMT2, a new member of the ammonium transporter family in the arbuscular mycorrhizal fungus *Glomus intraradices*. *Fungal Genet. Biol.* 48, 1044–1055.

Petutschnig, E. K., Jones, A. M. E., Serazetdinova, L., Lipka, U., and Lipka, V. (2010). The lysin motif receptor-like kinase (LysM-RLK) CERK1 Is a major chitin-binding protein in *Arabidopsis thaliana* and subject to chitin-induced phosphorylation. *J. Biol. Chem.* 285, 28902–28911.

Pfeffer, P. E., Douds, D. D., Becard, G., and Shachar-Hill, Y. (1999). Carbon uptake and the metabolism and transport of lipids in an arbuscular mycorrhiza. *Plant Physiol.* 120, 587–598.

Pini, F., Frascella, A., Santopolo, L., Bazzicalupo, M., Biondi, E. G., Scotti, C., et al. (2012). Exploring the plant-associated bacterial communities in *Medicago sativa* L. *BMC Microbiology* 12, 78.

Pratelli, J., Sutter, J. U., and Blatt, M. R. (2004). A new catch in the SNARE. *Trends Plant Sci.* 9, 187–195.

Prell, J., and Poole, P. (2006). Metabolic changes of rhizobia in legume nodules. *Trends Microbiol.* 14, 161–168.

Pumplin, N., and Harrison, M. J. (2009). Live-cell imaging reveals periarbuscular membrane domains and organelle location in *Medicago truncatula* roots during arbuscular mycorrhizal symbiosis. *Plant Physiol.* 151, 809–819.

Pumplin, N., Mondo, S. J., Topp, S., Starker, C. G., Gantt, J. S., and Harrison, M. J. (2010). *Medicago truncatula* Vapyrin is a novel protein required for arbuscular mycorrhizal symbiosis. *Plant J.* 61, 482–494.

Pumplin, N., Zhang, X., Noar, R. D., and Harrison, M. J. (2012). Polar localization of a symbiosis-specific phosphate transporter is mediated by a transient reorientation of secretion. *Proc. Natl. Acad. Sci. U.S.A.* 109, E665–E672.

Radutoiu, S., Madsen, L. H., Madsen, E. B., Felle, H. H., Umehara, Y., Gronlund, M., et al. (2003). Plant recognition of symbiotic bacteria requires two LysM receptor-like kinases. *Nature* 425, 585–592.

Radutoiu, S., Madsen, L. H., Madsen, E. B., Jurkiewicz, A., Fukai, E., Quistgaard, E. M. H., et al. (2007). LysM domains mediate lipochitin-oligosaccharide recognition and Nfr genes extend the symbiotic host range. *EMBO J.* 26, 3923–3935.

Ramos, A. C., Martins, M. A., Okorokova-Facanha, A. L., Olivares, F. L., Okorokov, L. A., Sepulveda, N., et al. (2009). Arbuscular mycorrhizal fungi induce differential activation of the plasma membrane and vacuolar H+ pumps in maize roots. *Mycorrhiza* 19, 69–80.

Rausch, C., Daram, P., Brunner, S., Jansa, J., Laloi, M., Leggewie, G., et al. (2001). A phosphate transporter expressed in arbuscule-containing cells in potato. *Nature* 414, 462–466.

Redecker, D., Kodner, R., and Graham, L. E. (2000). Glomalean fungi from the Ordovician. *Science* 289, 1920–1921.

Requena, N., Breuninger, M., Franken, P., and Ocón, A. (2003). Symbiotic status, phosphate, and sucrose regulate the expression of two plasma membrane H+-ATPase genes from the mycorrhizal fungus *Glomus mosseae*. *Plant Physiol.* 132, 1540–1549.

Riely, B. K., Lougnon, G., Ané, J. M., and Cook, D. R. (2007). The symbiotic ion channel homolog DMI1 is localized in the nuclear membrane of *Medicago truncatula* roots. *Plant J.* 49, 208–216.

Rivers, R. L., Dean, R. M., Chandy, G., Hall, J. E., Roberts, D. M., and Zeidel, M. L. (1997). Functional analysis of nodulin 26, an aquaporin in soybean root nodule symbiosomes. *J. Biol. Chem.* 272, 16256–16261.

Robertson, J. G., and Lyttleton, P. (1982). Coated and smooth vesicles in the biogenesis of cell walls, plasma membranes, infection threads and peribacteroid membranes in root hairs and nodules of white clover. *J. Cell. Sci.* 58, 63–78.

Rogato, A., D'Apuzzo, E., Barbulova, A., Omrane, S., Stedel, C., Simon-Rosin, U., et al. (2008). Tissue-specific down-regulation of LjAMT1;1 compromises nodule function and enhances nodulation in *Lotus japonicus*. *Plant Mol. Biol.* 68, 585–595.

Saalbach, G., Erik, P., and Wienkoop, S. (2002). Characterisation by proteomics of peribacteroid space and peribacteroid membrane preparations from pea (*Pisum sativum*) symbiosomes. *Proteomics* 2, 325–337.

Saito, C., Ueda, T., Abe, H., Wada, Y., Kuroiwa, T., Hisada, A., et al. (2002). A complex and mobile structure forms a distinct subregion within the continuous vacuolar membrane in young cotyledons of *Arabidopsis*. *Plant J.* 29, 245–255.

Saito, K., Yoshikawa, M., Yano, K., Miwa, H., Uchida, H., Asamizu, E., et al. (2007). NUCLEOPORIN85 is required for calcium spiking, fungal and bacterial symbioses, and seed production in *Lotus japonicus*. *Plant Cell* 19, 610–624.

Sekhara Reddy, D. M. R., Schorderet, M., Feller, U., and Reinhardt, D. (2007). A petunia mutant affected in intracellular accommodation and morphogenesis of arbuscular mycorrhizal fungi. *Plant J.* 51, 739–750.

Sharda, J. N., and Koide, R. T. (2008). Can hypodermal passage cell distribution limit root penetration by mycorrhizal fungi? *New Phytol.* 180, 696–701.

Shimizu, T., Nakano, T., Takamizawa, D., Desaki, Y., Ishii-Minami, N., Nishizawa, Y., et al. (2010). Two LysM receptor molecules, CEBiP and OsCERK1, cooperatively regulate chitin elicitor signaling in rice. *Plant J.* 64, 204–214.

Shinya, T., Motoyama, N., Ikeda, A., Wada, M., Kamiya, K., Hayafune, M., et al. (2012). Functional characterization of CEBiP and CERK1 homologs in Arabidopsis and rice reveals the presence of different chitin receptor systems in plants. *Plant Cell Physiol.* doi: 10.1093/pcp/pcs113. [Epub ahead of print].

Simon-Plas, F., Perraki, A., Bayer, E., Gerbeau-Pissot, P., and Mongrand, S. (2011). An update on plant membrane rafts. *Curr. Opin. Plant Biol.* 14, 642–649.

Simons, K., and Ikonen, E. (1997). Functional rafts in cell membranes. *Nature* 387, 569–572.

Singer, S. J., and Nicolson, G. L. (1972). Fluid mosaic model of structure of cell membranes. *Science* 175, 720–731.

Singh, S., and Parniske, M. (2012). Activation of calcium- and calmodulin-dependent protein kinase (CCaMK), the central regulator of plant root endosymbiosis. *Curr. Opin. Plant Biol.* 15, 444–453.

Smit, P., Limpens, E., Geurts, R., Fedorova, E., Dolgikh, E., Gough, C., et al. (2007). Medicago LYK3, an entry receptor in rhizobial nodulation factor signaling. *Plant Physiol.* 145, 183–191.

Smith, S., and Read, D. (2008). *Mycorrhizal Symbiosis.* New York, NY: Academic Press.

Smith, S. E., and Smith, F. A. (2011). Roles of arbuscular mycorrhizas in plant nutrition and growth: new paradigms from cellular to ecosystem scales. *Annu. Rev. Plant Biol.* 62, 227–250.

Soltis, D. E., Soltis, P. S., Morgan, D. R., Swensen, S. M., Mullin, B. C., Dowd, J. M., et al. (1995). Chloroplast gene sequence data suggest a single origin of predisposition for symbiotic nitrogen fixation in angiosperms. *Proc. Natl. Acad. Sci. U.S.A.* 92, 2647–2651.

Soto, M. J., Nogales, J., Perez-Mendoza, D., Gallegos, M. T., Olivares, J., and Sanjuan, J. (2011). Pathogenic and mutualistic plant-bacteria interactions: ever increasing similarities. *Central Eur. J. Biol.* 6, 911–917.

Spaink, H. P. (1995). The molecular basis of infection and nodulation by rhizobia - the ins and outs of sympathogenesis. *Annu. Rev. Phytopathol.* 33, 345–368.

Starker, C. G., Parra-Colmenares, A. L., Smith, L., Mitra, R. M., and Long, S. R. (2006). Nitrogen fixation mutants of *Medicago truncatula* fail to support plant and bacterial symbiotic gene expression. *Plant Physiol.* 140, 671–680.

Strack, D., and Fester, T. (2006). Isoprenoid metabolism and plastid reorganization in arbuscular mycorrhizal roots. *New Phytol.* 172, 22–34.

Stracke, S., Kistner, C., Yoshida, S., Mulder, L., Sato, S., Kaneko, T., et al. (2002). A plant receptor-like kinase required for both bacterial and fungal symbiosis. *Nature* 417, 959–962.

Tanner, W., Malinsky, J., and Opekarova, M. (2011). In plant and animal cells, detergent-resistant membranes do not define functional membrane rafts. *Plant Cell* 23, 1191–1193.

Tena, G., Boudsocq, M., and Sheen, J. (2011). Protein kinase signaling networks in plant innate immunity. *Curr. Opin. Plant Biol.* 14, 519–529.

Tian, C. J., Kasiborski, B., Koul, R., Lammers, P. J., Bucking, H., and Shachar-Hill, Y. (2010). Regulation of the nitrogen transfer pathway in the arbuscular mycorrhizal symbiosis: gene characterization and the coordination of expression with nitrogen flux. *Plant Physiol.* 153, 1175–1187.

Timmers, A. C. J., Auriac, M. C., De Billy, F., and Truchet, G. (1998). Nod factor internalization and microtubular cytoskeleton changes occur concomitantly during nodule differentiation in alfalfa. *Development* 125, 339–349.

Toth, K., Stratil, T. F., Madsen, E. B., Ye, J. Y., Popp, C., Antolin-Llovera, M., et al. (2012). Functional domain analysis of the remorin protein LjSYMREM1 in *Lotus japonicus*. *PLoS ONE* 7:e30817. doi: 10.1371/journal.pone.0030817

Tyerman, S. D., Whitehead, L. F., and Day, D. A. (1995). A channel-like transporter for NH4+ on the symbiotic interface of N2-fixing plants. *Nature* 378, 629–632.

Uehlein, N., Otto, B., Hanson, D. T., Fischer, M., McDowell, N., and Kaldenhoff, R. (2008). Function of *Nicotiana tabacum* aquaporins as chloroplast gas pores challenges the concept of membrane CO2 permeability. *Plant Cell* 20, 648–657.

Uetake, Y., Kojima, T., Ezawa, T., and Saito, M. (2002). Extensive tubular vacuole system in an arbuscular mycorrhizal fungus, *Gigaspora margarita*. *New Phytol.* 154, 761–768.

Van Brussel, A. A. N., Bakhuizen, R., Vanspronsen, P. C., Spaink, H. P., Tak, T., Lugtenberg, B. J. J., et al. (1992). Induction of preinfection thread structures in the leguminous host plant by mitogenic lipooligosaccharides of Rhizobium. *Science* 257, 70–72.

Van De Velde, W., Zehirov, G., Szatmari, A., Debreczeny, M., Ishihara, H., Kevei, Z., et al. (2010). Plant peptides govern terminal differentiation of bacteria in symbiosis. *Science* 327, 1122–1126.

Verma, D. P. S., Kazazian, V., Zogbi, V., and Bal, A. K. (1978). Isolation and characterization of membrane envelope enclosing bacteroids in soybean root-nodules. *J. Cell Biol.* 78, 919–936.

Walter, M. H., Floss, D. S., and Strack, D. (2010). Apocarotenoids: hormones, mycorrhizal metabolites and aroma volatiles. *Planta* 232, 1–17.

Wan, J., Tanaka, K., Zhang, X.-C., Son, G. H., Brechenmacher, L., Nguyen, T. H. N., et al. (2012). LYK4, a

LysM receptor-like kinase, is important for chitin signaling and plant innate immunity in Arabidopsis. *Plant Physiol.* 160, 396–406.

Wan, J. R., Zhang, X. C., Neece, D., Ramonell, K. M., Clough, S., Kim, S. Y., et al. (2008). A LysM receptor-like kinase plays a critical role in chitin signaling and fungal resistance in *Arabidopsis*. *Plant Cell* 20, 471–481.

Wang, B., and Qiu, Y. L. (2006). Phylogenetic distribution and evolution of mycorrhizas in land plants. *Mycorrhiza* 16, 299–363.

Wang, B., Yeun, L. H., Xue, J. Y., Liu, Y., Ane, J. M., and Qiu, Y. L. (2010a). Presence of three mycorrhizal genes in the common ancestor of land plants suggests a key role of mycorrhizas in the colonization of land by plants. *New Phytol.* 186, 514–525.

Wang, D., Griffitts, J., Starker, C., Fedorova, E., Limpens, E., Ivanov, S., et al. (2010b). A nodule-specific protein secretory pathway required for nitrogen-fixing symbiosis. *Science* 327, 1126–1129.

Wang, D., and Dong, X. N. (2011). A highway for war and peace: the secretory pathway in plant-microbe interactions. *Mol. Plant* 4, 581–587.

Wang, D., Yang, S. M., Tang, F., and Zhu, H. Y. (2012). Symbiosis specificity in the legume - rhizobial mutualism. *Cell. Microbiol.* 14, 334–342.

Wegmüller, S., Svistoonoff, S., Reinhardt, D., Stuurman, J., Amrhein, N., and Bucher, M. (2008). A transgenic dTph1 insertional mutagenesis system for forward genetics in mycorrhizal phosphate transport of Petunia. *Plant J.* 54, 1115–1127.

Willmann, R., Lajunen, H. M., Erbs, G., Newman, M.-A., Kolb, D., Tsuda, K., et al. (2011). *Arabidopsis* lysin-motif proteins LYM1 LYM3 CERK1 mediate bacterial peptidoglycan sensing and immunity to bacterial infection. *Proc. Natl. Acad. Sci. U.S.A.* 108, 19824–19829.

Yano, K., Yoshida, S., Muller, J., Singh, S., Banba, M., Vickers, K., et al. (2008). CYCLOPS, a mediator of symbiotic intracellular accommodation. *Proc. Natl. Acad. Sci. U.S.A.* 105, 20540–20545.

Yun, H. S., and Kwon, C. (2012). Trafficking at the host cell surface during plant immune responses. *J. Plant Biol.* 55, 185–190.

Yurgel, S. N., and Kahn, M. L. (2005). *Sinorhizobium meliloti* dctA mutants with partial ability to transport dicarboxylic acids. *J. Bacteriol.* 187, 1161–1172.

Zamioudis, C., and Pieterse, C. M. J. (2012). Modulation of host immunity by beneficial microbes. *Mol. Plant Microbe Interact.* 25, 139–150.

Zeng, L., Velasquez, A. C., Munkvold, K. R., Zhang, J., and Martin, G. B. (2012). A tomato LysM receptor-like kinase promotes immunity and its kinase activity is inhibited by AvrPtoB. *Plant J.* 69, 92–103.

Zeuthen, T. (2010). Water-transporting proteins. *J. Membr. Biol.* 234, 57–73.

Zhang, Q., Blaylock, L. A., and Harrison, M. J. (2010). Two *Medicago truncatula* half-ABC transporters are essential for arbuscule development in arbuscular mycorrhizal symbiosis. *Plant Cell* 22, 1483–1497.

Zhang, X. C., Cannon, S. B., and Stacey, G. (2009). Evolutionary genomics of LysM genes in land plants. *BMC Evol. Biol.* 9, 183.

Conflict of Interest Statement: The authors declare that the research was conducted in the absence of any commercial or financial relationships that could be construed as a potential conflict of interest.

Received: 03 July 2012; accepted: 14 September 2012; published online: 05 October 2012.

*Citation: Bapaume L and Reinhardt D (2012) How membranes shape plant symbioses: signaling and transport in nodulation and arbuscular mycorrhiza. Front. Plant Sci. **3**:223. doi: 10.3389/fpls.2012.00223*

This article was submitted to Frontiers in Plant Traffic and Transport, a specialty of Frontiers in Plant Science.

APPENDIX

Table A1 | Genes involved in regulation of arbuscular mycorrhiza and/or root nodule symbiosis.

Genes	Organism	Structural characteristics	(putative) Localization	Mutants/transformed lines analyzed	phenotypes of the mutants/transformed lines	Involvement in	(putative) Function	References
(Ph)PDR1	*P. hybrida*	ATP-binding cassette transporter subtype G (ABCG)	Plasma membrane	Transposon insertion mutant and KD RNAi lines in petunia plants; *A. thaliana* OE lines	Silenced lines: delay in AM colonization, strigolactone exudate levels affected; *A. thaliana* OE lines: higher tolerance to the synthetic strigolactone less retained into roots.	AM	Strigolactone exporter	Kretzschmar et al., 2012
(Lj)NFR1/(Mt)LYK3	*L. japonicus*/*M. truncatula*	LYK	Plasma membrane	(1,2,3) Mutants from a T-DNA insertion screen (*Ljnfr1-1/Ljsym1-1, Ljnfr1-2/Ljsym1-2*) (4) *M. truncatula* EMS-induced mutants *B56/hcl-1, W1/hcl-2, AF3/hcl-3* (5) KD RNAi transformed roots. (6) *M. truncatula* EMS-induced mutants *hcl-1, hcl-2, hcl-3, AC6/hcl-4/lyk3-4*	(1,2) Nod- phenotype, AM not affected (Ami+). (3) No root hair deformation, no root hair curling, no infection threads nor nodule primordia induced. (4) *HCL* stands for defective in root hair curling; only root hair deformation and reduced cortical cell division without meristematic cells. (5) Upon inoculation with a rhizobia strain mutated for the NF: root hair curling but decrease of IT number, ITs with a sac-like structure aborted in the root hair. (6) Concerning the fourth *lyk3* mutant *hcl-4*: normal root hair curling observed, ITs with a sac-like shape and often aborted, few nodules.	RNS	NF receptor	(1) Schauser et al., 1998; (2) Wegel et al., 1998; (3) Radutoiu et al., 2003; (4) Catoira et al., 2001; (5) Limpens et al., 2003; (6) Smit et al., 2007

(Continued)

Table A1 | Continued

Genes	Organism	Structural characteristics	(putative) Localization	Mutants/transformed lines analyzed	phenotypes of the mutants/transformed lines	Involvement in	(putative) Function	References
(Lj)NFR5/ (Mt)NFP/(Pa)NFP	*L. japonicus*/ *M. truncatula*/ *P. andersonii*	LYK	Plasma membrane	(1,3,4,5) Mutant from a T-DNA insertion mutants screen (*282-894/Ljnfr5-1/Ljsym5*), Ac-TE insertion mutant (*Ljnfr5-2*), (2) EMS-induced mutant (*EMS223/Ljnfr5-3/Ljsym25*); (6,7) EMS-induced mutants (*Mtnfp-1, Mtnfp-2*), KD RNAi transformed roots; (8) KD RNAi transformed roots (*PaNFP*)	(1,2) Nod- phenotype. (1,3) Ami+ phenotypes. (2) (4, 5) Nod- phenotype and unresponsiveness to inoculation with *M. loti* or application of NF (no root hair deformation). (6,7) EMS-induced mutants: Nod- phenotype, absolutely no sign of RNS, even root hair deformation. (7) Silenced lines: ITs abortions in root hair cells, with sac-like structures. (8) Impairment of both RNS and AM.	RNS (and AM for *P. andersonii*)	NF receptor	(1) Schauser et al., 1998; (2) Szczyglowski et al., 1998 (3) Wegel et al., 1998; (4) Madsen et al., 2003; (5) Radutoiu et al., 2003; (6) Ben Amor et al., 2003; (7) Arrighi et al., 2006; (8) Op Den Camp et al., 2011
(At)CERK1/ (Os)CERK1	*A. thaliana*/ *O. sativa*	LYK	Plasma membrane	(1) KO transposon and T-DNA insertion mutants *Atcerk1-1* and *Atcerk1-2*; (2,6) KO T-DNA insertion mutant *Atcerk1-2*; (3,4) KO T-DNA *Atcerk1-2* and *Atcerk1-3* mutants; (5) KD RNAi OsCERK1 lines	(1) No responses to chitin, including MAPK activation, ROS generation, and gene expression; impairment of disease resistance against the incompatible fungus *Alternaria brassicicola*. (2) Impairment of chitin-responsive genes, increase of fungal but not of bacterial growth (*Erysiphe cichoracearum* and *Alternaria brassicicola*; and *Pto* DC3000 respectively).	Defense	Chitin and PGN receptor	(1) Miya et al., 2007; (2) Wan et al., 2008; (3) Gimenez-Ibanez et al., 2009; (4) Willmann et al., 2011; (5) Shimizu et al., 2010; (6) Shinya et al., 2012

(Continued)

Table A1 | Continued

Genes	Organism	Structural characteristics	(putative) Localization	Mutants/transformed lines analyzed	phenotypes of the mutants/transformed lines	Involvement in	(putative) Function	References
					(3) Enhanced growth of the virulent bacterial strain *Pto* DC3000 and the non-pathogenic strain *Pto* DC3000 *hrcC*. (4) Impairment of FRK1 induction after chitin and PGN treatment, as well as PGN-responsive genes. (5) Impairment of specific ROS generation and of phytoalexins accumulation. (6) Impairment of ROS generation, defense-related genes.			
(At)LYM2/(Os)CEBiP	*A. thaliana*/*O. sativa*	LYM	Plasma membrane	(1) OsCEBiP KO RNAi lines; (2) transposon insertion mutants *lym2-2*, *lym2-3*	(1) Suppression of the specific ROS generation and impairment of gene responses induced by chitin. (2) No impairment of ROS generation.	Defense	Chitin receptor	(1) Kaku et al., 2006; (2) Shinya et al., 2012
(At)LYK4	*A. thaliana*	LYK	Plasma membrane	T-DNA insertion mutant *lyk4*	Impairment of chitin-responsive genes, increase of fungal and bacterial growth (*Alternaria brassicicola* and *Pto* DC3000 respectively).	Defense	Chitin receptor	Wan et al., 2012
(At)LYM1	*A. thaliana*	LYM	Plasma membrane	(1) T-DNA insertion mutants *lym1-1*, *lym1-2*; (2) T-DNA insertion mutant *lym1-1*, transposon insertion mutant *lym1-2*	Impairment of FRK1 induction after PGN treatment, as well as PGN-responsive genes; enhanced growth of *Pto* DC3000. (2) No impairment of ROS generation (*lym1-2*).	Defense	PGN receptor	(1) Willmann et al., 2011; (2) Shinya et al., 2012

(Continued)

Table A1 | Continued

Genes	Organism	Structural characteristics	(putative) Localization	Mutants/transformed lines analyzed	phenotypes of the mutants/transformed lines	Involvement in	(putative) Function	References
(At)LYM3	*A. thaliana*	LYM	Plasma membrane	(1,2) cs *lym3-1*, *lym3-2*	(1) Impairment of FRK1 induction after PGN treatment, as well as PGN-responsive genes; enhanced growth of *Pto* DC3000, *Pto* DC3000 hrcC- and the hypovirulent *Pto* DC3000 ΔavrPto/PtoB. (2) No impairment of ROS generation (*lym3-1*).	Defense	PGN receptor	(1) Willmann et al., 2011; (2) Shinya et al., 2012
(Lj)SYMRK/(Ms) NORK/(Mt)DMI2	*L. japonicus*/*M. sativa*/*M. truncatula*	LRR-RLK	Plasma membrane and IT	(1,2,7) *L. japonicus* EMS-induced mutant (*EMS61/Ljsym21-2*) and (1,3,4,7) mutants from a transposon/T-DNA insertion mutants screen (*282-287/Ljsym2-1*, *cac41.5*); (5,6) *M. sativa* MN-1008 mutant obtained from crosses between different cultivars; (8) *M. truncatula* KD RNAi transformed roots, transformed roots with the RNAi hairpin construct *ENOD12::DMI2i*, and *35S::DMI2*-transformed roots from the TR25 mutant (lowering DMI2 activity in the nodule apex)	(1) Nod- phenotype. (2) Amplified swelling and branching, but no curling of root hairs when inoculated with *M. loti*. No more induction of the leghaemoglobin gene. (3,4) Coi- and Nod- phenotypes. (5,6,7) Myc- and Nod- phenotypes. (8) RNAi transformed roots: few nodules formed, in which ITs but few symbiosomes were observed; transformed roots with the RNAi hairpin or *35S::DMI2* constructs: more nodules formed, ITs growth amplified, with enlarged and branched ITs, but no symbiosomes observed, Fix- phenotype.	Common SYM pathway	Required for accommodation in both symbioses; positioned between NF perception and calcium spiking in the common SYM pathway	(1) Szczyglowski et al., 1998 (2) Stracke et al., 2002; (3) Schauser et al., 1998; (4) Wegel et al., 1998; (5) Caetano-Anollés and Gresshoff, 1991; (6) Endre et al., 2002; (7) Kistner et al., 2005; (8) Limpens et al., 2005

(Continued)

Table A1 | Continued

Genes	Organism	Structural characteristics	(putative) Localization	Mutants/transformed lines analyzed	phenotypes of the mutants/transformed lines	Involvement in	(putative) Function	References
(Lj)SIP2	*L. japonicus*	MAPKK	Plasma membrane-associated and cytoplasm	KD RNAi transformed roots	Strong down-regulation of three marker genes for IT and nodule primordium formation; impairment of IT and nodulation formation.	RNS	Functional MAPKK interacting with SYMRK and that could be involved in the regulation of early symbiotic signal transduction and nodule organogenesis may be due to the inhibitory effect of SYMRK on its activity	Chen et al., 2012
(Lj)SINA4	*L. japonicus*	E3 ubiquitin ligase	Cytoplasm	OE transformed roots and OE transgenic lines	OE transformed roots: reduced SYMRK protein levels upon *M. loti* inoculation; OE transgenic lines: decrease of infection events and number of ITs, increase of white nodules, thick and branched ITs in both white and pink nodules, no or few bacteroids observed.	RNS	SYMRK turnover	Den Herder et al., 2012

(Continued)

Table A1 | Continued

Genes	Organism	Structural characteristics	(putative) Localization	Mutants/transformed lines analyzed	phenotypes of the mutants/transformed lines	Involvement in	(putative) Function	References
(Mt)PUB1	*M. truncatula*	E3 ubiquitin ligase	Plasma membrane-associated	OE and KD RNAi transformed roots in the wild-type background and in the *hcl-4 (lyk3-4)* background	OE transformed roots: delay in nodulation observed; KD transformed roots (wt background): number of nodules strongly increased only upon *S. meliloti* mutant strains (*nodL, nodFnodL*: NF modified at the non-reducing end); KD transformed roots (*hcl-4* background): impairment of nodulation and IT development observed in *hcl-4* mutant overcame.	RNS*	Functional E3 ubiquitin ligase that interacts with LYK3 physically and functionally by regulating negatively infection and nodulation	Mbengue et al., 2010
(Lj)SYMREM1/ (Mt)SYMREM1	*L. japonicus*/*M. truncatula*	Remorin	Host-derived membrane-associated with a localization to nodular ITs, more strongly at the tip where unwalled infection droplets form, and symbiosomes	(1) KD RNAi transformed roots, stable RNAi lines, *Tnt1*-transposon insertion mutants; (2) OE transformed roots	(1) RNAi transformed roots: no or few nodulation, often with small and white nodules, multiplication of IT formation, IT often aborted, highly branched or with a sac-like structure. Stable RNAi lines: enlargement of ITs and absence of symbiosome, suggesting a delay in rhizobia release into host cells; KO line: morphological change of nodule shape, enlarged and highly branched ITs, almost no symbiosomes formed. (2) Increase of mature nodules number but not in IT number.	RNS	Role in RNS accommodation and hypothesized to supervise localization, sorting and regulation of LjNFR1/MtLYK3, LjNFR5/MtNFP and LjSYMRK/MtDMI2 during RN symbiosis in plasma membrane sub-domains.	(1) Lefebvre et al., 2010; (2) Toth et al., 2012

(Continued)

Table A1 | Continued

Genes	Organism	Structural characteristics	(putative) Localization	Mutants/transformed lines analyzed	phenotypes of the mutants/transformed lines	Involvement in	(putative) Function	References
(Mt)HMGR1	*M. truncatula*	3-Hydroxy-3-Methylglutaryl Coenzyme A Reductase	Vesicle-like structures	Pharmacological inhibition and KD RNAi transformed roots	Pharmacological inhibition: decrease of nodule number; KD transformed roots: nodulation strongly decreased, with ITs and nodules development arrested at an early step, Fix- phenotype.	RNS*	HMGR1 activity is required for nodule development; four hypotheses were mentioned concerning the recruitment of HMGR1 by NORK and the link with the mevalonic acid (MVA) pathway	Kevei et al., 2007
(Mt)FLOT2	*M. truncatula*	Flotillin-like	Plasma membrane-associated microdomains	KD RNAi and amiRNA transformed roots	Few infection events, normal IT development but great part of small and white nodules; also decrease in primary root length as well as increase in lateral root length.	RNS	Required for IT initiation	Haney and Long, 2010
(Mt)FLOT4	*M. truncatula*	Flotillin-like	Plasma membrane-associated microdomains	KD RNAi and amiRNA transformed roots	Few infection events, ITs largely aborted in root hair, great part of small and white nodules; also increase in the number of secondary lateral roots.	RNS	Required for IT initiation and development	Haney and Long, 2010

(Continued)

Table A1 | Continued

Genes	Organism	Structural characteristics	(putative) Localization	Mutants/transformed lines analyzed	phenotypes of the mutants/transformed lines	Involvement in	(putative) Function	References
(Mt)MSBP1	*M. truncatula*	Membrane-bound steroid-binding protein	Nuclear membranes and surrounding ER	Transformed roots with KD RNAi lines	KD lines: frequency of mycorrhizal colonization unchanged but infection sites often aborted. In case of successful infection sites, septated hyphae and collapsed arbuscules observed.	AM	Sterol homeostasis	Kuhn et al., 2010
(Lj)CASTOR and (Lj)POLLUX/ (Mt)DMI1	*L. japonicus*/*M. truncatula*	Ion channel	Nuclear membranes, (5) preferentially the inner nuclear membrane	(3,4,5,6) EMS-induced mutant (*EMS1749/Ljsym4-2*); (2,3,4,5,6) mutant from a T-DNA insertion screen (*282-227/Ljsym4-1*); (1,5,6) EMS-induced mutant (*EMS46/Ljsym22-1*); (5) EMS-induced mutant, T-DNA insertion mutants, somaclonal variation-induced mutants; (7,9) EMS-induced mutants (*dmi1-1/C71, dmi1-2/B129*); (8,9) fast neutron bombardment-induced mutant (*dmi1-4*)	(1) Nod- phenotype. (2) Coi- phenotype. (3,6) Nod- phenotype. No root hair curling, no IT. (3,4,6) Myc- phenotype for *Ljsym4-2*, rare infection events and delay in arbuscule formation for *Ljsym4-1* and *Ljsym22-1*. (5) No penetration of endosymbionts, with no root hairs curling neither calcium spiking during RNS, and abortion of infection attempts in AM. (7,8) Nod- phenotype.	Common SYM pathway	Cation channel that could trigger a potassium influx at the nuclear envelope and be involved in a compensatory mechanism with the release of Ca^{2+} during calcium spiking around the nucleus	(1) Szczyglowski et al., 1998 (2) Wegel et al., 1998; (3) Bonfante et al., 2000; (4) Novero et al., 2002; (5) Imaizumi-Anraku et al., 2005; (6) Kistner et al., 2005; (7) Catoira et al., 2000; (8) Ané et al., 2004
(Lj)NUP85	*L. japonicus*	Nucleoporin	Nuclear membranes	EMS-induced mutants (1,3,4,5,6) *EMS76/Ljsym24-1/Ljnup85-1*, (3,2,7) *EMS1-1E/Ljnup85-2/Ljsym73* (3,7) *EMS1-6F/Ljnup85-3/Ljsym85*	(1) Nod- phenotype for *Ljsym24*. (2) Low nodulation and Ami+. (3) Nod- and Myc- phenotypes for *Ljsym24* and *Ljsym85*; low nodulation for *Ljsym73*. (4) No ITs, low nodulation with Fix- phenotype, arbuscule formation delayed. (6) Nod- Ami- phenotypes. (5) Root hair deformation but impairment of calcium spiking. (7) Root hair branching after NF treatment, few ITs, no calcium spiking recorded, Coi- phenotype. Less AM and RNS impairments at reduced temperatures.	Common SYM pathway	NPC component	(1) Szczyglowski et al., 1998 (2) Kawaguchi et al., 2002; (3) Kawaguchi et al., 2005; (4) Kistner et al., 2005; (5) Miwa et al., 2006; (6) Sandal et al., 2006; (7) Saito et al., 2007

(Continued)

Table A1 | Continued

Genes	Organism	Structural characteristics	(putative) Localization	Mutants/transformed lines analyzed	phenotypes of the mutants/transformed lines	Involvement in	(putative) Function	References
(Lj)NUP133	*L. japonicus*	Nucleoporin	Nuclear membranes	T-DNA insertion mutants (1,3,4) *5371-22/nup133-1/Ljsym3-1*, (1,2,4) *2557-1/nup133-2/Ljsym3-2*; (4) *nup133-4/Ljsym45*; (3,4) EMS-induced mutant *EMS247/nup133-3/Ljsym3-3*	(1) Nod- and Coi- phenotypes for *Ljsym3-2*. (2) Coi- phenotype. (3) No ITs, low nodulation with Fix- phenotype, Coi- phenotype, rarely arbuscules formation observed but strongly delayed. (4) No calcium spiking recorded for *Ljsym3-1*; for several *Ljnup133* mutants root hair swelling and branching, but not root hair curling, few ITs, strong defects in nodule development, from no nodules formed to small ineffective nodules (Fix- phenotype) with almost no infected cells. Less AM and RNS impairments at reduced temperatures.	Common SYM pathway	NPC component	(1) Schauser et al., 1998; (2) Wegel et al., 1998; (3) Kistner et al., 2005; (4) Kanamori et al., 2006
(Lj)NENA	*L. japonicus*	Nucleoporin	Nuclear membranes	EMS-induced mutants *nena-1* to *nena-5*, C6+ ion beam irradiated mutant *nena-6*	Coi- phenotype, rare successful colonization with normal arbuscules, no root hair infection, Nod- phenotype (*nena-1* and *nena-2*) to few nodules (*nena-3*), impairment of calcium spiking (*nena-1*). No symbiotic defects for *nena-4* and *nena-5*. Less AM and RNS impairments at reduced temperatures.	Common SYM pathway	NPC component proposed to be involved in import to the nucleus of proteins required for calcium spiking	Groth et al., 2010
(Mt)MCA8	*M. truncatula*	SERCA-type calcium ATPase	Nuclear membranes and ER	KD RNAi transformed roots	Silenced lines affected in NF-induced calcium spiking but no defects in nodulation, reduced AM colonization, with several aborted penetration attempts, and strongly reduced arbuscules and vesicles.	AM and RNS	Required for calcium oscillations with reloading nuclear envelope and ER lumen in calcium	Capoen et al., 2011

(Continued)

Table A1 | Continued

Genes	Organism	Structural characteristics	(putative) Localization	Mutants/transformed lines analyzed	phenotypes of the mutants/transformed lines	Involvement in	(putative) Function	References
(Mt)SYP132	*M. truncatula*	Syntaxin	Plasma membrane, IT, unwalled droplets and symbiosome	–	–	RNS	Vesicle trafficking during IT/symbiosome formation	Catalano et al., 2004, 2007; Limpens et al., 2009; Ivanov et al., 2012
(Mt)VAMP721d and (Mt)VAMP721e	*M. truncatula*	SNARE	Vesicles closed to unwalled droplets, near or on membranes of developing symbiosomes; over PAM, in particular thin branches	KD RNAi transformed roots concerning both VAMP721d and VAMP721e	Impairment of symbiosome formation, with numerous nodular ITs but no or rare symbiosomes observed, "unwalled droplets" actually with a thin cell wall, and impairment of arbuscule formation, stopped before mature arbuscule development	AM and RNS	Common symbiotic regulators in exocytotic vesicle trafficking	Ivanov et al., 2012
(Mt)DNF1	*M. truncatula*	22-kD subunit (SPC22) of the signal peptidase complex (SPC)	ER-like structures	Fast neutron bombardment mutants	(1) Accumulation of nodule-specific cysteine-rich (NCR) peptides in the ER. (2) No terminal differentiation of bacteroids, Fix- phenotype.	RNS	Proper secretion of components involved in functional symbiosomes	(1) Van De Velde et al., 2010; (2) Wang et al., 2010b
(Ph)PAM1/(Mt) VAPYRIN	*P. hybrida*/*M. truncatula*	MSP and ANK domains	Cytoplasm, mobile spherical structures, nucleus	(1,2) Transposon mutants; (3) KD RNAi transformed roots; (4) four fast-neutron mutants, tansposon mutant lines	(1,2,3,5) Difficulties to penetrate epidermis cells, no functional arbuscules found. (4) Normal root hair curling, but numerous infection events, abnormal IT development and small, white and uninfected nodules	AM and RNS	Role in RNS and AM fungal accommodation, acting downstream of the calcium signal of the common SYM pathway, may be involved in membrane and/or cargo trafficking	(1) Sekhara Reddy et al., 2007; (2) Feddermann et al., 2010; (3) Pumplin et al., 2010; (4) Murray et al., 2011

Ami, AM infection; Coi-, Absence of cortex invasion; Fix-, defective in nitrogen fixation; KD, Knockdown; KO, Knockout; Myc-, Non-mycorrhizal; Nod-, Non-nodulating; OE, Overexpression; PGN, peptidoglycan; Pto DC3000, Pseudomonas syringae pathovar tomato strain DC3000; RNAi, RNA interference; ROS, Reactive oxygen species

**up-regulated during AM.*

REFERENCES

Ané, J.-M., Kiss, G. B., Riely, B. K., Penmetsa, R. V., Oldroyd, G. E. D., Ayax, C., et al. (2004). *Medicago truncatula* DMI1 required for bacterial and fungal symbioses in legumes. *Science* 303, 1364–1367.

Bonfante, P., Genre, A., Faccio, A., Martini, I., Schauser, L., Stougaard, J., et al. (2000). The *Lotus japonicus* LjSym4 gene is required for the successful symbiotic infection of root epidermal cells. *Mol. Plant Microbe Interact.* 13, 1109–1120.

Caetano-Anollés, G., and Gresshoff, P. M. (1991). Efficiency of nodule initiation and autoregulatory responses in a supernodulating soybean mutant. *Appl. Environ. Microbiol.* 57, 2205–2210.

Catoira, R., Galera, C., De Billy, F., Penmetsa, R. V., Journet, E. P., Maillet, F., et al. (2000). Four genes of *Medicago truncatula* controlling components of a nod factor transduction pathway. *Plant Cell* 12, 1647–1665.

Catoira, R., Timmers, A. C. J., Maillet, F., Galera, C., Penmetsa, R. V., Cook, D., et al. (2001). The HCL gene of *Medicago truncatula* controls Rhizobium-induced root hair curling. *Development* 128, 1507–1518.

Haag, A. F., Baloban, M., Sani, M., Kerscher, B., Pierre, O., Farkas, A., et al. (2011). Protection of *Sinorhizobium* against host cysteine-rich antimicrobial peptides is critical for symbiosis. *PLoS Biol.* 9:e1001169. doi: 10.1371/journal.pbio.1001169

Haney, C. H., and Long, S. R. (2010). Plant flotillins are required for infection by nitrogen-fixing bacteria. *Proc. Natl. Acad. Sci. U.S.A.* 107, 478–483.

Imaizumi-Anraku, H., Takeda, N., Charpentier, M., Perry, J., Miwa, H., Umehara, Y., et al. (2005). Plastid proteins crucial for symbiotic fungal and bacterial entry into plant roots. *Nature* 433, 527–531.

Karandashov, V., Nagy, R., Wegmuller, S., Amrhein, N., and Bucher, M. (2004). Evolutionary conservation of a phosphate transporter in the arbuscular mycorrhizal symbiosis. *Proc. Natl. Acad. Sci.* 101, 6285–6290.

Kawaguchi, M., Imaizumi-Anraku, H., Koiwa, H., Niwa, S., Ikuta, A., Syono, K., et al. (2002). Root, root hair, and symbiotic mutants of the model legume *Lotus japonicus*. *Mol. Plant Microbe Interact.* 15, 17–26.

Kawaguchi, M., Pedrosa-Harand, A., Yano, K., Hayashi, M., Murooka, Y., Saito, K., et al. (2005). *Lotus burttii* takes a position of the third corner in the Lotus molecular genetics triangle. *DNA Res.* 12, 69–77.

Kistner, C., Winzer, T., Pitzschke, A., Mulder, L., Sato, S., Kaneko, T., et al. (2005). Seven *Lotus japonicus* genes required for transcriptional reprogramming of the root during fungal and bacterial symbiosis. *Plant Cell* 17, 2217–2229.

Limpens, E., Franken, C., Smit, P., Willemse, J., Bisseling, T., and Geurts, R. (2003). LysM domain receptor kinases regulating rhizobial Nod factor-induced infection. *Science* 302, 630–633.

Mergaert, P., Uchiumi, T., Alunni, B., Evanno, G., Cheron, A., Catrice, O., et al. (2006). Eukaryotic control on bacterial cell cycle and differentiation in the Rhizobium-legume symbiosis. *Proc. Natl. Acad. Sci. U.S.A.* 103, 5230–5235.

Miwa, H., Sun, J., Oldroyd, G. E. D., and Downie, J. A. (2006). Analysis of nod-factor-induced calcium signaling in root hairs of symbiotically defective mutants of *Lotus japonicus*. *Mol. Plant Microbe Interact.* 19, 914–923.

Novero, M., Faccio, A., Genre, A., Stougaard, J., Webb, K. J., Mulder, L., et al. (2002). Dual requirement of the *LjSym4* gene for mycorrhizal development in epidermal and cortical cells of *Lotus japonicus* roots. *New Phytol.* 154, 741–749.

Riely, B. K., Lougnon, G., Ané, J. M., and Cook, D. R. (2007). The symbiotic ion channel homolog DMI1 is localized in the nuclear membrane of *Medicago truncatula* roots. *Plant J.* 49, 208–216.

Sandal, N., Petersen, T. R., Murray, J., Umehara, Y., Karas, B., Yano, K., et al. (2006). Genetics of symbiosis in *Lotus japonicus*: recombinant inbred lines, comparative genetic maps, and map position of 35 symbiotic loci. *Mol. Plant Microbe Interact.* 19, 80–91.

Schauser, L., Handberg, K., Sandal, N., Stiller, J., Thykjaer, T., Pajuelo, E., et al. (1998). Symbiotic mutants deficient in nodule establishment identified after T-DNA transformation of *Lotus japonicus*. *Mol. Gen. Genet.* 259, 414–423.

Szczyglowski, K., Shaw, R. S., Wopereis, J., Copeland, S., Hamburger, D., Kasiborski, B., et al. (1998). Nodule organogenesis and symbiotic mutants of the model legume *Lotus japonicus*. *Mol. Plant Microbe Interact.* 11, 684–697.

Wegel, E., Schauser, L., Sandal, N., Stougaard, J., and Parniske, M. (1998). Mycorrhiza mutants of *Lotus japonicus* define genetically independent steps during symbiotic infection. *Mol. Plant Microbe Interact.* 11, 933–936.